RW1102
11.7.2019

Das Standardmodell der Elementarteilchenphysik

Roland Waldi

Universität Rostock

Inhalt

1. Vorwort

Dies ist ein Skriptfragment zu einer Vorlesung an der Universität Rostock, es ersetzt kein Lehrbuch, sondern ergänzt es. Da es aus verschiedenen anderen Skripten zusammengebaut ist, ist der Text teilweise deutsch und teilweise englisch.

Ergänzende Kapitel sind mit * gekennzeichnet.

In der vorliegenden Version können noch Fehler enthalten sein, Vorsicht und Kritik sind angebracht! Hinweise und Anregungen sind willkommen.

1.1 Konventionen

In diesem Skript werden die Konstanten $\hbar$ und c i. A. weggelassen, was kurz durch $\hbar = c = 1$ ausgedrückt wird. Genauer bedeutet es, dass sie in den Messgrößen absorbiert werden, z. B. messen wir einen Impuls normalerweise in Einheiten von GeV/c, wir definieren aber $p_{\text{old}} \to p_{\text{new}} = p_{\text{old}} \cdot c$ und verwenden den Impuls p_{new} mit der Einheit GeV. Der Unterschied zwischen p_{old} und p_{new} besteht offensichtlich lediglich in einer Konstanten, es handelt sich also um die gleichen physikalischen Größen. In der Literatur verwendet man allerdings die alten Größen und nutzt stattdessen $\hbar$ und c als Maßeinheiten.

Bei Matrizen bedeutet
$M^\dagger$ = transponiert: $(m^\dagger)_{\alpha\beta} = m_{\beta\alpha}$,
M^* = komplex konjugiert: $(m^*)_{\alpha\beta} = m^*_{\alpha\beta}$, und
M^+ = hermitesch konjugiert: $(m^+)_{\alpha\beta} = m^*_{\beta\alpha}$.

Total antisymmetrischer Tensor (Levi–Civita-Tensor) in 3 Dimensionen

$$\varepsilon_{ijk} = \begin{cases} 1 & ijk = 123, 231, 312 \\ -1 & ijk = 321, 213, 132 \\ 0 & \text{sonst} \end{cases} \tag{1.1}$$

1.2 Minkowskimetrik

Der verwendete metrische Tensor ist[1]

$$g_{\mu\nu} = g^{\mu\nu} = \begin{pmatrix} 1 & 0 & 0 & 0 \\ 0 & -1 & 0 & 0 \\ 0 & 0 & -1 & 0 \\ 0 & 0 & 0 & -1 \end{pmatrix} \qquad \text{(im Minkowski-Raum)} \tag{1.2}$$

$$g_\mu{}^\nu = \delta^\nu_\mu$$
$$g^\mu{}_\nu = \delta^\mu_\nu$$
$$g^{\mu\nu} g_{\mu\nu} = 4$$

Die ständige Benutzung des Metriktensors $g_{\mu\nu}$ lässt sich vermeiden, wenn man zwischen oberen und unteren Indizes unterscheidet. Durch die Definition

$$x_\mu = g_{\mu\nu} x^\nu$$

macht man aus dem *kontravarianten* Vektor $x^\nu = (t, x, y, z)$ den *kovarianten* Vektor $x_\mu = (ct, -x, -y, -z)$. Damit lässt sich das Skalarprodukt einfacher schreiben als

$$x_\nu y^\nu = g_{\mu\nu} x^\mu y^\nu = x^\mu y_\mu$$

[1] Kronecker-Symbol: $\delta^\nu_\mu = \begin{cases} 1 & \mu = \nu \\ 0 & \text{sonst} \end{cases}$

Um korrekte Resultate zu erhalten, summiert man stets über Indizes, die einmal oben und einmal unten vorkommen.

Tensor 2. Stufe:

$$M^{\mu\nu} = \begin{pmatrix} m_{00} & m_{01} & m_{02} & m_{03} \\ m_{10} & m_{11} & m_{12} & m_{13} \\ m_{20} & m_{21} & m_{22} & m_{23} \\ m_{30} & m_{31} & m_{32} & m_{33} \end{pmatrix}, \quad M_{\mu\nu} = \begin{pmatrix} m_{00} & -m_{01} & -m_{02} & -m_{03} \\ -m_{10} & m_{11} & m_{12} & m_{13} \\ -m_{20} & m_{21} & m_{22} & m_{23} \\ -m_{30} & m_{31} & m_{32} & m_{33} \end{pmatrix}$$

$$M^{\mu}{}_{\nu} = \begin{pmatrix} m_{00} & -m_{01} & -m_{02} & -m_{03} \\ m_{10} & -m_{11} & -m_{12} & -m_{13} \\ m_{20} & -m_{21} & -m_{22} & -m_{23} \\ m_{30} & -m_{31} & -m_{32} & -m_{33} \end{pmatrix}, \quad M_{\mu}{}^{\nu} = \begin{pmatrix} m_{00} & m_{01} & m_{02} & m_{03} \\ -m_{10} & -m_{11} & -m_{12} & -m_{13} \\ -m_{20} & -m_{21} & -m_{22} & -m_{23} \\ -m_{30} & -m_{31} & -m_{32} & -m_{33} \end{pmatrix}$$

Differentialoperator:

$$\partial^{\mu} = \frac{\partial}{\partial x_{\mu}} = (\partial_t, -\partial_x, -\partial_y, -\partial_z), \quad \partial_{\mu} = \frac{\partial}{\partial x^{\mu}} = (\partial_t, \partial_x, \partial_y, \partial_z)$$

$$\partial_{\mu} V^{\mu} = \partial_t V^0 + \nabla \boldsymbol{V}$$

Impulsoperator:

$$\vec{p} = -i\nabla = \begin{pmatrix} -i\frac{\partial}{\partial x} \\ -i\frac{\partial}{\partial y} \\ -i\frac{\partial}{\partial z} \end{pmatrix}$$

Energieoperator:

$$E = i\frac{\partial}{\partial t} = i\partial_t$$

$$p^{\mu} = i\partial^{\mu}$$

Ruhemasse (Invariante):

$$m^2 = p^{\mu} p_{\mu} = E^2 - \vec{p}^{\,2} \tag{1.3}$$

Total antisymmetrischer Tensor im Minkowskiraum

$$\varepsilon^{\mu\nu\rho\sigma} = \begin{cases} 1 & \mu\nu\rho\sigma = (0123) \text{ gerade}^2 \\ -1 & \mu\nu\rho\sigma = (0123) \text{ ungerade}^2 \\ 0 & \text{sonst} \end{cases} \tag{1.4}$$

Eigenschaften:

$$\begin{aligned} \varepsilon_{..\mu\nu..} &= -\varepsilon_{..\nu\mu..} \\ \varepsilon^{\mu\nu\rho\sigma} &= -\varepsilon_{\mu\nu\rho\sigma} \\ \varepsilon^{\mu\nu\rho\alpha}\varepsilon_{\mu\nu\rho}{}^{\beta} &= -6g^{\alpha\beta} \\ \varepsilon^{\mu\nu\rho\sigma}\varepsilon_{\mu\nu\rho\sigma} &= -24 \\ \varepsilon^{\mu\nu\alpha\beta}\varepsilon_{\rho\sigma\alpha\beta} &= 2(\delta^{\mu}_{\sigma}\delta^{\nu}_{\rho} - \delta^{\mu}_{\rho}\delta^{\nu}_{\sigma}) \end{aligned} \tag{1.5}$$

Herleitung von (1.5): Terme $\neq 0$ haben $\mu = \rho, \nu = \sigma$ oder $\nu = \rho, \mu = \sigma$, und es gibt jeweils zwei davon, da $\{\alpha, \beta\}$ verschieden von $\{\mu, \nu\}$ sind.

Für jede symmetrische Matrix $X_{\mu\nu} = X_{\nu\mu}$ ist

$$X_{\mu\nu}\varepsilon^{\mu\nu\alpha\beta} = 0 \tag{1.6}$$

[2] gerade: 0123, 0231, 0312, 1032, 1203, 1320, 2013, 2130, 2301, 3021, 3102, 3210;
ungerade: 0132, 0213, 0321, 1023, 1230, 1302, 2031, 2103, 2310, 3012, 3120, 3201.
Zyklisches Vertauschen wechselt hier das Vorzeichen!

2. Theoretische Grundlagen

2.1 Polarisation

Polarisationsvektor im Ruhesystem eines Teilchens:

$$\boldsymbol{P} = \begin{pmatrix} \langle s_x \rangle \\ \langle s_y \rangle \\ \langle s_z \rangle \end{pmatrix}$$
$$P = (0, \boldsymbol{P}) \tag{2.1}$$

Eigenschaften:

$$P^\mu p_\mu = 0$$

2.2 Relativistische Beschreibung von ganzzahligen Spinzuständen

Die Beschreibung von Drehimpuls- oder Spin-Eigenzuständen zum Spin J kann kovariant durch Tensoren der Stufe J erfolgen[3]. Die 4^J Komponenten werden durch die Bedingungen

- Symmetrie: $\varepsilon_{\ldots\mu\ldots\nu\ldots} = \varepsilon_{\ldots\nu\ldots\mu\ldots}$
- Spurfreiheit: $\varepsilon_{\ldots\mu\ldots\mu\ldots} = 0$
- Orthogonalität: $p^\mu \varepsilon_{\ldots\mu\ldots} = 0$

auf die $2J + 1$ Freiheitsgrade eines Spin-J Systems reduziert.

2.2.1 Spin-1

Für ein Spin-1-Teilchen mit Viererimpuls $p = (E, 0, 0, p)$ ist der Polarisationstensor

$$\begin{aligned} \varepsilon_\mu(J_z = +1) &= (0, -\frac{1}{\sqrt{2}}, -\frac{i}{\sqrt{2}}, 0) \\ \varepsilon_\mu(J_z = 0) &= (\frac{p}{m}, 0, 0, \frac{E}{m}) \\ \varepsilon_\mu(J_z = -1) &= (0, \frac{1}{\sqrt{2}}, -\frac{i}{\sqrt{2}}, 0) \end{aligned} \tag{2.2}$$

mit

$$\varepsilon_\mu p^\mu = 0 \tag{2.3}$$

und für alle drei Eigenzustände

$$\varepsilon^*_\mu \varepsilon^\mu = -1 \tag{2.4}$$

Drehimpulseigenzustände ± 1 entsprechen zirkular polarisierten Feldern.

Parität:

$$\mathrm{P}\ \varepsilon_\mu(\vec{p}) = -\varepsilon^\mu(-\vec{p})$$

($\vec{\varepsilon}$ ist ein Axialvektor, die räumlichen Anteile ändern ihr Vorzeichen nicht)

[3] siehe z. B. C. Zemach, Phys. Rev. **140B**, 97 u. 109 (1965).

2.2.2 Das Photon

Photonen (allgemein masselose Spin-1 Teilchen) haben nur transversale Polarisation, d. h. $J_z = \pm 1$. Damit gilt für den Polarisationsvektor

$$\varepsilon^0 = 0$$

Es genügt zur Beschreibung der Dreiervektor $\vec{\varepsilon}$, mit $\vec{\varepsilon}\vec{p} = 0$.

2.2.3 Spin-2

Für ein Spin-2-Teilchen mit Impuls $p = (E, 0, 0, p)$ ist der Polarisationstensor

$$\begin{aligned}
\varepsilon_{\mu\nu}(J_z = +2) &= \varepsilon_\mu(+1)\varepsilon_\nu(+1) \\
\varepsilon_{\mu\nu}(J_z = +1) &= \frac{1}{\sqrt{2}}\varepsilon_\mu(+1)\varepsilon_\nu(0) + \frac{1}{\sqrt{2}}\varepsilon_\mu(0)\varepsilon_\nu(+1) \\
\varepsilon_{\mu\nu}(J_z = 0) &= \frac{1}{\sqrt{6}}[\varepsilon_\mu(+1)\varepsilon_\nu(-1) + \varepsilon_\mu(-1)\varepsilon_\nu(+1)] + \sqrt{\frac{2}{3}}\varepsilon_\mu(0)\varepsilon_\nu(0) \\
\varepsilon_{\mu\nu}(J_z = -1) &= \frac{1}{\sqrt{2}}\varepsilon_\mu(-1)\varepsilon_\nu(0) + \frac{1}{\sqrt{2}}\varepsilon_\mu(0)\varepsilon_\nu(-1) \\
\varepsilon_{\mu\nu}(J_z = -2) &= \varepsilon_\mu(-1)\varepsilon_\nu(-1)
\end{aligned} \tag{2.5}$$

Polarisationstensoren zu höheren ganzzahligen Spins können analog mit Hilfe der Clebsch–Gordan-Koeffizienten konstruiert werden.

2.2.4 Spinsummen

$$\gamma_{\mu\nu} := g_{\mu\nu} - \frac{p_\mu p_\nu}{m^2}$$

Spin 1:

$$\sum_{J_z=-1,0,+1} \varepsilon_\mu \varepsilon_\nu^* = -g_{\mu\nu} + \frac{p_\mu p_\nu}{m^2} = -\gamma_{\mu\nu} \tag{2.6}$$

Masselose Teilchen (Photonen) mit $\vec{J} \perp \vec{p}$:

$$\begin{aligned}
\varepsilon_0 &= 0 \\
\sum_{J_z=-1,+1} \varepsilon_j \varepsilon_k^* &= \delta_{jk} - \frac{p_j p_k}{\vec{p}^2} \quad j,k = 1\ldots 3 \\
\sum_{J_z=-1,+1} \varepsilon_\mu \varepsilon_\nu^* &\to -g_{\mu\nu}
\end{aligned} \tag{2.7}$$

Spin 2:

$$\sum_\lambda \varepsilon_{\mu\nu}(\lambda)\varepsilon^*_{\mu'\nu'}(\lambda) = \frac{1}{2}(\gamma_{\mu\mu'}\gamma_{\nu\nu'} + \gamma_{\mu\nu'}\gamma_{\nu\mu'}) - \frac{1}{3}\gamma_{\mu\nu}\gamma_{\mu'\nu'}$$

2.3 Lagrange-Dichte

Lagrange-Dichte der Felder $\psi_i = \psi_i(x^\mu)$

$$\mathcal{L} = \mathcal{L}(\psi_i, \partial^\mu \psi_i, x^\mu)$$

Euler-Lagrange-Gleichungen:

$$\frac{\partial \mathcal{L}}{\partial \psi_i} = \frac{\mathrm{d}}{\mathrm{d}x^\mu} \frac{\partial \mathcal{L}}{\partial(\partial_\mu \psi_i)} \tag{2.8}$$

2.4 Noether-Theorem

Wenn die Wirkung $\mathcal{S}$ invariant unter einer Koordinaten- und/oder Feldtransformation ist, die von n Parametern abhängt, dann existieren n Erhaltungsgrößen[4] (erhaltene Ströme).

Wirkung $\mathcal{S}$ invariant[5]:

$$\mathcal{S}(V) = \int_V \mathcal{L}(\psi_i', \partial_\mu' \psi_i', x') \,\mathrm{d}^4 x' = \int_V \mathcal{L}(\psi_i, \partial_\mu \psi_i, x) \,\mathrm{d}^4 x \tag{2.9}$$

für alle Raumzeitgebiete V mit gleicher Begrenzung $\partial V'(x') = \partial V(x)$, oder (äquivalent)

$$\mathcal{L}(\psi_i', \partial_\mu' \psi_i', x') \left\| \frac{\partial x'}{\partial x} \right\| = \mathcal{L}(\psi_i, \partial_\mu \psi_i, x) \tag{2.10}$$

mit der Jacobideterminante

$$J = \left\| \frac{\partial x'}{\partial x} \right\|$$

infinitesimale Transformation:

$$\begin{aligned} x'^\mu &= x^\mu + \delta x^\mu \\ \psi_i'(x') &= \psi_i'(x) = \psi_i(x) + \delta\psi_i(x) \qquad \delta\psi_i = \partial_\mu \psi_i \, \delta x^\mu + \bar{\delta}\psi_i \\ J &= 1 + \partial_\mu \delta x^\mu \end{aligned}$$

die von n Parametern $\alpha_1 \ldots \alpha_n$ abhängt (die ihrerseits weder von x noch von ψ abhängen):

$$\begin{aligned} \delta x^\mu &= \left. \frac{\partial x'^\mu}{\partial \alpha_k} \right|_{\alpha_k = 0} \delta\alpha_k \\ \delta\psi_i &= \left. \frac{\partial \psi_i'}{\partial \alpha_k} \right|_{\alpha_k = 0} \delta\alpha_k \end{aligned} \tag{2.11}$$

Sonderfall **Transformation innerer Freiheitsgrade**:

$$\begin{aligned} x'^\mu &= x^\mu \\ \psi_i'(x') &= \psi_i(x) + \delta\psi_i(x) \qquad \bar{\delta}\psi_i = \delta\psi_i \\ J &= 1 \end{aligned}$$

[4] Emmi Noether, Kgl. Ges. d. Wiss. Nachrichten, Math.-phys. Klasse, S. 235 (Göttingen, 1918).

[5] tatsächlich genügt die schwächere Bedingung
$\mathcal{L}(\psi_i', \partial_\mu' \psi_i', x') \,\mathrm{d}^4 x' = \mathcal{L}(\psi_i, \partial_\mu \psi_i, x) \,\mathrm{d}^4 x + \partial_\nu \delta Q^\nu(x) \,\mathrm{d}^4 x$ mit beliebigem $\delta Q^\nu(x)$

Sonderfall **Ortstransformation** und skalare Felder:

$$\begin{aligned} x'^{\mu} &= x^{\mu} + \delta x^{\mu} \\ \psi_i'(x') &= \psi_i(x) \qquad \Longrightarrow \qquad \bar{\delta}\psi_i = -\partial_\mu \psi_i \, \delta x^{\mu} \\ J &= 1 + \partial_\mu \delta x^{\mu} \end{aligned}$$

Umformung von (2.9) ergibt:

$$\begin{aligned} &\int_V \{\mathcal{L}(x') \cdot J - \mathcal{L}(x) \cdot J + \mathcal{L}(x) \cdot (J-1)\} \, \mathrm{d}^4x = 0 \\ &\int_V \{\delta\mathcal{L} \cdot J + \mathcal{L}(x) \cdot (J-1)\} \, \mathrm{d}^4x = 0 \\ &\int_V \{\delta\mathcal{L} \cdot 1 + \mathcal{L}(x) \cdot \partial_\mu \delta x^{\mu}\} \, \mathrm{d}^4x = 0 \end{aligned} \tag{2.12}$$

mit

$$\begin{aligned} \delta\mathcal{L} &:= \mathcal{L}(\psi_i', \partial_\mu' \psi_i', x') - \mathcal{L}(\psi_i, \partial_\mu \psi_i, x) \\ &= \frac{\partial \mathcal{L}}{\partial \psi_i} \, \bar{\delta}\psi_i + \frac{\partial \mathcal{L}}{\partial(\partial_\mu \psi_i)} \, \partial_\mu \bar{\delta}\psi_i + \left(\frac{\mathrm{d}}{\mathrm{d}x^{\mu}} \mathcal{L}(x) \right) \delta x^{\mu} \\ &= \frac{\mathrm{d}}{\mathrm{d}x^{\mu}} \left(\frac{\partial \mathcal{L}}{\partial(\partial_\mu \psi_i)} \, \bar{\delta}\psi_i \right) + \left(\frac{\mathrm{d}}{\mathrm{d}x^{\mu}} \mathcal{L}(x) \right) \delta x^{\mu} \end{aligned}$$

wegen (2.8). Damit wird (2.12)

$$\begin{aligned} &\int_V \frac{\mathrm{d}}{\mathrm{d}x^{\mu}} \left(\frac{\partial \mathcal{L}}{\partial(\partial_\mu \psi_i)} \, \bar{\delta}\psi_i + \mathcal{L} \, \delta x^{\mu} \right) \mathrm{d}^4x = 0 \\ &\int_V \delta\alpha_k \cdot \frac{\mathrm{d}}{\mathrm{d}x^{\mu}} \left\{ \frac{\partial \mathcal{L}}{\partial(\partial_\mu \psi_i)} \frac{\partial \delta\psi_i}{\partial \alpha_k} + \left(\mathcal{L} \cdot \delta^{\mu}_{\nu} - \frac{\partial \mathcal{L}}{\partial(\partial_\mu \psi_i)} \partial_\nu \psi_i \right) \frac{\partial \delta x^{\nu}}{\partial \alpha_k} \right\} \mathrm{d}^4x = 0 \end{aligned}$$

Es existiert also für jedes k eine Stromdichte

$$j_k^{\mu} = \frac{\partial \mathcal{L}}{\partial(\partial_\mu \psi_i)} \frac{\partial \delta\psi_i}{\partial \alpha_k} + \left(\mathcal{L} \cdot \delta^{\mu}_{\nu} - \frac{\partial \mathcal{L}}{\partial(\partial_\mu \psi_i)} \partial_\nu \psi_i \right) \frac{\partial \delta x^{\nu}}{\partial \alpha_k} \tag{2.13}$$

(summiert wird über i und ν) die die Kontinuitätsgleichung

$$\partial_\mu j_k^{\mu} = 0$$

erfüllt und den Transport einer erhaltenen „Ladung“

$$Q_k = \int_{V_3} j_k^0 \, \mathrm{d}^3x$$

beschreibt.

2.4.1 Beispiel: Phaseninvarianz und erhaltener Strom

Für eine Symmetrie unter Phasentransformation der Felder

$$\begin{aligned}\psi' &= e^{i\alpha}\psi \\ \psi'^* &= e^{-i\alpha}\psi^* \\ \delta\psi &= \left.\frac{\partial\psi'}{\partial\alpha}\right|_{\alpha=0} = i\psi \\ \delta\psi' &= \left.\frac{\partial\psi'^*}{\partial\alpha}\right|_{\alpha=0} = -i\psi^*\end{aligned}$$

d. h.

$$\mathcal{L}(\psi'(x), \partial_\mu\psi'(x), x) = \mathcal{L}(\psi(x), \partial_\mu\psi(x), x) \qquad (J = 1)$$

folgt die Erhaltung einer „Ladung“ mit der Stromdichte nach Gl. 2.13

$$j^\mu = i\left(\frac{\partial\mathcal{L}}{\partial(\partial_\mu\psi)}\,\psi - \frac{\partial\mathcal{L}}{\partial(\partial_\mu\psi^*)}\,\psi^*\right) \tag{2.14}$$

(mit den zwei Komponenten $\psi_1 = \psi, \psi_2 = \psi^*$)

2.4.2 Beispiel: Translationsinvarianz und Energie-Impuls-Tensor

Für die Symmetrie unter Raum- und Zeittranslationen (statt k verwenden wir einen Minkowskiraum-Index ν) $x'^\nu = x^\nu + \alpha^\nu$

$$\begin{aligned}\delta x^\nu &= \alpha^\nu \\ \delta\psi &= 0\end{aligned}$$

d. h.

$$\mathcal{L}(\psi'(x'), \partial_\mu\psi'(x'), x') = \mathcal{L}(\psi(x), \partial_\mu\psi(x), x) \qquad (J = 1)$$

folgt die Impuls- und Energieerhaltung. Statt eines Stromes erhält man mit $\mathrm{d}\delta x^\nu / \mathrm{d}\alpha^\lambda = \delta^\nu_\lambda$ (für alle 4 unabhängigen Komponenten von α^λ gemeinsam) nach Gl. 2.13 einen symmetrischen Tensor

$$T^\mu{}_\nu = \left(\mathcal{L}\cdot\delta^\mu_\nu - \frac{\partial\mathcal{L}}{\partial(\partial_\mu\psi_i)}\partial_\nu\psi_i\right) \tag{2.15}$$

bzw.

$$T^{\mu\nu} = \left(\mathcal{L}\cdot g^{\mu\nu} - \frac{\partial\mathcal{L}}{\partial(\partial_\mu\psi_i)}\partial^\nu\psi_i\right)$$

Die T^{00}-Komponente ist die Energiedichte $\partial E/\partial V$ des Feldes, Die T^{0i}-Komponenten sind die Impulsdichten $\partial p_i/\partial V$ des Feldes, die raumartige 3×3-Submatrix ist der Spannungstensor

$$\mathbf{T} = \begin{pmatrix}\sigma_x & \tau_{xy} & \tau_{xz} \\ \tau_{yx} & \sigma_y & \tau_{yz} \\ \tau_{zx} & \tau_{zy} & \sigma_z\end{pmatrix}$$

mit den Schubspannungen $\tau_{ij} = \tau_{ji}$. Die Kraft auf ein Flächenelement ist

$$\mathrm{d}\vec{F} = \mathbf{T}\,\mathrm{d}\vec{A}, \qquad \mathrm{d}F_i = \sum_{j=1}^{3} T_{ij}\,\mathrm{d}A_j = \sigma_i\,\mathrm{d}A_i + \sum_{j\neq i}\tau_{ij}\,\mathrm{d}A_j \tag{2.16}$$

2.5 Die Schrödinger-Gleichung

Ein nichtrelativistisches freies Teilchen wird durch die Schrödinger-Gleichung

$$i\partial_t\psi = \mathcal{H}\psi = m\psi \tag{2.17}$$

in seinem Ruhesystem ($\vec{p} = \mathbf{0}$) beschrieben. Sie hat die Lösung

$$|\psi\rangle = |\psi_0\rangle e^{-imt}$$

Für ein instabiles Teilchen ist

$$i\partial_t\psi = (m - \frac{i}{2}\Gamma)\psi \tag{2.18}$$

mit der Lösung

$$|\psi\rangle = |\psi_0\rangle e^{-imt} e^{-\frac{1}{2}\Gamma t} \tag{2.19}$$

die auf das radioaktive Zerfallsgesetz $|\langle\psi_0|\psi\rangle|^2 = e^{-\Gamma t}$ führt. Der Hamiltonoperator $\mathbf{H}$ in (2.18) ist **nicht hermitesch** (d. h. als einfache Zahl nicht reell), da er ein „Verschwinden“ von Teilchen beschreibt.

2.6 Die Klein-Gordon-Gleichung

Analog zur zeitabhängigen **Schrödingergleichung** für freie Teilchen

$$i\partial_t\psi = E\psi = -\frac{\nabla^2}{2m}\psi$$

gilt relativistisch

$$E^2 - \vec{p}^2 = m^2$$

daraus ergibt sich die Klein-Gordon-Gleichung[6]

$$-\partial_\mu\partial^\mu\phi = m^2\phi \tag{2.20}$$

die als Bewegungsgleichung aus der Lagrangedichte

$$\mathcal{L} = (\partial_\mu\phi)(\partial^\mu\phi^*) - m^2\phi^*\phi \tag{2.21}$$

für komplexe Felder $\phi(x)$ abgeleitet werden kann.

Aufspaltung in zwei reelle Felder:

$$\phi = \frac{1}{\sqrt{2}}(\phi_r + i\phi_i)$$

Lösungen, die Impulseigenzustände sind (freie Teilchen), sind ebene Wellen

$$\phi = \mathcal{N}e^{-ip_\mu x^\mu} \tag{2.22}$$

mit

$$\partial_\mu\phi = -ip_\mu\phi$$

und 2 Lösungen für die Energie

$$E = p^0 = \pm\sqrt{\vec{p}^2 + m^2}$$

[6] Oskar Klein, Walter Gordon (1926), Publikationen: O. Klein, Z. Phys. **37**, 895 (1926); V. A. Fock, Z. Phys. **39**, 226 (1926); W. Gordon, Z. Phys. **40**, 117 (1926); wurde zuvor schon von Schrödinger gefunden, aber wieder verworfen, da sie das Wasserstoffatom nicht beschreibt (Fermionen benötigen die Dirac-Gleichung).

2.6.1 Stromdichte

Aus der Phasensymmetrie $\phi' = e^{i\alpha}\phi$ folgt nach dem Noether-Theorem die Wahrscheinlichkeitsstromdichte

$$j^\mu = i(\phi^* \partial^\mu \phi - \phi \partial^\mu \phi^*) \tag{2.23}$$

mit der Kontinuitätsgleichung

$$\partial_\mu j^\mu = 0$$

und der Wahrscheinlichkeitsdichte = Ladungsdichte

$$\rho = j^0 = i\left(\phi^* \frac{\partial}{\partial t}\phi - \phi \frac{\partial}{\partial t}\phi^*\right)$$

Für freie Teilchen (2.22) ist

$$j^\mu = i(-i)\mathcal{N}^*\mathcal{N}p^\mu\phi^*\phi - i^2\mathcal{N}\mathcal{N}^*p^\mu\phi\phi^* = 2|\mathcal{N}|^2 p^\mu$$

d. h. die Wahrscheinlichkeitsdichte hat **dasselbe Vorzeichen** wie die Energie.

2.6.2 Reelle Felder

Reeller Klein-Gordon-Lagrangian

$$\mathcal{L} = \tfrac{1}{2}(\partial_\mu\phi)(\partial^\mu\phi) - \tfrac{1}{2}m^2\phi^2 \tag{2.24}$$

Hier gilt keine Phasensymmetrie, die Felder haben keine (erhaltene) Ladung und beschreiben neutrale Teilchen, die ihre eigenen Antiteilchen sind.

2.7 Pauli-Matrizen

Halbzahlige Spins beschreiben die Pauli-Matrizen, aus denen man die Generatoren der Symmetriegruppe **SU(2)** gewinnt.

Pauli-Matrizen:

$$\sigma_1 = \begin{pmatrix} 0 & 1 \\ 1 & 0 \end{pmatrix}, \quad \sigma_2 = \begin{pmatrix} 0 & -i \\ i & 0 \end{pmatrix}, \quad \sigma_3 = \begin{pmatrix} 1 & 0 \\ 0 & -1 \end{pmatrix}$$

Eigenschaften der σ_k:

1. $\sigma_k^+ = \sigma_k$ (Hermiteizität)
2. $\sigma_k^+ = \sigma_k^{-1}$ (Unitarität)
3. $\mathrm{Sp}(\sigma_k) = 0$
4. $\sigma_k^2 = \mathbf{1}$, daher sind alle geraden Potenzen der σ_k gleich 1, alle ungeraden gleich σ_k und $\mathrm{Sp}(\sigma_k^2) = 2$
5. $\forall j \neq k$: $\sigma_j\sigma_k = i\varepsilon_{jkl}\sigma_l$ und $\mathrm{Sp}(\sigma_j\sigma_k) = 0$
6. Vertauschungsrelationen: $[\sigma_j, \sigma_k] = 2i\varepsilon_{jkl}\sigma_l$ das bedeutet für den Vektor der Pauli-Matrizen $\vec{\sigma} \times \vec{\sigma} = 2i\vec{\sigma}$

3. Quarkmodell und Symmetriegruppen

3.1 Überblick

Table 3.1 Die elementaren Fermionen (Spin $\frac{1}{2}$). Quarkmassen kann man nicht messen, da Quarks nur als Hadronen gebunden vorkommen. Die Masse eines Quarks als Baustein in einem Hadron ist etwa $350\,\mathrm{MeV}/c^2$ größer als die Strommasse.

Quarks	Strommasse	Q_{el} $[e]$	Colour	$(I_W, I_{W3})_L$	I_{WR}
d	$\sim 5\,\mathrm{MeV}$	$-\frac{1}{3}$	r, g, b	$(\frac{1}{2}, -\frac{1}{2})$	0
u	$\sim 2\,\mathrm{MeV}$	$\frac{2}{3}$	r, g, b	$(\frac{1}{2}, \frac{1}{2})$	0
s	$95\,\mathrm{MeV}$	$-\frac{1}{3}$	r, g, b	$(\frac{1}{2}, -\frac{1}{2})$	0
c	$1300\,\mathrm{MeV}$	$\frac{2}{3}$	r, g, b	$(\frac{1}{2}, \frac{1}{2})$	0
b	$4200 MeV$	$-\frac{1}{3}$	r, g, b	$(\frac{1}{2}, -\frac{1}{2})$	0
t	$173000\,\mathrm{MeV}$	$\frac{2}{3}$	r, g, b	$(\frac{1}{2}, \frac{1}{2})$	0
Leptonen	Masse	Q_{el} $[e]$	Colour	I_W, I_{W3L}	I_{WR}
e^-	$0.511\,\mathrm{MeV}$	-1	0	$(\frac{1}{2}, -\frac{1}{2})$	0
ν_e	~ 0	0	0	$(\frac{1}{2}, \frac{1}{2})$	0
μ^-	$105.7\,\mathrm{MeV}$	-1	0	$(\frac{1}{2}, -\frac{1}{2})$	0
ν_μ	~ 0	0	0	$(\frac{1}{2}, \frac{1}{2})$	0
τ^-	$1777\,\mathrm{MeV}$	-1	0	$(\frac{1}{2}, -\frac{1}{2})$	0
ν_τ	~ 0	0	0	$(\frac{1}{2}, \frac{1}{2})$	0

Antiteilchen haben entgegengestezte Ladungen $(-Q_{\mathrm{el}}, -I_{W3}, \bar{r}, \bar{g}, \bar{b})$.

3.1.1 Der Teilchenzoo

Alle an der starken Wechselwirkung teilnehmenden Teilchen bezeichnet man als Hadronen ($\acute{\alpha}\delta\rho\acute{o}\varsigma$ = stark). Unterklassen sind Baryonen (Fermionen) und Mesonen (Bosonen).

Historisch unterschied man schwere Teilchen: Baryonen ($\beta\breve{\alpha}\rho\acute{\upsilon}\varsigma$ = schwer), mittelschwere Teilchen: Mesonen ($\mu\acute{\varepsilon}\sigma o\varsigma$ = mittel) und leichte Teilchen: Leptonen ($\lambda\epsilon\pi\tau\acute{o}\varsigma$ = dünn, mager, leicht). Heute stimmen diese Zuordnungen nicht mehr. Das Lepton τ^- ist doppelt so schwer wie das Baryon Proton. Auch das „My-Meson“ μ^- ist nach heutiger Nomenklatur kein Meson, sondern ein Lepton, heißt also richtig My-Lepton oder Myon.

In den 1960ern kante man bereits über 200 Hadronen. Die beobachteten Symmetrien erlaubten, Ordung in diese Vielfalt zu bringen.

3.2 Lie-Gruppen und Quarkmodell

Lie-Gruppe $\mathbf{U(n)}$ = Gruppe der **unitären** Transformationen (Matrizen) des n-dimensionalen Vektorraums über $\mathbf{C}$. $\mathbf{U(n)}$ ist eine Untergruppe der vollen linearen Gruppe $\mathbf{G(n)}$.

Eigenschaften der $U \in \mathbf{U(n)}$:

1. $U^{\dagger} = U^{-1}$, Unitarität $(UU^+ = U^+U = \mathbf{1})$

2. $\|Uv\| = \|v\|$, v = Vektor aus $\mathbf{C}^n$
3. $\det U = e^{ir}$, r = reelle Zahl
4. Anzahl der reellen Parameter: n^2
   ($n \times n$-Matrizen mit komplexen Komponenten = $2n^2$ reelle Parameter, Unitarität = n^2 lineare Gleichungen)
5. zu jedem U existiert eine **hermitesche** Matrix H mit $U = e^{iH}$ und[7] $\det U = e^{i\,\mathrm{Sp}\,H}$
   ($e^{iH} = 1 + (iH)/1! + (iH)^2/2! + (iH)^3/3! + \ldots$)

Eigenschaften der $U \in \mathbf{SU(n)}$:

SU(n) = Untergruppe von **U(n)** mit der Zusatzbedingung $\det U = 1$

4. Anzahl der reellen Parameter: $n^2 - 1$
   (n^2 der **U(n)**, $\det U = 1$ = eine Gleichung)
5. zu jedem U existiert eine **hermitesche** Matrix H mit $U = e^{iH}$ und $\mathrm{Sp}\,H = 0$ (wegen $\det U = e^{\mathrm{Sp}\,H}$)

3.2.1 Infinitesimalring, Generatoren, Strukturkonstanten

Die allgemeine Form einer **SU(n)**-Matrix ist

$$U = e^{iT_a\theta_a}, \quad a = 1 \ldots (n^2 - 1)$$

mit reellen Parametern $\theta_a \in \mathbf{R}$.

Generatoren = die $n^2 - 1$ hermiteschen Matrizen T_a

Die obige Gleichung kann um 0 Taylor-entwickelt werden:

$$U = 1 + i\theta_a T_a + \ldots$$

Die $i\theta_a T_a$ bilden den *Infinitesimalring* (Lie-Ring) der **SU(n)** mit $\theta_a \in \mathbf{R}$.

- Ring-Addition: + (Matrixaddition)
- Ring-Multiplikation: [,] (Kommutator)

Die Elemente $i\theta_a T_a$ des Infinitesimalrings sind **schiefhermitesch** (oder anti-hermitesch): $(i\theta_a T_a)^+ = -i\theta_a T_a^+ = -(i\theta_a T_a)$.

$$[T_a, T_b] = i f_{abc} T_c$$

Die $f_{abc} \in \mathbf{R}$ sind die *Strukturkonstanten* der **SU(n)**

$$\begin{aligned} f_{abc} &= (1/4i)\,\mathrm{Sp}([T_a, T_b]T_c) \\ &= (1/4i)\,\mathrm{Sp}(T_a T_b T_c - T_b T_a T_c) \end{aligned}$$

Eigenschaften der Strukturkonstanten:

- $f_{abc} = 0$, falls $a = b$, $b = c$ oder $a = c$ (triviale Strukturkonstanten)
- Es gibt nur $(n^2 - 1)(n^2 - 2)(n^2 - 3)$ nichttriviale Strukturkonstanten, die in 6er-Gruppen mit $f_{abc} = f_{bca} = f_{cab} = -f_{cba} = -f_{bac} = -f_{acb}$ zusammenfallen
- die Anzahl 6er-Gruppen beträgt für die **SU(2)** 1, für die **SU(3)** 56 etc.

[7] $\mathrm{Sp}\,X$ = Spur der Matrix X

Übergang Gruppe → Infinitesimalring:

$$I(\theta_a) = \sum \theta_a \partial_a U(0)$$

Übergang Infinitesimalring → Gruppe:

$$U(\theta_a) = e^{I(\theta_a)}$$

Der Infinitesimalring ist ein (n^2-1)-dimensionaler Vektorraum über den reellen Zahlen $\mathbf{R}$, wenn wir die Generatoren T_a mit den Einheitsvektoren $\boldsymbol{e}_a$ identifizieren. Das Skalarprodukt $\boldsymbol{e}_a \cdot \boldsymbol{e}_b = \delta_{ab}$ ist dabei zu unterscheiden vom Matrixprodukt $T_a \cdot T_b$.

3.2.2 SU(2)-Generatoren

Generatoren:

$$T_1 = \tfrac{1}{2}\sigma_1, \quad T_2 = \tfrac{1}{2}\sigma_2, \quad T_3 = \tfrac{1}{2}\sigma_3$$

mit den Pauli-Matrizen σ_a (siehe 2.7).

3.2.2.1 Eigenschaften der T_a

gilt für alle **SU(n)**-Gruppen:

Hermiteizität:

$$T_a^+ = T_a$$

Spurfreiheit:

$$\mathrm{Sp}(T_a) = 0$$

$$\mathrm{Sp}(T_a T_b) = \tfrac{1}{2}\delta_{ab} \tag{3.1}$$

3.2.2.2 Strukturkonstanten

$f_{123} = 1$
damit ist allgemein $f_{ijk} = \varepsilon_{ijk}$ (total antisymmetrischer Tensor)
d. h. $[T_1, T_2] = iT_3$ etc.
und $f_{ijk} T_j T_k = \boldsymbol{T} \times \boldsymbol{T} = i\boldsymbol{T}$

3.2.2.3 SU(2)-Transformationen

$$U = e^{iT_a\theta_a} = e^{i\frac{1}{2}\sigma_a\theta_a}, \qquad a = 1,2,3$$

$\theta_1, \theta_2, \theta_3$ = reelle Parameter der Gruppe,
T_1, T_2, T_3 = **Generatoren** der **SU(2)**

Im folgenden gilt die rechte Matrix für getrennte Real- und Imaginärteile in der Reihenfolge $\mathcal{R}e\,x_1$, $\mathcal{I}m\,x_1$, $\mathcal{R}e\,x_2$, $\mathcal{I}m\,x_2$ und es ist $s = \sin\frac{\theta}{2}$, $c = \cos\frac{\theta}{2}$. Die Transformationen beziehen sich auf den 2-dimensionalen Hilbertraum.

Gemischte Transformationen (Generator T_1):

$$U(\theta) = e^{i\theta T_1} = \begin{pmatrix} \cos\frac{\theta}{2} & i\sin\frac{\theta}{2} \\ i\sin\frac{\theta}{2} & \cos\frac{\theta}{2} \end{pmatrix} = \begin{pmatrix} c & 0 & 0 & -s \\ 0 & c & s & 0 \\ 0 & -s & c & 0 \\ s & 0 & 0 & c \end{pmatrix}$$
$$= \begin{pmatrix} 1 & 0 \\ 0 & -i \end{pmatrix} \cdot \begin{pmatrix} \cos\frac{\theta}{2} & \sin\frac{\theta}{2} \\ -\sin\frac{\theta}{2} & \cos\frac{\theta}{2} \end{pmatrix} \cdot \begin{pmatrix} 1 & 0 \\ 0 & i \end{pmatrix}$$

Wir können auch das Produkt als

$$U(\theta) = e^{i\theta T_1} = e^{i\frac{\pi}{2}T_3} e^{i\theta T_2} e^{-i\frac{\pi}{2}T_3}$$

schreiben.

Nota bene: die T_i und $e^{i\theta_i T_i}$ kommutieren nicht, wir können daher das Produkt nicht als e-Funktion mit einer Summe im Exponenten schreiben.

Rotationen (Generator T_2):

$$R(\theta) = e^{i\theta T_2} = \begin{pmatrix} \cos\frac{\theta}{2} & \sin\frac{\theta}{2} \\ -\sin\frac{\theta}{2} & \cos\frac{\theta}{2} \end{pmatrix} = \begin{pmatrix} c & 0 & s & 0 \\ 0 & c & 0 & s \\ -s & 0 & c & 0 \\ 0 & -s & 0 & c \end{pmatrix}$$

Dabei entspricht $\frac{\theta}{2}$ dem Rotationswinkel in 2 Dimensionen, θ dem Rotationswinkel im geometrischen Raum (Spin-**SU(2)**) bzw. im Isoraum.

Relative Phasenänderungen (Generator T_3):

$$P(\theta) = e^{i\theta T_3} = \begin{pmatrix} e^{i\frac{\theta}{2}} & 0 \\ 0 & e^{-i\frac{\theta}{2}} \end{pmatrix} = \begin{pmatrix} c & s & 0 & 0 \\ -s & c & 0 & 0 \\ 0 & 0 & c & -s \\ 0 & 0 & s & c \end{pmatrix}$$

Alternative Form, α, β, θ reelle Parameter:

$$U(\alpha,\beta,\theta) = \begin{pmatrix} e^{+i\frac{\alpha}{2}} & 0 \\ 0 & e^{-i\frac{\alpha}{2}} \end{pmatrix} \cdot \begin{pmatrix} \cos\frac{\theta}{2} & \sin\frac{\theta}{2} \\ -\sin\frac{\theta}{2} & \cos\frac{\theta}{2} \end{pmatrix} \cdot \begin{pmatrix} e^{+i\frac{\beta}{2}} & 0 \\ 0 & e^{-i\frac{\beta}{2}} \end{pmatrix}$$
$$= \begin{pmatrix} e^{i(\alpha+\beta)/2}\cos\frac{\theta}{2} & e^{i(\alpha-\beta)/2}\sin\frac{\theta}{2} \\ -e^{-i(\alpha-\beta)/2}\sin\frac{\theta}{2} & e^{-i(\alpha+\beta)/2}\cos\frac{\theta}{2} \end{pmatrix} \tag{3.2}$$

Auf- und Absteige-Operatoren (Leiteroperatoren, *raising and lowering ladder operators*):

$$T_+ = T_1 + iT_2 = \begin{pmatrix} 0 & 1 \\ 0 & 0 \end{pmatrix}$$
$$T_- = T_1 - iT_2 = \begin{pmatrix} 0 & 0 \\ 1 & 0 \end{pmatrix}$$
$$T_+ = T_-^{\dagger}$$

die Vorzeichen + und − beziehen sich auf die Eigenwerte zu T_3: $T_+|-\tfrac{1}{2}\rangle = |+\tfrac{1}{2}\rangle$, $T_+|+\tfrac{1}{2}\rangle = 0$ etc.

3.2.3 Casimir-Operatoren

Definition: $C = f(T_a), \quad [C, T_a] = 0 \quad$ für alle a

Eigenschaften:

- C ist nur bis auf einen beliebigen Faktor definiert
- Jedes C hat genau einen Eigenwert (innerhalb einer irreduziblen Darstellung)
- Die Eigenwerte sind nur eine Funktion der Darstellung

SU(n) hat $(n-1)$ lin. unabh. Casimir-Operatoren

Casimir-Operator der **SU(2)**:

$$\begin{aligned} T^2 &= (T_1^2 + T_2^2 + T_3^2) \\ &= T_+ \cdot T_- + T_3^2 \end{aligned}$$

Eigenwerte von T^2 in der N-dimensionalen Darstellung

$$\frac{(N-1)\cdot(N+1)}{4}$$

Dies entspricht dem bekannten $j(j+1)$, da die Dimension (= Multiplizität) $N = 2j+1$ und damit $j = (N-1)/2$ ist.

3.3 Darstellungen von Gruppen

Eine Darstellung in N Dimensionen ist eine Menge von $N \times N$-Matrizen $M(U)$ zu jedem U aus der Gruppe mit der Eigenschaft

$$M(U_1 U_2) = M(U_1) M(U_2)$$

Damit ist

$$\begin{aligned} M(1) &= \mathbf{1} \\ M(U^{-1}) &= M^{-1}(U) \end{aligned}$$

- Die Menge $\{1\}$ ist die *triviale Darstellung* jeder Gruppe. Sie „tut nichts“ und wirkt auf den **eindimensionalen** Raum **C**. Sie beschreibt Spin 0, Colour-Ladung 0 etc.
- Die *kontragradiente Darstellung* $\bar{M}(U)$ wird durch die inversen transponierten Matrizen einer regulären Darstellung

  $$\bar{M}(U) = M^{\dagger}(U^{-1}) = \left(M^{-1}\right)^{\dagger}(U)$$

  gebildet.

$$\begin{aligned} M^{\dagger}(U_1 U_2) &= M^{\dagger}(U_2) M^{\dagger}(U_1) \\ M^{-1}(U_1 U_2) &= M^{-1}(U_2) M^{-1}(U_1) \\ \bar{M}(U_1 U_2) &= \bar{M}(U_1) \bar{M}(U_2) \end{aligned}$$

3.3.1 Darstellungen der SU(n)

Eine Darstellung der **SU(n)** in N Dimensionen ist eine Menge von $N \times N$-Matrizen $M(U)$ zu jedem $U \in \mathbf{SU(n)}$ mit der Eigenschaft

$$M(U_1 U_2) = M(U_1) M(U_2)$$

- Die Darstellung des Infinitesimalrings ist der Infinitesimalring der Darstellung. Die Beziehung $M = \exp(i\theta_a T'_a)$ gilt auch hier, sodass die Darstellung durch die Darstellung der Generatoren $T'_a(T_a)$ bestimmt ist.
- Jede **SU(n)** ist ihre eigene Darstellung in n Dimensionen, die *fundamentale Darstellung*.
- Die Darstellungen der **SU(n)** sind **unitär**.
- Daher ist die *kontragradiente Darstellung*

$$\bar{M}(U) = \left(M^{+}\right)^{\dagger}(U) = M^{*}(U)$$

  und reelle Darstellungen der **SU(n)** sind zu sich selbst kontragradient.

Äquivalente Darstellungen:

$$M \sim M' \quad \Longleftrightarrow \quad \exists A \; \forall U, \quad M'(U) = A M(U) A^{-1}$$

Äquivalente Darstellungen unterscheiden sich nur durch eine Transformation des Koordinatensystems.

3.3.1.1 Kontragradiente Fundamental-Darstellung der SU(2)

kontragradiente Darstellung $\mathbf{2}^*$:

Für jede **SU(2)**-Matrix ist

$$U^* = U^{+\dagger} = U^{-1\dagger} = \begin{pmatrix} U_{22} & -U_{21} \\ -U_{12} & U_{11} \end{pmatrix}$$

und

$$U^* = \begin{pmatrix} U_{22} & -U_{21} \\ -U_{12} & U_{11} \end{pmatrix} = \begin{pmatrix} 0 & -1 \\ 1 & 0 \end{pmatrix} \begin{pmatrix} U_{11} & U_{12} \\ U_{21} & U_{22} \end{pmatrix} \begin{pmatrix} 0 & 1 \\ -1 & 0 \end{pmatrix}$$

Damit wird aus dem Isospin-Dublett

$$\begin{pmatrix} u \\ d \end{pmatrix}$$

für Quarks das Dublett

$$\begin{pmatrix} 0 & -1 \\ 1 & 0 \end{pmatrix} \begin{pmatrix} \bar{u} \\ \bar{d} \end{pmatrix} = \begin{pmatrix} -\bar{d} \\ \bar{u} \end{pmatrix} \tag{3.3}$$

für Antiquarks.

Das ist konsistent mit der C-Operation auf Fermionen:

$$\psi_C = C\bar{\psi}^{\dagger} = C\gamma^0 \psi^*$$

Bei einem mit U transformierten Spinor werden alle Matrixelemente im transformierten $\psi' = U\psi$ komplex konjugiert.

3.3.2 Reduzibilität

Eine Darstellung heißt *vollständig reduzibel*, wenn der Vektorraum in orthogonale invariante Unterräume zerfällt (d. h. ein Vektor aus einem dieser Unterräume kann durch keine Matrix der Darstellung aus diesem heraus transformiert werden).

Die Matrizen zerfallen dann bei einer geeigneten Wahl der Basis in Blöcke (hier zwei):

$$M = \left(\begin{array}{c|c} A & 0 \\ \hline 0 & B \end{array}\right)$$

Bei unvollständiger Reduzibilität existiert nur ein invarianter Unterraum, einer der 0-Blöcke der Matrizen ist von 0 verschieden. Unitäre Darstellungen sind jedoch stets vollständig reduzibel oder irreduzibel.

Es gibt bis auf Äquivalenz maximal **zwei** irreduzible Darstellungen der **SU(n)** in N Dimensionen, die zueinander kontragradient sind (es können auch 0 oder 1 sein).

Sind $M_k(U)$ und $M_l(U)$ je k- und l-dimensionale Darstellungen, so ist die direkte Summe $M_k \oplus M_l$

$$M_{k\oplus l}(U) = \left(\begin{array}{c|c} M_k(U) & 0 \\ \hline 0 & M_l(U) \end{array}\right)$$

eine vollständig reduzible Darstellung in $k + l$ Dimensionen.

3.3.3 Adjungierte Darstellung

Alle $U \in \mathbf{SU(n)}$ (fundamentale Darstellung) definieren Abbildungen

$$X \to UXU^{\dagger}$$

die sowohl die **SU(n)** als auch den Infinitesimalring linear auf sich selbst abbilden.

Der Infinitesimalring ist ein $(n^2 - 1)$-dimensionaler Vektorraum über $\mathbf{R}$, d. h. diese Abbildung ist eine **reelle** Darstellung der **SU(n)** in $(n^2 - 1)$ Dimensionen = adjungierte Darstellung.

Die Basis des Infinitesimalrings bilden die Generatoren, ein Spaltenvektor $\boldsymbol{x} = \sum x_a T_a$ wird durch die adjungierte Darstellung transformiert in

$$\boldsymbol{x}' = M(U)\boldsymbol{x} \quad \text{mit} \quad \boldsymbol{x}' = \sum x_a U T_a U^{\dagger} = \sum x'_a T_a$$

- Die adjungierte Darstellung enthält nur Rotationen $\implies$ $\mathbf{SU(n)} \subset \mathbf{SO(n^2 - 1)}$.
- Nur die adjungierte Darstellung der **SU(2)** enthält jedoch **alle** Rotationen (in 3 Dimensionen) $\implies$ $\mathbf{SU(2)}/Z_2 \cong \mathbf{SO(3)}$, d. h. Zuordnung **SU(2)** $\leftrightarrow$ **SO(3)** ist zweideutig;

  Generatoren der **SO(3)**: $T_1 = \begin{pmatrix} 0 & 0 & 0 \\ 0 & 0 & i \\ 0 & -i & 0 \end{pmatrix}$, $T_2 = \begin{pmatrix} 0 & 0 & -i \\ 0 & 0 & 0 \\ i & 0 & 0 \end{pmatrix}$, $T_3 = \begin{pmatrix} 0 & i & 0 \\ -i & 0 & 0 \\ 0 & 0 & 0 \end{pmatrix}$.

3.3.4 Gewichte

Von den $n^2 - 1$ Generatoren der **SU(n)** sind $n - 1$ gleichzeitig diagonalisierbar (diese erzeugen die relativen Phasentransformationen, „Typ 3“).

Die **Gewichte** m sind die $(n-1)$-tupel aus den Eigenwerten dieser Generatoren.

Sie werden i. A. als Punkte im $(n-1)$-dimensionalen Gewichtsraum dargestellt. Eine N-dimensionale Darstellung hat N (nicht notwendig verschiedene) Gewichte. **Diese bestimmen die Darstellung bis auf Äquivalenz**.

In N Dimensionen gibt es (bis auf Äquivalenz) maximal **zwei** irreduzible Darstellungen, die zueinander *kontragradient* sind.

Definition:	$M(U) \to M^\dagger(U^{-1})$
$U \in \mathbf{SU(n)}$:	$U \to U^*$
$I \in$ Infinitesimalring:	$I \to -I^*$
$T =$ Generator:	$T \to -T^*$
$m =$ Gewicht:	$m \to -m$

Ist eine Darstellung reell (insbesondere die adjungierte Darstellung), gibt es in dieser Dimension nur eine Darstellung (bis auf Äquivalenz).

fundamentale Darstellungen = **SU(n)** selbst und die dazu kontragradiente Darstellung (n Dimensionen).

3.3.4.1 Gewichte der SU(2)

Die **SU(2)** hat nur einen diagonalen Generator, T_3, Gewichte sind also (eindimensionale) Zahlen.

T_3 hat die Eigenvektoren $\begin{pmatrix}1\\0\end{pmatrix}$ und $\begin{pmatrix}0\\1\end{pmatrix}$ mit Eigenwerten $\frac{1}{2}$ und $-\frac{1}{2}$ in der fundamentalen Darstellung.

Diese entsprechen 2 Zuständen $|\uparrow\rangle$ und $|\downarrow\rangle$.

Die kontragradiente Fundamental-Darstellung hat dieselben Gewichte.

3.3.5 Äußeres Produkt

Äußere Produkte $D = D' \otimes D''$ von Darstellungen D', D'' führen zu neuen Darstellungen in höheren Dimensionen. Dabei ensteht aus zwei Vektoren $(x, y, \ldots)$ und $(u, v, \ldots)$ der neue Vektor $(xu, xv, \ldots, yu, yv, \ldots, \ldots, \ldots)$.

Ein äußeres Produkt aus zwei Matrizen

$$M(U)_{ikjl} = M'(U)_{ij} M''(U)_{kl}$$

ist ein Tensor vierter Stufe, die Indizes $ijkl$ laufen von 1111 bis $NMNM$, wenn D', D'' Darstellungen in N bzw. M Dimensionen sind. Ordnet man jeweils $N \cdot M$ Elemente in einer Spalte oder Zeile mit Index von 1 bis $N \cdot M$ an, kann man aus dem Tensor wieder eine Matrix in $N \cdot M$ Dimensionen machen.

Die Matrizen

$$M' = \begin{pmatrix} a & b & \ldots \\ c & d & \ldots \\ . & . & \ldots \end{pmatrix} \qquad \text{und} \qquad M'' = \begin{pmatrix} p & q & \ldots \\ r & s & \ldots \\ . & . & \ldots \end{pmatrix}$$

werden zu

$$M = M' \otimes M'' = \begin{pmatrix} ap & aq & \dots & bp & bq & \dots \\ ar & as & \dots & br & bs & \dots \\ . & . & \dots & . & . & \dots \\ cp & cq & \dots & dp & dq & \dots \\ cr & cs & \dots & dr & ds & \dots \\ . & . & \dots & . & . & \dots \\ \dots & \dots & \dots & \dots & \dots & \dots \end{pmatrix}$$

Die diagonalen Generatoren („Typ 3“) transformieren sich dabei besonders einfach: Bedingt durch die Exponentialfunktion werden Produkte zu Summen, und die neuen Diagonalelemente ergeben sich aus den alten nach

$$\begin{aligned} & (a, b, \dots) \otimes (p, q, \dots) = (a+p, a+q, \dots, b+p, b+q, \dots, \dots) \\ \Longrightarrow \qquad & m = m' + m'' \end{aligned}$$

aus allen möglichen Kombinationen der m', m''.

Diese Darstellungen sind i. A. **reduzibel**!

3.3.5.1 Äußeres Produkt mit Leiteroperatoren

Beispiel: **SU(2)**, $\mathbf{2} \otimes \mathbf{2}$:

$$T_{4+} = \frac{1}{\sqrt{2}}(T_{2+} \otimes \mathbf{1} + \mathbf{1} \otimes T_{2+})$$

3.3.6 Irreduzible Darstellungen der SU(2)

Fundamentale Darstellung (2 Dimensionen) $\mathbf{2}$: Gewichte $\frac{1}{2}$ und $-\frac{1}{2}$. kontragradiente Darstellung $\mathbf{2}^*$: Gewichte $-\frac{1}{2}$ und $\frac{1}{2}$.

3.3.6.1 Addition von Spins/Drehimpulsen

Beispiel: 2 Spin-$\frac{1}{2}$-Teilchen, Basiszustände

$\mathbf{2} \otimes \mathbf{2} = \mathbf{3} \oplus \mathbf{1}$ mit Gewichten $1, 0, -1$ und 0.

$$|\uparrow\uparrow\rangle, |\uparrow\downarrow\rangle, |\downarrow\uparrow\rangle, |\downarrow\downarrow\rangle$$

Kombination zu neuen Zuständen definierter Symmetrie

$$\begin{aligned} \text{Triplett } (S=1): \quad & |\uparrow\uparrow\rangle \\ & \frac{1}{\sqrt{2}}(|\uparrow\downarrow\rangle + |\downarrow\uparrow\rangle) \\ & |\downarrow\downarrow\rangle \\ \text{Singulett } (S=0): \quad & \frac{1}{\sqrt{2}}(|\uparrow\downarrow\rangle - |\downarrow\uparrow\rangle) \end{aligned}$$

Beispiel: 2 Isospin-$\frac{1}{2}$-Teilchen, Basiszustände

$$|uu\rangle, |ud\rangle, |du\rangle, |dd\rangle \qquad (\text{oder } |pp\rangle, |pn\rangle, |np\rangle, |nn\rangle)$$

Kombination zu neuen Zuständen definierter Symmetrie

$$\begin{aligned}\text{Triplett } (I=1): &\quad |uu\rangle \\ &\quad \frac{1}{\sqrt{2}}(|ud\rangle + |du\rangle) \\ &\quad |dd\rangle \\ \text{Singulett } (I=0): &\quad \frac{1}{\sqrt{2}}(|ud\rangle - |du\rangle)\end{aligned}$$

Beispiel: Isospin-$\frac{1}{2}$-Quarks und Antiquarks, Basiszustände

$\mathbf{2} \otimes \mathbf{2} = \mathbf{3} \oplus \mathbf{1}$ mit Gewichten $1, 0, -1$ und 0.

$$|u\bar{d}\rangle, |u\bar{u}\rangle, |d\bar{d}\rangle|d\bar{u}\rangle, \qquad (\text{oder } |p\bar{n}\rangle, |p\bar{p}\rangle, |n\bar{n}\rangle, |n\bar{p}\rangle)$$

Kombination zu Isospin-Eigenzuständen, kontragradiente Darstellung für Antiquarks (3.3)

$$\begin{aligned}\text{Triplett } (I=1): &\quad -|u\bar{d}\rangle \\ &\quad \frac{1}{\sqrt{2}}(|u\bar{u}\rangle - |d\bar{d}\rangle) \\ &\quad |d\bar{u}\rangle \\ \text{Singulett } (I=0): &\quad \frac{1}{\sqrt{2}}(|u\bar{u}\rangle + |d\bar{d}\rangle)\end{aligned}$$

Beispiel: 2 Spin-1 Teilchen, Basiszustände $|1,-1\rangle$, $|1,0\rangle$, $|1,1\rangle$ zu neuen Zuständen definierter Symmetrie (gerade S = gerade Symmetrie, ungerade S = ungerade Symmetrie)

$\mathbf{3} \otimes \mathbf{3} = \mathbf{5} \oplus \mathbf{3} \oplus \mathbf{1}$ mit Gewichten $2, 1, 0, -1, -2$ und $1, 0, -1$ und 0.

$$\begin{aligned}\text{Quintett } (S=2): &\quad |1,1;1,1\rangle \\ &\quad |1,-1;1,-1\rangle \\ &\quad \frac{1}{\sqrt{2}}(|1,1;1,0\rangle + |1,0;1,1\rangle) \\ &\quad \frac{1}{\sqrt{2}}(|1,-1;1,0\rangle + |1,0;1,-1\rangle) \\ &\quad \frac{1}{\sqrt{6}}(|1,1;1,-1\rangle + |1,-1;1,1\rangle) + \sqrt{\frac{2}{3}}|1,0;1,0\rangle \\ \text{Triplett } (S=1): &\quad \frac{1}{\sqrt{2}}(|1,1;1,0\rangle - |1,0;1,1\rangle) \\ &\quad \frac{1}{\sqrt{2}}(|1,-1;1,0\rangle - |1,0;1,-1\rangle) \\ &\quad \frac{1}{\sqrt{2}}(|1,1;1,-1\rangle - |1,-1;1,1\rangle) \\ \text{Singulett } (S=0): &\quad \frac{1}{\sqrt{3}}(|1,1;1,-1\rangle + |1,-1;1,1\rangle - |1,0;1,0\rangle)\end{aligned}$$

Die genauen Vorfaktoren sind die Clebsch–Gordan-Koeffizienten Aus Symmetriegründen trägt $|1,0;1,0\rangle$ nicht zu $S=1$ bei. Analog gilt für alle $|S_1,0;S_2,0\rangle$, dass sie nur zu $|S,0\rangle$ beitragen, falls $S+S_1+S_2$ gerade ist.

3.3.6.2 Clebsch–Gordan Koeffizienten

Kombinationen von $|j_1 m_1\rangle$ und $|j_2 m_2\rangle$ zu $|jm\rangle$, mit

$$|j_1 - j_2| \leq j \leq j_1 + j_2$$

(Condon–Shortley Phasenkonvention)

$$\begin{aligned}\langle j_1, m_1; j_2, m_2 | j, m\rangle = \delta_{m,m_1+m_2} &\sqrt{\frac{(j_1+j_2-j)!(j+j_1-j_2)!(j+j_2-j_1)!(2j+1)}{(j+j_1+j_2+1)!}} \\ &\cdot \sqrt{(j_1+m_1)!(j_1-m_1)!(j_2+m_2)!(j_2-m_2)!(j+m)!(j-m)!} \\ &\cdot \sum_{k=k_{\min}}^{k_{\max}} \frac{(-1)^k}{(j_1+j_2-j-k)!(j_1-m_1-k)!(j_2+m_2-k)!(j-j_2+m_1+k)!(j-j_1-m_2+k)!}\end{aligned}$$

mit

$$\begin{aligned}k_{\min} &= \max\{j_2 - j - m_1, j_1 - j + m_2, 0\} \\ k_{\max} &= \min\{j_1 + j_2 - j, j_1 - m_1, j_2 + m_2\}\end{aligned}$$

Symmetrien:

$$\begin{aligned}\langle j_1, m_1; j_2, m_2 | j, m\rangle &= (-1)^{j_1+j_2-j} \langle j_1, -m_1; j_2, -m_2 | j, -m\rangle \\ \langle j_1, m_1; j_2, m_2 | j, m\rangle &= (-1)^{j_1+j_2-j} \langle j_1, m_2; j_2, m_1 | j, m\rangle \\ \langle j_1, m_1; j_2, m_2 | j, m\rangle &= \langle j_2, -m_2; j_1, -m_1 | j, -m\rangle\end{aligned}$$

Spezielle Werte:

$j_1 = \frac{1}{2},\ j = \ldots$	$m_1 = \frac{1}{2}$	$m_1 = -\frac{1}{2}$
$j_2 + \frac{1}{2}$	$\sqrt{\frac{j_2 + m + \frac{1}{2}}{2j_2+1}}$	$\sqrt{\frac{j_2 - m + \frac{1}{2}}{2j_2+1}}$
$j_2 - \frac{1}{2}$	$-\sqrt{\frac{j_2 - m + \frac{1}{2}}{2j_2+1}}$	$\sqrt{\frac{j_2 + m + \frac{1}{2}}{2j_2+1}}$

$j_1 = 1,$ $j = \ldots$	$m_1 = 1$ $m_2 = m-1$	$m_1 = 0$ $m_2 = m$	$m_1 = -1$ $m_2 = m+1$
$j_2 + 1$	$\sqrt{\frac{(j_2+m)(j_2+m+1)}{(2j_2+1)(2j_2+2)}}$	$\sqrt{\frac{(j_2-m+1)(j_2+m+1)}{(2j_2+1)(j_2+1)}}$	$\sqrt{\frac{(j_2-m)(j_2-m+1)}{(2j_2+1)(2j_2+2)}}$
j_2	$-\sqrt{\frac{(j_2+m)(j_2-m+1)}{2j_2(j_2+1)}}$	$\sqrt{\frac{m^2}{j_2(j_2+1)}}$	$\sqrt{\frac{(j_2-m)(j_2+m+1)}{2j_2(j_2+1)}}$
$j_2 - 1$	$\sqrt{\frac{(j_2-m)(j_2-m+1)}{2j_2(2j_2+1)}}$	$-\sqrt{\frac{(j_2-m)(j_2+m)}{j_2(2j_2+1)}}$	$\sqrt{\frac{(j_2+m+1)(j_2+m)}{2j_2(2j_2+1)}}$

$\langle j_1, 0; j_2, 0 | j, 0\rangle = 0$ falls $(j_1 + j_2 - j)$ ungerade

$\langle j_1, m_1; j_1, m_1 | j, 2m_1\rangle = 0$ falls j ungerade

Schema (mit $C = \langle l_1, m_1; l_2, m_2 | l, m\rangle$):

$l_1 \otimes l_2$	$\begin{matrix} l \\ m \end{matrix}$	$\begin{matrix} l \\ m \end{matrix}$	$\cdots$
m_1, m_2	$\operatorname{sgn} C \cdot \lvert C\rvert^2$	$\cdots$	$\cdots$
m_1, m_2	$\vdots$	$\ddots$	
$\vdots$	$\vdots$		$\ddots$

$\frac{1}{2}\otimes\frac{1}{2}$	$\begin{matrix}1\\-1\end{matrix}$	$\begin{matrix}1\\0\end{matrix}$	$\begin{matrix}0\\0\end{matrix}$	$\begin{matrix}1\\1\end{matrix}$
$+\frac{1}{2},+\frac{1}{2}$				1
$+\frac{1}{2},-\frac{1}{2}$		$\frac{1}{2}$	$\frac{1}{2}$	
$-\frac{1}{2},+\frac{1}{2}$		$\frac{1}{2}$	$-\frac{1}{2}$	
$-\frac{1}{2},-\frac{1}{2}$	1			

$1\otimes\frac{1}{2}$	$\begin{matrix}\frac{3}{2}\\-\frac{3}{2}\end{matrix}$	$\begin{matrix}\frac{3}{2}\\-\frac{1}{2}\end{matrix}$	$\begin{matrix}\frac{1}{2}\\-\frac{1}{2}\end{matrix}$	$\begin{matrix}\frac{3}{2}\\+\frac{1}{2}\end{matrix}$	$\begin{matrix}\frac{1}{2}\\+\frac{1}{2}\end{matrix}$	$\begin{matrix}\frac{3}{2}\\+\frac{3}{2}\end{matrix}$
$+1,+\frac{1}{2}$						1
$+1,-\frac{1}{2}$				$\frac{1}{3}$	$\frac{2}{3}$	
$0,+\frac{1}{2}$				$\frac{2}{3}$	$-\frac{1}{3}$	
$0,-\frac{1}{2}$		$\frac{2}{3}$	$\frac{1}{3}$			
$-1,+\frac{1}{2}$		$\frac{1}{3}$	$-\frac{2}{3}$			
$-1,-\frac{1}{2}$	1					

$\frac{3}{2}\otimes\frac{1}{2}$	$\begin{matrix}2\\-2\end{matrix}$	$\begin{matrix}2\\-1\end{matrix}$	$\begin{matrix}1\\-1\end{matrix}$	$\begin{matrix}2\\0\end{matrix}$	$\begin{matrix}1\\0\end{matrix}$	$\begin{matrix}2\\+1\end{matrix}$	$\begin{matrix}1\\+1\end{matrix}$	$\begin{matrix}2\\+2\end{matrix}$
$+\frac{3}{2},+\frac{1}{2}$								1
$+\frac{3}{2},-\frac{1}{2}$						$\frac{1}{4}$	$\frac{3}{4}$	
$+\frac{1}{2},+\frac{1}{2}$						$\frac{3}{4}$	$-\frac{1}{4}$	
$+\frac{1}{2},-\frac{1}{2}$				$\frac{1}{2}$	$\frac{1}{2}$			
$-\frac{1}{2},+\frac{1}{2}$				$\frac{1}{2}$	$-\frac{1}{2}$			
$-\frac{1}{2},-\frac{1}{2}$		$\frac{3}{4}$	$\frac{1}{4}$					
$-\frac{3}{2},+\frac{1}{2}$		$\frac{1}{4}$	$-\frac{3}{4}$					
$-\frac{3}{2},-\frac{1}{2}$	1							

$1\otimes 1$	$\begin{matrix}2\\-2\end{matrix}$	$\begin{matrix}2\\-1\end{matrix}$	$\begin{matrix}1\\-1\end{matrix}$	$\begin{matrix}2\\0\end{matrix}$	$\begin{matrix}1\\0\end{matrix}$	$\begin{matrix}0\\0\end{matrix}$	$\begin{matrix}2\\+1\end{matrix}$	$\begin{matrix}1\\+1\end{matrix}$	$\begin{matrix}2\\+2\end{matrix}$
$+1,+1$									1
$+1,0$							$\frac{1}{2}$	$\frac{1}{2}$	
$0,+1$							$\frac{1}{2}$	$-\frac{1}{2}$	
$+1,-1$				$\frac{1}{6}$	$\frac{1}{2}$	$\frac{1}{3}$			
$0,0$				$\frac{2}{3}$	0	$-\frac{1}{3}$			
$-1,+1$				$\frac{1}{6}$	$-\frac{1}{2}$	$\frac{1}{3}$			
$-1,0$		$\frac{1}{2}$	$-\frac{1}{2}$						
$0,-1$		$\frac{1}{2}$	$\frac{1}{2}$						
$-1,-1$	1								

3.3.7 Isospin-Wellenfunktionen

Diquark, $I = 0$:

$$\frac{1}{\sqrt{2}}(|ud\rangle - |du\rangle)$$

Diquark, $I = 1$:

$$|dd\rangle$$
$$\frac{1}{\sqrt{2}}(|ud\rangle + |du\rangle)$$
$$|uu\rangle$$

Proton p ($I = \frac{1}{2}$):

$$\frac{1}{\sqrt{2}}(|uud\rangle - |udu\rangle)$$
$$\frac{1}{\sqrt{2}}(|udu\rangle - |duu\rangle)$$

zwei Möglichkeiten eines **SU(3)**-Oktetts, die dritte Möglichkeit ist eine Linearkombination dieser beiden mit Spin (faktorisiert nicht):

$$\frac{1}{\sqrt{18}}\left[(2|u\uparrow u\uparrow d\downarrow\rangle - |u\uparrow d\uparrow u\downarrow\rangle - |d\uparrow u\uparrow u\downarrow\rangle) + (\ldots|\uparrow\downarrow\uparrow\rangle\ldots) + (\ldots|\downarrow\uparrow\uparrow\rangle\ldots)\right]$$

Δ^+ ($I = \frac{3}{2}$):

$$\frac{1}{\sqrt{3}}(|uud\rangle + |udu\rangle + |duu\rangle)$$

Σ^{*0} ($I = 1$, Dekuplett):

$$\frac{1}{\sqrt{6}}(|uds\rangle + |sud\rangle + |dsu\rangle + |sdu\rangle + |usd\rangle + |dus\rangle)$$

Σ^0 ($I = 1$):

$$\frac{1}{2}(|uds\rangle - |usd\rangle + |dus\rangle - |dsu\rangle)$$
$$\frac{1}{2}(|usd\rangle - |sud\rangle + |dsu\rangle - |sdu\rangle)$$

zwei Möglichkeiten eines **SU(3)**-Oktetts, die dritte Möglichkeit ist eine Linearkombination dieser beiden.
Λ ($I = 0$):

$$\frac{1}{\sqrt{12}}(2|uds\rangle + |usd\rangle + |sdu\rangle - 2|dus\rangle - |dsu\rangle - |sud\rangle)$$
$$\frac{1}{\sqrt{12}}(-|uds\rangle + |usd\rangle - 2|sdu\rangle + |dus\rangle - |dsu\rangle + 2|sud\rangle)$$

zwei Möglichkeiten eines **SU(3)**-Oktetts, die dritte Möglichkeit ist eine Linearkombination dieser beiden.

3.3.7.1 Antibaryonen

Für Antibaryonen gibt es zwei Namens-Konventionen, die oft zu Missverständnissen führen:

$$\overline{\Delta}^{--} \equiv \overline{\Delta^{++}}, \overline{\Sigma}^- \equiv \overline{\Sigma^+} \neq \overline{\Sigma}^+ \equiv \overline{\Sigma^-} \text{ etc.}$$

3.3.8 SU(3)-Generatoren

Die 8 Generatoren der **SU(3)** sind nicht mehr unitär. Eine Standardform (Gell-Mann-Matrizen, λ-Matrizen) ist

$$T_a = \tfrac{1}{2}\lambda_a$$

Gemischte Transformationen:

$$T_1 = \tfrac{1}{2}\begin{pmatrix} 0 & 1 & 0 \\ 1 & 0 & 0 \\ 0 & 0 & 0 \end{pmatrix}, \quad T_4 = \tfrac{1}{2}\begin{pmatrix} 0 & 0 & 1 \\ 0 & 0 & 0 \\ 1 & 0 & 0 \end{pmatrix}, \quad T_6 = \tfrac{1}{2}\begin{pmatrix} 0 & 0 & 0 \\ 0 & 0 & 1 \\ 0 & 1 & 0 \end{pmatrix}$$

Rotationen:

$$T_2 = \tfrac{1}{2}\begin{pmatrix} 0 & -i & 0 \\ i & 0 & 0 \\ 0 & 0 & 0 \end{pmatrix}, \qquad T_5 = \tfrac{1}{2}\begin{pmatrix} 0 & 0 & -i \\ 0 & 0 & 0 \\ i & 0 & 0 \end{pmatrix}, \qquad T_7 = \tfrac{1}{2}\begin{pmatrix} 0 & 0 & 0 \\ 0 & 0 & -i \\ 0 & i & 0 \end{pmatrix}$$

Relative Phasenänderungen:

$$T_3 = \tfrac{1}{2}\begin{pmatrix} 1 & 0 & 0 \\ 0 & -1 & 0 \\ 0 & 0 & 0 \end{pmatrix}, \qquad T_8 = \frac{1}{2\sqrt{3}}\begin{pmatrix} 1 & 0 & 0 \\ 0 & 1 & 0 \\ 0 & 0 & -2 \end{pmatrix}$$

Strukturkonstanten:

nichttriviale 6er-Gruppen $f_{abc} = f_{bca} = f_{cab} = -f_{cba} = -f_{bac} = -f_{acb}$ (je 1 Element):

$f_{123} = 1$
$f_{147} = f_{165} = f_{246} = f_{257} = f_{345} = f_{376} = \frac{1}{2}$
$f_{458} = f_{678} = \frac{\sqrt{3}}{2}$

alle andern 47 nichttrivialen 6er-Gruppen sind 0

weitere Eigenschaften:
$\mathrm{Sp}\,\lambda_a^2 = 2$, $\mathrm{Sp}\,T_a^2 = \frac{1}{2}$.

3.3.9 Irreduzible Darstellungen der SU(3)

Gewichte der fundamentalen Darstellungen **3** und $\mathbf{3}^*$ = Eigenwerte der Matrizen T_3 und T_8. Für **3**:

$$m_1 = (1/2, 1/2\sqrt{3}), \qquad m_2 = (-1/2, 1/2\sqrt{3}), \qquad m_3 = (0, -1/\sqrt{3})$$

Für die kontragradiente Darstellung $\mathbf{3}^*$ sind die Zahlen jeweils mit -1 zu multiplizieren.

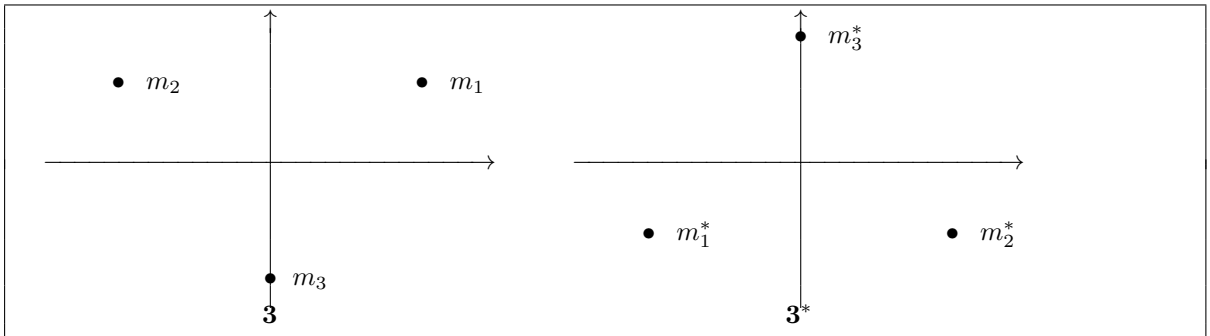

Fig. 3.1 Gewichte der fundamentalen **SU(3)**-Darstellungen. Sie bilden je ein gleichseitiges Dreieck im Gewichtsraum.

Der Abstand benachbarter Gewichte im Gewichtsraum ist 1.

Die erste Komponente des Gewichts ist das Gewicht einer **SU(2)**-Untergruppe und wird daher oft als Isospin-Komponente I_3 bezeichnet. Die zweite Komponente des Gewichts ist bis auf einen konstanten Faktor $\frac{\sqrt{3}}{2}$ die Hyperladung.

Jede **irreduzible** Darstellung hat im Gewichtsraum einen Rand der Form

Darst. $(p|q)$

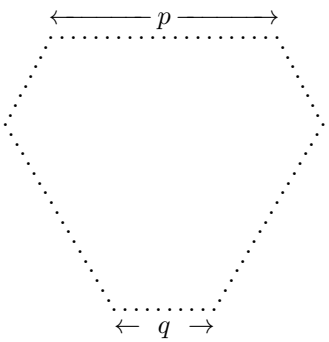

Dabei nimmt die Multiplizität der Punkte von außen nach innen solange um jeweils 1 zu, bis sich ein dreieckiger Rand ergibt, und bleibt dann konstant.

Darst. $(5|2)$

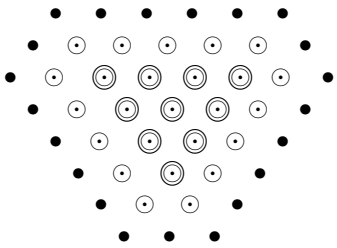

Fig. 3.2 Gewichtsdiagramme

3.3.10 Ausreduzieren von SU(3)-Darstellungen mit Gewichtsdiagrammen

Äußeres Produkt: alle Gewichtsvektor-Summen $m = m' + m''$.

Ausreduzieren: Iteratives Subtrahieren von Gewichtsdiagrammen nach den Regeln von Fig. 3.2, angefangen mit dem Diagramm mit größtem Rand (Beispiele in Fig. 3.3).

3.3.11 Young-Tableaux

Die irreduziblen Darstellungen der **SU(n)** kann man auch mit Hilfe der Young-Tableaux gewinnen.

Ein Young-Tableau ist eine Struktur aus Kästchen, die in Zeilen und Spalten so angeordnet sind, dass die Zahl der Kästchen in den Zeilen von oben nach unten, in den Spalten von links nach rechts nicht zunimmt. Beispiele:

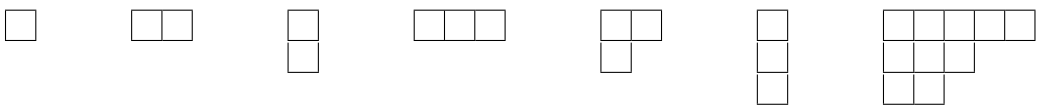

Zu jedem Young-Tableau gehört eine irreduzible Darstellung. Ihre Dimension kann auf folgende Weise gewonnen werden:

1. Zeichne Tableau zweimal.

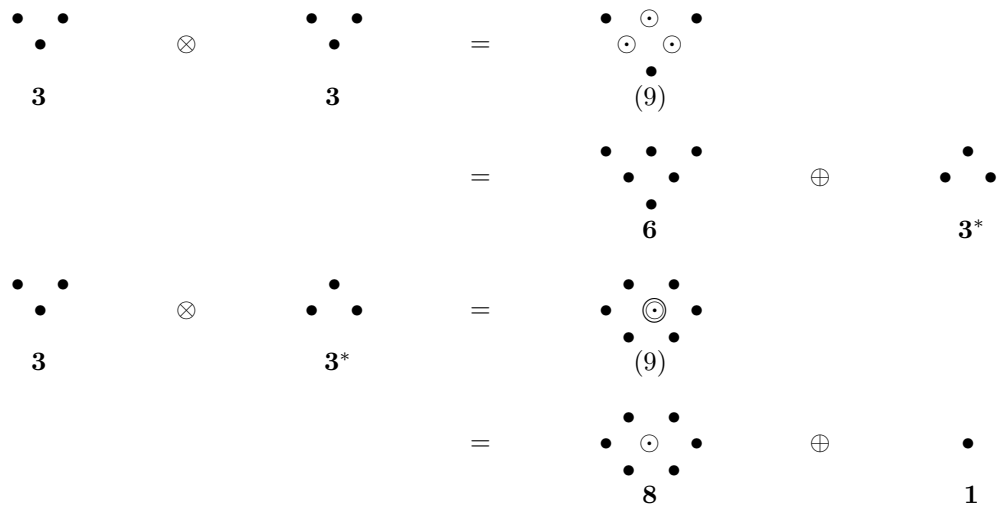

Fig. 3.3 Zwei Beispiele: Ausreduzieren von **SU(3)**-Darstellungen mit Gewichtsdiagrammen nach den Regeln von Fig. 3.2.

2. Trage in Tableau 1 die Zahlen

   n, $n+1$, $n+2$, ... in die erste Zeile,
   $n-1$, n, $n+1$, ... in die zweite Zeile,
   $n-2$, $n-1$, n, ... in die dritte Zeile usw. ein,

   d. h. jeweils in steigender Folge von links nach rechts und fallend von oben nach unten.

3. Trage in Tableau 2 die Anzahl der Kästchen ein, die in derselben Zeile rechts oder in derselben Spalte unter einem Kästchen stehen, plus 1 (= Länge der „Haken“).

4. Multipliziere alle Zahlen in Tableau 1 und dividiere durch alle Zahlen in Tableau 2. Das Resultat ist die Dimension der Darstellung.

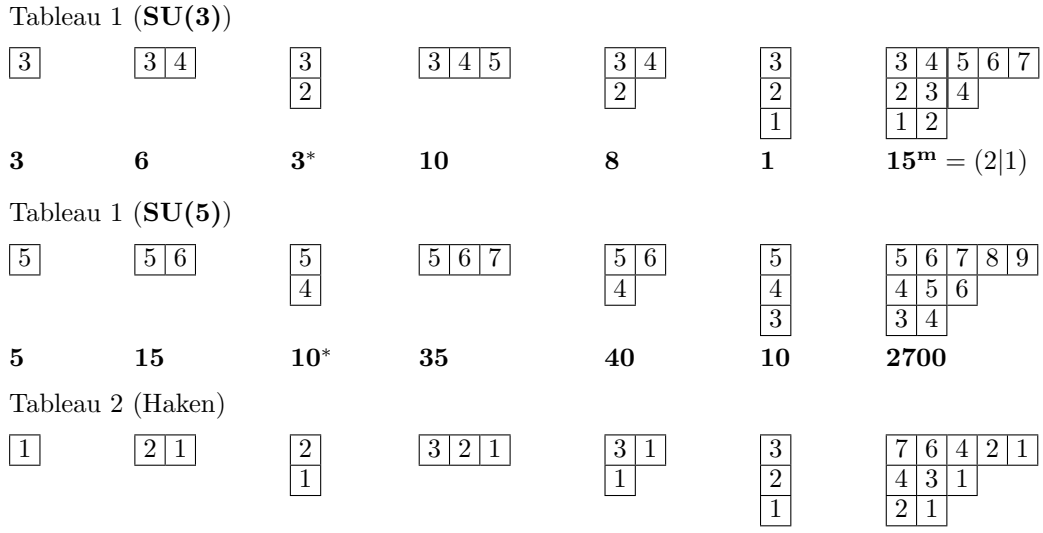

Fig. 3.4 Dimension einer Darstellung aus Young-Tableaux. Das untere Tableau mit den Längen der „Haken“ ist für alle **SU(n)** dasselbe.

Die so erhaltene Dimension ist gleich der Anzahl der Möglichkeiten, Zahlen $\in \{1 \dots n\}$ so in das Tableau zu schreiben, dass sie von links nach rechts nicht kleiner und von oben nach unten stets größer werden.

Die triviale Darstellung (Dimension = 1) gehört zum Young-Tableau mit einer Spalte aus n Kästchen.

Zu allen Young-Tableaux der **SU(n)** mit mehr als n Zeilen gehört keine Darstellung (Dimension = 0).

Die irreduziblen Darstellungen, in die das k-fache äußere Produkt der fundamentalen Darstellung zerfällt, entsprechen allen Young-Tableaux mit k Kästchen, aber höchstens n Zeilen.

Die Dimensionsberechnung kann vereinfacht werden, wenn man für die **SU(n)** alle **Spalten der Länge** n wegstreicht (die Dimension ändert sich nicht).

Durch das verbleibende Diagramm ist die Darstellung eindeutig bestimmt. Man bezeichnet dabei die Darstellung in der Form $(p_1|p_2|\dots|p_{n-1})$, wobei p_i die Anzahl Spalten der Länge i angibt, also z.B.

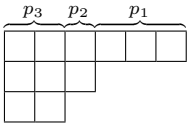

$= (3|1|2)$ der **SU(4)**

oder $(3|1|2|0)$ der **SU(5)** etc. Diese Bezeichnungsweise ist identisch mit der für Gewichtsdiagramme der **SU(3)** in Fig. 3.2.

Weitere Beispiele[8] der SU(3):


$= (2|0) = \mathbf{6}$


$= (3|0) = \mathbf{10}$


$= (4|0) = \mathbf{15}$

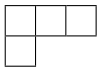
$= (2|1) = \mathbf{15^m}$

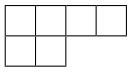
$= (2|2) = \mathbf{27}$


$= (0|2) = \mathbf{6}^*$


$= (0|3) = \mathbf{10}^*$

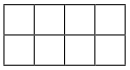
$= (0|4) = \mathbf{15}^*$


$= (1|2) = \mathbf{15^{m*}}$

3.3.12 Ausreduzieren äußerer Produkte mit Young-Tableaux

Ein äußeres Produkt aus zwei gegebenen irreduziblen Darstellungen $D = D' \otimes D''$ zerfällt wieder in irreduzible Darstellungen nach folgenden Regeln:

- Numeriere die Kästchen von D'' mit ihrer Zeilennummer.
- Hänge diese Kästchen (einzeln) an das Young-Tableau der Darstellung D' rechts oder unten so an, dass
  1. ein neues zulässiges Tableau entsteht,
  2. die Zahlen in einer Zeile von links nach rechts nicht abnehmen,
  3. in einer Spalte von oben nach unten zunehmen,
  4. und beim zeilenweisen Durchzählen **von rechts nach links** (wie Hebräisch oder Arabisch) keine Zahl häufiger auftritt als eine kleinere, d. h. an jeder Stelle müssen bereits mindestens so viele 1 wie 2, 2 wie 3 etc. aufgetreten sein.

[8] Es bedeutet * eine kontragradiente Darstellung und $^{\mathbf{m}}$ eine Darstellung, die die gleiche Multiplizität hat wie eine andere, zuvor definierte (Notation in Analogie zu metastabilen Isotopen in der Kernphysik; bei Darstellungen dient das m aber lediglich als Markierung mit der Bedeutung „alternativ“).

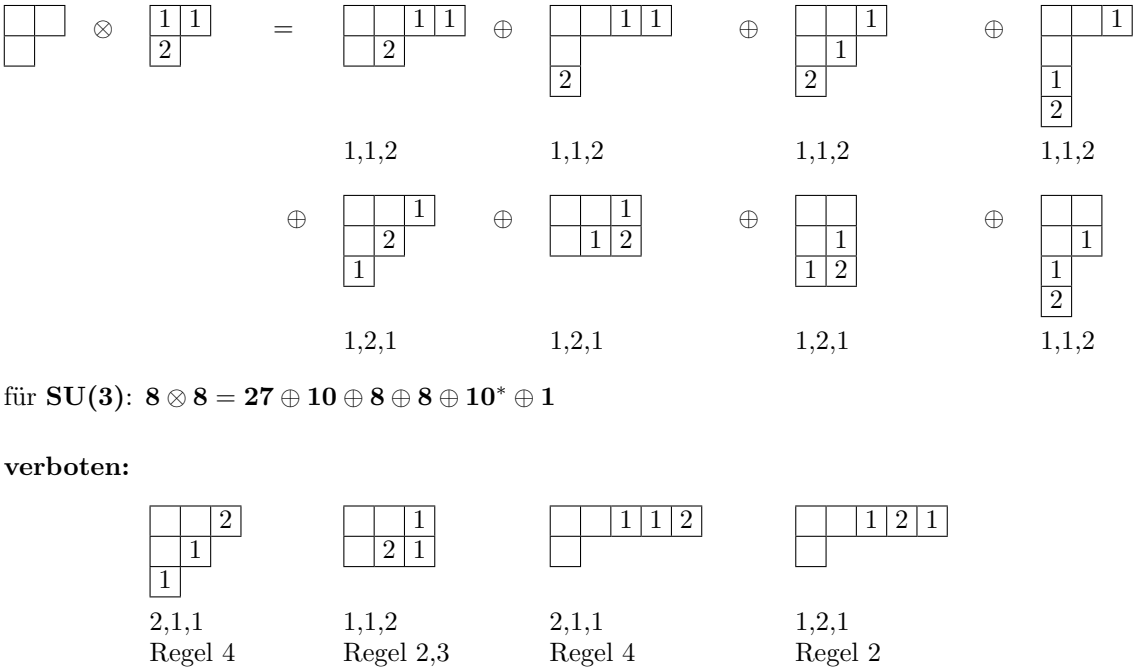

Fig. 3.5 Äußeres Produkt mit Young-Tableau. Die beiden Tableaux der letzten Spalte sind für die **SU(3)** ungültig, da sie vier Zeilen haben. Die Zahlenfolge beim Durchzählen nach Regel (4) ist jeweils darunter zu finden.

Weitere Beispiele der **SU(3)**:

$$\mathbf{10} \otimes \mathbf{8} = \mathbf{35} \oplus \mathbf{27} \oplus \mathbf{10} \oplus \mathbf{8}$$
$$\mathbf{6} \otimes \mathbf{6} = \mathbf{15} \oplus \mathbf{15^m} \oplus \mathbf{6^*}$$

3.4 Das Quarkmodell

Die Flavour-**SU(3)** der leichten Quarks[9] basiert auf Symmetriebetrachtungen von Ne'eman und Gell-Mann[10] und mit dem Namen „aces“ (Asse) auf Zweig[11].

Die Gewichte sind $(I_3, Y \cdot \sqrt{3}/2)$, Isospin und Hyperladung.

Die Gell-Mann–Nishijima-Formel[12] für die elektrische Ladung:

$$Q = I_3 + \frac{N_B + S + C + B + T}{2}$$

Irreduzible Multiplets von Zusammensetzungen aus Quarks:

$$\begin{aligned} qq: &\quad 3 \otimes 3 = 6 \oplus 3^* \\ qqqq: &\quad 3 \otimes 3 \otimes 3 \otimes 3 = (6 \oplus 3^*) \otimes (6 \oplus 3^*) = (15 \oplus 15^m \oplus 6^*) \oplus 2 \cdot (10 \oplus 8) \oplus (6^* \oplus 3) \\ &\quad = 15 \oplus 15^m \oplus 2 \cdot 10 \oplus 2 \cdot 8 \oplus 2 \cdot 6^* \oplus 3 \end{aligned}$$

[9] M. Gell-Mann, Phys. Lett. **8**, 214 (1964).
[10] Yuval Ne'eman, Nucl. Phys. **26**, 222 (1961); Murray Gell-Mann, Phys. Rev. **125**, 1067 (1962).
[11] George Zweig, CERN Reports Th-401 and Th-412, 1964, and Proceedings of the International School of Physics “Ettore Majorana”, Erice, Italy, 1963, ed. A. Zichichi (W. A. Benjamin, Inc., New York, 1964).
[12] Kazuhiko Nishijima, Progr. Theor. Phys. **13**, 285-304 (1955).

Table 3.2 Quantenzahlen der Quarks.

Quarks	I_3	Y	m	S	C	B	T
d	$-\frac{1}{2}$	$\frac{1}{3}$	$\left(-\frac{1}{2}, \frac{1}{2\sqrt{3}}\right)$	0	0	0	0
u	$\frac{1}{2}$	$\frac{1}{3}$	$\left(\frac{1}{2}, \frac{1}{2\sqrt{3}}\right)$	0	0	0	0
s	0	$-\frac{2}{3}$	$\left(0, -\frac{1}{\sqrt{3}}\right)$	-1	0	0	0
c	0	0	$(0,0)$	0	1	0	0
b	0	0	$(0,0)$	0	0	-1	0
t	0	0	$(0,0)$	0	0	0	1

Colour-Singuletts:

$$\begin{aligned}
q\bar{q}: &\quad 3 \otimes 3^* = 8 \oplus \mathbf{1} \\
qqq: &\quad 3 \otimes 3 \otimes 3 = (6 \oplus 3^*) \otimes 3 = 10 \oplus 8 \oplus 8 \oplus \mathbf{1} \\
qq\bar{q}\bar{q}: &\quad 3 \otimes 3 \otimes 3^* \otimes 3^* = 27 \oplus 10 \oplus 10^* \oplus 4 \cdot 8 \oplus 2 \cdot \mathbf{1} \\
qqqq\bar{q}: &\quad 3 \otimes 3 \otimes 3 \otimes 3 \otimes 3^* = 35 \oplus 3 \cdot 27 \oplus 4 \cdot 10 \oplus 2 \cdot 10^* \oplus 8 \cdot 8 \oplus 3 \cdot \mathbf{1}
\end{aligned}$$

Flavour-Singulett Meson:

$$u\bar{u} + d\bar{d} + s\bar{s} \tag{3.4}$$

Der Normierungsfaktor $1/\sqrt{3}$ ist weggelassen (auch in den folgenden Beispielen). Das Singulett-Meson ist symmetrisch unter Flavour-Austausch.

Flavour-Singulett Baryon:

$$\sum_{i,j,k} \varepsilon_{ijk} q_i q_j q_k \tag{3.5}$$

mit $q_1 \equiv u$, $q_2 \equiv d$, $q_3 \equiv s$. Das Singulett-Baryon ist antisymmetrisch unter Flavour-Austausch.

Coulour-Singuletts haben entsprechende Wellenfunktionen mit $u, d, s \to r, g, b$.

Die Wellenfunktion eines Spin-$\frac{1}{2}$ Flavour-Singulett Baryons ist

$$\begin{aligned}
\Psi \sim &\,(uds + dsu + sud - sdu - dus - usd) \times \\
&\times (rgb + gbr + brg - bgr - grb - rbg) \times (2\cdot \uparrow\uparrow\downarrow - \uparrow\downarrow\uparrow - \downarrow\uparrow\uparrow) \times f_L(123)
\end{aligned} \tag{3.6}$$

und ist symmetrisch unter der Vertauschung der Quarks 1 und 2, falls die Ortswellenfunktion $f_L(123)$ symmetrisch ist. Da die Gesamtwellenfuntion aber antisymmetrisch unter Vertauschung zweier Fermionen sein muss, verschwindet sie für den Grundzustand mit $L = 0$.

Für Spin-$\frac{3}{2}$ existiert im Grundzustand aus dem gleichen Grund nur das symmetrische Flavour-Dekuplett.

Triplett 3:

Darst. (1|0)

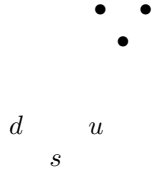

Anti-Triplett 3^*:

Darst. $(0|1)$

$$\begin{array}{ccc} & \bar{s} & \\ \bar{d} & & \bar{u} \end{array}$$

Sextett 6:

Darst. $(2|0)$

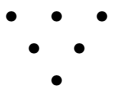

$$\begin{array}{ccccc} dd & & du+ud & & uu \\ & ds+sd & & us+su & \\ & & ss & & \end{array}$$

Anti-Sextett 6^*:

Darst. $(0|2)$

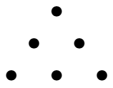

$$\begin{array}{ccccc} & & \bar{s}\bar{s} & & \\ & \bar{d}\bar{s}+\bar{s}\bar{d} & & \bar{u}\bar{s}+\bar{s}\bar{u} & \\ \bar{d}\bar{d} & & \bar{d}\bar{u}+\bar{u}\bar{d} & & \bar{u}\bar{u} \end{array}$$

Oktett 8:

Darst. $(1|1)$

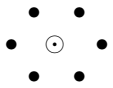

$$\begin{array}{ccccc} & d\bar{s} & & u\bar{s} & \\ d\bar{u} & & u\bar{u}-d\bar{d} & & u\bar{d} \\ & & 2s\bar{s}-u\bar{u}-d\bar{d} & & \\ & s\bar{u} & & s\bar{d} & \end{array}$$

Dekuplett 10:

Darst. $(3|0)$

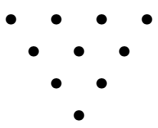

$$\begin{array}{ccccccc} ddd & & ddu & & duu & & uuu \\ & dds & & dus & & uus & \\ & & dss & & uss & & \\ & & & sss & & & \end{array}$$

Anti-Dekuplett 10^*:

Darst. (0|3)

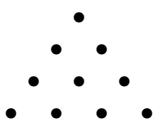

weitere Dreiecke: $15 = (4|0)$, $15^* = (0|4)$, $21 = (5|0)$. $21^* = (0|5)$ etc.
weitere Sechsecke: $15^m = (2|1)$, $15^{m*} = (1|2)$ etc.
27:

Darst. (2|2)

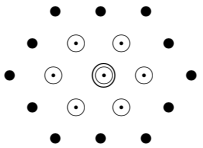

35:

Darst. (4|1)

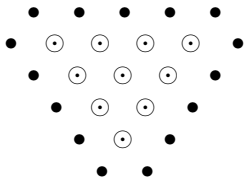

Pentaquark-Zustände:

	$dddd\bar{s}$		$dddu\bar{s}$		$dduu\bar{s}$		$duuu\bar{s}$		$uuuu\bar{s}$	
$dddd\bar{u}$		$dddu\bar{u}$		$dduu\bar{u}$		$duuu\bar{u}$		$uuuu\bar{u}$		
		$dddd\bar{d}$		$dddu\bar{d}$		$dduu\bar{d}$		$duuu\bar{d}$		$uuuu\bar{d}$
		$sddd\bar{s}$		$sddu\bar{s}$		$sduu\bar{s}$		$suuu\bar{s}$		
	$sddd\bar{u}$		$sddu\bar{u}$		$sduu\bar{u}$		$suuu\bar{u}$			
			$sddd\bar{d}$		$sddu\bar{d}$		$sduu\bar{d}$		$suuu\bar{d}$	
			$ssdd\bar{s}$		$ssdu\bar{s}$		$ssuu\bar{s}$			
		$ssdd\bar{u}$		$ssdu\bar{u}$		$ssuu\bar{u}$				
				$ssdd\bar{d}$		$ssdu\bar{d}$		$ssuu\bar{d}$		
				$sssd\bar{s}$		$sssu\bar{s}$				
			$sssd\bar{u}$		$sssu\bar{u}$					
					$sssd\bar{d}$		$sssu\bar{d}$			
					$ssss\bar{s}$					
				$ssss\bar{u}$						
						$ssss\bar{d}$				

Die Multiplizität der einzelnen Punkte erhält man aus der Zahl unterschiedlicher Permutationen der Quarks, z. B. $dddu\bar{s}, ddud\bar{s}, dudd\bar{s}, uddd\bar{s}$ ergibt einen vierfach besetzten Punkt:

		1		4		6		4		1	
1		9		22		22		9		1	
	4		22		36		22		4		
		6		22		22		6			
			4		9		4				
				1		1					

3.4.1 Wellenfunktionen aus Young-Tableaux

Die Permutationen der Colour oder Flavour eines **SU(n)**-Zustands werden

- bei Vertauschen in einer Spalte mit $-$
- bei Vertauschen in einer Zeile mit $+$

addiert.

So ist das folgende Dreiteilchensystem, das Dekuplett der **SU(3)** oder $I = \frac{3}{2}$ der **SU(2)**,

$$\begin{array}{|c|c|c|}\hline &&\\\hline\end{array} = \frac{1}{\sqrt{6}}\left(\begin{array}{|c|c|c|}\hline 1&2&3\\\hline\end{array}+\begin{array}{|c|c|c|}\hline 2&3&1\\\hline\end{array}+\begin{array}{|c|c|c|}\hline 3&1&2\\\hline\end{array}+\begin{array}{|c|c|c|}\hline 3&2&1\\\hline\end{array}+\begin{array}{|c|c|c|}\hline 1&3&2\\\hline\end{array}+\begin{array}{|c|c|c|}\hline 2&1&3\\\hline\end{array}\right)$$

oder

$$\frac{1}{\sqrt{3}}\left(\begin{array}{|c|c|c|}\hline 1&1&2\\\hline\end{array}+\begin{array}{|c|c|c|}\hline 1&2&1\\\hline\end{array}+\begin{array}{|c|c|c|}\hline 2&1&1\\\hline\end{array}\right)$$

eine total symmetrische Wellenfunktion. Dagegen ist das folgende Dreiteilchensystem, das Oktett der **SU(3)** oder $I = \frac{1}{2}$ der **SU(2)**,

$$\begin{array}{|c|c|}\hline &\\\hline \\\cline{1-1}\end{array} = \frac{1}{2}\left(\begin{array}{|c|c|}\hline 1&2\\\hline 3\\\cline{1-1}\end{array}+\begin{array}{|c|c|}\hline 1&3\\\hline 2\\\cline{1-1}\end{array}-\begin{array}{|c|c|}\hline 2&3\\\hline 1\\\cline{1-1}\end{array}-\begin{array}{|c|c|}\hline 3&2\\\hline 1\\\cline{1-1}\end{array}\right) \quad \text{oder} \quad \frac{1}{\sqrt{2}}\left(\begin{array}{|c|c|}\hline 1&1\\\hline 2\\\cline{1-1}\end{array}-\begin{array}{|c|c|}\hline 2&1\\\hline 1\\\cline{1-1}\end{array}\right)$$

eine Funktion mit gemischter Symmetrie. Wegen der Antisymmetrieregel können von den 6 möglichen immer nur maximal 4 Terme vorkommen.

Aus demselben Grund gibt es auch keine Oktett-Wellenfunktion mit drei gleichen Quarks, die Terme mit relativem Minuszeichen würden sich immer wegheben, die resultierende Wellenfunktion ist 0.

Beispiel Colour-**SU(3)**:

Singulett aus 3 Quarks: $\begin{array}{|c|}\hline \cdots\\\hline \cdots\\\hline \cdots\\\hline\end{array}$ ist total antisymmetrisch, Gleichung 3.5.

Aber: Singulett aus Quark und Antiquark ist symmetrisch, Gleichung 3.4.

Antitriplett $\bar{3} = \begin{array}{|c|}\hline \cdot\cdot\\\hline \cdot\cdot\\\hline\end{array}$

$$\frac{1}{\sqrt{2}}(|rg\rangle - |gr\rangle) \mathrel{\widehat{=}} |\bar{b}\rangle, \quad \frac{1}{\sqrt{2}}(|gb\rangle - |bg\rangle) \mathrel{\widehat{=}} |\bar{r}\rangle, \quad \frac{1}{\sqrt{2}}(|br\rangle - |rb\rangle) \mathrel{\widehat{=}} |\bar{g}\rangle$$

Sextett $6 = \begin{array}{|c|c|}\hline \cdot\cdot&\cdot\cdot\\\hline\end{array}$

$$|rr\rangle, \quad |gg\rangle, \quad |bb\rangle, \quad \frac{1}{\sqrt{2}}(|rg\rangle + |gr\rangle), \quad \frac{1}{\sqrt{2}}(|gb\rangle + |bg\rangle), \quad \frac{1}{\sqrt{2}}(|br\rangle + |rb\rangle)$$

Auch **SU(6)**-Wellenfunktionen aus $u\uparrow, u\downarrow, d\uparrow, d\downarrow, s\uparrow, s\downarrow$ lassen sich nach diesem Schema konstruieren.

Für Baryonen ist

$$\mathbf{6} \otimes \mathbf{6} \otimes \mathbf{6} = \mathbf{56} \oplus \mathbf{70} \oplus \mathbf{70} \oplus \mathbf{20}$$

wobei in **SU(3)**,**SU(2)**-Notation

$$\begin{aligned}\mathbf{56} &= (\mathbf{10},\mathbf{4}) + (\mathbf{8},\mathbf{2}) \quad \text{(symmetrisch)}\\ \mathbf{70} &= (\mathbf{10},\mathbf{2}) + (\mathbf{8},\mathbf{4}) + (\mathbf{8},\mathbf{2}) + (\mathbf{1},\mathbf{2})\\ \mathbf{20} &= (\mathbf{8},\mathbf{2}) + (\mathbf{1},\mathbf{4}) \quad \text{(antisymmetrisch)}\end{aligned}$$

Zweig-verbotene oder OZI-verbotene[13] Zerfälle sind Zerfälle ohne durchlaufende Quarklinien. In der QCD werden sie durch midestens 2 oder 3 s-Kanal-Gluonen vermittelt.

3.4.2 Symmetriebrechung

Die Flavour-**SU(3)**-Symmetrie wird durch die Masse des s-Quarks gebrochen.

Table 3.3 Quarkmassen.

Quark	Strommasse (current mass)	Konstituentenmasse
d	$4.5 \ldots 5.3\,\mathrm{MeV}$	$357\,\mathrm{MeV}$
u	$1.8 \ldots 3.0\,\mathrm{MeV}$	$354\,\mathrm{MeV}$
s	$(95 \pm 5)\,\mathrm{MeV}$	$530\,\mathrm{MeV}$
c	$(1275 \pm 25)\,\mathrm{MeV}$	$1585\,\mathrm{MeV}$
b	$(4180 \pm 30)\,\mathrm{MeV}$	$4930\,\mathrm{MeV}$
t	$(173200 \pm 900)\,\mathrm{MeV}$	$174000\,\mathrm{MeV}$

3.4.2.1 The Gell-Mann Okubo Mass Formula

Mass relations can be derived from a slightly broken SU(3) symmetry of the light quarks[14]: The heavier s-quark introduces a symmetry breaking proportional to λ_8:

$$m = m_0 + m_1 \cdot Y + m_2 \cdot [I(I+1) - \frac{1}{4}Y^2] \tag{3.7}$$

with coefficients $m_{0,1,2}$ depending on the multiplet.

Here Y is a linear function of the number of s quarks, so $(-)m_1$ is the linear contribution of its constituent mass. Since the isospin mass splitting is negligible, the mass can depend only on the eigenvalues of I^2 and Y^2. The term $[I(I+1) - \frac{1}{4}Y^2]$ is derived by Okubo from lengthy calculations with the involved symmetry transformations, breaking $\mathbf{SU(3)}$ to $\mathbf{SU(2)}_I \otimes \mathbf{U(1)}_Y$.

For the baryon decuplet, $I = 1 + \frac{1}{2}Y$, hence $I(I+1) - \frac{1}{4}Y^2 = 2 + \frac{3}{2}Y$ and only two coefficients $m'_{0,1}$ for $m = m_0 + m_1 \cdot Y$ are sufficient.

While for fermions the Hamiltonian is linear in mass, for bosons it is proportional to m^2, hence the formula should be used for squared masses for mesons. Also, since $\bar{s}$ and s have the same masses, the linear term vanishes for mesons, $m_1 = 0$, and instead the s quark mass enters via m_2. One relation directly derived from the Gell-Mann Okubo formula for the meson octet is:

$$3m_{\eta_8}^2 = 4m_K^2 - m_\pi^2 \tag{3.8}$$

or with linear masses

$$3m_{\eta_8} = 4m_K - m_\pi \tag{3.9}$$

[13] S. Okubo, Phys. Lett. **5**, 165 (1963); G. Zweig, CERN Report Th-412 (1964); J. Iizuka, Progr. Phys. Suppl. **37**, 21 (1966).

[14] S. Okubo, Progr. Theor. Phys. **27**, 949 (1962).

3.4.2.2 Singulett-Oktett-Mischung

Die leichten Mesonen werden durch das **SU(3)**-Oktett und das Singulett repräsentiert. Aufgrund der Symmetriebrechung mischt aber das Singulett

$$|\eta_1\rangle = \frac{1}{\sqrt{3}}\left(|u\bar{u}\rangle + |d\bar{d}\rangle + |s\bar{s}\rangle\right)$$

mit dem Oktett-Meson mit den gleichen Quantenzahlen

$$|\eta_8\rangle = \frac{1}{\sqrt{6}}\left(|u\bar{u}\rangle + |d\bar{d}\rangle - 2|s\bar{s}\rangle\right)$$

zu den physikalischen Mesonen.

Bei den neun $^1S_0$-Mesonen (Grundzustand, $S = L = 0$) sind die physikalischen Teilchen

$$\begin{aligned}
|\eta'\rangle &= \cos\theta|\eta_1\rangle + \sin\theta|\eta_8\rangle \\
&= \cos\alpha|s\bar{s}\rangle + \sin\alpha\frac{1}{\sqrt{2}}(|u\bar{u}\rangle + |d\bar{d}\rangle) \\
|\eta\rangle &= -\sin\theta|\eta_1\rangle + \cos\theta|\eta_8\rangle \\
&= -\sin\alpha|s\bar{s}\rangle + \cos\alpha\frac{1}{\sqrt{2}}(|u\bar{u}\rangle + |d\bar{d}\rangle)
\end{aligned}$$

mit einem Mischungswinkel $\theta \approx -11.5°$.

Bei den neun $^3S_1$-Mesonen (Grundzustand, $S = 1, L = 0$) sind die physikalischen Teilchen „η“: $\phi \approx |s\bar{s}\rangle$ und „η'“: $\omega \approx \frac{1}{\sqrt{2}}(|u\bar{u}\rangle + |d\bar{d}\rangle)$ fast ideal gemischt, d. h. das s-Quark zeigt seine Sonderrolle, mit einem Mischungswinkel $\alpha \approx 90°$ und $\theta \approx 38.7°$. Die *ideale Mischung* $\alpha = 90°$ entspricht $\theta = 35.3°$.

Bei angeregten Meson-Multipletts entspricht η: f', h' und η': f, h.

Die Massenmatrix

$$M = \begin{pmatrix} m_8 & H_{18} \\ H_{18} & m_1 \end{pmatrix}$$

hat die Eigenwerte $m_\eta, m_{\eta'}$. Die Diagonalisierung der Massenmatrix wird durch eine Rotation um den Winkel θ bewirkt, mit

$$\tan 2\theta = \frac{2H_{18}}{m_8 - m_1} \tag{3.10}$$

und

$$\tan\theta = \frac{m_8 - m_\eta}{H_{18}} \tag{3.11}$$

$$\begin{pmatrix} \cos\theta & \sin\theta \\ -\sin\theta & \cos\theta \end{pmatrix}\begin{pmatrix} m_8 & H_{18} \\ H_{18} & m_1 \end{pmatrix}\begin{pmatrix} \cos\theta & -\sin\theta \\ \sin\theta & \cos\theta \end{pmatrix} = \begin{pmatrix} m_\eta & 0 \\ 0 & m_{\eta'} \end{pmatrix}$$

Es ist daher

$$\begin{aligned}
m_\eta &= \cos^2\theta\, m_8 + 2\cos\theta\sin\theta\, H_{18} + \sin^2\theta m_1 \\
m_{\eta'} &= \sin^2\theta\, m_8 - 2\cos\theta\sin\theta\, H_{18} + \cos^2\theta m_1
\end{aligned}$$

und somit

$$\begin{aligned}
m_1 + m_8 &= m_\eta + m_{\eta'} \\
m_1 &= m_\eta + m_{\eta'} - m_8
\end{aligned}$$

Aus (3.9) erhält man m_8, und aus der Invarianz der Determinante

$$H_{18}^2 = m_1 m_8 - m_\eta m_{\eta'}$$

erhält man H_{18}. Daraus kann man den Mischungswinkel mit (3.10)

$$\tan 2\theta = \frac{2\sqrt{-(4m_K - m_\pi - 3m_\eta)(4m_K - m_\pi - 3m_{\eta'})}}{8m_K - 2m_\pi - 3m_\eta - 3m_{\eta'}}$$

oder (3.11)

$$\tan\theta = \sqrt{\frac{4m_K - m_\pi - 3m_\eta}{-4m_K + m_\pi + 3m_{\eta'}}}$$

berechnen.

Ohne die η'-Masse kommt man aus, wenn man im Flavourraum der Zustände $|u\bar{u}\rangle, |d\bar{d}\rangle, |s\bar{s}\rangle$ im Oktett die Massenmatrix

$$M = \begin{pmatrix} 2m_u + M_8 & 0 & 0 \\ 0 & 2m_d + M_8 & 0 \\ 0 & 0 & 2m_s + M_8 \end{pmatrix}$$

und wegen der Isospin-Symmetrie $m_u = m_d$ ansetzt. Dann kann man H_{18} aus Quarkmassen berechnen:

$$\begin{aligned} H_{18} &= \frac{1}{\sqrt{6}}\left(\langle u\bar{u}| + \langle d\bar{d}| - 2\langle s\bar{s}|\right) M \frac{1}{\sqrt{3}}\left(|u\bar{u}\rangle + |d\bar{d}\rangle + |s\bar{s}\rangle\right) \\ &= \frac{2}{3\sqrt{2}}(m_u + m_d - 2m_s) \\ &= \frac{4}{3\sqrt{2}}(m_u - m_s) \end{aligned}$$

$$\begin{aligned} m_K &= m_u + m_s + M_8 \\ m_\pi &= 2m_u + M_8 \\ \Longrightarrow \quad m_u - m_s &= m_\pi - m_K \\ \Longrightarrow \quad H_{18} &= \frac{4}{3\sqrt{2}}(m_\pi - m_K) \end{aligned}$$

Damit wird aus (3.11)

$$\tan\theta = \frac{4m_K - m_\pi - 3m_\eta}{2\sqrt{2}(m_\pi - m_K)}$$

Man wendet diese Formel – wie bei den Gell-Mann–Okubo-Beziehungen – meist auf Massenquadrate an, und erhält damit andere Mischungswinkel! Die oben angegebenen Zahlenwerte entsprechen weitgehend denen aus Massequadraten.

Zusatzinformationen zur Mischung erhält man aus Zerfällen wie $\phi \to \eta\gamma / \phi \to \eta'\gamma$.

3.5 Schwere Quarks

3.5.1 Quarkonia

Leading order QCD:

$$\begin{aligned} \Gamma(^3\mathrm{S}_1 \to ggg) &= \frac{40(\pi^2 - 9)\,\alpha_\mathrm{s}^3}{81\pi}\frac{|R(0)|^2}{M^2} \\ &= \frac{160(\pi^2 - 9)\,\alpha_\mathrm{s}^3}{81}\frac{|\Psi(0)|^2}{M^2} \\ &= \frac{10(\pi^2 - 9)\,\alpha_\mathrm{s}^3}{81\pi}\frac{|R(0)|^2}{m_q^2} \\ &= \frac{40(\pi^2 - 9)\,\alpha_\mathrm{s}^3}{81}\frac{|\Psi(0)|^2}{m_q^2} \end{aligned} \tag{3.12}$$

corresponding to orthopositronium

$$\Gamma(^3\mathrm{S}_1 \to \gamma\gamma\gamma) = \frac{4(\pi^2 - 9)\,\alpha^3}{9\pi}\frac{|R(0)|^2}{m_e^2}$$

Replacing one gluon with a photon gives

$$\Gamma(^3\mathrm{S}_1 \to \gamma gg) = \frac{32(\pi^2 - 9)\,\alpha\alpha_\mathrm{s}^2 Q_q^2}{9\pi}\frac{|R(0)|^2}{M^2} \tag{3.13}$$

Leading order QCD:

$$\Gamma(^1\mathrm{S}_0 \to gg) = \frac{8\pi\alpha_\mathrm{s}^2}{3m_q^2}|\Psi(0)|^2 \tag{3.14}$$

corresponding to parapositronium

$$\Gamma(^1\mathrm{S}_0 \to \gamma\gamma) = \frac{4\pi\alpha^2}{m_e^2}|\Psi(0)|^2$$

3.6 Exotische Hadronen

4. Dirac-Theorie

4.1 Die Dirac-Gleichung

Ansatz[15]:

- lineare Gleichung:
$$H\psi = (\vec{\alpha}\vec{p} + \beta m)\psi \tag{4.1}$$

- $H^2 = \vec{p}^2 + m^2$
$$H^2\psi = (\alpha_i p_i + \beta m)(\alpha_j p_j + \beta m)\psi = (\delta_{ij} p_i p_j + m^2)\psi$$
daraus erhält man durch Koeffizientenvergleich und $p_i p_j = p_j p_i$
$$\begin{aligned} \alpha_i\alpha_j + \alpha_j\alpha_i &= 0 \qquad (i \neq j) \\ \alpha_i\beta + \beta\alpha_i &= 0 \\ \alpha_i^2 &= 1 \\ \beta^2 &= 1 \end{aligned} \tag{4.2}$$

- $H = i\partial_t$, $\vec{p} = -i\nabla = (-i\partial_1, -i\partial_2, -i\partial_3)$

führt auf die Dirac-Gleichung (multipliziert mit β)
$$i\beta\partial_t\psi = -i\beta\alpha_i\partial_i\psi + m\psi$$
mit $\gamma^\mu := (\beta, \beta\vec{\alpha})$ erhält man die kovariante Form der **Dirac-Gleichung** mit γ-Matrizen:
$$\begin{aligned} (i\gamma^\mu\partial_\mu - m)\psi &= 0 \\ i\partial_\mu\bar{\psi}\gamma^\mu + m\bar{\psi} = (i{\gamma^\mu}^\dagger\partial_\mu + m)\bar{\psi} &= 0 \end{aligned} \tag{4.3}$$
die als Bewegungsgleichung aus der Lagrangedichte
$$\mathcal{L}_F = \bar{\psi}(i\gamma^\mu\partial_\mu - m)\psi \tag{4.4}$$
abgeleitet werden kann. Sie ist eine **lineare**, **kovariante** Differentialgleichung. Die Linearität erfordert Matrizen $\vec{\alpha}, \beta$ und damit mehrkomponentige Felder (Spinorfelder) ψ. Skalare Felder lassen sich nur durch eine **nichtlineare**, kovariante Differentialgleichung beschreiben (z. B. Klein-Gordon-Gleichung, s.o.)

Mit Hilfe der Gleichungen (4.2) erhält man
$$\begin{aligned} \gamma^0\gamma^0 &= \beta^2 = 1 \\ \gamma^1\gamma^1 &= \beta\alpha_1\beta\alpha_1 = -(\alpha_1)^2 = -1 \\ \gamma^0\gamma^1 + \gamma^1\gamma^0 &= \beta\beta\alpha_1 + \beta\alpha_1\beta = \alpha_1 - \alpha_1 = 0 \\ \gamma^1\gamma^2 + \gamma^2\gamma^1 &= \beta\alpha_1\beta\alpha_2 + \beta\alpha_2\beta\alpha_1 = -\alpha_1\alpha_2 - \alpha_2\alpha_1 = 0 \end{aligned}$$
etc. oder kurz
$$\{\gamma^\mu, \gamma^\nu\} = \gamma^\mu\gamma^\nu + \gamma^\nu\gamma^\mu = 2g^{\mu\nu} \tag{4.5}$$
Verschiedene Gamma-Matrizen ($\mu \neq \nu$) antikommutieren:
$$\gamma^\mu\gamma^\nu = -\gamma^\nu\gamma^\mu \text{ für } \mu \neq \nu$$

[15] P. A. M. Dirac, Proc. Roy. Soc. **A117**, 610 (London, 1928)

4.1.1 Spinoren und Gamma-Matrizen

Spinoren:

$$\begin{aligned} \psi &= (\psi_1; \psi_2; \psi_3; \psi_4) \\ \psi^{\dagger} = \psi^* &= (\psi_1^*; \psi_2^*; \psi_3^*; \psi_4^*) \end{aligned} \tag{4.6}$$

adjungierter Spinor:

$$\bar{\psi} = \psi^{\dagger}\gamma^0 \tag{4.7}$$

$$= \gamma^0\psi^* \tag{4.8}$$

$$\bar{\psi}\gamma^0 = \psi^{\dagger}$$

Wenn man Zeilen- und Spaltenvektoren unterscheidet, ist $\bar{\psi} = (\gamma^0\psi^*)^{\dagger}$.

Pauli–Dirac Darstellung der **γ-Matrizen**:

$$\vec{\alpha} = \begin{pmatrix} 0 & \vec{\sigma} \\ \vec{\sigma} & 0 \end{pmatrix}$$

$$\gamma^0 = \beta = \begin{pmatrix} 1 & 0 & 0 & 0 \\ 0 & 1 & 0 & 0 \\ 0 & 0 & -1 & 0 \\ 0 & 0 & 0 & -1 \end{pmatrix}, \quad \gamma^1 = \begin{pmatrix} 0 & 0 & 0 & 1 \\ 0 & 0 & 1 & 0 \\ 0 & -1 & 0 & 0 \\ -1 & 0 & 0 & 0 \end{pmatrix}, \quad \gamma^2 = \begin{pmatrix} 0 & 0 & 0 & -i \\ 0 & 0 & i & 0 \\ 0 & i & 0 & 0 \\ -i & 0 & 0 & 0 \end{pmatrix}$$

$$\gamma^3 = \begin{pmatrix} 0 & 0 & 1 & 0 \\ 0 & 0 & 0 & -1 \\ -1 & 0 & 0 & 0 \\ 0 & 1 & 0 & 0 \end{pmatrix}, \quad \gamma_5 \equiv i\gamma^0\gamma^1\gamma^2\gamma^3 = \begin{pmatrix} 0 & 0 & 1 & 0 \\ 0 & 0 & 0 & 1 \\ 1 & 0 & 0 & 0 \\ 0 & 1 & 0 & 0 \end{pmatrix} \tag{4.9}$$

$$\gamma_0 = \beta = \begin{pmatrix} 1 & 0 & 0 & 0 \\ 0 & 1 & 0 & 0 \\ 0 & 0 & -1 & 0 \\ 0 & 0 & 0 & -1 \end{pmatrix}, \quad \gamma_1 = \begin{pmatrix} 0 & 0 & 0 & -1 \\ 0 & 0 & -1 & 0 \\ 0 & 1 & 0 & 0 \\ 1 & 0 & 0 & 0 \end{pmatrix}, \quad \gamma_2 = \begin{pmatrix} 0 & 0 & 0 & i \\ 0 & 0 & -i & 0 \\ 0 & -i & 0 & 0 \\ i & 0 & 0 & 0 \end{pmatrix}$$

$$\gamma_3 = \begin{pmatrix} 0 & 0 & -1 & 0 \\ 0 & 0 & 0 & 1 \\ 1 & 0 & 0 & 0 \\ 0 & -1 & 0 & 0 \end{pmatrix}, \quad \gamma_5 \equiv -i\gamma_0\gamma_1\gamma_2\gamma_3 = \begin{pmatrix} 0 & 0 & 1 & 0 \\ 0 & 0 & 0 & 1 \\ 1 & 0 & 0 & 0 \\ 0 & 1 & 0 & 0 \end{pmatrix}$$

$$\vec{\gamma} = \begin{pmatrix} 0 & \vec{\sigma} \\ -\vec{\sigma} & 0 \end{pmatrix}$$

adjungierter Spinor:

$$\bar{\psi} = (\psi_1^*; \psi_2^*; -\psi_3^*; -\psi_4^*)$$

Weyl Darstellung der **γ-Matrizen** (die *chirale* Darstellung ist fast identisch mit dieser Darstellung, mit $\gamma^k \leftrightarrow -\gamma^k$):

$$\gamma^0 = \begin{pmatrix} 0 & 0 & 1 & 0 \\ 0 & 0 & 0 & 1 \\ 1 & 0 & 0 & 0 \\ 0 & 1 & 0 & 0 \end{pmatrix}, \quad \gamma^1 = \begin{pmatrix} 0 & 0 & 0 & -1 \\ 0 & 0 & -1 & 0 \\ 0 & 1 & 0 & 0 \\ 1 & 0 & 0 & 0 \end{pmatrix}, \quad \gamma^2 = \begin{pmatrix} 0 & 0 & 0 & i \\ 0 & 0 & -i & 0 \\ 0 & -i & 0 & 0 \\ i & 0 & 0 & 0 \end{pmatrix}$$

$$\gamma^3 = \begin{pmatrix} 0 & 0 & -1 & 0 \\ 0 & 0 & 0 & 1 \\ 1 & 0 & 0 & 0 \\ 0 & -1 & 0 & 0 \end{pmatrix}, \qquad \gamma_5 \equiv i\gamma^0\gamma^1\gamma^2\gamma^3 = \begin{pmatrix} 1 & 0 & 0 & 0 \\ 0 & 1 & 0 & 0 \\ 0 & 0 & -1 & 0 \\ 0 & 0 & 0 & -1 \end{pmatrix} \tag{4.10}$$

$$\vec{\gamma} = \begin{pmatrix} 0 & -\vec{\sigma} \\ \vec{\sigma} & 0 \end{pmatrix}$$

adjungierter Spinor:

$$\bar{\psi} = (\psi_3^*; \psi_4^*; \psi_1^*; \psi_2^*)$$

Tensor-Operator:

$$\begin{aligned} \sigma^{\mu\nu} &\equiv \frac{i}{2}(\gamma^\mu\gamma^\nu - \gamma^\nu\gamma^\mu) \\ &= i(\gamma^\mu\gamma^\nu - g^{\mu\nu}) \\ \Leftrightarrow\ [\gamma^\mu, \gamma^\nu] &= -2i\sigma^{\mu\nu} \end{aligned} \tag{4.11}$$

Beide Darstellungen der γ-Matrizen haben folgende Eigenschaften:
Unitarität: $\gamma^{\mu\dagger}\gamma^\mu = 1$ (nicht summieren über μ), $\gamma_5^\dagger\gamma_5 = 1$

$$\begin{aligned} {\gamma^0}^\dagger &= \gamma^0 \\ {\gamma^1}^\dagger &= -\gamma^1 \\ {\gamma^2}^\dagger &= \gamma^2 \\ {\gamma^3}^\dagger &= -\gamma^3 \\ {\gamma_5}^\dagger &= \gamma_5 \\ \Longrightarrow \qquad \gamma^0\psi = \psi\gamma^0, &\quad \gamma^1\psi = -\psi\gamma^1 \qquad \text{etc.} \end{aligned} \tag{4.12}$$

$$\{\gamma_5, \gamma^\mu\} = \gamma_5\gamma^\mu + \gamma^\mu\gamma_5 = 0 \tag{4.13}$$

$$(1 \pm \gamma_5)(1 \pm \gamma_5) = 2(1 \pm \gamma_5) \tag{4.14a}$$
$$(1 \pm \gamma_5)(1 \mp \gamma_5) = 0 \tag{4.14b}$$
$$(1 \pm \gamma_5)\gamma^\mu(1 \pm \gamma_5) = 0 \tag{4.14c}$$
$$(1 \pm \gamma_5)\gamma^\mu(1 \mp \gamma_5) = 2\gamma^\mu(1 \mp \gamma_5) \tag{4.14d}$$
$$(1 \pm \gamma_5)\gamma^\mu\gamma^\nu(1 \pm \gamma_5) = 2\gamma^\mu\gamma^\nu(1 \pm \gamma_5) \tag{4.14e}$$
$$(1 \pm \gamma_5)\gamma^\mu\gamma^\nu(1 \mp \gamma_5) = 0 \tag{4.14f}$$

$$\gamma_5 = \frac{i}{4!}\varepsilon_{\mu\nu\rho\sigma}\gamma^\mu\gamma^\nu\gamma^\rho\gamma^\sigma \tag{4.15}$$

$$\gamma^\mu\gamma_5 = \frac{i}{6}\varepsilon^{\mu\nu\rho\sigma}\gamma_\mu\gamma_\rho\gamma_\sigma \tag{4.16}$$

$$\begin{aligned} \gamma_\mu\gamma_\nu &= g_{\mu\nu} - i\sigma_{\mu\nu} \\ \gamma^\mu\gamma^\nu\gamma^\lambda &= g^{\mu\nu}\gamma^\lambda + g^{\nu\lambda}\gamma^\mu - g^{\lambda\mu}\gamma^\nu - i\gamma_5\gamma_\rho\varepsilon^{\rho\mu\nu\lambda} \\ \gamma^\lambda\gamma^\nu\gamma_\lambda &= 2g^{\lambda\nu}\gamma_\lambda - \gamma^\nu\gamma^\lambda\gamma_\lambda = -2\gamma^\nu \\ \gamma_5\sigma^{\mu\nu} &= \frac{i}{2}\varepsilon^{\mu\nu\rho\sigma}\sigma_{\rho\sigma} \end{aligned}$$

Aus (4.5) folgt $(\gamma^\mu)^2 = g^{\mu\mu}$:

$$\begin{aligned}(\gamma^0)^2 = (\gamma_5)^2 &= 1 \\ (\gamma^k)^2 &= -1\end{aligned} \tag{4.17}$$

$$\begin{aligned}(\gamma^0\gamma^k)^2 &= -(\gamma^0)^2(\gamma^k)^2 = 1 \\ (\gamma^j\gamma^k)^2 &= -(\gamma^j)^2(\gamma^k)^2 = -1\end{aligned} \tag{4.18}$$

$$\gamma^\mu\gamma_\mu = 4$$

Beweis: $\gamma^\mu\gamma_\mu = \frac{1}{2}\{\gamma^\mu,\gamma^\nu\}g_{\mu\nu} = \frac{1}{2}\cdot 2g^{\mu\nu}\mathbf{1}_{\text{Spinor}}g_{\mu\nu} = \delta^\mu_\mu\mathbf{1}_{\text{Spinor}} = (\operatorname{Sp}\mathbf{1}_{\text{Raumzeit}})\mathbf{1}_{\text{Spinor}} = 4\cdot\mathbf{1}_{\text{Spinor}}$

$$\begin{aligned}&\gamma^{0\dagger} = \gamma^0, \qquad \vec{\gamma}^\dagger = -\vec{\gamma} \\ \Longrightarrow \qquad &\gamma^{\mu\dagger} = \gamma^0\gamma^\mu\gamma^0 = \gamma_\mu \\ &\gamma_5^\dagger = -\gamma^0\gamma_5\gamma^0 = \gamma_5 \\ &(\gamma_5\gamma^\mu)^\dagger = \gamma^0(\gamma_5\gamma^\mu)\gamma^0 \\ &(\sigma^{\mu\nu})^\dagger = \gamma^0(\sigma^{\mu\nu})\gamma^0\end{aligned} \tag{4.19}$$

Feynmandagger (Slash):

$$\not{a} := a^\mu\gamma_\mu$$

Pauli–Dirac-Darstellung:

$$\not{a} = \begin{pmatrix} a^0 & 0 & -a^3 & -a_- \\ 0 & a^0 & -a_+ & a^3 \\ a^3 & a_- & -a^0 & 0 \\ a_+ & -a^3 & 0 & -a^0 \end{pmatrix} = \begin{pmatrix} a_0 & 0 & a_3 & -a_- \\ 0 & a_0 & -a_+ & -a_3 \\ -a_3 & a_- & -a_0 & 0 \\ a_+ & a_3 & 0 & -a_0 \end{pmatrix} = \begin{pmatrix} a^0\mathbf{1} & -\vec{\sigma}\vec{a} \\ \vec{\sigma}\vec{a} & -a^0\mathbf{1} \end{pmatrix}$$

mit $a_\pm = a_x \pm i a_y$

$$\not{a}\not{a} = a^\mu a_\mu \tag{4.20a}$$

$$\not{a}\not{b} = 2a^\mu b_\mu - \not{b}\not{a} \tag{4.20b}$$

$$\gamma^\nu\not{a}\gamma_\nu = -2\not{a} \tag{4.20c}$$

$$\gamma^\nu\not{a}\not{b}\gamma_\nu = 4a^\mu b_\mu \tag{4.20d}$$

4.1.1.1 Majorana-Darstellung

Majorana Darstellung der **γ-Matrizen**:

$$\gamma^0 = \begin{pmatrix} 0 & 0 & 0 & -i \\ 0 & 0 & i & 0 \\ 0 & -i & 0 & 0 \\ i & 0 & 0 & 0 \end{pmatrix}, \qquad \gamma^1 = \begin{pmatrix} i & 0 & 0 & 0 \\ 0 & -i & 0 & 0 \\ 0 & 0 & i & 0 \\ 0 & 0 & 0 & -i \end{pmatrix}, \qquad \gamma^2 = \begin{pmatrix} 0 & 0 & 0 & i \\ 0 & 0 & -i & 0 \\ 0 & -i & 0 & 0 \\ i & 0 & 0 & 0 \end{pmatrix}$$

$$\gamma^3 = \begin{pmatrix} 0 & -i & 0 & 0 \\ -i & 0 & 0 & 0 \\ 0 & 0 & 0 & -i \\ 0 & 0 & -i & 0 \end{pmatrix}, \qquad \gamma_5 \equiv i\gamma^0\gamma^1\gamma^2\gamma^3 = \begin{pmatrix} 0 & -i & 0 & 0 \\ i & 0 & 0 & 0 \\ 0 & 0 & 0 & i \\ 0 & 0 & -i & 0 \end{pmatrix} \tag{4.21}$$

adjungierter Spinor:

$$\bar{\psi} = (i\psi_4^*; -i\psi_3^*; i\psi_2^*; -i\psi_1^*)$$

4.1.2 Spursätze

Für alle Matrizen ist

$$\mathrm{Sp}(ABC) = \sum_{i,j,k} A_{ij}B_{jk}C_{ki} = \mathrm{Sp}(BCA) = \mathrm{Sp}(CAB) \tag{4.22}$$

d. h. man kann in Produkten die Matrizen zyklisch tauschen.

- Die Spur eines Produkts mit ungerader Anzahl von γ^μ ist 0 (Antikommutator!). Zum Beweis:

$$\mathrm{Sp}\,\gamma_5 \underbrace{\gamma^\mu \dots \gamma^\omega}_{m} = (-1)^m \,\mathrm{Sp}\underbrace{\gamma^\mu \dots \gamma^\omega}_{m}\gamma_5 = (-1)^m \,\mathrm{Sp}\,\gamma_5 \underbrace{\gamma^\mu \dots \gamma^\omega}_{m}$$

  wegen $\{\gamma^\mu, \gamma_5\} = 0$ und (4.22) und

$$\mathrm{Sp}\underbrace{\gamma^\mu \dots \gamma^\omega}_{m} = \mathrm{Sp}\underbrace{\gamma^\mu \dots \gamma^\omega}_{m}\gamma_5\gamma_5 = (-1)^m \,\mathrm{Sp}\,\gamma_5 \underbrace{\gamma^\mu \dots \gamma^\omega}_{m}\gamma_5 = (-1)^m \,\mathrm{Sp}\underbrace{\gamma^\mu \dots \gamma^\omega}_{m}\gamma_5\gamma_5$$

- γ_5 selbst ist ein Produkt aus einer geraden Zahl von Gammamatrizen (und zählt also bei dieser Regel nicht mit)
- $\mathrm{Sp}\,\gamma^\mu\gamma^\nu = 2g^{\mu\nu}\,\mathrm{Sp}\,\mathbf{1} - \mathrm{Sp}\,\gamma^\nu\gamma^\mu$
  $\mathrm{Sp}\,..\gamma^\mu\gamma^\nu.. = 2g^{\mu\nu}\,\mathrm{Sp}\,..\,.. - \mathrm{Sp}\,..\gamma^\nu\gamma^\mu..$

Mit (4.22) wird z. B. $\mathrm{Sp}\,\gamma^\mu\gamma^\nu = 2g^{\mu\nu}\,\mathrm{Sp}\,\mathbf{1} - \mathrm{Sp}\,\gamma^\nu\gamma^\mu = 2g^{\mu\nu}\,\mathrm{Sp}\,\mathbf{1} - \mathrm{Sp}\,\gamma^\mu\gamma^\nu$ oder $2\,\mathrm{Sp}\,\gamma^\mu\gamma^\nu = 2g^{\mu\nu}\,\mathrm{Sp}\,\mathbf{1} = 8g^{\mu\nu}$.

$$\begin{aligned}
\mathrm{Sp}\,\mathbf{1} &= 4 \\
\mathrm{Sp}\,\gamma_5 &= 0 \\
\mathrm{Sp}\,\gamma^\mu &= \mathrm{Sp}\,\gamma_5\gamma^\mu = \mathrm{Sp}\,\not{a} = \mathrm{Sp}\,\gamma_5\not{a} = 0 \\
\mathrm{Sp}\,\gamma^\mu\gamma^\nu\gamma^\rho &= \mathrm{Sp}\,\gamma_5\gamma^\mu\gamma^\nu\gamma^\rho = 0 && \text{(4.23a)} \\
&\vdots \\
\mathrm{Sp}\,\gamma^\mu\gamma^\nu &= 4g^{\mu\nu} && \text{(4.23b)} \\
\mathrm{Sp}\,\gamma^\mu\not{a} &= 4a^\mu \\
\mathrm{Sp}\,\not{a}\not{b} &= 4a^\mu b_\mu \\
\mathrm{Sp}\,\sigma^{\mu\nu} &= 0 \\
\mathrm{Sp}\,\gamma^\mu\gamma^\nu\gamma^\rho\gamma^\sigma &= 4(g^{\mu\nu}g^{\rho\sigma} - g^{\mu\rho}g^{\nu\sigma} + g^{\mu\sigma}g^{\nu\rho}) && \text{(4.23c)} \\
\mathrm{Sp}\,\gamma^\mu\not{a}\gamma^\nu\not{b} &= 4(a^\mu b^\nu - g^{\mu\nu}(ab) + a^\nu b^\mu) \\
\mathrm{Sp}\,\not{a}\not{b}\not{c}\not{d} &= 4(a^\mu b_\mu c^\nu d_\nu - a^\mu c_\mu b^\nu d_\nu + a^\mu d_\mu b^\nu c_\nu) \\
\mathrm{Sp}\,\sigma^{\mu\nu}\sigma^{\rho\sigma} &= 4(g^{\mu\rho}g^{\nu\sigma} - g^{\mu\sigma}g^{\nu\rho}) && \text{(4.23d)} \\
\mathrm{Sp}\,\gamma_5\gamma^\mu\gamma^\nu &= \mathrm{Sp}\,\gamma_5\not{a}\not{b} = 0 && \text{(4.23e)} \\
\mathrm{Sp}\,\gamma_5\gamma^\mu\gamma^\nu\gamma^\rho\gamma^\sigma &= -4i\varepsilon^{\mu\nu\rho\sigma} = 4i\varepsilon_{\mu\nu\rho\sigma} && \text{(4.23f)} \\
\mathrm{Sp}\,\gamma_5\not{a}\not{b}\not{c}\not{d} &= -4i\varepsilon_{\mu\nu\rho\sigma}a^\mu b^\nu c^\rho d^\sigma \\
\mathrm{Sp}\,\gamma_5\sigma^{\mu\nu}\sigma^{\rho\sigma} &= 4i\varepsilon^{\mu\nu\rho\sigma} \\
\mathrm{Sp}\,\not{a}_1\not{a}_2\cdots\not{a}_{2n} &= a_1a_2\,\mathrm{Sp}\,\not{a}_3\cdots\not{a}_{2n} - a_1a_3\,\mathrm{Sp}\,\not{a}_2\not{a}_4\cdots\not{a}_{2n} + \cdots + a_1a_{2n}\,\mathrm{Sp}\,\not{a}_2\cdots\not{a}_{2n-1} \\
\mathrm{Sp}\,\gamma^{\mu_1}\gamma^{\mu_2}\cdots\gamma^{\mu_{2n}} &= g^{\mu_1\mu_2}\,\mathrm{Sp}\,\gamma^{\mu_3}\cdots\gamma^{\mu_{2n}} - g^{\mu_1\mu_3}\,\mathrm{Sp}\,\gamma^{\mu_2}\gamma^{\mu_4}\cdots\gamma^{\mu_{2n}} + \cdots + g^{\mu_1\mu_{2n}}\,\mathrm{Sp}\,\gamma^{\mu_2}\cdots\gamma^{\mu_{2n-1}}
\end{aligned}$$

4.1.3 Stromdichte

Für die Dirac-Gleichung kann man nach dem Noether-Theorem eine Stromdichte

$$j^\mu = \bar{\psi}\gamma^\mu\psi \tag{4.24}$$

konstruieren, die der Kontinuitätsgleichung

$$\partial_\mu j^\mu = \partial_t j^0 + \nabla\vec{j} = 0 \tag{4.25}$$

genügt.

Dies ist der erhaltene Vektorstrom (CVC)

$$\partial_\mu j^\mu = (\partial_\mu\bar{\psi})\gamma^\mu\psi + \bar{\psi}\gamma^\mu\partial_\mu\psi = (im\bar{\psi})\psi + \bar{\psi}(-im\psi) = 0$$

der nach dem Noether-Theorem zu der Phasensymmetrie

$$\psi \to e^{i\alpha}\psi$$

gehört.

Ladungsstromdichte des Elektrons:

$$j^\mu = -e\,\bar{\psi}\gamma^\mu\psi \tag{4.26}$$

Der Axialvektorstrom

$$a^\mu = \bar{\psi}\gamma^\mu\gamma_5\psi \tag{4.27}$$

ergibt dagegen

$$\partial_\mu a^\mu = im\bar{\psi}\gamma_5\psi - (-im\bar{\psi}\gamma_5\psi) = 2im\bar{\psi}\gamma_5\psi$$

und ist nur für masselose Fermionen ein erhaltener Strom, der nach dem Noether-Theorem zu der Symmetrie

$$\psi \to e^{i\alpha\gamma_5}\psi$$

gehört (PCAC = partially conserved axial current baut auf einer Fast-Erhaltung für kleine Massen auf).

4.1.4 Lösung der freien Dirac-Gleichung

Die **stationären** Zustände (Impulseigenzustände = ebene Wellen) findet man mit dem Ansatz:

$$\psi(\vec{x},t) = u(\vec{p})\cdot e^{i\vec{p}\vec{x}}\cdot e^{-iEt} = u(\vec{p})\cdot e^{-ip^\mu x_\mu} \tag{4.28}$$

Dabei ist E ein zunächst noch freier Parameter, der die zeitliche Entwicklung der Wellenfunktion beschreibt.

Für den Viererspinor $u(\vec{p})$ wird die Diracgleichung (4.3) zu

$$\gamma^\mu p_\mu\, u = m\, u$$

bzw.

$$(\not{p} - m)u = 0 \tag{4.29}$$

Gleichung (4.29) in der Pauli–Dirac-Darstellung:

$$\begin{pmatrix} E-m & 0 & -p_z & -p_- \\ 0 & E-m & -p_+ & p_z \\ p_z & p_- & -E-m & 0 \\ p_+ & -p_z & 0 & -E-m \end{pmatrix} u = 0$$

mit $p_\pm = p_x \pm i p_y$

Den Viererspinor u zerlegt man in zwei Anteile u_A und u_B:

$$u = \begin{pmatrix} u_1 \\ u_2 \\ \hline u_3 \\ u_4 \end{pmatrix} \equiv \left\{ \begin{matrix} u_A \\ u_B \end{matrix} \right\} \tag{4.30}$$

In die Dirac-Gleichung eingesetzt, ergibt sich folgendes Gleichungssystem für u_A und u_B:

$$\begin{aligned} \vec{\sigma} \cdot \vec{p} \cdot u_B &= (E - m)\, u_A \\ \vec{\sigma} \cdot \vec{p} \cdot u_A &= (E + m)\, u_B \end{aligned} \tag{4.31}$$

mit $\vec{\sigma}\vec{p} = \begin{pmatrix} p_z & p_- \\ p_+ & -p_z \end{pmatrix}$.

Dieses Gleichungssystem ist nur lösbar, wenn die Koeffizientendeterminante verschwindet. Man betrachtet die 2×2-Koeffizientendeterminante

$$[\vec{\sigma} \cdot \vec{p}]^2 - (E + m)(E - m) = 0$$

Es ergibt sich mit $[\vec{\sigma} \cdot \vec{p}]^2 = \vec{p}^{\,2} \cdot \mathbf{1}$ für den Parameter E

$$E = \pm\sqrt{m^2 + \vec{p}^{\,2}} \tag{4.32}$$

Die relativistische Beziehung (für die Quadrate) wurde in die Konstruktion der Dirac-Gleichung gesteckt!

Der Parameter der zeitlichen Entwicklung darf also zwei Werte annehmen, die der **positiven** und der **negativen** Energie entsprechen. Für den Spinor u erhalten wir vier linear unabhängige Lösungen, je zwei zu negativer und positiver Energie:

Spinor für $E > 0$:

$$u^{(1,2)} = \mathcal{N} \cdot \left\{ \begin{matrix} \chi^{(1,2)} \\ \dfrac{\vec{\sigma}\vec{p}}{E + m} \cdot \chi^{(1,2)} \end{matrix} \right\} \tag{4.33}$$

mit $u_A = \mathcal{N}\chi,\ u_B = \mathcal{N}\dfrac{\vec{\sigma}\vec{p}}{E + m}\chi$.

Spinor für $E < 0$ ($|E| = -E$):

$$u^{(3,4)} = \mathcal{N} \cdot \left\{ \begin{matrix} \dfrac{-\vec{\sigma}\vec{p}}{-E + m} \cdot \chi^{(1,2)} \\ \chi^{(1,2)} \end{matrix} \right\} \tag{4.34}$$

mit $\chi^{(1)} = \binom{1}{0}$ (Spin $s_z = +\frac{1}{2}$) und $\chi^{(2)} = \binom{0}{1}$ (Spin $-\frac{1}{2}$). Ein Boost in z-Richtung ändert die Spinrichtung nicht (aber u. U. die Helizität).

$$\psi_{(1)} = \mathcal{N} \begin{pmatrix} 1 \\ 0 \\ \frac{p_z}{E+m} \\ \frac{p_x + i p_y}{E+m} \end{pmatrix} e^{-ip^\mu x_\mu} \tag{4.35}$$

$$\psi_{(2)} = \mathcal{N} \begin{pmatrix} 0 \\ 1 \\ \frac{p_x - i p_y}{E+m} \\ -\frac{p_z}{E+m} \end{pmatrix} e^{-ip^\mu x_\mu}$$

$$\psi_{(3)} = \mathcal{N} \begin{pmatrix} -\frac{p_z}{-E+m} \\ -\frac{p_x + i p_y}{-E+m} \\ 1 \\ 0 \end{pmatrix} e^{-ip^\mu x_\mu}$$

$$\psi_{(4)} = \mathcal{N} \begin{pmatrix} -\frac{p_x - i p_y}{-E+m} \\ \frac{p_z}{-E+m} \\ 0 \\ 1 \end{pmatrix} e^{-ip^\mu x_\mu}$$

Da für $\psi_{(3,4)}$ $E < 0$ ist, ist der Divisor $-E + m = |E| + m > 0$.

4.1.4.1 Normierung von Spinoren

Die Stromdichte ist

$$j^\mu = \bar\psi_{(1)}\gamma^\mu\psi_{(1)} = \bar\psi_{(2)}\gamma^\mu\psi_{(2)} = \frac{2|\mathcal{N}|^2}{E+m}p^\mu$$

und der Skalar

$$\bar\psi_{(1)}\psi_{(1)} = \bar\psi_{(2)}\psi_{(2)} = \frac{2|\mathcal{N}|^2}{E+m}m$$

Der **Normierungsfaktor** $\mathcal{N}$ hängt von der gewählten Normierung ab. Zwei oft benutzte Normierungen sind: 1. die $2E$-Normierung:

$$\int j^0\,\mathrm{d}V = 2|E|\cdot V \qquad \Longrightarrow \qquad \mathcal{N} = \sqrt{|E|+m} \tag{4.36}$$

Hier ist die Dichte j^0 proportional zu $E = p^0$, hat also das richtige Verhalten unter Lorentztransformationen. Der Faktor $\frac{2|\mathcal{N}|^2}{E+m}$ ist 2.

2. die kovariante Normierung:

$$\int j^0\,\mathrm{d}V = 1\cdot V \qquad \Longrightarrow \qquad \mathcal{N} = \sqrt{\frac{|E|+m}{2|E|}} \tag{4.37}$$

Der Faktor $\frac{2|\mathcal{N}|^2}{E+m}$ ist $\frac{1}{E}$.

Nota bene: $\int j^0\,\mathrm{d}V$ divergiert $\sim V$ für ebene Wellen, man benötigt also eigentlich ein Wellenpaket mit einer normierbaren Ortsfunktion! Dann ist z. B.

$$\psi'_{(1)} = \psi_{(1)}\cdot f(x^\mu), \qquad \int j^0\,\mathrm{d}V = \psi^{+}_{(1)}\psi_{(1)}\int |f(x^\mu)|^2\,\mathrm{d}V$$

4.1.4.2 Skalarprodukte im Spinorraum

Der Spinorraum ist ein $\mathbf{C}^4$-Vektorraum. Ein Skalarprodukt im Spinorraum kann man als $\phi^{+}\psi$ oder $\bar\phi\psi$ definieren.

Das Standard-Skalarprodukt eines Spinors mit sich selbst ist die 0-Komponente eines Minkowskivektors, die Dichte

$$j^0 = \bar\psi\gamma^0\psi = \psi^{+}\gamma^0\gamma^0\psi = \psi^{+}\psi = |\psi_1|^2 + |\psi_2|^2 + |\psi_3|^2 + |\psi_4|^2$$

Die Variante, die ein Lorentz-invariantes Skalarprodukt in der $2E$-Normierung ergibt, benutzt den **adjungierten Spinor**

$$\bar\psi := \psi^{+}\gamma^0 = (\gamma^0\psi^*)^\dagger = (\psi_1^*;\psi_2^*;-\psi_3^*;-\psi_4^*) \tag{4.38}$$

Da der Skalar $\bar\psi\phi = \phi^\dagger\bar\psi^\dagger = (\bar\phi\psi)^*$ ein Skalarprodukt zweier Vierervektoren mit einfacher Metrik ist, hat eine Unterscheidung zwischen Zeilenvektoren $\psi^\dagger$ und Spaltenvektoren ψ keine weitergehende Bedeutung, deshalb wird der Transpositionsoperator † bei Spinoren in diesem Skript i. a. weggelassen.

In der Pauli-Dirac-Dtrstellung ist $\bar\psi\psi = |\psi_1|^2 + |\psi_2|^2 - |\psi_3|^2 - |\psi_4|^2$, in der Weyl-Darstellung $\bar\psi\psi = 2\,\mathcal{R}e(\psi_1\psi_3^* + \psi_2\psi_4^*)$.

Die Norm eines Spinors ist für dieses Skalarprodukt

$$\bar\psi\psi = \mathcal{N}^2\frac{2m}{|E|+m}$$

und mit $\mathcal{N} = \sqrt{|E|+m}$ ist $\bar\psi\psi = 2m$ eine Lorentz-Invariante (ein Skalar).

4.1.5 Fermion in Ruhe

Für ein Fermion in Ruhe ($\vec{p} = \mathbf{0}$) gilt mit $E = m > 0$

$$u^{(1)} = \mathcal{N}(1,0,0,0)$$
$$u^{(2)} = \mathcal{N}(0,1,0,0)$$

und mit $E = -m < 0$

$$u^{(3)} = \mathcal{N}(0,0,1,0)$$
$$u^{(4)} = \mathcal{N}(0,0,0,1)$$

Dabei ist $\mathcal{N}$ entweder $\sqrt{2m}$ oder 1.
Daraus wird z. B.

$$u^{(1,2)}(\vec{p}) = \frac{\not{p} + m}{E + m} u^{(1,2)}(\mathbf{0})$$

4.1.6 Zuordnung der Lösungen zu $E > 0$ und $E < 0$

Die Zuordnung der Lösungen zu $E > 0$ und $E < 0$ ergibt sich aus dem Hamilton-Operator (4.1)

$$H\psi = (\vec{\alpha}\vec{p} + \beta m)\psi = E\psi$$

Für $\vec{p} = \mathbf{0}$ wird damit

$$E\psi = m\beta\psi = m\gamma_0\psi$$

mit den Lösungen $+m$ für $u^{(1,2)}$ und $-m$ für $u^{(3,4)}$ (in Ruhe).

4.1.7 Ultrarelativistisches Fermion

Für $\beta \to 1$ oder $m = 0$ werden die Lösungen

$$\psi_{(1)} = \mathcal{N} \begin{pmatrix} 1 \\ 0 \\ \frac{p_z}{p} \\ \frac{p_x + ip_y}{p} \end{pmatrix} e^{-ip^\mu x_\mu} \tag{4.39}$$

$$\psi_{(2)} = \mathcal{N} \begin{pmatrix} 0 \\ 1 \\ \frac{p_x - ip_y}{p} \\ -\frac{p_z}{p} \end{pmatrix} e^{-ip^\mu x_\mu}$$

$$\psi_{(3)} = \mathcal{N} \begin{pmatrix} \frac{p_z}{p} \\ \frac{p_x + ip_y}{p} \\ 1 \\ 0 \end{pmatrix} e^{-ip^\mu x_\mu}$$

$$\psi_{(4)} = \mathcal{N} \begin{pmatrix} \frac{p_x - ip_y}{p} \\ -\frac{p_z}{p} \\ 0 \\ 1 \end{pmatrix} e^{-ip^\mu x_\mu}$$

mit Impuls in z-Richtung:

$$\psi_{(1)} = \mathcal{N} \begin{pmatrix} 1 \\ 0 \\ 1 \\ 0 \end{pmatrix} e^{-ip^\mu x_\mu} \tag{4.40}$$

$$\psi_{(2)} = \mathcal{N} \begin{pmatrix} 0 \\ 1 \\ 0 \\ -1 \end{pmatrix} e^{-ip^\mu x_\mu}$$

$$\psi_{(3)} = \mathcal{N} \begin{pmatrix} 1 \\ 0 \\ 1 \\ 0 \end{pmatrix} e^{-ip^\mu x_\mu} = \psi_{(1)}$$

$$\psi_{(4)} = \mathcal{N} \begin{pmatrix} 0 \\ -1 \\ 0 \\ 1 \end{pmatrix} e^{-ip^\mu x_\mu} = -\psi_{(2)}$$

Die reinen Spinoren erhält man durch Abspaltung des Ebene-Welle-Faktors

$$u_{(1)} = \mathcal{N} \begin{pmatrix} 1 \\ 0 \\ 1 \\ 0 \end{pmatrix} = u_{(3)}, \qquad u_{(2)} = \mathcal{N} \begin{pmatrix} 0 \\ 1 \\ 0 \\ -1 \end{pmatrix} = -u_{(4)}$$

Mit $v^{(2,1)}(\vec{p}) := u^{(3,4)}(-\vec{p})$ wird

$$v_{(1)} = \mathcal{N} \begin{pmatrix} 0 \\ 1 \\ 0 \\ 1 \end{pmatrix}, \qquad v_{(2)} = \mathcal{N} \begin{pmatrix} -1 \\ 0 \\ 1 \\ 0 \end{pmatrix}$$

Lösungen mit Impuls $p(\sin\theta; 0; \cos\theta)$ (aber Spins in $\pm z$-Richtung):

$$\psi_{(1)} = \mathcal{N} \begin{pmatrix} 1 \\ 0 \\ \cos\theta \\ \sin\theta \end{pmatrix} e^{-ip^\mu x_\mu} \tag{4.41}$$

$$\psi_{(2)} = \mathcal{N} \begin{pmatrix} 0 \\ 1 \\ \sin\theta \\ -\cos\theta \end{pmatrix} e^{-ip^\mu x_\mu}$$

$$\psi_{(3)} = \mathcal{N} \begin{pmatrix} \cos\theta \\ \sin\theta \\ 1 \\ 0 \end{pmatrix} e^{-ip^\mu x_\mu}$$

$$\psi_{(4)} = \mathcal{N} \begin{pmatrix} \sin\theta \\ -\cos\theta \\ 0 \\ 1 \end{pmatrix} e^{-ip^\mu x_\mu}$$

4.1.8 Interpretation der Lösungen

Die Dirac-Gleichung (wie auch die Klein-Gordon-Gleichung) hat als Lösungen ebene Wellen, die Zustände mit konstantem Impuls beschreiben, und als freie Teilchen betrachtet werden. Es gibt jedoch stets zwei Lösungen, mit positiver und negativer Energie $E = \pm\sqrt{p^2 + m^2}$. Die Lösungen negativer Energie werden mit der Existenz von Antiteilchen assoziiert. Es gibt zwei anschauliche Deutungen.

Dirac's Interpretation: Alle möglichen Energiezustände eines Fermions der Masse m reichen von $-\infty$ bis $-m$ und von m bis ∞. Im *Vakuum* sind alle Zustände negativer Energie besetzt („Dirac-See"), die Zustände positiver Energie aber leer.

Mit einer Energie $\Delta E > 2m$ kann ein Teilchen negativer Energie in den Bereich positiver Energie angehoben werden; es entsteht ein freies Teilchen und ein Loch (ähnlich wie im Bändermodell eines Halbleiters). Das Loch kann sich selbst wie ein freies Teilchen ausbreiten, es hat aber die entgegengesetzten Quantenzahlen. Es wird als Antiteilchen beobachtet, das die positive Energie trägt, die erforderlich war, um das Teilchen aus dem Loch herauszulösen.

Die Lösungen negativer Energie haben lediglich die Funktion, Zustände zu definieren, die im *Vakuum* alle besetzt sind.

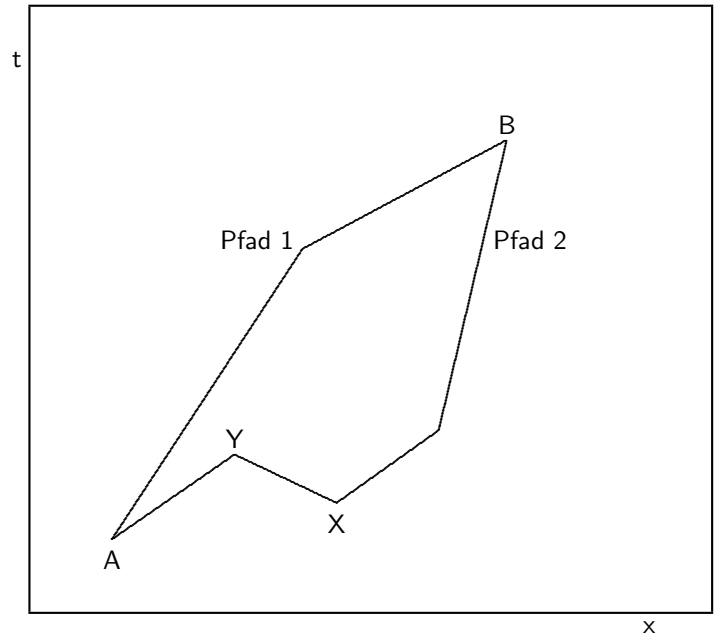

Fig. 4.1 Zwei mögliche Pfade von A:(x_A, t_A) nach B:(x_B, t_B)

Feynman's Interpretation: Wegen $E = i\partial/\partial t$ bedeuten Zustände negativer Energie Teilchen, die in der Zeit rückwärts laufen (zuerst vorgeschlagen 1941 von Stückelberg). Ein in der Zeit rückwärts laufendes Teilchen wird als in der Zeit vorwärts laufendes Antiteilchen mit positiver Energie beobachtet.

Die Transformation, die ein in der Zeit vorwärts laufendes Teilchen in ein in der Zeit rückwärts laufendes Antiteilchen mit gleichem Impuls verwandelt, ist CPT. Darin manifestiert sich die CPT-Invarianz als notwendige Voraussetzung einer Feldtheorie.

Insbesondere gehören zu einer vollständigen Beschreibung der Ausbreitung eines Teilchens von $(\vec{x}_A, t_A)$ nach $(\vec{x}_B, t_B)$ auch Pfade, die teilweise rückwärts in der Zeit laufen (Pfad 2 in Fig. 4.1). Solche Pfade kann man dann folgendermaßen interpretieren: Am Punkt Y vernichten sich das Teilchen und ein Antiteilchen, das am Punkt X entstanden ist. Das korrespondierende Teilchen von X wandert nach Punkt B.

4.1.9 Bilineare Kovarianten

Man benötigt bilineare Kovarianten, um die allgemeinste Form der Ströme lorentz-kovariant zu formulieren. Für die Bilinearform $\bar{\psi}(4\times 4)\phi$ mit unveränderter Norm gibt es insgesamt 16 linear unabhängige Möglichkeiten, die in der folgenden Tabelle zusammengefasst sind.

Komplexe 4×4-Matrizen haben 32 Matrizen als Basisvektoren, unitäre Matrizen erfüllen 16 Gleichungen $UU^{+}=\mathbf{1}$, sie haben daher nur 16 Basisvektoren. Die Bilinearformen sollen die Wahrscheinlichkeit (Teilchenzahl) erhalten und können daher nur mit unitären Matrizen gebildet werden.

Table 4.1 Bilineare Kovarianten

Form	Transformationsverhalten	Anzahl der Komponenten
$\bar{\psi}\phi$	Skalar	1
$\bar{\psi}\gamma^{\mu}\phi$	Vektor	4
$\bar{\psi}\sigma^{\mu\nu}\phi$	Tensor	6
$\bar{\psi}\gamma^{\mu}\gamma_5\phi$	Axialvektor	4
$\bar{\psi}\gamma_5\phi$	Pseudoskalar	1

Aufgrund der Eigenschaften der γ-Matrizen (4.16,4.17) führt jede weitere Multiplikation zu einer Linearkombination der in der Tabelle angegebenen Formen.

Komplexe Konjugation ergibt

$$(\bar{\psi}O\phi)^{*}=\bar{\phi}\gamma_0 O^{+}\gamma_0\psi$$

und explizit

$$\begin{aligned}(\bar{\psi}\phi)^{*}&=\bar{\phi}\psi\\(\bar{\psi}\gamma^{\mu}\phi)^{*}&=\bar{\phi}\gamma^{\mu}\psi\\(\bar{\psi}\sigma^{\mu\nu}\phi)^{*}&=\bar{\phi}\sigma^{\mu\nu}\psi\\(\bar{\psi}\gamma^{\mu}\gamma_5\phi)^{*}&=\bar{\phi}\gamma^{\mu}\gamma_5\psi\\(\bar{\psi}\gamma_5\phi)^{*}&=-\bar{\phi}\gamma_5\psi\end{aligned}$$

Daher wird gerne statt $\bar{\psi}\gamma_5\phi$ die Kombination $i\bar{\psi}\gamma_5\phi$ genommen, mit

$$(i\bar{\psi}\gamma_5\phi)^{*}=i\bar{\phi}\gamma_5\psi$$

Beispiel eines Minkowskivektors (Pauli-Dirac-Darstellung):

$$\bar{\psi}_{\alpha}\gamma^{\mu}_{\alpha\beta}\phi_{\beta}=\begin{pmatrix}\bar{\psi}_1\phi_1+\bar{\psi}_2\phi_2-\bar{\psi}_3\phi_3-\bar{\psi}_4\phi_4\\ \bar{\psi}_1\phi_4+\bar{\psi}_2\phi_3-\bar{\psi}_3\phi_2-\bar{\psi}_4\phi_1\\ -i\bar{\psi}_1\phi_4+i\bar{\psi}_2\phi_3+i\bar{\psi}_3\phi_2-i\bar{\psi}_4\phi_1\\ \bar{\psi}_1\phi_3-\bar{\psi}_2\phi_4-\bar{\psi}_3\phi_1+\bar{\psi}_4\phi_2\end{pmatrix} \tag{4.42}$$

4.1.10 Spinoperator

Der Spinoperator im Spinorraum ist[16]

$$\begin{aligned}\tfrac{1}{2}\vec{\Sigma}=\frac{i}{4}\vec{\gamma}\times\vec{\gamma}&=\tfrac{1}{2}\begin{pmatrix}\vec{\sigma}&0\\0&\vec{\sigma}\end{pmatrix}\\&=\tfrac{1}{2}\gamma_5\gamma^0\vec{\gamma}\end{aligned} \tag{4.43}$$

[16] Man könnte auch $\frac{1}{2}\vec{\Sigma}\to\vec{\Sigma}$ wählen, es hat sich aber eingebürgert, den Faktor $\frac{1}{2}$ abzuspalten.

$$\tfrac{1}{2}\Sigma_3 = \tfrac{1}{2}\begin{pmatrix} 1 & 0 & 0 & 0 \\ 0 & -1 & 0 & 0 \\ 0 & 0 & 1 & 0 \\ 0 & 0 & 0 & -1 \end{pmatrix}$$

d. h. $\chi^{(1)} = \binom{1}{0}$ hat $S_3 = +\frac{1}{2}$ und $\chi^{(2)} = \binom{0}{1}$ hat $S_3 = -\frac{1}{2}$.

$$(\tfrac{1}{2}\vec{\Sigma})^2 = \frac{3}{4}$$

$$\begin{aligned} \tfrac{1}{2}\Sigma_i &= \frac{1}{4}\varepsilon_{ijk}\sigma^{jk} \\ &= \frac{i}{4}\varepsilon_{ijk}\gamma^j\gamma^k \\ &= \tfrac{1}{2}\gamma_5\gamma^0\gamma^i \end{aligned}$$

$$\tfrac{1}{2}\Sigma_3\psi_{(1)} = \tfrac{1}{2}\mathcal{N}\begin{pmatrix} 1 \\ 0 \\ \frac{p_z}{E+m} \\ -\frac{p_x+ip_y}{E+m} \end{pmatrix} e^{-ip^\mu x_\mu}$$

$$\tfrac{1}{2}\Sigma_3\psi_{(2)} = -\tfrac{1}{2}\mathcal{N}\begin{pmatrix} 0 \\ 1 \\ -\frac{p_x-ip_y}{E+m} \\ -\frac{p_z}{E+m} \end{pmatrix} e^{-ip^\mu x_\mu}$$

d. h. $\psi_{(1,2)}$ aus (4.35) sind Eigenzustände mit Spin $s_z = \pm\frac{1}{2}$, falls $p_x = p_y = 0$.

4.2 Transformationen des Minkowskiraums

4.2.1 Poincaré-Gruppe

Poincaré Transformation:

$$\Pi = \Pi(a^\mu, \boldsymbol{\beta}, \Omega) = T(a^\mu) \circ \Lambda(\boldsymbol{\beta}) \circ R(\Omega) \circ S$$

Translation ∘ echte Lorentz-Transformation ∘ Rotation ∘ Parität/Zeitumkehr

$$\begin{aligned} x' &= \Pi x \\ x'^\mu &= \Lambda^\mu{}_\nu(\boldsymbol{\beta})\, R^\nu{}_\rho(\Omega)\, x^\rho + a^\mu \end{aligned}$$

$R \in \mathbf{SO(3)}$, $\Lambda \in \mathbf{SO(3,1)}$

Die *eigentliche Lorentzgruppe* $\mathbf{SO(3,1)}$ enthält alle Transformationen

$$\Lambda(\boldsymbol{\beta}) \circ R(\Omega)$$

die *allgemeine Lorentzgruppe* $\mathbf{O(3,1)}$ enthält noch Spiegelungen (Parität, Zeitumkehr). Transformationen der eigentliche Lorentzgruppe werden durch 6 reelle Parameter beschrieben: 3 Winkel und 3 Geschwindigkeitskomponenten (Rapiditäten).

Die echten Lorentztransformationen (Boosts) bilden keine Gruppe, zwei sukzessive Boosts entsprechen i. a. einem Boost ∘ einer Rotation.

4.2.2 Darstellung von Transformationen des Minkowskiraums

Transformation $x'^{\mu} = \Pi^{\mu}{}_{\nu} x^{\nu}$

Impuls $p'^{\mu} = \Pi^{\mu}{}_{\nu} p^{\nu}$

ein Vektor $V^{\mu} = \bar{\psi}(\boldsymbol{p}_1)\gamma^{\mu}\phi(\boldsymbol{p}_2)$ transformiert sich

$$V'^{\mu} = \Pi^{\mu}{}_{\nu} V^{\nu}$$

Das erreicht man entweder durch eine

- Transformation der γ-Matrizen, also $V'^{\mu} = \bar{\psi}(\boldsymbol{p}_1)\gamma'^{\mu}\phi(\boldsymbol{p}_2)$:

$$\gamma'^{\mu} = \Pi^{\mu}{}_{\nu}\gamma^{\nu} = S^{-1}(\Pi)\,\gamma^{\mu}\,S(\Pi) \tag{4.44}$$

  wobei $S(\Pi)$ eine Darstellung der Transformation im Spinorraum ist,

oder besser durch eine

- Transformation der Spinoren (die γ-Matrizen sind dann **in jedem System gleich**), also $V'^{\mu} = \bar{\psi}'(\boldsymbol{p}'_1)\gamma^{\mu}\phi'(\boldsymbol{p}'_2))$:

$$\begin{aligned}\phi'(\boldsymbol{p}'_2) &= S(\Pi)\,\phi(\boldsymbol{p}_2)\\ \psi'(\boldsymbol{p}'_1) &= S(\Pi)\,\psi(\boldsymbol{p}_1)\end{aligned}$$

  und

$$\begin{aligned}\bar{\psi}' &= (S\,\psi)^{+}\gamma^0\\ &= \bar{\psi}(\gamma^0\,S^{+}\,\gamma^0)\end{aligned}$$

  d. h. $S^{-1} = \gamma^0 S^{+}\gamma^0$

Für **infinitesimale** Transformationen

$$\Pi^{\mu}{}_{\nu} = \delta^{\mu}_{\nu} + \omega^{\mu}{}_{\nu}$$

(die $\omega^{\mu}{}_{\nu}$ bilden den Infinitesimalring). Die Darstellung im Spinorraum ist

$$\begin{aligned}S(\Pi) &= 1 - \frac{i}{4}\sigma^{\mu\nu}\omega_{\mu\nu}\\ &= 1 + \frac{1}{4}\gamma^{\mu}\gamma^{\nu}\omega_{\mu\nu}\end{aligned} \tag{4.45}$$

(wegen $\mathrm{Sp}\,\boldsymbol{\omega} = \omega^{\nu}{}_{\nu} = g^{\mu\nu}\omega_{\mu\nu} = 0$ fällt der $g^{\mu\nu}$-Term weg).

Für infinitesimale Transformation des Bezugssystems ist

$$\omega^{\mu}{}_{\nu} = \begin{pmatrix} 0 & -\delta\beta_1 & -\delta\beta_2 & -\delta\beta_3\\ -\delta\beta_1 & 0 & \delta\theta_{12} & \delta\theta_{31}\\ -\delta\beta_2 & -\delta\theta_{12} & 0 & \delta\theta_{23}\\ -\delta\beta_3 & -\delta\theta_{31} & -\delta\theta_{23} & 0 \end{pmatrix}$$

$$\omega_{\mu\nu} = \begin{pmatrix} 0 & -\delta\beta_1 & -\delta\beta_2 & -\delta\beta_3\\ \delta\beta_1 & 0 & -\delta\theta_{12} & -\delta\theta_{31}\\ \delta\beta_2 & \delta\theta_{12} & 0 & -\delta\theta_{23}\\ \delta\beta_3 & \delta\theta_{31} & \delta\theta_{23} & 0 \end{pmatrix} = \begin{pmatrix} 0 & -\delta y_1 & -\delta y_2 & -\delta y_3\\ \delta y_1 & 0 & -\delta\theta_{12} & -\delta\theta_{31}\\ \delta y_2 & \delta\theta_{12} & 0 & -\delta\theta_{23}\\ \delta y_3 & \delta\theta_{31} & \delta\theta_{23} & 0 \end{pmatrix}$$

(infinitesimale Transformation des Teilchens/Feldes bedeutet $\omega^{\mu\nu} \to -\omega^{\mu\nu}$)

Auch die integrierte allgemeine Form hat in der Taylorreihe nur gerade Anzahlen von Gamma-Matrizen. Für die Rotationen sind $\mu, \nu \neq 0$, daher ist

$$S^{-1} = \gamma^0 S^{+}\gamma^0 = S^{+}$$

d. h. die Darstellungen von Rotationen sind unitär.

Eine beliebige einfache Transformation $\omega_{\mu\nu} = -\omega_{\nu\mu} = \omega$ für ein Paar μ, ν kann in N kleine infinitesimale Transformationen um ω/N zerlegt werden, daher ist

$$S(\omega) = [S(\omega/N)]^N = \left(1 + \frac{1}{4}(\gamma^\mu\gamma^\nu - \gamma^\nu\gamma^\mu)\frac{\omega}{N}\right)^N = \left(1 + \frac{1}{2}\gamma^\mu\gamma^\nu\frac{\omega}{N}\right)^N \to e^{\gamma^\mu\gamma^\nu\frac{\omega}{2}} \tag{4.46}$$

im Grenzfall $N \to \infty$ eine e-Funktion. Wegen (4.5) ist hier $\gamma^\mu\gamma^\nu = -\gamma^\nu\gamma^\mu\gamma$.

4.2.3 Lorentztransformation in z-Richtung

Für $\Lambda(\beta)$ ist

$$\begin{aligned} S(\beta) &= e^{-\gamma^0\gamma^3\frac{y}{2}} \\ &= \cosh\frac{y}{2} - \gamma^0\gamma^3\sinh\frac{y}{2} \\ &= \begin{pmatrix} \cosh\frac{y}{2} & 0 & -\sinh\frac{y}{2} & 0 \\ 0 & \cosh\frac{y}{2} & 0 & \sinh\frac{y}{2} \\ -\sinh\frac{y}{2} & 0 & \cosh\frac{y}{2} & 0 \\ 0 & \sinh\frac{y}{2} & 0 & \cosh\frac{y}{2} \end{pmatrix} \end{aligned} \tag{4.47}$$

mit der Rapidität $y = \operatorname{Artanh}\beta$ (infinitesimal $\delta y \approx \delta\beta$)

$$S^{-1}(\beta) = S(-\beta) = \cosh\frac{y}{2} - \gamma^0\gamma^3\sinh\frac{y}{2} = \gamma^0 S\gamma^0$$

$S = S^+$ ist hermitesch.

Das ist die Transformation des Bezugssystems um β oder die Transformation des Teilchens um $-\beta$.

4.2.4 Rotation um die z-Achse

Für

$$R_z(\theta) = \begin{pmatrix} 1 & 0 & 0 & 0 \\ 0 & \cos\theta & \sin\theta & 0 \\ 0 & -\sin\theta & \cos\theta & 0 \\ 0 & 0 & 0 & 1 \end{pmatrix}$$

ist

$$\begin{aligned} S_z(\theta) &= e^{-\gamma^1\gamma^2\frac{\theta}{2}} \\ &= \cos\frac{\theta}{2} - \gamma^1\gamma^2\sin\frac{\theta}{2} \\ &= \begin{pmatrix} \cos\frac{\theta}{2} + i\sin\frac{\theta}{2} & 0 & 0 & 0 \\ 0 & \cos\frac{\theta}{2} - i\sin\frac{\theta}{2} & 0 & \\ 0 & 0 & \cos\frac{\theta}{2} + i\sin\frac{\theta}{2} & 0 \\ 0 & 0 & 0 & \cos\frac{\theta}{2} - i\sin\frac{\theta}{2} \end{pmatrix} \end{aligned} \tag{4.48}$$

$$S_z^{-1}(\theta) = S_z(-\theta) = \cos\frac{\theta}{2} + \gamma^1\gamma^2\sin\frac{\theta}{2}$$

S_z ist unitär: $S_z^+ = S_z^{-1}$

infinitesimal ist

$$S(\delta\theta) = 1 - \gamma^1\gamma^2\frac{\delta\theta}{2} = 1 + i\sigma^{12}\frac{\delta\theta}{2}$$

4.2.5 Rotation um die y-Achse

Für

$$R_y(\theta) = \begin{pmatrix} 1 & 0 & 0 & 0 \\ 0 & \cos\theta & 0 & \sin\theta \\ 0 & 0 & 1 & 0 \\ 0 & -\sin\theta & 0 & \cos\theta \end{pmatrix}$$

ist

$$\begin{aligned} S_y(\theta) &= e^{-\gamma^3\gamma^1\frac{\theta}{2}} \\ &= \cos\frac{\theta}{2} - \gamma^3\gamma^1 \sin\frac{\theta}{2} \\ &= \begin{pmatrix} \cos\frac{\theta}{2} & \sin\frac{\theta}{2} & 0 & 0 \\ -\sin\frac{\theta}{2} & \cos\frac{\theta}{2} & 0 & 0 \\ 0 & 0 & \cos\frac{\theta}{2} & \sin\frac{\theta}{2} \\ 0 & 0 & -\sin\frac{\theta}{2} & \cos\frac{\theta}{2} \end{pmatrix} \end{aligned} \tag{4.49}$$

4.2.6 Infinitesimale Rotation um eine beliebige Achse

Für eine infinitesimale Rotation

$$\begin{aligned} \boldsymbol{x}' &= \boldsymbol{x} + \boldsymbol{x} \times \delta\boldsymbol{\theta} \\ x'_j &= x_j + \varepsilon_{jkl} x_k \delta\theta_l \\ \delta x_j &= \varepsilon_{jkl} x_k \delta\theta_l \end{aligned}$$

ist

$$\begin{aligned} S(\delta\boldsymbol{\theta}) &= 1 - \frac{1}{4}\varepsilon_{jkl}\gamma^j\gamma^k\delta\theta_l = 1 - \frac{1}{4}(\boldsymbol{\gamma}\times\boldsymbol{\gamma})\,\delta\boldsymbol{\theta} \\ \delta\psi &= -\frac{1}{4}(\boldsymbol{\gamma}\times\boldsymbol{\gamma})\,\delta\boldsymbol{\theta}\,\psi \end{aligned}$$

Rotationsinvarianz der Diracgleichung und das Noether-Theorem (2.13) führen auf eine erhaltene Dichte

$$\boldsymbol{J}^0 = \psi^* i \left[\frac{1}{4}(\boldsymbol{\gamma}\times\boldsymbol{\gamma}) + (\boldsymbol{x}\times\nabla)\right]\psi$$

deren Integral dem Drehimpulsvektor-Erwartungswert entspricht. Daraus ergibt sich der Spinoperator (4.43).

4.3 Chiralität und Helizität

Projektionsoperator auf Eigenzustände der „Chiralität“ (kovariantes Analogon zur Helizität)

$$\begin{aligned} O_L &= \tfrac{1}{2}(1-\gamma_5) \\ O_R &= \tfrac{1}{2}(1+\gamma_5) \end{aligned}$$

In der Pauli-Dirac Darstellung:

$$O_L = \tfrac{1}{2}\begin{pmatrix} 1 & 0 & -1 & 0 \\ 0 & 1 & 0 & -1 \\ -1 & 0 & 1 & 0 \\ 0 & -1 & 0 & 1 \end{pmatrix} \qquad O_R = \tfrac{1}{2}\begin{pmatrix} 1 & 0 & 1 & 0 \\ 0 & 1 & 0 & 1 \\ 1 & 0 & 1 & 0 \\ 0 & 1 & 0 & 1 \end{pmatrix}$$

$$
\begin{aligned}
O_L^2 = O_L, \qquad & O_R^2 = O_R \\
O_L + O_R = 1, \qquad & O_L^2 + O_R^2 = 1 \\
O_L^+ = O_L, \qquad & O_R^+ = O_R \\
\tfrac{1}{2}(1-\gamma_5)\gamma^\mu = \tfrac{1}{2}\gamma^\mu(1+\gamma_5) & \\
\gamma_5 O_L = O_L\gamma_5 = -O_L, \qquad & \gamma_5 O_R = O_R\gamma_5 = O_R \\
\gamma^\mu O_L = O_R\gamma^\mu, \qquad & \gamma^\mu O_R = O_L\gamma^\mu
\end{aligned}
\tag{4.50}
$$

$$
\begin{aligned}
\psi &= \left\{ \begin{matrix} u_A \\ u_B \end{matrix} \right\} \cdot e^{-ip^\mu x_\mu} \\
\psi_L := O_L\psi &= \left\{ \begin{matrix} \frac{1}{2}(u_A - u_B) \\ \frac{1}{2}(u_B - u_A) \end{matrix} \right\} \cdot e^{-ip^\mu x_\mu} \\
\psi_R := O_R\psi &= \left\{ \begin{matrix} \frac{1}{2}(u_A + u_B) \\ \frac{1}{2}(u_A + u_B) \end{matrix} \right\} \cdot e^{-ip^\mu x_\mu} \\
\bar\psi_L = \overline{(O_L\psi)} &= (O_L\psi)^+\gamma^0 = \psi^* O_L\gamma^0 = \psi^*\gamma^0 O_R \\
&= \bar\psi O_R \\
\bar\psi_R &= \bar\psi O_L
\end{aligned}
$$

$$
\psi_{(1)L} = \tfrac{1}{2}\mathcal{N} \begin{pmatrix} \frac{E-p_z+m}{E+m} \\ \frac{p_x+ip_y}{E+m} \\ -\frac{E-p_z+m}{E+m} \\ -\frac{p_x+ip_y}{E+m} \end{pmatrix} e^{-ip^\mu x_\mu}
$$

$$
\psi_{(2)L} = \tfrac{1}{2}\mathcal{N} \begin{pmatrix} \frac{p_x-ip_y}{E+m} \\ \frac{E+p_z+m}{E+m} \\ -\frac{p_x-ip_y}{E+m} \\ -\frac{E+p_z+m}{E+m} \end{pmatrix} e^{-ip^\mu x_\mu}
$$

Bilineare Kovarianten:

$$
\begin{aligned}
\psi &= \psi_R + \psi_L \\
\bar\psi\psi &= \bar\psi_L\psi_R + \bar\psi_R\psi_L \\
&= \bar\psi O_R O_R\psi + \bar\psi O_L O_L\psi \\
&= \bar\psi(O_R + O_L)\psi \\
\bar\psi\gamma_5\psi &= \bar\psi_L\psi_R - \bar\psi_R\psi_L \\
\bar\psi\gamma^\mu\psi &= \bar\psi_R\gamma^\mu\psi_R + \bar\psi_L\gamma^\mu\psi_L \\
\bar\psi\gamma^\mu\gamma_5\psi &= \bar\psi_R\gamma^\mu\psi_R - \bar\psi_L\gamma^\mu\psi_L \\
\bar\psi\sigma^{\mu\nu}\psi &= \bar\psi_R\sigma^{\mu\nu}\psi_L + \bar\psi_L\sigma^{\mu\nu}\psi_R
\end{aligned}
$$

Chiralitätsoperator (kovariant, Gl. 4.50)

$$
O_\chi = \gamma_5 \tag{4.51}
$$

$$
\begin{aligned}
\gamma_5\, O_L\psi = -O_L\psi, \quad & \gamma_5\, O_R\psi = +O_R\psi \\
\gamma_5\bar\psi_R = \gamma_5\,\bar\psi O_L = -\bar\psi O_L, \quad & \gamma_5\bar\psi_L = \gamma_5\,\bar\psi O_R = +\bar\psi O_R \\
\bar\psi_L\psi_R = (\bar\psi_L\gamma_5)(\gamma_5\psi_R) = \bar\psi_L\psi_R, \quad & \bar\psi_R\psi_L = (\bar\psi_R\gamma_5)(\gamma_5\psi_L) = (-\bar\psi_R)(-\psi_L) \\
\bar\psi_L\psi_L = (\bar\psi_L\gamma_5)(\gamma_5\psi_L) = \bar\psi_L(-\psi_L) = 0, \quad & \bar\psi_R\psi_R = (\bar\psi_R\gamma_5)(\gamma_5\psi_R) = -\bar\psi_R\psi_R = 0
\end{aligned}
\tag{4.52}
$$

Die Chiralität adjungierter Spinoren ist der Eigenwert zu $-\gamma_5$.

Helizitätsoperator (nicht kovariant!)

$$\lambda = \boldsymbol{\Sigma}\hat{\boldsymbol{p}} = \frac{\boldsymbol{\sigma p}}{p} = \frac{1}{p}\begin{pmatrix} p_z & p_- & 0 & 0 \\ p_+ & -p_z & 0 & 0 \\ 0 & 0 & p_z & p_- \\ 0 & 0 & p_+ & -p_z \end{pmatrix} \tag{4.53}$$

Nach (4.31) ist

$$\lambda\psi_L = \left\{ \begin{array}{l} -\frac{E}{p}\frac{1}{2}(u_A - u_B) + \frac{m}{p}\frac{1}{2}(u_A + u_B) \\ -\frac{E}{p}\frac{1}{2}(u_B - u_A) - \frac{m}{p}\frac{1}{2}(u_A + u_B) \end{array} \right\} \cdot e^{-ip^\mu x_\mu} \tag{4.54}$$

$$\lambda\psi_R = \left\{ \begin{array}{l} \frac{E}{p}\frac{1}{2}(u_A + u_B) + \frac{m}{p}\frac{1}{2}(u_A - u_B) \\ \frac{E}{p}\frac{1}{2}(u_A + u_B) + \frac{m}{p}\frac{1}{2}(u_A - u_B) \end{array} \right\} \cdot e^{-ip^\mu x_\mu} \tag{4.55}$$

Für **masselose** Fermionen ist $\frac{E\pm m}{p} = 1$ mit den Spinoren (4.40); damit sind ψ_L und ψ_R Eigenzustände zu λ mit Helizität $+1$ und -1 und $p_z = +E$:

$$u_R = u_{(1)} = \mathcal{N}\begin{pmatrix} 1 \\ 0 \\ 1 \\ 0 \end{pmatrix}, \quad u_L = u_{(2)} = \mathcal{N}\begin{pmatrix} 0 \\ 1 \\ 0 \\ -1 \end{pmatrix}, \quad u_{(3)} = \mathcal{N}\begin{pmatrix} -1 \\ 0 \\ 1 \\ 0 \end{pmatrix}, \quad u_{(4)} = \mathcal{N}\begin{pmatrix} 0 \\ 1 \\ 0 \\ 1 \end{pmatrix} \tag{4.56}$$

und

$$\begin{aligned} \bar{u}_R &= \mathcal{N}\,(1 \quad 0 \quad -1 \quad 0\,) \\ \bar{u}_L &= \mathcal{N}\,(0 \quad 1 \quad 0 \quad 1\,) \end{aligned}$$

Für Teilchenspinoren ist die z-Komponente des Spins $u_R : +\frac{1}{2}$, $u_L : -\frac{1}{2}$, $\bar{u}_R : +\frac{1}{2}$, $\bar{u}_L : -\frac{1}{2}$, daher beschreibt R Helizität $+1$ und L Helizität -1.

Eigenzustände für massive Teilchen sind[17]

$$\psi_\pm = \left\{ \begin{array}{c} \chi \\ \frac{\pm p}{E+m}\chi \end{array} \right\} \cdot e^{-ip^\mu x_\mu} \tag{4.57}$$

Mittlere Helizität eines Chiralitätseigenzustands:

$$\langle\lambda\psi_R\rangle = \beta, \qquad \langle\lambda\psi_L\rangle = -\beta \tag{4.58}$$

entspricht den Anteilen

$$\begin{aligned} &\langle\lambda\rangle = A\cdot(+1) + B\cdot(-1) \\ &\quad 1 = A + B \\ \Longrightarrow \qquad &\langle\lambda\rangle = \frac{1+\beta}{2}(+1) + \frac{1-\beta}{2}(-1) = \beta \qquad \text{mit} \qquad A = \frac{1+\beta}{2}, \qquad B = \frac{1-\beta}{2} \end{aligned}$$

Für freie Fermionen ist die Helizität in einem festen Inertialsystem erhalten, da Impuls und Spin erhalten sind. Chiralität ist dagegen keine Erhaltungsgröße für massive Teilchen. Nur für masselose Fermionen ist Chiralität = Helizität eine Erhaltungsgröße.

[17] $\frac{p}{E+m} = \frac{E-m}{p}$ wegen $E^2 - m^2 = p^2$

Während der Vektorstrom (4.24) erhalten ist, ist der Axialvektorstrom

$$a^\mu = \bar{\psi}\gamma^\mu\gamma_5\psi \tag{4.59}$$

mit

$$\partial_\mu a^\mu = 2im\bar{\psi}\gamma_5\psi$$

nur für masselose Fermionen ein erhaltener Strom, die Eigenzustände zu γ_5 sind (PCAC = partially conserved axial vector current). Er gehört nach dem Noethertheorem zur chiralen Symmetrie

$$\psi \to e^{i\theta\gamma_5}\psi$$

Der kinetische Term des Dirac-Lagrangian (4.4) ist symmetrisch unter chiralen Transformationen, der Masseterm dagegen nicht.

4.3.1 Weyl-Spinoren

In der Weyl-Darstellung ist

$$O_L = \tfrac{1}{2}\begin{pmatrix} 0 & 0 & 0 & 0 \\ 0 & 0 & 0 & 0 \\ 0 & 0 & 1 & 0 \\ 0 & 0 & 0 & 1 \end{pmatrix} \qquad O_R = \tfrac{1}{2}\begin{pmatrix} 1 & 0 & 0 & 0 \\ 0 & 1 & 0 & 0 \\ 0 & 0 & 0 & 0 \\ 0 & 0 & 0 & 0 \end{pmatrix} \qquad \gamma_5 = \begin{pmatrix} 1 & 0 & 0 & 0 \\ 0 & 1 & 0 & 0 \\ 0 & 0 & -1 & 0 \\ 0 & 0 & 0 & -1 \end{pmatrix}$$

und die Basis-Spinoren sind Eigenzustände zur Chiralität.

4.3.2 Invarianz der Chiralität

Wegen (4.13) und (4.45) kommutiert γ_5 mit allen Transformationen S:

$$[S(\omega), \gamma_5] = [1, \gamma_5] + \tfrac{1}{2}\omega[\gamma^\mu\gamma^\nu, \gamma_5] = 0$$

d. h. Chiralität ist eine Invariante, die sich unter Rotationen und Lorentztransformationen nicht ändert.

4.3.3 Fermion in z-Richtung

Mit $\boldsymbol{p} = (0, 0, p)$ wird

$$\psi_{(1)} = \mathcal{N}\begin{pmatrix} 1 \\ 0 \\ \frac{p}{E+m} \\ 0 \end{pmatrix} e^{-ip^\mu x_\mu} \tag{4.60}$$

$$\psi_{(2)} = \mathcal{N}\begin{pmatrix} 0 \\ 1 \\ 0 \\ -\frac{p}{E+m} \end{pmatrix} e^{-ip^\mu x_\mu}$$

$$\lambda = \begin{pmatrix} 1 & 0 & 0 & 0 \\ 0 & -1 & 0 & 0 \\ 0 & 0 & 1 & 0 \\ 0 & 0 & 0 & -1 \end{pmatrix}$$

$$\lambda\psi_{(1)} = \psi_{(1)}$$

$$\lambda\psi_{(2)} = -\psi_{(2)}$$
$$\psi_{(1)L} = \frac{\mathcal{N}}{2}\begin{pmatrix} 1-\frac{p}{E+m} \\ 0 \\ -1+\frac{p}{E+m} \\ 0 \end{pmatrix} e^{-ip^\mu x_\mu}$$
$$\psi_{(2)L} = \frac{\mathcal{N}}{2}\begin{pmatrix} 0 \\ 1+\frac{p}{E+m} \\ 0 \\ -1-\frac{p}{E+m} \end{pmatrix} e^{-ip^\mu x_\mu}$$
$$\lambda\psi_{(1)L} = \psi_{(1)L}$$
$$\lambda\psi_{(2)L} = -\psi_{(2)L}$$

4.3.4 Vollständigkeitsrelationen (Spinsummen)

in der $2E$-Normierung[18]:

$$\sum_{s=-\frac{1}{2},+\frac{1}{2}} u(\boldsymbol{p},s)\,\bar{u}(\boldsymbol{p},s) = \not{p} + m$$
$$\sum_{s=-\frac{1}{2},+\frac{1}{2}} v(\boldsymbol{p},s)\,\bar{v}(\boldsymbol{p},s) = \not{p} - m \tag{4.61}$$

4.4 Elektromagnetische Wechselwirkung

Die elektromagnetische Wechselwirkung kann durch einen Zusatzterm in der Diracgleichung berücksichtigt werden:

$$[\gamma^\mu(i\partial_\mu + eA_\mu) - m]\,\psi = 0 \tag{4.62}$$

Wenn man die Diracgleichung als Bewegungsgleichung (Euler-Lagrange-Gleichung) einer Lagrangedichte auffasst, erhält man als Wechselwirkungskomponente

$$eA_\mu\bar{\psi}\gamma^\mu\psi \tag{4.63}$$

Dabei ist A^μ das elektromagnetische Viererpotenzial

$$A^\mu = (\Phi, \vec{A})$$

aus dem man den Feldstärketensor berechnen kann:

$$F^{\mu\nu} = \partial^\mu A^\nu - \partial^\nu A^\mu = \begin{pmatrix} 0 & -E_x & -E_y & -E_z \\ E_x & 0 & -B_z & B_y \\ E_y & B_z & 0 & -B_x \\ E_z & -B_y & B_x & 0 \end{pmatrix}$$

Mit

$$F_{\mu\nu} = \begin{pmatrix} 0 & E_x & E_y & E_z \\ -E_x & 0 & -B_z & B_y \\ -E_y & B_z & 0 & -B_x \\ -E_z & -B_y & B_x & 0 \end{pmatrix}$$

[18] Indices ausgeschrieben: $\sum_{s=-\frac{1}{2},+\frac{1}{2}} u_\alpha(\boldsymbol{p},s)\,\bar{u}_\beta(\boldsymbol{p},s) = \not{p}_{\alpha\beta} + m\delta_{\alpha\beta}$

wird die Energiedichte des elektromagnetischen Feldes

$$\tfrac{1}{2}\vec{E}\vec{B}^2 - \tfrac{1}{2}\vec{B}^2 = -\tfrac{1}{4}F^{\mu\nu}F_{\mu\nu}$$

Aus dem Noether-Theorem erhält man damit die Energiedichte als Komponente des Energie-Impuls-Tensors mit der Energiedichte $T^{00} = \frac{1}{2}\vec{E}^2 + \frac{1}{2}\vec{B}^2$ und der Impulsdichte $\vec{E} \times \vec{B}$ (Poynting-Vektor).

Die ersten beiden Maxwellgleichungen

$$\nabla\vec{E} = \rho, \qquad \nabla \times \vec{B} - \frac{\partial\vec{E}}{\partial t} = \vec{j}$$

sind

$$\partial^\mu F_{\mu\nu} = j_\nu \tag{4.64}$$

Die beiden übrigen Gleichungen

$$\nabla\vec{B} = 0, \qquad \nabla \times \vec{E} + \frac{\partial\vec{B}}{\partial t} = \vec{0}$$

nehmen die folgende Form an:

$$\partial_\lambda F_{\mu\nu} + \partial_\nu F_{\lambda\mu} + \partial_\mu F_{\nu\lambda} = 0 \tag{4.65}$$

Die 3 Indices können je 4 Werte annehmen, d. h. (4.65) entspricht $4^3 = 64$ skalaren Gleichungen. Wegen der Antisymmetrie von $F_{\mu\nu}$ sind aber die mit $\lambda = \mu$ oder $\lambda = \nu$ oder $\mu = \nu$ trivial, die Indizes müssen also alle drei verschieden sein, sodass tatsächlich nur 4 unabhängige Gleichungen mit $\lambda\mu\nu = 012, 123, 230, 301$ übrigbleiben. Diese kann man mit dem total antisymmetrischen Tensor als

$$\varepsilon^{\rho\lambda\mu\nu}\partial_\lambda F_{\mu\nu} = 0 \tag{4.66}$$

schreiben ($\rho = 0, 1, 2, 3$). Sie unterscheidet sich von (4.65) um einen Faktor 2.

4.5 Die Proca-Gleichung

Für Vektorbosonen gilt analog zur Klein-Gordon-Gleichung die Proca-Gleichung[19]

$$\partial_\mu F^{\mu\nu} + m^2 A^\nu = 0 \tag{4.67}$$

mit $F_{\mu\nu} = \partial_\mu A_\nu - \partial_\nu A_\mu$, die als Bewegungsgleichung aus der Lagrangedichte

$$\mathcal{L} = -\frac{1}{4}F_{\mu\nu}F^{\mu\nu} + \frac{1}{2}m^2 A_\mu A^\mu \tag{4.68}$$

abgeleitet werden kann.

Für das masselose Photon entfällt jeweils der zweite Term, und die Proca-Gleichung

$$\partial_\mu F^{\mu\nu} = 0$$

entspricht den ersten beiden Maxwellgleichungen (4.64) bei Abwesenheit elektrischer Ladungen.

[19] Alexandru Proca, rumänischer Physiker 1897–1955. A. Proca, „Sur la théorie ondulatoire des électrons positifs et négatifs“, J. Phys. Radium 7, 347-353 (1936).

5. Discrete Symmetries

The history of particle physics is a history of discoveries of **symmetries**. It is remarkable, that most of the symmetries discovered have, however, finally turned out to be only "almost-symmetries", i. e. to be more or less broken.

The only unbroken symmetries so far discovered are the U(1) charge-phase symmetry and the SU(3) colour symmetry. One consequence is that the electric and colour charges are exactly conserved in all observed reactions. All quantities which obey a strict symmetry cannot be observed. Hence another consequence is that the position in SU(3)-space cannot be determined, e. g. a "red" and a "blue" quark cannot be distinguished. Likewise, the electromagnetic phase is unobservable.

When we talk about symmetry, we imagine typically a geometric figure, as in figure 5.1a. A definition of symmetry (both geometric and general) is **invariance under a transformation**. If a system S is said to be symmetric with respect to a transformation T, we have

$$\mathrm{T}(S) = S \tag{5.1}$$

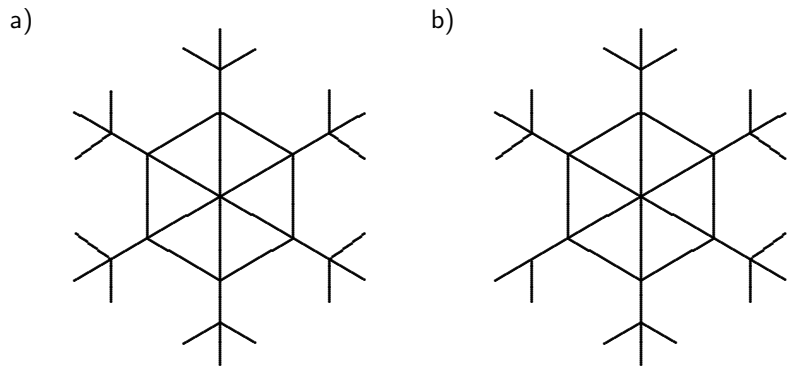

Fig. 5.1 Geometrical discrete symmetry.

The transformation applying to figure 5.1a is a rotation about its centre by any multiple of 60°. The figure does not change under such a rotation. It is a **discrete** symmetry, since only angles of $60°, 120°, 180°, 240°, 300°$, and 360° leave the shape invariant, in contrast to the **continuous** symmetry of a circle that is invariant under a rotation of any angle about its centre. A continuous symmetry, for example, would be rotation about any angle. A circle is an example of a shape with such a symmetry with respect to its centre.

The topic of this chapter is the transformations C, P and T which are even simpler discrete transformation, since they already reproduce any system when applied twice in sequence.

The symmetries we are concerned with are not symmetries of an object as in figure 5.1, but are **symmetries of the laws of physics** which are invariant under physics transformations. For example, rotational symmetry implies that the laws of physics read the same independent of the orientation of the coordinate system. This is true even if our world is usually nowhere (where we make experiments) of a rotaionally symmetric shape.

As for the geometric shape, this invariance implies **indistinguishability**. There is no special direction which is distinguished from all other directions. Perfect colour symmetry in strong interaction makes it impossibly to measure the actual colour of a quark, i. e. to invent a prescription by which the colour "red", for example, can be defined. Such a procedure would inevitably distinguish it from "green" and "blue" and hence would require a breaking of the symmetry.

In figure 5.1b the symmetry is broken since the symmetry transformation does not lead to the same flake due to the lower left arm that is marked by a missing branch, and thus distinguishable from the other branches. The symmetry transformation applied to this flake leads to a similar, but not identical shape, corresponding to a small symmetry breaking.

Just as the shape of the snow flake 5.1b is no longer invariant under a certain symmetry transformation, broken symmetries in particle physics are symmetry transformations that do not leave the laws of physics invariant.

For instance, the symmetries between leptons and quarks of different flavour is broken by the different masses and electro-weak charges of these particles, and is best approximated in strong interactions as isospin symmetry between the u and d quark due to their almost identical constituent mass.

Although physics laws are strictly symmetric under translation or rotation, space-time translational and rotational symmetry is broken through matter: The fact that matter is not distributed homogeneously throughout the universe at small scales introduces a locally asymmetric structure of space-time, or asymmetric boundary conditions to any microscopic system. This makes a prove of symmetry more subtle, since symmetric experimental conditions are only approximated on a macroscopic scale—the whole universe—or for microscopic systems isolated from other matter by large distances. The laws of physics are, however, still perfectly symmetric for these transformations. To observe this symmetry in an asymmetric environment, even as a symmetry in shape, we have to introduce the idea of a **statistical symmetry**: translation and rotation of a certain volume makes it the same "on average". This means, for instance, that the orientation of the axes of spiral galaxies is uniformly distributed over the whole solid angle.

Statistical observation of the symmetry of processes is not restricted to physics. The growth of a tree, for instance, is governed by the laws of biology and the external conditions. External conditions are gravity and light, which break the vertical symmetry and hence determine the upward growing of the stem and the downward growing of the roots. There is, however, an azimuthal symmetry about the stem. So, when a tree grows a new branch, it is **spontaneously breaking** this symmetry. That the symmetry still exists in the biological laws that govern this growth is seen only statistically: The orientation of all branches of many trees is **uniformly distributed** in azimuth.

These laws are, however, not mirror symmetric. This can be observed in organisms as ourselves. Human beings have (except for a very rare anomaly) their hearts all at the left side! If growth were symmetric and symmetry broken only spontaneously for each individual, we should observe about as many people with their heart at the right side than those with their heart on the left.

This **parity violation** in biology is observed already on the level of molecules. Amino acids, sugars and many other organic substances occur in two stereo-isomers. When we synthesize these substances in the laboratory, these isomers are produced in equal proportion. This proves that the laws of chemistry are symmetric about the operation of mirror imaging (parity). If they are produced by enzymes in living organisms, however, only one form is produced. This asymmetry is already present in the substance that contains the genetic information of an organism: The DNA is realized in living organisms as an α-helix, which is a right-turning helix. Its mirror image, a left-turning helix, does not occur in living organisms.

This chapter describes the fundamental discrete symmetries parity (P), charge conjugation (C) and time reversal (T). These symmetries are intact for the strong and electromagnetic interactions, but are all broken in weak interaction. Indeed, the breaking of mirror symmetry is indispensible for the unique definition of left and right.

For instance, left with respect to the facing direction of a human being is the position of his heart. Left or right can only be defined on a three-dimensional object that is not point-symmetric. Communicating this term to aliens at a very distant galaxy would require the same asymmetric object at their place. This will, therefore, only be possible if an asymmetry exists in a fundamental object in nature—biology is not fundamental enough to rely on its asymmetry to hold at the alien's place in the same way as in our place. But (if the laws of physics are universal as we assume) we can use the orientation of weak interaction decay processes to communicate the meaning of left and right to them unambiguously.

We will show in the further course of this script, that not only symmetries, but even more symmetry violations are essential ingredients for a world to be like our universe.

5.1 Antiparticles and Charge Conjugation

5.1.1 The general operator C

In general there is an operator of *charge conjugation*

$$\begin{aligned} \mathrm{C}\,|X\rangle &= e^{i\phi_C(X)}|\overline{X}\rangle \\ \mathrm{C}\,|\overline{X}\rangle &= e^{-i\phi_C(X)}|X\rangle \end{aligned} \tag{5.2}$$

with

$$\mathrm{C}^2 = \mathrm{C}\circ\mathrm{C} = 1$$

and a convention dependent phase $\phi_C(\overline{X}) = -\phi_C(X)$. This operator inverts all charge quantum numbers.

There exist particles with all charge quantum numbers 0. These **eigenstates** X^0 of C have an eigenvalue (called *C-parity*) which is $\zeta_C(X_0) = e^{i\phi_C(X_0)} = e^{-i\phi_C(X_0)} = \pm 1$, i. e. $\phi_C = 0$ or π.

5.1.2 Antifermions

To account for the antiparticle interpretation of the negative energy solutions, we have to introduce positive energy solutions. To this end we define a **antifermion spinor** $v(\vec{p})$ as:

$$v^{(2,1)}(\vec{p}) \equiv u^{(3,4)}(-\vec{p}) \tag{5.3}$$

positron-spinor for $E > 0$:

$$v^{(2,1)} = \mathcal{N}\cdot\left\{\begin{array}{c} \frac{\vec{\sigma}\vec{p}}{(E+m)}\cdot\chi^{(1,2)} \\ \chi^{(1,2)} \end{array}\right\} \tag{5.4}$$

This yields the wave function of a free positron:

$$\psi_{(3)}(-E,-\vec{p}) = \mathcal{N}\begin{pmatrix} \frac{p_z}{E+m} \\ \frac{p_x+ip_y}{E+m} \\ 1 \\ 0 \end{pmatrix} e^{ip^\mu x_\mu} = v^{(2)}e^{ip^\mu x_\mu} \tag{5.5}$$

$$\psi_{(4)}(-E,-\vec{p}) = \mathcal{N}\begin{pmatrix} \frac{p_x-ip_y}{E+m} \\ -\frac{p_z}{E+m} \\ 0 \\ 1 \end{pmatrix} e^{ip^\mu x_\mu} = v^{(1)}e^{ip^\mu x_\mu}$$

The Dirac equation for the spinors u (4.29) and v has the form

$$(\not{p} - m)\,u(\vec{p}) = 0 \qquad \text{bzw.} \qquad (\not{p} + m)\,v(\vec{p}) = 0 \tag{5.6}$$

mit $\not{p} \equiv \gamma^\mu p_\mu$ und $p^0 = E > 0$.

The wavefunctions for electron (ψ) and positron ($\psi_C = \mathrm{C}\,\psi$) are related as

$$\psi_C = C\bar{\psi} = C\gamma^0\psi^* \tag{5.7}$$

where C is[20] in the chosen spinor representation the following (4×4) matrix including an arbitrary phase $e^{i\phi_C}$:

$$C = e^{i\phi_C} \begin{pmatrix} 0 & 0 & 0 & -1 \\ 0 & 0 & 1 & 0 \\ 0 & -1 & 0 & 0 \\ 1 & 0 & 0 & 0 \end{pmatrix} \qquad \text{(in spinor space)} \tag{5.8}$$

We choose $\phi_C = 0$ and obtain

$$C = -i\gamma^0\gamma^2 = i\gamma_0\gamma_2 \tag{5.9}$$

and $\psi_C = i\gamma^2\psi^*$.

This yields e. g.

$$\psi_{C(1)} = \begin{pmatrix} 0 & 0 & 0 & 1 \\ 0 & 0 & -1 & 0 \\ 0 & -1 & 0 & 0 \\ 1 & 0 & 0 & 0 \end{pmatrix} \psi^*_{(1)} = \mathcal{N} \begin{pmatrix} \frac{p_x - ip_y}{E+m} \\ -\frac{p_z}{E+m} \\ 0 \\ 1 \end{pmatrix} e^{ip^\mu x_\mu} = \psi_{(4)}(-p^\mu)$$

$$\psi_{C(2)} = \begin{pmatrix} 0 & 0 & 0 & 1 \\ 0 & 0 & -1 & 0 \\ 0 & -1 & 0 & 0 \\ 1 & 0 & 0 & 0 \end{pmatrix} \psi^*_{(2)} = \mathcal{N} \begin{pmatrix} -\frac{p_z}{E+m} \\ -\frac{p_x + ip_y}{E+m} \\ -1 \\ 0 \end{pmatrix} e^{ip^\mu x_\mu} = -\psi_{(3)}(-p^\mu)$$

i. e. an e^- with momentum $\vec{p}$ and spin $+\frac{1}{2}$ is transformed into an e^- with negative energy, momentum $-\vec{p}$ und spin $-\frac{1}{2}$. This "hole" in the Dirac sea corresponds to an e^+ with positive energy, momentum $\vec{p}$ and spin $+\frac{1}{2}$.

The latter implies that the v spinors are defined with exchanged $\chi^{(1,2)}$, or explicitely

positron-spinor for $E > 0$:

$$v^{(1,2)} = \mathcal{N} \cdot \begin{Bmatrix} \frac{\vec{\sigma}\vec{p}}{(E+m)} \cdot \tilde{\chi}^{(1,2)} \\ \tilde{\chi}^{(1,2)} \end{Bmatrix} \quad \text{with} \quad \tilde{\chi}^k = \begin{pmatrix} 0 & 1 \\ 1 & 0 \end{pmatrix} \chi^k \tag{5.10}$$

and that the Spin operator $\Sigma_3 \to \bar{\Sigma}_3 = -\Sigma_3$ for antifermions, i. e.

$$\bar{\Sigma}_3 = \begin{pmatrix} -1 & 0 & 0 & 0 \\ 0 & 1 & 0 & 0 \\ 0 & 0 & -1 & 0 \\ 0 & 0 & 0 & 1 \end{pmatrix} \tag{5.11}$$

The ultrarelativistic spinors for antiparticles are derived from $-u_{(3)} \to v_{(2)}$ and $u_{(4)} \to v_{(1)}$ in (4.56):

$$v_L = v_{(1)} = \mathcal{N} \begin{pmatrix} 0 \\ -1 \\ 0 \\ 1 \end{pmatrix}, \; v_R = v_{(2)} = \mathcal{N} \begin{pmatrix} -1 \\ 0 \\ -1 \\ 0 \end{pmatrix}, \quad \bar{v}_L = \mathcal{N}\,(0 \quad -1 \quad 0 \quad -1), \; \bar{v}_R = \mathcal{N}\,(-1 \quad 0 \quad 1 \quad 0)$$

and have, consequently, momentum $p_z = +E$ and spins $v_L : +\frac{1}{2}$, $v_R : -\frac{1}{2}$, $\bar{v}_L : +\frac{1}{2}$, $\bar{v}_R : -\frac{1}{2}$, therefore R is helicity -1 und L helicity $+1$.

Note that $\gamma_5 v_L = -v_L$, $\gamma_5 v_R = v_R$, $\bar{v}_L\gamma_5 = \bar{v}_L$, and $\bar{v}_R\gamma_5 = -\bar{v}_R$. Helicity and chirality are opposite.

[20] we distinguish the abstract operator C and the spinor representation C by their font style, the latter being a slanted character.

5.1.3 Properties of C

The spinor operator C has the following properties:

$$C^\dagger = C^+ = C^{-1} \tag{5.12}$$

i. e. C is a **unitary** matrix with

$$C^+ = -C \tag{5.13}$$

Including the arbitrary phase, we have

$$C^+ = C^{-1} = -C^* \tag{5.14}$$

Apparently this leads to

$$C^2 = -1 \tag{5.15}$$

which is another pecularity of fermions, like the factor (-1) from a rotation by 360°, and does not lead to $CC = 1$ (which would hold for bosons).

Including the distinction between row and column spinors we have

$$\begin{aligned}
\psi_C &= C\bar{\psi}^\dagger = C\gamma^0\psi^* \\
\psi_C^\dagger &= (C\bar{\psi}^\dagger)^\dagger = \bar{\psi}C^\dagger = -\bar{\psi}C \\
\bar{\psi}_C &= \psi^\dagger C^\dagger = (C\psi)^\dagger \\
\bar{\psi}_C^\dagger &= C\psi
\end{aligned} \tag{5.16}$$

Equation (5.16) implies that $\overline{\psi_C} = -\bar{\psi}_C$ which is another of the pecularities from the application of C to $\bar{\psi}$ related to $CC = -1$.

Using (5.15), we can derive the C-eigenvalue of quarkonia: Using the phase conventions

$$\mathrm{C}\,|q\rangle = |\bar{q}\rangle, \quad \mathrm{C}\,|\bar{q}\rangle = -|q\rangle$$

we obtain for a spin-0 an additional factor (-1) for the exchange of two quarks, in contrast to a symmetric spin-1 state:

$$\begin{aligned}
\text{Triplett } (S=1): \quad & |\uparrow\uparrow\rangle \\
& \frac{1}{\sqrt{2}}(|\uparrow\downarrow\rangle + |\downarrow\uparrow\rangle) \\
& |\downarrow\downarrow\rangle \\
\text{Singulett } (S=0): \quad & \frac{1}{\sqrt{2}}(|\uparrow\downarrow\rangle - |\downarrow\uparrow\rangle)
\end{aligned}$$

i. e., an $S = 0, L = 0$ quarkonium has

$$\mathrm{C}(|q\uparrow\ \bar{q}\downarrow\rangle - |q\downarrow\ \bar{q}\uparrow\rangle) = (-|\bar{q}\uparrow\ q\downarrow\rangle + |\bar{q}\downarrow\ q\uparrow\rangle) = +(|q\uparrow\ \bar{q}\downarrow\rangle - |q\downarrow\ \bar{q}\uparrow\rangle)$$

This corresponds to a pseudoscalar meson, and must therefore resemble the C transformation of $\bar{\psi}\gamma_5\psi \to +\bar{\psi}\gamma_5\psi$.

If the two quarks have an orbital angular momentum L, their exchange involves an additional factor $(-1)^L$, so in general we have

$$\mathrm{C}\,|q\bar{q}, S, L\rangle = (-1)^{S+L}|q\bar{q}, S, L\rangle \tag{5.17}$$

Further properties of C are

$$\begin{aligned} C^{+}\gamma^{\mu}C &= (-\gamma^{\mu})^{\dagger} \\ C^{+}\gamma_5 C &= (\gamma_5)^{\dagger} \end{aligned} \tag{5.18}$$

that can be verified by explicit calculation.

Using (5.18) and keeping in mind that the spinors are here not used as operators (i. e. we need not distinguish ψ and $\psi^{\dagger}$), we can calculate the behaviour of bilinear covariants under the C operation as given in table 5.1. These quantities are important because observables on fermions are always calculated from those bilinear covariants. An example for the transformation of a Lorentz scalar is:

$$\begin{aligned} \mathrm{C}\{\bar{\psi}\phi\} &= \bar{\psi}_C\phi_C = (C\psi)^{\dagger}C\bar{\phi}^{\dagger} \\ &= (\bar{\phi}C^{\dagger})(C\psi) = \bar{\phi}(C^{\dagger}C)\psi \\ &= \bar{\phi}\psi \end{aligned}$$

The same calculation can be shown using indices instead of transposed spinors:

$$\begin{aligned} \mathrm{C}\{\bar{\psi}\phi\} &= (\bar{\psi}_C)_\alpha(\phi_C)_\alpha \\ &= C_{\alpha\beta}\psi_\beta C_{\alpha\kappa}\bar{\phi}_\kappa = \bar{\phi}_\kappa C^{\dagger}_{\beta\alpha}C_{\alpha\kappa}\psi_\beta = \bar{\phi}_\kappa\delta_{\kappa\beta}\psi_\beta \\ &= \bar{\phi}_\kappa\psi_\kappa \end{aligned}$$

Table 5.1 Transformation of bilinear covariants under C (using eqn.s 4.17,5.9)

term	transformed term
$\bar{\psi}\phi$	$\bar{\psi}_C\phi_C = +\bar{\phi}\psi$
$\bar{\psi}\gamma^{\mu}\phi$	$\bar{\psi}_C\gamma^{\mu}\phi_C = -\bar{\phi}\gamma^{\mu}\psi$
$\bar{\psi}\sigma^{\mu\nu}\phi$	$\bar{\psi}_C\sigma^{\mu\nu}\phi_C = -\bar{\phi}\sigma^{\mu\nu}\psi$
$\bar{\psi}\gamma^{\mu}\gamma_5\phi$	$\bar{\psi}_C\gamma^{\mu}\gamma_5\phi_C = +\bar{\phi}\gamma^{\mu}\gamma_5\psi$
$\bar{\psi}\gamma_5\phi$	$\bar{\psi}_C\gamma_5\phi_C = +\bar{\phi}\gamma_5\psi$

5.1.4 Vektorfelder

Das Photon ist sein eigenes Antiteilchen. Den C-Eigenwert können wir aus der klassischen Maxwellgleichung (4.64)

$$\partial^{\mu}F_{\mu\nu} = \partial^{\mu}\partial_{\mu}A_{\nu} - \partial_{\nu}\partial^{\mu}A_{\mu} = j_{\nu} \tag{5.19}$$

Unter C ändern Ladungen und Ströme ihr Vorzeichen, also $\mathrm{C}\, j^{\mu} = -j^{\mu}$, während Raum-Zeit-Koordinaten unverändert bleiben. Das Vorzeichen von $\mathrm{C}\, A^{\mu}$ wird also durch Raum-Zeit-Ableitungen nicht verändert und damit

$$\mathrm{C}\, A^{\mu} = -A^{\mu}$$

bzw. $\mathrm{C}\,|\gamma\rangle = -|\gamma\rangle$.

The electromagnetic interaction is described by a vector current term in the Hamiltonian (or Lagrangian) $eA_{\mu}\bar{\psi}\gamma^{\mu}\psi$ (4.63). If we apply the C operation to this term, we find that it is **invariant**. Therefore, matrix elements derived from this term have equal magnitude if we exchange particles with antiparticles. The interaction is C symmetric.

5.2 Parity

The operator P defines a reflection about a point:

$$\mathrm{P}\,\vec{x} = -\vec{x}$$

This implies $\mathrm{P}^2 = \mathrm{P} \circ \mathrm{P} = 1$, i. e. a twofold application of the transformation reestablishes the original state.

For a Minkowski vector we have

$$\mathrm{P}\,x^\mu = x_\mu \tag{5.20}$$

and correspondingly $\mathrm{P}\,x_\mu = x^m u$, $\mathrm{P}\,p^\mu = p_\mu$, and a scalar is invariant under P: $\mathrm{P}\,p^\mu x_\mu = p_\mu x^\mu = p^\mu x + \mu$.

One can replace it with a product of three planar mirror reflections,

$$\mathrm{P} = S_x \circ S_y \circ S_z$$

where $S_x \psi(x, y, z) = \psi(-x, y, z)$ is a reflection at the yz-plane, and S_y, S_z reflections at the xz-, xy-plane, respectively. To built your own "point-mirror", you can construct a rectangular corner from three planar mirrors. If you look into the direction of this corner, you can see the parity-transformed real world.

Alternatively, a parity transformation can be composed of a plane mirror transformation and a rotation of 180° within the mirror plane.

$$\mathrm{P} = S_x \circ R_x(\pi) = S_y \circ R_y(\pi) = S_z \circ R_z(\pi) \tag{5.21}$$

Many essential properties of parity can therefore be illustrated by one plane mirror transformation that is more easy to imagine.

An important feature of a mirror is the exchange of right $\leftrightarrow$ left: $\mathrm{P}\,|R\rangle = |L\rangle$. This allows the construction of eigenstates:

$$\begin{aligned} |+\rangle &= |R\rangle + |L\rangle \qquad \text{mit} \qquad \mathrm{P}\,|+\rangle = +|+\rangle \\ |-\rangle &= |R\rangle - |L\rangle \qquad \text{mit} \qquad \mathrm{P}\,|-\rangle = -|-\rangle \end{aligned}$$

They are eigenstates with eigenvalues $\zeta_P = +1$ (even parity) and -1 (odd parity).

For a scalar function $\Psi(\vec{x})$, e. g. a classical mass distribution or a quantum mechanical wave function, the operator simply modifies the function argument.

$$\mathrm{P}\,\Psi(\vec{x}) = \Psi(-\vec{x})$$

In classical physics, any three-dimensional vector is associated with three-dimensional space: The velocity is the derivative of a space vector, the momentum is the product of a scalar (mass) with the velocity, the electric field has an orientation in space given by Coulomb's law as $\vec{E} \propto \hat{r}/r^2$ etc. These are all examples of polar vectors. The action of P on any polar vector is

$$\mathrm{P}\,\vec{v} = -\vec{v}$$

i. e. a polar vector has always odd parity. However, an axial vector such as an angular momentum or a vector product behaves differently:

$$\vec{a} = \vec{v}_1 \times \vec{v}_2 \qquad \Longrightarrow \qquad \mathrm{P}\,\vec{a} = -\vec{v}_1 \times (-\vec{v}_2) = \vec{a}$$

i. e. an axial vector has always even parity.

Some examples from classical physics are given in the following list:

$$\begin{aligned}
\mathrm{P}\,\vec{r} &= -\vec{r} \\
\mathrm{P}(r;\theta;\phi) &= (r;\pi-\theta;\pi+\phi) \\
\mathrm{P}\,\vec{p} &= \mathrm{P}(m\dot{\vec{r}}) = -\vec{p} \\
\mathrm{P}\,\vec{F} &= \mathrm{P}(m\ddot{\vec{r}}) = -\vec{F} \\
\mathrm{P}\,\vec{L} &= \mathrm{P}(\vec{r}\times\vec{p}) = \vec{L} \\
\mathrm{P}\,h &= \mathrm{P}(\vec{L}\vec{p}) = -h \\
\mathrm{P}\,\vec{E} &= \mathrm{P}(\frac{q\vec{r}}{r^3}) = -\vec{E} \\
\mathrm{P}\,\vec{B} &= \mathrm{P}(\vec{v}\times\vec{E}) = \vec{B} \\
\mathrm{P}\,\vec{F} &= \mathrm{P}(q\vec{E}+\vec{v}\times\vec{B}) = -\vec{F} \\
\mathrm{P}\,V_S &= \mathrm{P}((\vec{x_1}\times\vec{x_2})\vec{x_3}) = -V_S \\
\mathrm{P}\,V &= \mathrm{P}\,|V_S| = V \\
\mathrm{P}\,\rho(\vec{r}) &= \mathrm{P}(Q/V) = \rho(-\vec{r})
\end{aligned} \tag{5.22}$$

To investigate spatial wave functions of bound states, we consider the spherical harmonics

$$Y_l^m(\theta,\phi) = \sin^m\theta\,\left.\frac{\mathrm{d}^m P_l(\xi)}{\mathrm{d}\xi^m}\right|_{\xi=\cos\theta} e^{im\phi}$$

Parity transforms $\theta\to\pi-\theta$ ($\sin\theta\to\sin\theta$), $\xi=\cos\theta\to-\xi$, $\phi\to\phi+\pi$. So we find

$$\begin{aligned}
\mathrm{P}\,Y_l^m(\theta,\phi) &= \sin^m\theta\,\left.\frac{\mathrm{d}^m P_l(\xi)}{\mathrm{d}\xi^m}\right|_{\xi=-\cos\theta} e^{im\phi}e^{im\pi} \\
&= \sin^m\theta\,\left.\frac{\mathrm{d}^m P_l(-\xi)}{\mathrm{d}(-\xi)^m}\right|_{\xi=\cos\theta} e^{im\phi}(-1)^m \\
&= Y_l^m\cdot\zeta_P(l)
\end{aligned}$$

where $\zeta_P(l)$ is the eigenvalue of

$$\mathrm{P}\,P_l(\xi) = \zeta_P(l)\cdot P_l(\xi)$$

The Legendre polynomials

$$\begin{aligned}
P_0(\xi) &= 1 \\
P_1(\xi) &= \xi \\
P_2(\xi) &= \frac{3\xi^2-1}{2} \\
P_3(\xi) &= \frac{5\xi^3-3\xi}{2} \\
P_4(\xi) &= \frac{35\xi^4-30\xi^2+3}{8} \\
P_5(\xi) &= \frac{63\xi^5-70\xi^3+15\xi}{8} \\
&\vdots \\
P_l(\xi) &= \frac{1}{2^l l!}\,\left.\frac{\mathrm{d}^l(x^2-1)^l}{\mathrm{d}x^l}\right|_{x=\xi}
\end{aligned}$$

are parity eigenfunctions with eigenvalues

$$\zeta_P(l) = (-1)^l \tag{5.23}$$

Therefore also Y_l^m are eigenfunctions with the same eigenvalues $(-1)^l$. The spatial distribution of states with orbital angular momentum L, L_z are described by $Y_L^{L_z}$, hence the parity of these states is given by their intrinsic parity times $(-1)^L$.

5.2.1 Parity of Particle Fields

For all fields one has

$$\mathrm{P}\,\Phi(x) = \Phi'(x')$$

where $x'^\mu = x_\mu = (x^0, -x^1, -x^2, -x^3)$. The parity operator changes the location $x \to x'$ as well as the "spatial orientation" of the field.

A scalar or pseudoscalar field has no spatial orientation. Hence the transformation is simply

$$\mathrm{P}\,\Phi(x) = \pm\Phi(x')$$

with $\Phi' = +\Phi$ for a scalar field and $\Phi' = -\Phi$ for a pseudoscalar field. The distinction between the two is just the behaviour under parity transformation.

For other fields, like spinors, vectors or tensors, the change by the parity transformation is more substantial. Spinor fields have a spin orientation in space (in classical physics this would be an axial vector), vector fields are represented by a spatial four-vector.

5.2.2 Spinor-Representation

To investigate the effect of a parity transformation on a spinor, we need to find a representation P of the parity operator P in the spinor space with

$$\psi'(x') = P\psi(x) \tag{5.24}$$

which acts on the gamma matrices as

$$P^{-1}\gamma^\mu P = \boldsymbol{P}^\mu{}_\nu \gamma^\nu \tag{5.25}$$

where $\boldsymbol{P}$ is the matrix representing the parity operator in Minkowski space

$$\boldsymbol{P}^\mu{}_\nu = \begin{pmatrix} 1 & 0 & 0 & 0 \\ 0 & -1 & 0 & 0 \\ 0 & 0 & -1 & 0 \\ 0 & 0 & 0 & -1 \end{pmatrix} = g_{\mu\nu} \tag{5.26}$$

This leads to

$$P^\dagger \gamma^0 P = \gamma^0$$
$$P^\dagger \gamma^k P = -\gamma^k$$

with the solution $P = e^{i\phi_P}\gamma^0$ or in general

$$P\psi(x_\mu) = e^{i\phi_P}\gamma^0\psi(x'_\mu), \qquad \bar\psi(x_\mu)P^\dagger = e^{-i\phi_P}\bar\psi(x'_\mu)\gamma^0$$

There is a phase ϕ_P that can be chosen, and will be discussed below. For the solutions of the free particle Dirac equation the relations

$$Pu(\vec p) = e^{i\phi_P}u(-\vec p), \qquad Pv(\vec p) = -e^{i\phi_P}v(-\vec p)$$

hold.

Using the Pauli-Dirac representation of gamma matrices, we adopt the convention

$$P = \gamma^0 = \begin{pmatrix} 1 & 0 & 0 & 0 \\ 0 & 1 & 0 & 0 \\ 0 & 0 & -1 & 0 \\ 0 & 0 & 0 & -1 \end{pmatrix} \qquad \text{(in spinor space)} \tag{5.27}$$

with $\phi_P = 0$. Then we have

$$\psi' = \begin{pmatrix} \psi'_1 \\ \psi'_2 \\ \psi'_3 \\ \psi'_4 \end{pmatrix} = \gamma^0 \begin{pmatrix} \psi_1 \\ \psi_2 \\ \psi_3 \\ \psi_4 \end{pmatrix} = \begin{pmatrix} \psi_1 \\ \psi_2 \\ -\psi_3 \\ -\psi_4 \end{pmatrix} \tag{5.28}$$

which implies that particles and antiparticles have opposite parity.

Example: solution (1) of the Dirac equation in (4.35) transforms as

$$\mathrm{P}\,\psi_{(1)}(\vec{p}) = \gamma^0 \psi_{(1)}(-\vec{p}) = \mathcal{N} \begin{pmatrix} 1 \\ 0 \\ \frac{p_z}{E+m} \\ \frac{p_x+ip_y}{E+m} \end{pmatrix} e^{-ip^\mu x_\mu} = \psi_{(1)}(\vec{p}) \tag{5.29}$$

and solution (3) as

$$\mathrm{P}\,\psi_{(3)}(\vec{p}) = \gamma^0 \psi_{(3)}(-\vec{p}) = \mathcal{N} \begin{pmatrix} \frac{p_z}{-E+m} \\ \frac{p_x+ip_y}{-E+m} \\ -1 \\ 0 \end{pmatrix} e^{-ip^\mu x_\mu} = -\psi_{(3)}(\vec{p}) \tag{5.30}$$

Note that $P^\dagger \gamma_5 P = -\gamma_5$, i. e. the parity operation flips the chirality. This is necessary, since it also flips the helicity (eq. 5.22).

We may also consider

$$CP = -i\gamma^0\gamma^2\gamma^0 = i\gamma^0\gamma^0\gamma^2 = -PC \tag{5.31}$$

to see that the parity eigenvalue of fermion and anti-fermion are related by a factor -1.

Apparently, this representation also fulfills

$$P^2 = 1, \quad P^\dagger = P = P^{-1}$$

Another choice of the phase is motivated by (5.21). The sequential operation of two P operations on a fermion is similar to a total rotation by 2π. This induces a factor -1 due to the spin $\frac{1}{2}$ of a fermion. Therefore, the phase could be chosen to be $\phi_P = \frac{\pi}{2}$ leading to eigenvalues $\pm i$, with the consequence that $\mathrm{P}^2 = -1$ for fermions. We will, however, adopt the simpler convention with real eigenvalues.

The transformation of all bilinear covariants of fermion fields is obtained from

$$P\bar{\psi}O\phi P^\dagger = (\bar{\psi}P^\dagger)O(P\phi) = \bar{\psi}(P^\dagger O P)\phi$$

and given in table 5.2. Here, we adopt the convention of equal parity for all fermions, otherwise the signs would only be correct for $\phi = \psi$.

Table 5.2 Transformation of bilinear covariants under P. These transformations are independent of the choice of the phase ϕ_P. A change of indices ${}^{\mu} \leftrightarrow {}_{\mu}$ corresponds to a factor (-1) for all spacelike components, which is the parity transformation of a vector.

term	transformed term
$\bar{\psi}\phi$	$\bar{\psi}P^{+}P\phi = +\bar{\psi}\phi$
$\bar{\psi}\gamma^{\mu}\phi$	$\bar{\psi}P^{+}\gamma^{\mu}P\phi = +\bar{\psi}\gamma_{\mu}\phi$
$\bar{\psi}\sigma^{\mu\nu}\phi$	$\bar{\psi}P^{+}\sigma^{\mu\nu}P\phi = +\bar{\psi}\sigma_{\mu\nu}\phi$
$\bar{\psi}\gamma^{\mu}\gamma_5\phi$	$\bar{\psi}P^{+}\gamma^{\mu}\gamma_5 P\phi = -\bar{\psi}\gamma_{\mu}\gamma_5\phi$
$\bar{\psi}\gamma_5\phi$	$\bar{\psi}P^{+}\gamma_5 P\phi = -\bar{\psi}\gamma_5\phi$

5.2.3 Vector Fields

Parity transformation on vector fields is straightforward:

$$\boldsymbol{P}^{\mu}{}_{\nu}A^{\nu}(x_\lambda) = A_{\mu}(x'_\lambda)$$

i. e. $A^{\mu} \to A_{\mu} = (A^0, -A^1, -A^2, -A^3)$. This leaves the interaction term (4.63) invariant. It corresponds to the transformation of the electromagnetic field tensor that makes $\vec{E}$ a polar vector and $\vec{B}$ an axial vector.

All vector fields, including the W and Z^0 bosons, transform accordingly.

5.2.4 Parity Sign Conventions

We have shown in (5.31) that the parity of an anti-fermion is (-1) times the parity of a fermion. The absolute eigenvalue of a fermion, however, is merely a convention. A **meaningfull** convention is to assign the same parity to all particles. Then, a bound system of a fermion and an anti-fermion has always parity $(-1)\cdot(-1)^L$, e. g. the quark parities $\zeta_P(q) = +1, \zeta_P(\bar{q}) = -1$ imply $\zeta_P(\pi^0) = \zeta_P(\pi^+) = \zeta_P(\pi^-) = -1$. An S wave of three quarks has the parity of a single quark, which is by convention $+1$, hence $\zeta_P(p) = \zeta_P(n) = +1$ etc. and accordingly, $\zeta_P(\bar{p}) = \zeta_P(\bar{n}) = -1$.

Also **possible** is, however, a convention where each particle gets assigned an individual parity eigenvalue. Then, the parity of a bound fermion-anti-fermion state is not defined and depends on this assignment. Nevertheless, it is a conserved quantum number in processes that conserve all flavour quantum numbers. Example: $\zeta_P(u) = +1, \zeta_P(\bar{u}) = -1$, and $\zeta_P(d) = -1, \zeta_P(\bar{d}) = +1$ with $\zeta_P(\pi^0) = -1$, but $\zeta_P(\pi^+) = \zeta_P(\pi^-) = +1$, $\zeta_P(p) = -1$, $\zeta_P(n) = +1$ etc.

5.3 Zeitumkehr

Die Zeitumkehr T : $t \to -t$ dreht im Minkowskiraum die Zeitrichtung. Da ein Boost durch den Lichtkegel begreznt ist, gibt es keine stetige Transformation, die das bewirken kann.

Die Schrödingergleichung transformiert sich in ihr komplex konjugiertes

$$-i\partial_t\psi_T = H^{+}\psi_T \tag{5.32}$$

Ein Zeitumkehr-invarianter Hamiltonian H ist hermitesch, d. h. $H^{+} = H$.

Die Zeitumkehr-Invarianz wird mikroskopisch durch magnetische Monopole oder elementare elektrische Dipole verletzt. Diese verletzen gleichzeitig P. Sie erhalten C und damit auch CPT.

Makroskopische Verletzung der Zeitumkehrsymmetrie bewirken **dissipative** (absorptive) Prozesse. Ein Beispiel ist das Ohmsche Gesetz:

$$\vec{j} = \frac{1}{\rho}\vec{E}$$

Während die Stromdichte $\vec{j}$ ihr Vorzeichen unter T wechselt, behält das elektrische Feld $\vec{E}$ die Richtung bei. Die Gleichung beschreibt einen thermodynamischen Prozess, die Umwandlung elektrischer Energie in Wärme.

Streuprozesse

$$\langle f|\mathbf{S}|i\rangle$$

transformieren sich unter T zu

$$\langle Ti|\mathbf{S}^*|Tf\rangle$$

d. h. Anfangs- und Endzustand werden vertauscht, und alle Größen, die zu t oder $1/t$ proportional sind, wechseln ihr Vorzeichen.

Beispiel:

$$e^+(\boldsymbol{p}_+) + e^-(\boldsymbol{p}_-) \to \mu^+(\boldsymbol{q}_+) + \mu^-(\boldsymbol{q}_-) + \gamma(\boldsymbol{q})$$

(mit $\boldsymbol{q} = \boldsymbol{p}_+ + \boldsymbol{p}_- - \boldsymbol{q}_+ - \boldsymbol{q}_-$) wird unter T zu

$$\mu^+(-\boldsymbol{q}_+) + \mu^-(-\boldsymbol{q}_-) + \gamma(-\boldsymbol{q}) \to e^+(-\boldsymbol{p}_+) + e^-(-\boldsymbol{p}_-)$$

Nur falls $\mathbf{S}^* = \mathbf{S}$, d. h. $\mathcal{I}m\,\mathbf{S} = 0$, ist auch der Prozess

$$e^+(-\boldsymbol{p}_+) + e^-(-\boldsymbol{p}_-) \to \mu^+(-\boldsymbol{q}_+) + \mu^-(-\boldsymbol{q}_-) + \gamma(-\boldsymbol{q})$$

ein zeitgespiegelter Prozess („naive Zeitumkehr“ $\tilde{\mathrm{T}}$).

Der Zeitumkehroperator T hat keine eindeutige Darstellung im Minkowskiraum, da

$$\begin{aligned}\boldsymbol{T}x^\mu &= (-t, x, y, z) = -\boldsymbol{P}^\mu{}_\nu x^\nu \\ \boldsymbol{T}p^\mu &= (E, -p_x, -p_y, -p_z) = +\boldsymbol{P}^\mu{}_\nu p^\nu\end{aligned}$$

Eine Darstellung mit Hilfe des Operators K der komplexen Konjugation

$$\begin{aligned}Kf &= f^* \\ Kf\ldots &= f^*K\ldots\end{aligned}$$

im Minkowskiraum mit $\boldsymbol{x}$ und $i\boldsymbol{p}$ ist

$$T = \begin{pmatrix} -1 & 0 & 0 & 0 \\ 0 & 1 & 0 & 0 \\ 0 & 0 & 1 & 0 \\ 0 & 0 & 0 & 1 \end{pmatrix} K \qquad \text{(im Minkowskiraum)} \tag{5.33}$$

bei gleichzeitiger Klassifizierung in reelle und imaginäre Vierer-Vektoren kann man die Transformation allgemein definieren. Zeitartige imaginäre Größen ändern dann ihr Vorzeichen unter T nicht.

Eine Darstellung im Spinorraum ist

$$T = i\gamma^2\gamma_5 K = \begin{pmatrix} 0 & 1 & 0 & 0 \\ -1 & 0 & 0 & 0 \\ 0 & 0 & 0 & -1 \\ 0 & 0 & 1 & 0 \end{pmatrix} K \qquad \text{(im Spinorraum)} \tag{5.34}$$

Er ist antiunitär und antilinear, d. h.

$$\begin{aligned} T^\dagger T &= 1 \\ T(a\psi + b\phi) &= a^* T\psi + b^* T\phi \\ [T, c] &= (c^* - c)T = (-2\mathcal{I}m\, c)T \\ \mathrm{T}\,|\Psi\rangle &= \langle \mathrm{T}\,\Psi| \end{aligned}$$

Damit ist auch CPT ein antiunitärer Operator.

Nota bene: C ist linear und unitär, d. h.

$$C(a\psi + b\phi) = aC\psi + bC\phi$$

Eigenschaften:

$$T^2 = -1, \quad T^{+} = -T$$

Zweimaliges Anwenden von T auf Fermionen erzeugt also eine Phase von π, wie bei der Drehung um $360°$.

Table 5.3 Transformation der bilinearen Kovarianten unter T

Form	Transformationsverhalten
$\bar\psi\phi$	$\bar\psi T^{-1} T\phi = +\bar\phi\psi$
$\bar\psi\gamma^\mu\phi$	$\bar\psi T^{-1}\gamma^\mu T\phi = +\bar\phi\gamma_\mu\psi$
$\bar\psi\sigma^{\mu\nu}\phi$	$\bar\psi T^{-1}\sigma^{\mu\nu} T\phi = -\bar\phi\sigma_{\mu\nu}\psi$
$\bar\psi\gamma^\mu\gamma_5\phi$	$\bar\psi T^{-1}\gamma^\mu\gamma_5 T\phi = +\bar\phi\gamma_\mu\gamma_5\psi$
$\bar\psi\gamma_5\phi$	$\bar\psi T^{-1}\gamma_5 T\phi = +\bar\phi\gamma_5\psi$
$i\bar\psi\gamma_5\phi$	$i\bar\psi T^{-1}\gamma_5 T\phi = -i\bar\phi\gamma_5\psi$

5.4 CPT-Theorem

Eine Quantenfeldtheorie ist symmetrisch[21] unter CPT.

5.4.1 Observablen

Table 5.4 Transformationsverhalten physikalischer Observablen.

		C	P	T	CP	CPT
Ladung	Q	−	+	+	−	−
Abstand	$\boldsymbol{x}$	+	−	+	−	−
Zeitdifferenz	t	+	+	−	+	−
Geschwindigkeit	$\boldsymbol{v} = \dot{\boldsymbol{x}}$	+	−	−	−	+
Beschleuigung	$\boldsymbol{a} = \dot{\boldsymbol{v}}$	+	−	+	−	−
Impuls	$\boldsymbol{p}$	+	−	−	−	+
Energie	E	+	+	+	+	+
Drehimpuls	$\boldsymbol{L} = \boldsymbol{x} \times \boldsymbol{p}$	+	+	−	+	−
Helizität	$h \sim \boldsymbol{L} \cdot \boldsymbol{p}$	+	−	+	−	−
elektrisches Feld	$\vec{E}$	−	−	+	+	+
magnetisches Feld	$\vec{B}$	−	+	−	−	+

[21] G. Lüders, Math. Fysik. Medd. Kgl. Danske Akad. Ved. **28**, 5 (1954).

5.5 Irreduzible Darstellung der SU(2) in 3 Dimensionen

Generatoren:

$$T_1 = \frac{1}{\sqrt{2}}\begin{pmatrix} 0 & 1 & 0 \\ 1 & 0 & 1 \\ 0 & 1 & 0 \end{pmatrix} \qquad T_2 = \frac{1}{\sqrt{2}}\begin{pmatrix} 0 & i & 0 \\ -i & 0 & i \\ 0 & -i & 0 \end{pmatrix} \qquad T_3 = \begin{pmatrix} 1 & 0 & 0 \\ 0 & 0 & 0 \\ 0 & 0 & -1 \end{pmatrix}$$

$$T_+ = \begin{pmatrix} 0 & 0 & 0 \\ 1 & 0 & 0 \\ 0 & 1 & 0 \end{pmatrix} \qquad T_- = \begin{pmatrix} 0 & 1 & 0 \\ 0 & 0 & 1 \\ 0 & 0 & 0 \end{pmatrix}$$

Beispiel einer **SU(2)**-Matrix:

$$\begin{aligned} R_2(x) &= e^{ixT_2} \\ &= 1 + \sum_{n=1}^{\infty} \frac{(ix)^{2n-1}}{(2n-1)!} \frac{1}{\sqrt{2}} \begin{pmatrix} 0 & i & 0 \\ -i & 0 & i \\ 0 & -i & 0 \end{pmatrix} + \sum_{n=1}^{\infty} \frac{(ix)^{2n}}{(2n)!} \begin{pmatrix} \frac{1}{2} & 0 & -\frac{1}{2} \\ 0 & 1 & 0 \\ -\frac{1}{2} & 0 & \frac{1}{2} \end{pmatrix} \\ &= \begin{pmatrix} \frac{1}{2} + \frac{1}{2}\cos x & -\frac{1}{\sqrt{2}}\sin x & \frac{1}{2} - \frac{1}{2}\cos x \\ \frac{1}{\sqrt{2}}\sin x & \cos x & -\frac{1}{\sqrt{2}}\sin x \\ \frac{1}{2} - \frac{1}{2}\cos x & \frac{1}{\sqrt{2}}\sin x & \frac{1}{2} + \frac{1}{2}\cos x \end{pmatrix} \end{aligned}$$

5.5.1 Rotation im Isoraum um 180°

Rotation um die **SO(3)**-y-Achse um 180°

$$R_2(\pi) = \begin{pmatrix} -1 & 0 & 0 \\ 0 & 1 & 0 \\ 0 & 0 & -1 \end{pmatrix} \quad \text{in der adjungierten Darstellung}$$

SU(2):

$$\begin{aligned} R_2(\pi) &= e^{i\pi T_2} \\ &= \text{Rotation im 2-dim. Raum um } 90° \\ &= \begin{pmatrix} 0 & 1 \\ -1 & 0 \end{pmatrix} \quad \text{in 2 Dimensionen} \\ &= \begin{pmatrix} 0 & 0 & 1 \\ 0 & -1 & 0 \\ 1 & 0 & 0 \end{pmatrix} \quad \text{in 3 Dimensionen} \end{aligned} \tag{5.35}$$

z. B. Darstellung $uu, ud + du, dd$, Vorzeichenwechsel bei $-u\bar{d}, u\bar{u} - d\bar{d}, d\bar{u}$.

$$\begin{aligned} R_{2,\pi} T_1 R_{2,\pi}^{+} &= -T_1 \\ R_{2,\pi} T_2 R_{2,\pi}^{+} &= T_2 \\ R_{2,\pi} T_3 R_{2,\pi}^{+} &= -T_3 \\ R_{2,\pi} T_+ R_{2,\pi}^{+} &= -T_- \\ R_{2,\pi} T_- R_{2,\pi}^{+} &= -T_+ \end{aligned}$$

$$\begin{aligned} R_2(-\pi) &= e^{-i\pi T_2} \\ &= \text{Rotation im 2-dim. Raum um } -90^\circ \\ &= \begin{pmatrix} 0 & -1 \\ 1 & 0 \end{pmatrix} \quad \text{in 2 Dimensionen} \end{aligned}$$

Iso-Dublett und Antidublett (kontragradiente Darstellung)

$$R_{2,\pi}|u\rangle = -|d\rangle, \quad R_{2,\pi}|d\rangle = |u\rangle$$
$$R_{2,\pi}|\bar{d}\rangle = \begin{pmatrix} 0 & 1 \\ -1 & 0 \end{pmatrix}\begin{pmatrix} -1 \\ 0 \end{pmatrix} = |\bar{u}\rangle, \quad R_{2,\pi}|\bar{u}\rangle = \begin{pmatrix} 0 & 1 \\ -1 & 0 \end{pmatrix}\begin{pmatrix} 0 \\ 1 \end{pmatrix} = -|\bar{d}\rangle$$

5.5.2 G-Parität

G-Parität = Ladungskonjugation ∘ Rotation um die 2-Achse im 3-dimensionalen Isoraum[22]

$$\mathrm{G} = \mathrm{C}\, R_{2,\pi}$$

Isospin 0:

$$\mathrm{G}(|u\bar{u}\rangle + |d\bar{d}\rangle) = \mathrm{C}(|d\bar{d}\rangle + |u\bar{u}\rangle)$$

Isospin 1:

$$\begin{aligned} \mathrm{G}(-|u\bar{d}\rangle) &= \mathrm{C}(|d\bar{u}\rangle) \\ \mathrm{G}(|u\bar{u}\rangle - |d\bar{d}\rangle) &= \mathrm{C}(|d\bar{d}\rangle - |u\bar{u}\rangle) \\ \mathrm{G}(|d\bar{u}\rangle) &= \mathrm{C}(-|u\bar{d}\rangle) \end{aligned}$$

Daher ist für Mesonen aus u und d Quarks, die durch die G-Parität in sich selbst überführt werden, der Eigenwert $G = (-1)^{L+S+I}$.

Insbesondere ist $\mathrm{G}|\pi\rangle = -|\pi\rangle$.

Für Mesonen, die C-Eigenzustände sind, ist $C = (-1)^{L+S}$ und $G = C(-1)^I$.

Eine alternative Herleitung benutzt den 3-dimensionalen Isoraum (adjungierte Darstellung) und die Rotation um die 2-Achse mit

$$\begin{aligned} R_{2,\pi}\pi_1 &= -\pi_1 \\ R_{2,\pi}\pi_2 &= \pi_2 \\ R_{2,\pi}\pi_3 &= -\pi_3 \\ \pi^0 = \pi_3 \qquad & R_{2,\pi}\pi^0 = -\pi^0 \\ \pi^+ = \frac{1}{\sqrt{2}}(\pi_1 + i\pi_2) \qquad & R_{2,\pi}\pi^+ = -\pi^- \\ \pi^- = \frac{1}{\sqrt{2}}(\pi_1 - i\pi_2) \qquad & R_{2,\pi}\pi^- = -\pi^+ \end{aligned}$$

Die Darstellung (5.35) lässt sich auch anwenden, wenn man beachtet, das die Wellenfunktionen $|\pi^+\rangle$ und $|\pi^-\rangle$ ein relatives Minuszeichen haben. In der Literatur wird das oft umgangen, da man in

[22] T. D. Lee, C. N. Yang, Il Nuovo Cim. **Ser. 10 Vol. 3**, 749–753 (1956).

$\mathrm{C}\,|\pi^+\rangle = e^{i\phi_{\mathrm{CP}\,\pi}}|\pi^-\rangle$ eine nicht-physikalische Phase $\phi_{\mathrm{CP}\,\pi}$ so wählen kann, dass $\mathrm{C}\,|\pi^+\rangle = \pm|\pi^-\rangle$ ist und ein Plus bei der Iso-Rotation durch ein Minus bei C ausgeglichen werden kann.

Für Paare von Mesonen XY ist der Eigenwert $G = (-1)^{I+L}$ mit dem Gesamtisospin $I(XY)$ und dem Drehimpuls L_{XY}.

Da Pionen Bosonen sind, ist ihre Gesamtwellenfunktion symmetrisch. Für alle Paare müssen daher entweder L und I beide gerade oder beide ungerade sein, und G ist stets $+1$.

Ein einzelnes Pion hat $G = -1$, n Pionen haben daher $G = (-1)^n$.

5.6 Zwei reelle Photonen

Ein Zustand aus zwei rellen Photonen erfüllt folgende Bedingungen (im CMS, z-Achse in Flugrichtung):

- Charge conjugation $C = +1$.
- Parität $P = (-1)^L$ (Bahndrehimpuls L)
- Ein Zwei-Boson-Zustand ist **symmetrisch** unter Austausch, i.e. die Spinwellenfunktion muss *symmetrisch* für $L = \textit{gerade}$ und *antisymmetrisch* für $L = \textit{ungerade}$ sein.
- Reelle Photonen sind **transversal** polarisiert, i.e. $|S, S_z\rangle = |1, +1\rangle$ oder $|1, -1\rangle$. Daher haben zwei Photonen nur $S_z = 0, \pm 2$.
- Es gibt keine Drehimpulskomponente in Flugrichtung, i.e. $|L, L_z\rangle = |L, 0\rangle$. Das gilt schon klassisch: $\vec{L} = \vec{r} \times \vec{p}$.

Drehimpulsaddition: $\langle S, 0; L, 0|J, 0\rangle = 0$ falls $(S + L - J)$ *ungerade*

Damit sind folgende Kombinationen erlaubt:

1) $\sqrt{\frac{1}{2}}\,(|1,-1\rangle|1,+1\rangle + |1,+1\rangle|1,-1\rangle) = \sqrt{\frac{2}{3}}|0,0\rangle + \sqrt{\frac{1}{3}}|2,0\rangle$ falls $L = \textit{gerade}$

$\longleftarrow\!\Leftarrow\!\!-\ L\ -\!\!\Rightarrow\!\longrightarrow \quad + \quad \longleftarrow\!\Rightarrow\!\!-\ L\ -\!\!\Leftarrow\!\longrightarrow$

	$S=0$	$S=2$
$L=0$	0^{++}	2^{++}
$L=2$	2^{++}	$0^{++}, 2^{++}, 4^{++}$
$L=4$	4^{++}	$2^{++}, 4^{++}, 6^{++}$
$\dots$	$\dots$	

2) $\sqrt{\frac{1}{2}}\,(|1,-1\rangle|1,+1\rangle - |1,+1\rangle|1,-1\rangle) = |1,0\rangle$ falls $L = \textit{ungerade}$

$\longleftarrow\!\Leftarrow\!\!-\ L\ -\!\!\Rightarrow\!\longrightarrow \quad - \quad \longleftarrow\!\Rightarrow\!\!-\ L\ -\!\!\Leftarrow\!\longrightarrow$

$L=1$	$0^{-+}, 2^{-+}$
$L=3$	$2^{-+}, 4^{-+}$
$L=5$	$4^{-+}, 6^{-+}$
$\dots$	$\dots$

3) $|1,+1\rangle|1,+1\rangle = |2,+2\rangle$ falls $L = \textit{gerade}$

$\longleftarrow\!\Rightarrow\!\!-\ L\ -\!\!\Rightarrow\!\longrightarrow$

$L=0$	2^{++}
$L=2$	$2^{++}, 3^{++}, 4^{++}$
$L=4$	$4^{++}, 5^{++}, 6^{++}$
$\dots$	$\dots$

ebenso $|1,-1\rangle|1,-1\rangle = |2,-2\rangle$

$$\longleftarrow\!\!\Leftarrow\!\!- \; L \; -\!\!\Leftarrow\!\!\longrightarrow$$

Erlaubte Quantenzahlen J^{PC} sind

$$J^{++} \; (J \neq 1), \quad \textit{gerade}^{-+}$$

Klassische Herleitung aus den Eigenschaften des Photonfeldes (Landau–Yang-Theorem [23]).

[23] L. D. Landau, Sov. Phys. Dok. **60**, 207 (1948) und C. N. Yang, Phys. Rev. **77**, 242 (1950).

6. QCD und QED

Die Symmetriegruppe im Farb-Ladungsraum der starken Wechselwirkung ist die **SU(3)**.
Die Generatoren $T_{1\ldots8}$ werden auch mit Hilfe der Gell-Mann Matrizen $\lambda_{1\ldots8}$ als

$$T_a := \tfrac{1}{2}\lambda_a$$

geschrieben oder mit Colour-Quantenzahlen als Auf- und Absteige-Operatoren:

$$G_{r\bar{b}} = T_1 + iT_2 = \begin{pmatrix} 0 & 1 & 0 \\ 0 & 0 & 0 \\ 0 & 0 & 0 \end{pmatrix}, \quad G_{r\bar{g}} = \begin{pmatrix} 0 & 0 & 1 \\ 0 & 0 & 0 \\ 0 & 0 & 0 \end{pmatrix}, \quad G_{b\bar{r}} = \begin{pmatrix} 0 & 0 & 0 \\ 1 & 0 & 0 \\ 0 & 0 & 0 \end{pmatrix}$$

$$G_{b\bar{g}} = \begin{pmatrix} 0 & 0 & 0 \\ 0 & 0 & 1 \\ 0 & 0 & 0 \end{pmatrix}, \quad G_{g\bar{r}} = \begin{pmatrix} 0 & 0 & 0 \\ 0 & 0 & 0 \\ 1 & 0 & 0 \end{pmatrix}, \quad G_{g\bar{b}} = \begin{pmatrix} 0 & 0 & 0 \\ 0 & 0 & 0 \\ 0 & 1 & 0 \end{pmatrix}$$

$$G_{r\bar{r}-b\bar{b}} = \frac{1}{\sqrt{2}} \begin{pmatrix} 1 & 0 & 0 \\ 0 & -1 & 0 \\ 0 & 0 & 0 \end{pmatrix}, \quad G_{r\bar{r}+b\bar{b}-2g\bar{g}} = \frac{1}{\sqrt{6}} \begin{pmatrix} 1 & 0 & 0 \\ 0 & 1 & 0 \\ 0 & 0 & -2 \end{pmatrix}$$

6.1 Casimir-Operatoren der SU(3)

Es gibt zwei, der wichtigste ist

$$T^2 = \sum_a T_a^2$$

Er entspricht in der Colour-**SU(3)** einem Colour-Ladungsquadrat und gibt die relative Stärke der Kraft zwischen zwei (gleichen) Farbladungen an.

Der zweite ist

$$C_2 = d_{abc} T_a T_b T_c$$

Eigenwerte von T^2 und C_2 in der Darstellung $(p|q)$:

$$T^2: \qquad \frac{p^2 + q^2 + pq + 3(p+q)}{3}$$

$$C_2: \qquad \frac{2(p-q)\cdot[2(p+q)^2 + pq + 9(p+q+1)]}{9}$$

Beispiele:

Singulett	$(0\|0)$	$T^2 = 0$	$C_2 = 0$
Triplett	$(1\|0)$	$T^2 = \frac{4}{3}$	$C_2 = \frac{40}{9}$
Sextett	$(2\|0)$	$T^2 = \frac{10}{3}$	$C_2 = \frac{70}{9}$
Oktett	$(1\|1)$	$T^2 = 3$	$C_2 = 0$

6.2 Yang–Mills-Theorie

6.2.1 Freie Fermionen

Der Lagrangian (Lagrangedichte, mit der Dimension Energie/Volumen = Energie^4) für ein freies Fermion ist

$$\mathcal{L}_F = \bar{\psi}(i\gamma^\mu \partial_\mu - m)\psi \tag{6.1}$$

Die Euler-Lagrange-Gleichung dazu ist die Dirac-Gleichung.

Dabei ist ψ ein Spinor eines Fermionfeldes und ein Vektor in n inneren Freiheitsgraden, bzgl. deren die Fermionen eine Symmetrie haben, die durch eine Liegruppe beschrieben wird. Eine Symmetrietransformation U aus der Gruppe wird charakterisiert durch ein N-tupel $(\theta_a | a = 1 \dots N)$ und dargestellt durch die unitäre $n \times n$-Matrix $\boldsymbol{U}(\theta)$

$$\boldsymbol{U} = \exp(i\boldsymbol{T}_a\theta_a)$$

(Summation über mehrfach vorkommende Indices).

Die Exponentialfunktion wird als Taylorreihe berechnet

$$\boldsymbol{U} = e^{iT_a\theta_a} = 1 + \sum_a \frac{i}{1!}\theta_a\boldsymbol{T}_a + \frac{i^2}{2!}\sum_{a,b}\theta_a\theta_b\boldsymbol{T}_a\boldsymbol{T}_b + \frac{i^3}{3!}\sum_{a,b,c}\theta_a\theta_b\theta_c\boldsymbol{T}_a\boldsymbol{T}_b\boldsymbol{T}_c + \dots \tag{6.2}$$

Da die Generatoren hermitesch sind, $\boldsymbol{T}_a^+ = \boldsymbol{T}_a$, ist

$$\boldsymbol{U}^+ = 1 + \sum_a \frac{-i}{1!}\theta_a\boldsymbol{T}_a + \frac{i^2}{2!}\sum_{a,b}\theta_a\theta_b\boldsymbol{T}_b\boldsymbol{T}_a + \frac{-i^3}{3!}\sum_{a,b,c}\theta_a\theta_b\theta_c\boldsymbol{T}_c\boldsymbol{T}_b\boldsymbol{T}_a + \dots = e^{-iT_a\theta_a}$$

wobei in den Summen $a, b \to b, a$, $a, b, c \to c, b, a$ etc. umbenannt werden muss ($(T_aT_bT_c)^+ = T_c^+T_b^+T_a^+ = T_cT_bT_a$ etc.).

Die Matrizen $\boldsymbol{T}_a$ $(a = 1 \dots N)$ sind die Generatoren der Gruppe. Die reelle unitäre (orthogonale) $N \times N$-Matrix (U_{ab}) der *adjungierten Darstellung* zu U beschreibt das Transformationsverhalten im von den T_a aufgespannten Infinitesimalring.

6.2.2 Globale Transformationen

Transformation der Fermionfelder:

$$\begin{aligned} \psi' &= \boldsymbol{U}\psi \\ \bar{\psi}' &= \bar{\psi}\boldsymbol{U}^+ \end{aligned} \tag{6.3}$$

allgemeine Generatoren:

$$\boldsymbol{G} := G_a\boldsymbol{T}_a \tag{6.4}$$

Vektorfelder $\boldsymbol{G}_\mu$ werden entsprechend definiert mit Komponenten $G_{\mu(a)}$. Transformationsverhalten von Generator-Koeffizienten:

$$G'_a = U_{ab}G_b \tag{6.5}$$

$$G'_a\boldsymbol{T}_a = G_b\boldsymbol{U}\boldsymbol{T}_b\boldsymbol{U}^+$$

Transformation des Lagrangian:

$$\mathcal{L}_F(\psi') = \mathcal{L}_F(\psi) \qquad \textbf{invariant} \tag{6.6}$$

6.2.3 Lokale Transformationen

Lokale Transformation:

$$\boldsymbol{U} = \boldsymbol{U}(x_\mu) = e^{i\mathbf{T}_a\theta_a(x_\mu)}$$
$$\boldsymbol{U}^+(x_\mu) = e^{-i\mathbf{T}_a\theta_a(x_\mu)}$$

Wegen $\boldsymbol{U}^+\boldsymbol{U} = \mathbf{1}$ ist

$$(\partial_\mu \boldsymbol{U}^+)\boldsymbol{U} = -\boldsymbol{U}^+\partial_\mu \boldsymbol{U}$$

und für abelsche Gruppen, z. B. $\mathbf{U(1)}$, ist

$$\partial_\mu \boldsymbol{U} = i\boldsymbol{T}_a\boldsymbol{U}\partial_\mu\theta_a, \quad \partial_\mu \boldsymbol{U}^+ = -i\boldsymbol{T}_a\boldsymbol{U}^+\partial_\mu\theta_a$$

dagegen kann man für nicht-abelsche Gruppen die Kettenregel nicht anwenden, da die Matrizen $\boldsymbol{T}_a$ nicht kommutieren.

6.2.3.1 Physikalische Interpretation

Die Forderung nach Invarianz unter lokalen Transformationen drückt die Willkür eines Bezugssystems für innere Freiheitsgrade beim Transport in Raum und Zeit aus. Da die inneren Freiheitsgrade keinerlei Bezug zu Raumzeitrichtungen haben, kann es auch keine ausgezeichnete Vorschrift geben, wie ein Koordinatensystem für diese Freiheitsgrade sich beim Transport durch Raum und Zeit verhält. Mit anderen Worten, es ist prinzipiell nicht unterscheidbar, ob ein „rotes Quark“ nach einer bestimmten Zeit immer noch „rot“ ist, oder jetzt „blau“. Einzig und allein die relative Orientierung in einem transportierten System ist eine physikalisch sinnvolle Größe: Ein zweites Quark „derselben Farbe“, das auf dem gleichen Pfad mittransportiert wird, behält „dieselbe Farbe“.

Jeder Transport eines Bezugssystems für innere Freiheitsgrade muss gewährleisten, dass beim Umlauf längs eines geschlossenen Pfades in der Raumzeit das ursprüngliche System wieder erhalten wird. Ein geschlossener Pfad im Raum mit Anfang und Ende zu verschiedenen Zeiten macht dagegen keine Einschränkung.

6.2.3.2 Eine geometrische Analogie

Eine anschauliche Analogie zur lokalen Transformation innerer Freiheitsgrade ist die lokale Transformation eines Koordinatensystems, etwa zur Beschreibung der Oberfläche einer Kugel:

Zur Illustration des Unterschiedes zwischen globalen und lokalen Symmetrien betrachte man einen idealen kugelförmigen Ballon, auf dem Längen- und Breitenkreise eingezeichnet sind, so dass die Lage der Punkte auf der Oberfläche durch Angabe von Länge und Breite bestimmt ist.

Wenn man dieses Koordinatensystem um irgendeine durch den Mittelpunkt gehende Achse dreht, erhält man eine Symmetrietransformation: Das neue Koordinatensystem beschreibt denselben, unveränderten Ballon. Sie ist global, weil die Lagen aller Punkte auf der Oberfläche durch die Drehung um einen Winkel in gleicher Weise verändert werden.

Würde man andererseits die Knoten im Koordinatennetz unabhängig voneinander auf der Ballonfläche zu neuen Positionen verschieben, dann wäre dies auch eine Symmetrietransformation, denn der Ballon bleibt unverändert. Weil aber jeder Punkt anders als seine Nachbarn transformiert wird, handelt es sich dabei um eine lokale Symmetrietransformation.

Bemerkenswert ist, dass bei der lokalen Symmetrieoperation die Ballonhaut verspannt wird und somit elastische Kräfte zwischen den gegeneinander verschobenen Punkten auftreten. Tatsächlich treten Scheinkräfte auf, da ja nicht der Ballon, sondern nur das Koordinatensystem verändert wurde. Ein

Beobachter, der das nicht von einem unverzerrten Koordinatennetz unterscheiden kann, sieht das lineare Kraft/Abstands-Gesetz verletzt, und schließt daher auf das Wirken zusätzlicher Kräfte.

In ähnlicher Weise treten Kräfte immer dann auf, wenn eine physikalische Theorie eine lokale Symmetrie (Eichsymmetrie) besitzt. Wenn ein physikalisches Gesetz einer globalen Symmetrie genügt, kann die stärkere Forderung nach Invarianz gegenüber den lokalen Transformationen nur durch die Einführung neuer Felder erfüllt werden, und es tritt eine durch diese Eichfelder vermittelte Wechselwirkung auf.

6.2.4 Transformation des Lagrangian

infinitesimal $\delta_a \ll 1$:

$$\begin{aligned} \boldsymbol{U} &= 1 + i\boldsymbol{T}_a\delta_a \\ \boldsymbol{U}^+ &= 1 - i\boldsymbol{T}_a\delta_a \end{aligned}$$

Transformation der Fermionfelder:

$$\psi' = \boldsymbol{U}\psi, \quad \bar{\psi}' = \bar{\psi}\boldsymbol{U}^+ \tag{6.7}$$

Transformation des Lagrangian:

$$\begin{aligned} \mathcal{L}_F(\psi') &= \bar{\psi}\boldsymbol{U}^+(i\gamma^\mu\partial_\mu - m)\boldsymbol{U}\psi \\ &= i\bar{\psi}\gamma^\mu\boldsymbol{U}^+\partial_\mu(\boldsymbol{U}\psi) - \bar{\psi}\boldsymbol{U}^+\boldsymbol{U}m\psi \\ &= \bar{\psi}(i\gamma^\mu\partial_\mu - m)\psi + i\bar{\psi}\gamma^\mu\boldsymbol{U}^+(\partial_\mu\boldsymbol{U})\psi \\ &= \mathcal{L}_F(\psi) + i\bar{\psi}\gamma^\mu(\boldsymbol{U}^+\partial_\mu\boldsymbol{U})\psi \qquad \textbf{nicht invariant!} \\ &= \mathcal{L}_F(\psi) - i\bar{\psi}\gamma^\mu(\partial_\mu\boldsymbol{U}^+)\boldsymbol{U}\psi \end{aligned}$$

Der letzte Term hat die Form einer Kopplung des Fermionfeldes an ein Vektorfeld:

$$i\bar{\psi}\gamma^\mu(\partial_\mu\boldsymbol{U}^+)\boldsymbol{U}\psi = -i\bar{\psi}\gamma^\mu\boldsymbol{U}^+(\partial_\mu\boldsymbol{U})\psi = \bar{\psi}\gamma^\mu\tilde{\boldsymbol{G}}_\mu(x)\psi$$

mit

$$\tilde{\boldsymbol{G}}_\mu = -ie^{-i\mathbf{T}_a\theta_a(x_\nu)}(\partial_\mu e^{i\mathbf{T}_a\theta_a(x_\mu)})$$

Im Fall einer Abelschen Gruppe ist

$$\mathcal{L}_F(\psi') = \mathcal{L}_F(\psi) - \bar{\psi}\gamma^\mu\boldsymbol{T}_a\psi\partial_\mu\theta_a$$

Dabei wurde $[\boldsymbol{U}, \boldsymbol{T}_a] = 0$ verwendet. Diese Matrizen kommutieren, da alle Generatoren kommutieren und

$$\boldsymbol{U} = e^{iT_a\theta_a} = 1 + \frac{i}{1!}\sum_a \theta_a\boldsymbol{T}_a + \frac{i^2}{2!}\left(\sum_a \theta_a\boldsymbol{T}_a\right)^2 + \ldots$$

enthält nur Produkte aus Generatoren.

Einführung einer minimalen Kopplung an Vektorfelder[24] (Eichbosonen) $G_{\mu(a)}$, mit Transformationsverhalten:

$$\begin{aligned} \boldsymbol{G}'_\mu = \sum_a G'_{\mu(a)}\boldsymbol{T}_a &= \sum_b G_{\mu(b)}\boldsymbol{U}\boldsymbol{T}_b\boldsymbol{U}^+ + \frac{1}{ig}\boldsymbol{U}\partial_\mu\boldsymbol{U}^+ \\ &= \boldsymbol{U}\boldsymbol{G}_\mu\boldsymbol{U}^+ + \frac{1}{ig}\boldsymbol{U}\partial_\mu\boldsymbol{U}^+ \end{aligned}$$

[24] C. N. Yang, R. L. Mills, Phys. Rev. **96**, 191 (1954).

für abelsche Gruppen sind die $\boldsymbol{T}_a = \boldsymbol{U}\boldsymbol{T}_a\boldsymbol{U}^+$ invariant und es ist

$$G'_{\mu(a)} = U_{ab}G_{\mu(b)} - \frac{1}{g}\partial_\mu\theta_a \tag{6.8}$$
$$\boldsymbol{G}'_\mu = \sum_a G'_{\mu(a)}\boldsymbol{T}_a = \sum_a G_{\mu(a)}\boldsymbol{T}_a - \frac{1}{g}\sum_a \partial_\mu\theta_a\boldsymbol{T}_a$$

wobei $g \neq 0$ beliebig und ein Parameter der Theorie ist. Der zweite Term beschreibt die Eichfreiheit des Vektorpotenzials einer klassischen Theorie.

Lagrangian $\mathcal{L} = \mathcal{L}_F + \mathcal{L}_K$ mit dem Kopplungsbeitrag

$$\mathcal{L}_K = -g\bar{\psi}\left(\gamma^\mu \sum_a \boldsymbol{T}_a G_{\mu(a)}\right)\psi = -g\bar{\psi}\gamma^\mu\boldsymbol{G}_\mu\psi \tag{6.9}$$

Transformation des Kopplungs-Lagrangian:

$$\begin{aligned}\mathcal{L}_K(\psi', G') &= -g\bar{\psi}\boldsymbol{U}^+(\gamma^\mu[\boldsymbol{U}\boldsymbol{G}_\mu\boldsymbol{U}^+ + \frac{1}{ig}\boldsymbol{U}\partial_\mu\boldsymbol{U}^+])\boldsymbol{U}\psi \\ &= -g\bar{\psi}(\gamma^\mu\boldsymbol{G}_\mu)\psi + i\bar{\psi}\boldsymbol{U}^+\gamma^\mu\boldsymbol{U}(\partial_\mu\boldsymbol{U}^+)\boldsymbol{U}\psi \\ &= \mathcal{L}_K(\psi, G) + i\bar{\psi}\gamma^\mu(\partial_\mu\boldsymbol{U}^+)\boldsymbol{U}\psi\end{aligned} \tag{6.10}$$

oder für abelsche Gruppen

$$\begin{aligned}\mathcal{L}_K(\psi', G') &= -g\bar{\psi}\boldsymbol{U}^+(\gamma^\mu\boldsymbol{T}_a[G_{\mu(a)} - \frac{1}{g}\partial_\mu\theta_a]\boldsymbol{U}\psi \\ &= -g\bar{\psi}(\gamma^\mu\boldsymbol{T}_a G_{\mu(a)})\psi + \bar{\psi}\gamma_\mu\boldsymbol{T}_a(\partial_\mu\theta_a)\psi \\ &= \mathcal{L}_K(\psi, G) + \bar{\psi}\gamma_\mu\boldsymbol{T}_a\psi\partial_\mu\theta_a\end{aligned} \tag{6.11}$$

$$\mathcal{L}_{F+K}(\psi', G') = \mathcal{L}_{F+K}(\psi, G) \qquad \textbf{invariant} \tag{6.12}$$

Kovariante Ableitung:

$$D_\mu := \partial_\mu\mathbf{1} + ig\boldsymbol{G}_\mu = \partial_\mu\mathbf{1} + ig\boldsymbol{T}_a G_{\mu(a)} \tag{6.13}$$
$$i\gamma^\mu D_\mu = i\gamma^\mu\partial_\mu - g\gamma^\mu\boldsymbol{G}_\mu$$

Transformationsverhalten:

$$D'_\mu = \boldsymbol{U}D_\mu\boldsymbol{U}^+ \tag{6.14}$$

wobei der Differentialoperator auch auf $\boldsymbol{U}^+$ wirkt.

Lagrangian:

$$\mathcal{L}_{F+K} = \bar{\psi}(i\gamma^\mu D_\mu - m)\psi \tag{6.15}$$

6.2.5 Euler-Lagrange-Gleichungen

$$\frac{\partial \mathcal{L}}{\partial \bar{\psi}} = \frac{\mathrm{d}}{\mathrm{d}x^\mu} \frac{\partial \mathcal{L}}{\partial(\partial_\mu \bar{\psi})}$$

$$(i\gamma^\mu D_\mu - m)\psi = 0 \tag{6.16}$$

(= Diracgleichung für ψ unter Einschluss der Eichfelder)

$$\frac{\partial \mathcal{L}}{\partial \psi} = \frac{\mathrm{d}}{\mathrm{d}x^\mu} \frac{\partial \mathcal{L}}{\partial(\partial_\mu \psi)}$$

$$\bar{\psi}(m + g\gamma^\mu \boldsymbol{T}_a G_{\mu(a)}) = i\frac{\mathrm{d}}{\mathrm{d}x_\mu}(\bar{\psi}\gamma^\mu) \tag{6.17}$$

(= Diracgleichung für $\bar{\psi}$)
Die dritte Gleichung

$$\frac{\partial \mathcal{L}}{\partial G_{\nu(a)}} = \frac{\mathrm{d}}{\mathrm{d}x^\mu} \frac{\partial \mathcal{L}}{\partial(\partial_\mu G_{\nu(a)})}$$

ergibt

$$\begin{aligned} & \bar{\psi}(g\gamma^\mu \boldsymbol{T}_a)\psi = 0 \\ \Longrightarrow \quad & \psi \equiv 0 \qquad \text{oder} \qquad g = 0 \end{aligned} \tag{6.18}$$

Da $g = 0$ wegen $1/g$ im Kopplungsterm nicht möglich ist, kann der Lagrangian noch nicht vollständig sein. Es fehlen kinetische Terme der Eichfelder ($\partial_\mu G_{\nu(a)} \ldots$).

6.2.6 Der vollständige Yang–Mills-Lagrangian

$$\mathcal{L}_{YM} = \mathcal{L}_F + \mathcal{L}_K + \mathcal{L}_E$$

Dabei beschreibt $\mathcal{L}_E$ den Lagrangian freier Eichfelder. Als Vektorbosonen erfüllen Sie die Proca-Gleichung (4.68) und haben damit kin. Energie und Massenterme. Die kin. Energie der Eichfelder:

$$\mathcal{L}_E = -\frac{1}{2} \operatorname{Sp} \boldsymbol{F}_{\mu\nu} \boldsymbol{F}^{\mu\nu} \tag{6.19}$$

Feldtensor:

$$\boldsymbol{F}_{\mu\nu} := \frac{i}{g}[D_\mu, D_\nu]\mathbf{1} \tag{6.20}$$

$$\begin{aligned} D_\mu D_\nu X = {} & \partial_\mu \partial_\nu \mathbf{1} X - ig\boldsymbol{T}_a[\partial_\mu(G_{\nu(a)}X) + G_{\mu(a)}(\partial_\nu X)] \\ & - g^2 \boldsymbol{T}_a \boldsymbol{T}_b G_{\mu(a)} G_{\nu(b)} X \end{aligned} \tag{6.21}$$

$$\begin{aligned} = {} & \partial_\mu \partial_\nu X - ig\boldsymbol{T}_a[(\partial_\mu G_{\nu(a)})X + G_{\nu(a)}(\partial_\mu X) + G_{\mu(a)}(\partial_\nu X)] \\ & - g^2 \boldsymbol{T}_a \boldsymbol{T}_b G_{\mu(a)} G_{\nu(b)} X \\ D_\mu D_\nu 1 = {} & - ig\boldsymbol{T}_a(\partial_\mu G_{\nu(a)}) - g^2 \boldsymbol{T}_a \boldsymbol{T}_b G_{\mu(a)} G_{\nu(b)} \end{aligned}$$

Mit (6.21) ergibt (6.20):

$$\begin{aligned}\boldsymbol{F}_{\mu\nu} &= (\partial_\mu G_{\nu(a)} - \partial_\nu G_{\mu(a)})\boldsymbol{T}_a - igG_{\mu(a)}G_{\nu(b)}[\boldsymbol{T}_a, \boldsymbol{T}_b] \\ &= (\partial_\mu G_{\nu(a)} - \partial_\nu G_{\mu(a)})\boldsymbol{T}_a + g \cdot f_{abc}G_{\mu(a)}G_{\nu(b)}\boldsymbol{T}_c\end{aligned} \tag{6.22}$$

mit

$$\boldsymbol{F}_{\mu\nu} = F_{\mu\nu(a)}\boldsymbol{T}_a$$

und den Komponenten ($f_{abc} = f_{bca} = f_{cab}$)

$$F_{\mu\nu(a)} = (\partial_\mu G_{\nu(a)} - \partial_\nu G_{\mu(a)}) + g \cdot f_{abc}G_{\mu(b)}G_{\nu(c)} \tag{6.23}$$

Damit wird mit (3.1)

$$\begin{aligned}\mathcal{L}_E &= -\left[\partial_\mu G_{\nu(a)} - \partial_\nu G_{\mu(a)} + g \cdot f_{abc}G_{\mu(b)}G_{\nu(c)}\right]\left[(\partial^\mu G^\nu_{(d)} - \partial^\nu G^\mu_{(d)} + g \cdot f_{def}G^\mu_{(e)}G^\nu_{(f)}\right] \operatorname{Sp}\frac{\boldsymbol{T}_a\boldsymbol{T}_d}{2} \\ &= -\frac{1}{4}\left[\partial_\mu G_{\nu(a)} - \partial_\nu G_{\mu(a)} + g \cdot f_{abc}G_{\mu(b)}G_{\nu(c)}\right]\left[(\partial^\mu G^\nu_{(a)} - \partial^\nu G^\mu_{(a)} + g \cdot f_{aef}G^\mu_{(e)}G^\nu_{(f)}\right]\end{aligned} \tag{6.24}$$

Mit

$$\begin{aligned}D'_\mu D'_\nu &= \boldsymbol{U}D_\mu\boldsymbol{U}^+\boldsymbol{U}D_\nu\boldsymbol{U}^+ \\ &= \boldsymbol{U}D_\mu D_\nu\boldsymbol{U}^+ \\ &= \boldsymbol{U}\boldsymbol{U}^+\partial_\mu\partial_\nu + \boldsymbol{U}(\partial_\nu\boldsymbol{U}^+)\partial_\mu + \boldsymbol{U}(\partial_\mu\boldsymbol{U}^+)\partial_\nu + \boldsymbol{U}(\partial_\mu\partial_\nu\boldsymbol{U}^+) \\ &\quad + ig\boldsymbol{U}(\partial_\mu\boldsymbol{G}_\nu)\boldsymbol{U}^+ + ig\boldsymbol{U}\boldsymbol{G}_\nu(\partial_\mu\boldsymbol{U}^+) + ig\boldsymbol{U}\boldsymbol{G}_\nu\boldsymbol{U}^+\partial_\mu \\ &\quad + ig\boldsymbol{U}\boldsymbol{G}_\mu(\partial_\nu\boldsymbol{U}^+) + ig\boldsymbol{U}\boldsymbol{G}_\mu\boldsymbol{U}^+\partial_\nu \\ &\quad - g^2\boldsymbol{U}\boldsymbol{G}_\mu\boldsymbol{G}_\nu\boldsymbol{U}^+ \\ D'_\mu D'_\nu 1 &= \boldsymbol{U}(\partial_\mu\partial_\nu\boldsymbol{U}^+) \\ &\quad + ig\boldsymbol{U}(\partial_\mu\boldsymbol{G}_\nu)\boldsymbol{U}^+ + ig\boldsymbol{U}\boldsymbol{G}_\nu(\partial_\mu\boldsymbol{U}^+) \\ &\quad + ig\boldsymbol{U}\boldsymbol{G}_\mu(\partial_\nu\boldsymbol{U}^+) \\ &\quad - g^2\boldsymbol{U}\boldsymbol{G}_\mu\boldsymbol{G}_\nu\boldsymbol{U}^+ \\ D'_\nu D'_\mu 1 &= \boldsymbol{U}(\partial_\mu\partial_\nu\boldsymbol{U}^+) \\ &\quad + ig\boldsymbol{U}(\partial_\nu\boldsymbol{G}_\mu)\boldsymbol{U}^+ + ig\boldsymbol{U}\boldsymbol{G}_\mu(\partial_\nu\boldsymbol{U}^+) \\ &\quad + ig\boldsymbol{U}\boldsymbol{G}_\nu(\partial_\mu\boldsymbol{U}^+) \\ &\quad - g^2\boldsymbol{U}\boldsymbol{G}_\nu\boldsymbol{G}_\mu\boldsymbol{U}^+ \\ [D'_\mu, D'_\nu]1 &= ig\boldsymbol{U}(\partial_\mu\boldsymbol{G}_\nu - \partial_\nu\boldsymbol{G}_\mu)\boldsymbol{U}^+ \\ &\quad - g^2\boldsymbol{U}[\boldsymbol{G}_\mu, \boldsymbol{G}_\nu]\boldsymbol{U}^+\end{aligned}$$

(hier wirken die ∂ nach Anwendung der Produktregel nur auf Argumente innerhalb der Klammer) ergibt sich die Transformation der $\boldsymbol{F}_{\mu\nu}$:

$$\boldsymbol{F}'_{\mu\nu} = \boldsymbol{U}\boldsymbol{F}_{\mu\nu}\boldsymbol{U}^+ \tag{6.25}$$

als einfache Matrixmultiplikation mit $\boldsymbol{U}$ und $\boldsymbol{U}^+$. Für die Komponenten hat nur die infinitesimale Transformation eine einfache Form:

$$F'_{\mu\nu(a)} = F_{\mu\nu(a)} + f_{abc}\delta_b F_{\mu\nu(c)}$$

Transformation des Lagrangian:

$$\mathcal{L}_E(G') = \mathcal{L}_E(G) \qquad \textbf{invariant} \tag{6.26}$$

wegen (6.25) und $\operatorname{Sp} \boldsymbol{U}\boldsymbol{X}\boldsymbol{U}^{+} = \operatorname{Sp} \boldsymbol{X}$ und

$$\mathcal{L}_{YM}(\psi', G') = \mathcal{L}_{YM}(\psi, G) \qquad \textbf{invariant} \tag{6.27}$$

Die Euler-Lagrange-Gleichung

$$\frac{\partial \mathcal{L}}{\partial G_{\nu(a)}} = \frac{\mathrm{d}}{\mathrm{d}x^{\mu}} \frac{\partial \mathcal{L}}{\partial(\partial_{\mu} G_{\nu(a)})}$$

für den vollständigen Yang-Mills-Lagrangian $\mathcal{L}_{YM}$ ergibt

$$\bar{\psi}(g\gamma^{\mu}\boldsymbol{T}_a)\psi + \partial^{\mu} F_{\mu\nu(a)} + g f_{abc} G^{\mu}_{(b)} F_{\mu\nu(c)} = 0 \tag{6.28}$$

Dabei bezeichnet der Term $\bar{\psi}(g\gamma^{\mu}\boldsymbol{T}_a)\psi$ die Ladungsstromdichte, also die Quelle des Feldes. Zur Herleitung schreibt man

$$\mathcal{L}_E = -\frac{1}{4}\left[F_{(a)\mu\nu}\right]\left[\partial^{\mu} G^{\nu}_{(a)} - \partial^{\nu} G^{\mu}_{(a)} + g \cdot f_{abc} G^{\mu}_{(b)} G^{\nu}_{(c)}\right] = -\frac{1}{4}\left[F_{(b)\mu\nu}\right]\left[\partial^{\mu} G^{\nu}_{(b)} - \partial^{\nu} G^{\mu}_{(b)} - g \cdot f_{abc} G^{\mu}_{(a)} G^{\nu}_{(c)}\right]$$

und beachtet die Symmetrie der beiden [ ]-Terme und $F_{\mu\nu} = -F_{\nu\mu}$.

6.2.7 Massenterme

Massenterme nach (4.68) der Form

$$\mathcal{L}_M = \tfrac{1}{2} M_a^2 G^{\mu}_{(a)} G_{\mu(a)} \operatorname{Sp}(\boldsymbol{T}_a^2)$$

sind nicht eichinvariant:

$$\begin{aligned}
\mathcal{L}_M(G') &= \tfrac{1}{2}\boldsymbol{M}^2 \operatorname{Sp}(\boldsymbol{U}\boldsymbol{G}^{\mu}\boldsymbol{U}^{+} + \frac{1}{ig}\boldsymbol{U}\partial^{\mu}\boldsymbol{U}^{+})(\boldsymbol{U}\boldsymbol{G}_{\mu}\boldsymbol{U}^{+} + \frac{1}{ig}\boldsymbol{U}\partial_{\mu}\boldsymbol{U}^{+}) \\
&= \tfrac{1}{2}\boldsymbol{M}^2 \left[\operatorname{Sp} \boldsymbol{G}^{\mu}\boldsymbol{G}_{\mu} + \frac{1}{ig}\operatorname{Sp}[\boldsymbol{U}\boldsymbol{G}^{\mu}\partial_{\mu}\boldsymbol{U}^{+} + (\partial^{\mu}\boldsymbol{U}^{+})\boldsymbol{U}\boldsymbol{G}_{\mu}] - \frac{1}{g^2}\operatorname{Sp}(\boldsymbol{U}\partial^{\mu}\boldsymbol{U}^{+})(\boldsymbol{U}\partial_{\mu}\boldsymbol{U}^{+})\right]
\end{aligned}$$

Wegen (3.1) sind für $\mathbf{SU(n)}$-Symmetrien in einer Massenmatrix

$$\begin{aligned}
\mathcal{L}_M &= \tfrac{1}{2}\boldsymbol{M}^2 \operatorname{Sp} \boldsymbol{G}^{\mu}\boldsymbol{G}_{\mu} \\
&= \tfrac{1}{2} M_{ab}^2 G^{\mu}_{(a)} G_{\mu(b)} \operatorname{Sp}(\boldsymbol{T}_a\boldsymbol{T}_b)
\end{aligned}$$

nur die Diagonalelemente relevant, und die globale Symnmetrie erfordert gleiche Masse für alle Eichbosonen, $\boldsymbol{M} = m_g\mathbf{1}$.

Beispiel für abelsche Gruppen:

$$\begin{aligned}
\mathcal{L}_M(G') &= \tfrac{1}{2} M^2 \operatorname{Sp}[G^{\mu}_{(a)}\boldsymbol{U}\boldsymbol{T}_a\boldsymbol{U}^{+} + \frac{1}{g}\partial^{\mu}\theta_a\boldsymbol{T}_a][G_{\mu(a)}\boldsymbol{U}\boldsymbol{T}_a\boldsymbol{U}^{+} + \frac{1}{g}\partial_{\mu}\theta_a\boldsymbol{T}_a] \\
&= \tfrac{1}{2} M^2 \left[G^{\mu}_{(a)} G_{\mu(a)} + 2G_{\mu(a)}\frac{1}{g}\partial^{\mu}\theta_a + \frac{1}{g^2}(\partial^{\mu}\theta_a)(\partial_{\mu}\theta_a)\right] \operatorname{Sp}(\boldsymbol{T}_a^2)
\end{aligned}$$

D. h. Eichbosonen sind **masselos**.

6.3 Spezialfall: elektromagnetisches Feld

Die QED ist eine Yang-Mills-Theorie. Im elektromagnetischen Feld mit dem Vierervektorpotenzial $A^\mu = (\Phi, \boldsymbol{A})$ und der abelschen Eichgruppe $\mathbf{U(1)}$ ist für ein geladenes Fermion mit Ladungsquantenzahl Q

$$\begin{aligned}
\boldsymbol{G}_\mu &= A_\mu \\
\boldsymbol{T} &= 1 \\
\boldsymbol{U} &= e^{i\theta(x)} \\
\boldsymbol{U}^+ &= e^{-i\theta(x)} \\
\partial_\mu \boldsymbol{U}^+ &= -ie^{-i\theta(x)}\partial_\mu\theta(x) \\
\psi' &= e^{iQ\theta(x)}\psi \\
g &= e \approx 0.3 \\
D_\mu &= \partial_\mu + iQeA_\mu \\
iD_\mu &= i\partial_\mu - QeA_\mu \\
\boldsymbol{F}_{\mu\nu} = \partial_\mu A_\nu - \partial_\nu A_\mu &= \begin{pmatrix} 0 & -E_x & -E_y & -E_z \\ E_x & 0 & -B_z & B_y \\ E_y & B_z & 0 & -B_x \\ E_z & -B_y & B_x & 0 \end{pmatrix}
\end{aligned}$$

mit

$$\alpha = \frac{e^2}{4\pi}$$

Der Feld-Lagrangian ist

$$\mathcal{L}_E = -\tfrac{1}{4}F^{\mu\nu}F_{\mu\nu}$$

Damit wird die Dirac-Gleichung 6.16 für ein Elektron ($Q = -1$) zu:

$$(\gamma^\mu(i\partial_\mu + eA_\mu) - m)\,\psi = 0 \tag{6.29}$$

mit dem Kopplungsterm (4.63). Die entsprechende Gleichung für das Positron ist

$$(\gamma^\mu(i\partial_\mu - eA_\mu) - m)\,\psi_C = 0 \tag{6.30}$$

Die Euler-Lagrange-Gleichung (6.28) ist die Maxwell-Gleichung

$$eQ\bar{\psi}\gamma^\mu\psi + \partial^\mu F_{\mu\nu} = 0$$

Eichtransformation $U(x) = e^{i\theta(x)}$ und

$$A'_\mu = A_\mu - \frac{1}{e}\partial_\mu\theta(x)$$

Massenterme sind auch hier nicht eichinvariant:

$$\begin{aligned}
\mathcal{L}_M(A) &= M^2 A^\mu A_\mu \\
\mathcal{L}_M(A') &= \mathcal{L}_M(A) + 2A_\mu\partial^\mu\theta + (\partial^\mu\theta)(\partial_\mu\theta)
\end{aligned}$$

aber das Photon ist masselos ($M = 0$).

6.4 Wechselwirkungen und Feynmandiagramme

Wechselwirkungen sind Streureaktionen und Zerfälle.

Man beschreibt sie durch die *Quantenfeldtheorie*. Die Quantenfeldtheorie der elektromagnetischen Wechselwirkung ist die *Quantenelektrodynamik* (QED).

Die Berechnung durch Störungsrechnung lässt sich graphisch darstellen: die *Feynmandiagramme* sind Graphen, deren Beitrag mit zunehmender Komplexität geringer wird.

In der Quantenmechanik sind wir gewohnt, Teilaspekte der Natur durch einfache Bilder zu beschreiben, wie im Teilchenbild oder im Wellenbild. In diesem Sinn stellen die Feynman-Graphen Beiträge zur Gesamtamplitude eines Prozesses im Teilchenbild dar. Berechnet werden sie aber im Wellenbild (ebene Wellen = Impulszustände).

6.4.1 Feynmanregeln der QED

für ein Matrixelement $-i\mathcal{M}$

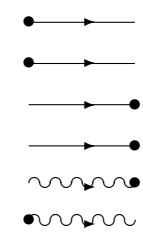

$\bar{u}(\boldsymbol{p})$	auslaufendes Fermion
$\bar{v}(\boldsymbol{p})$	einlaufendes Antifermion
$u(\boldsymbol{p})$	einlaufendes Fermion
$v(\boldsymbol{p})$	auslaufendes Antifermion
$\varepsilon_\mu(\boldsymbol{k})$	einlaufendes Photon
$\varepsilon^*_\mu(\boldsymbol{k})$	auslaufendes Photon

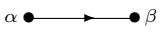

$\dfrac{i}{\not{q}-m} = i\,\dfrac{\not{q}+m}{q^2-m^2}{}_{\beta\alpha}$	inneres Fermion
$\dfrac{-ig^{\mu\nu}}{q^2}$	inneres Photon

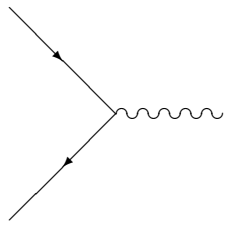

$iQe\gamma_\mu$	Photon-Fermion-Vertex

Für jeden Vertex hat man ein $(2\pi)^4\,\delta^4(\sum p_{\text{in}} - \sum p_{\text{aus}})$, wobei die Impulsrichtung virtueller Teilchen im Diagramm beliebig konsistent festgelegt werden kann.

Aber: innere Fermionlinien haben Impuls in Pfeilrichtung, und Spinorindices „entgegen“ der Pfeilrichtung, d. h. sie tragen Impuls vom Vertex rechts zum Vertex links im Matrixelement.

Über alle Impulse innerer Linien steht im **Matrixelement** ein

$$\int \mathrm{d}^4 q(\ldots)$$

Die meisten Integrale eliminieren die Deltafunktionen, pro Loop bleibt ein nichttriviales Integral.

Die Kopplungskonstante ist mit

$$\alpha = \frac{e^2}{4\pi} = \frac{1}{137.036}$$

$e = 0.3028$ (bei $q^2 = 0$).

6.5 Gebrauch der Spinoren

Ein Spinor im Operatorraum (Erzeugungs- und Vernichtungsoperatoren)

ψ_L = vernichtet ein linkshändiges Fermion / erzeugt ein rechtshändiges Antifermion
ψ_R = vernichtet ein rechtshändiges Fermion / erzeugt ein linkshändiges Antifermion
$\bar{\psi}_L$ = erzeugt ein linkshändiges Fermion / vernichtet ein rechtshändiges Antifermion
$\bar{\psi}_R$ = erzeugt ein rechtshändiges Fermion / vernichtet ein linkshändiges Antifermion

u = einlaufendes Fermion
$\bar{u}$ = auslaufendes Fermion
v = auslaufendes Antifermion
$\bar{v}$ = einlaufendes Antifermion
$u_L = O_L u$ = einlaufendes linkshändiges Fermion
$\bar{u}_L = \bar{u} O_R = \overline{O_L u}$ = auslaufendes linkshändiges Fermion
$v_L = O_L v$ = auslaufendes rechtshändiges Antifermion
$\bar{v}_L = \bar{v} O_R = \overline{O_L v}$ = einlaufendes rechtshändiges Antifermion

Beispiele: Zerfall eines Skalars ϕ in Fermion-Antifermion

$\phi \bar{u}_L v_R + \phi \bar{u}_R v_L$ 

Zerfall eines Vektors A^μ in Fermion-Antifermion

$A^\mu \bar{u}_L \gamma_\mu v_L + A^\mu \bar{u}_R \gamma_\mu v_R$ 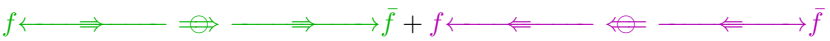

Streuung eines Skalars ϕ an einem Fermion

$\phi \bar{u}_L u_R \phi$ 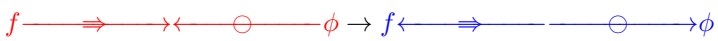

6.6 Zerfälle

$\lambda = \Gamma$ ist die Zerfallswahrscheinlichkeit pro Zeiteinheit. Zerfallswahrscheinlichkeit in der Zeit $\mathrm{d}t$: $dP = \lambda \cdot \mathrm{d}t$

$\Longrightarrow$ Zerfallsgesetz:

$$N(t) = N(0) \cdot e^{-\lambda \cdot t} \tag{6.31}$$

Zerfallsrate:

$$\lambda = 1/\tau \quad (\tau = \textstyle\int_0^\infty t e^{-\lambda t}\,\mathrm{d}t = \text{mittl. Lebensdauer})$$

Zusammenhang mit Übergangswahrscheinlichkeit in Ebene-Wellen-Endzustände (Fermi's Goldene Regel)

$$\mathrm{d}\Gamma = \frac{1}{2m} \cdot |\overline{\mathcal{M}}|^2 \,\mathrm{dPS}$$

dabei ist m die Masse des zerfallenden Teilchens, und PS = phase space „der Phasenraum“, oder präziser die Zustandsdichte im Phasenraum.

6.6.1 Zerfall quantenmechanisch betrachtet

Im Ruhesystem eines Teilchens erfüllt seine Wellenfunktion die zeitabhängige Schrödingergleichung

$$i \cdot \hbar \cdot \partial_t \psi = H \cdot \psi = mc^2 \cdot \psi \tag{6.32}$$

oder mit $\hbar = c = 1$:

$$i\partial_t \psi = m\psi$$

Lösung:

$$\psi(t) = e^{-imt} \tag{6.33}$$

und

$$|\psi(t)|^2 = 1 \tag{6.34}$$

Die Wahrscheinlichkeit, ein Teilchen zur Zeit t anzutreffen ist genauso groß wie zur Zeit 0.

Ist das Teilchen instabil, so wird $|\psi(t)|^2$ eine Funktion der Zeit sein, welche dem Zerfallsgesetz entspricht

$$|\psi(t)|^2 = e^{-\lambda \cdot t} \tag{6.35}$$

Für ψ finden wir dann die Form einer gedämpften Schwingung

$$\psi(t) = e^{-(\lambda/2+im)\cdot t} \tag{6.36}$$

Fouriertransformierte:

$$\begin{aligned} \Psi(E) &= \int_0^\infty \psi(t) \cdot e^{iEt}\,\mathrm{d}t \\ &= \int e^{-[\lambda/2+i\cdot(m-E)]t}\,\mathrm{d}t \\ &= \frac{-1}{i(E-m)-\lambda/2} \cdot \Big[e^{\cdots}\Big]_0^\infty \end{aligned} \tag{6.37}$$

Für $t = \infty$ macht die e-Funktion alles zu Null

$$\Psi(E) = \frac{1}{i(E-m)-\lambda/2} \tag{6.38}$$

und für das Betragsquadrat

$$|\Psi(E)|^2 = \frac{1}{(E-m)^2 + (\lambda/2)^2} \tag{6.39}$$

$|\Psi(E)|^2$ = Wahrscheinlichkeit, mit der die Energie E im Zustand Ψ vorkommt.

Die Funktion (6.39) heißt *Breit-Wigner*-Funktion. Sie hat zwei Parameter, die Breite Γ auf halber Höhe (FWHM) und den Energiewert E_0, bei welchem das Maximum liegt. Normierte Breit-Wigner-Verteilung:

$$B(x) = \frac{\Gamma}{2\pi} \cdot \frac{1}{(x-E_0)^2 + (\Gamma/2)^2} \tag{6.40}$$

$$\int B(x)\,\mathrm{d}x = 1$$

Durch Vergleich sehen wir:

$$\Gamma = \lambda = 1/\tau \tag{6.41}$$

$$\text{und} \qquad E_0 = m$$

Beispiel: Das Υ-Meson ($m_\Upsilon = 9460\,\mathrm{MeV}$) hat eine Breite $\Gamma = 0.042\,\mathrm{MeV} \implies \tau \approx 1.6 \cdot 10^{-20}\,\mathrm{s}$.

$\Gamma =$	$1\,\mathrm{GeV}$	$1\,\mathrm{MeV}$	$1\,\mathrm{keV}$	$1\,\mathrm{eV}$	$1\,\mathrm{meV}$	$1\,\mu\mathrm{eV}$	$1\,\mathrm{neV}$
$\tau \approx$	$\frac{2}{3}\cdot 10^{-24}\,\mathrm{s}$	$\frac{2}{3}\cdot 10^{-21}\,\mathrm{s}$	$\frac{2}{3}\cdot 10^{-18}\,\mathrm{s}$	$\frac{2}{3}\cdot 10^{-15}\,\mathrm{s}$	$\frac{2}{3}\cdot 10^{-12}\,\mathrm{s}$	$\frac{2}{3}\cdot 10^{-9}\,\mathrm{s}$	$\frac{2}{3}\cdot 10^{-6}\,\mathrm{s}$

6.7 Der Phasenraum

Den (nichtrelativistischen) Phasenraum erhält man als Integral über $\mathrm{d}x\,\mathrm{d}y\,\mathrm{d}z\,\mathrm{d}p_x\,\mathrm{d}p_y\,\mathrm{d}p_z$. Das Phasenraumvolumen ist gequantelt in Einheiten h^3 oder in natürlichen Einheiten ($\hbar = 1$) $(2\pi)^3$ (Beispiel unendlich hoher Potenzialtopf), die Anzahl möglicher Zustände ist daher dem Phasenraumvolumen proportional.

Da Wellenfunktionen zu festen Impulsen verwendet werden, also ebene Wellen, ist das Volumen V stets unendlich. Solche Wellenfunktionen sind nicht normierbar, aber $|\Psi|^2$ ist überall im Raum konstant. Daher wird das Integral über dem Volumen als ausgeführt betrachtet (womit man das Problem der Normierung umgeht), und es bleibt als Phasenraum lediglich der Impulsraum.

In kovarianter Verallgemeinerung ist

$$\mathrm{dPS} = \frac{1}{(2\pi)^3}\delta(p_\mu p^\mu - m^2)\,\mathrm{d}^4p\,\Theta(p^0) = \frac{\mathrm{d}^3p}{(2\pi)^3 2E} \tag{6.42}$$

Der Faktor $\Theta(p^0)$ garantiert positive Energie. Eine ebene Welle $\Psi(x) = \sqrt{\frac{1}{V}}e^{-ik_\mu x^\mu}$ im Volumen V (mit $\lim_{V\to\infty}$) hat die Viererstromdichte

$$j^\mu = i(\Psi^*\partial^\mu\Psi - \Psi\partial^\mu\Psi^*) = \frac{2}{V}k^\mu \tag{6.43}$$

Der Faktor E in der Dichte $\rho = j^0 = 2E/V$ kompensiert die Lorentzkontraktion des Volumens V bei einem Boost. Setzt man $\rho = |\tilde{\Psi}|^2$, so muß man die Normierung $\tilde{\Psi}(x^\mu) = \sqrt{\frac{2k^0}{V}}e^{-ik_\mu x^\mu}$ wählen.

In dieser Beschreibung ist kein Spin berücksichtigt; die analoge Beschreibung für Spin-$\frac{1}{2}$-Fermionen haben wir bereits in (4.36) und (4.24) kennengelernt.

6.7.1 Lorentzinvarianter Phasenraum (L.I.P.S.) für n Teilchen

n freie Teilchen

$$\mathrm{dPS} = \frac{1}{(2\pi)^{3n}}\prod_1^n \delta(p_\mu p^\mu - m^2)\Theta(p^0)\,\mathrm{d}^4p \tag{6.44}$$

n Teilchen aus Anfangszustand mit Viererimpuls p_in (Die Viererimpulserhaltung wird aber oft auch zu $\mathcal{M}|^2$ gerechnet):

$$\mathrm{dPS} = \frac{1}{(2\pi)^{3n-4}}\prod_1^n \delta(p_\mu p^\mu - m^2)\Theta(p^0)\,\mathrm{d}^4p\cdot\delta^4(\sum p - p_\mathrm{in}) \tag{6.45}$$

$$\mathrm{PS} = \int \mathrm{dPS} \tag{6.46}$$

Dimension: $3n-4$
Einheit: GeV^{2n-4}

$$\begin{aligned}
\delta(p_\mu p^\mu - m^2)\,\Theta(p^0)\,\mathrm{d}^4p &= \mathrm{d}^3p/2E && (6.47a)\\
&= p^2/2E\,\mathrm{d}p\,\mathrm{d}\Omega && (6.47b)\\
&= p/2\,\mathrm{d}E\,\mathrm{d}\Omega && (6.47c)\\
&= p_\perp/2E\,\mathrm{d}p_\parallel\,\mathrm{d}p_\perp\,\mathrm{d}\phi && (6.47d)\\
&= 1/4E\,\mathrm{d}p_\parallel\,\mathrm{d}p_\perp^2\,\mathrm{d}\phi && (6.47e)\\
&= 1/4\,\mathrm{d}y\,\mathrm{d}p_\perp^2\,\mathrm{d}\phi && (6.47f)
\end{aligned}$$

mit $\mathrm{d}p_\perp^2 = \mathrm{d}m_\perp^2$ und $\mathrm{d}\Omega = \mathrm{d}\xi\,\mathrm{d}\phi = \sin\theta\,\mathrm{d}\theta\,\mathrm{d}\phi$ $(\xi := \cos\theta)$

Herleitung (6.47a):

$$\begin{aligned}\delta(p^2 - m^2)\,\Theta(p^0)\,\mathrm{d}^4p &= \delta(E^2 - \boldsymbol{p}^2 - m^2)\,\Theta(E)\,\mathrm{d}E\,\mathrm{d}^3p \\ &= \delta(E^2 - \boldsymbol{p}^2 - m^2)\frac{\mathrm{d}E^2}{2E}\,\mathrm{d}^3p \\ &= \frac{1}{2E}\,\mathrm{d}^3p\end{aligned}$$

Die Energie wird von 0 bis ∞ integriert, es wird beim Übergang zu E^2 nur ein Parabel-Ast verwendet (sonst hätte man einen zusätzlichen Faktor 2). Formal ist das von Anfang an in (6.42) durch die Heaviside-Funktion $\Theta(p^0)$ berücksichtigt.

6.7.2 2-Körper-Phasenraum

$$\begin{aligned}\mathrm{dPS} &= \frac{1}{(2\pi)^2}\,\delta^4(p_\mathrm{in} - p_1 - p_2)\,\delta(p_1^2 - m_1^2)\,\delta(p_2^2 - m_2^2)\Theta(p_1^0)\Theta(p_2^0)\,\mathrm{d}^4p_1\,\mathrm{d}^4p_2 \\ &= \frac{1}{(2\pi)^2}\,\delta\big((p_\mathrm{in} - p_2)^2 - m_1^2\big)\,\frac{\mathrm{d}^3p_2}{2E_2}\end{aligned}$$

im CMS mit $p_\mathrm{in} = (W, \mathbf{0})$, $p_2 = (E_2, \boldsymbol{p})$ und $(p_\mathrm{in} - p_2)^2 = W^2 - 2E_2W + m_2^2$:

$$\begin{aligned}&= \frac{1}{(2\pi)^2}\,\delta(W^2 + m_2^2 - m_1^2 - 2E_2W)\,\frac{p\,\mathrm{d}E_2\,\mathrm{d}\Omega}{2} \\ &= \frac{p}{16\pi^2 W}\,\mathrm{d}\Omega\end{aligned} \tag{6.48}$$

$(W = \sqrt{s})$

Bei konstantem Matrixelement (isotroper Zerfall):

$$\mathrm{PS} = \int \mathrm{dPS} = p/4\pi W \tag{6.49}$$

$$\begin{aligned}p = p_\mathrm{CMS} &= \sqrt{\frac{(m_1^2 - m_2^2)^2 - 2s(m_1^2 + m_2^2) + s^2}{4s}} \\ &= \sqrt{\frac{[s - (m_1 - m_2)^2]\cdot[s - (m_1 + m_2)^2]}{4s}}\end{aligned} \tag{6.50}$$

mit $s = W^2$. Falls $m_1 = m_2 = m$:

$$p = \frac{1}{2}\sqrt{s - 4m^2} \tag{6.51}$$

Kinematik im Zweikörper-Zerfall:

$M \to m_1 + m_2$, Impuls- und Energieerhaltung im Schwerpunktsystem $(W = M)$:

$$\begin{aligned}p_1 &= (E_1, \boldsymbol{p}) \\ p_2 &= (E_2, -\boldsymbol{p}) \\ p_1 + p_2 &= (M, \mathbf{0}) \\ (p_1 - p_2)\cdot(p_1 + p_2) = (E_1 - E_2)M &= p_1^2 - p_2^2 = m_1^2 - m_2^2\end{aligned}$$

$$
\begin{aligned}
\Longrightarrow \qquad E_1 - E_2 &= \frac{m_1^2 - m_2^2}{M} \\
E_1 + E_2 &= M \\
\Longrightarrow \qquad E_1 &= \frac{M^2 + m_1^2 - m_2^2}{2M} = \frac{M}{2}\left[1 + \frac{m_1^2 - m_2^2}{M^2}\right] \\
E_2 &= \frac{M^2 + m_2^2 - m_1^2}{2M} = \frac{M}{2}\left[1 - \frac{m_1^2 - m_2^2}{M^2}\right] \\
\boldsymbol{p}^2 &= E_1^2 - m_1^2 \\
&= E_2^2 - m_2^2 \\
&= \frac{[M^2 - (m_1 - m_2)^2][M^2 - (m_1 + m_2)^2]}{4M^2} \\
|\boldsymbol{p}| &= \frac{M}{2}\sqrt{\left[1 - \left(\frac{m_1 - m_2}{M}\right)^2\right]\left[1 - \left(\frac{m_1 + m_2}{M}\right)^2\right]}
\end{aligned}
$$

Spezialfälle:

$m_1 = m$, $m_2 = 0$:

$$E_1 = (M^2 + m^2)/2M, \qquad E_2 = p = (M^2 - m^2)/2M$$

$m_1 = m_2 = m$:

$$E_1 = E_2 = M/2, \qquad p = \sqrt{M^2 - 2m^2}/2$$

6.7.3 3-Körper-Phasenraum

$$
\begin{aligned}
\mathrm{dPS} &= \frac{1}{(2\pi)^5}\delta^4(p_{\mathrm{in}} - p_1 - p_2 - p_3)\,\delta(p_1^2 - m_1^2)\,\delta(p_2^2 - m_2^2)\,\delta(p_3^2 - m_3^2)\,\mathrm{d}^4p_1\,\mathrm{d}^4p_2\,\mathrm{d}^4p_3 \\
&= \frac{1}{(2\pi)^5}\delta\big((p_{\mathrm{in}} - p_2 - p_3)^2 - m_1^2\big)\,\frac{\mathrm{d}^3p_2}{2E_2}\,\frac{\mathrm{d}^3p_3}{2E_3}
\end{aligned}
\tag{6.52}
$$

im CMS mit $p_{\mathrm{in}} = (W, \mathbf{0})$, $p_2 = (E_2, \boldsymbol{p}_2)$, $p_3 = (E_3, \boldsymbol{p}_3)$ ist

$$
\begin{aligned}
p_1^2 &= (p_{\mathrm{in}} - p_2 - p_3)^2 \\
&= W^2 - 2E_2W - 2E_3W + m_2^2 + m_3^2 + 2E_2E_3 - 2|\boldsymbol{p}_2||\boldsymbol{p}_3|\cos\theta_{23}
\end{aligned}
$$

damit wird

$$
\begin{aligned}
\mathrm{dPS} &= \frac{1}{(2\pi)^5}\delta(\ldots - 2|\boldsymbol{p}_2||\boldsymbol{p}_3|\cos\theta_{23})\,\frac{|\boldsymbol{p}_2|\,\mathrm{d}E_2\,\mathrm{d}\Omega_2}{2}\,\frac{|\boldsymbol{p}_3|\,\mathrm{d}E_3\,\mathrm{d}\cos\theta_{23}\,\mathrm{d}\phi_{23}}{2} \\
&= \frac{1}{(2\pi)^5}\,\frac{dE_2\,\mathrm{d}\Omega_2\,\mathrm{d}E_3\,\mathrm{d}\phi_{23}}{8}
\end{aligned}
\tag{6.53}
$$

Integration über alle Winkel ergibt (Dalitzplot)

$$
\begin{aligned}
\mathrm{dPS} &= \frac{1}{32\pi^3}\,\mathrm{d}E_2\,\mathrm{d}E_3 \\
&= \frac{1}{64\pi^3 W}\,\mathrm{d}m_{13}^2\,\mathrm{d}E_3 \\
&= \frac{1}{128\pi^3 W^2}\,\mathrm{d}m_{13}^2\,\mathrm{d}m_{12}^2
\end{aligned}
\tag{6.54}
$$

mit $m_{12}^2 = W^2 + m_3^2 - 2WE_3$ etc.

6.8 Wirkungsquerschnitt

Die Wahrscheinlichkeit einer „Teilchen-Reaktion“ wird in der Physik als effektive Querschnittsfläche angegeben. Diese Fläche – der **Wirkungsquerschnitt** – kann dabei interpretiert werden als die tatsächliche Querschnittsfläche in folgendem Ersatz-Bild:

Man denke sich das Projektil-Teilchen als idealen Punkt, das Target-Teilchen als Fläche von der Größe des Wirkungsquerschnitts, die so ausgerichtet ist, dass das Projektil entweder auf ihr senkrecht auftrifft oder vorbeifliegt. Die betrachtete Reaktion findet dann beim Auftreffen **immer**, beim Vorbeifliegen **nie** statt.

Fig. 6.1 Streuquerschnitt zweier Billardkugeln

Was ist dann der Wirkungsquerschnitt für die Streuung (= Streuquerschnitt) zweier Billardkugeln vom Radius r, die – ausnahmsweise – frei durch den Raum fliegen (Fig. 6.1)? Die Streuung findet offensichtlich genau dann statt, wenn die Kugelmittelpunkte in einem Abstand $d \leq 2r$ aneinander vorbeifliegen. Die gleiche Streuwahrscheinlichkeit haben aber ein Punkt und eine zur Flugrichtung senkrechte Scheibe vom Radius $2r$. Also ist der Streuquerschnitt

$$\sigma = \pi \cdot (2r)^2 = 4\pi r^2$$

Als zweites Beispiel betrachten wir den Wirkungsquerschnitt für die Absorption (= Absorptionsquerschnitt) eines Photons in einem „grauen“ Glasplättchen von $1\,\mathrm{cm}^2$ Fläche. Wenn das Glasplättchen genau 70% des Lichts durchlässt, ist die Absorptionswahrscheinlicheit genauso groß wie bei einem schwarzen Plättchen mit 30% der Querschnittsfläche. Also ist der Absorptionsquerschnitt

$$\sigma = 30\% \cdot 1\,\mathrm{cm}^2 = 0.3\,\mathrm{cm}^2$$

Allgemein gilt für einen beliebigen Reaktionsquerschnitt

$$\sigma = \int P(x,y)\,\mathrm{d}x\,\mathrm{d}y$$

wobei $P(x,y)$ die Reaktionswahrscheinlichkeit ist, falls die Gerade, längs der sich der Schwerpunkt des Projektils vor der Reaktion bewegt, die zu ihr senkrechte Ebene durch den Schwerpunkt des Targets an der Stelle (x,y) schneidet.

6.8.1 Messtechnische Definition

Die Wahrscheinlichkeit, dass ein Projektil mit einem Target wechselwirkt, ist

$$P = \frac{\mathrm{d}n_{\mathrm{Targ}}}{\mathrm{d}A} \cdot \sigma = \rho \cdot d \cdot \sigma$$

wobei ρ die (Anzahl-)Dichte der Targetteilchen ist, d die Dicke des Target (d. h. ρd ist die Targetflächendichte $\mathrm{d}n_{\mathrm{Targ}}/\,\mathrm{d}A$) und σ der Wirkungsquerschnitt. Bei einem einfallenden Projektilstrom

$$J = \frac{\mathrm{d}n_{\mathrm{Proj}}}{\mathrm{d}t}$$

ist die Zahl der Wechselwirkungen pro Zeit

$$\dot{N} = \frac{\mathrm{d}n_{\mathrm{Targ}}\,\mathrm{d}n_{\mathrm{Proj}}}{\mathrm{d}A\,\mathrm{d}t}\sigma = J\rho d\,\sigma \tag{6.55}$$

Alternativ, wenn der Fluss der Projektile das ganze Target überstreicht, ist

$$\dot{N} = \frac{n_{\mathrm{Targ}}\,\mathrm{d}^2 n_{\mathrm{Proj}}}{\mathrm{d}A\,\mathrm{d}t}\sigma = \Phi\, n_{\mathrm{Targ}}\,\sigma \tag{6.56}$$

mit dem Fluss

$$\Phi = \frac{\mathrm{d}^2 n_{\mathrm{Proj}}}{\mathrm{d}A\,\mathrm{d}t}$$

und der Gesamtzahl n_{Targ} der Targetteilchen.

6.8.2 Luminosität

$$L := \dot{N}/\sigma \tag{6.57}$$

$$L = \int j(x,y)\cdot a(x,y)\,\mathrm{d}x\,\mathrm{d}y \tag{6.58}$$

j = Teilchenstromdichte (Strahl),
a = Target-Teilchen-Flächendichte

Beam-Target (6.55)

$$L = J\cdot\rho\cdot d \tag{6.59}$$

J = Teilchenstrom (Strahlteilchen pro Zeiteinheit),
ρ = Target-Teilchendichte
d = Target-Dicke

Beam-Beam: 2 **einzelne** ellipsoidale Bunche mit allseitig Gaußschem Dichteprofil

$$f(x,y,z) = \frac{1}{\sqrt{2\pi}^3\sigma_x\sigma_y\sigma_z} e^{-\frac{x^2}{2\sigma_x^2}} e^{-\frac{y^2}{2\sigma_y^2}} e^{-\frac{(z\pm ct)^2}{2\sigma_z^2}}$$

und $N_{1,2}$ Teilchen. Dabei ist c die Geschwindigkeit und σ_z die RMS-Länge **im Laborsystem**. Kollision der Bunchmitten bei $x = y = z = t = 0$, (scheinbare) Relativgeschwindigkeit $2c$:

$$\begin{aligned}
L &= \iiint 2cN_1 f_1(x,y,z) N_2 f_2(x,y,z)\,\mathrm{d}x\,\mathrm{d}y\,\mathrm{d}z \\
&= \frac{2cN_1N_2}{(2\pi)^3\sigma_x^2\sigma_y^2\sigma_z^2}\int e^{-\frac{2x^2}{2\sigma_x^2}}\,\mathrm{d}x \int e^{-\frac{2y^2}{2\sigma_y^2}}\,\mathrm{d}y \int e^{-\frac{(z-ct)^2}{2\sigma_z^2}} e^{-\frac{(z+ct)^2}{2\sigma_z^2}}\,\mathrm{d}z \\
&= \frac{2cN_1N_2}{(2\sqrt{\pi})^3\sigma_x\sigma_y\sigma_z} e^{-\frac{(ct)^2}{\sigma_z^2}} \\
&= \frac{N_1N_2}{4\pi\sigma_x\sigma_y}\frac{c}{\sqrt{\pi}\sigma_z} e^{-\frac{(ct)^2}{\sigma_z^2}}
\end{aligned}$$

integriert über alle Zeiten (= Beitrag eines Bunches)

$$L_{\mathrm{int,b}} = \frac{N_1N_2}{4\pi\sigma_x\sigma_y}$$

Die Verteilung der Wechselwirkungspunkte ist

$$f_{\mathrm{IP}}(x,y,z) = \frac{1}{\sqrt{\pi}^3 \sigma_x \sigma_y \sigma_z} e^{-\frac{x^2}{\sigma_x^2}} e^{-\frac{y^2}{\sigma_y^2}} e^{-\frac{z^2}{\sigma_z^2}}$$

mit jeweils auf $1/\sqrt{2}$ reduzierten RMS-Werten $\sigma_x/\sqrt{2}$, $\sigma_y/\sqrt{2}$ und $\sigma_z/\sqrt{2}$.
Für n_b Bunche im Ring und Umlauffrequenz f bzw. bunch spacing d_b ist dann

$$\begin{aligned} L &= f n_\mathrm{b} L_{\mathrm{int,b}} \\ &= \frac{c}{d_\mathrm{b}} L_{\mathrm{int,b}} \\ &= \frac{f n_\mathrm{b} N_1 N_2}{4\pi \sigma_x \sigma_y} \\ &= \frac{I_1 I_2}{4\pi e^2 \sigma_x \sigma_y f n_\mathrm{b}} \end{aligned} \tag{6.60}$$

mit I_1, I_2 = el. Strom (Beam 1 und 2).
integrierte Luminosität

$$L_{\mathrm{int}} := N/\sigma \tag{6.61}$$

6.8.3 Mandelstam-Variable

Mandelstam-Variable für $a + b \to 1 + 2$:
Schwerpunktsenergiequadrat

$$s = W^2 = \sum p^\mu_{\mathrm{in}} p_{\mu \mathrm{in}} \tag{6.62}$$

CMS:

$$s = (E_a + E_b)^2 = (E_1 + E_2)^2$$

Beam-Target:

$$s = (E_{\mathrm{Beam}} + m_{\mathrm{Target}})^2 - p^2_{\mathrm{Beam}}$$

Viererimpulsübertrag

$$\begin{aligned} t &= (p_1 - p_a)_\mu (p_1 - p_a)^\mu \\ &= (p_2 - p_b)_\mu (p_2 - p_b)^\mu \\ &= (E_1 - E_a)^2 - (\boldsymbol{p}_1 - \boldsymbol{p}_a)^2 \end{aligned}$$

$$\begin{aligned} u &= (p_2 - p_a)_\mu (p_2 - p_a)^\mu \\ &= (p_1 - p_b)_\mu (p_1 - p_b)^\mu \end{aligned}$$

$$s + t + u = m_a^2 + m_b^2 + m_1^2 + m_2^2 \tag{6.63}$$

Im Schwerpunktsystem

$$t = m_a^2 + m_1^2 - 2E_a E_1 + 2|\boldsymbol{p}_a||\boldsymbol{p}_1| \cos\theta^*$$

Sonderfall $m_a = m_b$, $m_1 = m_2$, im CMS:

$$s = 4E^2$$

mit $E = E_a = E_b = E_1 = E_2$

$$\begin{aligned} t &= (p_1 - p_a)_\mu (p_1 - p_a)^\mu \\ &= -(2E^2 - m_a^2 - m_1^2 - 2p_a^* p_1^* \cos\theta^*) \\ &= -(\boldsymbol{p}_1^* - \boldsymbol{p}_a^*)^2 \\ &\approx -2E^2(1 - \cos\theta^*) \end{aligned}$$

$$\begin{aligned} u &= (p_2 - p_a)_\mu (p_2 - p_a)^\mu \\ &= -(2E^2 - m_a^2 - m_1^2 + 2p_a^* p_1^* \cos\theta^*) \\ &= -(\boldsymbol{p}_1^* + \boldsymbol{p}_a^*)^2 \\ &\approx -2E^2(1 + \cos\theta^*) \end{aligned}$$

mit $\sphericalangle(\boldsymbol{p}_1, \boldsymbol{p}_a) = \theta^*$ (im CMS), $\boldsymbol{p}_2^* = -\boldsymbol{p}_1^*$.
In diesem Fall wird das Phasenraumelement (6.47)

$$\delta(p_\mu p^\mu - m^2)\, \mathrm{d}^4 p = \frac{p}{4E^2}\, \mathrm{d}E\, \mathrm{d}\phi\, \mathrm{d}t$$

Zweikörperphasenraum, berechnet im CMS:

$$\begin{aligned} t &= m_1^2 + m_a^2 - 2E_1 E_a + 2p_1 p_a \cos\theta \\ &= m_1^2 + m_a^2 - \frac{s}{2} + 2p_1 p_a \cos\theta \\ \mathrm{d}t &= 2p_1 p_a\, \mathrm{d}\cos\theta \\ \mathrm{dPS} &= \frac{p_1\, \mathrm{d}\phi\, \mathrm{d}\cos\theta}{16\pi^2\sqrt{s}} \\ &= \frac{\mathrm{d}\phi\, \mathrm{d}t}{32\pi^2 p_a \sqrt{s}} \end{aligned}$$

mit

$$p_a = \frac{\sqrt{\left[\sqrt{s} - (m_a - m_b)^2\right]\left[\sqrt{s} - (m_a + m_b)^2\right]}}{2}$$

Bei Isotropie in ϕ, $\int \mathrm{d}\phi = 2\pi$:

$$\mathrm{dPS} = \frac{\mathrm{d}t}{16\pi p_a \sqrt{s}} \tag{6.64}$$

6.8.4 Streuquerschnitt

Prozess: $a + b \to 1 + 2 + \ldots + n$

$$\mathrm{d}\sigma = F^{-1} \cdot S \cdot |\mathcal{M}|^2 \cdot \mathrm{dPS} \tag{6.65}$$

(Fermi's Goldene Regel)
F = Flussfaktor
S = statistischer Faktor = $1/k!$ für k identische Teilchen
$\mathcal{M}$ = Übergangsmatrixelement für $a + b \to 1 + \ldots + n$
PS = Phasenraum

$$F = 4\sqrt{(p_a^\mu p_{\mu\, b})^2 - (m_a m_b)^2} \qquad (6.66)$$
$$= 4 v_{ab} E_a E_b \qquad (v_{ab} = \text{Relativgeschw.})$$

CMS ($\vec{p} = \vec{p}_a = -\vec{p}_b$): $= 4p \cdot \sqrt{s}$ (6.67)

($m_a = m_b = m$): $= 2\sqrt{s - 4m^2} \cdot \sqrt{s}$

Beam-Target: $= 4\sqrt{E_{\text{Beam}}^2 m_{\text{Target}}^2 - m_{\text{Beam}}^2 m_{\text{Target}}^2}$

$= 4 p_{\text{Beam}} \cdot m_{\text{Target}}$

6.8.5 Produktionsquerschnitt

Formationsprozess: $a + b \to M \to 1 + 2 + \ldots + n$

Resonanz der Masse M, Breite Γ_{tot}, Spin J

$$\sigma(W) = \frac{4\pi}{W^2} \cdot \frac{2J+1}{(2J_a+1)(2J_b+1)} \cdot \frac{\Gamma(M \to ab)\Gamma(M \to 12\ldots n)}{(W-M)^2 + \Gamma_{\text{tot}}^2/4} \qquad (6.68)$$

$$\int \sigma(W)\, \mathrm{d}W = \frac{8\pi}{M^2} \cdot \frac{2J+1}{(2J_a+1)(2J_b+1)} \cdot \frac{\Gamma(M \to ab)\Gamma(M \to 12\ldots n)}{\Gamma_{\text{tot}}} \qquad (6.69)$$

Produktionsprozess: $a + b \to M + X$

6.8.6 Paarproduktion

Der Wirkungsquerschnitt für $e^+e^- \to \mu^+\mu^-$, $e^+e^- \to \tau^+\tau^-$, $e^+e^- \to q\bar{q}$ lässt sich aus der allgemeinen Formel für $l_i^+ l_i^- \to l_f^+ l_f^-$ mit elektrischen Ladungen Q_i und Q_f berechnen.

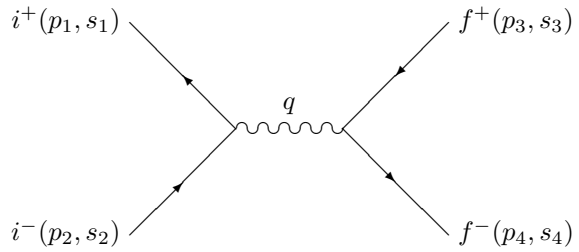

Notation: p = Energie-Impuls-Vektor, s = Spin, $u(p_i, s_i) = u_i$

Photonimpuls: $q = p_1 + p_2 = p_3 + p_4$

Feynmanregeln:

$$\begin{aligned} -i\mathcal{M} &= \bar{u}_\alpha(p_4, s_4)\, iQ_f e \gamma^\mu_{\alpha\beta}\, v_\beta(p_3, s_3) \frac{-ig_{\mu\nu}}{q^2} \bar{v}_\gamma(p_1, s_1)\, iQ_i e \gamma^\nu_{\gamma\delta}\, u_\delta(p_2, s_2) \\ &= \frac{iQ_i Q_f e^2}{q^2} \bar{u}_{4,\alpha}\, \gamma^\mu_{\alpha\beta}\, v_{3,\beta} \bar{v}_{1,\gamma}\, \gamma_{\mu,\gamma\delta}\, u_{2,\delta} \\ &= \frac{iQ_i Q_f e^2}{q^2} (\bar{u}_L \gamma^\mu\, v_L + \bar{u}_R \gamma^\mu\, v_R)_f \cdot (\bar{v}_L \gamma_\mu\, u_L + \bar{v}_R \gamma_\mu\, u_R)_i \qquad (6.70) \\ i\mathcal{M}^* &= -\frac{iQ_i Q_f e^2}{q^2} \bar{u}_{2,\epsilon}\, \gamma^\nu_{\epsilon\zeta}\, v_{1,\zeta} \bar{v}_{3,\eta}\, \gamma_{\nu,\eta\theta}\, u_{4,\theta} \end{aligned}$$

$$
\begin{aligned}
|\mathcal{M}|^2 &= (-i\mathcal{M})(i\mathcal{M}^*) \\
&= \frac{e^4 Q_i^2 Q_f^2}{q^4} \left[\bar{u}_{4,\alpha}\gamma_{\mu,\alpha\beta} v_{3,\beta} \bar{v}_{3,\eta}\gamma_{\nu,\eta\theta} u_{4,\theta} \bar{v}_{1,\gamma}\gamma^{\mu}_{\gamma\delta} u_{2,\delta} \bar{u}_{2,\epsilon}\gamma^{\nu}_{\epsilon\zeta} v_{1,\zeta}\right] \\
&= \frac{e^4 Q_i^2 Q_f^2}{q^4} \left[u_{4,\theta}\bar{u}_{4,\alpha}\gamma_{\mu,\alpha\beta} v_{3,\beta} \bar{v}_{3,\eta}\gamma_{\nu,\eta\theta} v_{1,\zeta} \bar{v}_{1,\gamma}\gamma^{\mu}_{\gamma\delta} u_{2,\delta} \bar{u}_{2,\epsilon}\gamma^{\nu}_{\epsilon\zeta}\right]
\end{aligned}
$$

6.8.6.1 Spinbetrachtung

Die Kopplung an ein Photon (Vektor γ^μ) geht nur mit einem LL- oder RR-Fermion-Antifermion-Paar. Das bedeutet im ultrarelativistischen Limit entgegengesetzte Helizität, also parallele Spins, Gesamtspin $(S, S_z) = (1, \pm 1)$ und $(S, S_{z'}) = (1, \pm 1)$ für das e^+e^--Paar im Anfangszustand und das Fermionpaar im Endzustand. Die Winkelverteilung ergibt sich daraus durch die Projektion von $(1, 1)$ auf $(1, 1)$ und $(1, -1)$ durch die Rotation um θ von z nach z'. Diese ist

$$
|d^1_{1,1}|^2 + |d^1_{1,-1}|^2 = \left(\frac{1+\cos\theta}{2}\right)^2 + \left(\frac{1-\cos\theta}{2}\right)^2 = \frac{1+\cos^2\theta}{2} \tag{6.71}
$$

Für ultrarelativistische Fermionen kann man (6.70) leicht ausrechnen. Die einlaufenden Elektronen in z-Richtung ergeben

$$
\bar{v}_L \gamma^\mu u_L = \mathcal{N}^2 \begin{pmatrix} 0 \\ 2 \\ -2i \\ 0 \end{pmatrix}
$$

$$
\bar{v}_R \gamma^\mu u_R = \mathcal{N}^2 \begin{pmatrix} 0 \\ 2 \\ 2i \\ 0 \end{pmatrix}
$$

Die auslaufenden Fermionen unter dem Winkel θ können durch eine Rotation um die y-Achse erzeugt werden:

$$
u_R = \mathcal{N} \begin{pmatrix} \cos\frac{\theta}{2} \\ -\sin\frac{\theta}{2} \\ \cos\frac{\theta}{2} \\ -\sin\frac{\theta}{2} \end{pmatrix}
$$

$$
u_L = \mathcal{N} \begin{pmatrix} \sin\frac{\theta}{2} \\ \cos\frac{\theta}{2} \\ -\sin\frac{\theta}{2} \\ -\cos\frac{\theta}{2} \end{pmatrix}
$$

$$
v_R = \mathcal{N} \begin{pmatrix} \sin\frac{\theta}{2} \\ \cos\frac{\theta}{2} \\ \sin\frac{\theta}{2} \\ \cos\frac{\theta}{2} \end{pmatrix}
$$

$$
v_L = \mathcal{N} \begin{pmatrix} -\cos\frac{\theta}{2} \\ \sin\frac{\theta}{2} \\ \cos\frac{\theta}{2} \\ -\sin\frac{\theta}{2} \end{pmatrix}
$$

$$\bar{u}_L = \mathcal{N} \begin{pmatrix} \sin\frac{\theta}{2} \\ \cos\frac{\theta}{2} \\ \sin\frac{\theta}{2} \\ \cos\frac{\theta}{2} \end{pmatrix}$$
$$\dots$$

Damit wird (Spaltenvektoren im Minkowskiraum, Gl. 4.42)

$$\bar{u}_L \gamma^\mu v_L = \mathcal{N}^2 \begin{pmatrix} 0 \\ 2\cos\theta \\ 2i \\ 2\sin\theta \end{pmatrix}$$
$$\bar{u}_R \gamma^\mu v_R = \mathcal{N}^2 \begin{pmatrix} 0 \\ 2\cos\theta \\ -2i \\ 2\sin\theta \end{pmatrix}$$

Die Produkte (LL)(LL) und (RR)(RR) ergeben Terme mit $\mathcal{M} \sim 1 + \cos\theta$. Die Produkte (LL)(RR) und (RR)(LL) ergeben Terme mit $\mathcal{M} \sim 1 - \cos\theta$.

Der spingemittelte Wirkungsquerschnitt ist

$$\frac{\mathrm{d}\sigma}{\mathrm{d}\Omega} \sim (1+\cos\theta)^2 + (1-\cos\theta)^2 = 2(1+\cos^2\theta)$$

6.8.6.2 Das exakte Matrixelement

Spinsummen (4.61):

$$\sum_{s=\pm\frac{1}{2}} u_\alpha(\boldsymbol{p}, s)\, \bar{u}_\beta(\boldsymbol{p}, s) = \not{p}_{\alpha\beta} + m\mathbf{1}_{\alpha\beta}$$
$$\sum_{s=\pm\frac{1}{2}} v_\alpha(\boldsymbol{p}, s)\, \bar{v}_\beta(\boldsymbol{p}, s) = \not{p}_{\alpha\beta} - m\mathbf{1}_{\alpha\beta}$$

$$\begin{aligned}
\frac{1}{4}\sum_{s_1,s_2}\sum_{s_3,s_4}|\mathcal{M}|^2 &= \frac{e^4 Q_i^2 Q_f^2}{4q^4}\left\{(\not{p}_4 + m_f)_{\theta\alpha}\gamma_{\mu,\alpha\beta}(\not{p}_3 - m_f)_{\beta\eta}\gamma_{\nu,\eta\theta}(\not{p}_1 - m_i)_{\zeta\gamma}\gamma^\mu_{\gamma\delta}(\not{p}_2 + m_i)_{\delta\epsilon}\gamma^\nu_{\epsilon\zeta}\right\} \\
&= \frac{e^4 Q_i^2 Q_f^2}{4q^4}\left\{\mathrm{Sp}[(\not{p}_4 + m_f)\gamma_\mu(\not{p}_3 - m_f)\gamma_\nu]\,\mathrm{Sp}[(\not{p}_1 - m_i)\gamma^\mu(\not{p}_2 + m_i)\gamma^\nu]\right\} \\
&= \frac{e^4 Q_i^2 Q_f^2}{4q^4}\left\{\mathrm{Sp}[\not{p}_4\gamma_\mu\not{p}_3\gamma_\nu - m_f^2\gamma_\mu\gamma_\nu]\,\mathrm{Sp}[\not{p}_1\gamma^\mu\not{p}_2\gamma^\nu - m_i^2\gamma^\mu\gamma^\nu]\right\} \\
&= \frac{e^4 Q_i^2 Q_f^2}{4q^4}\cdot 4[p_{4,\mu}p_{3,\nu} + p_{3,\mu}p_{4,\nu} - g_{\mu\nu}(p_3p_4) - m_f^2 g_{\mu\nu}] \\
&\qquad \cdot 4[p_1^\mu p_2^\nu + p_2^\mu p_1^\nu - g^{\mu\nu}(p_1p_2) - m_i^2 g^{\mu\nu}] \\
&= \frac{e^4 Q_i^2 Q_f^2}{4q^4}\big\{16[2(p_4p_1)(p_3p_2) + 2(p_4p_2)(p_3p_1) + 4(p_1p_2)(p_3p_4) + 4m_i^2 m_f^2 \\
&\qquad - 4(p_1p_2)(p_3p_4) + 4(p_1p_2)m_f^2 + 4(p_3p_4)m_i^2 - 2(p_1p_2)m_f^2 - 2(p_3p_4)m_i^2]\big\} \\
&= \frac{2e^4 Q_i^2 Q_f^2}{q^4}\left\{4(p_4p_1)(p_3p_2) + 4(p_4p_2)(p_3p_1) + 4(p_1p_2)m_f^2 + 4(p_3p_4)m_i^2 + 8m_i^2 m_f^2\right\}
\end{aligned}$$

Etwas Kinematik:

$$\begin{aligned} q^2 &= s \\ (p_1+p_2)^2 = (p_3+p_4)^2 &= s \\ \Longrightarrow \qquad 2p_1p_2 = s-2m_i^2, &\quad 2p_3p_4 = s-2m_f^2 \end{aligned}$$

Kinematik im CMS:

$$\begin{aligned} \boldsymbol{p}_1^* &= \boldsymbol{p}_i = -\boldsymbol{p}_2^* \\ \boldsymbol{p}_3^* &= \boldsymbol{p}_f = -\boldsymbol{p}_4^* \\ E_i = E_f &= \sqrt{s}/2 \\ p_3p_1 &= E_iE_f - p_ip_f\cos\theta = \frac{s}{4}(1-\beta_i\beta_f\cos\theta) \\ p_4p_2 &= E_iE_f - p_ip_f\cos\theta = \frac{s}{4}(1-\beta_i\beta_f\cos\theta) \\ p_4p_1 &= E_iE_f + p_ip_f\cos\theta = \frac{s}{4}(1+\beta_i\beta_f\cos\theta) \\ p_3p_2 &= E_iE_f + p_ip_f\cos\theta = \frac{s}{4}(1+\beta_i\beta_f\cos\theta) \\ |\boldsymbol{p}_i| &= \frac{\sqrt{s}}{2}\beta_i = \sqrt{\frac{s}{4}-m_i^2} \\ |\boldsymbol{p}_f| &= \frac{\sqrt{s}}{2}\beta_f = \sqrt{\frac{s}{4}-m_f^2} \end{aligned}$$

$$\begin{aligned} \frac{1}{4}\sum_{s_1,s_2}\sum_{s_3,s_4}|\mathcal{M}|^2 &= \frac{e^4Q_i^2Q_f^2}{4s^2}\big\{2s^2(1-\beta_i\beta_f\cos\theta)^2 + 2s^2(1+\beta_i\beta_f\cos\theta)^2 \\ &\qquad + 16(s-2m_f^2)^2m_f^2 + 16(s-2m_i^2)^2m_i^2 + 64m_i^2m_f^2\big\} \\ &= e^4Q_i^2Q_f^2\left\{1+\beta_i^2\beta_f^2\cos^2\theta + \frac{4m_f^2}{s} + \frac{4m_i^2}{s}\right\} \end{aligned}$$

Der spingemittelte Wirkungsquerschnitt ist mit $e^4 = \alpha^2 16\pi^2$

$$\begin{aligned} \frac{\mathrm{d}\sigma}{\mathrm{d}\Omega} &= \frac{1}{4p_i\sqrt{s}}\cdot 16\pi^2\alpha^2Q_i^2Q_f^2\left\{1+\beta_i^2\beta_f^2\cos^2\theta + \frac{4m_f^2}{s} + \frac{4m_i^2}{s}\right\}\cdot\frac{p_f}{16\pi^2\sqrt{s}} \\ &= \frac{Q_i^2Q_f^2\alpha^2}{4s}\cdot\frac{\beta_f}{\beta_i}\cdot\{1+\mu_i^2+\mu_f^2+\beta_i^2\beta_f^2\cos^2\theta\} \end{aligned}$$

mit $\mu_X = m_X/E$ ($E = \sqrt{s}/2$ = Energie von i oder f im CMS = halbe Schwerpunktsenergie). Die Geschwindigkeit (im CMS) ist

$$\beta = \sqrt{1-\mu^2} = \frac{\sqrt{(E-m)(E+m)}}{E}$$

Damit wird

$$\frac{\mathrm{d}\sigma}{\mathrm{d}\Omega} = \frac{Q_i^2Q_f^2\alpha^2}{4s}\cdot\frac{\beta_f}{\beta_i}\cdot\{3-\beta_i^2-\beta_f^2+\beta_i^2\beta_f^2\cos^2\theta\}$$

Bereits an der Schwelle zur μ-Paar-Erzeugung ist $\mu_e \lesssim 1/200$. Für $i \equiv e$ und $Q_f = 1$ ist dann

$$\frac{\mathrm{d}\sigma}{\mathrm{d}\Omega} = \frac{\alpha^2}{4s} \cdot \beta_f \cdot [2 - \beta_f^2 + \beta_f^2 \cos^2\theta] \approx \frac{\alpha^2}{4s} \cdot [1 + \cos^2\theta]$$

für $\mu_f \to 0$. Quarks haben einen zusätzlichen Statistikfaktor $N_C = 3$ für die Colour-Freiheitsgrade. Der integrierte Wirkungsquerschnitt ist[25]

$$\begin{aligned}
\sigma_0(s) &= \int_{-1}^{1} \frac{\mathrm{d}\sigma}{\mathrm{d}\Omega}\, 2\pi\, \mathrm{d}\cos\theta \\
&= \frac{4\pi\alpha^2}{3s} \cdot \beta_f \cdot \left[\frac{3}{2} - \frac{1}{2}\beta_f^2\right] \\
&\approx \frac{4\pi\alpha^2}{3s} \\
&= \frac{86.86\,\mathrm{nb\,GeV}^2}{s}
\end{aligned} \tag{6.72}$$

6.8.6.3 Kovarianter Wirkungsquerschnitt

(= bezugssystemunabhängiger Wirkungsquerschnitt)
Kinematik-Invarianten (Mandelstam-Variable):

$$\begin{aligned}
2p_3p_1 &= -(p_3 - p_1)^2 + m_f^2 + m_i^2 = m_f^2 + m_i^2 - t \\
2p_4p_2 &= m_f^2 + m_i^2 - t \\
2p_4p_1 &= 2p_3p_2 = m_f^2 + m_i^2 - u \\
2p_1p_2 &= (p_1 + p_2)^2 - 2m_i^2 = s - 2m_i^2 \\
2p_3p_4 &= s - 2m_f^2 \\
s + t + u &= 2(m_i^2 + m_f^2)
\end{aligned}$$

$$\begin{aligned}
\frac{1}{4}\sum_{s_1,s_2}\sum_{s_3,s_4} |\mathcal{M}|^2 &= \frac{2e^4Q_i^2Q_f^2}{q^4}\left\{4(p_4p_1)(p_3p_2) + 4(p_4p_2)(p_3p_1) + 4(p_1p_2)m_f^2 + 4(p_3p_4)m_i^2 + 8m_i^2m_f^2\right\} \\
&= \frac{2e^4Q_i^2Q_f^2}{s^2}\left\{(u - m_f^2 - m_i^2)^2 + (t - m_f^2 - m_i^2)^2\right. \\
&\qquad \left. + 2(s - 2m_i^2)m_f^2 + 2(s - 2m_f^2)m_i^2 + 8m_i^2m_f^2\right\} \\
&= \frac{2e^4Q_i^2Q_f^2}{s^2}\left\{u^2 + t^2 - 2(m_i^2 + m_f^2)(u + t) + 4m_i^2m_f^2\right. \\
&\qquad \left. + 2m_i^4 + 2m_f^4 + 2s(m_i^2 + m_f^2) - 8m_i^2m_f^2 + 8m_i^2m_f^2\right\} \\
&= \frac{2e^4Q_i^2Q_f^2}{s^2}\left\{s^2 + 2t^2 + 2st - 4t(m_f^2 + m_i^2) + 2(m_i^2 + m_f^2)^2\right\} \\
&= \frac{2e^4Q_i^2Q_f^2}{s^2}\left\{u^2 + t^2 - 4t(m_f^2 + m_i^2) + 2(m_i^2 + m_f^2)^2\right\}
\end{aligned}$$

[25] $(\hbar c)^2 = 389386\,\mathrm{nb\,GeV}^2$, $1\,GeV^{-2} \mathrel{\widehat{=}} 3.89386 \cdot 10^5 nb$, $\alpha = 1/137.036$

Wirkungsquerschnitt mit (6.64)

$$\begin{aligned}\frac{\mathrm{d}\sigma}{\mathrm{d}t} &= \frac{1}{4p_i\sqrt{s}}\frac{2e^4Q_i^2Q_f^2}{s^2}\left\{s^2+2t^2+2st-4t(m_f^2+m_i^2)+2(m_i^2+m_f^2)^2\right\}\frac{1}{16\pi p_i\sqrt{s}}\\ &= \frac{2\alpha^2Q_i^2Q_f^2\pi}{(s-4m_i^2)s}\left\{1+2\frac{t^2}{s^2}+2\frac{t}{s}+2\frac{(-2t+m_i^2+m_f^2)(m_f^2+m_i^2)}{s^2}\right\}\\ &\approx \frac{2\alpha^2Q_i^2Q_f^2\pi}{s^2}\left\{1+2\frac{t^2}{s^2}+2\frac{t}{s}\right\} = \frac{2\alpha^2Q_i^2Q_f^2\pi}{s^2}\cdot\frac{t^2+u^2}{s^2}\end{aligned}$$

6.8.6.4 Polarisierte Fermionen

Falls man polarisierte Strahlen streut, ist der Polarisationsvektor s^μ mit $s^\mu s_\mu = -P^2$, $s^\mu p_\mu = 0$ nicht der Nullvektor. Im Ruhesystem ist $s^\mu = (0, P_x, P_y, P_z)$ (vgl. Abschnitt 2.1).

In der $2E$-Normierung ist dann

$$\begin{aligned}u(p,s)\,\bar{u}(p,s) &= (\not{p}+m)\frac{1+\gamma_5\not{s}}{2}\\ v(p,s)\,\bar{v}(p,s) &= (\not{p}-m)\frac{1+\gamma_5\not{s}}{2}\end{aligned} \tag{6.73}$$

Analog ersetzt man Spinsummen für die auslaufenden Fermionen, wenn man deren Spin misst und den Wirkungsquerschnitt spinabhängig berechnen will.

6.8.7 Energieabhängigkeit bei Austausch eines virtuellen Teilchens

Kann eine Reaktion durch Austausch eines virtuellen Teilchens (im s- oder t-Kanal) ablaufen, wird die Reaktionswahrscheinlichkeit durch die Heisenbergsche Unschärferelation eingeschränkt:

$$\begin{aligned}\Delta p\cdot\Delta r &\le 1\\ \Delta E\cdot\Delta t &\le 1\end{aligned}$$

Die Reichweite des virtuellen Teilchens Δr ist umgekehrt proportional zur Verletzung des Energiesatzes, der seine „Virtualität“ ausmacht. Ein On-shell-Teilchen erfüllt

$$E^2+p^2 = q^2 = m^2$$

ein virtuelles Teilchen verletzt entweder die Energie- oder die Impulserhaltung, mit $\Delta E^2 = q^2-m^2$ oder $\Delta p^2 = 2p\Delta p = q^2-m^2$. Dabei haben p, E und q die gleiche Unschärfe $\Delta p \approx \Delta E \approx \Delta q \approx \sqrt{|q^2|}$, falls $m^2 \ll |q^2|$.

Der Wirkungsquerschnitt masseloser Austauschteilchen ist daher

$$\sigma \sim (\Delta r)^2 \sim \frac{1}{q^2} \approx \frac{1}{E^2}$$

6.8.8 Das anomale magnetische Moment von Elektron und Myon

Ein Beispiel von Präzisionsmessungen und QED-Rechnungen ist das anomale magnetische Moment von Elektron oder Myon.

Beispielexperiment: Präzessionsmessung in einem Myon-Speicherring. Die Zyklotronfrequenz (Umlauffrequenz) ist

$$\omega_C = \frac{eB}{\gamma m}$$

Die Spinpräzessionsfrequenz (Larmor nichtrelativistisch, Thomas relativistisch) ist

$$\omega_s = \frac{g}{2}\frac{eB}{m} + \left(\frac{1}{\gamma} - 1\right)\frac{eB}{m} = \omega_C + \frac{g-2}{2}\frac{eB}{m}$$

Die Spinrichtung wird über die Zahl schneller, vorwärts emittierter Elektronen aus dem Myonzerfall gemessen. Die Häufigkeit ist maximal, wenn der Myonspin entgegen der Flugrichtung zeigt.

Technische Details:

Der Spin eines bewegten Myons präzediert auch in einem äußeren elektrischen Feld. Die gesamte Präzessionsfrequenz ist[26]

$$\vec{\omega}_s = \omega_C + \frac{g-2}{2}\frac{e\vec{B}}{m} + \left(\frac{g-2}{2} + \frac{1}{\gamma^2-1}\right)\frac{e\vec{\beta}\times\vec{E}}{m}$$

Für die *magische Geschwindigkeit* $\gamma = 29.3$ ($p_\mu = 3.094\,\mathrm{GeV}$) wird $\left(\frac{g-2}{2} + \frac{1}{\gamma^2-1}\right) = 0$ und die Frequenz hängt nur noch von B ab. Dann kann man problemlos elektrische Felder, beispielsweise zur vertikalen Fokussierung im Ring, verwenden.

Experiment (E821 at Brookhaven BNL[27]):

$$\begin{aligned} a(\mu^+) &= 11659204(6)(5)\cdot 10^{10} \\ a(\mu^-) &= 11659215(8)(3)\cdot 10^{10} \\ a(\mu) &= 11659209(5)(3)\cdot 10^{10} \end{aligned}$$

Theorie (PDG 2015):

$$a(\mu) = 11659180(4)(3)\cdot 10^{-10}$$

[26] Zuerst gerechnet von Thomas 1927; Publikation: V. Bargmann, L. Michel, and V. L. Telegdi, Precession of the Polarization of Particles Moving in a Homogeneous Electromagnetic Field, Phys. Rev. Lett. **2**, 435 (1959).

[27] G. W. Bennett et al., Phys. Rev. **D73**, 072003 (2006).

7. Die Schwache Wechselwirkung

7.1 Vier-Fermion Theorie der Schwachen Wechselwirkung

Fermi's ansatz for the description of weak interaction was a coupling of 4 fermions at a point. This 4-fermion-interaction can be described in the most general way by a set of parameters first presented by Louis Michel[28] in 1950.

It can be investigated without being obscured by strong interaction effects in purely leptonic decays of heavy leptons:

$$\mu^- \to e^- \overline{\nu}_e \nu_\mu$$
$$\tau^- \to e^- \overline{\nu}_e \nu_\tau$$
$$\tau^- \to \mu^- \overline{\nu}_\mu \nu_\tau$$

Very precise measurements of muon decays are available, and the precision for τ decays is steadily improving.

7.1.1 Fierz-Transformationen *

Für Spinoren a, b, c, d:

$$\begin{aligned}
\bar{a}b \cdot \bar{c}d &= -\frac{1}{4}\bar{a}d \cdot \bar{c}b - \frac{1}{4}\bar{a}\gamma^\mu d \cdot \bar{c}\gamma_\mu b - \frac{1}{8}\bar{a}\sigma^{\mu\nu} d \cdot \bar{c}\sigma_{\mu\nu} b \\
&\quad + \frac{1}{4}\bar{a}\gamma^\mu\gamma_5 d \cdot \bar{c}\gamma_\mu\gamma_5 b - \frac{1}{4}\bar{a}\gamma_5 d \cdot \bar{c}\gamma_5 b \\
\bar{a}\gamma^\mu b \cdot \bar{c}\gamma_\mu d &= -\bar{a}d \cdot \bar{c}b + \frac{1}{2}\bar{a}\gamma^\mu d \cdot \bar{c}\gamma_\mu b + \frac{1}{2}\bar{a}\gamma^\mu\gamma_5 d \cdot \bar{c}\gamma_\mu\gamma_5 b + \bar{a}\gamma_5 d \cdot \bar{c}\gamma_5 b \\
\bar{a}\sigma^{\mu\nu} b \cdot \bar{c}\sigma_{\mu\nu} d &= -3\bar{a}d \cdot \bar{c}b + \frac{1}{2}\bar{a}\sigma^{\mu\nu} d \cdot \bar{c}\sigma_{\mu\nu} b - 3\bar{a}\gamma_5 d \cdot \bar{c}\gamma_5 b \\
\bar{a}\gamma^\mu\gamma_5 b \cdot \bar{c}\gamma_\mu\gamma_5 d &= \bar{a}d \cdot \bar{c}b + \frac{1}{2}\bar{a}\gamma^\mu d \cdot \bar{c}\gamma_\mu b + \frac{1}{2}\bar{a}\gamma^\mu\gamma_5 d \cdot \bar{c}\gamma_\mu\gamma_5 b - \bar{a}\gamma_5 d \cdot \bar{c}\gamma_5 b \\
\bar{a}\gamma_5 b \cdot \bar{c}\gamma_5 d &= -\frac{1}{4}\bar{a}d \cdot \bar{c}b + \frac{1}{4}\bar{a}\gamma^\mu d \cdot \bar{c}\gamma_\mu b - \frac{1}{8}\bar{a}\sigma^{\mu\nu} d \cdot \bar{c}\sigma_{\mu\nu} b \\
&\quad - \frac{1}{4}\bar{a}\gamma^\mu\gamma_5 d \cdot \bar{c}\gamma_\mu\gamma_5 b - \frac{1}{4}\bar{a}\gamma_5 d \cdot \bar{c}\gamma_5 b
\end{aligned}$$

Damit kann eine Vier-Fermion-Theorie immer mehrdeutig interpretiert werden, zum Beispiel eine $V-A$-Theorie mit den Termen $VV - VA - AV + AA$ durch Austausch geladener W-Bosonen mit Spin 1, die nur an linkshändige Fermionen koppeln, oder neutraler Bosonen mit Spin 1, was den Fierz-transformierten Termen einer $V-A$-Theorie entspricht.

7.1.2 Michel Parameters

Using a general matrix element for $\mu^- \to e^- \overline{\nu}_e \nu_\mu$ (or $\tau^- \to e^- \overline{\nu}_e \nu_\tau, \tau^- \to \mu^- \overline{\nu}_\mu \nu_\tau$)

$$\mathcal{M} = \frac{G_F}{\sqrt{2}} \sum_{i=S,P,V,A,T} \bar{\psi}(e) O_i \psi(\overline{\nu}_e) \cdot \bar{\psi}(\nu_\mu)(G_i O_i + G_i' O_i \gamma_5)\psi(\mu) \tag{7.1a}$$
$$= \frac{G_F}{\sqrt{2}} \sum_{i=S,P,V,A,T} \bar{\psi}(e) O_i \psi(\mu) \cdot \bar{\psi}(\nu_\mu)(C_i O_i + C_i' O_i \gamma_5)\psi(\overline{\nu}_e) \tag{7.1b}$$

[28] Louis Michel Proc. Phys. Soc. **A63**, 514 (1950); C. Bouchiat, L. Michel, Phys. Rev. **106**, 170 (1957).

$$= 4\frac{G_F}{\sqrt{2}} \sum_{\substack{i=S,V,T \\ \lambda_e=L,R \\ \lambda_\mu=L,R}} g^i_{\lambda_e\lambda_\mu}\, \bar\psi(e)_{\lambda_e} O_i \psi(\overline{\nu}_e) \cdot \bar\psi(\nu_\mu) O_i \psi(\mu)_{\lambda_\mu} \tag{7.1c}$$

where all possible combinations of Dirac matrices ($O_i = 1, \gamma_5, \gamma_\mu, \gamma_\mu\gamma_5, \sigma_{\mu\nu}$) are allowed, i. e. with scalar, pseudoscalar, vector, axial vector and tensor couplings[29]. The corresponding 10 complex parameters are determined by 19 real numbers, since one phase is arbitrary.

In (7.1c) g^T_{RR}, g^T_{LL} are unphysical, since the corresponding terms lead to $|\mathcal{M}|^2 \equiv 0$, reducing the number again to 10 complex coefficients.

We can parametrize the decay amplitude by the Michel parameters (the G-terms are only for $G_T = G'_T = 0$):

$$\begin{aligned}
\rho &= \frac{3}{A}(|C_A|^2 + |C'_A|^2 + |C_V|^2 + |C'_V|^2 + 2|C_T|^2 + 2|C'_T|^2) \\
&= \frac{3}{4A}(2|G_A|^2 + 2|G'_A|^2 + 2|G_V|^2 + 2|G'_V|^2 + 4\,\mathcal{R}e(G^*_A G_V + {G'_A}^* G'_V) \\
&\quad + |G_P|^2 + |G'_P|^2 + |G_S|^2 + |G'_S|^2) \\
&= \frac{3}{4} - \frac{12}{A}\left[|g^V_{LR}|^2 + |g^V_{RL}|^2 + 2|g^T_{LR}|^2 + 2|g^T_{RL}|^2 + \mathcal{R}e\left(g^S_{LR}\, {g^*}^T_{LR} + g^S_{RL}\, {g^*}^T_{RL}\right)\right] \qquad (7.2) \\
&= \frac{3}{4}(b^+ + b^-) + (c^+ + c^-) \\
\eta &= \frac{1}{A}(3|C_S|^2 + 3|C'_S|^2 - |C_P|^2 - |C'_P|^2 + 2|C_A|^2 + 2|C'_A|^2 - 2|C_V|^2 - 2|C'_V|^2) \\
&= \frac{2}{A}\,\mathcal{R}e(G^*_P G_A - {G'_P}^* G'_A + G^*_S G_V - {G'_S}^* G'_V)) \\
&= \frac{8}{A}\,\mathcal{R}e\left[6 g^V_{LR} {g^*}^T_{RL} + 6 g^V_{RL} {g^*}^T_{LR} + g^S_{RR} {g^*}^V_{LL} + g^S_{RL} {g^*}^V_{LR} + g^S_{LR} {g^*}^V_{RL} + g^S_{LL} {g^*}^V_{RR}\right] \qquad (7.3) \\
\xi &= \frac{2}{A}[3\,\mathcal{R}e(C^*_S C'_P + C'_S C^*_P) - 4\,\mathcal{R}e(C^*_A C'_V + C'_A C^*_V) + 14\,\mathcal{R}e(C'_T C^*_T)] \\
&= \frac{2}{A}[\mathcal{R}e(G^*_P G'_P + G^*_S G'_S) - 4\,\mathcal{R}e(G^*_A G'_A + G^*_V G'_V) + 8\,\mathcal{R}e(G^*_A G'_V + G^*_V G'_A)] \\
&= \frac{4}{A}[|g^S_{RR}|^2 - |g^S_{LL}|^2 + |g^S_{LR}|^2 - |g^S_{RL}|^2 + 4(|g^V_{RR}|^2 - |g^V_{LL}|^2 + 3|g^V_{RL}|^2 - 3|g^V_{LR}|^2) \\
&\qquad - 20(|g^T_{LR}|^2 - |g^T_{RL}|^2) + 16\,\mathcal{R}e(g^S_{RL} {g^*}^T_{RL} - g^S_{LR} {g^*}^T_{LR})] \qquad (7.4) \\
&= 3(a^- - a^+) + (b^- - b^+) + \frac{7}{3}(c^+ - c^-) \\
\kappa &= \xi\delta \\
&= \frac{6}{A}[-\mathcal{R}e(C^*_A C'_V + C'_A C^*_V) + 2\,\mathcal{R}e(C'_T C^*_T)] \\
&= \frac{3}{2A}[\mathcal{R}e(G^*_P G'_P + G^*_S G'_S) + 2\,\mathcal{R}e(G^*_A G'_A + G^*_V G'_V) + 2\,\mathcal{R}e(G^*_A G'_V + G^*_V G'_A)] \\
&= \frac{3}{A}[(|g^S_{RR}|^2 - |g^S_{LL}|^2 + |g^S_{LR}|^2 - |g^S_{RL}|^2) + 4(|g^V_{RR}|^2 - |g^V_{LL}|^2) \\
&\qquad - 4(|g^T_{RL}|^2 - |g^T_{LR}|^2) + 4\,\mathcal{R}e(g^S_{RL} {g^*}^T_{RL} - g^S_{LR} {g^*}^T_{LR})] \qquad (7.5) \\
&= \frac{3}{4}(b^- - b^+) + (c^+ - c^-)
\end{aligned}$$

with the normalization

$$A = |C_S|^2 + |C'_S|^2 + |C_P|^2 + |C'_P|^2 + 4|C_V|^2 + 4|C'_V|^2 + 4|C_A|^2 + 4|C'_A|^2$$

[29] Some authors use the tensor $\sigma^{\mu\nu}/\sqrt{2}$.

$$
\begin{aligned}
&+ 6|C_T|^2 + 6|C'_T|^2 \\
&= |G_S|^2 + |G'_S|^2 + |G_P|^2 + |G'_P|^2 + 4|G_V|^2 + 4|G'_V|^2 + 4|G_A|^2 + 4|G'_A|^2 \\
&= 4\left(|g^S_{RR}|^2 + |g^S_{RL}|^2 + |g^S_{LR}|^2 + |g^S_{LL}|^2\right) \\
&\quad + 16\left(|g^V_{RR}|^2 + |g^V_{RL}|^2 + |g^V_{LR}|^2 + |g^V_{LL}|^2\right) + 48\left(|g^T_{RL}|^2 + |g^T_{LR}|^2\right) \qquad (7.6) \\
&= 16(a^+ + a^- + b^+ + b^- + c^+ + c^-) \qquad (7.7)
\end{aligned}
$$

The C and G coefficients in equation (7.1) are linear combinations of each other and related by Fierz transformations (section 7.1.1). This represents a feature of the four-fermion interaction: It can be a low-energy limit for the exchange of a heavy neutral or charged intermediate boson. Today, we know that the flavour changing weak interaction is described by the exchange of the charged W^+ and W^- boson. At the time when Michel introduced his parametrization, it was more natural to group the leptons of same charge together as shown in (7.1b).

The lower versions of the Michel parameter equations and (7.7) use the parameters

$$
\begin{aligned}
a^+ &= |g^V_{RL}|^2 + \frac{1}{16}|g^S_{RL} + 6g^T_{RL}|^2 \\
a^- &= |g^V_{LR}|^2 + \frac{1}{16}|g^S_{LR} + 6g^T_{LR}|^2 \\
b^+ &= |g^V_{RR}|^2 + \frac{1}{4}|g^S_{RR}|^2 \\
b^- &= |g^V_{LL}|^2 + \frac{1}{4}|g^S_{LL}|^2 \\
c^+ &= \frac{3}{16}|g^S_{RL} - 2g^T_{RL}|^2 \\
c^- &= \frac{3}{16}|g^S_{LR} - 2g^T_{LR}|^2
\end{aligned}
$$

The Standard Model has a normalization $A = 16$, and small corrections from additional non-standard physics contribution can be searched for via deviations of the total width, so $A > 16$ is a convenient way to parametrize this effect.

The allowed range for ρ is $0 \le \rho \le 1$. The range of (ρ, η) pairs is shown in figure 7.1, for (ρ, ξ) pairs in figure 7.2.

In the Standard Model we have the decay diagram

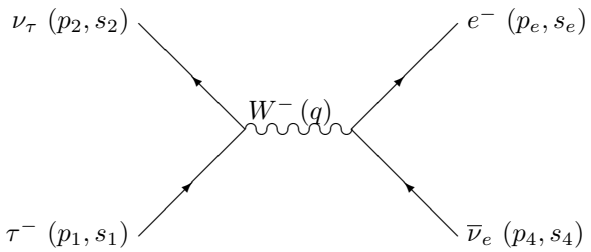

with a $V-A$ coupling, i. e. $C_V = C'_A = 1$, $C_A = C'_V = -1$ and all others 0, or correspondingly $G_V = G_A = 1$, $G'_V = G'_A = -1$ and all others 0, or $g^V_{LL} = 1$ and all others 0 in the Fetscher notation. The values for the Michel parameters are

$$\rho = \frac{3}{4}, \quad \kappa = -\frac{3}{4}, \quad \eta = 0, \quad \xi = -1, \quad A = 16$$

Other cases are given in table 7.1.

Table 7.1 Michel parameters for different couplings (for admixtures we assume $\varepsilon \ll 1$). The sign convention for ξ is sometimes opposite in the literature.

coupling $(\tau \times l)$		ρ	η	ξ	κ
$(V-A)\times(V-A)$	LL	3/4	0	-1	$-3/4$
$(V+A)\times(V+A)$	RR	3/4	0	$+1$	3/4
$V\times V$		3/8	0	0	0
$A\times A$		3/8	0	0	0
$(V-A)\times(V+A)$	LR	0	0	-3	0
$(V+A)\times(V-A)$	RL	0	0	$+3$	0
$V\times(V-A)$		3/8	0	-2	$-3/8$
$A\times(V-A)$		3/8	0	$+2$	3/8
$(V-rA)\times(V-rA)$		$3/8\left[1+\left(\frac{2r}{1+r^2}\right)^2\right]$	0	$-\frac{2r}{1+r^2}$	$3\xi/4$
$(V-A)\times(V-A)\ldots$					
$\ldots+\varepsilon^2(V+A)\times(V+A)$		3/4	0	$2\varepsilon^2-1$	$3\xi/4$
$\ldots+\varepsilon^2(S-P)\times(S-P)$	LL	3/4	0	-1	$-3/4$
$\ldots+\varepsilon^2(S+P)\times(S+P)$		3/4	$\mathcal{R}e\,\varepsilon/2$	$\frac{\varepsilon^2}{2}-1$	$3\xi/4$
$\ldots+\varepsilon^2\,S\times S$		3/4	$\mathcal{R}e\,\varepsilon/8$	$\frac{\varepsilon^2}{16}-1$	$3\xi/4$
$\ldots+\varepsilon^2\,T\times T$	[a])	$\frac{3}{4}(1-2\varepsilon^2)$	0	$-1+f\varepsilon^2$	$-\frac{3}{4}(1-2\varepsilon^2)$

[a] $f=+8,+3,-2$ for LR,(LR+RL),RL.

If the Standard Model $V-A$ is true, a significant reduction in couplings can be achieved by measurement of ξ, ρ and ξ' (see below). The relations

$$2-\frac{2}{3}\xi+\frac{32}{9}\kappa=|g^S_{RR}|^2+|g^S_{LR}|^2+4(|g^V_{RR}|^2+|g^V_{LR}|^2)+12|g^T_{LR}|^2$$
$$2(1-\xi')=|g^S_{RR}|^2+|g^S_{RL}|^2+4(|g^V_{RR}|^2+|g^V_{RL}|^2)+12|g^T_{RL}|^2$$

allow to exclude 8 complex couplings (all with righthanded τ, e, μ), if the left hand sides are found to be 0.

From (7.7) and the rewriting of ρ, ξ and κ, the allowed region for these three Michel parameters is a tetrahedron. The projections of this tetrahedron are shown in figs. 7.2, 7.3 and 7.6.

The Standard Model matrix element will be given below.

7.1.3 Energy Distributions

The exact, Lorentz invariant partial width in the four-fermion theory for massless neutrinos is

$$\frac{\mathrm{d}\Gamma(\tau(\mu)\to l\bar{\nu}\nu)}{\mathrm{d}E_l}=\frac{4G_F^2}{3m_\tau(2\pi)^3}\,|\boldsymbol{p}|\left\{\left(3-\frac{10\rho}{3}\right)Q^2(Pp)+\frac{4\rho}{3}(Qp)(QP)+3\eta m_\tau m_l Q^2\right\} \tag{7.8}$$

where the four-momenta are $P(\tau$ or $\mu)$, $p(l)$ and $Q=P-p$. In the tau rest frame, this can be rewritten using

$$Q^2=m_\tau^2+m_l^2-2m_\tau E_l$$
$$QP=(m_\tau-E_l)m_\tau$$
$$Qp=m_\tau E_l-m_l^2$$
$$Pp=m_\tau E_l$$

For the $\tau\to\mu\bar{\nu}\nu$ and different values for ρ and η, this is shown in figures 7.7, 7.8and 7.9.

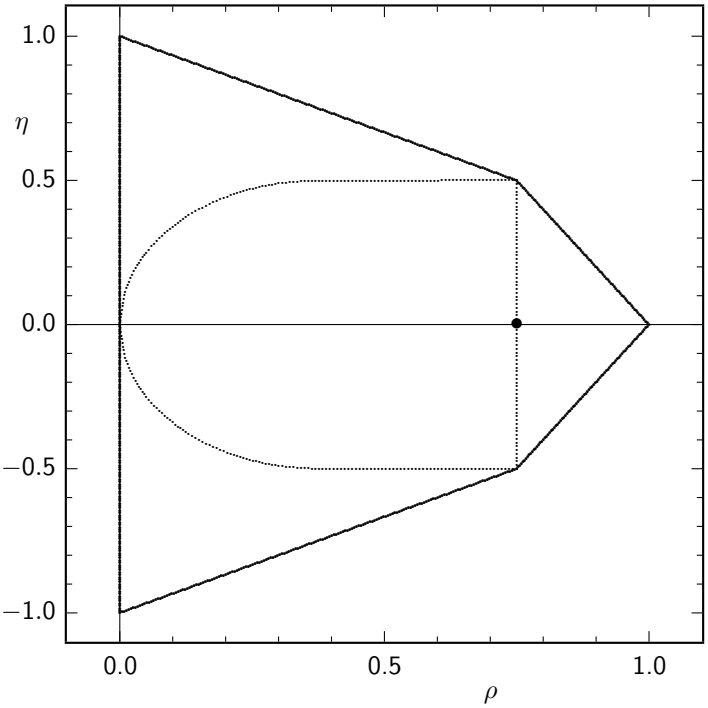

Fig. 7.1 Limits for the Michel parameters ρ and η. The dotted line defines the allowed region without any tensor couplings (in charge-exchange notation). The solid bounds are for all possible couplings without any restriction. • denotes the Standard Model prediction.

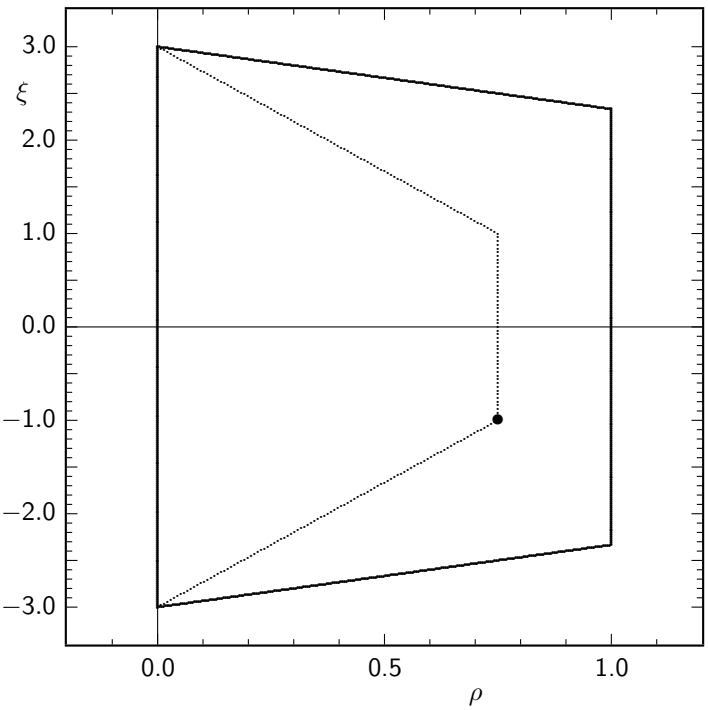

Fig. 7.2 Limits for the Michel parameters ρ and ξ. The dotted line defines the allowed region without any tensor couplings (in charge-exchange notation). • denotes the Standard Model prediction.

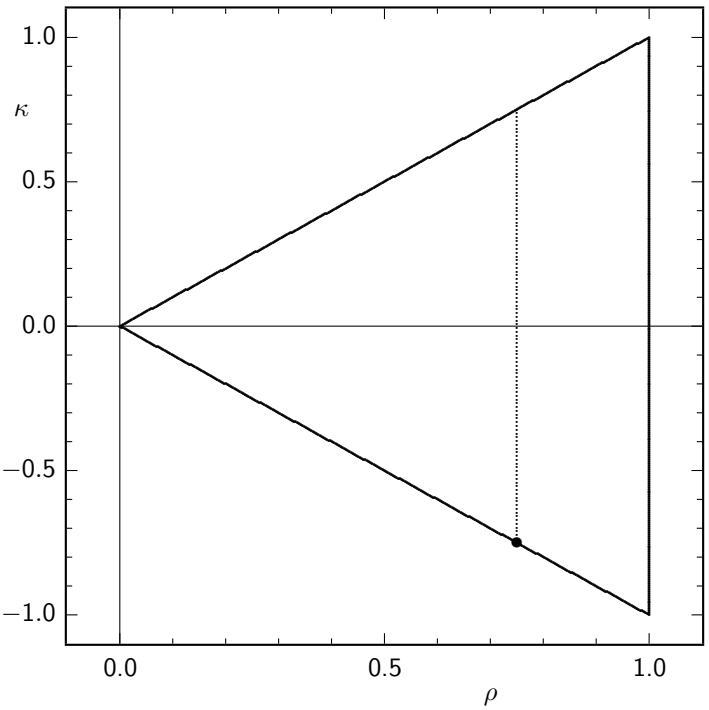

Fig. 7.3 Limits for the Michel parameters ρ and $\kappa = \xi\delta$. The dotted line defines the allowed region without any tensor couplings (in charge-exchange notation). In both cases, $|\kappa| < \rho$. • denotes the Standard Model prediction.

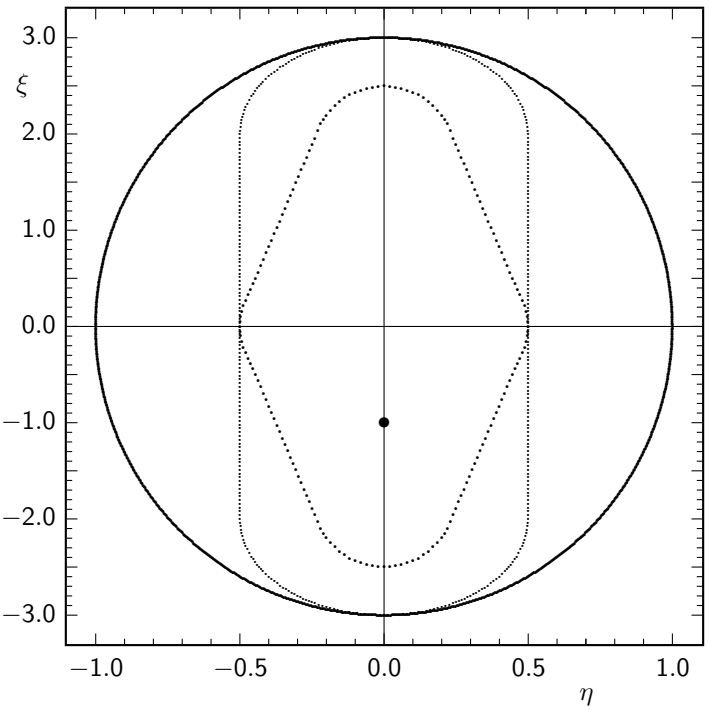

Fig. 7.4 Limits for the Michel parameters η and ξ, fulfilling $(3\eta)^2 + \xi^2 < 9$. The thin-dotted line defines the allowed region without any tensor couplings (in charge-exchange notation). The thick-dotted line defines the limits for $\rho = 3/4$. • denotes the Standard Model prediction.

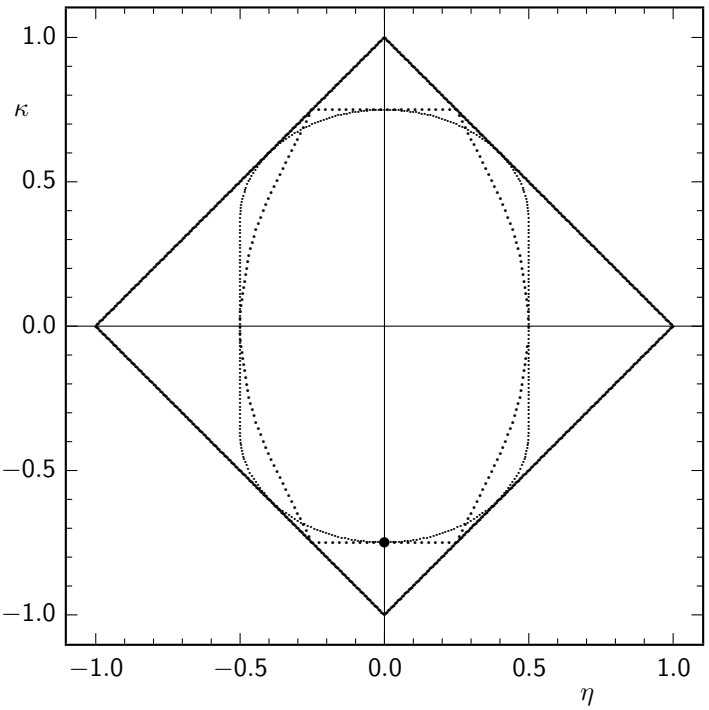

Fig. 7.5 Limits for the Michel parameters η and $\kappa = \xi\delta$, fulfilling $|\kappa| + |\eta| < 1$. The thin-dotted line defines the allowed region without any tensor couplings (in charge-exchange notation). The thick-dotted line defines the limits for $\rho = 3/4$. • denotes the Standard Model prediction.

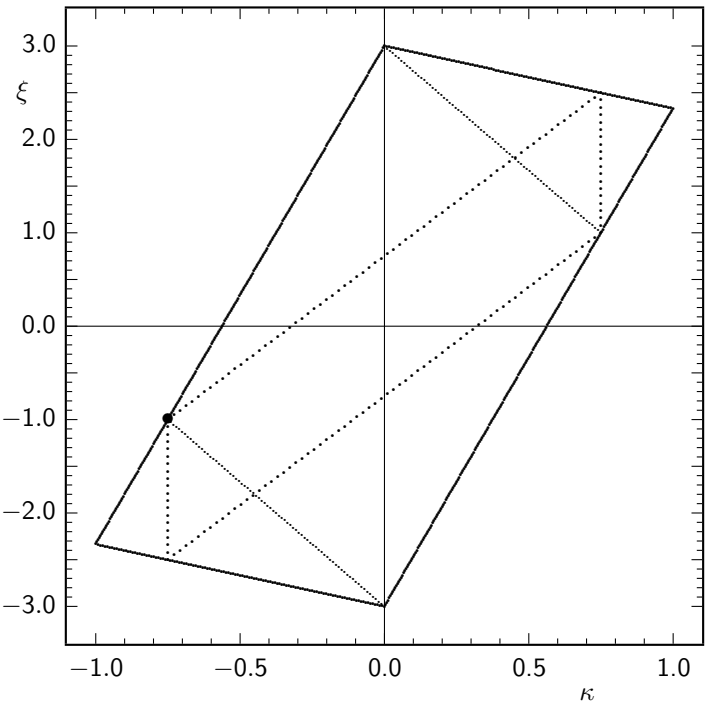

Fig. 7.6 Limits for the Michel parameters ξ and $\kappa = \xi\delta$. The thin-dotted line defines the allowed region without any tensor couplings (in charge-exchange notation). The thick-dotted line defines the limits for $\rho = 3/4$. • denotes the Standard Model prediction.

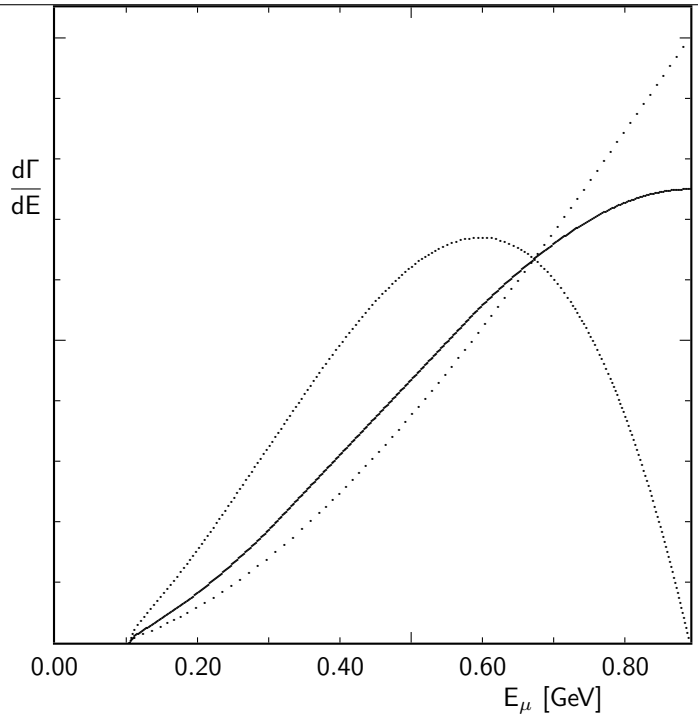

Fig. 7.7 Energy and momentum distributions of the μ in the τ rest frame, for $\rho = 3/4$ (——), $\rho = 0$ (·····) and $\rho = 1$ (· · · · ·) and $\eta = 0$. The scale is arbitrary; the marks allow to read ρ directly from the right edge at maximum energy.

If we neglect terms of order $(m_l/m_\tau)^2$ and add a term for the leading radiative corrections the energy spectrum can be written as

$$\frac{1}{\Gamma}\frac{\mathrm{d}\Gamma}{\mathrm{d}x} = x^2\left[\frac{1+a(x)}{1+4\eta\cdot(m_l/m_\tau)}\Big(12(1-x)+\frac{4}{3}\rho(8x-6)+24\eta\frac{m_l}{m_\tau}\frac{1-x}{x}\Big)\right] \tag{7.9}$$

with radiative corrections $a(x)$ and using a scaling variable for the energy of the charged light lepton (e or μ)

$$x = E_l/E_{\max} \tag{7.10}$$

Since $|a(x)| \ll 1$ and $m_l \ll m_\tau$ this reduces to

$$\frac{1}{\Gamma}\frac{\mathrm{d}\Gamma}{\mathrm{d}x} \approx 12x^2\Big[1-x+\frac{2}{3}\rho\Big(\frac{4}{3}x-1\Big)\Big] \tag{7.11}$$

with the Michel parameter $\rho = 3/4$ for standard $V{-}A$ coupling.

Of special interest in this context is a $V{+}A$ structure in contrast to the $V{-}A$ of the Standard Model.

If both the electron and the tau couple to the W as a $V{+}A$ current, we expect the same ρ. If only the tau couples as $V{+}A$ and the light lepton as $V{-}A$, we obtain $\rho = 0$, and the electron energy distribution has to go to zero at $E_l = E_{\max}$.

This can also be understood from helicity arguments: If both the electron and the tau are described by left-handed currents, i. e. $V{-}A$, the electron's helicity is $-1/2$ (ignoring its non-zero mass), the electron antineutrino's helicity is $+1/2$ and the tau neutrino's helicity is $-1/2$. The total spin for the configuration with maximum electron energy, where the electron goes back-to-back with both neutrinos, is $1/2$. If, on the contrary, the tau couples right-handed ($V{+}A$), the tau neutrino has helicity $+1/2$. Therefore, in this case, the spin adds to $3/2$, which requires $L = 1$ in spin-1/2-particle decay, and hence ($L_z \equiv 0$) has no back-to-back configuration as required for $x = 1$.

$x = 1$:

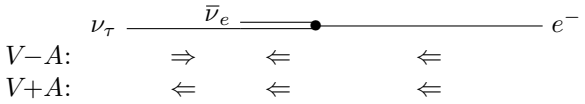

7.1.4 Polarized Taus

A more general amplitude for $\tau^- \to l^- \nu_\tau \overline{\nu}_l$ can be given for polarised taus[30]

$$\begin{aligned}\frac{\mathrm{d}\Gamma}{\mathrm{d}\Omega\,\mathrm{d}x} =& \frac{G_F^2 m_\tau^5}{192\pi^3} \cdot \frac{A}{64\pi} \cdot x^2 \\ & \cdot \Big\{ [1 + a(x)] \Big(12(1-x) + \frac{4}{3}\rho(8x-6) + 24\eta \frac{m_l}{m_\tau} \frac{1-x}{x} \Big) \\ & + P \cos\theta \Big(4\xi(1-x) + \frac{4}{3}\kappa(8x-6) + \xi \frac{\alpha}{2\pi} \frac{b(x)}{x^2} \Big) \Big\} \end{aligned} \tag{7.12}$$

where $a(x)$ and $b(x)$ are radiative corrections, and θ is the angle of the light lepton momentum with respect to the tau polarisation, and the polarisation is $P = \frac{\#(\tau\uparrow) - \#(\tau\downarrow)}{\#(\tau)} \in [-1, 1]$. Using $m_l/m_\tau \ll 1$ and ignoring radiative corrections, this simplifies to

$$\frac{\mathrm{d}\Gamma}{\mathrm{d}\Omega\,\mathrm{d}x} = \frac{G_F^2 m_\tau^5}{192\pi^3} \cdot \frac{A}{64\pi} \cdot x^2 \cdot \Big\{ 12(1-x) + \frac{4}{3}\rho(8x-6) + + \cos\theta \Big(4\xi(1-x) + \frac{4}{3}\kappa(8x-6) \Big) \Big\} \tag{7.13}$$

Integrating over $\mathrm{d}\Omega$ makes the $\cos\theta$-term vanish and gives

$$\frac{\mathrm{d}\Gamma}{\mathrm{d}x} = \frac{G_F^2 m_\tau^5}{192\pi^3} \cdot \frac{3A}{4} \cdot x^2 \cdot \Big(1 - x + \frac{2}{3}\rho(\frac{4}{3}x - 1) \Big) \tag{7.14}$$

which is identical to (7.11) for $A = 16$.

7.1.5 Polarized Decay Products *

For the muon decay, also the electron polarisation is accessible by experiment. This leads to some new parameters, the most important being

$$\begin{aligned}\xi' &= 1 - \frac{1}{A}[(a + a') + 4(b + b') + 6(c + c')] \\ &= 1 - \frac{1}{A}[32|g_{RL}^V|^2 + 2|g_{RL}^S + 6g_{RL}^T|^2 + 6|g_{RL}^S - 2g_{RL}^T|^2 + 32|g_{RR}^V|^2 + 8|g_{RR}^S|^2] \\ \xi'' &= 1 + \frac{2}{A}[10c - a]\end{aligned}$$

[30] ξ has to be replaced with $-\xi$ for τ^+ decays. The sign convention for ξ in W. Fetscher, Phys. Rev. **D42**, 1544 (1990) is opposite to the one used here.

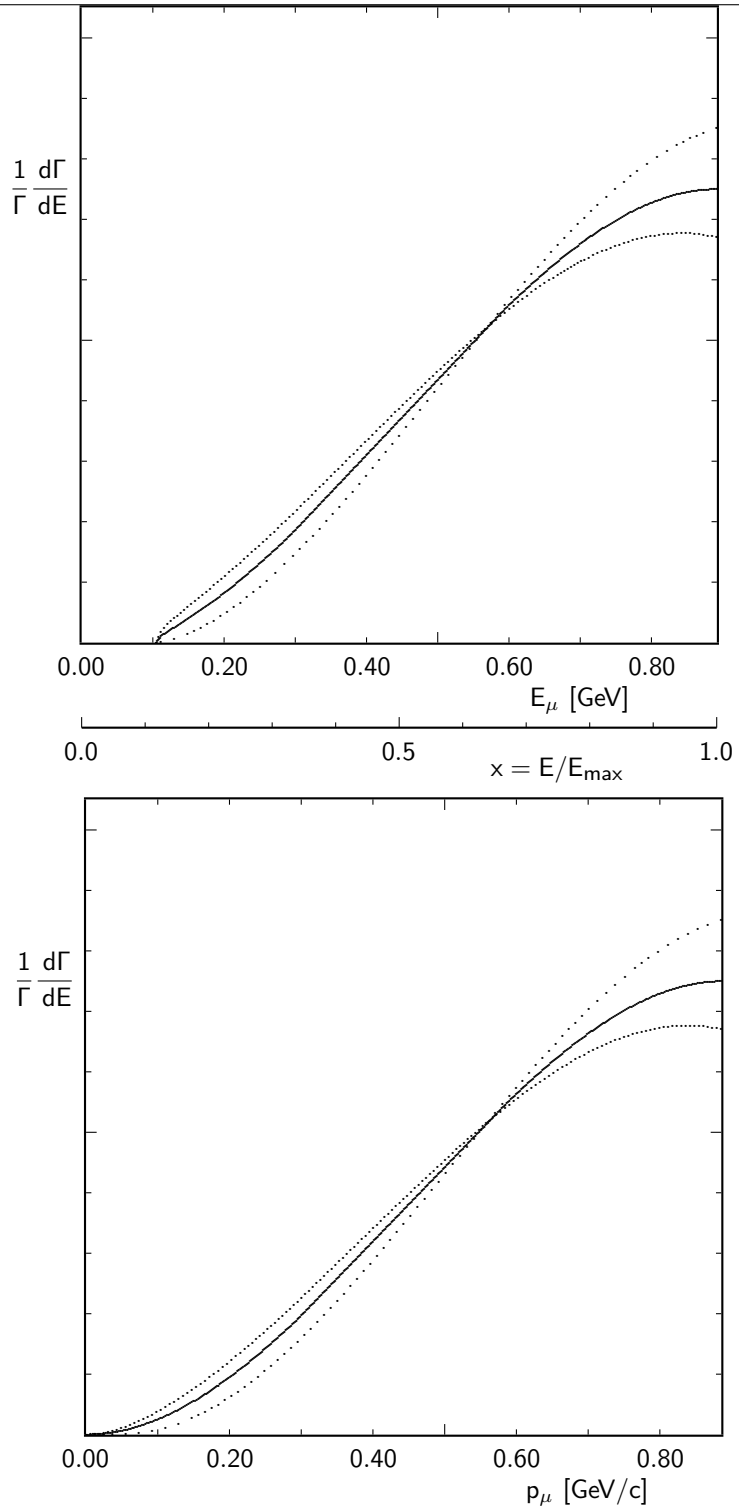

Fig. 7.8 Shape of the μ energy and momentum distributions in the τ rest frame, for $\rho = 3/4$ and $\eta = 0$ (——), $\eta = 0.5$ (·····) and $\eta = -0.5$ (· · · · ·).

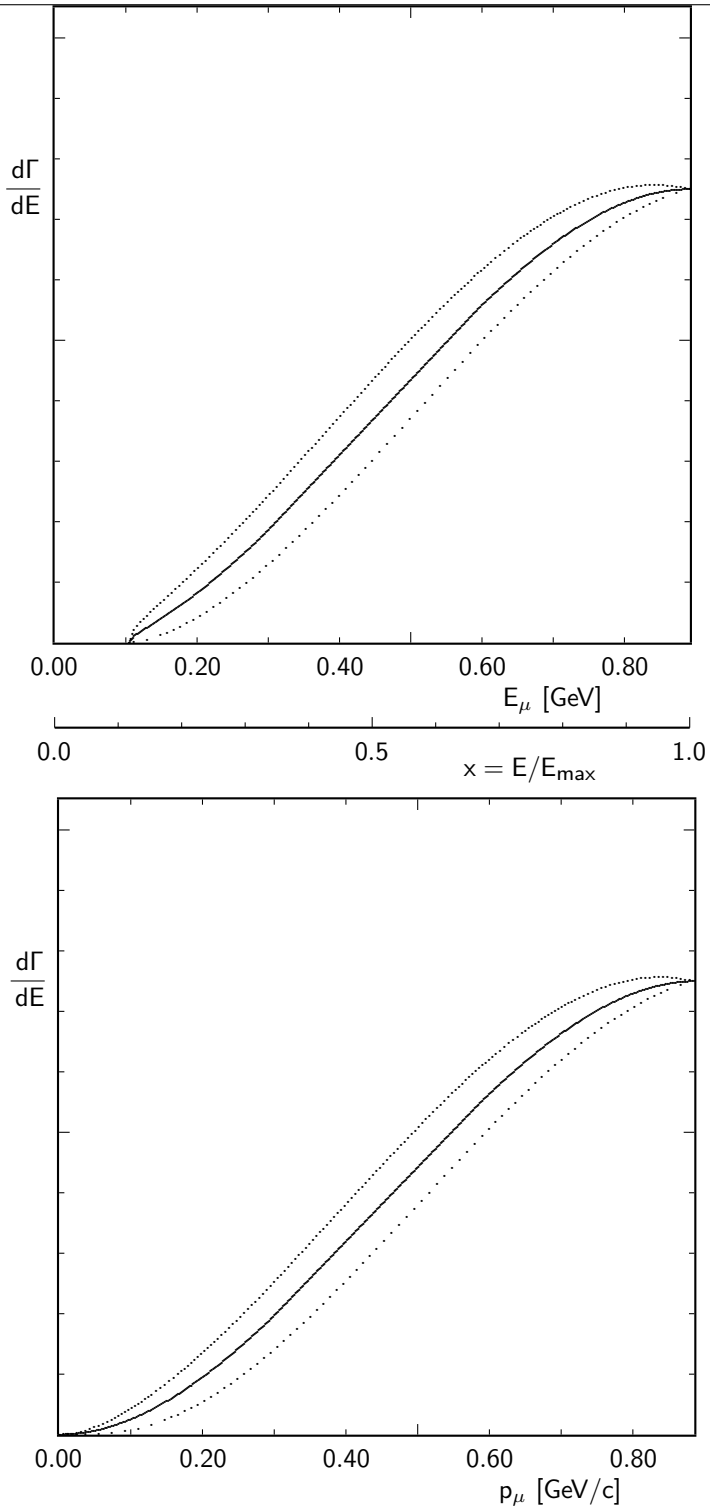

Fig. 7.9 Differential partial width of the $\tau \to \mu\nu\bar{\nu}$ decay in the τ rest frame, for $\rho = 3/4$ and $\eta = 0$ (——), $\eta = 0.5$ (·····) and $\eta = -0.5$ (· · · · ·).

7.1.6 Experimental Results on Tau Decays

The results on τ decaus come mainly from e^+e^- storage rings, at cms energies close to threshold (BES at BEPC, Beijing), at 10 GeV (CLEO at CESR, Ithaca NY, and until 1992 ARGUS at DORIS, Hamburg; BABAR at PEP II, Stanford and BELLE at KEK-B, Tsukuba), and at the Z^0 resonance (ALEPH, DELPHI, L3, and OPAL at LEP, Geneva). At energies much above 10 GeV the cross section is too low to provide large samples, except at the Z^0 resonance, which contributes more than 1 nb to τ pair production. This high energy has also the advantage of a significantly cleaner separation of τ pairs from background, as illustrated in table 7.2, where efficiencies of ARGUS and ALEPH for samples of similar purity are compared.

Table 7.2 Background fractions from different τ channels and from other events, and efficiencies for typical τ decay channels at 10 GeV cms energy (ARGUS) and 90 GeV (ALEPH).

τ^+/τ^- channel	10 GeV	90 GeV
$e\nu\overline{\nu}/\mu\nu\overline{\nu}$	$\tau : (2.6 \pm 0.1)\%,\ \text{other} : (0.8 \pm 0.8)\%$ $\varepsilon = 16\%$	$\tau : (3.2 \pm 0.2)\%,\ \text{other} : (0.6 \pm 0.1)\%$ $\varepsilon = 70\%$
$\mu\nu\overline{\nu}/\pi^+\pi^-\pi^-\nu$	$\tau : (10 \pm 2)\%,\ \text{other} : (0.4 \pm 0.3)\%$ $\varepsilon = 13\%$	$\tau : (9.4 \pm 0.5)\%,\ \text{other} : (0.1 \pm 0.1)\%$ $\varepsilon = 50\%$
$\pi^+\pi^0\overline{\nu}/\pi^-\pi^0\nu$	$\tau : (28 \pm 2)\%,\ \text{other} : (1.9 \pm 0.7)\%$ $\varepsilon = 6.7\%$	$\tau : (12 \pm 1)\%,\ \text{other} : (2.4 \pm 0.4)\%$ $\varepsilon = 30\%$

The first reasonable measurement of the Michel parameter ρ was already in 1979 by the DELCO collaboration, but only in the 1990s all four parameters became known. The precision of the measurements has already reached errors below 0.10 in the worst case.

The most interesting parameter for scalar couplings, e. g. through a charged Higgs boson, is η. Assuming that only lefthanded neutrinos participate in the interaction, we expect a lefthanded τ and μ/e for the Standard Model vector part, but a righthanded τ and μ/e for the scalar. Coupling constants would therefore be $g^V_{LL} = 1$ and $g^S_{RR} \neq 0$ for a small scalar contribution. The interference term leads to $\eta = \frac{8}{A}\,\mathcal{R}e\, g^S_{RR}$ depending linearly on g^S_{RR} while $A = 16 + 4|g^S_{RR}|^2$ receives only a small correction. Since η goes always with m_l/m_τ, even the maximum $|\eta| = 0.5$ (for $\rho = 0.75$) leads to a coefficient of $1.4 \cdot 10^{-4}$ for the decay to an electron, which will hardly be observable within the foreseeable future. The effect on the muon spectrum is still small, with a maximum coefficient of 0.06, but accessible with large data samples. Looking at the spectra, one finds that the most sensitive region to η is at low laboratory momenta, while the τ rest system would provide more information close to the endpoint. On the other hand, background from the channel $\tau \to \pi^-\nu$ can only be suppressed using muon identification, which is accomplished via high-energetic muons passing a substantial thickness of iron absorber. At 90 GeV cms energy, the implied cut $E \gtrsim 2\,\text{GeV}$ still leaves most of the interesting part of the spectrum, while at 10 GeV even a cut of 1 GeV removes the sensitive part entirely. A more elaborate method has to be used there, finding a good approximation to the tau rest system and using the spectrum of figure 7.9.

A more precise calculation for the ratio gives

$$\frac{\mathcal{B}(\tau \to \mu\nu\overline{\nu})}{\mathcal{B}(\tau \to e\nu\overline{\nu})} \approx 1 + 4\eta\frac{m_\mu - m_e}{m_\tau} - 8\frac{m_\mu^2}{m_\tau^2} = 0.973 + 0.239\eta \tag{7.15}$$

Experimental results on Michel parameters are summarized in table 7.3.

7.1.7 Experimental Results on Muon Decays

Many detailed measurements on the muon decay have been performed since the 1950s, and information on the structure of this coupling has also been obtained from the inverse process $\nu_\mu + e^- \to \mu^- + \nu_e$. The present status of experimental results is given in table 7.3.

The best existing measurements for the ξ' and ξ'' parameters of the muon are also given in table 7.3

Table 7.3 Experimentelle Resultate über Michelparameter in Myon- and Tau-Zerfällen (Stand 2000).

	$\mu \to e\nu\bar{\nu}$	$\tau \to \mu\nu\bar{\nu}$	$\tau \to e\nu\bar{\nu}$	Standard Model
ρ	0.7518 ± 0.0026	0.758 ± 0.023	0.745 ± 0.023	0.75
η	-0.007 ± 0.013	0.06 ± 0.20		0
η^a		0.019 ± 0.033		0
ξ	$-1.0027 \pm 0.0079 \pm 0.0030$	-1.08 ± 0.07	-0.99 ± 0.04	-1
κ	$-0.7486 \pm 0.0026 \pm 0.0028$	-0.78 ± 0.04	-0.73 ± 0.05	-0.75
ξ'	1.04 ± 0.04			1
ξ''	0.65 ± 0.36			1

[a] from the ratio (7.15)

7.2 Parity Violation in the Weak Interaction

Parity conservation in an interaction means

$$[\mathrm{P}, \mathcal{H}_\mathrm{K}] = [\mathcal{H}_\mathrm{K}, \mathrm{P}] = 0$$

where the interaction is described by the operator $\mathcal{H}_\mathrm{K}$. Equivalently, $\mathrm{P}\,\mathcal{H}_\mathrm{K}\,\mathrm{P}^{-1} = \mathcal{H}_\mathrm{K}$, and thereby $\mathrm{P}(\mathcal{H}_\mathrm{K}|\pm\rangle) = \pm\mathcal{H}_\mathrm{K}|\pm\rangle$, i. e. the product of the interactions has the same eigenvalue as the initial state (if it was an eigenstate).

This implies that parity violation can be established as different effects

1) $\mathrm{P}(\mathcal{H}_\mathrm{K}|\pm\rangle) = \mp\mathcal{H}_\mathrm{K}|\pm\rangle$, i. e. the eigenvalue has changed during the interaction.
2) $\mathrm{P}(\mathcal{H}_\mathrm{K}|\psi\rangle) \neq \mathcal{H}_\mathrm{K}|\,\mathrm{P}\,\psi\rangle$, e. g. the interaction in a left-handed system differs from the mirror-image of the interaction in a right-handed system.
3) Starting from a parity eigenstate of any eigenvalue, a parity-odd observable O with $\mathrm{P}\,O\,\mathrm{P}^{-1} = -O$ has a non-zero expectation value $\langle O\rangle$. An example is any pseudoscalar variable like the helicity.

   For a parity eigenstate $|\Psi\rangle$ with $\mathrm{P}\,|\Psi\rangle = \pm|\Psi\rangle$ we have

$$\langle\Psi|O|\Psi\rangle = \langle \mathrm{P}\,\Psi|\,\mathrm{P}\,O\,\mathrm{P}^{-1}\,|\,\mathrm{P}\,\Psi\rangle = \pm\langle\Psi|\,\mathrm{P}\,O\,\mathrm{P}^{-1}(\pm1)|\Psi\rangle = \langle\Psi|\,\mathrm{P}\,O\,\mathrm{P}^{-1}\,|\Psi\rangle$$

   which implies $\langle\Psi|O|\Psi\rangle = \langle\Psi|\,\mathrm{P}\,O\,\mathrm{P}^{-1}\,|\Psi\rangle = -\langle\Psi|O|\Psi\rangle$. Therefore, parity odd operators must have an expectation value of 0.

As a striking and simple example to demonstrate parity violation, we use the decay of the τ lepton to $\pi\nu$.

For a general coupling with different vector and axial vector coupling constants

$$\mathcal{H}_\mathrm{K} = W^{+,\mu}\,\bar{u}(g_V\,\gamma_\mu - g_A\,\gamma_5\gamma_\mu)u + \text{c.c.}$$

the angular distribution ($\theta = \sphericalangle\boldsymbol{s}, \boldsymbol{p}_\pi$) for the decay of polarised taus in the τ rest system is

$$\frac{\mathrm{d}\Gamma}{\mathrm{d}\cos\theta} \propto 1 + P \cdot h \cdot \cos\theta$$

where P is the τ polarisation and

$$h = -\frac{2\,\mathcal{R}e\, g_A g_V^*}{|g_V|^2 + |g_A|^2} = 1$$

in the Standard Model.

This is immediately seen in the τ rest frame for 100% polarised taus, $P = 1$:

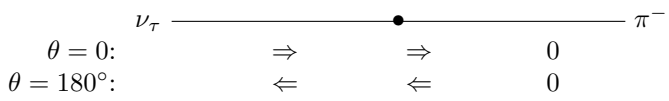

The decay of a spin $\frac{1}{2}$ particle into spin 0 and spin $\frac{1}{2}$ daughters must conserve total angular momentum, and can therefore proceed only with $L = 0$ or $L = 1$. For $L = 1$ we have $L_z = 0$ in the direction of flight ($\boldsymbol{L} \perp \boldsymbol{p}$), therefore S_z must be equal for the neutrino and the τ. To get the angular distribution with respect to the τ spin direction, we must therefore evaluate the projection

$$|\langle \tfrac{1}{2}, \theta | \tfrac{1}{2}, 0 \rangle|^2 = \cos^2 \frac{\theta}{2} = \frac{1}{2}(1 + \cos\theta)$$

An indication for a given neutrino helicity $h = \pm 1$ is the distribution

$$\frac{\mathrm{d}\Gamma}{\mathrm{d}\cos\theta(\nu)} \propto 1 \pm \cos\theta(\nu)$$

or for the pion with $\theta = \theta(\pi)$

$$\frac{\mathrm{d}\Gamma}{\mathrm{d}\cos\theta} \propto 1 \mp \cos\theta$$

which is a linear function rising from 0 in the direction where τ and ν spin would be aligned or opposite (0° or 180°) to its maximum at the other end of the distribution (180° or 0°).

Even for the most general couplings, h can be interpreted as the average polarisation of the tau neutrino: The fraction of lefthanded neutrinos at angle θ to a lefthanded τ is $\propto (1 - \cos\theta)$, the fraction of righthanded neutrinos at angle θ to a lefthanded τ is $\propto (1 + \cos\theta)$. Therefore, a polarisation $h = \frac{\#(\nu_L) - \#(\nu_R)}{\#(\nu)}$ yields an angular distribution $\propto 1 - h\cos\theta$. The τ polarisation enters accordingly.

At large τ energies, in the approximation $m_\pi^2 \ll m_\tau^2 \ll E_\tau^2$, the width can be expressed in $x := E_\pi / E_\tau$ (in the laboratory) as

$$\frac{\mathrm{d}\Gamma}{\mathrm{d}x} \propto 2Ph \cdot x + (1 - Ph) \tag{7.16}$$

A source of polarised taus, although not completely polarised, is the decay $Z^0 \to \tau^+\tau^-$. Decays of taus from this source to pions have been investigated at the LEP storage ring. Taking into account the actual polarisation of taus, figure 7.10 shows clearly the linear distribution from DELPHI data[31]. Data from ALEPH[32]. show the same with increasing accuracy. A quantitative analysis by many experiments leads to a neutrino helicity $h = -0.992 \pm 0.046$ [33] compatible with -1 as expected in the Standard Model for τ^- decays, and the opposite for τ^+.

If the weak interaction were P symmetric, we would observe a flat distribution. The result can be interpreted as P violation of type (2) or (3). The mirror image of the experiment would invert all momenta (polar vectors), but keep the spins (axial vectors). Therefore, the asymmetry in momentum with respect to the tau spin orientation would be inverted. Any non-flat distribution is not invariant

[31] DELPHI Collab., Eur. Phys. J. **C14**, 585 (2000)

[32] ALEPH Coll., Phys. Lett. **B265**, 430 (1991); Z. Phys. **C59**, 369 (1993); Z. Phys. **C69**, 183 (1996); Eur. Phys. J. **C20**, 401 (2001).

[33] PDG 2000

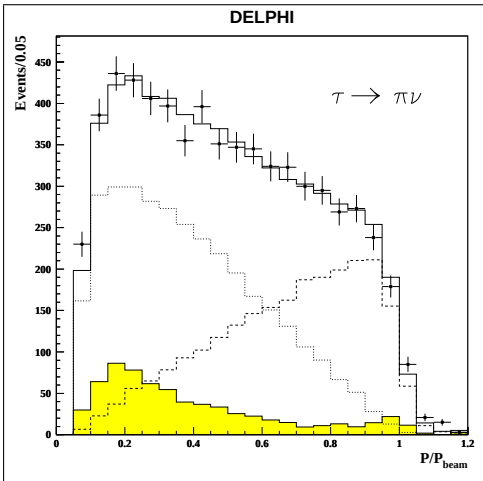

Fig. 7.10 Momentum distributions of charged pions from $\tau^- \to \pi^-\nu_\tau$. This was actually a measurement of τ polarisation at LEP, but taking the polarisation as given, it can also serve as a demonstration of parity violation in the decay. A parity symmetric decay would for any polarisation result in a flat distribution.

under this inversion, so the mirror-image result can not be achieved with true taus. Alternatively, we can say that the experiment observes a non-zero expectation value of a pseudoscalar, i. e. a parity-odd variable. Both interpretations manifest parity violation.

This experiment demonstrates C violation at the same time, since the asymmetry is opposite for the decay of the antiparticle $\tau^+ \to \pi^+\overline{\nu}_\tau$.

7.2.1 Another P-odd Variable in τ Physics

There is another simple way to demonstrate P violation in the decay $\tau^- \to a_1^-\nu_\tau \to \pi^-\pi^-\pi^+\nu_\tau$. Here, the mixed product (parallelepipedial product)

$$\boldsymbol{p}_1 \cdot (\boldsymbol{p}_2 \times \boldsymbol{p}_3)\,\mathrm{sign}(m_{13} - m_{23})$$

where 1,2 are the π^- and 3 is the π^+, is also a pseudoscalar. The factor $\mathrm{sign}(m_{13}-m_{23})$ ensures a unique definition when the two π^- are exchanged. It has been suggested[34] for a quantitative determination of the neutrino helicity, and has been measured for the first time by ARGUS in 1990 [35]. Its average as a function of $Q^2 = m^2(a_1) = (p_1 + p_2 + p_3)^2$ is shown in figure 7.11.

This observable allows, in fact, to measure the sign of the neutrino helicity with unpolarized τ leptons. The mixed product sign reflects the sign of the helicity of the a_1 meson which is the intermediate resonance decaying into three pions. It has spin 1 and can therefore allow for the following configurations in its rest frame:

$J, J_z = 1, +1$

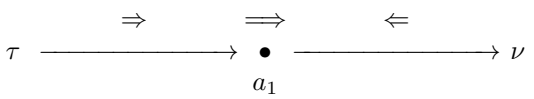

τ_L with helicity $+1$
(suppressed)

$$\propto \frac{1-\beta^*}{2} = \frac{m_a^2}{m_\tau^2 + m_a^2}$$

$J, J_z = 1, 0$

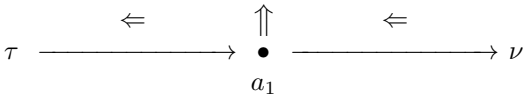

τ_L with helicity -1
(allowed)

$$\propto \frac{1+\beta^*}{2} = \frac{m_\tau^2}{m_\tau^2 + m_a^2}$$

[34] J. H. Kühn, F. Wagner, Nucl. Phys. **B236**, 16 (1984).
[35] H. Albrecht et al. (ARGUS), Phys. Lett. **B250**, 164 (1990).

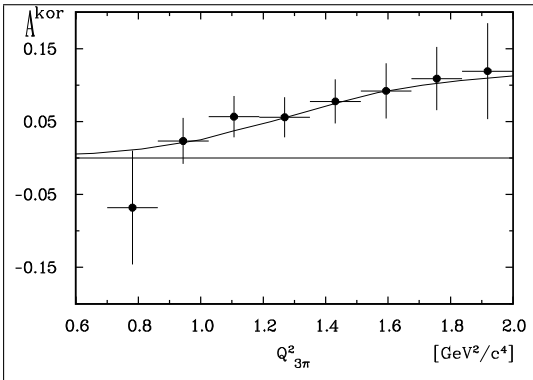

Fig. 7.11 Average asymmetry of the mixed product of pion momenta in the P and C violating decay $\tau^- \to \pi^-\pi^-\pi^+\nu_\tau$, which has been used to determine that the tau neutrino helicity is -1.

for lefthanded neutrinos and

$$J, J_z = 1, -1 \qquad\qquad J, J_z = 1, 0$$

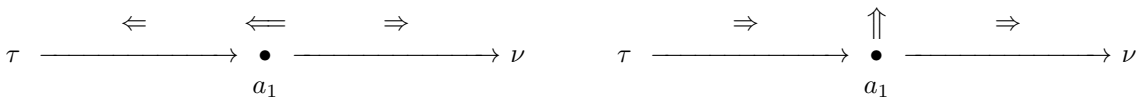

τ_R with helicity -1 (suppressed)

$$\propto \frac{1-\beta^*}{2} = \frac{m_a^2}{m_\tau^2 + m_a^2}$$

τ_R with helicity $+1$ (allowed)

$$\propto \frac{1+\beta^*}{2} = \frac{m_a^2}{m_\tau^2 + m_a^2}$$

for righthanded neutrinos.

7.2.2 History

For long time, parity was believed to be a fundamental symmetry of all physical laws. First ideas of a violation of this symmetry in weak interaction emerged as a solution of the "Θ τ puzzle".

The observation leading to this puzzle was of kaon decays both to P $= +1$ and P $= -1$ eigenstates. The most prominent were the decays $K^0 \to \pi^+\pi^-$ and $K^+ \to \pi^+\pi^0$, which involve only particles of spin 0 and hence require also zero angular momentum. The final states are, therefore, necessarily states of even parity, P $= +1$. Before the angular momentum of this so called Θ^+ meson was determined, parity and angular momentum conservation allowed the combinations $J^P = 0^+, 1^-, 2^+ \ldots$.

Another decay of a particle with the same mass and with the same strange long lifetime was the decay $K^0 \to \pi^+\pi^-\pi^0$, and $K^+ \to \pi^+\pi^+\pi^-$ for the charged particle. Three spinless particles could, in principle, be of both parity eigenvalues, depending on the relative angular momenta. However, since the two π^+ in the K^+ decay are two identical bosons, they must have an even wave function and therefore $L^P_{++} = 0^+, 2^+, 4^+ \ldots$. If the K has spin 0, the orbital angular momentum of the third pion must then be identical to L_{++} to compensate and therefore the total parity is determined by the intrinsic parity of the pions, leading to P $= -1$. Again, without knowledge of the spin of this τ^+ meson (not to be mixed with the τ lepton mentioned above, which was discovered 22 years later) the possible combinations are $J^P = 0^-, 2^-, 4^- \ldots$. None of these combintions is in the list of possibilities for the Θ^+ above.

Therefore, the K particles were assumed to be two different ones, with the only distinction in their parity eigenvalue. The P $= +1$ states were called Θ^+ and Θ^0 and the P $= -1$ states were called τ^+ and τ^0.

Since there was no other difference observed, Lee and Yang [36] suggested a different solution to the puzzle: Parity is **not conserved** in weak decays.

[36] T. D. Lee, C. N. Yang, Phys. Rev. **104**, 254 (1956).

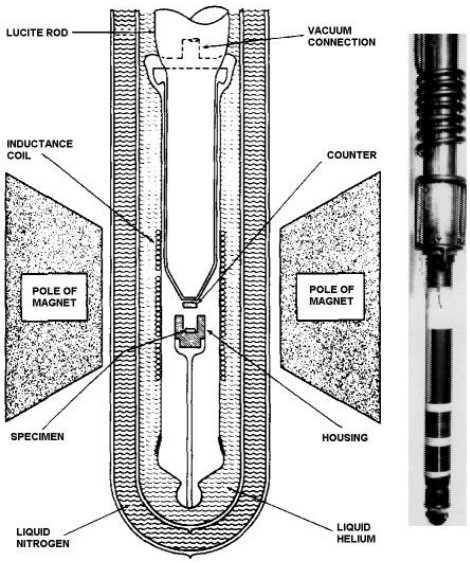

Fig. 7.12 Apparatus used in the historical experiment establishing parity violation in weak beta decay.

Parity violation in weak interaction is most pronounced in the almost massless neutrinos, which are produced in weak interactions only with left-handed helicity, or right-handed in the case of anti-neutrinos (violating the charge-conjugation symmetry C at the same time).

7.2.2.1 The Wu Experiment

A direct observation of parity violation in weak decays as a left-right-asymmetry followed soon. It is the observation of a non-zero expectation value of a P-odd observable in a nuclear beta decay by Chieng-Shiung Wu and collaborators [37].

The ground state of the ^{60}Co nucleus is $J^P = 5^+$, corresponding to a large magnetic moment. A sample of ^{60}Co at 0.01 K was placed inside a solenoid. The external magnetic field was amplified by using cobalt inside a paramagnetic salt. At this low temperature, the Co magnetic moments are aligned to a high degree. The beta decay[38] $^{60}\mathrm{Co}(J = 5) \rightarrow {}^{60}\mathrm{Ni}^*(J = 4)\, e^- \,\overline{\nu}_e$ of polarised Co nuclei was investigated. The degree of alignment of the Co atoms was measured from the angular distribution of the γ rays from the $^{60}\mathrm{Ni}^* \rightarrow \gamma\,\gamma\,{}^{60}\mathrm{Ni}$ (see figure 7.12).

The electrons were detected in an anthrazene scintillator, its light is transmitted by a light-guide to a photomultiplier. The photons were detected at 0° and 90° with respect to the polarising field by a NaI(Tl) crystal detector.

The P operation was applied by inverting the current to create the polarising magnetic field. This corresponds in fact to $\mathrm{P} \circ R_\pi$, a parity transformation followed by a 180° rotation, since the apparatus was always aligned vertically and the detector on the upper side.

The relative electron intensities in parallel and opposite to the magnetic field directions were observed qualitatively to be consistent with a distribution of the form

$$\frac{\mathrm{d}n}{\mathrm{d}\cos\theta} = 1 + \alpha\beta\cos\theta$$

with $\alpha = -1$, where $\beta = v/c$ is the velocity of the electrons and θ is the angle of emission with respect to the Co polarisation vector $\boldsymbol{J}$. The variation with β was checked in the range $0.4 < \beta < 0.8$.

[37] C. S. Wu et al., Phys. Rev. **105**, 1413 (1957).

[38] This is a $\Delta J = 1$ transition or Gamow-Teller transition with a spin flip of the dacaying neutron, in contrast to the $\Delta J = 0$ Fermi transition.

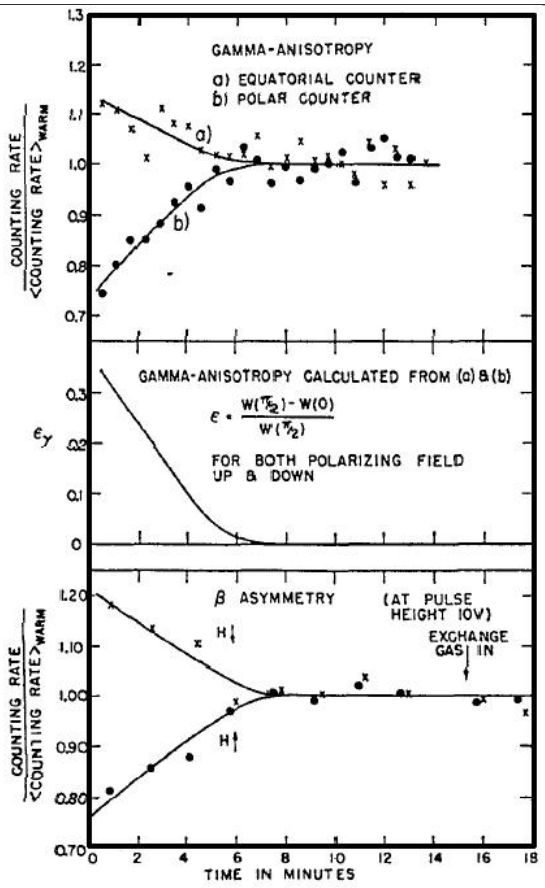

Fig. 7.13 The results of the parity violation experiment by Wu et al.: The top diagram shows the polarisation of the Ni nuclei from the gamma ray anisotropy, and the lower plot shows the counting rate for electrons, both as a function of time. Two series with opposite orientation of the magnetic field are shown (• and ×). While the sample warms up, the polarisation decreases, and the counting rate asymmetry of electrons decreases accordingly.

The years 1956/57 were indeed an exciting time. Several groups were working on proposed experiments by Lee and Yang on parity violation. The Wu group wanted to verify their results from December 27, repeating the experiment. Their original finding of a large asymmetry in the beta ray distribution was not consistently reproducible. However, after a week of solving problems with the apparatus, consistent results were obtained. And the results pointed to parity violation. Much consideration was given to the question of the origin of the beta ray asymmetry—was it really an indication of the failure of parity or some result intrinsic to the experiment? The group worked around the clock, assembling the apparatus many times, and took their breaks for a few hours sleep when the superfluid helium spoiled their vacuum by finding its way around the stopper at the bottom of the cryostat. Hoppes then slept beside the apparatus, telephoning to the others as soon as its temperature was low enough to begin their experiments again. Finally, on Januray 9th, at 2 o'clock in the morning, Hudson brought out a bottle of Chateau Lafite-Rothschild, 1949, and they drank to the overthrow of the law of parity.

The results are shown in figure 7.13, where one can see that the low temperature persisted only a few minutes, and the nuclei were completely depolarised again afterwards.

The helicity $h = \beta\chi$ of the observed electrons corresponds to chirality $\chi = -1$ which is a maximum parity violation.

7.2.3 Pion Decay

The tau decay discussed in section 7.2 is described by the diagram

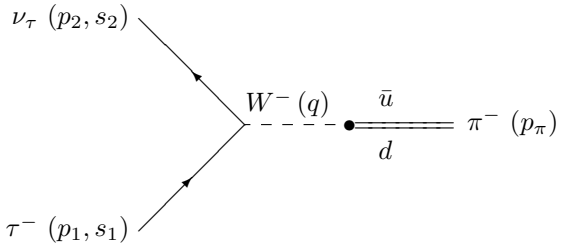

which also describes the pion decay to $\mu\overline{\nu}$ or $e\overline{\nu}$, where $1 = l = e$ or μ and $2 = \overline{\nu}$. The matrix element is

$$\begin{aligned}|\mathcal{M}|^2 &= \frac{G_F^2 f_\pi^2}{4}|V_{ud}|^2 \,\mathrm{Sp}\{\not{p}_2\not{p}_\pi(1-\gamma_5)\not{p}_1\not{p}_\pi(1-\gamma_5)\} \\ &= G_F^2 f_\pi^2 |V_{ud}|^2 \cdot m_l^2(m_\pi^2 - m_l^2)\end{aligned}$$

for a massless neutrino.

The ratio of mass factors for $l = e$ and μ is

$$\frac{m_e^2}{m_\mu^2} \cdot \frac{m_\pi^2 - m_e^2}{m_\pi^2 - m_\mu^2} = 2.34 \cdot 10^{-5} \cdot 2.34 = 5.48 \cdot 10^{-5}$$

The spin-0 pion decays to a right-handed anti-neutrino.

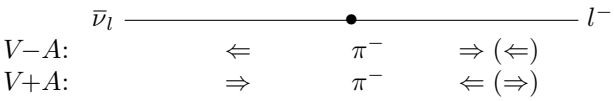

Angular momentum conservation requires that the charged lepton is also right-handed. The ratio can be obtained approximately by the probability that a helicity $+1$ fermion can have a chirality of -1 in the interaction

$$|\mathcal{M}|^2 \propto \frac{E}{E+m}(1-\beta) = \frac{E-p}{E+m} = \frac{2m_l^2}{m_\pi^2 + m_l^2} \approx \frac{2m_l^2(m_\pi^2 - m_l^2)}{m_\pi^4}$$

The ratio of phase space factors is

$$\frac{p_e^*}{p_\mu^*} = \frac{69.8\,\mathrm{MeV}}{29.8\,\mathrm{MeV}} = 2.34$$

resulting in a predicted ratio of widths of $1.283 \cdot 10^{-4}$. The experimental ratio $(1.230 \pm 0.004) \cdot 10^{-4}$ is in good agreement, taking into account radiative corrections.

This does support the existing model of a $V{-}A$ structure, but is not a prove of parity violation. A pure V interaction which is P-symmetric can be described by a sum of $V{-}A$ and $V{+}A$, which both have the same helicity suppression. The same suppression is seen in $\pi^0 \to e^+e^-$ which has a branching fraction of $6 \cdot 10^{-8}$. There is no parity violation involved in this electromagnetic decay.

Parity violation in charged pion decay is, however, observed in the fact that the decay product (muon or electron) is polarised. This can be observed in an asymmetry in the decay chain

$$\pi^- \to \mu^-\overline{\nu}_\mu, \mu^- \to e^-\overline{\nu}_e\nu_\mu$$

This asymmetry of electron emission in the muon centre of mass system with respect to the pion direction was observed [39] in the same year as the first parity violation. The asymmetry involves in fact parity violation in both steps of the cascade: the first producing a polarised muon, and the second identifying this polarisation by a forward-backward asymmetry that is itself parity violating.

The muon in pion decay is polarized: the righthanded antineutrino implies also a righthanded muon, so its spin points into the direction of flight. In the experiment by Garvin et al. the pion is stopped, and decays at rest, so the polarization of the muon is known from its direction. Then the muon is stopped, too, inside a magnetic field that can be varied in strength. The muon spin will precess, and can be observed through the anisotropy of the electron direction in muon decay. Using a delayed coincidence measurement, the electron rate is measured as a function of the magnetic field strength, and an oscillationg behaviour is observed indicating parity violation in both decays.

7.2.4 Parity Violation in Λ Decay

Parity violation in Λ decay has also been observed in the year 1957 in a purely hadronic decay. Again a pseudoscalar, a P-odd observable, has been measured to have a nonzero expectation value. The reaction

$$\pi^- p \to \Lambda K^0,\ \Lambda \to p\pi^-$$

has been investigated [40]. The pseudoscalar is the mixed product

$$(\boldsymbol{p}_{\text{beam}} \times \boldsymbol{p}_\Lambda) \cdot \boldsymbol{p}_\pi$$

Eisler et al. showed the distribution of the angle $\theta = \sphericalangle \boldsymbol{n}_{\text{plane}}, \boldsymbol{p}_\pi$ which is the angle between the normal to the reaction plane (represented in the mixed product by $\boldsymbol{p}_{\text{beam}} \times \boldsymbol{p}_\Lambda$) and the outgoing pion. The Λ hyperon is polarised perpedicular to the reaction plane and the asymmetry is in the decay direction with respect to the Λ polarisation.

They find 158 up-going pions versus 105 down-going. This is about three sigma evidence for parity violation in the decay of polarized Λ baryons.

The decay may proceed as an S wave (p spin = Λ spin) or a P wave (p spin opposite to Λ spin). The angular asymmetry with respect to the Λ spin direction arises due to the interference of S and P wave. The pion is preferentially emitted opposite to the Λ spin direction, but in the direction of the $\overline{\Lambda}$ spin (P violation = C violation).

$$\frac{\mathrm{d}\Gamma}{\mathrm{d}\Omega} \sim 1 + \alpha \hat{\boldsymbol{s}} \hat{\boldsymbol{p}} = 1 + \alpha \cos\theta_{s,p}$$

with $\boldsymbol{s} = \Lambda$ spin, $\boldsymbol{p} = p$ momentum in Λ rest frame, and $\alpha_\Lambda = -\alpha_{\overline{\Lambda}} \approx 0.64$.

The same asymmetry holds for $\Lambda \to n\pi^0$.

[39] R. L. Garvin, L. M. Lederman, M. Weinrich, Phys. Rev. **105**, 1415 (1957);
J. J. Friedman, V. L. Telegdi, Phys. Rev. **105**, 1681 (1957).

[40] F. Eisler et al., Phys. Rev. **108**, 1353 (1957).

8. Elektroschwache Wechselwirkung

Das Glashow–Weinberg–Salam-Modell[41] ist eine Yang-Mills-Theorie zur Symmetrie $\mathbf{SU(2)} \times \mathbf{U(1)}$: schwacher Isospin I_W, I_{W3} und schwache Hyperladung Y_W mit

$$\begin{aligned} Q &= \frac{Y_W}{2} + I_{W3} \\ Y_W &= 2(Q - I_{W3}) \end{aligned} \tag{8.1}$$

Eichfelder W_1, W_2, W_3 und B

Table 8.1 Elektroschwache Ladungen der Fermionen

Fermionen	Q	I_W, I_{W3}	Y_W
e_L^-, μ_L^-, τ_L^-	-1	$\frac{1}{2}, -\frac{1}{2}$	-1
$\nu_{eL}, \nu_{\mu L}, \nu_{\tau L}$	0	$\frac{1}{2}, +\frac{1}{2}$	-1
e_R^-, μ_R^-, τ_R^-	-1	$0, 0$	-2
$\nu_{eR}, \nu_{\mu R}, \nu_{\tau R}$	0	$0, 0$	0
$d_{rL}, d_{gL}, d_{bL},\ s_{rL}, s_{gL}, s_{bL},\ b_{rL}, b_{gL}, b_{bL}$	$-\frac{1}{3}$	$\frac{1}{2}, -\frac{1}{2}$	$\frac{1}{3}$
$u_{rL}, u_{gL}, u_{bL},\ c_{rL}, c_{gL}, c_{bL},\ t_{rL}, t_{gL}, t_{bL}$	$\frac{2}{3}$	$\frac{1}{2}, +\frac{1}{2}$	$\frac{1}{3}$
$d_{rR}, d_{gR}, d_{bR},\ s_{rR}, s_{gR}, s_{bR},\ b_{rR}, b_{gR}, b_{bR}$	$-\frac{1}{3}$	$0, 0$	$-\frac{2}{3}$
$u_{rR}, u_{gR}, u_{bR},\ c_{rR}, c_{gR}, c_{bR},\ t_{rR}, t_{gR}, t_{bR}$	$\frac{2}{3}$	$0, 0$	$\frac{4}{3}$

Lagrangian:

$$L_{F+K} = \bar{\psi}_L i\gamma^\mu D_{\mu(L)} \psi_L + \bar{\psi}_R i\gamma^\mu D_{\mu(R)} \psi_R - \bar{\psi}_L m \psi_R - \bar{\psi}_R m \psi_L \tag{8.2}$$

mit $\psi_L = \frac{1}{2}(1 - \gamma_5)\psi$, $\psi_R = \frac{1}{2}(1 + \gamma_5)\psi$ und

$$\begin{aligned} D_{\mu(L)} &= \partial_\mu - ig \sum_{j=1}^{3} W_{j,\mu} \frac{\sigma_j}{2} - ig' B_\mu \frac{Y_W}{2} \\ D_{\mu(R)} &= \partial_\mu - ig' B_\mu \frac{Y_W}{2} \end{aligned}$$

und der Hyperladung Y_W aus Tabelle 8.1.

$$\begin{aligned} W^+ &= \frac{1}{\sqrt{2}}(W_1 - iW_2) \\ W^- &= \frac{1}{\sqrt{2}}(W_1 + iW_2) \\ W_1 &= \frac{1}{\sqrt{2}}(W^+ + W^-) \\ W_2 &= \frac{-i}{\sqrt{2}}(W^+ - W^-) \\ W^{+\dagger} &= W^- \end{aligned}$$

[41] S. L. Glashow, Nucl. Phys. **22**, 579 (1961); S. Weinberg, Phys. Rev. Lett. **19**, 1264 (1967); A. Salam in N. Svartholm (Ed.), Proc. 8-th Nobel Symp., Almquist and Wiksell, Stockholm (1968), p. 367.

8.1 Elektroschwache Mischung

Weinbergwinkel θ_W

$$\tan\theta_W := g'/g \tag{8.3}$$

(Experiment: $\sin^2\theta_W \approx 0.23$)
Physikalische Felder Z^0 und A (Photon):

$$\begin{aligned} Z^0 &= W_3\cos\theta_W - B\sin\theta_W \\ A &= W_3\sin\theta_W + B\cos\theta_W \end{aligned} \tag{8.4}$$

$$\begin{aligned} W_3 &= Z^0\cos\theta_W + A\sin\theta_W \\ B &= -Z^0\sin\theta_W + A\cos\theta_W \end{aligned}$$

Setzt man

$$e = g\sin\theta_W \tag{8.5}$$

ist

$$\begin{aligned} W_3 &= Z^0 e/g' + Ae/g \\ B &= -Z^0 e/g + Ae/g' \end{aligned} \tag{8.6}$$

$$\frac{1}{2}\left(W_1\sigma_1 + W_2\sigma_2\right) = \frac{1}{\sqrt{2}}\begin{pmatrix} 0 & \frac{1}{\sqrt{2}}(W_1 - iW_2) \\ \frac{1}{\sqrt{2}}(W_1 + iW_2) & 0 \end{pmatrix} = \frac{1}{\sqrt{2}}\begin{pmatrix} 0 & W^+ \\ W^- & 0 \end{pmatrix}$$

hier ist z. B. der Aufsteigeoperator $I_+ = \begin{pmatrix} 0 & 1 \\ 0 & 0 \end{pmatrix}$ durch die Kombination $W^+ \sim W_1 - iW_2$ repräsentiert.

$$\begin{aligned} \frac{1}{2}\left(gW_3\sigma_3 + g'BY_W\right) &= \frac{1}{2}\begin{pmatrix} gW_3 + g'BY_W & 0 \\ 0 & -gW_3 + g'BY_W \end{pmatrix} \\ &= e\begin{pmatrix} A\frac{1+Y_W}{2} + Z^0\frac{\cos^2\theta_W - Y_W\sin^2\theta_W}{2\sin\theta_W\cos\theta_W} & 0 \\ 0 & A\frac{1-Y_W}{2} + Z^0\frac{-\cos^2\theta_W - Y_W\sin^2\theta_W}{2\sin\theta_W\cos\theta_W} \end{pmatrix} \end{aligned}$$

$$\begin{aligned} D_{\mu(L)} &= \partial_\mu - ig\sum_{j=1}^{3} W_{j,\mu}\frac{\sigma_j}{2} - ig'B_\mu\frac{Y_W}{2} \\ &= \partial_\mu - \frac{i}{2}\begin{pmatrix} gW_{3,\mu} + g'B_\mu Y_W & g\sqrt{2}W_\mu^- \\ g\sqrt{2}W_\mu^+ & -gW_{3,\mu} + g'B_\mu Y_W \end{pmatrix} \\ &= \partial_\mu - \frac{i}{2}\begin{pmatrix} e(1+Y_W)A_\mu + eZ_\mu\frac{\cos^2\theta_W - Y_W\sin^2\theta_W}{\sin\theta_W\cos\theta_W} & g\sqrt{2}W_\mu^- \\ g\sqrt{2}W_\mu^+ & e(1-Y_W)A_\mu + eZ_\mu\frac{-\cos^2\theta_W - Y_W\sin^2\theta_W}{\sin\theta_W\cos\theta_W} \end{pmatrix} \end{aligned}$$

Die Terme für linkshändige Fermionen $\frac{1}{2}\frac{\pm\cos^2\theta_W - Y_W\sin^2\theta_W}{\sin\theta_W\cos\theta_W}$ lassen sich mit (8.1) als

$$\frac{I_{W3}\cos^2\theta_W - \frac{Y_W}{2}\sin^2\theta_W}{\sin\theta_W\cos\theta_W} = \frac{I_{W3} - Q\sin^2\theta_W}{\sin\theta_W\cos\theta_W}$$

schreiben. Das ist die effektive Ladung für die Wechselwirkung eines linkshändigen Fermions mit dem Z-Boson (wobei der Nenner Teil der Kopplungskonstanten ist).

Daraus ergibt sich der Wechselwirkungsterm

$$\begin{aligned}\mathcal{L}_{WW} &= e\cdot\left\{A^\mu {J_\mu}^{em} + \frac{1}{\sin\theta_W\cos\theta_W} Z^\mu {J_\mu}^{nc} + \frac{1}{\sqrt{2}\sin\theta_W}(W^{+,\mu}{J_\mu}^{cc} + W^{-,\mu}{J_\mu^+}^{cc})\right\}\\ &= eA^\mu {J_\mu}^{em} + \frac{g}{\cos\theta_W} Z^\mu {J_\mu}^{nc} + \frac{g}{\sqrt{2}}(W^{+,\mu}{J_\mu}^{cc} + W^{-,\mu}{J_\mu^+}^{cc})\end{aligned}$$

Ströme:

$${J_\mu}^{em} = -\begin{pmatrix}\bar e\\ \bar\mu\\ \bar\tau\end{pmatrix}\gamma_\mu\begin{pmatrix}e\\ \mu\\ \tau\end{pmatrix} + \frac{2}{3}\sum_{r,g,b}\begin{pmatrix}\bar u\\ \bar c\\ \bar t\end{pmatrix}\gamma_\mu\begin{pmatrix}u\\ c\\ t\end{pmatrix} - \frac{1}{3}\sum_{r,g,b}\begin{pmatrix}\bar d\\ \bar s\\ \bar b\end{pmatrix}\gamma_\mu\begin{pmatrix}d\\ s\\ b\end{pmatrix} \tag{8.7}$$

$${J_\mu}^{cc} = \begin{pmatrix}\bar\nu_e\\ \bar\nu_\mu\\ \bar\nu_\tau\end{pmatrix}\gamma_\mu\frac{1-\gamma_5}{2}\begin{pmatrix}e\\ \mu\\ \tau\end{pmatrix} + \sum_{r,g,b}\begin{pmatrix}\bar u\\ \bar c\\ \bar t\end{pmatrix}\gamma_\mu\frac{1-\gamma_5}{2}\ \boldsymbol{V}\cdot\begin{pmatrix}d\\ s\\ b\end{pmatrix} \tag{8.8}$$

$$\begin{aligned}{J_\mu}^{nc} = {}& \tfrac{1}{2}\begin{pmatrix}\bar\nu_e\\ \bar\nu_\mu\\ \bar\nu_\tau\end{pmatrix}\gamma_\mu\frac{1-\gamma_5}{2}\begin{pmatrix}\nu_e\\ \nu_\mu\\ \nu_\tau\end{pmatrix} - \tfrac{1}{2}\begin{pmatrix}\bar e\\ \bar\mu\\ \bar\tau\end{pmatrix}\gamma_\mu\frac{1-\gamma_5}{2}\begin{pmatrix}e\\ \mu\\ \tau\end{pmatrix}\\ &+ \tfrac{1}{2}\sum_{r,g,b}\begin{pmatrix}\bar u\\ \bar c\\ \bar t\end{pmatrix}\gamma_\mu\frac{1-\gamma_5}{2}\begin{pmatrix}u\\ c\\ t\end{pmatrix} - \tfrac{1}{2}\sum_{r,g,b}\begin{pmatrix}\bar d\\ \bar s\\ \bar b\end{pmatrix}\gamma_\mu\frac{1-\gamma_5}{2}\begin{pmatrix}d\\ s\\ b\end{pmatrix}\\ &- \sin^2\theta_W J_\mu^{em}\end{aligned} \tag{8.9}$$

Als Summe aus Vektor- und Axialvektoranteil für ein Fermion-dublett (x, y):

$$\begin{aligned}\mathcal{L}_{WW}^{\text{schwach}} = {}& Z^\mu\,\bar\psi_x(g_v^{nc}(x)\,\gamma_\mu - g_a^{nc}(x)\,\gamma_5\gamma_\mu)\psi_x + Z^\mu\,\bar\psi_y(g_v^{nc}(y)\,\gamma_\mu - g_a^{nc}(y)\,\gamma_5\gamma_\mu)\psi_y\\ &+ W^{+,\mu}\,\bar\psi_y(g_v^{cc}(x)\,\gamma_\mu - g_a^{cc}(x)\,\gamma_5\gamma_\mu)\psi_x + W^{-,\mu}\,\bar\psi_x(g_v^{cc}(x)\,\gamma_\mu - g_a^{cc}(x)\,\gamma_5\gamma_\mu)\psi_y\end{aligned}$$

Kopplungskonstanten:

elektromagnetisch: $g_e = e\cdot Q$

geladener Vektorstrom (W): $g_v^{cc} = \dfrac{e}{\sqrt{2}\sin\theta_W}\cdot I_W$

geladener Axialvektorstrom (W): $g_a^{cc} = \dfrac{e}{\sqrt{2}\sin\theta_W}\cdot I_W$

neutraler Vektorstrom (Z^0): $g_v = g_v^{nc} = \dfrac{e}{\sin\theta_W\cos\theta_W}\cdot\left(\dfrac{I_{W3}}{2} - Q\sin^2\theta_W\right)$

neutraler Axialvektorstrom (Z^0): $g_a = g_a^{nc} = \dfrac{e}{\sin\theta_W\cos\theta_W}\cdot\dfrac{I_{W3}}{2}$

Table 8.2 Ladungen und Kopplungskonstanten, experimentelle Werte mit Fehlern

Fermionen	Q	I_{W3}	$c_v = \dfrac{2g_v\sin\theta_W\cos\theta_W}{e}$	$c_a = \dfrac{2g_a\sin\theta_W\cos\theta_W}{e}$
e^-, μ^-, τ^-	-1	$-\frac{1}{2}$	$-\frac{1}{2} + 2\sin^2\theta_W \quad = -0.038$	$-\frac{1}{2}$
ν_e, ν_μ, ν_τ	0	$+\frac{1}{2}$	$+\frac{1}{2} \quad = +0.500$	$+\frac{1}{2}$
$d_r, d_g, d_b,\ s_r, s_g, s_b$ b_r, b_g, b_b	$-\frac{1}{3}$	$-\frac{1}{2}$	$-\frac{1}{2} + \frac{2}{3}\sin^2\theta_W \quad = -0.346(-0.33\pm0.06)$	$-\frac{1}{2}$
$u_r, u_g, u_b,\ c_r, c_g, c_b$ t_r, t_g, t_b	$+\frac{2}{3}$	$+\frac{1}{2}$	$+\frac{1}{2} - \frac{4}{3}\sin^2\theta_W \quad = 0.192(+0.29\pm0.09)$	$+\frac{1}{2}$

Table 8.3 L- und R-Kopplungskonstanten

Fermionen	$c_L = c_v + c_a = 2(I_{W3} - Q\sin^2\theta_W)$	$c_R = c_v - c_a = -2Q\sin^2\theta_W$
e^-, μ^-, τ^-	$2\sin^2\theta_W - 1 \quad = -0.538$	$2\sin^2\theta_W \quad = 0.462$
ν_e, ν_μ, ν_τ	1	0
$d_r, d_g, d_b,\ s_r, s_g, s_b$ b_r, b_g, b_b	$\frac{2}{3}\sin^2\theta_W - 1 \quad = -0.846$	$\frac{2}{3}\sin^2\theta_W \quad = 0.154$
$u_r, u_g, u_b,\ c_r, c_g, c_b$ t_r, t_g, t_b	$1 - \frac{4}{3}\sin^2\theta_W \quad = 0.692$	$-\frac{4}{3}\sin^2\theta_W \quad = -0.308$

$\sin^2\theta_W(m_Z) = 0.2312 \pm 0.0001$ (bei $Q^2 = m_Z^2$ und abhängig vom Renormierungsschema, hier $\overline{MS}$), bei kleinen Energien ist $\sin^2\theta_W = 0.228 \pm 0.001$.

Links- und rechtshändige Kopplungskonstanten:

$$
\begin{aligned}
g_R^{cc} &= 0 \\
g_L^{cc} &= g_v^{cc} + g_a^{cc} = \frac{e\sqrt{2}I_W}{\sin\theta_W} \approx 1.47e \\
g_R^{nc} &= g_v - g_a = eQ\tan\theta_W \approx 0.547e \cdot Q \\
g_L^{nc} &= g_v + g_a = e\frac{I_{W3} - Q\sin^2\theta_W}{\sin\theta_W\cos\theta_W} \\
\left(g_L^{nc} = e\frac{-1 + 2\sin^2\theta_W}{2\sin\theta_W\cos\theta_W} \approx -0.640e \quad \text{für das Elektron}\right)
\end{aligned}
$$

Die Kopplungen werden durch individuelle Ladungen der Fermionen modifiziert, g_L^{nc} kann nicht teilchenunabhängig faktorisiert werden (vgl. Tab. 8.3).

8.1.1 Bosonmassen

Ersetzt man in (8.4) die Felder durch Massen, erhält man

$$
\begin{aligned}
m_Z &= m_W\cos\theta_W - m_B\sin\theta_W \\
m_\gamma &= m_W\sin\theta_W + m_B\cos\theta_W
\end{aligned}
$$

Aus $m_\gamma = 0$ folgt $m_Z = m_W/\cos\theta_W$ oder

$$
\cos\theta_W = \frac{m_W}{m_Z} \tag{8.10}
$$

und

$$
\rho := \frac{m_W^2}{m_Z^2\cos^2\theta_W} = 1
$$

Zum Beweis betrachtet man den Proca-Massenterm des Lagrangian

$$
\mathcal{L}_M = \tfrac{1}{2}m_Z^2\,\mathrm{Sp}\,\boldsymbol{Z}^\mu\boldsymbol{Z}_\mu + m_W^2\,\mathrm{Sp}\,\boldsymbol{W}^{+\mu}\boldsymbol{W}^-{}_\mu = \tfrac{1}{2}m_B^2B^\mu B_\mu + \tfrac{1}{2}m_W^2\sum_{j=1}^{3}\mathrm{Sp}\,\boldsymbol{W}_j^\mu\boldsymbol{W}_{j,\mu}
$$

mit $\boldsymbol{W}_j^\mu = \frac{1}{2}W_j^\mu\sigma_j$ etc. Für das Photon ist $m_\gamma = 0$, es trägt daher nicht zu $\mathcal{L}_M$ bei.

Der Beitrag des Z^0 ist

$$
\mathcal{L}_M = \tfrac{1}{2}m_Z^2\,\mathrm{Sp}\,\boldsymbol{Z}^\mu\boldsymbol{Z}_\mu
$$

Da W_3 die gleiche Masse wie W_1 und W_2 haben muss, deren Proca-Terme

$$\mathcal{L}_M = \tfrac{1}{2} m_W^2 \,\mathrm{Sp}(\tfrac{1}{2} W_{1\mu}\sigma_1)(\tfrac{1}{2} W_1^\mu \sigma_1) = \tfrac{1}{4} m_W^2 W_1^\mu W_{1\mu}$$

sind, ist $\frac{1}{4} m_Z^2 \cos^2\theta_W$, der Koeffizient von $W_3^\mu W_{3\mu}$, gleich $\frac{1}{4} m_W^2$, dem Koeffizienten von $W_1^\mu W_{1\mu}$. Daraus folgt (8.10).

8.2 Entdeckung des W-Bosons

Die erste Beobachtung reeller W-Bosonen publizierte 1983 das UA1-Experiment[42] (Sprecher: C. Rubbia) am Sp$\bar{\text{p}}$S Speicherring (CERN):

$$p\bar{p} \to WX, W \to e\nu$$

Das Neutrino wird als fehlender Transversalimpuls und fehlende transversale Energie rekonstruiert. Man erhält eine Untergrenze für die Masse

$$\begin{aligned} m_W^2 \geq m_\perp^2 &= (E_{e\perp} + E_{\nu\perp})^2 - (\vec{p}_{e\perp} + \vec{p}_{\nu\perp})^2 \\ &= 2E_{e\perp}E_{\nu\perp}(1 - \cos\phi_{e\nu}) \\ &= 2E_e E_\nu \sin\theta_e \sin\theta_\nu (1 - \cos\phi_{e\nu}) \end{aligned}$$

wobei $\phi_{e\nu}$ der Winkel zwischen $\vec{p}_{e\perp}$ und $\vec{p}_{\nu\perp}$ in der Ebene senkrecht zur Strahlachse ist (Koordinaten: Strahlachse z, Elektron in xz-Ebene, $\vec{p}_\nu/E_\nu = (\cos\phi_{e\nu}\sin\theta_\nu, \sin\phi_{e\nu}\sin\theta_\nu, \cos\theta_\nu)$; für die leichten Leptonen ist $|\vec{p}| = E$). Die wirkliche W-Masse ist gegeben durch

$$\begin{aligned} m_W^2 &= (E_e + E_\nu)^2 - (\vec{p}_e + \vec{p}_\nu)^2 \\ &= 2E_e E_\nu (1 - \cos\phi_{e\nu}\sin\theta_e \sin\theta_\nu - \cos\theta_e \cos\theta_\nu) \\ m_W^2 - m_\perp^2 &= 2E_e E_\nu \,(1 - \cos(\theta_e - \theta_\nu)) \end{aligned}$$

Für $\theta_e = \theta_\nu$ ist $m_\perp = m_W$, sonst ist es immer kleiner.

8.3 Neutrale Ströme

Neutrale Ströme (8.9), die über das Z^0-Boson miteinander koppeln, wurden 1973 zum ersten Mal beobachtet. Die Gargamelle-Blasenkammer am CERN, die mit 12000 Liter Freon gefüllt war, stand in einem Neutronenstrahl. In einer Datenmenge von über 700000 Aufnahmen fand man eine elastische Streuung eines Neutrinos an einem Elektron.

8.3.1 Z^0-Zerfall

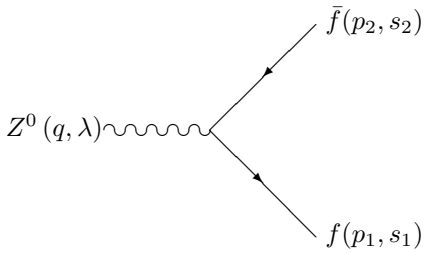

[42] UA1 Collab., Phys. Lett. **122B**, 103 (1983).

Notation: p, q = Energie-Impuls-Vektor, s = Fermionspin, λ = Bosonspin

Feynmanregeln $\Longrightarrow$

$$-i\mathcal{M} = \varepsilon_\mu(q,\lambda)\,\bar{u}(p_1,s_1)\,\frac{-ig}{\cos\theta_W}\gamma_\mu\tfrac{1}{2}(c_v - c_a\gamma_5)v(p_2,s_2)$$

Spinmittelung beim Z_0, Spinsummen im Endzustand $\frac{1}{3}\sum_{\lambda,s_1,s_2}|\mathcal{M}|^2$ führt auf die Breite

$$\Gamma_{f\bar{f}} = m_Z\frac{g^2}{48\pi\cos^2\theta_W}[c_v^2(f)+c_a^2(f)] = \frac{m_Z^3 G_F}{6\sqrt{2}\,\pi}[c_v^2(f)+c_a^2(f)]$$

$$\Gamma_{\text{tot}} = \sum_{e,\mu,\tau,\nu_e,\nu_\mu,\nu_\tau,u,d,s,c,b}\Gamma_{f\bar{f}} \approx 2\,\text{GeV}$$

bei den Quarks jeweils 3 Colours

8.4 Der Higgs-Mechanismus

Der Higgs-Mechanismus wurde in den Jahren 1964–66 von verschiedenen Autoren[43] formuliert, und nach der Entdeckung des Higgs-Bosons[44] 2013 mit dem Nobelpreis and Englert und Higgs gewürdigt.

Ausgangspunkt ist ein Lagrangian eines skalaren Feldes[45]

$$\mathcal{L}_H = (\partial_\mu\phi)^*(\partial^\mu\phi) + \mu^2\phi^*\phi - \lambda(\phi^*\phi)^2 \tag{8.11}$$

mit Selbstkopplung (ϕ^4-Term) und negativer Masse ($+\mu^2$ statt $-\mu^2$), dem „Wine bottle potential“. Das zugehörige Potenzial

$$V(\phi) = \pm\mu^2\phi^*\phi + \lambda(\phi^*\phi)^2$$

ist das allgemeinste renormierbare skalare Potenzial.

Als einfaches Modellbeispiel diskutieren wir einen Higgsmechanismus für die $\mathbf{U(1)}$-Symmetrie. Dazu benötigen wir ein komplexes skalares Feld

$$\phi = \frac{1}{\sqrt{2}}(\phi_1 - i\phi_2) \tag{8.12}$$

mit elektrischer Ladung $Q = 1$, das sich unter $\mathbf{U(1)}$-Transformationen wie

$$\phi' = e^{i\alpha(x)}\phi$$

transformiert. Dann ist mit $D_\mu = \partial_\mu + ieQA_\mu$ und $A'_\mu = A_\mu - \frac{1}{e}\partial_\mu\alpha(x)$

$$\begin{aligned} D'_\mu\phi' &= (\partial_\mu + ieA'_\mu)e^{i\alpha(x)}\phi \\ &= e^{i\alpha(x)}\partial_\mu\phi + i(\partial_\mu\alpha(x))e^{i\alpha(x)}\phi + ie\left(A_\mu - \frac{1}{e}\partial_\mu\alpha(x)\right)e^{i\alpha(x)}\phi \\ &= e^{i\alpha(x)}\partial_\mu\phi + ieA_\mu e^{i\alpha(x)}\phi = e^{i\alpha(x)}D_\mu\phi \end{aligned}$$

[43] F. Englert, R. Brout, „Broken Symmetry and the Mass of Gauge Vector Mesons“, Phys. Rev. Lett. **13**, 321 (1964); Peter W. Higgs, „Broken Symmetries, Massless Particles and Gauge Fields“, Phys. Lett. **12**, 132 (1964); P. W. Higgs, „Broken Symmetries and the Masses of Gauge Bosons“, Phys. Rev. Lett. **13**, 508 (1964); G. S. Guralnik, C. R. Hagen, Tom W. B. Kibble, „Global Conservation Laws and Massless Particles“, Phys. Rev. Lett. **13**, 585 (1964).

[44] vorhergesagt von Peter Higgs, „Spontaneous Symmetry Breakdown without Massless Bosons“, Phys. Rev. **145**, 1156 (1966).

[45] Jeffrey Goldstone, „Field Theories with ‘Superconductor’ Solutions“, Il Nuovo Cim. **19**, 154 (1961).

und

$$(D'_\mu \phi')^* (D'^\mu \phi') = (D_\mu \phi)^* (D^\mu \phi)$$

ist lokal eichinvariant, ebenso wie $\phi'^* \phi' = \phi^* e^{-i\alpha(x)} e^{i\alpha(x)} \phi = \phi^* \phi$.

Lagrangian, invariant unter **U(1)**:

$$\mathcal{L}_H = (D_\mu \phi)^* (D^\mu \phi) - V(\phi^* \phi) \tag{8.13}$$

Das Higgs-Potenzial (potenzielle Energiedichte)

$$V(\phi^* \phi) = -\mu^2 \phi^* \phi + \lambda (\phi^* \phi)^2 \tag{8.14}$$

Dimensionsbetrachtung: Eine Energiedichte hat die Dimension $[E/x^3] = [E^4]$ in natürlichen Einheiten, μ und ϕ haben jeweils die Dimension $[E]$, λ ist dimensionslos, also eine Kopplungskonstante.

V hat ein Minimum bei

$$-\mu^2 + 2\lambda \phi^* \phi = 0 \qquad \Longrightarrow \qquad \phi^* \phi = \frac{\mu^2}{2\lambda}, \qquad |\phi| = \tilde{v} = \frac{\mu}{\sqrt{2\lambda}}$$

mit

$$\min V = V_0 = -\mu^4 / 4\lambda = -\tfrac{1}{2} \mu^2 \tilde{v}^2$$

Ein beliebiges Higgsfeld im Minimum ist dann $e^{i\alpha(x)} \tilde{v}$.

Ein beliebiges Higgsfeld ist

$$\phi(x) = \left(\tilde{v} + \frac{1}{\sqrt{2}} h(x) \right) e^{i\alpha(x)}$$

Eine Eichtransformation

$$e^{-i\alpha(x)}$$

macht daraus das reelle Feld

$$\phi'(x) = \tilde{v} + \frac{1}{\sqrt{2}} h(x) = \frac{v + h(x)}{\sqrt{2}} \tag{8.15}$$

d. h. die zweite Komponente kann **weggeeicht** werden.

In den meisten Lehrbüchern findet man statt $\tilde{v}$ den Wert $v = \sqrt{2}\, \tilde{v}$, den Wert der Komponente ϕ_1 aus (8.12) im Minimum.

Eine Entwicklung um $\tilde{v}$ ergibt

$$\phi(x) = \tilde{v} + \frac{1}{\sqrt{2}} h(x) + i \tilde{v} \alpha(x) + \mathcal{O}(\alpha^2, h\alpha)$$

Eine lokale Eichtransformation ändert also in niedrigster Ordnung den Imaginärteil (ϕ_2) des Feldes. In der umgeeichten Version (8.15) ist die imaginäre Komponente ϕ_2 verschwunden. Die Feldanregung $\phi_2 = -\sqrt{2}\, \tilde{v} \alpha(x)$ ist ein *Goldstone-Boson*[46], das aber weggeeicht werden kann und daher keinem beobachtbaren Teilchen entspricht. Die Feldanregung $\phi_1 = h(x)$ ein *Higgs-Boson*.

[46] Fußnote [45] on page 125 und J. Goldstone, A. Salam, S. Weinberg, Phys. Rev. **127**, 965 (1962).

Die Lagrangedichte (8.13) ist eichinvariant, daher können wir für ϕ das reelle Feld (8.15) einsetzen:

$$\begin{aligned}
\mathcal{L}_H &= (D_\mu\phi)^*(D^\mu\phi) - V(\phi^*\phi) \\
&= \left(\frac{1}{\sqrt{2}}\partial_\mu h - ie\tilde{v}A_\mu - i\frac{e}{\sqrt{2}}A_\mu h\right)\left(\frac{1}{\sqrt{2}}\partial^\mu h + ie\tilde{v}A^\mu + i\frac{e}{\sqrt{2}}A^\mu h\right) \\
&\quad + \mu^2\left(\tilde{v}^2 + \frac{1}{2}h^2 + \sqrt{2}\,\tilde{v}h\right) - \lambda\left(\tilde{v}^4 + \frac{1}{4}h^4 + 2\tilde{v}^2h^2 + \tilde{v}^2h^2 + \sqrt{2}\,\tilde{v}h^3 + 2\sqrt{2}\,\tilde{v}^3h\right) \\
&= \frac{1}{2}(\partial_\mu h)(\partial^\mu h) + e^2\tilde{v}^2A_\mu A^\mu + \frac{e^2}{2}h^2A_\mu A^\mu + \frac{2e^2\tilde{v}}{\sqrt{2}}hA_\mu A^\mu \\
&\quad + \mu^2\left(\tilde{v}^2 + \frac{1}{2}h^2 + \sqrt{2}\,\tilde{v}h\right) - \frac{\mu^2}{2\tilde{v}^2}\left(\tilde{v}^4 + \frac{1}{4}h^4 + 2\tilde{v}^2h^2 + \tilde{v}^2h^2 + \sqrt{2}\,\tilde{v}h^3 + 2\sqrt{2}\,\tilde{v}^3h\right) \\
&= \frac{1}{2}(\partial_\mu h)(\partial^\mu h) + e^2\tilde{v}^2A_\mu A^\mu + \frac{e^2}{2}h^2A_\mu A^\mu + \frac{2e^2\tilde{v}}{\sqrt{2}}hA_\mu A^\mu \\
&\quad - V_0 - \mu^2h^2 - \mu\sqrt{\lambda}\,h^3 - \frac{\lambda}{4}h^4
\end{aligned}$$

Durch Vergleich mit dem Lagrangian zur Proca-Gleichung (4.68)

$$\mathcal{L} = -\frac{1}{4}F_{\mu\nu}F^{\mu\nu} + \frac{1}{2}m^2A_\mu A^\mu$$

sieht man, dass das Photonfeld A_μ die Masse $m_A = \sqrt{2}\,e\tilde{v}$ erhalten hat.

Es sind auch neue Kopplungen dazugekommen: ein Dreiervertex $h\gamma\gamma$ mit Kopplungskonstante em_A proportional zur Photonmasse, und ein Vierervertex $hh\gamma\gamma$ mit Kopplungskonstante $e^2/2$.

Das Residualfeld h, das physikalische Higgs-Boson, ist ein reellwertiges Feld ohne Phasensymmetrie, also auch ohne elektrische Ladung. Wir haben also aus dem ursprünglich geladenen Teilchen nach der spontanen Symmetriebrechung ein neutrales Teilchen gewonnen. Es koppelt an das massive Photon mit einer Kopplungsstärke, die proportional zur Masse ist.

Durch Vergleich mit der Lagrangedichte für reelle skalare Felder (2.24) erhält man die Higgsmasse $m_h = \sqrt{2}\mu$.

8.4.1 Das Standardmodell-Higgsfeld

Das Higgsfeld $\phi = \begin{pmatrix}\phi^+\\ \phi^0\end{pmatrix} = \frac{1}{\sqrt{2}}\begin{pmatrix}\phi_1 - i\phi_2\\ \phi_3 - i\phi_4\end{pmatrix}$ besteht aus 4 reellen skalaren Feldern ϕ_1, ϕ_2, ϕ_3, ϕ_4.

Ladungskonjugation:

$$\mathrm{C}\,\phi = i\sigma_2\phi^* = \begin{pmatrix}\bar{\phi}^0\\ \phi^-\end{pmatrix} = \frac{1}{\sqrt{2}}\begin{pmatrix}\phi_3 + i\phi_4\\ -\phi_1 - i\phi_2\end{pmatrix} \tag{8.16}$$

mit dem total-antisymmetrischen Tensor der Dimension 2

$$\epsilon = \begin{pmatrix}0 & 1\\ -1 & 0\end{pmatrix} = i\sigma_2$$

Table 8.4 Elektroschwache Ladungen der Higgsfelder

Feldkomponenten	Q	I_W, I_{W3}	Y_W
ϕ^+	$+1$	$\frac{1}{2}, +\frac{1}{2}$	1
ϕ^0	0	$\frac{1}{2}, -\frac{1}{2}$	1
ladungskonjugierte Feldkomponenten	Q	I_W, I_{W3}	Y_W
$\bar{\phi}^0$	0	$\frac{1}{2}, +\frac{1}{2}$	-1
ϕ^-	-1	$\frac{1}{2}, -\frac{1}{2}$	-1

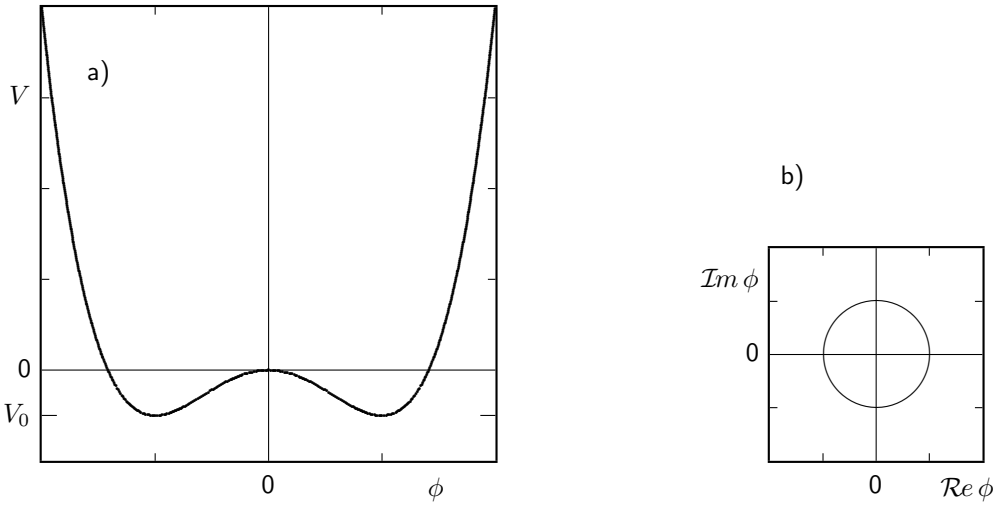

Fig. 8.1 Higgs-Potenzial für $\begin{pmatrix}0\\ \phi\end{pmatrix}$ mit reellem ϕ-Feld (a) und Ortslinie der Minima für komplexe ϕ (b)

Die Komponenten ϕ_1, ϕ_2, ϕ_3, ϕ_4 haben keine wohldefinierten Quantenzahlen. So ist etwa $\phi_1 = \frac{1}{\sqrt{2}}(\phi^+ - \phi^-)$ aus einer positiv und einer negativ geladenen Komponente zusammengesetzt (analog zum Vektorfeld W_1).

Lagrangian, invariant unter $\mathbf{SU(2)} \times \mathbf{U(1)}$:

$$\mathcal{L}_H = (D_\mu \phi)^\dagger (D^\mu \phi) - V(\phi^\dagger \phi)$$

mit

$$D_\mu = \partial_\mu - ig \sum_{j=1}^{3} W_{j,\mu} \frac{\sigma_j}{2} - ig' B_\mu \frac{Y_W}{2} = \partial_\mu - \frac{i}{2} \begin{pmatrix} gW_{3,\mu} + g' B_\mu Y_W & g\sqrt{2} W_\mu^- \\ g\sqrt{2} W_\mu^+ & -gW_{3,\mu} + g' B_\mu Y_W \end{pmatrix}$$

und ($Y_W = 1$)

$$\begin{aligned} D_\mu \phi &= \frac{1}{\sqrt{2}} \begin{pmatrix} \partial_\mu(\phi_1 - i\phi_2) \\ \partial_\mu(\phi_3 - i\phi_4) \end{pmatrix} - \frac{i}{2\sqrt{2}} \begin{pmatrix} (gW_{3,\mu} + g' B_\mu)(\phi_1 - i\phi_2) + g\sqrt{2} W_\mu^-(\phi_3 - i\phi_4) \\ g\sqrt{2} W_\mu^+(\phi_1 - i\phi_2) - (gW_{3,\mu} - g' B_\mu)(\phi_3 - i\phi_4) \end{pmatrix} \\ &= \frac{1}{\sqrt{2}} \begin{pmatrix} \partial_\mu(\phi_1 - i\phi_2) \\ \partial_\mu(\phi_3 - i\phi_4) \end{pmatrix} - \frac{i}{2\sqrt{2}} \begin{pmatrix} e(2A_\mu + \frac{\sin^2\theta_W - \cos^2\theta_W}{\sin\theta_W \cos\theta_W} Z_\mu)(\phi_1 - i\phi_2) + g\sqrt{2} W_\mu^-(\phi_3 - i\phi_4) \\ g\sqrt{2} W_\mu^+(\phi_1 - i\phi_2) + \frac{e}{\sin\theta_W \cos\theta_W} Z_\mu(\phi_3 - i\phi_4) \end{pmatrix} \end{aligned}$$

und

$$\phi^\dagger \phi = \frac{1}{2}(\phi_1^2 + \phi_2^2 + \phi_3^2 + \phi_4^2)$$

Potenzielle Energie(dichte)[47]:

$$V(\phi^\dagger \phi) = -\mu^2 \phi^\dagger \phi + \lambda (\phi^\dagger \phi)^2 \tag{8.17}$$

Eigenschaften:

- renormierbare skalare Theorie (maximale Potenz ϕ^4)

[47] andere Konventionen sind $\mu^2 \to -\mu^2$, $\lambda \to \frac{1}{2}\lambda$, $\lambda \to \frac{1}{2}\lambda^2$ und $\phi = \frac{1}{\sqrt{2}} \begin{pmatrix} \phi_1 + i\phi_2 \\ \phi_3 + i\phi_4 \end{pmatrix}$

- Energieminimum[48] (Vakuumzustand) ist nicht im Symmetriezentrum, sondern auf einer Hypersphäre mit

$$|\phi|^2 = \tilde{v}^2 = \frac{\mu^2}{2\lambda}$$

Alle Feldkonfigurationen dieser minimalen Energie ($V_0 = -\mu^4/4\lambda$) lassen sich als

$$\phi = \boldsymbol{U} \begin{pmatrix} 0 \\ \tilde{v} \end{pmatrix}$$

darstellen, mit allen $\boldsymbol{U} \in \mathbf{SU(2)} \times \mathbf{U(1)}$.

8.4.2 Spontane Symmetriebrechung

Die Auswahl einer Feldkonfiguration mit minimaler Energie V_0 im Vakuum,

$$\langle 0|\phi^{+}\phi|0\rangle = \tilde{v}^2 \neq 0\,,$$

enspricht einer **spontanen Symmetriebrechung**. In den meisten Lehrbüchern findet man statt $\tilde{v}$ den Wert $v = \sqrt{2}\,\tilde{v}$, den Wert der Komponente ϕ_3 im Minimum.

Das Higgsfeld

$$\phi(x) = \boldsymbol{U}(x) \begin{pmatrix} 0 \\ \tilde{v} + h(x)/\sqrt{2} \end{pmatrix} = \frac{1}{\sqrt{2}} \boldsymbol{U}(x) \begin{pmatrix} 0 \\ v + h(x) \end{pmatrix}$$

hat – bei geeigneter Wahl der $\mathbf{SU(2)}\times\mathbf{U(1)}$-Eichung $\boldsymbol{U}(x)$ – nur **eine** physikalische Komponente h, das neutrale Higgs-Boson, $h = \frac{1}{\sqrt{2}}(\phi^0 + \bar{\phi}^0)$. Es ist sein eigenes Antiteilchen und trägt keine Ladung.

Tatsächlich genügt ein $\boldsymbol{U} \in \mathbf{SU(2)}$ mit 3 Freiheitsgraden, weil eine globale Phasenänderung durch die $\mathbf{U(1)}$-Transformation $e^{\frac{i}{2}\alpha}$ auch durch die $\mathbf{SU(2)}$-Transformation $e^{-i\frac{1}{2}\sigma_3\alpha}$ bewirkt wird, da die 1. Komponente des Isovektors 0 ist.

Die verbleibenden Beiträge zur potenziellen Energie sind

$$\begin{aligned}
\phi^{+}\phi &= \tilde{v}^2 + \sqrt{2}\,\tilde{v}h + \tfrac{1}{2}h^2 \\
(\phi^{+}\phi)^2 &= \tilde{v}^4 + 2\tilde{v}^2h^2 + \frac{1}{4}h^4 + 2\sqrt{2}\,\tilde{v}^3h + \tilde{v}^2h^2 + \sqrt{2}\,\tilde{v}h^3 \\
V(\phi^{+}\phi) &= -\mu^2\phi^{+}\phi + \lambda(\phi^{+}\phi)^2 \\
&= -\mu^2\tilde{v}^2 - \mu^2\sqrt{2}\,\tilde{v}h - \tfrac{1}{2}\mu^2h^2 + \frac{\mu^2}{2\tilde{v}^2}(\tilde{v}^4 + 2\tilde{v}^2h^2 + \frac{1}{4}h^4 + 2\sqrt{2}\,\tilde{v}^3h + \tilde{v}^2h^2 + \sqrt{2}\,\tilde{v}h^3) \\
&= V_0 + \mu^2h^2 + \frac{\mu^2h^3}{\sqrt{2}\,\tilde{v}} + \frac{\mu^2h^4}{8\tilde{v}^2}
\end{aligned}$$

Die drei verschwundenen Freiheitsgrade des Higgsfeldes erscheinen als neue longitudinale Freiheitsgrade von W^+, W^- und Z^0, die durch die Massenterme ($m \neq 0$) hinzugekommen sind.

Damit wird

$$\begin{aligned}
\mathcal{L}_H &= (D_\mu\phi)^{+}(D^\mu\phi) - V(\phi^{+}\phi) \\
&= \frac{1}{2}g^2\tilde{v}^2W_\mu^+W^{-\mu} + \frac{1}{4}g^2\tilde{v}^2W_{3\mu}W_3^\mu + \frac{1}{4}g'^2\tilde{v}^2B_\mu B^\mu - \frac{1}{2}gg'\tilde{v}^2W_{3\mu}B^\mu
\end{aligned}$$

[48] $\frac{\partial V}{\partial|\phi|^2} = -\mu^2 + 2\lambda|\phi|^2 = 0$ im Minimum

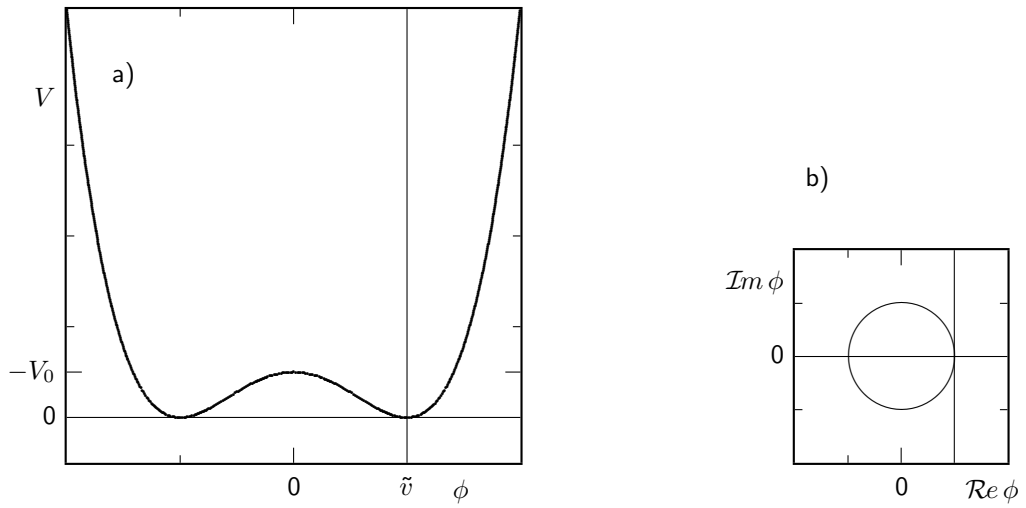

Fig. 8.2 Das Higgs-Potenzial vom Vakuum als Zentrum: die Symmetrie ist verloren.

$$
\begin{aligned}
&+\left[\frac{1}{4}g^2W_\mu^+W^{-\mu}+\frac{1}{8}g^2W_{3\mu}W_3^\mu+\frac{1}{8}g'^2B_\mu B^\mu-\frac{1}{4}gg'W_{3\mu}B^\mu\right]\left(h^2+2\sqrt{2}hv\right)\\
&+\frac{1}{2}(\partial_\mu h)(\partial^\mu h)-\mu^2h^2-\mu\sqrt{\lambda}\,h^3-\frac{\lambda}{4}h^4\\
=\;&\frac{1}{2}g^2\tilde{v}^2W_\mu^+W^{-\mu}+\frac{1}{4}\frac{g^2\tilde{v}^2}{\cos^2\theta_W}Z_\mu Z^\mu\\
&+\frac{g^2}{4}h^2W_\mu^+W^{-\mu}+\frac{g^2}{8\cos^2\theta_W}h^2Z_\mu Z^\mu+\frac{g^2\tilde{v}}{2\sqrt{2}}hW_\mu^+W^{-\mu}+\frac{g^2\tilde{v}}{4\sqrt{2}\cos^2\theta_W}hZ_\mu Z^\mu\\
&+\frac{1}{2}(\partial_\mu h)(\partial^\mu h)-\mu^2h^2-\mu\sqrt{\lambda}\,h^3-\frac{\lambda}{4}h^4
\end{aligned}
$$

wobei das Vakuumpotenzial $V_0 = 0$ gewählt wurde. Zur Umrechnung wird (8.4) und $g' = g\tan\theta_W$ eingesetzt. Man sieht, daß alle Terme mit A^μ herausfallen, d. h. das Higgsfeld macht keine elektromagnetische Wechselwirkung und das Photon hat keine Masse!

Der Vakuumerwartungswert bricht die $\mathbf{SU(2)}_W$ und die $\mathbf{U(1)}_{Y_W}$ Symmetrie, nicht aber die Linearkombination $I_{W3}+Y_W/2$, die dem elektrischen Ladungsoperator entspricht.

Dagegen sind folgende Massenterme enthalten:

$$\ldots\tfrac{1}{2}m_W^2(W_\mu^+W^{+\mu}+W_\mu^-W^{-\mu})+\tfrac{1}{2}m_Z^2Z_\mu Z^\mu+\ldots+\tfrac{1}{2}m_H^2h^2$$

Durch Vergleich mit dem Lagrangian zur Proca-Gleichung (4.68) für ein massives Vektorfeld ohne innere Symmetrie und mit dem zur Klein-Gordon-Gleichung (2.24) für ein relles skalares Feld (ohne Ladung) erhält man

$$m_H=\sqrt{2}\mu=2\sqrt{\lambda}\tilde{v},\qquad m_W=\frac{g\tilde{v}}{\sqrt{2}}=\frac{gv}{2}=\frac{g\mu}{2\sqrt{\lambda}},\qquad m_Z=m_W/\cos\theta_W$$

und keine Masse für das Photonfeld A^μ.

Mit der W-Masse $m_W\approx 80.4\,\mathrm{GeV}$, $\sin^2\theta_W=0.23$ und der Higgs-Masse $m_H\approx 126\,\mathrm{GeV}$ wird

$$\tilde{v}=\frac{\sqrt{2}\,m_W\sin\theta_W}{e}=\frac{1}{\sqrt{2\sqrt{2}G_F}}=174\,\mathrm{GeV}$$
$$v=\sqrt{2}\,\tilde{v}=\frac{2m_W\sin\theta_W}{e}=246\,\mathrm{GeV}$$

$$\mu = \frac{m_H}{\sqrt{2}} = 89\,\mathrm{GeV}$$
$$\lambda = \frac{\mu^2}{2\tilde{v}^2} = \frac{\mu^2}{v^2} = 0.13$$
$$V_0 = -\mu^4/4\lambda = -\tfrac{1}{2}\mu^2\tilde{v}^2 = 1.2 \cdot 10^8\,\mathrm{GeV}^4$$

Die drei Goldstone-Bosonen existieren nicht als masselose Teilchen, stattdessen führt ihre lokale Eichung durch die W- und Z-Felder zu den Massen dieser Vektorbosonen. Sie verstecken sich im zusätzlichen Polarisations-Freiheitsgrad, den ein massives Spin-1-Teilchen im Vergleich zum masselosen besitzt.

Die Brechung der $\mathbf{SU(2)}_W$- und $\mathbf{U(1)}_{Y_W}$-Symmetrien bedeutet auch, dass die zugehörigen Ladungen nicht erhalten sein müssen. So hat das Photon keinen schwachen Isospin, obwohl es eine W_3-Komponente mit $I_W = 1$ enthält. Auch das physikalische Higgsfeld h hat keine wohldefinierten Quantenzahlen der schwachen Wechselwirkung, nur seine elektrische Ladung ist definitiv 0.

Das Higgs-Potenzial (8.17) kann um sein Minimum bei $\phi = \tilde{v} = \mu/\sqrt{2\lambda}$ entwickelt werden[49]:

$$V(\Delta\phi) = V_0 + 4\mu^2\Delta\phi^2 + \mathcal{O}(\Delta\phi^3) \tag{8.18}$$

Eine Feldanregung kann als (eindimensionaler) harmonischer Oszillator betrachtet werden mit dem Oszillatorpotenzial $V(\Delta\phi) = \frac{1}{2}\omega^2\Delta\phi^2$ ($\omega = \sqrt{8}\mu$) und den Energieniveaus

$$E_n = \left(n + \frac{1}{2}\right) \cdot \omega$$

Die minimale Anregung $n = 0$ hat die Energie

$$E_0 = m_H = \frac{1}{2} \cdot \omega = \sqrt{2}\mu \tag{8.19}$$

Die freigesetzte Energiedichte bei der spontanen Symmetriebrechung durch das Higgsfeld ist

$$-V_0 = \frac{\mu^4}{4\lambda} = \frac{m_H^2\tilde{v}^2}{4}$$

Für $m_H = 125\,\mathrm{GeV}$ ist[50] das $-V_0 = 1.2 \cdot 10^8\,\mathrm{GeV}^4 \approx 1.6 \cdot 10^{55}\,\mathrm{GeV/m^3} \approx 3 \cdot 10^{28}\,\mathrm{kg/m^3}$!

8.4.3 Fermion-Massen

Massenterme in der Lagrangedichte müssen wie alle Terme reelle Zahlen sein. Wegen der Paritätsverletzung der schwachen Wechselwirkung gilt das aber nicht für Fermionen. Beispiel (für Elektronmasse):

$$m\bar{\psi}\psi = m\bar{\psi}_L\psi_R + m\bar{\psi}_R\psi_L = m\begin{pmatrix}\bar{\nu}_L\\ \bar{e}_L\end{pmatrix}e_R + m\bar{e}_R\begin{pmatrix}\nu_L\\ e_L\end{pmatrix} = m\begin{pmatrix}\bar{\nu}_L e_R + \bar{e}_R\nu_L\\ \bar{e}_L e_R + \bar{e}_R e_L\end{pmatrix}$$

Auch hier hilft das Higgsfeld.

Fermion-Massen können durch Kopplungen an das Higgsfeld eingeführt werden:

$$\begin{aligned}\mathcal{L}_{FH} &= g_f(\bar{\psi}_R\phi^{+}\psi_L + \bar{\psi}_L\phi\psi_R)\\ &= g_f\tilde{v}\bar{\psi}\psi + g_f(\bar{\psi}_R h\psi_L + \bar{\psi}_L h\psi_R)\end{aligned}$$

[49] $\frac{\partial^2 V}{\partial\phi^2} = -2\mu^2 + 12\lambda\phi^2 = 4\mu^2$ im Minimum, $\frac{\partial^3 V}{\partial\phi^3} = 24\lambda\phi$.

[50] $1\,\mathrm{GeV}^4 = 1.3 \cdot 10^{47}\,\mathrm{GeV/m^3} = 2.3 \cdot 10^{20}\,\mathrm{kg/m^3}$

Unter **SU(2)**-Transformationen ist

$$\begin{aligned}\psi'_L &= \boldsymbol{U}\psi_L \\ \psi'_R &= \psi_R \\ \phi' &= \boldsymbol{U}\phi\end{aligned}$$

und somit $\mathcal{L}_{FH}$ invariant.

Auch unter **U(1)**-Transformationen $\sim e^{iY_W\alpha(x)}$ ist dieser Term invariant, solange die Summe der Y_W Null ergibt.

Beispiel (für Elektronmasse):

$$g_e \begin{pmatrix}\bar\nu_L \\ \bar e_L\end{pmatrix}\begin{pmatrix}0 \\ \tilde v\end{pmatrix} e_R + g_e\bar e_R \begin{pmatrix}0 \\ \tilde v\end{pmatrix}\begin{pmatrix}\nu_L \\ e_L\end{pmatrix} = g_e\tilde v(\bar e_L e_R + \bar e_R e_L)$$

mit $Y_W(\bar l_L) = 1$, $Y_W(\phi) = 1$, $Y_W(e_R) = -2$. Dagegen wäre ein Term

$$g_X \begin{pmatrix}\bar\nu_L \\ \bar e_L\end{pmatrix}\begin{pmatrix}0 \\ \tilde v\end{pmatrix}\nu_R$$

nicht invariant unter (globalen und lokalen) **U(1)**-Transformationen, da $Y_W(\nu_R) = 0$ ist. Schwache Hyperladung und elektrische Ladung wären bei dieser Kopplung nicht erhalten.

Analoge Terme erhält man für Down-Quarks.

Um auch dem Neutrino und den Up-Quarks eine Masse zu geben, brauchen wir eine weitere Kopplung

$$g_\nu \begin{pmatrix}\bar\nu_L \\ \bar e_L\end{pmatrix}\begin{pmatrix}0 & 1 \\ -1 & 0\end{pmatrix}\begin{pmatrix}0 \\ \tilde v\end{pmatrix}\nu_R + g_\nu\bar\nu_R \begin{pmatrix}0 & 1 \\ -1 & 0\end{pmatrix}\begin{pmatrix}0 \\ \tilde v\end{pmatrix}\begin{pmatrix}\nu_L \\ e_L\end{pmatrix} = g_\nu\tilde v(\bar\nu_L\nu_R + \bar\nu_R\nu_L)$$

Dieser Term beschreibt die Kopplung des C-konjugierten Higgsfeldes (8.16)

$$g_\nu \begin{pmatrix}\bar\nu_L \\ \bar e_L\end{pmatrix}\frac{1}{\sqrt2}\begin{pmatrix}\phi_3 + i\phi_4 \\ -\phi_1 - i\phi_2\end{pmatrix}\nu_R = g_\nu \begin{pmatrix}\bar\nu_L \\ \bar e_L\end{pmatrix}\begin{pmatrix}\tilde v + \frac{1}{\sqrt2}h \\ 0\end{pmatrix}\nu_R$$

Damit wird

$$\begin{aligned}\mathcal{L}_{FH} &= g_{f-\frac12}(\bar\psi_R\boldsymbol{\phi}^+\boldsymbol{\psi}_L + \bar{\boldsymbol{\psi}}_L\boldsymbol{\phi}\psi_R) + g_{f+\frac12}(\bar\psi_R\boldsymbol{\phi}^+ i\sigma_2\boldsymbol{\psi}_L + \bar{\boldsymbol{\psi}}_L i\sigma_2\boldsymbol{\phi}\psi_R) \\ &= g_{f-\frac12}\tilde v(\bar\psi\psi)_{f-\frac12} + g_{f+\frac12}\tilde v(\bar\psi\psi)_{f+\frac12} + g_{f-\frac12}h(\bar\psi\psi)_{f-\frac12} + g_{f+\frac12}h(\bar\psi\psi)_{f+\frac12}\end{aligned}$$

Jedes Fermion hat seine eigene Kopplungskonstante $g_f = m_f/\tilde v$

8.5 Feynmanregeln

für ein Matrixelement $-i\mathcal{M}$

	$\varepsilon_\mu(\boldsymbol{k})$	einlaufendes W oder Z
	$\varepsilon^*_\mu(\boldsymbol{k})$	auslaufendes W oder Z
	$\dfrac{-i(g^{\mu\nu} - q^\mu q^\nu/M^2)}{q^2 - M^2}$	inneres W oder Z $(M = m_W, m_Z)$

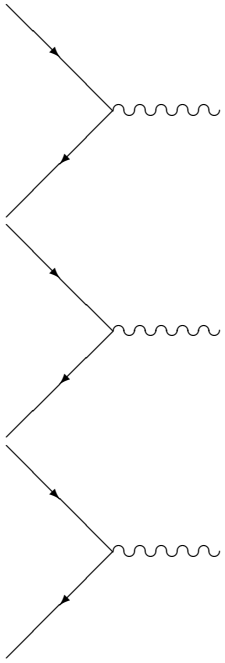

$-\frac{ig}{\sqrt{2}}\gamma_\mu \frac{1}{2}(1-\gamma_5)$ W-Fermion-Vertex

$-\frac{ig}{\sqrt{2}}\, V_{ab}\, \gamma_\mu \frac{1}{2}(1-\gamma_5)$ W-Quark-Vertex $b \to a$, $\bar{a} \to \bar{b}$

$-\frac{ig}{\cos\theta_W}\gamma_\mu \frac{1}{2}(c_v - c_a\gamma_5)$ Z-Fermion-Vertex

Dabei ist

$$e = g \sin\theta_W \tag{8.20}$$

8.5.1 Der 3-Vektorboson-Vertex

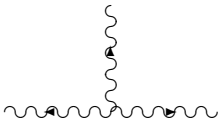

$$\begin{aligned} g\big\{ & f_{abc} g_{\mu\nu}(k_{(a)} - k_{(b)})_\rho \\ & + f_{bca} g_{\nu\rho}(k_{(b)} - k_{(c)})_\mu \\ & + f_{cab} g_{\rho\mu}(k_{(c)} - k_{(a)})_\nu \big\} \end{aligned}$$

Für $W_{(1)}W_{(2)}\gamma$ ist der Vertex-Faktor

$$e\{g_{\mu\nu}(k_{(1)} - k_{(2)})_\rho - g_{\nu\rho}(k_{(2)} - k_{(\gamma)})_\mu - g_{\rho\mu}(k_{(\gamma)} - k_{(1)})_\nu\}$$

Für $W_{(1)}W_{(2)}Z^0$ ist der Vertex-Faktor

$$g\cos\theta_W\{g_{\mu\nu}(k_{(1)} - k_{(2)})_\rho - g_{\nu\rho}(k_{(2)} - k_{(Z)})_\mu - g_{\rho\mu}(k_{(Z)} - k_{(1)})_\nu\}$$

8.5.2 Der 4-Vektorboson-Vertex

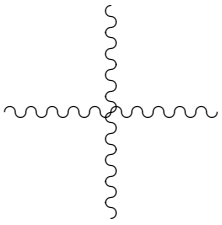

$$\begin{aligned} -ig^2\big\{ & f_{abe} f_{ecd}(g_{\mu\sigma} g_{\nu\rho} - g_{\mu\rho} g_{\nu\sigma}) \\ & + f_{ade} f_{ebc}(g_{\mu\rho} g_{\nu\sigma} - g_{\mu\nu} g_{\rho\sigma}) \\ & + f_{ace} f_{edb}(g_{\mu\nu} g_{\rho\sigma} - g_{\mu\sigma} g_{\nu\rho}) \big\} \end{aligned}$$

Für $W_{(1)}W_{(2)}W_{(3)}W_{(4)}$ ist der Vertex-Faktor

$$ig^2\{2g_{\mu\nu}g_{\rho\sigma} - g_{\sigma\nu}g_{\mu\rho} - g_{\mu\sigma}g_{\rho\nu}\}$$

Analog WWZ^0Z^0 $(-ig^2\cos\theta_W)$, $WWZ^0\gamma$ $(-ieg\cos\theta_W)$, $WW\gamma\gamma$ $(-ie^2)$.

8.5.3 Higgs-Kopplungen

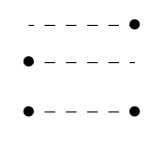

1 einlaufendes Higgs

1 auslaufendes Higgs

$\dfrac{i}{q^2 - m_H^2}$ inneres Higgs

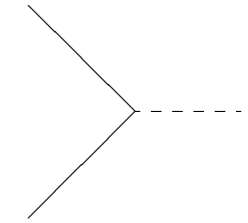

$-i\dfrac{g}{2}\dfrac{m_f}{m_W}$ Higgs-Fermion-Vertex

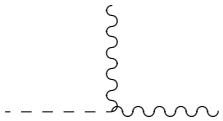

$WWh : igm_W g_{\mu\nu}$

$ZZh : ig\dfrac{m_Z}{\cos\theta_W} g_{\mu\nu}$

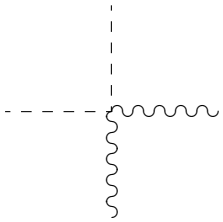

$WWhh : \dfrac{ig^2}{2} g_{\mu\nu}$

$ZZhh : \dfrac{ig^2}{2\cos^2\theta_W} g_{\mu\nu}$

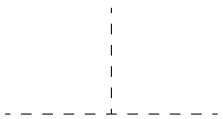

$hhh : -\dfrac{3ig}{2}\dfrac{m_H^2}{m_W}$

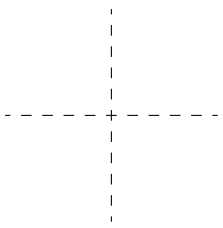

$hhhh : -\dfrac{3ig^2}{4}\dfrac{m_H^2}{m_W^2}$

8.5.4 Schwache Wechselwirkung bei kleinen q^2

Bei niedrigen Energien $E \ll m_W, m_Z$ ist $q^2 \ll M^2$ und somit

$\dfrac{ig^{\mu\nu}}{M^2}$ inneres W oder Z

$$\mathcal{L}_{WW}{}^{cc} = \frac{4G_F}{\sqrt{2}}(J_\mu{}^{cc} J^{\mu +cc} + J^{\mu cc} J_\mu^{+cc})$$

$$\mathcal{L}_{WW}{}^{nc} = \frac{4G_F m_W^2}{\sqrt{2}\, m_Z^2} J_\mu{}^{nc} J^{\mu +nc}$$

mit der Fermi-Kopplungskonstanten

$$
\begin{aligned}
G_F &= \frac{g^2}{4\sqrt{2}\; m_W^2} && (8.21)\\
&= \frac{\pi\alpha}{\sqrt{2}\; m_W^2\; \sin^2\theta_W}\\
&= \frac{\pi\alpha}{\sqrt{2}\; m_W^2\; (1-\frac{m_W^2}{m_Z^2})(1-\Delta r)}\\
&= \frac{g^2}{4\sqrt{2}\; m_Z^2 \cos^2\theta_W} && (8.22)\\
&= 1.16637\cdot 10^{-5} GeV^{-2}
\end{aligned}
$$

Daraus kann man den Vakuumerwartungswert des Higgsfeldes ausrechnen:

$$G_F = \frac{1}{2\sqrt{2}\bar{v}^2} = \frac{1}{\sqrt{2}v^2}$$

8.6 Der Myonzerfall

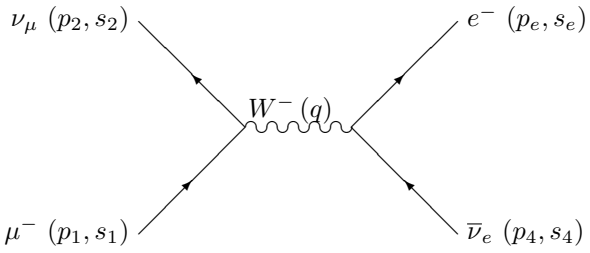

Notation: p = Energie-Impuls-Vektor, s = Spin, $m = m_1 = m(\mu)$
Feynmanregeln $\Longrightarrow$

$$
\begin{aligned}
-i\mathcal{M} = \bar{u}(p_2,s_2)\,\frac{-ig}{\sqrt{2}}\frac{1}{2}\gamma^\mu(1-\gamma_5)\,u(p_1,s_1)\\
\cdot(-i)\frac{g_{\mu\nu}-q_\mu q_\nu/m_W^2}{q^2-m_W^2}\,\cdot\\
\cdot\,\bar{u}(p_e,s_e)\,\frac{-ig}{\sqrt{2}}\frac{1}{2}\gamma^\nu(1-\gamma_5)\,v(p_4,s_4)
\end{aligned}
$$

kleine $q^2 \ll m_W^2$ (Gl. 8.21) $\Longrightarrow$

$$
\begin{aligned}
-i\mathcal{M} &= -i\frac{G_F}{\sqrt{2}}\big\{\bar{u}(p_2,s_2)\,\gamma_\mu(1-\gamma_5)\,u(p_1,s_1)\big\}\big\{\bar{u}(p_e,s_e)\,\gamma^\mu(1-\gamma_5)\,v(p_4,s_4)\big\}\\
|\mathcal{M}|^2 &= \frac{G_F^2}{2}\big\{\bar{u}(p_2,s_2)\,\gamma_\mu(1-\gamma_5)\,u(p_1,s_1)\,\bar{u}(p_1,s_1)\,\gamma_\nu(1-\gamma_5)\,u(p_2,s_2)\big\}\\
&\quad\cdot\big\{\bar{u}(p_e,s_e)\,\gamma^\mu(1-\gamma_5)\,v(p_4,s_4)\,\bar{v}(p_4,s_4)\,\gamma^\nu(1-\gamma_5)\,u(p_e,s_e)\big\}
\end{aligned}
$$

Spinmittelung beim μ, Spinsummen im Endzustand (4.61) $\Longrightarrow$

$$\frac{1}{2}\sum_{s_1,s_4}|\mathcal{M}|^2 = \frac{G_F^2}{4}\big\{\bar{u}_a(p_2,s_2)\,[\gamma_\mu(1-\gamma_5)(\not{p}_1+m)\gamma_\nu(1-\gamma_5)]_{ab}\,u_b(p_2,s_2)\big\}$$

$$\cdot\,\big\{\bar{u}_c(p_e,s_e)\,[\gamma^\mu(1-\gamma_5)(\not{p}_4-m_4)\gamma^\nu(1-\gamma_5)]_{cd}\,u_d(p_e,s_e)\big\}$$

$$\frac{1}{2}\sum_{s_1,s_4}\sum_{s_2,s_e}|\mathcal{M}|^2 = \frac{G_F^2}{4}\,\mathrm{Sp}\big\{(\not{p}_2+m_2)\gamma_\mu(1-\gamma_5)(\not{p}_1+m)\gamma_\nu(1-\gamma_5)\big\}$$

$$\cdot\,\mathrm{Sp}\big\{(\not{p}_e+m_e)\gamma^\mu(1-\gamma_5)(\not{p}_4-m_4)\gamma^\nu(1-\gamma_5)\big\}$$

Alle expliziten Massenterme fallen weg wegen (4.14c).
Einsetzen von (4.14e) und der Spursätze (4.23c,f) $\Longrightarrow$

$$\begin{aligned}
|\overline{\mathcal{M}}|^2 &= \frac{G_F^2}{4}\,\mathrm{Sp}\big\{\not{p}_2\gamma_\mu(1-\gamma_5)\not{p}_1\gamma_\nu(1-\gamma_5)\big\}\,\mathrm{Sp}\big\{\not{p}_e\gamma^\mu(1-\gamma_5)\not{p}_4\gamma^\nu(1-\gamma_5)\big\}\\
&= G_F^2\,\mathrm{Sp}\big\{\not{p}_2\gamma_\mu\not{p}_1\gamma_\nu(1-\gamma_5)\big\}\,\mathrm{Sp}\big\{\not{p}_e\gamma^\mu\not{p}_4\gamma^\nu(1-\gamma_5)\big\}\\
&= 16G_F^2\big\{p_{2\mu}p_{1\nu}+p_{2\nu}p_{1\mu}-(p_2p_1)g_{\mu\nu}+i\varepsilon_{\alpha\mu\beta\nu}p_2^\alpha p_1^\beta\big\}\\
&\qquad\cdot\big\{p_e^\mu p_4^\nu+p_e^\nu p_4^\mu-(p_ep_4)g^{\mu\nu}+i\varepsilon^{\alpha\mu\beta\nu}p_{e\alpha}p_{4\beta}\big\}\\
&= 64G_F^2\big\{(p_2p_e)(p_1p_4)\big\}
\end{aligned}\tag{8.23}$$

In (8.23) ergeben die gemischten Produkte mit dem ε-Tensor 0, da $g_{\mu\nu}$ und $p_{2\mu}p_{1\nu}+p_{2\nu}p_{1\mu}$ etc. symmetrische Matrizen sind und für jede symmetrische Matrix $X_{\mu\nu}=X_{\nu\mu}$

$$X_{\mu\nu}\varepsilon^{\mu\nu\alpha\beta}=0\tag{8.24}$$

ist.

8.6.1 Breite

im μ^--Ruhesystem mit $r := m_e/m$ ist

$$\begin{aligned}
\mathrm{d}\Gamma &= \frac{1}{2m}\cdot|\overline{\mathcal{M}}|^2\,\mathrm{dPS}\\
&= \frac{1}{2m}\,\frac{64G_F^2}{2}m^2[mE_4(1-r^2)-2E_4^2]\,\frac{1}{(2\pi)^5}\,\frac{dE_4\,\mathrm{d}\Omega_4\,\mathrm{d}E_e\,\mathrm{d}\phi_{e4}}{8}
\end{aligned}$$

Integration über alle Winkel und Phasenraumelement (6.54) ergibt

$$\mathrm{d}\Gamma = \frac{1}{2m}\,\frac{64G_F^2}{2}m^2[mE_4(1-r^2)-2E_4^2]\,\frac{1}{64\pi^3m}\,\mathrm{d}q^2\,\mathrm{d}E_e = \frac{G_F^2}{4\pi^3}[mE_4(1-r^2)-2E_4^2]\,\mathrm{d}q^2\,\mathrm{d}E_e$$

mit $q = p_e + p_4$.
Mit (6.53) und (für $m_2 = m_4 = 0$):

$$\begin{aligned}
p_1p_4 &= mE_4\\
(p_2+p_e)^2 &= m_e^2+2p_2p_e\\
=(p_1-p_4)^2 &= m(m-2E_4)\\
\Longrightarrow\qquad p_2p_e &= \tfrac{1}{2}m[m(1-r^2)-2E_4]\\
&\approx \tfrac{1}{2}m[m-2E_4]
\end{aligned}$$

Für $r \approx 0$:
Kinematische Grenzen $0 < E_2 = m - E_e - E_4 < \frac{1}{2}m$, $0 < E_4 < \frac{1}{2}m$

Integration $\int \ldots \frac{dE_4\,\mathrm{d}\Omega_4\,\mathrm{d}\phi_{e4}}{8} = \pi^2 \int_{m/2-E_e}^{m/2} \ldots \mathrm{d}E_4$ ergibt

$$\mathrm{d}\Gamma = \frac{G_F^2}{12\pi^3} m^2 E_e^2 \left[3 - 4\frac{E_e}{m}\right] \mathrm{d}E_e$$

totale Breite

$$\begin{aligned}\Gamma &= \frac{G_F^2}{12\pi^3} m^2 \int_0^{m/2} \left[3E_e^2 - 4\frac{E_e^3}{m}\right] \mathrm{d}E_e \\ &= \frac{G_F^2 m^5}{192\pi^3}\end{aligned} \tag{8.25}$$

8.7 The Standard Model Matrix Element for $\tau^- \to l^- \nu_\tau \bar{\nu}_l$

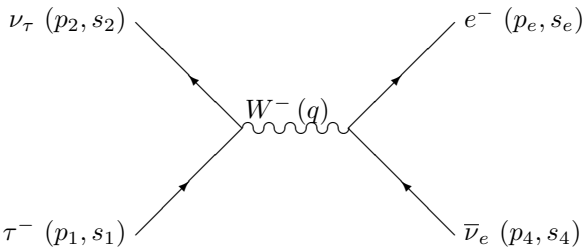

Notation: p = Energie-Impuls-Vektor, s = Spin, $m = m_1 = m(\tau)$

$$\begin{aligned}-i\mathcal{M} = \bar{u}(p_2, s_2)\, &\frac{-ig}{\sqrt{2}} \frac{1}{2} \gamma^\mu (1 - \gamma_5)\, u(p_1, s_1) \\ &\cdot (-i) \frac{g_{\mu\nu} - q_\mu q_\nu / m_W^2}{q^2 - m_W^2} \cdot \\ &\cdot \bar{u}(p_e, s_e)\, \frac{-ig}{\sqrt{2}} \frac{1}{2} \gamma^\nu (1 - \gamma_5)\, v(p_4, s_4)\end{aligned}$$

for $q^2 \ll m_W^2 \quad \Longrightarrow$

$$\begin{aligned}-i\mathcal{M} &= -i\frac{G_F}{\sqrt{2}} \big\{\bar{u}(p_2, s_2)\, \gamma_\mu (1 - \gamma_5)\, u(p_1, s_1)\big\} \big\{\bar{u}(p_e, s_e)\, \gamma^\mu (1 - \gamma_5)\, v(p_4, s_4)\big\} \\ |\mathcal{M}|^2 &= 64 G_F^2 \big\{(p_2 p_e)(p_1 p_4)\big\}\end{aligned}$$

in the mother (μ or τ) rest system and $r := m_e/m$ we have

$$\begin{aligned}\mathrm{d}\Gamma &= \frac{1}{2m} \cdot |\overline{\mathcal{M}}|^2\, \mathrm{dPS} \\ &= \frac{1}{2m} \frac{64 G_F^2}{2} m^2 [m E_4 (1 - r^2) - 2E_4^2] \frac{1}{(2\pi)^5} \frac{dE_4\,\mathrm{d}\Omega_4\,\mathrm{d}E_e\,\mathrm{d}\phi_{e4}}{8}\end{aligned}$$

Integrating over all angles gives

$$\mathrm{d}\Gamma = \frac{1}{2m} \frac{64 G_F^2}{2} m^2 [m E_4 (1 - r^2) - 2E_4^2] \frac{1}{64\pi^3 m}\, \mathrm{d}q^2\, \mathrm{d}E_e = \frac{G_F^2}{4\pi^3} [m E_4 (1 - r^2) - 2E_4^2]\, \mathrm{d}q^2\, \mathrm{d}E_e$$

with $q = p_e + p_4$.
Using (6.53) and $m_2 = m_4 = 0$:

$$\begin{aligned} p_1 p_4 &= mE_4 \\ (p_2 + p_e)^2 &= m_e^2 + 2p_2 p_e \\ = (p_1 - p_4)^2 &= m(m - 2E_4) \\ \Longrightarrow \qquad p_2 p_e &= \tfrac{1}{2} m[m(1 - r^2) - 2E_4] \\ &\approx \tfrac{1}{2} m[m - 2E_4] \end{aligned}$$

For $r \approx 0$:
the kinematical limits are $0 < E_2 = m - E_e - E_4 < \frac{1}{2}m$, $0 < E_4 < \frac{1}{2}m$
Integrating $\int \ldots \frac{dE_4 \, \mathrm{d}\Omega_4 \, \mathrm{d}\phi_{e4}}{8} = \pi^2 \int_{m/2-E_e}^{m/2} \ldots \, \mathrm{d}E_4$ yields

$$\mathrm{d}\Gamma = \frac{G_F^2}{12\pi^3} m^2 E_e^2 \left[3 - 4\frac{E_e}{m}\right] \mathrm{d}E_e$$

and the total width

$$\begin{aligned} \Gamma &= \frac{G_F^2}{12\pi^3} m^2 \int_0^{m/2} \left[3E_e^2 - 4\frac{E_e^3}{m}\right] \mathrm{d}E_e \\ &= \frac{G_F^2 m^5}{192\pi^3} \end{aligned} \tag{8.26}$$

8.7.1 Corrections

Including the leading corrections the integrated width for the τ decay is

$$\begin{aligned} \Gamma_\mu = \frac{G_F^2 m_\tau^5}{192\pi^3} \Bigg[& 1 - 8\frac{m_\mu^2}{m_\tau^2} - 8\frac{m_{\nu_\tau}^2}{m_\tau^2} + 4\eta g\left(\frac{m_\mu}{m_\tau}\right) + 4\lambda\frac{m_{\nu_\tau}}{m_\tau} + 8\sigma\frac{m_\mu m_{\nu_\tau}}{m_\tau^2} \\ & + \frac{3}{5}\frac{m_\tau^2}{m_W^2} - \frac{\alpha}{2\pi}(\pi^2 - \frac{25}{4}) \Bigg] \end{aligned} \tag{8.27}$$

with the function

$$g(z) = z + 9z^2 - 9z^3 - z^4 + 6z^2(1 + z)\ln z \approx z$$

and

$$\begin{aligned} \lambda &= \frac{1}{2} \mathcal{R}e \left[g^S_{RR} g^{*S}_{\ LR} + g^S_{RR} g^{*S}_{\ RL} - 2g^V_{LL} g^{*V}_{\ LR} - 2g^V_{RR} g^{*V}_{\ RL} \right] \\ \sigma &= \frac{1}{2} \mathcal{R}e \left[-6g^V_{LL} g^{*T}_{\ RL} - 6g^V_{RR} g^{*T}_{\ LR} + g^S_{RR} g^{*V}_{\ LR} + g^S_{RL} g^{*V}_{\ LL} + g^S_{LR} g^{*V}_{\ RR} + g^S_{LL} g^{*V}_{\ RL} \right] \end{aligned}$$

Eq. 8.27 is used to calculate (7.15) to determine the Michel parameter η.

8.8 Fermion Mass Generation and the CKM Matrix

The quark mass generating part of the Lagrangian may be written as scalar $\bar{\psi}\psi = \bar{\psi}_L\psi_R + \bar{\psi}_R\psi_L$ couplings

$$\mathcal{L} = \ldots - \sum_{r,g,b} \begin{pmatrix} \bar{u} \\ \bar{c} \\ \bar{t} \end{pmatrix} \mathbf{M}_u \begin{pmatrix} u \\ c \\ t \end{pmatrix} - \sum_{r,g,b} \begin{pmatrix} \bar{d} \\ \bar{s} \\ \bar{b} \end{pmatrix} \mathbf{M}_d \begin{pmatrix} d \\ s \\ b \end{pmatrix} + \text{h.c.} \tag{8.28}$$

where the diagonal matrices $\mathbf{M}_u$ and $\mathbf{M}_d$ are applied to the mass eigenstates. This can be rewritten as

$$\mathcal{L} = \ldots - \sum_{r,g,b} \begin{pmatrix} \bar{u} \\ \bar{c} \\ \bar{t} \end{pmatrix} \mathbf{M}_u \begin{pmatrix} u \\ c \\ t \end{pmatrix} - \sum_{r,g,b} \begin{pmatrix} \bar{d}' \\ \bar{s}' \\ \bar{b}' \end{pmatrix} \mathbf{V}\mathbf{M}_d\mathbf{V}^{\dagger} \begin{pmatrix} d' \\ s' \\ b' \end{pmatrix} + \text{h.c.} \tag{8.29}$$

where the matrices $\mathbf{M}_u$ and $\mathbf{V}\mathbf{M}_d\mathbf{V}^{\dagger}$ are applied to the eigenstates of the weak interaction, i. e. with diagonal transition matrix between (d', s', b') and (u, c, t) through the intermediate W boson. While for one triplet, here the (u, c, t) one, a diagonal mass matrix

$$\mathbf{M}_u = \begin{pmatrix} m_u & 0 & 0 \\ 0 & m_c & 0 \\ 0 & 0 & m_t \end{pmatrix}$$

is sufficient, the other triplet needs a more general one, since the weak partners of (u, c, t) are not the mass eigenstates. If the mass matrix

$$\mathbf{M}_d = \begin{pmatrix} m_d & 0 & 0 \\ 0 & m_s & 0 \\ 0 & 0 & m_b \end{pmatrix}$$

is diagonal, the corresponding matrix between the weak eigenstates $\mathbf{V}\mathbf{M}_d\mathbf{V}^{\dagger}$ is not. The d-type quarks have to be transformed using the CKM matrix $\mathbf{V}$ to form the weak eigenstates. In general, both u- and d-type quarks can have their own complex mass matrices, still leaving the W-mediated interaction diagonal. This moves the question of the origin of the CKM matrix elements into the realm of mass generation, which belongs still to the more "mysterious" parts[51] of the Standard Model, the mass generation via the couplings to the scalar Higgs field, or, more precisely, to the vacuum expectation value v of the single component of this field that is not eaten up by gauge symmetries:

$$m_i = y_{ii} v$$

where y_{ii} is the Yukawa coupling constant specific to quark i.

The origin of these coupling constants is not understood. Without these couplings the three families of massless fermions were quite symmetric. The hierarchy of the family masses is only brought in by the interactions with the Higgs field.

We must start with the most general Yukawa couplings of the full four-component Higgs field ϕ to (initially degenerate) quarks in an arbitrary basis in both up and down flavour spaces, (u'', c'', t'') and (d'', s'', b''),

$$\mathcal{L} = \ldots - \sum_{r,g,b} (\bar{u}''_R, \bar{c}''_R, \bar{t}''_R)\, \mathbf{Y}''_u \, (\,\bar{\phi}^0, -\phi^-\,) \begin{pmatrix} \begin{pmatrix} u''_L \\ d''_L \end{pmatrix} \\ \begin{pmatrix} c''_L \\ s''_L \end{pmatrix} \\ \begin{pmatrix} t''_L \\ b''_L \end{pmatrix} \end{pmatrix}$$

[51] C. Jarlskog, "Mysteries in the Standard Model", Proc. of the Int. Symp. on Production and Decay of Heavy Flavours, Heidelberg 1996, p. 331.

$$-\sum_{r,g,b}(\bar{d}''_R,\bar{s}''_R,\bar{b}''_R)\,\mathbf{Y}''_d\,(\,\phi^+,\phi^0\,)\begin{pmatrix}\begin{pmatrix}u''_L\\d''_L\end{pmatrix}\\\begin{pmatrix}c''_L\\s''_L\end{pmatrix}\\\begin{pmatrix}t''_L\\b''_L\end{pmatrix}\end{pmatrix} \tag{8.30}$$

with arbitrary complex 3×3 matrices $\mathbf{Y}''_u$, $\mathbf{Y}''_d$ for an arbitrary basis of left- and righthanded quark fields in the three-dimensional family space. While the left-handed fields go in doublets and can only be transformed in pairs due to the SU(2) gauge invariance, we can arbitrarily transform the right-handed singlet fields.

There is no *a priori* restriction in the number of parameters in $\mathbf{Y}''_u$ and $\mathbf{Y}''_d$, and this implies that they need not (and, in fact, do not) have eigenvalues. However, these matrices can be reduced to a real, diagonal matrix $\mathbf{Y}_u$, and a matrix $\mathbf{Y}_d$ with a minimum number of parameters that correspond to the mass matrices $\mathbf{M}=v\mathbf{Y}$

$$\mathbf{M}_u=v\mathbf{U}_{uR}\mathbf{Y}''_u\mathbf{U}_L^{\dagger},\qquad \mathbf{V}\mathbf{M}_d\mathbf{V}^{\dagger}=v\mathbf{U}_{dR}\mathbf{Y}''_d\mathbf{U}_L^{\dagger},\qquad \mathbf{M}_d=v\mathbf{V}^{\dagger}\mathbf{U}_{dR}\mathbf{Y}''_d\mathbf{U}_L^{\dagger}\mathbf{V} \tag{8.31}$$

via the unitary transformations

$$\begin{pmatrix}u_R\\c_R\\t_R\end{pmatrix}=\mathbf{U}_{uR}\begin{pmatrix}u''_R\\c''_R\\t''_R\end{pmatrix},\quad \begin{pmatrix}u_L\\c_L\\t_L\end{pmatrix}=\mathbf{U}_L\begin{pmatrix}u''_L\\c''_L\\t''_L\end{pmatrix}$$
$$\begin{pmatrix}d'_R\\s'_R\\b'_R\end{pmatrix}=\mathbf{U}_{dR}\begin{pmatrix}d''_R\\s''_R\\b''_R\end{pmatrix},\quad \begin{pmatrix}d'_L\\s'_L\\b'_L\end{pmatrix}=\mathbf{U}_L\begin{pmatrix}d''_L\\s''_L\\b''_L\end{pmatrix}$$
$$\begin{pmatrix}d_R\\s_R\\b_R\end{pmatrix}=\mathbf{V}^{\dagger}\mathbf{U}_{dR}\begin{pmatrix}d''_R\\s''_R\\b''_R\end{pmatrix}\quad \begin{pmatrix}d_L\\s_L\\b_L\end{pmatrix}=\mathbf{V}^{\dagger}\mathbf{U}_L\begin{pmatrix}d''_L\\s''_L\\b''_L\end{pmatrix}$$

which transform family space to a coordinate system where the up-type quarks u,c,t are mass eigenstates, while the down-type quarks d',s',b' are the weak-isospin partners of u,c,t.

There is only one $\mathbf{U}_L$ since the lefthanded quarks are weak iso-doublets that transform as one entity. Therefore, $\mathbf{Y}_u$ and $\mathbf{Y}_d$ cannot be diagonalized simultaneously by unitary transformations in the two R and one L family spaces. The unitary transformations $\mathbf{U}_{uR}$ and $\mathbf{U}_L$ are chosen to diagonalize $\mathbf{Y}_u$ (which corresponds to a reduction of 18 real parameters to 3, the up-type quark masses, absorbing 9 in $\mathbf{U}_{uR}$ and 6 more in $\mathbf{U}_L$). Since a common phase can be arbitrarily distributed between $\mathbf{U}_{uR}$ and $\mathbf{U}_L$, the effective sum of parameters of both is $9+8$. In the second term, $\mathbf{U}_{dR}$ can be used to reduce the number of parameters of $\mathbf{Y}_d$ from 18 real numbers to 9 (absorbing 9 in $\mathbf{U}_{dR}$) and further using the remaining 2 of $\mathbf{U}_L$ to finally 7. These 7 parameters correspond to the three down-type quark masses and the four non-trivial parameters of the CKM matrix $\mathbf{V}$.

These transformations isolate the mass term (8.29) from the Higgs coupling term (8.30) using the vacuum expectation value of the Higgs field $(\phi^+,\phi^0)=(0,v)$.

Using the physical quark fields coupling to the W boson, and the vacuum field $(\phi^+,\phi^0)=(0,v)$, we can rewrite (8.30) as

$$\mathcal{L}=\ldots-\sum_{r,g,b}(\bar{u}_R,\bar{c}_R,\bar{t}_R)\,\mathbf{Y}_u\,(\,v,0\,)\begin{pmatrix}\begin{pmatrix}u_L\\d'_L\end{pmatrix}\\\begin{pmatrix}c_L\\s'_L\end{pmatrix}\\\begin{pmatrix}t_L\\b'_L\end{pmatrix}\end{pmatrix}-\sum_{r,g,b}(\bar{d}'_R,\bar{s}'_R,\bar{b}'_R)\,\mathbf{Y}'_d\,(\,0,v\,)\begin{pmatrix}\begin{pmatrix}u_L\\d'_L\end{pmatrix}\\\begin{pmatrix}c_L\\s'_L\end{pmatrix}\\\begin{pmatrix}t_L\\b'_L\end{pmatrix}\end{pmatrix} \tag{8.32}$$

with $\mathbf{Y}_u v = \mathbf{M}_u$ and $\mathbf{Y}'_d v = \mathbf{V}^+ \mathbf{M}_d \mathbf{V}$.

After the discovery of the Higgs boson at the LHC storage ring at CERN in 2012, this origin of quark masses and mixing is established, and the Standard Model is thus complete. There is still the open question about the origin of these parameters, 10 independent numbers that are not related within the theory. There are even (at least) 10 more for the mass generation in the lepton sector.

8.9 Discovery of the Higgs Boson

The physical Higgs boson has been discovered[52] by the experiments ATLAS and CMS at the CERN Large Hadron Collider LHC. In July 2012, the observation of a new boson was announced, decaying into two photons or into one on-shell and one virtual Z boson, at a mass around 125 GeV. About one year later, additional properties of this boson lead to the conclusion that it is indeed the Higgs boson of the Standard Model.

[52] ATLAS Collab., "Observation of a new particle in the search for the Standard Model Higgs boson with the ATLAS detector at the LHC", Phys. Lett. **B716**, 1–29 (2012); CMS Collab., "Observation of a new boson at a mass of 125 GeV with the CMS experiment at the LHC", Phys. Lett. **B716**, 30–61 (2012).

9. Quark Mixing, CP and T Violation

9.1 The Unitary CKM Matrix

The charged current weak interactions responsible for flavour changes are described in the Standard Model by the couplings $gW^\mu J_\mu^{cc}$ of the W boson to the current

$$J_\mu^{cc} = \begin{pmatrix} \overline{\nu}_e \\ \overline{\nu}_\mu \\ \overline{\nu}_\tau \end{pmatrix} \gamma_\mu \frac{1-\gamma_5}{2} \begin{pmatrix} e \\ \mu \\ \tau \end{pmatrix} + \sum_{r,g,b} \begin{pmatrix} \bar{u} \\ \bar{c} \\ \bar{t} \end{pmatrix} \gamma_\mu \frac{1-\gamma_5}{2} \, \mathbf{V} \cdot \begin{pmatrix} d \\ s \\ b \end{pmatrix} \tag{9.1}$$

with a non-trivial transformation matrix $\mathbf{V}$ in the quark sector, the Cabibbo–Kobayashi–Maskawa (CKM) Matrix[53]

$$\mathbf{V} = \begin{pmatrix} V_{ud} & V_{us} & V_{ub} \\ V_{cd} & V_{cs} & V_{cb} \\ V_{td} & V_{ts} & V_{tb} \end{pmatrix}$$

A coupling via a scalar boson would allow a general 3×3 coupling matrix. However, local gauge invariance which is realized via the gauge bosons $W^\pm$ requires that one universal coupling constant connects the triplet of up-type quarks with the triplet of down-type quarks. The only complication permitted is a unitary transformation to another basis of states, which is accomplished by the CKM matrix.

If there were more than three quark families, this would not hold for the 3×3 submatrix. However, this possibility is unlikely, given the limit on neutrino flavours from LEP experiments, who find[54] $n_\nu = 2.984 \pm 0.008$ for neutrinos with mass much below the Z^0 mass. Thus, if a fourth generation exists, it must incorporate a massive neutrino which is more than a factor 10^{10} heavier than the masses of the known three neutrinos, as can be inferred from the upper limit of the electron neutrino mass of 2eV and the m^2 differences measured in neutrino oscillations.

From the 9 real parameters of a general unitary matrix, 5 can be absorbed in 1 global phase, 2 relative phases between u, c, t and 2 relative phases between d, s, b which are all subject to convention and in principle unobservable. If two quarks within one of these two groups were degenerate in mass, even the sixth phase could be removed by redefining the basis in their two-dimensional subspace.

Rephasing may be accomplished by applying a phase factor to every row and column:

$$V_{jk} \to e^{i(\phi_j - \phi_k)} V_{jk} \tag{9.2}$$

Note that $j = u, c, t$, $k = d, s, b$, and the six numbers $\phi_u, \phi_c, \phi_t, \phi_d, \phi_s, \phi_b$ represent only five independent phases in the CKM matrix, since different sets of $\{\phi_j, \phi_k\}$ yield the same result. Any product where each row and column enters once as V_{ij} and once via a complex conjugate V_{kl}^* like $V_{ij} V_{kl} V_{il}^* V_{kj}^*$ is **invariant** under the transformation (9.2). This implies that observable phases must always correspond to similar products of CKM matrix elements with equal numbers of V and V^* factors and appropriate combination of indices.

Removing as much unphysical phases as possible, the CKM matrix is described by **4 real parameters**, where only one is a phase parameter, while the other three are rotation angles in flavour space. The physical phase is not one unique number due to the arbitrary choice of the unphysical phases. Unambiguous representations of this phase as the angles of unitarity triangles will be discussed below. The standard parametrization[55] uses a choice of phases, that leave V_{ud} and V_{cb} real:

$$\mathbf{V} = \begin{pmatrix} 1 & 0 & 0 \\ 0 & c_{23} & s_{23} \\ 0 & -s_{23} & c_{23} \end{pmatrix} \begin{pmatrix} c_{13} & 0 & s_{13} e^{-i\delta_{13}} \\ 0 & 1 & 0 \\ -s_{13} e^{i\delta_{13}} & 0 & c_{13} \end{pmatrix} \begin{pmatrix} c_{12} & s_{12} & 0 \\ -s_{12} & c_{12} & 0 \\ 0 & 0 & 1 \end{pmatrix}$$

[53] N. Cabibbo, Phys. Rev. Lett. **10**, 531 (1963); M. Kobayashi, T. Maskawa, Progr. Theor. Phys. **49**, 652 (1973).
[54] PDG 2010
[55] following the Particle Data Group, first proposed in L.-L. Chau, W.-Y. Keung, Phys. Rev. Lett. **53**, 1802 (1984), notation follows H. Harari, M. Leurer, Phys. Lett. **B181**, 123 (1986).

$$= \begin{pmatrix} c_{12}c_{13} & s_{12}c_{13} & s_{13}e^{-i\delta_{13}} \\ -s_{12}c_{23} - c_{12}s_{13}s_{23}e^{i\delta_{13}} & c_{12}c_{23} - s_{12}s_{13}s_{23}e^{i\delta_{13}} & c_{13}s_{23} \\ s_{12}s_{23} - c_{12}s_{13}c_{23}e^{i\delta_{13}} & -c_{12}s_{23} - s_{12}s_{13}c_{23}e^{i\delta_{13}} & c_{13}c_{23} \end{pmatrix} \tag{9.3}$$

with $c_{ij} = \cos\theta_{ij}$, $s_{ij} = \sin\theta_{ij}$, and $s_{ij} > 0$, $c_{ij} > 0$ ($0 \le \theta_{ij} \le \pi/2$). The angle $\theta_C = \theta_{12}$ is the Cabibbo-angle.

A convenient substitution[56] is $s_{12} = \lambda$, $s_{23} = A\lambda^2$, $s_{13}\sin\delta_{13} = A\lambda^3\eta$, and $s_{13}\cos\delta_{13} = A\lambda^3\rho$, which reflects the apparent hierarchy in the size of mixing angles via orders of a parameter λ. This leads to

$$\begin{aligned} \mathbf{V} &= \begin{pmatrix} 1 & 0 & 0 \\ 0 & \sqrt{1-A^2\lambda^4} & A\lambda^2 \\ 0 & -A\lambda^2 & \sqrt{1-A^2\lambda^4} \end{pmatrix} \cdot \\ &\quad \cdot \begin{pmatrix} \sqrt{1-A^2\lambda^6(\rho^2+\eta^2)} & 0 & A\lambda^3(\rho - i\eta) \\ 0 & 1 & 0 \\ -A\lambda^3(\rho + i\eta) & 0 & \sqrt{1-A^2\lambda^6(\rho^2+\eta^2)} \end{pmatrix} \cdot \begin{pmatrix} \sqrt{1-\lambda^2} & \lambda & 0 \\ -\lambda & \sqrt{1-\lambda^2} & 0 \\ 0 & 0 & 1 \end{pmatrix} \\ &= \begin{pmatrix} 1 - \frac{\lambda^2}{2} - \frac{\lambda^4}{8} & \lambda & A\lambda^3(\rho - i\eta) \\ -\lambda - A^2\lambda^5(\rho + i\eta - \frac{1}{2}) & 1 - \frac{\lambda^2}{2} - (\frac{1}{8} + \frac{A}{2})\lambda^4 & A\lambda^2 \\ A\lambda^3[1 - (\rho + i\eta)(1 - \frac{\lambda^2}{2})] & -A\lambda^2 - A\lambda^4(\rho + i\eta - \frac{1}{2}) & 1 - \frac{1}{2}A^2\lambda^4 \end{pmatrix} + \mathcal{O}(\lambda^6) \end{aligned} \tag{9.4}$$

and agrees to $\mathcal{O}(\lambda^3)$ with the Wolfenstein approximation[57]:

$$\mathbf{V} = \begin{pmatrix} 1 - \frac{\lambda^2}{2} & \lambda & A\lambda^3(\rho - i\eta + \frac{i}{2}\eta\lambda^2) \\ -\lambda & 1 - \frac{\lambda^2}{2} - i\eta A^2\lambda^4 & A\lambda^2(1 + i\eta\lambda^2) \\ A\lambda^3(1 - \rho - i\eta) & -A\lambda^2 & 1 \end{pmatrix} \tag{9.5}$$

$$\mathbf{V} \approx \begin{pmatrix} 1 - \frac{\lambda^2}{2} & \lambda & A\lambda^3(\rho - i\eta) \\ -\lambda & 1 - \frac{\lambda^2}{2} & A\lambda^2 \\ A\lambda^3(1 - \rho - i\eta) & -A\lambda^2 & 1 \end{pmatrix} \tag{9.6}$$

Equation (9.4) is more convenient in higher orders than the original proposal of Wolfenstein, or an exact parametrization[58] using the Wolfenstein parameters.

9.1.1 Unitarity Triangles

If nature provides us with just these three families of fermions, unitarity requires the following 12 conditions to be fulfilled:

$$\begin{aligned} &\text{rows } 1\times 1,\ uu && |V_{ud}|^2 + |V_{us}|^2 + |V_{ub}|^2 = 1 && \text{(9.7a)} \\ &\text{rows } 2\times 2,\ cc && |V_{cd}|^2 + |V_{cs}|^2 + |V_{cb}|^2 = 1 && \text{(9.7b)} \\ &\text{rows } 3\times 3,\ tt && |V_{td}|^2 + |V_{ts}|^2 + |V_{tb}|^2 = 1 && \text{(9.7c)} \\ &\text{columns } 1\times 1,\ dd && |V_{ud}|^2 + |V_{cd}|^2 + |V_{td}|^2 = 1 && \text{(9.7d)} \\ &\text{columns } 2\times 2,\ ss && |V_{us}|^2 + |V_{cs}|^2 + |V_{ts}|^2 = 1 && \text{(9.7e)} \\ &\text{columns } 3\times 3,\ bb && |V_{ub}|^2 + |V_{cb}|^2 + |V_{tb}|^2 = 1 && \text{(9.7f)} \\ &\text{rows } 1\times 2,\ cu && V_{ud}^*V_{cd} + V_{us}^*V_{cs} + V_{ub}^*V_{cb} = 0 && \text{(9.7g)} \\ &\text{rows } 1\times 3,\ tu && V_{ud}^*V_{td} + V_{us}^*V_{ts} + V_{ub}^*V_{tb} = 0 && \text{(9.7h)} \end{aligned}$$

[56] A. J. Buras, M. E. Lautenbacher, G. Ostermaier, Phys. Rev. **D50**, 3433 (1994). An equivalent choice is $\lambda = s_{12}c_{13}$ which leads to the same parametrization to $\mathcal{O}(\lambda^5)$.

[57] L. Wolfenstein, Phys. Rev. Lett. **51**, 1945 (1984), using $\lambda := V_{us} = s_{12}c_{13}$, $A\lambda^2 := V_{cb} = s_{23}c_{13}$ and unitarity at $\mathcal{O}(\lambda^3)$ to define ρ, η, and using a phase convention that leaves V_{ud}, V_{us}, V_{tb}, V_{ts}, and especially V_{cd} real to $\mathcal{O}(\lambda^5)$.

[58] M. Kobayashi, Progr. Theor. Phys. **92**, 287 (1994).

rows 2×3, tc	$V_{cd}^*V_{td} + V_{cs}^*V_{ts} + V_{cb}^*V_{tb} = 0$	(9.7i)
columns 1×2, sd	$V_{ud}V_{us}^* + V_{cd}V_{cs}^* + V_{td}V_{ts}^* = 0$	(9.7j)
columns 1×3, bd	$V_{ud}V_{ub}^* + V_{cd}V_{cb}^* + V_{td}V_{tb}^* = 0$	(9.7k)
columns 2×3, bs	$V_{us}V_{ub}^* + V_{cs}V_{cb}^* + V_{ts}V_{tb}^* = 0$	(9.7l)

The conditions a–f are redundant, three are sufficient to establish unitarity together with g–l. An arbitrary phase for the whole matrix cancels in $\mathbf{V^+V}$. A phase common to all elements in a line (column), corresponding to arbitrary phases between u, c, t (d, s, b) will vanish in eqns. 9.7j–l (9.7g–i) and become a common factor in eqns. 9.7g–i (9.7j–l).

Dividing (9.7k) by $A\lambda^3 \approx -V_{cd}V_{cb}^*$ yields the unitarity triangle[59] as shown in figure 9.1a. In the Wolfenstein approximation, it corresponds to

$$(\rho + i\eta) - 1 + (1 - \rho - i\eta) = 0 \tag{9.8}$$

A second one from (9.7h) is shown in figure 9.1b. Dividing by $A\lambda^3 \approx -V_{us}^*V_{ts}$ and using the approximation $V_{ud} \approx 1$ gives the same triangle (9.8). A closer look, however, reveals slightly different lengths and angles to $\mathcal{O}(\lambda^2)$.

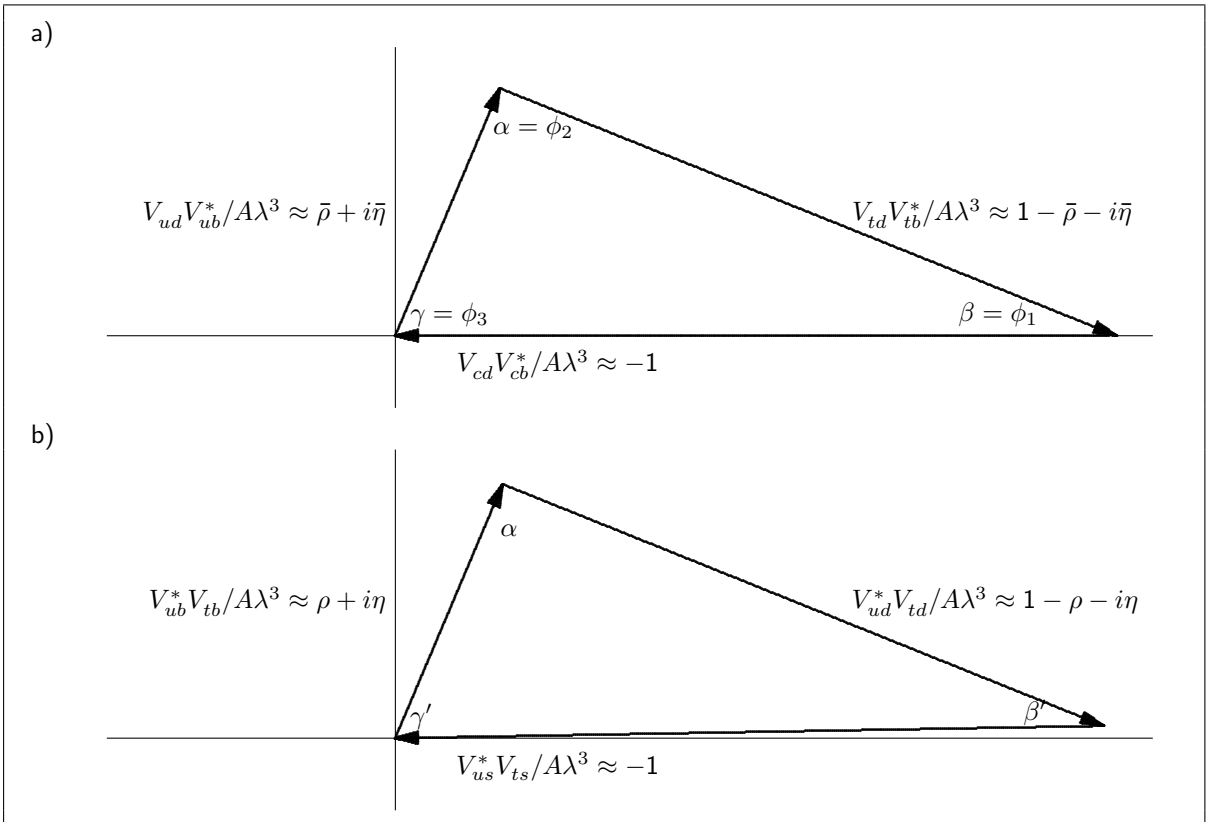

Fig. 9.1 Unitarity triangles bd and tu in the complex plane, corresponding to **a**: (9.7k) and **b**: (9.7h), respectively. Up to corrections of $\mathcal{O}(\lambda^4)$ the top points are (ρ, η) in **(b)**, but $(\bar\rho = [1 - \frac{\lambda^2}{2}]\rho, \bar\eta = [1 - \frac{\lambda^2}{2}]\eta)$ in **(a)**, and the rightmost points are $(1, 0)$ in **(a)**, but $(1 - \lambda^2[\frac{1}{2} - \rho], \lambda^2\eta)$ in **(b)**. The angles are related via $\gamma - \gamma' = \beta' - \beta \approx \beta_s \approx \lambda^2\eta$. Changing the phase convention for the CKM matrix will rotate the triangles in the complex plain, but their shape is invariant under those transformations. To avoid this, we may use $-V_{cd}V_{cb}^*$ instead of $A\lambda^3$ as scale factor, which makes the baseline of the triangle (a) exactly -1.

[59] This geometric interpretation has been pointed out by Bjorken ∼1986; its first documentation in printed form is in conference proceedings 1987 by K. R. Schubert, C. Hamzaoui, J. L. Rosner, and A. I. Sanda.

The angles[60] of the unitarity triangles bd and tu (9.7k and h) in figure 9.1 are defined by[61]

$$e^{i\alpha} = -\frac{V_{td}V_{ub}V_{ud}^*V_{tb}^*}{|V_{td}V_{ub}V_{ud}V_{tb}|}$$
$$e^{i\beta} = -\frac{V_{td}^*V_{cb}^*V_{cd}V_{tb}}{|V_{td}V_{cb}V_{cd}V_{tb}|} \approx e^{i\beta'} = -\frac{V_{td}^*V_{us}^*V_{ts}V_{ud}}{|V_{td}V_{us}V_{ts}V_{ud}|}$$
$$e^{i\gamma} = -\frac{V_{ub}^*V_{cd}^*V_{cb}V_{ud}}{|V_{ub}V_{cd}V_{cb}V_{ud}|} \approx e^{i\gamma'} = -\frac{V_{ub}^*V_{ts}^*V_{us}V_{tb}}{|V_{ub}V_{ts}V_{us}V_{tb}|}$$

These are rephasing invariant expressions, hence the angles resemble physical quantities independent of the CKM parametrization. It was first emphasized by Jarlskog[62], that CP violation can be described via a rephasing invariant quantity

$$J = \pm\mathcal{I}m\, V_{ij}V_{kl}V_{il}^*V_{kj}^* \approx A^2\lambda^6\eta$$

which is up to a sign independent of i, j, k, l, provided $i \neq k$, $j \neq l$.

$$\begin{array}{rrr}
J &= \mathcal{I}m(V_{ud}V_{cs}V_{us}^*V_{cd}^*) &= -\mathcal{I}m(V_{ud}V_{cb}V_{ub}^*V_{cd}^*) = -\mathcal{I}m(V_{ud}V_{ts}V_{us}^*V_{td}^*) \\
&= \mathcal{I}m(V_{ud}V_{tb}V_{ub}^*V_{td}^*) &= -\mathcal{I}m(V_{us}V_{cd}V_{ud}^*V_{cs}^*) = \mathcal{I}m(V_{us}V_{cb}V_{ub}^*V_{cs}^*) \\
&= \mathcal{I}m(V_{us}V_{td}V_{ud}^*V_{ts}^*) &= -\mathcal{I}m(V_{us}V_{tb}V_{ub}^*V_{ts}^*) = \mathcal{I}m(V_{ub}V_{cd}V_{ud}^*V_{cb}^*) \\
&= -\mathcal{I}m(V_{ub}V_{cs}V_{us}^*V_{cb}^*) &= -\mathcal{I}m(V_{ub}V_{td}V_{ud}^*V_{tb}^*) = \mathcal{I}m(V_{ub}V_{ts}V_{us}^*V_{tb}^*) \\
&= \mathcal{I}m(V_{cd}V_{ts}V_{cs}^*V_{td}^*) &= -\mathcal{I}m(V_{cd}V_{tb}V_{cb}^*V_{td}^*) = -\mathcal{I}m(V_{cs}V_{td}V_{cd}^*V_{ts}^*) \\
&= \mathcal{I}m(V_{cs}V_{tb}V_{cb}^*V_{ts}^*) &= \mathcal{I}m(V_{cb}V_{td}V_{cd}^*V_{tb}^*) = -\mathcal{I}m(V_{cb}V_{ts}V_{cs}^*V_{tb}^*)
\end{array}$$

These terms are all products of the type $\mathcal{I}m\, AB^* = |A||B|\,\mathcal{I}m\, e^{i(\arg A - \arg B)} = |A||B|\sin(\arg A - \arg B)$, which is twice the area of a triangle in the complex plain with sides A and B. The A and B here are sides of a unitarity triangle. The equality of these terms is easily seen, e. g. for the last line replacing d with s is equivalent to applying the unitarity condition (9.7i)

$$V_{td}V_{cd}^* = -V_{ts}V_{cs}^* - V_{tb}V_{cb}^*$$

which yields

$$\mathcal{I}m(V_{cb}V_{td}V_{cd}^*V_{tb}^*) = -\mathcal{I}m(V_{cb}V_{ts}V_{cs}^*V_{tb}^*) - \mathcal{I}m(V_{cb}V_{tb}V_{cb}^*V_{tb}^*)$$

and the last argument is real, i. e. $\mathcal{I}m(V_{cb}V_{tb}V_{cb}^*V_{tb}^*) = \mathcal{I}m\,|V_{cb}|^2|V_{tb}|^2 = 0$. Hence the areas of all six unitarity triangles defined by (9.7g–l) are equal and have the value $J/2$. This corresponds to an area $\approx \eta/2$ for the ones in figure 9.1, since their sides have been reduced by the factor $A\lambda^3$. As will be shown below, CP violating observables are typically proportional to the sine of the angles in unitarity triangles, like

$$\sin\gamma = \mathcal{I}m\, e^{i\gamma} = -\frac{\mathcal{I}m(V_{ub}^*V_{cd}^*V_{cb}V_{ud})}{|V_{ub}V_{cd}V_{cb}V_{ud}|} = -\frac{J}{|V_{ub}V_{cd}V_{cb}V_{ud}|}$$

and vanish for $J = 0$, i. e. if all triangles collapse into lines. If the non-trivial phase in the CKM matrix is 0 or π, the parameter η is 0 and hence $J = 0$. This would also be the case if two quarks of a given charge had the same mass, since then a rotation between these two flavours could be chosen that removes the phase factors, as can be seen in (9.3) where $\theta_{13} = 0$ would remove all terms with the phase δ_{13}.

All six unitarity triangles are shown approximately to scale in figure 9.2. Their angles—which are still largely unknown—can be determined using the standard parametrization (9.3) in a rewritten form

$$\mathbf{V} = \begin{pmatrix} |V_{ud}| & |V_{us}| & |V_{ub}|e^{-i\tilde{\gamma}} \\ -|V_{cd}|e^{i\tilde{\phi}_4} & |V_{cs}|e^{-i\tilde{\phi}_6} & |V_{cb}| \\ |V_{td}|e^{-i\tilde{\beta}} & -|V_{ts}|e^{i\tilde{\phi}_2} & |V_{tb}| \end{pmatrix} \tag{9.9}$$

[60] Another naming convention is $\phi_1 = \beta$, $\phi_2 = \alpha$ and $\phi_3 = \gamma$.

[61] In the complex plane, the angle $\alpha - \beta$ between two vectors $A = ae^{i\alpha}$ and $B = be^{i\beta}$ is given by $e^{i(\alpha-\beta)} = AB^*/|AB|$ and $\sin(\alpha-\beta) = \mathcal{I}m(AB^*)/|AB| = (AB^* - A^*B)/(2i|AB|)$.

[62] C. Jarlskog, Phys. Rev. Lett. **55**, 1039 (1985); Z. Phys. **C29**, 491 (1985).

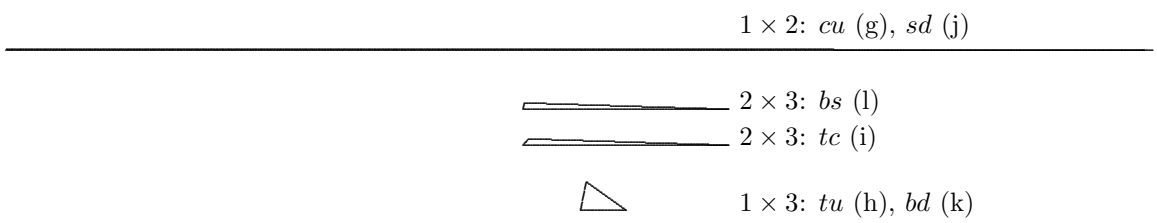

Fig. 9.2 The three types of unitarity triangles, approximately to scale (assuming some allowed values for ρ, η that differ from those assumed in figure 9.1). Their areas are equal.

with $\tilde{\gamma} \equiv \delta_{13}$. Here, absolute values and phases are given as separate factors. The angles $\tilde{\phi}_2 \approx \eta\lambda^2$, $\tilde{\phi}_4 \approx \eta A^2\lambda^4$, and $\tilde{\phi}_6 \approx \eta A^2\lambda^6$ are all positive and very small and their subscript indicates the order in λ of their magnitude. The unitarity triangles in figure 9.1 have angles

$$\begin{aligned} \beta &= \tilde{\beta} + \tilde{\phi}_4, \qquad & \beta' &= \tilde{\beta} + \tilde{\phi}_2 = \beta + \tilde{\phi}_2 - \tilde{\phi}_4 \\ \gamma &= \tilde{\gamma} - \tilde{\phi}_4, \qquad & \gamma' &= \tilde{\gamma} - \tilde{\phi}_2 = \gamma - \tilde{\phi}_2 + \tilde{\phi}_4 \\ \alpha &= \pi - \tilde{\beta} - \tilde{\gamma} = \pi - \beta - \gamma = \pi - \beta' - \gamma' \\ & & \beta_s &= \tilde{\phi}_2 + \tilde{\phi}_6 \end{aligned}$$

In the Wolfenstein approximation, the unitarity relations read (all terms given to order λ^3)

$$\begin{aligned} -\lambda + \tfrac{1}{2}\lambda^3 + \lambda - \tfrac{1}{2}\lambda^3 + \quad 0 + \mathcal{O}(\lambda^5) \quad &= 0 && (9.7\mathrm{g}') \\ A\lambda^3(1-\rho-i\eta) - \quad A\lambda^3 \quad + \quad A\lambda^3(\rho+i\eta) \quad &= 0 && (9.7\mathrm{h}') \\ 0 + \mathcal{O}(\lambda^4) - \quad A\lambda^2 \quad + \quad A\lambda^2 \quad &= 0 && (9.7\mathrm{i}') \\ \lambda - \tfrac{1}{2}\lambda^3 - \lambda + \tfrac{1}{2}\lambda^3 - \quad 0 + \mathcal{O}(\lambda^5) \quad &= 0 && (9.7\mathrm{j}') \\ A\lambda^3(\rho+i\eta) - \quad A\lambda^3 \quad + A\lambda^3(1-\rho-i\eta) \quad &= 0 && (9.7\mathrm{k}') \\ 0 + \mathcal{O}(\lambda^4) + \quad A\lambda^2 \quad - \quad A\lambda^2 \quad &= 0 && (9.7\mathrm{l}') \end{aligned}$$

and define three pairs of unitarity triangles, 6 in total:

- (9.7h′) and (9.7k′) are the ones shown in figure 9.1 with three sides of similar length, all of order $A\lambda^3$. This is "**the unitarity triangle**". The other ones are quite flat, and it will require very high precision to prove experimentally that they are not degenerate to a line. They are all shown to approximate scale in figure 9.2.
- (9.7i′) and (9.7l′) have two sides of length $A\lambda^2$ and one much shorter of order $A\lambda^4$. This limits the small angles, which are $\tilde{\phi}_2 + \tilde{\phi}_6$ and $\tilde{\phi}_2 - \tilde{\phi}_6$, respectively. They are close to the differences of angles in the large triangles $\gamma - \gamma' = \beta' - \beta = \tilde{\phi}_2 - \tilde{\phi}_4$.

  The other two angles are for (9.7i′) $\sim \beta$ and $\sim \pi - \beta$, and for (9.7l′) $\sim \gamma$ and $\sim \pi - \gamma$.
- (9.7g′) and (9.7j′) have two sides of length λ and one very much shorter of order $A^2\lambda^5$, with a small angle $\tilde{\phi}_4 - \tilde{\phi}_6$ and $\tilde{\phi}_4 + \tilde{\phi}_6$, respectively. Both are of order λ^4.

  The other two angles are for (9.7j′) $\sim \beta$ and $\sim \pi - \beta$, and for (9.7g′) $\sim \gamma$ and $\sim \pi - \gamma$.

Tiny differences between the two standard unitarity triangles are $\mathcal{O}(\lambda^2)$ corrections,

$$\begin{aligned} A\lambda^3(1-\rho-i\eta) \quad &+ \quad -A\lambda^3 \quad + \quad A\lambda^3(\rho+i\eta) \quad = 0 \\ +A\lambda^5(\rho+i\eta-\tfrac{1}{2}) \quad &+ A\lambda^5(\tfrac{1}{2}-\rho-i\eta) \quad + \mathcal{O}(\lambda^7) \\ +\mathcal{O}(\lambda^7) \quad &+ \mathcal{O}(\lambda^7) \end{aligned} \qquad (9.7\mathrm{h}'')$$

$$\begin{aligned} A\lambda^3(\rho+i\eta) \quad &+ \quad -A\lambda^3 \quad + \quad A\lambda^3(1-\rho-i\eta) = 0 \\ -\tfrac{1}{2}A\lambda^5(\rho+i\eta) \quad &+ \mathcal{O}(\lambda^7) \quad + \tfrac{1}{2}A\lambda^5(\rho+i\eta) \\ +\mathcal{O}(\lambda^7) \quad & \quad + \mathcal{O}(\lambda^7) \end{aligned} \qquad (9.7\mathrm{k}'')$$

The angles in these two triangles can be estimated from experimental constraints on a 3×3 unitary CKM matrix element magnitudes, and directly measured in CP violation in B meson decays. However, deviations from or extensions to the Standard Model may imply that the two triangles are dissimilar, or even that they are no closed triangles at all. Therefore, it is important to distinguish measurements of different parameters, even if they are expected to have identical or close values within the three family Standard Model.

9.1.1.1 Phases and Observables

The fact that phases of quark fields are unobservable numbers has been used to show that phases in the CKM matrix are not observables either, and there remains some arbitrariness in the parametrization for this matrix. Any valid CKM matrix is obtained from (9.9) with five independent arbitrary phase angles $\zeta_1 \ldots \zeta_5$ as

$$\mathbf{V} = \begin{pmatrix} |V_{ud}|e^{i\zeta_1} & |V_{us}|e^{i(\zeta_1+\zeta_2)} & |V_{ub}|e^{i(\zeta_1+\zeta_3-\tilde{\gamma})} \\ -|V_{cd}|e^{i(\zeta_4+\tilde{\phi}_4)} & |V_{cs}|e^{i(\zeta_4+\zeta_2-\tilde{\phi}_6)} & |V_{cb}|e^{i(\zeta_4+\zeta_3)} \\ |V_{td}|e^{i(\zeta_5-\tilde{\beta})} & -|V_{ts}|e^{i(\zeta_5+\zeta_2+\tilde{\phi}_2)} & |V_{tb}|e^{i(\zeta_5+\zeta_3)} \end{pmatrix} \tag{9.10}$$

The freedom to choose quark phases may be extended to antiquarks, with six more phases $\bar{\phi}_u, \bar{\phi}_c, \bar{\phi}_t, \bar{\phi}_d, \bar{\phi}_s, \bar{\phi}_b$. With the new quark states

$$q'_j = e^{i\phi_j} q, \;\; \bar{q}'_j = e^{i\bar{\phi}_j} \bar{q}_j, \;\; j = u, c, t, d, s, b$$

also the phase induced by the CP operation is changed. The transition

$$\mathrm{CP}\,|q_j\rangle = e^{i\phi_{\mathrm{CP}\,j}}|\bar{q}_j\rangle \quad \rightarrow \quad \mathrm{CP}\,|q'_j\rangle = e^{i\phi'_{\mathrm{CP}\,j}}|\bar{q}'_j\rangle$$

requires

$$\phi'_{\mathrm{CP}\,j} = \phi_{\mathrm{CP}\,j} + \phi_j - \bar{\phi}_j$$

This equation leaves $\phi'_{\mathrm{CP}\,j}$ still completely undefined, since all three phases on the right-hand side are not observable, and therefore subject to arbitrary changes. It becomes meaningful, however, if it is applied to observables, like CP eigenvalues. Two CP eigenstates constructed from a meson and antimeson state with eigenvalues ± 1 are related accordingly:

$$|q_j\bar{q}_k\rangle \pm e^{i\phi_{\mathrm{CP}\,jk}}|q_k\bar{q}_j\rangle \;\; = \;\; e^{-i(\phi_j+\bar{\phi}_k)}\left[|q'_j\bar{q}'_k\rangle \pm e^{i\phi'_{\mathrm{CP}\,jk}}|q'_k\bar{q}'_j\rangle\right]$$

The new states $|q'_j\bar{q}'_k\rangle \pm e^{i\phi'_{\mathrm{CP}\,jk}}|q'_k\bar{q}'_j\rangle$ have the same eigenvalues, and differ by an overall unobservable phase from the old ones.

The CP operation on a meson, e. g. the pseudoscalar B^0 meson $|\bar{b}d\rangle$, is

$$\mathrm{CP}\,|B^0\rangle = e^{i\phi_{\mathrm{CP}\,B}}|\overline{B}^0\rangle \tag{9.11}$$

where the phase factor $e^{i\phi_{\mathrm{CP}\,B}} = \langle\overline{B}^0|\,\mathrm{CP}\,|B^0\rangle$ depends on the parity of the bound-state wave function, and the chosen quark and antiquark phase convention.

Quark phase changes could be compensated by phase changes of the CKM matrix elements according to (9.2), leaving terms like

$$\langle q_j|V_{jk}|q_k\rangle$$

invariant. However, the phase of this matrix element is **not** an observable. Hence the choice of phases in the CKM matrix parametrization can be made **independent** of the choice of quark phases.

Phase conventions will also enter into relations among decay amplitudes. An amplitude for a weak decay $B^0 \to X$ via a single well defined process can be written as

$$A = \langle X|\mathcal{H}|B^0\rangle = \langle X|\boldsymbol{O}V|B^0\rangle \tag{9.12}$$

where V is a product of the appropriate CKM matrix elements and $\boldsymbol{O}$ is an operator describing the rest of the weak and possibly also subsequent strong interaction processes involved in the transition. Since strong interaction (also weak interaction except for nontrivial phases in V) are CP invariant, the charge conjugate mirror process $\overline{B}^0 \to \overline{X}$ has an amplitude

$$\begin{aligned}\overline{A} = \langle \overline{X}|\mathcal{H}|\overline{B}^0\rangle &= \langle \overline{X}|\,\mathrm{CP}^{+}\,\mathrm{CP}\,\mathcal{H}\,\mathrm{CP}^{+}\,\mathrm{CP}\,|\overline{B}^0\rangle \\ &= e^{i\phi_{\mathrm{CP}X}}\langle X|\,\mathrm{CP}\,\boldsymbol{O}V\,\mathrm{CP}^{+}\,e^{-i\phi_{\mathrm{CP}B}}|B^0\rangle \\ &= e^{i(\phi_{\mathrm{CP}X}-\phi_{\mathrm{CP}B})}\langle X|\boldsymbol{O}V^*|B^0\rangle \\ &= e^{i(\phi_{\mathrm{CP}X}-\phi_{\mathrm{CP}B})}\frac{V^*}{V}A\end{aligned} \tag{9.13}$$

where also

$$\frac{V^*}{V} = e^{-2i\arg V}$$

is just a phase. Especially, if X is a CP eigenstate with eigenvalue $\zeta_X^{CP} = \pm 1$,

$$\overline{A} = \zeta_X^{CP} e^{-i(\phi_{\mathrm{CP}B}+2\arg V)}A \tag{9.14}$$

relates the two amplitudes, and the ratio $\overline{A}/A$ flips sign with the CP eigenvalue.

All physical observables must be independent of the choice of phases. This is the case if only absolute values of amplitudes are involved, but for interference terms the phase convention cancels often in a more subtle way. Some examples will be shown in the following chapters, one is the ratio

$$r := \frac{\eta_m \overline{A}}{A}$$

where the $e^{i\phi_{\mathrm{CP}B}}$ factors cancel from

$$\eta_m = \frac{q}{p} = \frac{\langle \overline{B}^0|B_L\rangle}{\langle B^0|B_L\rangle} = e^{i\phi_{\mathrm{CP}B}}\ldots$$

and only rephasing invariant products of CKM matrix elements remain.

On the other hand, expressions where the arbitrary phases are still present cannot be observables.

9.1.1.2 Reasonable Phase Conventions

Once the distinction of unobservable and observable phases is clear, it is reasonable to choose phases in a way that simplifies calculations.

So it is sensible to use only one phase in the CKM matrix as in (9.3), and not six as in (9.10). If a choice of phases were possible where all CKM matrix elements can be made real, also charged current weak interactions would not violate CP symmetry.

A natural choice for CP phases requires all $J^{PC} = 0^{-+}$ mesons to have $\mathrm{CP}\,|X\rangle = -|\overline{X}\rangle$, fixing $\phi_{\mathrm{CP}B} = \pi$. However, it has become fashionable to use the opposite sign convention, i. e. $\phi_{\mathrm{CP}B} = 0$.

The appearance of an additional phase factor in $e^{i\phi_{\mathrm{CP}\,kj}}\langle \bar{q}_j|V_{jk}^*|\bar{q}_k\rangle$ can be avoided by the restriction $\bar{\phi}_j = -\phi_j$ for quark phase changes, and an appropriate phase convention which makes terms related by a CPT transformation relatively real.

9.1.1.3 An Example of a Different Phase Convention

The standard phase convention (9.9)

$$V = \begin{pmatrix} |V_{ud}| & |V_{us}| & |V_{ub}|e^{-i\tilde{\gamma}} \\ -|V_{cd}|e^{i\tilde{\phi}_4} & |V_{cs}|e^{-i\tilde{\phi}_6} & |V_{cb}| \\ |V_{td}|e^{-i\tilde{\beta}} & -|V_{ts}|e^{i\tilde{\phi}_2} & |V_{tb}| \end{pmatrix}$$

puts large phases into the smallest CKM matrix elements, V_{ub} and V_{td}. A phase transformation of the u and d quark leads immediately to another phase convention

$$V = \begin{pmatrix} -|V_{ud}|e^{-i\alpha} & |V_{us}|e^{i\tilde{\gamma}} & |V_{ub}| \\ -|V_{cd}|e^{i(\tilde{\phi}_4+\tilde{\beta})} & |V_{cs}|e^{-i\tilde{\phi}_6} & |V_{cb}| \\ |V_{td}| & -|V_{ts}|e^{i\tilde{\phi}_2} & |V_{tb}| \end{pmatrix} \tag{9.15}$$

where $\alpha = \pi - \tilde{\beta} - \tilde{\gamma}$ has been used to simplify the phase of V_{ud}. In this representation big phases are associated with V_{ud}, V_{us}, and V_{cd}, while V_{ub} and V_{td} are real.

9.1.1.4 More Parameters

The parametrization (9.4) can be rewritten as

$$\begin{pmatrix} 1-\frac{\lambda^2}{2}-\frac{\lambda^4}{8} & \lambda & A\lambda^3(\rho-i\eta) \\ -\lambda - A^2\lambda^5(\rho+i\eta-\frac{1}{2}) & 1-\frac{\lambda^2}{2}-(\frac{1}{8}+\frac{A}{2})\lambda^4 & A\lambda^2 \\ A\lambda^3[1-(\bar{\rho}+i\bar{\eta})] & -A\lambda^2 - A\lambda^4(\rho+i\eta-\frac{1}{2}) & 1-\frac{1}{2}A^2\lambda^4 \end{pmatrix}$$

using the new parameters

$$\bar{\rho} := \rho(1-\frac{\lambda^2}{2}), \qquad \bar{\eta} := \eta(1-\frac{\lambda^2}{2}) \tag{9.16}$$

which can be used to write the bd unitarity triangle (9.7k) as

$$A\lambda^3(\bar{\rho}+i\bar{\eta}) + (-A\lambda^3) + A\lambda^3(1-\bar{\rho}-i\bar{\eta}) = 0 + \mathcal{O}(\lambda^7) \tag{9.7k'''}$$

The tip shown in figure 9.1a has the coordinates $(\bar{\rho}, \bar{\eta})$. The sides are given by

$$R_u := \left|\frac{V_{ub}^* V_{ud}}{V_{cb}^* V_{cd}}\right| = \sqrt{\bar{\rho}^2+\bar{\eta}^2}$$

and

$$R_t := \left|\frac{V_{td} V_{tb}^*}{V_{cb}^* V_{cd}}\right| = \sqrt{(1-\bar{\rho})^2+\bar{\eta}^2}.$$

9.2 Quark Mixing and Particle Antiparticle Oscillations

Mesons are neither particles nor antiparticles in a strict sense, since they are composed of a quark and an antiquark. This implies the existence of mesons with vacuum quantum numbers (e. g. f_0). More important is the existence of pairs of charge-conjugate mesons, which can be transformed into each other via flavour changing weak interaction transitions. These are $K^0/\overline{K}^0$ ($\bar{s}d/s\bar{d}$), $D^0/\overline{D}^0$ ($c\bar{u}/\bar{c}u$), $B^0/\overline{B}^0$ ($\bar{b}d/b\bar{d}$), and $B_s/\overline{B}_s$ ($\bar{b}s/b\bar{s}$). These are sometimes referred to by the term *meson antimeson pair*.

An unstable meson at rest can be described by the Schrödinger equation[63] $i\partial_t\psi = (m - \frac{i}{2}\Gamma)\psi$, with the solution

$$|\psi\rangle = |\psi_0\rangle e^{-imt} e^{-\frac{1}{2}\Gamma t} \tag{9.17}$$

which reproduces the exponential law of radioactive decay, since $|\langle\psi_0|\psi\rangle|^2 = e^{-\Gamma t}$. Since it describes the decay of a particle by its "vanishing", the Hamiltonian $H = m - \frac{i}{2}\Gamma$ is not real (i. e. not hermitian).

The four meson pairs $K^0/\overline{K}^0$, $D^0/\overline{D}^0$, $B^0/\overline{B}^0$, and $B_s/\overline{B}_s$ can be described as decaying two-component quantum states obeying the Schrödinger equation

$$i\partial_t\psi = \mathcal{H}\psi$$

with a general, non-hermitian Hamiltonian[64]

$$\mathcal{H} = \mathbf{M} - \tfrac{i}{2}\mathbf{\Gamma} = \begin{pmatrix} m_{11} - \frac{i}{2}\Gamma_{11} & m_{12} - \frac{i}{2}\Gamma_{12} \\ m_{12}^* - \frac{i}{2}\Gamma_{12}^* & m_{22} - \frac{i}{2}\Gamma_{22} \end{pmatrix} \tag{9.18}$$

written as a sum of the **hermitian** matrices $\mathbf{M}$ and $\mathbf{\Gamma}$. Even when the $\frac{i}{2}\Gamma_{jj}$ of the decay is removed, $\mathcal{H}$ is not hermitian!

The off-diagonal elements describe the transition $X^0 \leftrightarrow \overline{X}^0$ that are possible through the flavour-changing charged current and the non-zero angles in the CKM matrix.

If the $B^0/\overline{B}^0$ system is taken as a representative to illustrate the behaviour of oscillating meson pairs, the indices 1 and 2 correspond to base vectors

$$|B^0\rangle = \begin{pmatrix} 1 \\ 0 \end{pmatrix} \quad \text{and} \quad |\overline{B}^0\rangle = \begin{pmatrix} 0 \\ 1 \end{pmatrix}$$

These states are orthogonal, i. e. $\langle B^0|\overline{B}^0\rangle = 0$ and they are assumed to be normalized, i. e. $\langle\overline{B}^0|\overline{B}^0\rangle = \langle B^0|B^0\rangle = 1$.

CPT invariance is assumed for all following calculations unless noted otherwise. This requires $m_{11} = m_{22} := m$ and $\Gamma_{11} = \Gamma_{22} := \Gamma$, reducing the number of real parameters of the Hamiltonian to six.

$$\mathcal{H} = \begin{pmatrix} H & H_{12} \\ H_{21} & H \end{pmatrix} = \begin{pmatrix} m - \frac{i}{2}\Gamma & m_{12} - \frac{i}{2}\Gamma_{12} \\ m_{12}^* - \frac{i}{2}\Gamma_{12}^* & m - \frac{i}{2}\Gamma \end{pmatrix} \tag{9.19}$$

CPT invariance is one of the indispensable premises of any relativistic field theory within or beyond the Standard Model. The generalized phenomenology including CPT violation[65] will therefore not be considered here, but can be found in textbooks.

The parametrization of the off diagonal elements is convenient for calculation, but it is still the most general case, since 4 real parameters suffice to describe any H_{12} and H_{21}:

$$\begin{aligned}
m_{12} &= \tfrac{1}{2}(H_{12} + H_{21}^*) \\
\mathcal{R}e\, m_{12} &= \tfrac{1}{2}(\mathcal{R}e\, H_{12} + \mathcal{R}e\, H_{21}) \\
\mathcal{I}m\, m_{12} &= \tfrac{1}{2}(\mathcal{I}m\, H_{12} - \mathcal{I}m\, H_{21}) \\
\Gamma_{12} &= i(H_{12} - H_{21}^*) \\
\mathcal{R}e\, \Gamma_{12} &= \mathcal{I}m\, H_{12} + \mathcal{I}m\, H_{21} \\
\mathcal{I}m\, \Gamma_{12} &= \mathcal{R}e\, H_{12} - \mathcal{R}e\, H_{21} \\
\mathcal{R}e\, H_{12} &= \mathcal{R}e\, m_{12} + \tfrac{1}{2}\,\mathcal{I}m\, \Gamma_{12} \\
\mathcal{R}e\, H_{21} &= \mathcal{R}e\, m_{12} - \tfrac{1}{2}\,\mathcal{I}m\, \Gamma_{12} \\
\mathcal{I}m\, H_{12} &= \mathcal{I}m\, m_{12} - \tfrac{1}{2}\,\mathcal{R}e\, \Gamma_{12} \\
\mathcal{I}m\, H_{21} &= \mathcal{I}m\, m_{12} - \tfrac{1}{2}\,\mathcal{R}e\, \Gamma_{12}
\end{aligned}$$

[63] This is also a relativistic description of a particle at rest, i. e., without kinetic energy.

[64] T. T. Wu, C. N. Yang, Phys. Rev. Lett. **13**, 380 (1964).

[65] Indeed CPT can be violated in modern string or d-brane theories, so it is definitely worthwhile to search for CPT violation in experiment.

The Schrödinger equation for meson pairs is a set of two coupled differential equations. Its solutions can be composed of single particle solutions (9.17) for the eigenstates of the Hamiltonian (9.19). Solving the eigenvalue problem $\det(\mathcal{H} - a \cdot \mathbf{1}) = (H-a)^2 - H_{12}H_{21} = 0$, one obtains two eigenstates with eigenvalues

$$a_{L,H} = H \mp \sqrt{H_{12}H_{21}}$$

or explicitly

$$\begin{aligned} a_L &= m_L - \tfrac{i}{2}\Gamma_L = m - \tfrac{i}{2}\Gamma - \sqrt{\left(m_{12} - \tfrac{i}{2}\Gamma_{12}\right)\left(m_{12}^* - \tfrac{i}{2}\Gamma_{12}^*\right)} \\ a_H &= m_H - \tfrac{i}{2}\Gamma_H = m - \tfrac{i}{2}\Gamma + \sqrt{\left(m_{12} - \tfrac{i}{2}\Gamma_{12}\right)\left(m_{12}^* - \tfrac{i}{2}\Gamma_{12}^*\right)} \end{aligned} \tag{9.20}$$

where L, H stands for "light" and "heavy". It is immediately seen that m and Γ are the average mass $\frac{1}{2}(m_H + m_L)$ and width $\frac{1}{2}(\Gamma_H + \Gamma_L)$. The differences are

$$\begin{aligned} \frac{\Delta m}{2} &= \frac{m_H - m_L}{2} = \mathcal{R}e\,\sqrt{H_{12}H_{21}} \\ \frac{\Delta\Gamma}{2} &= \frac{\Gamma_H - \Gamma_L}{2} = -2\,\mathcal{I}m\,\sqrt{H_{12}H_{21}} \\ \frac{\Delta a}{2} &= \frac{a_H - a_L}{2} = \sqrt{\left(m_{12} - \tfrac{i}{2}\Gamma_{12}\right)\left(m_{12}^* - \tfrac{i}{2}\Gamma_{12}^*\right)} = \sqrt{|m_{12}|^2 - \tfrac{1}{4}|\Gamma_{12}|^2 - i\,\mathcal{R}e(m_{12}\Gamma_{12}^*)} \end{aligned} \tag{9.21}$$

The connection between mass and lifetime (width) differences[66] and the off-diagonal elements in the mass matrix are showing up in these equations, especially $\Delta m = 0$ if $m_{12} = 0$ and $\Delta\Gamma = 0$ if $\Gamma_{12} = 0$. Squaring the last line leads to the useful relation

$$\Delta m \cdot \Delta\Gamma = 4\,\mathcal{R}e(m_{12}\Gamma_{12}^*) \tag{9.22}$$

which relates the sign of Δm and $\Delta\Gamma$ with the off-diagonal elements m_{12} and Γ_{12}.

It is convenient to define the dimensionless parameters

$$x = \frac{\Delta m}{\Gamma}, \qquad y = \frac{\Delta\Gamma}{2\Gamma} = \frac{\Gamma_H - \Gamma_L}{\Gamma_H + \Gamma_L} = \frac{\Gamma - \Gamma_L}{\Gamma} = \frac{\tau_L - \tau_H}{\tau_L + \tau_H} \tag{9.23}$$

where x is a non-negative real number, and y may only assume values between -1 and 1. It is an asymmetry parameter in the widths or, equivalently, in the lifetimes τ_L, τ_H.

The widths of the eigenstates are then

$$\Gamma_H = \Gamma \cdot (1+y), \qquad \Gamma_L = \Gamma \cdot (1-y)\,. \tag{9.24}$$

The eigenvectors $|B_{L,H}\rangle = \begin{pmatrix} p \\ \pm q \end{pmatrix}$ are found by inserting (9.20) into

$$\begin{aligned} \mathcal{H}|B_{\mathrm{L,H}}\rangle &= a_{\mathrm{L,H}}|B_{\mathrm{L,H}}\rangle \\ \mathcal{H}\begin{pmatrix} p \\ q \end{pmatrix} &= a_{\mathrm{L}}\begin{pmatrix} p \\ q \end{pmatrix} \\ (m - \tfrac{i}{2}\Gamma)p + H_{12}\,q &= (m - \tfrac{i}{2}\Gamma - \sqrt{H_{12}H_{21}})p \\ H_{12}\,q &= -\sqrt{H_{12}H_{21}}\cdot p \end{aligned}$$

[66] Note that in the literature $\Delta\Gamma \leftrightarrow -\Delta\Gamma$ is often interchanged. This will change the sign of the dimensionless parameter y likewise.

giving the ratio

$$\eta_m := \frac{q}{p} = \frac{1-\epsilon_m}{1+\epsilon_m} = \frac{\sqrt{H_{21}H_{12}}}{-H_{12}} = \frac{-H_{21}}{\sqrt{H_{21}H_{12}}} = -2\frac{m_{12}^* - \frac{i}{2}\Gamma_{12}^*}{\Delta m - \frac{i}{2}\Delta\Gamma} \tag{9.25}$$

which includes the phase ambiguity in $H_{12} = \langle B^0|\mathcal{H}|\overline{B}^0\rangle$ and is therefore usually defined to have $\mathcal{R}e\,\eta_m > 0$. This implies $\mathcal{R}e\,H_{12} < 0$ and

$$\eta_m = +\sqrt{\frac{H_{21}}{H_{12}}}$$

and leads to

$$\begin{aligned}\epsilon_m &= \frac{1-\eta_m}{1+\eta_m} = \frac{p-q}{p+q} \\ &= \frac{\sqrt{H_{12}} - \sqrt{H_{21}}}{\sqrt{H_{12}} + \sqrt{H_{21}}} = \frac{H_{12} - H_{21}}{H_{12} + H_{21} + 2\sqrt{H_{12}H_{21}}}\end{aligned}$$

Normalization requires $|p|^2 + |q|^2 = 1$, i. e.

$$\begin{aligned}p &= \frac{1+\epsilon_m}{\sqrt{2(1+|\epsilon_m|^2)}} \\ q &= \frac{1-\epsilon_m}{\sqrt{2(1+|\epsilon_m|^2)}}\end{aligned}$$

and single particle eigenstates are described by one complex parameter η_m. This parameter[67] is defined only up to an arbitrary phase, and only $|\eta_m|$ is a measurable quantity. The value of the phase depends on conventions, one of them is the definition of the phase $\phi_{\mathrm{CP}B} = \arg\langle\overline{B}^0|\,\mathrm{CP}\,|B^0\rangle$. This makes also ϵ_m (sometimes also denoted $\bar{\epsilon}$ or $\tilde{\epsilon}$) an arbitrary quantity. The standard choice of the CKM matrix (9.3) and $\phi_{\mathrm{CP}K} = 0$ make $|\epsilon_m|$ small in the $K^0/\overline{K}^0$ system, but a consistent convention $\phi_{\mathrm{CP}B} = 0$ leaves it at $\mathcal{O}(0.1\ldots1)$ in the $B^0/\overline{B}^0$ system.

The dependence on unphysical phases can also be seen if the parameters are expressed in terms of matrix elements as

$$\eta_m = \frac{q}{p} = \frac{\langle\overline{B}^0|B_L\rangle}{\langle B^0|B_L\rangle} = -\frac{\langle\overline{B}^0|B_H\rangle}{\langle B^0|B_H\rangle} \tag{9.26}$$

and

$$\epsilon_m = \frac{\langle B^0|B_L\rangle - \langle\overline{B}^0|B_L\rangle}{\langle B^0|B_L\rangle + \langle\overline{B}^0|B_L\rangle} = \frac{\langle B^0|B_H\rangle + \langle\overline{B}^0|B_H\rangle}{\langle B^0|B_H\rangle - \langle\overline{B}^0|B_H\rangle}$$

Obviously, relative phases between $|B_L\rangle$ and $|B_H\rangle$ are irrelevant, while relative phases between $|B^0\rangle$ and $|\overline{B}^0\rangle$ occur as a phase factor in η_m and in a more involved way in ϵ_m.

There exist different definitions of ϵ for the kaon system that are independent of arbitrary phases, but not easily generalized to B mesons. However, convention independent parameters can always be defined if specific decays are involved. They can usually be expressed via the unitarity angles (see fig. 9.1) and will be given for the B and K systems at the appropriate places below.

[67] η_m or $-\eta_m$ is sometimes called α in the literature, e. g. in T. Nakada, Proc. of the XVIth Int. Symp. on Lepton-Photon Interactions, Ithaca 1993, eds. P. S. Drell, D. L. Rubin, AIP, New York 1994, p. 425, or in A. J. Buras, R. Fleischer, TUM-HEP-275/97, in Heavy Flavours II, ed. by A. J. Buras, M. Lindner, World Scientific 1997, p. 65.

A convenient choice of phases is to have p real, then we can rewrite

$$p = \frac{1}{\sqrt{1+|\eta_m|^2}}$$
$$q = \frac{\eta_m}{\sqrt{1+|\eta_m|^2}}$$

We can use (9.25) to rewrite

$$H_{21} = -\eta_m \frac{\Delta m - \frac{i}{2}\Delta\Gamma}{2}, \quad H_{12} = -\frac{1}{\eta_m}\frac{\Delta m - \frac{i}{2}\Delta\Gamma}{2}$$

and the original Hamiltonian as

$$\mathcal{H} = \begin{pmatrix} m - \frac{i}{2}\Gamma & -\frac{\Delta m - \frac{i}{2}\Delta\Gamma}{2\eta_m} \\ -\eta_m \frac{\Delta m - \frac{i}{2}\Delta\Gamma}{2} & m - \frac{i}{2}\Gamma \end{pmatrix} = \begin{pmatrix} m - \frac{i}{2}\Gamma & -\frac{\Gamma}{2}\frac{1}{\eta_m}(x - iy) \\ -\frac{\Gamma}{2}\eta_m(x - iy) & m - \frac{i}{2}\Gamma \end{pmatrix} \tag{9.27}$$

and the mass and flavour eigenstates are related by the equations

$$\begin{aligned} |B_L\rangle &= p|B^0\rangle + q|\overline{B}^0\rangle \\ |B_H\rangle &= p|B^0\rangle - q|\overline{B}^0\rangle \end{aligned} \tag{9.28}$$

$$\begin{aligned} |B^0\rangle &= \frac{1}{2p}\left(|B_L\rangle + |B_H\rangle\right) \\ |\overline{B}^0\rangle &= \frac{1}{2q}\left(|B_L\rangle - |B_H\rangle\right) \end{aligned}$$

Due to normalization $|p|^2 + |q|^2 = 1$ we may choose

$$\begin{aligned} |B^0\rangle &= \frac{\sqrt{1+|\eta_m|^2}}{2}\left(|B_L\rangle + |B_H\rangle\right) \\ |\overline{B}^0\rangle &= \frac{\eta_m^*\sqrt{1+|\eta_m|^2}}{2|\eta_m|}\left(|B_L\rangle - |B_H\rangle\right) \end{aligned}$$

The choice of the phase for $|B^0\rangle$ is arbitrary, so there may be a common phase factor in the two latter equations.

The eigenstates for a Hamiltonian with $\Gamma_{12} \neq 0$ are **not orthogonal**:

$$\langle B_H|B_L\rangle = \delta_\epsilon := \begin{pmatrix} p^* \\ -q^* \end{pmatrix} \cdot \begin{pmatrix} p \\ q \end{pmatrix} = |p|^2 - |q|^2 = \frac{1-|\eta_m|^2}{1+|\eta_m|^2} = \frac{2\,\mathcal{R}e\,\epsilon_m}{1+|\epsilon_m|^2} \tag{9.29}$$

In contrast to ϵ_m the real number δ_ϵ is an observable. The phase of $\langle B_H|B_L\rangle$ is no observable, though. The choice of the same coefficient p in the definitions of $|B_L\rangle$ and $|B_H\rangle$ is a convenient but arbitrary one. If we define instead

$$|B_H\rangle = e^{i\phi_{HL}}(p|B^0\rangle - q|\overline{B}^0\rangle)$$

which is an equally valid solution for B_H, we must define

$$\delta_\epsilon = \langle B_H|B_L\rangle \frac{\langle B_L|B^0\rangle}{\langle B_H|B^0\rangle}$$

to be a real number. In general, we have

$$\begin{aligned} p &= \langle B^0|B_L\rangle = e^{-i\phi_{HL}}\langle B^0|B_H\rangle \\ q &= \langle \overline{B}^0|B_L\rangle = -e^{-i\phi_{HL}}\langle \overline{B}^0|B_H\rangle \end{aligned} \tag{9.30}$$

Useful exact relations are

$$\frac{|\eta_m|^2}{1+|\eta_m|^2} = |q|^2 = \frac{1-\delta_\epsilon}{2}, \qquad \frac{1}{1+|\eta_m|^2} = |p|^2 = \frac{1+\delta_\epsilon}{2}, \qquad |\eta_m|^2 = \frac{1-\delta_\epsilon}{1+\delta_\epsilon} \tag{9.31}$$

for normalized p, q.
The deviation of $|\eta_m|$ from one (also called d_α) is

$$|\eta_m| - 1 = \sqrt{\frac{1-\delta_\epsilon}{1+\delta_\epsilon}} - 1 \approx -\delta_\epsilon$$

9.2.1 Special Cases

We may illustrate the properties of the eigenstates by three special cases. First we assume $\Gamma_{12} = 0$, i. e.

$$\mathcal{H} = \begin{pmatrix} m - \frac{i}{2}\Gamma & m_{12} \\ m_{12}^* & m - \frac{i}{2}\Gamma \end{pmatrix} \tag{9.32}$$

where the off-diagonal elements are from an Hermitian operator. Then we obtain

$$\begin{aligned} \Delta m &= 2|m_{12}| \\ \Delta\Gamma &= 0 \\ \eta_m &= -\frac{m_{12}^*}{|m_{12}|} \\ |\eta_m| = 1, &\qquad \delta_\epsilon = 0 \end{aligned}$$

As a second case we assume $m_{12} = 0$, i. e.

$$\mathcal{H} = \begin{pmatrix} m - \frac{i}{2}\Gamma & H_{12} \\ -H_{12}^* & m - \frac{i}{2}\Gamma \end{pmatrix} \tag{9.33}$$

Then

$$\begin{aligned} \Delta m &= 0 \\ \Delta\Gamma &= 4|H_{12}| \\ \eta_m &= -\frac{iH_{12}^*}{|H_{12}|} \\ |\eta_m| = 1, &\qquad \delta_\epsilon = 0 \end{aligned}$$

In both cases, η_m is a simple phase factor. Since it includes unphysical phases, only its phase relation to other amplitudes is relevant.

Finally, for real m_{12}, Γ_{12} the term $\frac{\Delta a}{2} = \sqrt{(m_{12} - \frac{i}{2}\Gamma_{12})(m_{12}^* - \frac{i}{2}\Gamma_{12}^*)}$ is replaced by $(m_{12} - \frac{i}{2}\Gamma_{12})$ and in the phase convention with $m_{12} < 0$ we have

$$\begin{aligned}
\Delta m &= 2|m_{12}| = -2m_{12} \\
\Delta\Gamma &= 2|\Gamma_{12}| \\
\eta_m &= +1 \\
\delta_\epsilon &= 0 \\
|B^0\rangle &= \frac{1}{\sqrt{2}}\left(|B_L\rangle + |B_H\rangle\right) \\
|\overline{B}^0\rangle &= \frac{1}{\sqrt{2}}\left(-|B_L\rangle + |B_H\rangle\right)
\end{aligned}$$

The same holds if $\arg(m_{12}) = \arg(\Gamma_{12})$, i. e., if they have the same phase. Hence, $\delta_\epsilon \neq 0$ implies that both $m_{12} \neq 0$ and $\Gamma_{12} \neq 0$, and they have **different** phases.

9.2.2 Time Evolution

For an arbitrary initial state

$$|\psi(0)\rangle = b_H|B_H\rangle + b_L|B_L\rangle = a|B^0\rangle + \bar{a}|\overline{B}^0\rangle$$

where the amplitudes are related via

$$\begin{aligned}
b_{L,H} &= \frac{1}{2}\left(\frac{a}{p} \pm \frac{\bar{a}}{q}\right) = \frac{a \pm \bar{a}/\eta_m}{2p} \\
a &= p\,(b_L + b_H), \quad \bar{a} = q\,(b_L - b_H)
\end{aligned}$$

its time evolution may be described using a scaled time variable

$$T := \Gamma t \tag{9.34}$$

where Γ is the average width of the eigenstates B_H and B_L. These states have a simple exponential development with time. Their masses $m_{H,L} = m \pm x\frac{\Gamma}{2}$ and widths $\Gamma_{H,L} = \Gamma(1 \pm y)$ can be expressed with the dimensionless parameters x and y defined in (9.23).

$$\begin{aligned}
|\psi(t)\rangle &= b_H e^{-i\,(m_H - i\Gamma_H/2)\,t}|B_H\rangle + b_L e^{-i\,(m_L - i\Gamma_L/2)\,t}|B_L\rangle \\
&= e^{-imt - T/2}\left[\frac{e^{i\,(x-iy)\,T/2} + e^{-i\,(x-iy)\,T/2}}{2}(a|B^0\rangle + \bar{a}|\overline{B}^0\rangle)\right. \\
&\quad \left. + \frac{e^{i\,(x-iy)\,T/2} - e^{-i\,(x-iy)\,T/2}}{2}\left(\frac{\bar{a}}{\eta_m}|B^0\rangle + a\eta_m|\overline{B}^0\rangle\right)\right] \qquad (9.35a) \\
&= e^{-imt - T/2}\left[\left(a|B^0\rangle + \bar{a}|\overline{B}^0\rangle\right)\cos(x-iy)\frac{T}{2} + i\left(\frac{\bar{a}}{\eta_m}|B^0\rangle + a\eta_m|\overline{B}^0\rangle\right)\sin(x-iy)\frac{T}{2}\right] \qquad (9.35b)
\end{aligned}$$

Starting with pure B^0 mesons at $T = 0$ corresponds to $\bar{a} = 0$ and

$$|\psi(t)\rangle = ae^{-imt - T/2}\left[\cos(x-iy)\frac{T}{2}|B^0\rangle + i\eta_m \sin(x-iy)\frac{T}{2}|\overline{B}^0\rangle\right] \tag{9.36}$$

Starting with pure $\overline{B}^0$ mesons at $T = 0$ is described by replacing $\eta_m \longleftrightarrow 1/\eta_m$. This case corresponds to $a = 0$ and

$$|\psi(t)\rangle = \bar{a}e^{-imt - T/2}\left[\cos(x-iy)\frac{T}{2}|\overline{B}^0\rangle + \frac{i}{\eta_m}\sin(x-iy)\frac{T}{2}|B^0\rangle\right] \tag{9.37}$$

The numbers of B^0 and $\overline{B}^0$ at time T for N_0 pure B^0 mesons at $T = 0$ are[68]

$$\begin{aligned} N_{B^0}(t) &= N_0|\langle B^0|\psi(t,\bar{a}=0,a=1)\rangle|^2 = N_0\frac{e^{-T}}{2}(\cosh yT + \cos xT) \\ N_{\overline{B}^0}(t) &= N_0|\langle \overline{B}^0|\psi(t,\bar{a}=0,a=1)\rangle|^2 = N_0|\eta_m|^2\,\frac{e^{-T}}{2}(\cosh yT - \cos xT) \end{aligned} \tag{9.38}$$

and the numbers of B^0 and $\overline{B}^0$ at time T for $\overline{N}_0$ pure $\overline{B}^0$ mesons at $T = 0$ are

$$\begin{aligned} \overline{N}_{B^0}(t) &= \overline{N}_0|\langle B^0|\psi(t,\bar{a}=1,a=0)\rangle|^2 = \overline{N}_0\frac{1}{|\eta_m|^2}\,\frac{e^{-T}}{2}(\cosh yT - \cos xT) \\ \overline{N}_{\overline{B}^0}(t) &= \overline{N}_0|\langle \overline{B}^0|\psi(t,\bar{a}=1,a=0)\rangle|^2 = \overline{N}_0\frac{e^{-T}}{2}(\cosh yT + \cos xT) \end{aligned} \tag{9.39}$$

These numbers, however, can not be observed. What is accessible by experiment is only the rate of decays to flavour specific final states X and $\overline{X}$ at a given time T. These decay modes are often called **tagging modes**, since they serve as a "tag" to indicate the flavour of the mother particle at decay time. The rates can be obtained from (9.36) by multiplying with $\langle X|\mathcal{H}$ or $\langle \overline{X}|\mathcal{H}$, respectively, to obtain the amplitudes. They are converted into rates[69]

$$\begin{aligned} \dot{N}_{B^0\to X}(t) &= N_0\int \mathrm{dPS}\,|\langle X|\mathcal{H}|\psi(t,\bar{a}=0)\rangle|^2 = \tfrac{1}{2}N_0 e^{-T}\Gamma_X(\cosh yT + \cos xT) \\ \dot{N}_{\overline{B}^0\to \overline{X}}(t) &= N_0\int \mathrm{dPS}\,|\langle \overline{X}|\mathcal{H}|\psi(t,\bar{a}=0)\rangle|^2 = \tfrac{1}{2}N_0|\eta_m|^2\,e^{-T}\Gamma_X(\cosh yT - \cos xT) \end{aligned} \tag{9.40}$$

where

$$\Gamma_X = \int \mathrm{dPS}\,|\langle X|\mathcal{H}|B^0\rangle|^2 = \int \mathrm{dPS}\,|\langle \overline{X}|\mathcal{H}|\overline{B}^0\rangle|^2$$

is the partial width for a non-oscillating meson. It agrees in value for the two CP conjugate processes if the amplitudes differ only by one phase factor (no CP violation in decay). Integrating over all times the total number of decays for initial B^0 mesons are

$$\begin{aligned} N_{B^0\to X} &= \int_0^\infty \dot{N}_{B^0\to X}(t)\,\mathrm{d}t = N_0\frac{\Gamma_X}{\Gamma}\left[\frac{1}{2(1-y^2)} + \frac{1}{2(1+x^2)}\right] \\ N_{\overline{B}^0\to \overline{X}} &= \int_0^\infty \dot{N}_{\overline{B}^0\to \overline{X}}(t)\,\mathrm{d}t = N_0\frac{\Gamma_X}{\Gamma}\left[\frac{|\eta_m|^2}{2(1-y^2)} - \frac{|\eta_m|^2}{2(1+x^2)}\right] \end{aligned} \tag{9.41}$$

The corresponding numbers for initial $\overline{B}^0$ mesons are obtained with the replacement $\eta_m \to 1/\eta_m$. If we ignore CP violating effects in the oscillation, i. e. for $|\eta_m| = 1$, we can define a meaningful branching fraction as

$$\mathcal{B}(B^0 \to X) = \frac{1}{N_0}\int_0^\infty [\dot{N}_{B^0\to X}(t) + \dot{N}_{\overline{B}^0\to \overline{X}}(t)]\,\mathrm{d}t = \frac{\Gamma_X}{\Gamma(1-y^2)} = \frac{1}{2}\frac{\Gamma_X}{\Gamma_H} + \frac{1}{2}\frac{\Gamma_X}{\Gamma_L}$$

which agrees with $\mathcal{B}(\overline{B}^0 \to \overline{X})$.

---

[68] for example, $\cos u = \frac{1}{2}(e^{iu} + e^{-iu})$, $(\cos u)^* = \frac{1}{2}(e^{iu^*} + e^{-iu^*})$, therefore

$$|\cos u|^2 = \frac{1}{4}\left(e^{i(u+u^*)} + e^{i(u-u^*)} + e^{i(u^*-u)} + e^{-i(u+u^*)}\right) = \tfrac{1}{2}(\cos 2\,\mathcal{R}e\,u + \cosh 2\,\mathcal{I}m\,u)$$

[69] Note that the decay rates denoted $\dot{N}$ include only dacays and are not $\mathrm{d}N(t)/\,\mathrm{d}t$ because the number of one B flavour changes by decay and by the transition to the opposite flavour.

The asymmetry is

$$a(T) := \left.\frac{\dot{N}(X \to X) - \dot{N}(X \to \overline{X})}{\dot{N}(X \to X) + \dot{N}(X \to \overline{X})}\right|_T = \frac{(1 - |\eta_m|^2)\cosh yT + (1 + |\eta_m|^2)\cos xT}{(1 + |\eta_m|^2)\cosh yT + (1 - |\eta_m|^2)\cos xT} \tag{9.42}$$

for a meson produced at $T = 0$ as a flavour eigenstate X, and decaying to a flavour-specific final state as X or $\overline{X}$ at a later time T. Expressed via the small real parameter δ_ϵ instead of $|\eta_m|$ this reads

$$a(T) = \frac{\cos xT + \delta_\epsilon \cosh yT}{\cosh yT + \delta_\epsilon \cos xT} \tag{9.43}$$

For an antimeson produced at $T = 0$ as a flavour eigenstate $\overline{X}$, and decaying to a flavour-specific final state as X or $\overline{X}$ at time T, we obtain a similar expression:

$$\bar{a}(T) := \left.\frac{\dot{N}(\overline{X} \to X) - \dot{N}(\overline{X} \to \overline{X})}{\dot{N}(\overline{X} \to X) + \dot{N}(\overline{X} \to \overline{X})}\right|_T = -\frac{\cos xT - \delta_\epsilon \cosh yT}{\cosh yT - \delta_\epsilon \cos xT} \tag{9.44}$$

The fraction of "mixed" decays at time T (i. e. decays where the flavour has changed from $T = 0$ to the actual decay time T) is

$$\begin{aligned}
\chi(T) &:= \left.\frac{\dot{N}(X \to \overline{X})}{\dot{N}(X \to \overline{X}) + \dot{N}(X \to X)}\right|_T = \frac{1 - a(T)}{2} = \frac{1 - \delta_\epsilon}{2}\frac{\cosh yT - \cos xT}{\cosh yT + \delta_\epsilon \cos xT} \\
\bar{\chi}(T) &:= \left.\frac{\dot{N}(\overline{X} \to X)}{\dot{N}(\overline{X} \to X) + \dot{N}(\overline{X} \to \overline{X})}\right|_T = \frac{1 + \bar{a}(T)}{2} = \frac{1 + \delta_\epsilon}{2}\frac{\cosh yT - \cos xT}{\cosh yT - \delta_\epsilon \cos xT}
\end{aligned} \tag{9.45}$$

The integrated mixing probability depends on the initial flavour. It is

$$\chi = \frac{|\eta_m|^2(x^2 + y^2)}{2 + x^2(1 + |\eta_m|^2) - y^2(1 - |\eta_m|^2)} = \frac{(1 - \delta_\epsilon)(x^2 + y^2)}{2[1 + x^2 + \delta_\epsilon(1 - y^2)]} \tag{9.46a}$$

for an initial X and

$$\bar{\chi} = \frac{(x^2 + y^2)}{2|\eta_m|^2 + x^2(1 + |\eta_m|^2) + y^2(1 - |\eta_m|^2)} = \frac{(1 + \delta_\epsilon)(x^2 + y^2)}{2[1 + x^2 - \delta_\epsilon(1 - y^2)]} \tag{9.46b}$$

for an initial $\overline{X}$ (which is χ with $|\eta_m|$ replaced by $1/|\eta_m|$ or, correspondingly, δ_ϵ by $-\delta_\epsilon$). This exhibits CP violation, since the probabilities $P(X \to \overline{X})$ and $P(\overline{X} \to X)$ are different. It is also T violation, since the transition $X \to \overline{X}$ is the time reversed process $\overline{X} \to X$.

The approximation $|\eta_m| = 1$ corresponding to $\delta_\epsilon = 0$, i. e., the absence of CP violation in the oscillation itself, leads to simpler expressions

$$a(T) = \frac{\cos xT}{\cosh yT} = -\bar{a}(T) \tag{9.47}$$

where x is clearly seen as the oscillation parameter, and y as the damping parameter, and

$$\chi(T) = \bar{\chi}(T) = \frac{1}{2} - \frac{\cos xT}{2\cosh yT} \tag{9.48}$$

with the integrated mixing probability

$$\chi = \bar{\chi} = \frac{x^2 + y^2}{2(1 + x^2)} \tag{9.49}$$

9.2.3 Mechanical Analogon

Equation (9.19) characterizes also the mechanical system of two coupled pendula of the same length[70]: Without coupling, they are both described by an oscillation frequency m and a damping constant Γ. They correspond to the meson X^0 and its antiparticle $\overline{X}^0$.

If they are coupled by a spring whose elasticity is proportional to a **non-negative real** number m_{12}, and a **non-negative real** damping constant Γ_{12}, the solutions correspond to a "long-lived" (= low damping), "light" (= low frequency) eigenstate where the pendula oscillate strictly in phase, and a "short-lived" (= high damping), "heavy" (= high frequency) eigenstate where one pendulum oscillates as a mirror image of the other, i. e. with phase difference 180°. The differences in frequency and damping are $\Delta m = 2m_{12}$ and $\Delta\Gamma = 2\Gamma_{12}$, respectively.

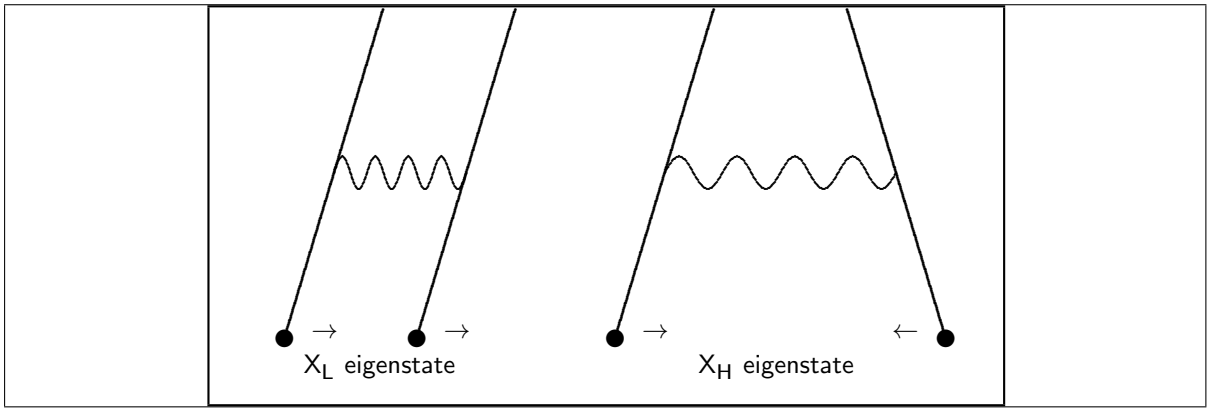

When one pendulum is excited, it will slowly transfer its energy to the other and back. This beating corresponds to the oscillation between a meson X^0 and its antiparticle $\overline{X}^0$. The beat frequency is $2\pi f_{12} = \Delta m$.

For the mechanical system, the frequencies m, Δm, and the damping constants Γ, $\Delta\Gamma$ can all be measured. For mesons, the oscillating part e^{-imt} in (9.17) is an unobservable phase factor (the mass can, of course, still be measured from kinematics), but in meson antimeson oscillation a mass difference can actually be observed as a frequency! The $B^0\overline{B}^0$ oscillation beat has $2\pi f \approx 0.5/\,\mathrm{ps}$ or a frequency of $f \approx 80\,\mathrm{GHz}$.

Due to the restriction of m_{12} and Γ_{12} to non-negative real values, this system has always $\Delta m \Delta\Gamma \geq 0$ (in contrast to the oscillating mesons), and can also not simulate CP violation since there are no non-trivial phases.

9.2.4 Coherence

The time evolution derived above assumes that eigenstates with different energy (or mass) can interfere. This is not a trivial assumption, and has to be checked. In classical physics, if a certain energy E is given to a B meson (as in fragmentation or $\Upsilon(4S)$ decay) its momentum and velocity depend on the mass, and will therefore slightly vary for B_L and B_H. In quantum mechanics, this variation can only be detected, if the variation of momentum p and location x according to the different velocities complies with the uncertainty limit $\Delta p \Delta x \gtrsim 1$. If this condition is not met, i. e. if $\Delta p \Delta x \lesssim 1$, we have to add both amplitudes coherently, as we did in the calculations shown above. Since the two are related via

$$\Delta x = \frac{\Delta p}{E} t$$

[70] A detailed discussion is found in K. R. Schubert, J. Stiewe, J. Phys. **G39**, 033101 (2012)

for a given lifetime t, the coherence condition for interfering mass eigenstates can be written as

$$\frac{(\Delta p)^2}{E} t \leq 1$$

The simple kinematical calculation

$$\Delta p = p_L - p_H = p_L - p_L \sqrt{1 - \frac{2m_L \Delta m + \Delta m^2}{p_L^2}} \approx \frac{m_B \Delta m}{p_B}$$

yields as coherence condition

$$t \leq \frac{E}{(\Delta p)^2} = \frac{E p^2}{m^2 (\Delta m)^2} \tag{9.50}$$

for the time in the laboratory, or for proper time

$$t' = \frac{t}{\gamma} \leq \frac{p^2}{m(\Delta m)^2}$$

which is for B mesons produced in $\Upsilon(4\mathrm{S}) \to B\overline{B}$ decay $t \lesssim 0.1\,\mathrm{s}$. This is so large compared to the lifetime of a B meson ($\sim 1.5\,\mathrm{ps}$) that it will always be fulfilled.

Similar calculations can be performed for the other oscillating mesons.

9.2.5 Standard Model Predictions

The Hamiltonian (9.19) can be obtained using

$$\mathcal{H} = \mathcal{H}_0 + \mathcal{H}_w$$

where $\mathcal{H}_0$ is the strong and electromagnetic Hamiltonian

$$\mathcal{H}_0 = \begin{pmatrix} E_0 & 0 \\ 0 & E_0 \end{pmatrix}$$

which has the stable flavour eigenstates B^0 and $\overline{B}^0$, and $\mathcal{H}_w$ is the weak interaction perturbation. The Wigner-Weisskopf approximation for small $\mathcal{H}_w$ leads to[71]

$$H_{jk} = H_{0\,jk} + \langle j|\mathcal{H}_w|k\rangle + \sum_X \mathcal{P} \int \mathrm{dPS}\, \langle j|\mathcal{H}_w|X\rangle\langle X|\mathcal{H}_w|k\rangle \left[\frac{1}{E_0 - E_X} - i\pi\delta(E_0 - E_X)\right] \tag{9.51}$$

where the sum runs over all multiparticle states X which are eigenstates of $\mathcal{H}_0$, and $\mathcal{P}$ denotes the principal value of the integral. The mass (hermitian) and decay (antihermitian) parts defined by (9.18) are

$$m_{jk} = \tfrac{1}{2}(H_{jk} + H^*_{kj}) = E_0\,\delta_{jk} + \langle j|\mathcal{H}_w|k\rangle + \sum_X \mathcal{P} \int \mathrm{dPS}\, \frac{\langle j|\mathcal{H}_w|X\rangle\langle X|\mathcal{H}_w|k\rangle}{E_0 - E_X}$$

and

$$\Gamma_{jk} = i(H_{jk} - H^*_{kj}) = 2\pi \sum_X \int \mathrm{dPS}\, \langle j|\mathcal{H}_w|X\rangle\langle X|\mathcal{H}_w|k\rangle\, \delta(E_0 - E_X)$$

[71] V. F. Weisskopf, E. P. Wigner, Z. Phys. **63**, 54 (1930)and Z. Phys. **65**, 18 (1930). A detailed discussion is in the textbook by O. Nachtmann.

The off-diagonal elements $H_{12,21}$ have non-zero contributions in the sum from states X which can be reached in weak decays of both B^0 and $\overline{B}^0$. In contrast to the neutral kaon system, for $B^0/\overline{B}^0$ these are only a small fraction of all B decays, and they contribute with alternating signs. Therefore $H_{12,21}$ are dominated by the leading term $\langle B^0|\mathcal{H}_w|\overline{B}^0\rangle$ which corresponds to the box diagrams

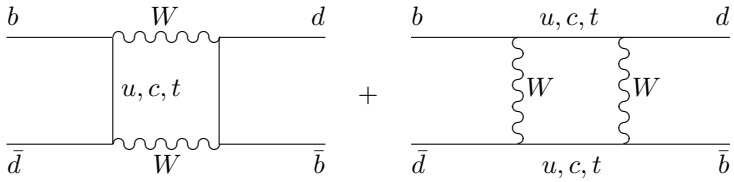

Their evaluation using the Feynman rules is usually simplified in two ways. The inner fermions in the loop may be u-, c- or t-quarks, leading to a total of 9 terms to be summed up (Π = propagator):

$$\begin{aligned}
\mathcal{M} \sim\ & V_{tb}V_{td}^*\Pi_t \cdot V_{tb}V_{td}^*\Pi_t && tt\\
&+ V_{cb}V_{cd}^*\Pi_c \cdot V_{tb}V_{td}^*\Pi_t && ct\\
&+ V_{ub}V_{ud}^*\Pi_u \cdot V_{tb}V_{td}^*\Pi_t && ut\\
&+ V_{tb}V_{td}^*\Pi_t \cdot V_{cb}V_{cd}^*\Pi_c && tc\\
&+ V_{tb}V_{td}^*\Pi_t \cdot V_{ub}V_{ud}^*\Pi_u && tu\\
&+ V_{cb}V_{cd}^*\Pi_c \cdot V_{cb}V_{cd}^*\Pi_c && cc\\
&+ V_{ub}V_{ud}^*\Pi_c \cdot V_{ub}V_{ud}^*\Pi_u && uu\\
&+ V_{cb}V_{cd}^*\Pi_c \cdot V_{ub}V_{ud}^*\Pi_u && cu\\
&+ V_{ub}V_{ud}^*\Pi_u \cdot V_{cb}V_{cd}^*\Pi_c && uc
\end{aligned}$$

Setting $m_c = m_u = 0$ one can play a trick similar to the GIM mechanism, since this yields $\Pi_c = \Pi_u = \Pi_0$ and

$$\begin{aligned}
\mathcal{M} \sim\ & V_{tb}V_{td}^*\Pi_t \cdot V_{tb}V_{td}^*\Pi_t\\
&+ (V_{cb}V_{cd}^* + V_{ub}V_{ud}^*)\Pi_0 \cdot V_{tb}V_{td}^*\Pi_t\\
&+ V_{tb}V_{td}^*\Pi_t \cdot (V_{cb}V_{cd}^* + V_{ub}V_{ud}^*)\Pi_0\\
&+ (V_{cb}V_{cd}^* + V_{ub}V_{ud}^*)\Pi_0 \cdot (V_{cb}V_{cd}^* + V_{ub}V_{ud}^*)\Pi_0
\end{aligned}$$

Using further unitarity (9.7k) this simplifies to

$$\begin{aligned}
\mathcal{M} &\sim (V_{td}V_{tb}^*)^2[\Pi_t\Pi_t - \Pi_0\Pi_t - \Pi_t\Pi_0 + \Pi_0\Pi_0]\\
&= (V_{td}V_{tb}^*)^2[\Pi_t - \Pi_0][\Pi_t - \Pi_0]
\end{aligned}$$

i. e. the sum corresponds to a single matrix element with inner fermions "$t - u$" where u represents a massless quark.

The second simplification is the vacuum insertion which is corrected for by the *bag parameter* B_B:

$$\langle B^0|J_\mu J^\mu|\overline{B}^0\rangle = \sum_X \langle B^0|J_\mu|X\rangle\,\langle X|J^\mu|\overline{B}^0\rangle = B_B \cdot \langle B^0|J_\mu|0\rangle\,\langle 0|J^\mu|\overline{B}^0\rangle = B_B f_B^2 p_\mu p^\mu \tag{9.52}$$

where f_B is the B decay constant. A big uncertainty is the product $f_B^2\,B_B$, where the most reliable calculations now come from lattice gauge theory with values around[72] $f_B\sqrt{B_B} \approx (227 \pm 19)\,\mathrm{MeV}$.

With these simplifications, the box diagrams give approximately

$$H_{12} = \langle B^0|\mathcal{H}|\overline{B}^0\rangle \approx m_{12} = -\frac{G_F^2}{12\pi^2}\, e^{-i\phi_{\mathrm{CP}B}} V_{tb}^2 V_{td}^{*\,2} m_W^2\, m_B\, [f_B^2\, B_B] \cdot [S(m_t^2/m_W^2) \cdot \eta_{\mathrm{QCD}}] \tag{9.53}$$

The CP phase is introduced during the evaluation of the hadronic part of the matrix element. The Inami–Lim function

$$S(x) = x\left[\frac{1}{4} + \frac{9}{4(1-x)} - \frac{3}{2(1-x)^2} - \frac{3x^2\ln x}{2(1-x)^3}\right] \tag{9.54}$$

from the loop[73] is to lowest order a factor m_t^2/m_W^2. An evaluation of the product $S(m_t^2/m_W^2)$ and η_{QCD}

[72] Average from `http://latticeaverages.org/` end of 2011.

[73] T. Inami, C. S. Lim, Progr. Theor. Phys. **65**, 297 (1981), and erratum Progr. Theor. Phys. **65**, 1772 (1981).

within a consistent renormalization scheme yields $S \approx 2.3$, $\eta_{\rm QCD} \approx 0.55$. The highest order correction[74] to $\eta_{\rm QCD}$ already included is $\sim 2\%$, the precision is estimated to be better than 0.5%.

In this approximation, we have for the B system

$$\Delta m = 2|m_{12}|$$

which can be used to determine $|V_{td}|$ (since $V_{tb} = 1$) from experimental results on $B^0/\overline{B}^0$ mixing. The eigenstates are determined by

$$\eta_m = -\frac{m_{12}^*}{|m_{12}|} = e^{i\phi_{{\rm CP}B}} \frac{V_{tb}^{*2} V_{td}^2}{|V_{tb}^2 V_{td}^2|} = e^{i(\phi_{{\rm CP}B} - 2\tilde{\beta})} \tag{9.55}$$

with $-\tilde{\beta} = \arg V_{tb}^* V_{td}$. This phase depends on the CKM parametrization and is—like the CP phase—not an observable: if we use the more general parametrization (9.10) we have instead $\arg V_{tb}^* V_{td} = -\tilde{\beta} - \zeta_3$ with an arbitrary ζ_3 (the arbitrariness cancels only in physical observables, which include decay amplitudes with further CKM elements and a CP phase). The corresponding

$$\epsilon_m = -i \frac{\sin \arg \eta_m}{1 + \cos \arg \eta_m} = -i \tan \frac{\arg \eta_m}{2} \tag{9.56}$$

is purely imaginary, i. e. $\mathcal{R}e\, \epsilon_m = 0$ and therefore $\delta_\epsilon = 0$. In the standard parametrization and for $\phi_{{\rm CP}B} = 0$, it is $\epsilon_m = i \tan \tilde{\beta}$.

Within the same framework, for the $B_s/\overline{B}_s$ system

$$\eta_{ms} = e^{i(\phi_{{\rm CP}B_s} + 2\tilde{\phi}_2)} \tag{9.57}$$

It must be emphasized, however, that there exist common final states for all four meson pairs, and Γ_{12} never vanishes completely, leaving always a small δ_ϵ, and also a small $\Delta\Gamma$. Within the Standard Model Γ_{12} can be approximated by the absorptive part of the box diagram, corresponding to a quark representation of the final states. This is a poor approximation to light hadronic final states which are dominating in the $K/\overline{K}$ system, and may still change the prediction for $B/\overline{B}$ considerably. The box calculation yields

$$\Gamma_{12} \approx -m_{12} \cdot \frac{3\pi}{2S(m_t^2/m_W^2)} \frac{m_b^2}{m_W^2} \left[1 + \frac{8}{3} \frac{m_c^2}{m_b^2} \frac{V_{cb} V_{cd}^*}{V_{tb} V_{td}^*} + \mathcal{O}\left(\frac{m_c^4}{m_b^4}\right)\right] \tag{9.58}$$

and $\Delta\Gamma$ and Δm have **opposite signs**[75]. The ratio can be estimated using (9.22) to be

$$\frac{\Delta\Gamma}{\Delta m} = \frac{2y}{x} \approx -\frac{3\pi}{2} \frac{m_b^2}{m_t^2} \sim -\frac{1}{250} \tag{9.59}$$

This ratio applies to both the B^0 and B_s systems.

[74] Part of the QCD corrections is absorbed in B_B, therefore $\eta_{\rm QCD}(\alpha_{\rm s} = 0) \neq 1$. The correction to the product $\eta_{\rm QCD} \cdot B_B \cdot S(m_t^2/m_W^2)$ is $\sim 18\%$.

[75] Note that some authors redefine $\Delta\Gamma \mapsto -\Delta\Gamma$ to obtain a positive sign in the Standard Model!

9.2.6 Predictions for x_s and y_s

Since the lifetimes of B^0 and B_s agree within present precision, a first approximation using (9.53) is

$$\frac{x_s}{x_d} \sim \frac{|V_{ts}|^2}{|V_{td}|^2}$$

which gives an estimate of the expected x_s range between 3 and 100. It suffers from the poor knowledge on V_{td}, which has to be obtained from the measured x_d. With the top mass known and lattice calculations giving more reliable numbers for f_B, f_{B_s}, B_B and B_{B_s}, theoretical predictions for x_s become more precise. The Standard Model allows numbers between 11 and 40.

The B_s meson eigenstates are expected to have also different widths at an observable level. $\Delta\Gamma$ is caused by final states to which both B and $\overline{B}$ can decay. For the B_s these include with the Cabibbo-allowed final states from the $b \to c\bar{c}s$ decay a substantial fraction, while their number is much smaller in B^0 decays. A value of $2y_s = \Delta\Gamma/\Gamma \approx 0.18 \left(\frac{f_{B_s}}{200\,\mathrm{MeV}}\right)^2$ is predicted from quark level QCD calculations, a similar number $2y_s \approx 0.15$ is obtained using exclusive decay channels. In the naive quark model a larger value around 0.20 is expected, and a QCD evaluation gives $2y_s = 0.16 \pm {}^{0.11}_{0.09}$. It can be related to bag parameters evaluated on the lattice which predicts lower values $2y_s \approx (0.022 \ldots 0.070) \left(\frac{f_{B_s}}{210\,\mathrm{MeV}}\right)^2$.

The refined ratio (9.59) is

$$\frac{\Delta\Gamma}{\Delta m} = \frac{2y_s}{x_s} \approx -\frac{\pi}{2}\frac{m_b^2}{m_t^2}\frac{3 - 8m_c^2/m_b^2}{0.54 \pm 0.02} \approx -\frac{1}{(200 \ldots 250)} \tag{9.60}$$

and corresponds to a lowest order estimate neglecting QCD corrections. The range given reflects only a variation of quark masses.

9.2.7 Behaviour of the Four Neutral Meson Antimeson Systems

All four meson pairs $K^0/\overline{K}^0$, $D^0/\overline{D}^0$, $B^0/\overline{B}^0$, and $B_s/\overline{B}_s$ show a different oscillation behaviour, since they have all different relations of Γ, $\Delta\Gamma$, and Δm. The same symbols will be used for all four systems. Only when two specific systems shall be compared, their parameters will be distinguished by the subscripts K, D, d, and s, respectively. The dimensionless parameters x and y give the ratios of time constants involved: $\tau = 1/\Gamma$ is the harmonic average of the lifetimes, $t_{\mathrm{osc}} = 2\pi/\Delta m = 2\pi\tau/x$ is the period of the oscillation, and $t_{\mathrm{rel}} = 2/\Delta\Gamma = \tau/y$ is the lifetime of the oscillation amplitude, i. e. the damping time constant of a relaxation process. Numerical values are summarized in table 9.1.

Table 9.1 Parameters of the four neutral oscillating meson pairs.

	$K^0/\overline{K}^0$	$D^0/\overline{D}^0$	$B^0/\overline{B}^0$	$B_s/\overline{B}_s$
τ [ps]	89.5 ± 0.1; 51200 ± 200	$0.4101 \pm .0015$	1.520 ± 0.004	1.510 ± 0.006
Γ [s^{-1}]	$5.59 \cdot 10^9$	$2.4 \cdot 10^{12}$	$6.56 \cdot 10^{11}$	$6.62 \cdot 10^{11}$
$y = \frac{\Delta\Gamma}{2\Gamma}$	-0.9965	$0.0069 \pm {}^{0.0006}_{0.0007}$	$\lvert y\rvert \lesssim 0.01^*$	-0.067 ± 0.004
Δm [s^{-1}]	$(5.292 \pm 0.009) \cdot 10^9$	$(7.8 \pm 3.4) \cdot 10^9$	$(5.10 \pm 0.03) \cdot 10^{11}$	$(17.76 \pm 0.02) \cdot 10^{12}$
Δm [eV]	$3.48 \cdot 10^{-6}$	$5.1 \cdot 10^{-6}$	$3.3 \cdot 10^{-4}$	$1.2 \cdot 10^{-2}$
$x = \frac{\Delta m}{\Gamma}$	0.946	0.0032 ± 0.0014	0.775	26.8
δ_ϵ	$(3.32 \pm 0.06) \cdot 10^{-3}$	0.12 ± 0.09	$(-0.8 \pm 0.8) \cdot 10^{-3}$	$(-3 \pm 14) \cdot 10^{-4}$
$\lvert\eta_m\rvert^2$	0.9934	$0.89 \pm {}^{0.08}_{0.07}$	$1 \ldots 1.002^*$	≈ 1.001

* Standard Model expectation

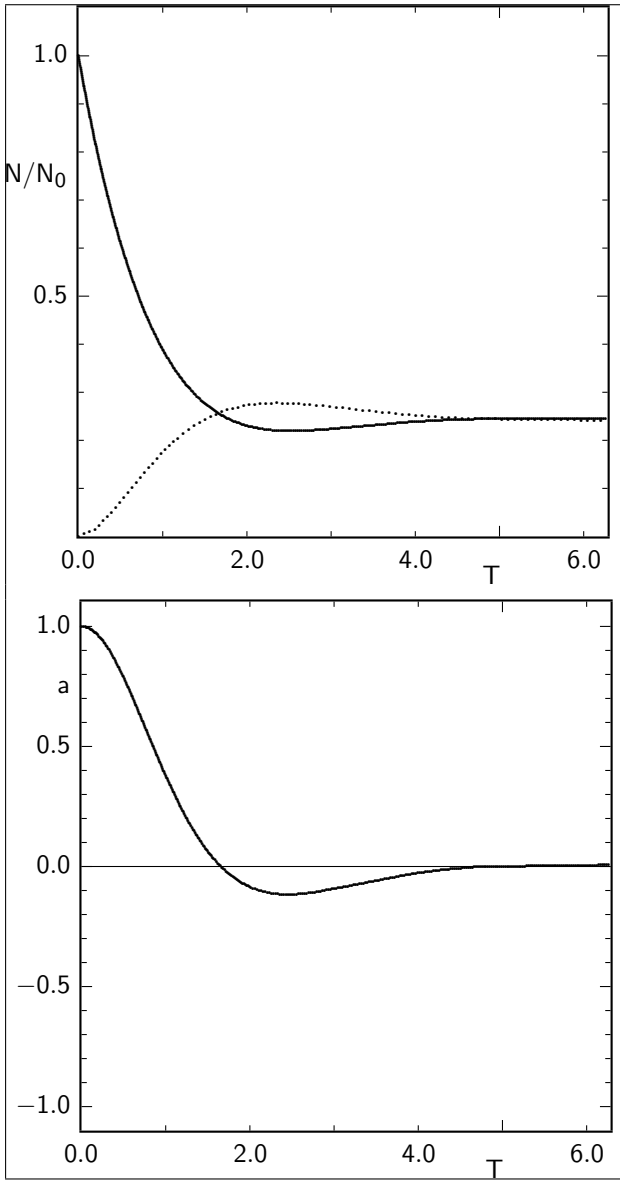

Fig. 9.3 $K^0/\overline{K}^0$ mixing is determined by the parameters $x = 0.945$, $y = 0.997$, and $|\eta_m|^2 = 0.994$ (see table 9.1). $T = t/\bar{\tau}$ is the lifetime in units of $\bar{\tau} \approx 2\tau_S$, the inverse of the average width of K_L^0 and K_S^0. The upper diagram shows the number of K^0 (solid) and $\overline{K}^0$ (dotted) as a function of T for a sample starting with 100% K^0 mesons. The lower diagram shows the asymmetry $a = (N_K - N_{\overline{K}})/(N_K + N_{\overline{K}})$. The relaxation process soon dominates, leaving only K_L^0 after not much more than one oscillation.

While the parameters of the $K^0/\overline{K}^0$ system are well measured, theoretical assumptions enter into the D and B meson columns.

Figures 9.3–9.6show the number of mesons and antimesons as a function of the scaling lifetime variable $T = t/\tau$ and the asymmetry $a(T)$.

9.2.8 $K^0\overline{K}^0$ Oscillation

The kaon has both $x \approx 1$ and $y \approx -1$, i. e. the long-living state K_L^0 is the heavier mass eigenstate K_H. With these parameters one half of a sample of kaons of either flavour decays rapidly, mainly into two pions with CP $= +1$, and the other half transforms to a sample of the long-living K_L^0 states, which decay (aside from the small CP violation effects) to CP $= -1$ eigenstates and to flavour-specific states. The ratio of lifetimes of the two states (table 9.1) is approximately 580. The time evolution of an initially pure K^0 flavour eigenstate is shown in figure 9.3. The upper diagram shows the number of remaining K^0 and $\overline{K}^0$ after a scaled time $T = \Gamma t$, where $\Gamma \approx \Gamma_S/2 = 1/(2\tau_S)$ is the average width of the short-

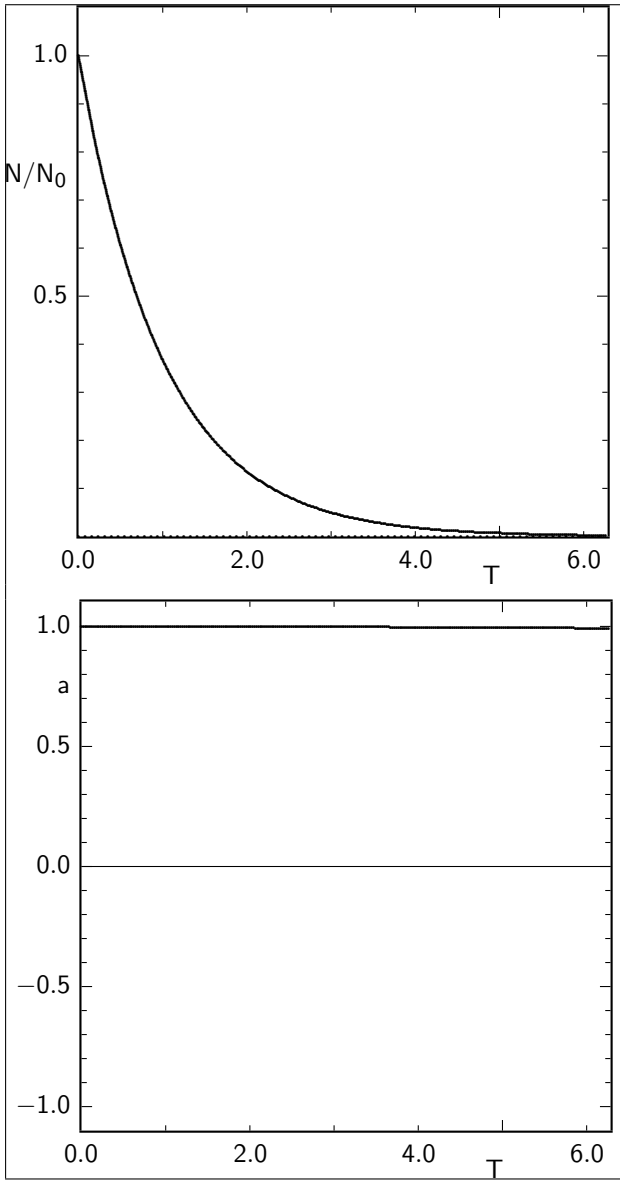

Fig. 9.4 $D^0/\overline{D}^0$ oscillations have not yet been observed, and are hardly visible even with $x = 0.02$ which is twice the observed value and was used for these plots together with $y = 0$ and $|\eta_m| = 1$.

and long-living state. The decay rate into flavour-specific final states is proportional to these numbers, while the dominant decays to CP eigenstates follow different evolution functions due to CP violation, and will be discussed below.

9.2.9 $D^0\overline{D}^0$ Oscillation

The D^0 meson decays mainly to flavour specific states with well defined strangeness, with only a few decays to CP $= +1$ eigenstates, as $\pi\pi$, $K\overline{K}$, $K^0_L\pi^0$ and CP $= -1$ states, as $K^0_S\pi^0$, $K^0_S\phi$ or $K^0_S\omega$. This leads to almost equal lifetimes for the two eigenstates, i. e. $y \approx 0$. The corresponding box graph has a b quark as the heaviest particle in the loop, which is accompanied by the small CKM elements V_{cb} and V_{ub}, or an s quark with the larger CKM elements V_{cs} and V_{us}. The mass difference induced that way by the Standard Model is very small, $x \approx 0.002$. Therefore, almost no asymmetry is visible in figure 9.4, although the number $x = 0.02$ used for the plot is at the upper range of possible values.

The three possible quarks in the loop lead to the following factors in the contribution to Δm.

$d: |V_{cd}V_{ud}| \approx 0.21 \quad m_d \approx 0.005\,\text{GeV} \quad d/s: \ 0.03$
$s: |V_{cs}V_{us}| \approx 0.21 \quad m_s \approx 0.15\,\text{GeV} \quad s/s: \ 1$
$b: |V_{cb}V_{ub}| \approx 0.00016 \quad m_b \approx 4.5\,\text{GeV} \quad b/s: \ 0.02e^{-i\gamma}$

The dominant contribution to the $D^0\overline{D}^0$ oscillation is the box diagram with an s quark in the loop.
The Taylor expansion of the asymmetry (9.43) in T and δ_ϵ is

$$a(T) = \left.\frac{\dot{N}(D\to D) - \dot{N}(D\to \overline{D})}{\dot{N}(D\to D) + \dot{N}(D\to \overline{D})}\right|_T = 1 - \tfrac{1}{2}(x^2+y^2)(1-2\delta_\epsilon)T^2 \tag{9.61}$$

and

$$\bar{a}(T) = \left.\frac{\dot{N}(\overline{D}\to D) - \dot{N}(\overline{D}\to \overline{D})}{\dot{N}(\overline{D}\to D) + \dot{N}(\overline{D}\to \overline{D})}\right|_T = -1 + \tfrac{1}{2}(x^2+y^2)(1+2\delta_\epsilon)T^2$$

The mixed fraction is

$$\chi(T) = \frac{1}{4}(x^2+y^2)(1-2\delta_\epsilon)T^2$$
$$\bar{\chi}(T) = \frac{1}{4}(x^2+y^2)(1+2\delta_\epsilon)T^2$$

as a function of lifetime and is in total given by (9.46) as

$$\chi = \frac{N(D^0\to \overline{D}^0\to \overline{X})}{N(D^0\to X) + N(D^0\to \overline{D}^0\to \overline{X})} = \frac{(1-\delta_\epsilon)(x^2+y^2)}{2[1+x^2+\delta_\epsilon(1-y^2)]}$$
$$\bar{\chi} = \frac{N(\overline{D}^0\to D^0\to X)}{N(\overline{D}^0\to \overline{X}) + N(\overline{D}^0\to D^0\to X)} = \frac{(1+\delta_\epsilon)(x^2+y^2)}{2[1+x^2-\delta_\epsilon(1-y^2)]}$$

A value $x = 0.002$ corresponds to a total mixed fraction of initially pure D^0 states of $\chi \approx 2\cdot 10^{-6}$.
For channels that can also originate from $\overline{D}^0$ decays with a small fraction $r' \ll 1$ (e. g. doubly Cabibbo suppressed decays) we can start from (9.36) to order $\{x,y\}^2$ (and $a=1$)

$$|\psi(t)\rangle = e^{-imt-T/2}\left[\left(1-(x-iy)^2\frac{T^2}{8}\right)|D^0\rangle + i\eta_m(x-iy)\frac{T}{2}|\overline{D}^0\rangle\right] \tag{9.62}$$

and using $A = \langle X|\mathcal{H}|D^0\rangle$ and $\overline{A} = \langle X|\mathcal{H}|\overline{D}^0\rangle = r'e^{i\delta}A$, i. e., if there is a phase difference δ between the Amplitudes $A(D\to X) = A(\overline{D}\to \overline{X})$ and $\overline{A}(D\to \overline{X}) = \overline{A}(\overline{D}\to X)$, we obtain to order $\{x,y,r'\}^2$

$$\langle X|\mathcal{H}|\psi(t)\rangle = e^{-imt-T/2}\left[1-(x-iy)^2\frac{T^2}{8} + i\eta_m(x-iy)\frac{T}{2}r'e^{i\delta} + \mathcal{O}(\{x,y\}^3)\right]A$$
$$\langle \overline{X}|\mathcal{H}|\psi(t)\rangle = e^{-imt-T/2}\left[r'e^{i\delta} + i\eta_m(x-iy)\frac{T}{2} + \mathcal{O}(\{x,y,r'\}^3)\right]A$$
$$|\langle X|\mathcal{H}|\psi(t)\rangle|^2 = e^{-T}|A|^2\left[1-(x^2-y^2)\frac{T^2}{4} + 2\,\mathcal{R}e\left(\eta_m e^{i\delta}(ix+y)\right)\frac{T}{2}r' + \mathcal{O}(\{x,y,r'\}^3)\right]$$
$$|\langle \overline{X}|\mathcal{H}|\psi(t)\rangle|^2 = e^{-T}|A|^2\left[r'^2 + 2\,\mathcal{R}e\left(\eta_m e^{i\delta}(ix+y)\right)\frac{T}{2}r' + |\eta_m|^2(x^2+y^2)\frac{T^2}{4} + \mathcal{O}(\{x,y\}^3)\right]$$

If $\eta_m = 1$ this simplifies to

$$|\langle X|\mathcal{H}|\psi(t)\rangle|^2 = e^{-T}|A|^2\left[1-(x^2-y^2)\frac{T^2}{4} + (-x\sin\delta + y\cos\delta)\,r'T\right]$$
$$|\langle \overline{X}|\mathcal{H}|\psi(t)\rangle|^2 = e^{-T}|A|^2\left[r'^2 + (-x\sin\delta + y\cos\delta)\,r'T + (x^2+y^2)\frac{T^2}{4}\right]$$

and the observed asymmetry is

$$a(T) = \frac{|\langle X|\mathcal{H}|\psi(t)\rangle|^2 - |\langle \overline{X}|\mathcal{H}|\psi(t)\rangle|^2}{|\langle X|\mathcal{H}|\psi(t)\rangle|^2 + |\langle \overline{X}|\mathcal{H}|\psi(t)\rangle|^2} = \frac{1 - 2x^2\frac{T^2}{4} - r'^2}{1 + 2y^2\frac{T^2}{4} + r'^2 + 2(-x\sin\delta + y\cos\delta)r'T}$$
$$\approx 1 - 2r'^2 - 2r'(y\cos\delta - x\sin\delta)T - \frac{x^2+y^2}{2}T^2 \tag{9.63}$$

where terms of order $\{x, y, r'\}^3$, i. e., products of three or more small numbers have been dropped.

Often effective parameters

$$x' := x\cos\delta + y\sin\delta$$
$$y' := -x\sin\delta + y\cos\delta$$
$$x'^2 + y'^2 = x^2 + y^2$$

are used, replacing x, y in (9.63) with x', y', and

$$a(T) \approx 1 - 2r'^2 - 2r'y'T - \frac{x'^2+y'^2}{2}T^2$$

For $\delta = 0$, we have $y' = y$ and $x' = x$.

The fraction of apparently mixed decays is

$$\chi(T) = r'^2 + r'y'T + \frac{x^2+y^2}{4}T^2 \tag{9.64}$$

Neglecting CP violation, $y = y_{\mathrm{CP}}$ can be determined from the lifetime difference of eigenstates with different CP eigenvalue and flavour-specific final states:

$$y_{\mathrm{CP}} = \frac{\Gamma - \Gamma_L}{\Gamma} = 1 - \frac{\tau}{\tau_L} \tag{9.65}$$

9.2.10 The Neutral B Mesons

The parameters of the $B^0/\overline{B}^0$ system have been introduced above. A good approximation is $y = 0$ and $\delta_\epsilon = 0$, which leads for N_0 pure B^0 at $T = 0$ to

$$N_{B^0}(T) = \tfrac{1}{2}N_0 e^{-T}(1 + \cos xT)$$
$$N_{\overline{B}^0}(T) = \tfrac{1}{2}N_0 e^{-T}(1 - \cos xT) \tag{9.66}$$

as shown in figure 9.5. The decay rate for flavour-specific final states (which are the majority of B^0 decays) follows the same time evolution. The asymmetry function is simply

$$a(T) = \cos xT \tag{9.67}$$

This asymmetry can be observed using a flavour-tagging decay, like $B^0 \to D^- l^+ \nu$. The rate of mesons decaying at time T into the channel X are given by (9.40) where $y = 0$ makes $\cosh yT = 1$ leading to the same asymmetry function $a(T) = \cos xT$. Integrating over all times, the observed numbers are

$$N_{B^0\to X} = \int \dot{N}_{B^0\to X}(T)\,\mathrm{d}t = \tfrac{1}{2}N_0\frac{\Gamma_X}{\Gamma}\frac{2+x^2}{1+x^2}$$
$$N_{\overline{B}^0\to \overline{X}} = \int \dot{N}_{\overline{B}^0\to \overline{X}}(T)\,\mathrm{d}t = \tfrac{1}{2}N_0\frac{\Gamma_X}{\Gamma}\frac{x^2}{1+x^2}$$

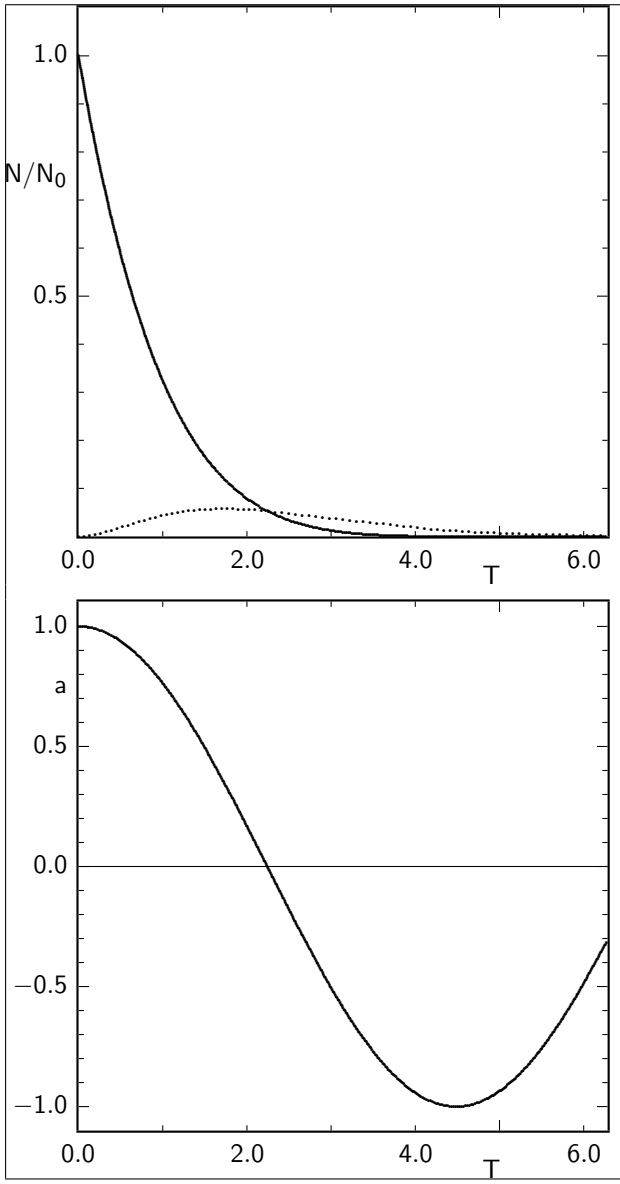

Fig. 9.5 $B^0/\overline{B}^0$ evolution is dominated by the oscillating part, with the parameters $x = 0.70$, $y = 0$, and $|\eta_m| = 1$. The ratio of the areas under the dotted and solid curve in the upper plot is the mixing probability χ. The zero transition in the asymmetry, which marks the crossover point in the upper plot, is at $T = \frac{\pi}{2x}$.

Their asymmetry becomes

$$a_{\text{int}} = \frac{N_{\overline{B}^0 \to \overline{X}} - N_{B^0 \to X}}{N_{\overline{B}^0 \to \overline{X}} + N_{B^0 \to X}} = \frac{1}{1+x^2}$$

and the mixing probability is

$$\chi = \frac{N_{B^0 \to \overline{B}^0 \to \overline{X}}}{N_{B^0 \to X} + N_{\overline{B}^0 \to \overline{X}}} = \frac{x^2}{2(1+x^2)} \tag{9.68}$$

It was this net effect which gave the first proof for a sizeable mixing parameter[76] $x \approx 0.7$ in the B^0 meson system in 1987. The time-dependent particle antiparticle oscillations of the neutral B meson have been first seen six years later by experiments at LEP (ALEPH experiment, 1993). With $x \approx 0.7$, about one period is visible before most of the mesons are decayed.

[76] ARGUS Collab., Phys. Lett. **B192**, 245 (1987).

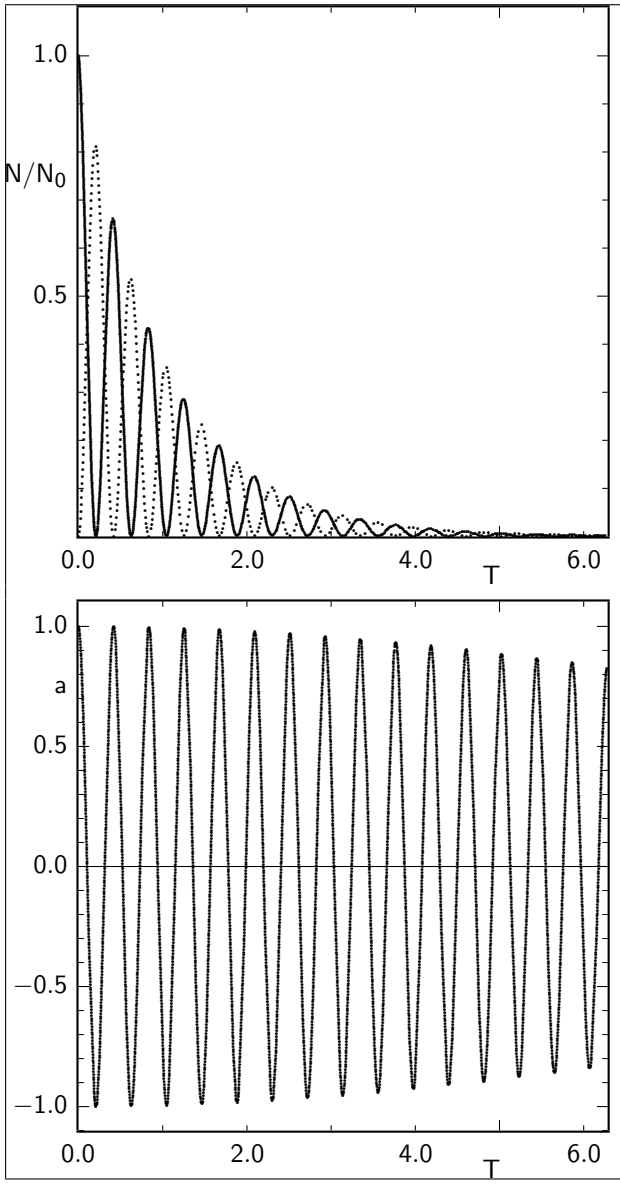

Fig. 9.6 $B_s/\overline{B}_s$ is expected to be the most rapidly oscillating system, with a longer relaxation time. This plot assumes $x_s = 15$, $y_s = 0.10$, and $|\eta_m| = 1$.

The B_s meson is a very interesting case, since there is a small y and a very large x. Figure 9.6 is plotted with $x_s = 15$, which is lower than the experimental value $x_s \approx 25$. The time-integrated mixing probability is for $|\eta_m| = 1$

$$\chi = \frac{x^2 + y^2}{2(1 + x^2)}$$

For $x_s \gg 1$, this approaches its maximum value of 0.5, where a measurement of this quantity has no sensitivity on x any more. To observe the rapid oscillations, a very good lifetime resolution is required.

9.2.11 Oscillation at the $\Upsilon(4S)$

The $B\overline{B}$ system from strong interaction $\Upsilon(4S)$ decay is in an odd C and P eigenstate with angular momentum $L = 1$, retaining the quantum numbers $J^{PC} = 1^{--}$ of the mother particle. This system has to be treated as a coherent quantum state. The time evolution of a state with odd symmetry is different

from that of one with even symmetry. This is due to the fact, that only one antisymmetric $X\overline{X}$ state,

$$|\overline{X}(1)X(2)\rangle - |X(1)\overline{X}(2)\rangle$$

is possible, so it has to stay constant. There are, however, three symmetric states,

$$|\overline{X}(1)X(2)\rangle + |X(1)\overline{X}(2)\rangle$$
$$|X(1)X(2)\rangle$$
$$|\overline{X}(1)\overline{X}(2)\rangle$$

and their relative amplitudes may change with time. The quantum numbers characterizing the two different mesons, which are represented by (1) and (2) here, can be thought of as the spatial wave functions $\psi(\boldsymbol{x})$ and $\psi(-\boldsymbol{x})$ or alternatively the states in momentum space $|\boldsymbol{p}\rangle$ and $|-\boldsymbol{p}\rangle$.

Explicitly, for initial $B\overline{B}$ states of well defined symmetry,

$$\psi(0) = |B^0(1)\overline{B}^0(2)\rangle \pm |B^0(2)\overline{B}^0(1)\rangle$$

the time evolution from (9.35b) translates into

$$\begin{aligned}\psi(t) = e^{-2imt}e^{-T}\cdot\\ \Big[\Big(c^2|B^0(1)\overline{B}^0(2)\rangle + i\eta_m sc|\overline{B}^0(1)\overline{B}^0(2)\rangle + \frac{i}{\eta_m}sc|B^0(1)B^0(2)\rangle - s^2|\overline{B}^0(1)B^0(2)\rangle\Big)\\ \pm\Big(c^2|\overline{B}^0(1)B^0(2)\rangle + i\eta_m sc|\overline{B}^0(1)\overline{B}^0(2)\rangle + \frac{i}{\eta_m}sc|B^0(1)B^0(2)\rangle - s^2|B^0(1)\overline{B}^0(2)\rangle\Big)\Big]\end{aligned} \tag{9.69}$$

for $-$:

$$\psi_-(t) = e^{-2imt}e^{-T}\left[|B^0(1)\overline{B}^0(2)\rangle - |\overline{B}^0(1)B^0(2)\rangle\right] \tag{9.69a}$$

for $+$:

$$\begin{aligned}\psi_+(t) = e^{-2imt}e^{-T}\Big[&\cos(x-iy)T\left(|B^0(1)\overline{B}^0(2)\rangle + |\overline{B}^0(1)B^0(2)\rangle\right)\\ &+ i\sin(x-iy)T\left(\frac{1}{\eta_m}|B^0(1)B^0(2)\rangle + \eta_m|\overline{B}^0(1)\overline{B}^0(2)\rangle\right)\Big]\end{aligned} \tag{9.69b}$$

where the shorthand notation $s = \sin(x-iy)T/2$, $c = \cos(x-iy)T/2$ has been used in (9.69). This means, the antisymmetric state stays always a 100% correlated $B\overline{B}$, as long as none of them has decayed. It is a typical example of an entangled quantum state, where both mesons always have exactly opposite flavour, although none of the single mesons is in a flavour eigenstate. Only when one decays into a state revealing its flavour (not necessarily the first one that decays) the state "collapses" into either $|B^0(1)\overline{B}^0(2)\rangle$ or $|\overline{B}^0(1)B^0(2)\rangle$ and the second meson continues as a one-particle state evolving in time according to (9.35).

The second case (9.69b) of an even wave function leads to a probability oscillating with twice the single-B frequency between a like-sign (BB or $\overline{B}\overline{B}$) and opposite-sign ($B\overline{B}$) flavour state.

For different times T_1 and T_2 of B meson (1) and (2) we have for the antisymmetric state

$$\begin{aligned}|\psi_-(T_1,T_2)\rangle &= e^{-(im/\Gamma+\frac{1}{2})(T_1+T_2)}\cdot\\ &\quad\Big[\cos\frac{(x-iy)(T_1-T_2)}{2}\left(|B^0(1)\overline{B}^0(2)\rangle - |B^0(2)\overline{B}^0(1)\rangle\right)\\ &\quad - i\sin\frac{(x-iy)(T_1-T_2)}{2}\left(\frac{1}{\eta_m}|B^0(1)B^0(2)\rangle - \eta_m|\overline{B}^0(1)\overline{B}^0(2)\rangle\right)\Big]\end{aligned} \tag{9.70a}$$

$$\begin{aligned}&= \frac{e^{-(im/\Gamma+\frac{1}{2})(T_1+T_2)}}{2pq}\cdot\\ &\quad\Big[\cos\frac{(x-iy)(T_1-T_2)}{2}\left(-|B_L(1)B_H(2)\rangle + |B_L(2)B_H(1)\rangle\right)\\ &\quad - i\sin\frac{(x-iy)(T_1-T_2)}{2}\left(|B_L(1)B_H(2)\rangle + |B_L(2)B_H(1)\rangle\right)\Big]\end{aligned} \tag{9.70b}$$

This is observable if we associate the times T_1 and T_2 with the times of decay of the two B mesons. Again it is seen that for $T_1 = T_2$ only the antisymmetric state is present, and mixed states, i. e. two final states indicating the same beauty flavour, will show up only at $T_1 \neq T_2$.

An explicit probability is

$$\begin{aligned}\langle B^0(T_1)B^0(T_2)|\psi_-(T_1,T_2)\rangle &= e^{-(im/\Gamma+\frac{1}{2})(T_1+T_2)} \cdot \left[-\frac{i}{\eta_m}\sin\frac{(x-iy)(T_1-T_2)}{2}\right]\\ \left|\langle B^0(T_1)B^0(T_2)|\psi_-(T_1,T_2)\rangle\right|^2 &= e^{-(T_1+T_2)}\frac{1}{|\eta_m|^2}\left[\left|\sin\frac{(x-iy)(T_1-T_2)}{2}\right|^2\right]\\ &= e^{-(T_1+T_2)}\frac{1}{2|\eta_m|^2}[\cosh y(T_1-T_2)-\cos x(T_1-T_2)]\end{aligned}$$

which is the mixing behaviour of a single B meson when T is replaced by the time difference $T_1 - T_2$.

The mixing probability (B and $\overline{B}$ denote the flavour at decay time)

$$\frac{N(BB)+N(\overline{B}\,\overline{B})}{N(BB)+N(B\overline{B})+N(\overline{B}B)+N(\overline{B}\,\overline{B})} = \chi \tag{9.71}$$

is identical to that for a single B meson. This can be understood from the fact that the second B meson is in a flavour eigenstate exactly when the first one decays into a tagging mode, and then evolves in time as a single oscillating B meson until it decays. The probability can also be obtained from equation (9.70a) using $N(BB) = \mathcal{N}\int\left|\langle B^0(1)B^0(2)|\psi_-(T_1,T_2)\rangle\right|^2 \mathrm{d}T_1\,\mathrm{d}T_2$, and $N(\overline{B}\,\overline{B})$, $N(B\overline{B})$, $N(\overline{B}B)$ accordingly. The normalization factor $\mathcal{N}$ depends on the branching fractions into tagging modes and in general on the parameters y, δ_ϵ and x, but cancels anyway in the ratio.

For incoherent $B^0\overline{B}^0$ pair production, e. g. in $b\bar{b}$ jet fragmentation, the integrated mixed-rate is determined by two independent mixing probabilities

$$\frac{N(B^0B^0)+N(\overline{B}^0\overline{B}^0)}{N(B^0B^0)+N(B^0\overline{B}^0)+N(\overline{B}^0B^0)+N(\overline{B}^0\overline{B}^0)} = 2\chi(1-\chi)$$

Note that the other b quark may hadronize into any b-hadron, and only a small fraction of events is found with two $B^0/\overline{B}^0$.

The actual distribution of observables is obtained from (9.70) multiplying with an appropriate bra vector, and computing the absolute square, $|\langle \mathit{final} \leftarrow BB|\psi_-\rangle|^2$. One is left with a function of T_1, T_2, or rather the more useful variables $T_+ = T_1 + T_2$ and $T_- = T_1 - T_2$. Integrating over all T_+ in the allowed range $|T_1 - T_2|$ to infinity yields

$$\int_{|T_-|}^{\infty} e^{-T_+} f(T_-)\,\mathrm{d}T_+ = e^{-|T_-|} f(T_-)$$

which adds a factor $e^{-|T_-|}$ to the function of the decay time difference. Thus, assuming $T = T_-$ and replacing the factor e^{-T} with $e^{-|T|}$ will transform most distributions for single B^0 time dependence into distributions in time difference at the $\Upsilon(4\mathrm{S})$. This feature is used below to write universal distributions valid for two definitions of T: $T = t_s/\tau$ defined by the signal B lifetime t_s for incoherent $b\bar{b}$ production, and $T = (t_s - t_t)/\tau$ for coherent $B\overline{B}$ production on the $\Upsilon(4\mathrm{S})$, where t_t denotes the second B meson in the $\Upsilon(4\mathrm{S})$ decay in a flavour tagging decay mode.

Equation (9.70b) is an expansion in the two mass eigenstates. The antisymmetric wave function is always composed of two different states, there will be never B_HB_H or B_LB_L, even at different decay times.

The same formalism applies to $\psi(3770) \to D^0\overline{D}^0$ and $\phi \to K^0\overline{K}^0$. The latter is indeed a decay $\phi \to K_L^0K_S^0$.

There is no wave function of CP eigenstates, because the CP properties are undefined before both B mesons have decayed. They involve the phases in decay amplitudes, and include all effects of CP violation which will be discussed in detail below.

For the symmetric state, the wave function is

$$
\begin{aligned}
|\psi_+(T_1,T_2)\rangle &= e^{-(im/\Gamma+\frac{1}{2})(T_1+T_2)}\cdot \\
&\quad \left[\cos\frac{(x-iy)(T_1+T_2)}{2}\left(|B^0(1)\overline{B}^0(2)\rangle + |B^0(2)\overline{B}^0(1)\rangle\right)\right. \\
&\quad \left. + i\sin\frac{(x-iy)(T_1+T_2)}{2}\left(\frac{1}{\eta_m}|B^0(1)B^0(2)\rangle + \eta_m|\overline{B}^0(1)\overline{B}^0(2)\rangle\right)\right] \qquad (9.72a)\\
&= \frac{e^{-(im/\Gamma+\frac{1}{2})(T_1+T_2)}}{2pq}\cdot \\
&\quad \left[\cos\frac{(x-iy)(T_1+T_2)}{2}\left(|B_L(1)B_L(2)\rangle - |B_H(1)B_H(2)\rangle\right)\right. \\
&\quad \left. + i\sin\frac{(x-iy)(T_1+T_2)}{2}\left(|B_L(1)B_L(2)\rangle + |B_H(1)B_H(2)\rangle\right)\right] \qquad (9.72b)
\end{aligned}
$$

This is very similar to the function of an antisymmetric state, but the oscillation is in the **sum** of the two lifetimes instead of the lifetime difference.

In the approximation $|\eta_m| = 1$ and $y = 0$, the integrated mixed-rate is

$$
\frac{N(BB)+N(\overline{B}\overline{B})}{N(BB)+N(B\overline{B})+N(\overline{B}B)+N(\overline{B}\overline{B})} = \frac{x^2(3+x^2)}{2(1+x^2)^2} = \chi(3-4\chi)
$$

In the general case, it is

$$
\frac{N(BB)+N(\overline{B}\overline{B})}{N(BB)+N(B\overline{B})+N(\overline{B}B)+N(\overline{B}\overline{B})} = \frac{(1+\delta_\epsilon^2)(x^2+y^2)[3-y^2+x^2(1+y^2)]}{2\left[(1+x^2)^2(1+y^2)-\delta_\epsilon^2(1-x^2)(1-y^2)^2\right]}
$$

but cannot be related to the mixing probabilities of single mesons χ and $\bar{\chi}$.

The expansion in mass eigenstates shows, that the symmetric wave functions consists always of two eigenstates with the same mass, i. e. B_HB_H or B_LB_L.

9.2.12 Experimental Determination of the Mixing Parameters of B Mesons

The asymmetry (9.42) in its simplified form (9.67) can be detected, if the flavour of B^0 mesons is known at production and at decay time. The flavour at decay time can be inferred from the reconstruction of its decay products. The flavour at production time can not directly be observed, but can be deduced from the flavour of the second b-hadron in $b\bar{b}$ pair production. At the $\Upsilon(4S)$, this is another neutral B meson and their coherent oscillation can be observed as a function of their decay time difference.

While only a small fraction of B meson decays can be fully reconstructed, the flavour of a B meson can be identified by various "tags". These are reconstructed particles from B meson decays that determine the beauty (or bottomness) flavour of the B meson by a measureable property, predominantly by their electric charge.

The first observation of a then unexpected large $B^0\overline{B}^0$ mixing by ARGUS in 1987 used the best flavour tags available: In multihadron events on the $\Upsilon(4S)$ resonance, like-sign lepton pairs were observed which could not be attributed to other sources but semileptonic B decays. The charge of the lepton from $\bar{b} \to l^+\nu\bar{c}$ in these decays is identical to the beauty quantum number of the meson, and these events had to be attributed to B^0B^0 and $\overline{B}^0\overline{B}^0$ final states from $\Upsilon(4S)$ decays.

9.2.12.1 Flavour Tagging

Flavour tagging exploits always a correlation between the beauty flavour of the parent b-hadron and a charge—in most cases the electric charge of the tagging particle, but e. g. for Λ hyperons the baryon number or strangeness and for D^0 mesons the charm.

This correlation is perfect for all fully reconstructed beauty baryons and charged B mesons, and almost all fully reconstructed neutral B mesons. However, a complete reconstruction of B decays will only be possible in a very limited number of events. A more universal approach is to collect this information via certain characteristics of the particles which are able to identify the flavour. In the first measurement of $B\overline{B}$ mixing only leptons have been used, with a charge correlated to the beauty flavour via semileptonic decays $\bar{b} \to l^+\nu\bar{c}$. This is not a perfect correlation since a substantial fraction of leptons from other sources have the "wrong" charge and thereby dilute the oscillation amplitude. If the fraction of oppositely charged leptons is w, the observed numbers of pairs with one unambiguously identified B meson and one lepton are

$$\begin{aligned} N_1 &\equiv N(Bl^- + \overline{B}l^+) = (1-w)\cdot N(B\overline{B}) + w\cdot N(BB \text{ or } \overline{B}\overline{B}) \\ N_2 &\equiv N(Bl^+ + \overline{B}l^-) = (1-w)\cdot N(BB \text{ or } \overline{B}\overline{B}) + w\cdot N(B\overline{B}) \end{aligned}$$

and the observed asymmetry is

$$\begin{aligned} a_{\text{obs}} &= \frac{N_1 - N_2}{N_1 + N_2} \\ &= \frac{(1-2w)\cdot N(B\overline{B}) - (1-2w)\cdot N(BB \text{ or } \overline{B}\overline{B})}{N(B\overline{B}) + N(BB \text{ or } \overline{B}\overline{B})} \\ &= (1-2w)\cdot a \end{aligned} \tag{9.73}$$

i. e. the true asymmetry a is **diluted** by a factor $D_t = 1-2w$. Likewise, the observed mixing probability

$$\chi_{\text{obs}} = \frac{N_2}{N_1 + N_2} = (1-2w)\cdot\chi + w$$

is a function of w and the true mixing probability χ. In the case of lepton pairs, we have

$$\begin{aligned} N_1 &\equiv N(l^+l^-) = [(1-w)^2 + w^2]\cdot N(B\overline{B}) + 2w(1-w)\cdot N(BB \text{ or } \overline{B}\overline{B}) \\ N_2 &\equiv N(l^+l^+ + l^-l^-) = [(1-w)^2 + w^2]\cdot N(BB \text{ or } \overline{B}\overline{B}) + 2w(1-w)\cdot N(B\overline{B}) \end{aligned}$$

and

$$\chi_{\text{obs}} = \frac{N_2}{N_1 + N_2} = (1-2w)^2\cdot\chi + 2w(1-w)$$

is reduced by the square of the lepton-tag dilution factor and also shifted by an offset $2w(1-w)$.

For the determination of a mixing probability, a fit of the lepton momentum distribution is used to determine the fraction of primary leptons.

For a lifetime-dependent measurement of mixing via the oscillation frequency, the time-dependence of the asymmetry is observed. Although this asymmetry will experience a constant dilution from each tag, this dilution is irrelevant for the measurement of the frequency. It is obtained from a fit to the asymmetry $a(T) = D\cos xT$ as amplitude of the osillation.

9.2.13 Mixing of B and $\overline{B}$

The first observation of $B^0\overline{B}^0$ mixing by ARGUS[76] on page 166in 1987 was the observation of 25 like-sign lepton pairs at the $\Upsilon(4S)$ energy. These could not be attributed to other sources but to B^0B^0 and $\overline{B}^0\overline{B}^0$ final states with semileptonic decay of both B mesons.

In addition, this observation was supported by four events with one fully reconstructed B meson plus a lepton of "wrong" sign, and one exclusive event $\Upsilon(4S) \to B^0B^0$ with both B^0 mesons reconstructed.

This measurement was the first in a series of "mixing" measurements, where the fraction χ of oscillated events is determined without lifetime information. The mixing probability χ can be calculated from the number of like- and opposite-sign dilepton events as

$$\chi = \frac{[N(l^+l^+) + N(l^-l^-)] \cdot (1+f)}{N(l^+l^+) + N(l^-l^-) + N(l^+l^-)}$$

where N are numbers corrected for mistags from secondary leptons, and the ratio of semileptonic branching fractions of neutral and charged B mesons and of their production rates enters as

$$f = \frac{[\mathcal{B}(B^+ \to l^+\nu X)]^2 \cdot \mathcal{B}(\Upsilon(4S) \to B^+B^-)}{[\mathcal{B}(B^0 \to l^+\nu X)]^2 \cdot \mathcal{B}(\Upsilon(4S) \to B^0\overline{B}^0)}$$

in a background dilution factor $D_\pm = 1/(1+f)$. In all analyses, the factor f is taken to be 1 consistent with measured numbers and theoretical expectation.

In addition to leptons and fully reconstructed B mesons as flavour tags also fully reconstructed $D^{*\pm}$ mesons, partially reconstructed $D^{*\pm} \to (D^0/\overline{D}^0)\pi^\pm$, partially reconstructed $B^0 \to D^{*-}l^+\nu$, and charged kaons have been used. The most precise single measurement uses $B^0 \to D^{*-}\pi^+(\pi^0)$ where the $D^{*-} \to \overline{D}^0\pi^-$ is partially reconstructed using the soft π^-. The flavour of the second B is determined by a lepton with $p > 1.4\,\mathrm{GeV}$. The average value from ARGUS and CLEO measurements is $\chi = 0.182 \pm 0.015$.

9.2.14 Oscillations in Time-Dependent Measurements

While only the integrated effect can be observed on the $\Upsilon(4S)$ at symmetric colliders, an observation of the oscillating behaviour was first possible at the Z^0, where the lifetime can be measured. This yields directly the frequency ν as $2\pi\nu = \Delta m$ from the asymmetry

$$a(t) = \left.\frac{\dot{N}(B) - \dot{N}(\overline{B})}{\dot{N}(B) + \dot{N}(\overline{B})}\right|_t = \cos\Delta m\, t$$

First results from LEP have been later augmented at asymmetric colliders on the $\Upsilon(4S)$ by the B meson factories PEP II/BABAR and KEKB/BELLE.

The measurements differ mostly in the tagging method used. Reconstructing hadronic final states of $B^0/\overline{B}^0$ decays requires a large number of B mesons and is therefore only used at the asymmetric B factories at PEP II and KEKB. The same holds for the channel $B^0 \to D^{*-}l^+\nu$.

The experiments at LEP use charged leptons (l), fully (D^*) or partially (π) reconstructed decays of $D^{*+} \to D^0\pi^+$, alone and associated with a lepton indicating a $B^0 \to D^{*-}(X)l^+\nu$ final state, and various definitions of a jet charge. The C and P asymmetry of polarized Z^0 decays is exploited at the Stanford Linear Collider by SLD.

As in the time integrated measurement, also in measurements of the lifetime dependent oscillation there is a background fraction $f_\pm$ from other b hadrons, predominantly charged $B^\pm$ which do not oscillate. This modifies (9.66) for N_0 initial B mesons at $T = 0$ to

$$\begin{aligned} N_B(T) &= \tfrac{1}{2}N_0e^{-T}(1 + \cos xT + f_\pm) \\ N_{\overline{B}}(T) &= \tfrac{1}{2}N_0e^{-T}(1 - \cos xT) \end{aligned} \qquad (9.74)$$

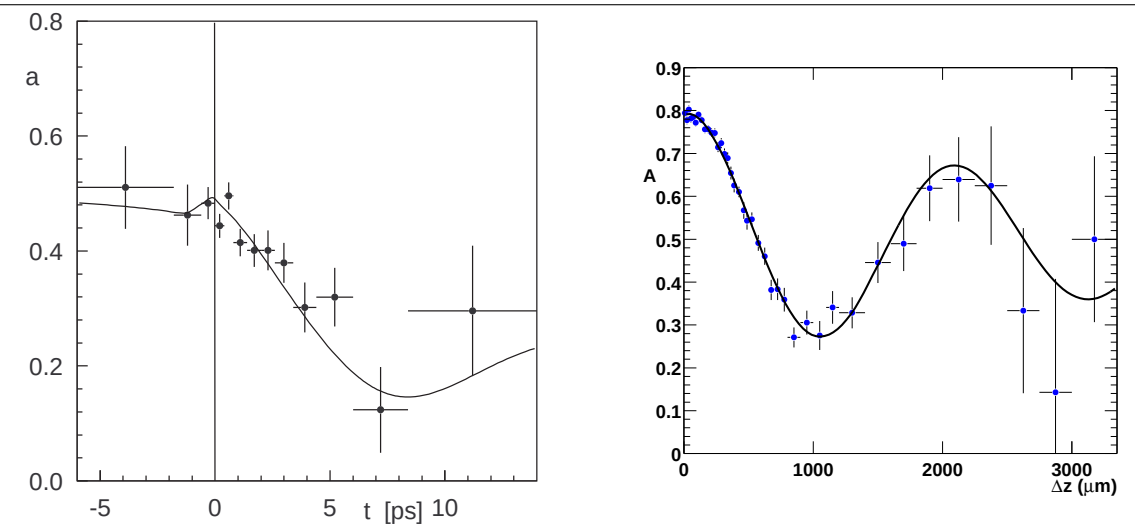

Fig. 9.7 Two measurements of $B^0\overline{B}^0$ oscillation using dilepton events at LEP (ALEPH Collab., Z. Phys. **C75**, 397 (1997), left) and the PEP II B factory (BABAR Collab., Phys. Rev. Lett. **88**, 221803 (2002), right). Both show the asymmetry defined in (9.67), the left figure has been derived from one showing the like-sign fraction $\chi_{\rm obs}(t)$ using $a(t) = 1 - 2\chi_{\rm obs}(t)$.

which corresponds to an asymmetry

$$a(T) = \frac{\cos xT}{1 + f_\pm/2} + \frac{f_\pm}{2 + f_\pm} = D_\pm \cos xT + I_\pm \tag{9.75}$$

corresponding to an effective dilution factor $D_\pm = \frac{1}{1+f_\pm/2}$ and an offset $I_\pm = \frac{f_\pm}{2+f_\pm}$. The value $a(0) = D_\pm + I_\pm = 1$ is independent of $f_\pm$.

If the flavour of one B meson is assigned wrong with probability w, the asymmetry is given by

$$\begin{aligned} N_B(T) &= \tfrac{1}{2} N_0 e^{-T} \left[(1-w)(1 + \cos xT + f_\pm) + w(1 - \cos xT)\right] \\ N_{\overline{B}}(T) &= \tfrac{1}{2} N_0 e^{-T} \left[(1-w)(1 - \cos xT) + w(1 + \cos xT + f_\pm)\right] \\ a(T) &= (1-2w)\left[\frac{\cos xT}{1 + f_\pm/2} + \frac{f_\pm}{2 + f_\pm}\right] \\ &= D_t D_\pm \cos xT + D_t I_\pm \end{aligned}$$

with a tagging dilution factor $D_t = a(0) = 1 - 2w$. The mistag probability at $b\bar{b}$ experiments includes the fraction of B^0 tags that have changed their flavour by their own, independent oscillation.

Two examples are shown in figure 9.7.

9.2.14.1 Lifetime Resolution

A limited error in vertex reconstruction leads to a smearing of the T distribution. This implies an

amplitude reduction factor D_r. Assuming a Gaussian resolution in Δt of σ_t, we have[77]

$$D_r = e^{-\frac{1}{2}(x\sigma_t/\tau)^2} \tag{9.76}$$

which is multiplied to the tagging dilution. A resolution function described by two Gaussians as

$$r(t) = \frac{f}{\sqrt{2\pi}\sigma_n} e^{-\frac{(t-t')^2}{2\sigma_n^2}} + \frac{1-f}{\sqrt{2\pi}\sigma_w} e^{-\frac{(t-t')^2}{2\sigma_w^2}}$$

yields

$$D_r = f e^{-\frac{1}{2}(x\sigma_n/\tau)^2} + (1-f) e^{-\frac{1}{2}(x\sigma_w/\tau)^2} \tag{9.77}$$

This approach to time smearing ignores the asymmetry entered by the exponential decay distribution. If the true distributions

$$f(T) = e^{-|T|}(1 \pm \cos xT)$$

are convolved with a Gaussian, and the asymmetry is calculated from the smeared distributions, there is in addition to the reduction in amplitude also a distortion.

At the b jet experiments, the distance between the primary vertex of $b\bar{b}$ jet production and the B decay vertex is measured with high precision silicon detectors. The primary vertex is determined from the interaction region, which has an RMS in the transverse plane of $150\,\mu\text{m} \times 10\,\mu\text{m}$ at LEP, $1\,\mu\text{m} \times 1\,\mu\text{m}$ at SLC and $25\,\mu\text{m} \times 25\,\mu\text{m}$ at the Tevatron. The wide x region at LEP is compensated by the use of fragmentation tracks to fit an event by event vertex. The time resolution is dominated by the B^0 decay vertex which is reconstructed with accuracies varying between 50 and $200\,\mu\text{m}$. These values are small compared to a typical distance of flight of $\sim 3\,\text{mm}$ (both at the Z^0 and the Tevatron).

Since

$$t = \frac{\Delta s \cdot m_B}{p}$$

where Δs is the distance between the secondary and primary vertices, and p the momentum of the B meson, the error is

$$\frac{\delta t}{t} = \frac{\delta \Delta s}{\Delta s} \oplus \frac{\delta p}{p}, \qquad \delta t = \delta \Delta s \frac{m_B}{p} \oplus \frac{\delta p}{p} t$$

with a constant term from vertex resolution and a linear term from momentum resolution. The measurements with B^0 mesons in b jets have been performed without full reconstruction of the B^0 meson. In this case, an important effect on the lifetime resolution is the error on the B^0 momentum, and since $\delta p/p \approx$ const ($\gtrsim 10\%$ at LEP) or $\delta t \propto t$, the lifetime becomes increasingly smeared. This leads to a progressive reduction in the amplitude of the observable asymmetry.

In contrast to this behaviour, oscillation measurements at asymmetric colliders at the $\Upsilon(4\text{S})$ energy have a dominantly constant resolution

$$\delta \Delta t \approx \frac{\delta \Delta z}{\beta\gamma} \approx \text{const}$$

due to the short distance between the two B decay vertices of $\sim 260\,\mu\text{m}$ (BABAR) and $\sim 200\,\mu\text{m}$ (BELLE). The velocity of the centre of mass system (the $\Upsilon(4\text{S})$) fluctuates by less than one per mille, the

[77] The measured asymmetry function is

$$\begin{aligned} f(\Delta t) &= \int_{-\infty}^{\infty} \cos x \frac{\Delta t'}{\tau} \cdot e^{-\frac{(\Delta t - \Delta t')^2}{2\sigma_t^2}} \, \mathrm{d}(\Delta t') \\ &= e^{-\frac{1}{2}(x\sigma_t/\tau)^2} \cos x \frac{\Delta t}{\tau} \end{aligned}$$

momentum uncertainty due to the proper motion of the B in the $\Upsilon(4S)$ cms causes a small contribution to the lifetime error that is visible at large lifetimes.

The constant and time-dependent resolution effects differ from experiment to experiment, and depend on the method of B identification. They are convolved with the full time dependence, including the exponential which makes the effective "smearing" of the true lifetime asymmetric. These together with a possible bias from cascade charm decays, resolution tails and background effects are modelled for each experiment and are taken into account in the fit functions, leading to shapes, of which two examples are shown in figure 9.7. The proper modelling of the distortions is crucial for a bias-free extraction of the oscillation frequency.

9.2.15 Summary of Experimental Results on the B^0 Meson

The average of all measurements is

$$\Delta m(B^0) = (0.507 \pm 0.004)/\,\mathrm{ps}$$

corresponding to an oscillation frequency $\nu = \Delta m/2\pi = (80.7 \pm 0.6)\,\mathrm{GHz}$ and a mass difference $\Delta m = (0.334 \pm 0.003)\,\mathrm{meV}$. This is a fraction of $6 \cdot 10^{-14} \cdot m(B^0)$.

The dimensionless mixing parameter x can be calculated from the mixing probability using (9.68) and from the oscillation frequency as $x = \Delta m\,\tau$ which requires also precise knowledge on the average lifetime $\tau_d = (1.519 \pm 0.007)\,\mathrm{ps}$ of the B^0 meson. It is

$$x = \Delta m\,\tau = 0.770 \pm 0.007$$
$$x = \sqrt{\frac{\chi}{\frac{1}{2} - \chi}} = 0.757 \pm 0.048$$

The two independent methods agree very well. The average is identical to the more precise value within the figures given, and the precision is better than 1%.

There is no observation of $\Delta\Gamma$ of the B^0 mass eigenstates. In the Standard Model, a value $y \sim 10^{-3}$ is expected.

9.2.16 Experimental Results on the B_s Meson

The first hint on large B_s mixing was obtained[78] by UA1 even before $B^0\overline{B}^0$ oscillation was established. They observed an average mixing probability $\chi = 0.12 \pm 0.05$ in b jets from $\bar{p}p$ annihilation. From the same quantity measured at e^+e^- annihilation and Z^0 decay, a value $\chi_s \approx 0.5$ can be inferred with large errors due to the small B_s fraction in b jets. Direct (non-) observations of the oscillation leads to more stringent limits on the frequency.

To determine a limit, the LEP Working group on B oscillations combined the fit results of the B_s asymmetry amplitude a (which is 1 for true oscillations) for a series of assumed values of Δm_s from 13 measurements by the five experiments ALEPH, CDF, DELPHI, OPAL, and SLD. A 95%CL lower limit is calculated using the point where the hypothesis $a = 1$ is excluded at 5% significance level in a one-sided Gaussian test. This means all values of Δm_s for which the combined amplitude a plus $1.645 \cdot \sigma(a)$ is smaller than 1 are excluded at 95%CL, where $\sigma(a)$ is the total error on a.

The same amplitude plot is also used in the first observations of $B_s\overline{B}_s$ oscillation. In 2006, a positive signal has been extracted by the CDF collaboration[79] leading to $\Delta m_s = (17.77 \pm 0.10 \pm 0.07)\,\mathrm{ps}^{-1}$ and is corroborated by the amplitude distribution from other experiments (fig. 9.8).

[78] UA1 Collab., Phys. Lett. **B186**, 247 (1987).
[79] CDF Collaboration, Phys. Rev. Lett. **97**, 242003 (2006).

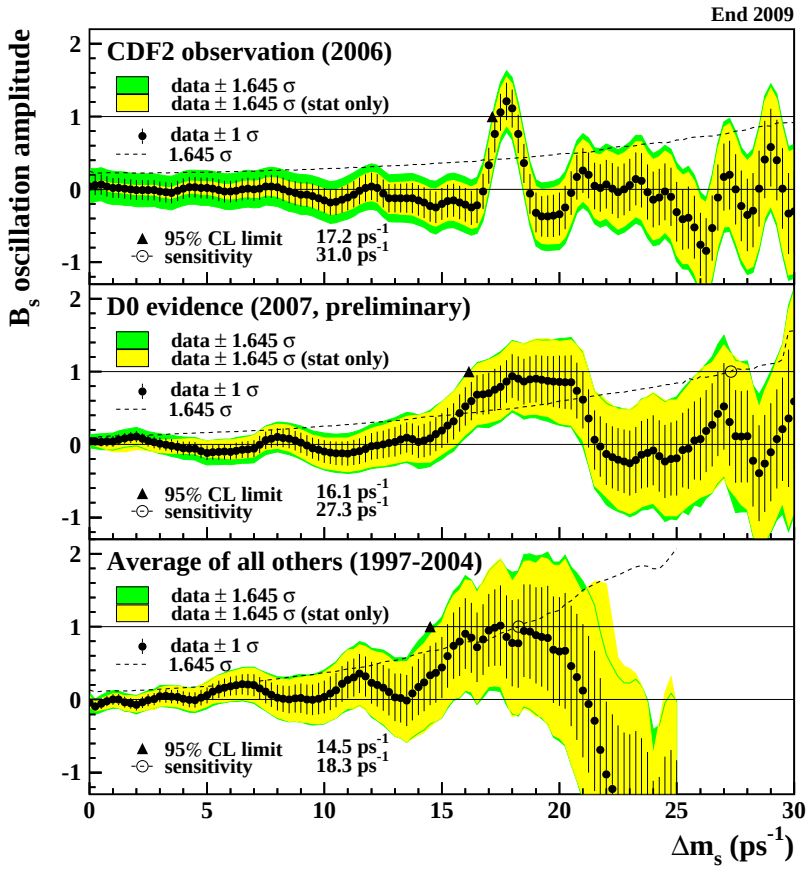

Fig. 9.8 Average amplitude for $B_s\overline{B}_s$ oscillation fits as a function of the oscillation frequency Δm_s from measurements by the CDF and D0 experiments, and average from ALEPH, DELPHI, OPAL and SLD. The shaded areas are the 90%CL intervals (with and without systematics), corresponding to a significance level of 5% for a one-sided test.

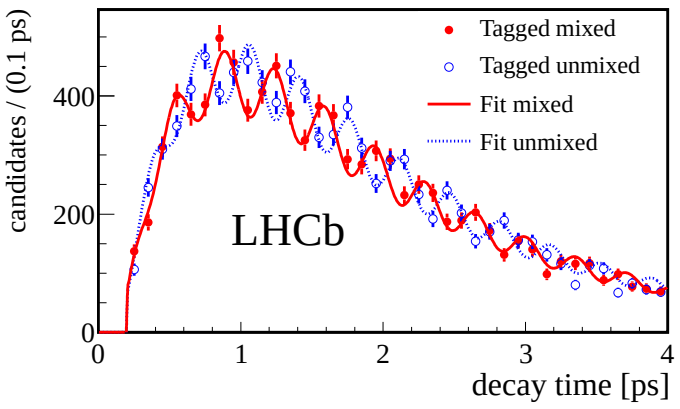

Fig. 9.9 $B_s\overline{B}_s$ oscillation observed in the LHCb experiment, corresponding to $\Delta m_s = (17.768 \pm 0.023 \pm 0.006)\,\mathrm{ps}^{-1}$.

A direct observation of the oscillation (with large dilution, as expected) has been achieved by the LHCb experiment[80] (fig. 9.9).

[80] LHCb Coll., New J. Phys. **15**, 053021 (2013).

The present world average is

$$\Delta m_s = (17.762 \pm 0.023)\,\mathrm{ps}^{-1}$$

and is dominated by the LHCb measurement. For the $B_s/\overline{B}_s$ system, using this value for the oscillation frequency and the B_s lifetime value $\tau_s = (1.516 \pm 0.011)\,\mathrm{ps}$, we obtain limit is

$$x_s = 26.9 \pm 0.2$$

It corresponds to a mixing probability $\chi_s > 0.499$.

The available results on the B_s lifetime are average lifetimes which can all have different weights of τ_H and τ_L due to the different mixture of final states used. The experimental information on the lifetime difference of the mass eigenstates is still weak and no significant lifetime difference has been observed. All flavour specific decays—like the semileptonic decays—have a time distribution (9.40)

$$\dot{N}(T) \propto e^{-T} \cosh yT = e^{-t/\tau_L} + e^{-t/\tau_H}$$

in the approximation $\delta_\epsilon = 0$. The kink in this distribution cannot be observed with the presently available data samples.

Other methods rely on Standard Model assumptions:

- the light eigenstate B_{sL} is the short lived one as suggested by the sign in (9.59), and
- this state decays dominantly into the CP $= +1$ final states, like K^+K^-, and the heavy state into CP $= -1$ final states.

The latter assumption is discussed in more detail in the next chapter on CP violation. A fit to lifetime measurements for CP-odd, CP-even and flavor specific final states by the Heavy Flavour Averaging Group[81] gives

$$y_s = 0.075 \pm 0.010$$

corresponding to $\Delta\Gamma/\Gamma = 0.15 \pm 0.02$. The Particle Data Group 2013 average is $\Delta\Gamma/\Gamma = 0.123 \pm 0.017$.

[81] Web page `http://www.slac.stanford.edu/xorg/hfag/`, June 2012.

9.3 CP Violation

Standard Model weak interactions are long known to violate parity and charge conjugation symmetries, in most cases even maximally. However, the combined symmetry operation CP leads generally to transitions identical to the original ones, i. e. CP symmetry is conserved. A typical example is the weak decay of a τ lepton into $\pi\nu_\tau$, as shown in figure 9.10. While a τ^- lepton can decay into a left-handed neutrino and a pion, the charge-conjugate decay of a τ^+ into a left-handed antineutrino is forbidden. However, if one looks at the mirror-image, i. e. one applies a parity transformation at the same time, the decay is allowed, and even more the amplitudes for both decays are equal. If we extend our definition of "antiparticle" to mean not only sign-flip of all charge-like quantities, but also of the spin, we have the CP operation and a perfect symmetry even for most weak-interaction processes. CP violation, on the contrary, is a true violation of particle antiparticle symmetry, which can not be restored by a mirror.

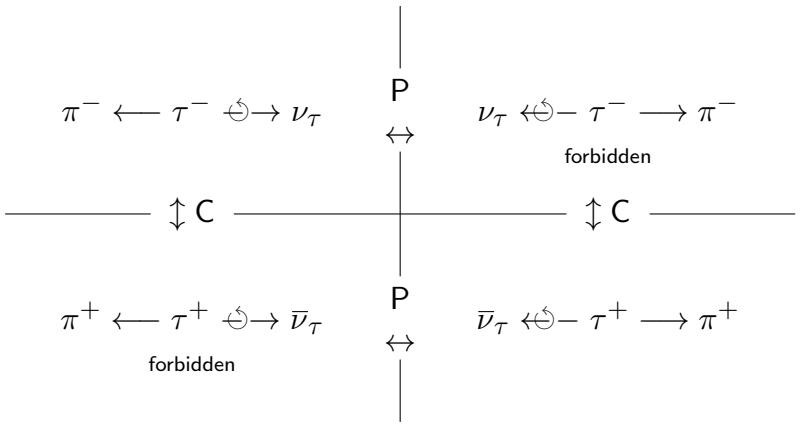

Fig. 9.10 Parity (P) and charge conjugation (C) operations on $\tau^- \rightarrow \pi^-\nu_\tau$. The upper right and lower left processes are forbidden.

If all interactions were CP symmetric, we had no way to distinguish left-/right-handedness, positive/negative charge etc. Parity and charge conjugation violation in weak interaction connects handedness with charge, but still does not allow a distinction between the two members of a pair. CP violating K^0 decays, however, provide a different decay rate function of time for K^0 and $\overline{K}^0$, which could be used to explicitly distinguish them by a dip or bump in this function.

Although we are presently not able to observe the difference of matter and antimatter at far regions of the universe, the absence of regions of matter antimatter annihilation boundaries suggests that the whole universe is made of matter, violating CP asymmetry to a large extent.

It has been suggested by Sakharov[82] already in 1967 that this global asymmetry must result from three facts:

(1) violation of CP and C symmetry,

(2) violation of baryon number conservation, and

(3) non-equilibrium (non-stationary expansion of the early universe).

Small asymmetries of the order 10^{-10} at the early universe are sufficient to explain this present situation, however, it is difficult to create these from the CP violation in the Standard Model which has particle antiparticle asymmetry only in mesons, whereas baryon number violation is observed in the universe. If one assumes baryon number violating processes at phase boundaries of the early universe, e. g. at the symmetry breaking phase transition to the electroweak interaction in the Standard Model, still the

[82] citesakh

CP asymmetry via the CKM phase is many orders of magnitude smaller than the observed number of baryons per background photon. Thus, CP violating mechanisms beyond the Standard Model are likely to exist, and we will possibly observe them as small deviations from the Standard Model predictions.

The origin of CP violation in K and B mesons may be only within the Standard Model, but other possibilities are not ruled out. Almost any extension of the Standard Model introduces new phases which result in CP violation. This can only be avoided by some fine tuning of parameters which seems unnatural.

Complementary searches for CP violation will give additional constraints: Only small CP violating effects are predicted by the Standard Model in weak decays of other particles, like D^0 mesons or strange baryons. CP asymmetries in neutrino oscillations or CP violation in lepton decay are potential windows to alternative models. All these are examples of C violating processes, while P does not compensate for that as in figure 9.10.

A different way to violate the CP symmetry is by C conserving parity violation. The search for magnetic monopoles or electric dipole in pointlike or spherically symmetric particles, e. g. in leptons, quarks or the neutron, is a way to find non-standard CP violation of this kind. At present, only upper limits on these effects exist, and no glimpse beyond the Standard Model has been obtained.

9.3.1 CP Violation in Extended Electrodynamics

While classical electrodynamics and QED both conserve the CP symmetry, it may be instructive to see how CP violation can be introduced in macroscopic systems extending classical electrodynamics by magnetic charges.

While CP violation discussed below is mostly C violation, we now give two examples of conserved C symmetry where CP violation occurs from a violation of parity P. The first example is the movement of a + (positive) electric charge in the field of a magnetic N (north) monopole as shown in figure 9.11. The Lorentz force will confine it to a circular orbit, rotating lefthanded with respect to the field lines. The mirror image is, however, a righthanded rotation, which does not occur through electromagnetic forces.

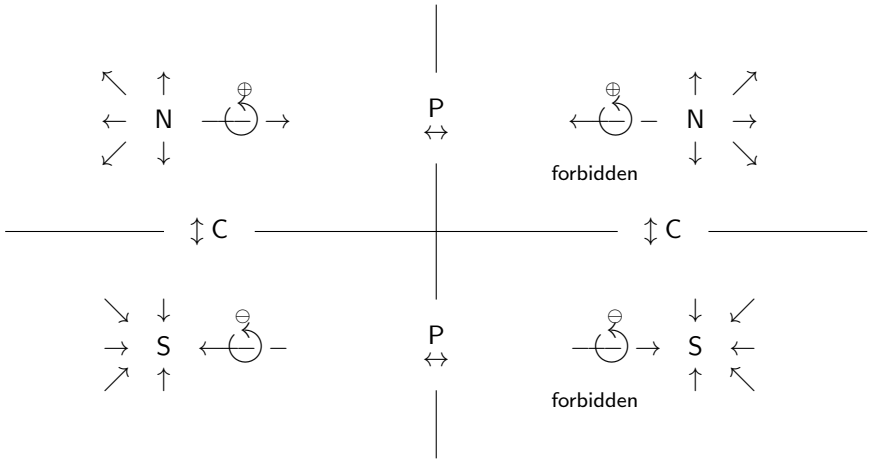

Fig. 9.11 Parity (P) and charge conjugation (C) operations on a charged particle moving in a magnetic monopole field. The upper right and lower right processes show the wrong movement of charge, opposite to the real one, and do therefore not occur in nature.

Why is this not observed with a magnetic dipole field? The answer is simple: a dipole field is generated by moving charges and their rotation and hence the field direction will also be inverted in the mirror. For a static (monopole) charge, this is not the case, leading to a maximum parity violation.

The C operation will transform the N monopole to a S monopole and the + to a − charge, and the motion will be unchanged. Thus CP = C ∘ P is violated.

A similar example is an elementary electric dipole with a dipole moment proportional to the particle spin. In the macroscopic world such a field can be created by a rotating magnetic monopole. In contrast to an induced electric dipole moment from shifted charges, an intrinsic electric dipole moment of any pointlike particle like the electron or s-wave bound system like the neutron is T and P violating, because it has to be aligned with the spin (Wigner–Eckart theorem). Table 9.2 shows experimental limits.

Table 9.2 Electric dipole moments. All measurements are compatible with $d = 0$.

particle	Experiment	d [e cm]
n	ILL, 2006	$(0.2 \pm 1.5 \pm 0.7) \cdot 10^{-26}$
e	YbF molecules, 2011	$(-2.4 \pm 5.7 \pm 1.5) \cdot 10^{-28}$

9.3.2 CP Eigenstates Versus Mass Eigenstates *

The following discussion will again use $B^0/\overline{B}^0$ as an example, but is applicable to each of the four systems accordingly. Independent of any convention two orthogonal CP eigenstates

$$\begin{aligned} |B^0_+\rangle &= \frac{1}{\sqrt{2}}\left(|B^0\rangle + \mathrm{CP}\,|B^0\rangle\right) = \frac{1}{\sqrt{2}}\left(|B^0\rangle + e^{i\phi_{\mathrm{CP}B}}|\overline{B}^0\rangle\right) \\ |B^0_-\rangle &= \frac{1}{\sqrt{2}}\left(|B^0\rangle - \mathrm{CP}\,|B^0\rangle\right) = \frac{1}{\sqrt{2}}\left(|B^0\rangle - e^{i\phi_{\mathrm{CP}B}}|\overline{B}^0\rangle\right) \end{aligned} \tag{9.78}$$

with $\mathrm{CP}\,|B^0_+\rangle = |B^0_+\rangle$ and $\mathrm{CP}\,|B^0_-\rangle = -|B^0_-\rangle$ can be defined. If a state agrees with one of these except for a phase factor, it will be a CP eigenstate. However, due to the arbitrariness of $\phi_{\mathrm{CP}B}$ this is not an observable property.

The mass eigenstates of the $B^0/\overline{B}^0$ system are not CP eigenstates (this statement is valid for any $X^0/\overline{X}^0$ system including $K^0/\overline{K}^0$). Using $\mathrm{CP}\,|B^0\rangle = e^{i\phi_{\mathrm{CP}B}}|\overline{B}^0\rangle$, they are transformed by a CP operation as

$$\begin{aligned} \mathrm{CP}\,|B_L\rangle &= \left(\frac{e^{i\phi_{\mathrm{CP}B}}}{2\,\eta_m} + \frac{e^{-i\phi_{\mathrm{CP}B}}\eta_m}{2}\right)|B_L\rangle - \left(\frac{e^{i\phi_{\mathrm{CP}B}}}{2\,\eta_m} - \frac{e^{-i\phi_{\mathrm{CP}B}}\eta_m}{2}\right)|B_H\rangle \\ &\approx \cos 2\tilde{\beta}\,|B_L\rangle - \sin 2\tilde{\beta}\,|B_H\rangle \\ \mathrm{CP}\,|B_H\rangle &= -\left(\frac{e^{i\phi_{\mathrm{CP}B}}}{2\,\eta_m} + \frac{e^{-i\phi_{\mathrm{CP}B}}\eta_m}{2}\right)|B_H\rangle + \left(\frac{e^{i\phi_{\mathrm{CP}B}}}{2\,\eta_m} - \frac{e^{-i\phi_{\mathrm{CP}B}}\eta_m}{2}\right)|B_L\rangle \\ &\approx -\cos 2\tilde{\beta}\,|B_H\rangle + \sin 2\tilde{\beta}\,|B_L\rangle \end{aligned}$$

where the approximation for the $B^0/\overline{B}^0$ system uses (9.55) and depends on the phase convention for the CKM matrix which determines the angle $\tilde{\beta}$. If $\tilde{\beta} = 0$ as in the alternative phase convention (9.15) (accompanied by a phase redefinition for the d field), these states would be eigenstates with CP = ±1, respectively. Still, there would be CP violation in their decay, and the CP eigenvalue of the final state would be different. Therefore, the question of which of the mass eigenstates is closest to which CP eigenstate has no convention independent answer. Only the CP eigenvalue of a decay product of one of these states is an observable. Since the weak interaction does not conserve CP, it is not legitimate to deduce from the final state's eigenvalue an eigenvalue of the decaying state.

A meaningful question is which of B_H or B_L **decays** more often into CP = ±1 eigenstates. In contrast to the neutral kaon system, most final states from B decays are flavour-specific, and both mass eigenstates

decay into them via either their B^0 or their $\overline{B}^0$ component. The small fraction of states that can be reached both by B^0 and $\overline{B}^0$ includes the contribution from CP eigenstates which appear mainly through three processes. On the tree level, there are two main decay channels that can produce CP eigenstates: $b \to c\bar{c}d$ with the $c\bar{c}d\bar{d}$ final state, and $b \to u\bar{u}d$ with the quark content $u\bar{u}d\bar{d}$. A state of the first kind with CP eigenvalue ζ_X^{CP} will have decay amplitudes

$$A = \langle X_{c\bar{c}}|\mathcal{H}|B^0\rangle = V_{cb}^* V_{cd} A_0, \qquad \bar{A} = \langle X_{c\bar{c}}|\mathcal{H}|\overline{B}^0\rangle = \zeta_X^{CP} e^{-i\phi_{\mathrm{CP}B}} V_{cb} V_{cd}^* A_0$$

where $\zeta_X^{CP} = \pm 1$ is the CP eigenvalue of the state. The corresponding decay amplitudes of B_H and B_L are

$$\begin{aligned} A_{L,H} &= \langle X_{c\bar{c}}|\mathcal{H}|B_{L,H}\rangle = pA \pm q\bar{A} \\ &= pA\left(1 \pm \eta_m \zeta_X^{CP} e^{-i\phi_{\mathrm{CP}B}} \frac{V_{cb}V_{cd}^*}{V_{cb}^* V_{cd}}\right) = pA\left(1 \pm |\eta_m| \zeta_X^{CP} e^{-2i\beta}\right) \end{aligned}$$

The decay ratio is then (in the approximation $|\eta_m| = 1$)

$$\frac{|A_H|^2}{|A_L|^2} = \frac{|1 - \zeta_X^{CP} e^{-2i\beta}|^2}{|1 + \zeta_X^{CP} e^{-2i\beta}|^2} = \frac{1 - \zeta_X^{CP} \cos 2\beta}{1 + \zeta_X^{CP} \cos 2\beta} = (\tan^2 \beta)^{\zeta_X^{CP}} \tag{9.79}$$

which is for $\beta < \frac{\pi}{4}$ less than 1 for $\zeta_X^{CP} = +1$ and *vice versa*. In this case, the heavier state B_H will decay more often into states with negative CP eigenvalue, $\zeta_X^{CP} = -1$.

The value $\tan\beta$ is also a parameter of CP violation in the interference of mixed and unmixed decay amplitudes: One convention-independent parameter that describes CP violation for the given final state is $\eta_X = i\zeta_X^{CP} \tan\beta$ which corresponds to the small "ϵ" parameter for the K meson.

Some decays with an intermediate state $c\bar{c}d\bar{s}$ or $c\bar{c}\bar{d}s$ proceed into K^0 or $\overline{K}^0$, which finally result in $c\bar{c}d\bar{d}$ via a K_L^0 or K_S^0 consecutive decay. Among those is the favourite decay $B^0 \to J/\psi K_S^0$. The total decay chain involves almost the same CKM element phase factors as the direct $b \to c\bar{c}d$ decay, leading to the same answers as for this decay mode (a more detailed discussion follows below).

Accordingly, for the $u\bar{u}d\bar{d}$ states

$$A_{L,H} = \langle X_{u\bar{u}}|\mathcal{H}|B_{L,H}\rangle = pA\left(1 \pm |\eta_m| \zeta_X^{CP} e^{2i\alpha}\right)$$

and the ratio

$$\frac{|A_H|^2}{|A_L|^2} = \frac{|1 - \zeta_X^{CP} e^{2i\alpha}|^2}{|1 + \zeta_X^{CP} e^{2i\alpha}|^2} = \frac{1 - \zeta_X^{CP} \cos 2\alpha}{1 + \zeta_X^{CP} \cos 2\alpha} = (\tan^2 \alpha)^{\zeta_X^{CP}} \tag{9.80}$$

depends on the angle α, which is larger than $\frac{\pi}{4}$. This gives the opposite answer, i. e. the heavier state B_H will decay more often into states with positive CP eigenvalue, $\zeta_X^{CP} = +1$.

For decays via W exchange, like $b\bar{d} \to c\bar{c}$ or $b\bar{d} \to u\bar{u}$, the same CKM elements are involved, and the same arguments lead to the same answers as above. Also, the favoured penguin-type transition $b \to s$ with subsequent hadronization into a K_L^0 or K_S^0 has a net phase close to β' leading to the ratio (9.79).

CP eigenstates with quark content $d\bar{d}$ can be reached via CKM-suppressed penguin-type loops. Due to the top quark dominance the amplitudes are

$$A = \langle X_{d\bar{d}}|\mathcal{H}|B^0\rangle \approx V_{tb}^* V_{td} A_0, \qquad \bar{A} = \langle X_{d\bar{d}}|\mathcal{H}|\overline{B}^0\rangle \approx \zeta_X^{CP} e^{-i\phi_{\mathrm{CP}B}} V_{tb} V_{td}^* A_0$$

and the CKM element phases cancel, which gives

$$\frac{|A_H|^2}{|A_L|^2} = \frac{1 - \zeta_X^{CP}}{1 + \zeta_X^{CP}}$$

i. e. B_H decays exclusively into states with negative CP eigenvalue, $\zeta_X^{CP} = -1$, and B_L into states with $\zeta_X^{CP} = +1$.

All these results receive corrections from non-leading terms, like c quark loops in the last case, or $b \to d$ penguin corrections to the $b \to u$ transition final states. The general case for an arbitrary ratio

$$r := \frac{\eta_m \bar{A}}{A}$$

leads to

$$A_{L,H} = pA \pm q\bar{A} = pA(1 \pm r)$$

and a ratio of rates

$$\frac{|A_H|^2}{|A_L|^2} = \frac{1 - \Omega_0}{1 + \Omega_0} \qquad \text{with} \qquad \Omega_0 := \frac{2\,\mathcal{R}e\, r}{1 + |r|^2} \tag{9.81}$$

Since systems with a $c\bar{c}$ pair probably constitute the major part for both CP eigenvalues, the heavy mass eigenstate can be said to be the one which decays more often into final states with CP $= -1$, and the light one into those with CP $= +1$, but both have also substantial branching fractions into final states with the opposite CP value. This is a consequence of the CP violating phase in the CKM matrix, but is not a CP violating decay, since none of the two B mass eigenstates was a CP eigenstate before it decayed.

The dominant decays of the B_s to CP eigenstates is to the quark state $c\bar{c}s\bar{s}$, which yields

$$\frac{|A_H|^2}{|A_L|^2} \approx (\tan^2 \beta_s)^{\zeta_X^{CP}} \tag{9.82}$$

Since $\tan^2 \beta_s \ll 1$, the heavy state, which is supposed to have the longer lifetime, will decay dominantly to $c\bar{c}s\bar{s}$ states with CP $= -1$, and the light, short-lived into CP $= +1$. This property is used to estimate the lifetime difference by measuring τ_{sL} from CP $= +1$ final states and τ_{sH} from CP $= -1$ final states.

9.3.2.1 The Formalism for Conserved CP

The situation would be different if a purely real CKM matrix could be achieved by choice of appropriate unphysical (quark) phases. In this case, all unitarity triangles would be degenerate to lines, and their angles would be 0 or π. Therefore, $\tan\alpha = \tan\beta = 0$, and the heavier state would be the **only** to decay to CP $= -1$, while CP $= +1$ final states would be reached exclusively via decays of B_L. For decay products which are CP eigenstates this situation would correspond to a perfectly predictable CP eigenvalue corresponding to the mass eigenstate B_L or B_H. A natural choice of phases in this case would force all terms of the weak interaction Hamiltonian to be real, corresponding to $\eta_m = e^{i\phi_{\mathrm{CP}B}}$. Then $\mathrm{CP}\,|B_L\rangle = +|B_L\rangle = |B_+\rangle$ and $\mathrm{CP}\,|B_H\rangle = -|B_H\rangle = -|B_-\rangle$, and CP is conserved in decays where this quantum number is meaningful.

In general, if CP is conserved η_m is a phase factor

$$\eta_m = e^{-i\phi_{\eta_m}}$$

as in (9.56). The Hamiltonian is then

$$\mathcal{H} = \begin{pmatrix} m - \frac{i}{2}\Gamma & -\frac{e^{i\phi_{\eta_m}}}{2}\left[\Delta m - \frac{i}{2}\Delta\Gamma\right] \\ -\frac{e^{-i\phi_{\eta_m}}}{2}\left[\Delta m - \frac{i}{2}\Delta\Gamma\right] & m - \frac{i}{2}\Gamma \end{pmatrix} = \begin{pmatrix} m - \frac{i}{2}\Gamma & -e^{i\phi_{\eta_m}}\frac{\Gamma}{2}(x - iy) \\ -e^{-i\phi_{\eta_m}}\frac{\Gamma}{2}(x - iy) & m - \frac{i}{2}\Gamma \end{pmatrix} \tag{9.83}$$

and

$$m_{12} = \tfrac{1}{2}(H_{12} + H_{21}^*) = -e^{i\phi_{\eta_m}} \frac{\Delta m}{2}$$
$$\Gamma_{12} = i(H_{12} - H_{21}^*) = -e^{i\phi_{\eta_m}} \frac{\Delta \Gamma}{2}$$

i. e. m_{12} and Γ_{12} have the same (unobservable) phase and the ratio Γ_{12}/m_{12} is real.

Starting from this situation, CP violation can be introduced as a perturbation via a small phase difference between m_{12} and Γ_{12}.

A more general approach starts from the Wigner-Weisskopf approximation (9.51). If CP is conserved, $\mathcal{H}_w = \mathrm{CP}^+ \mathcal{H}_w \mathrm{CP}$ and therefore the mixing Hamiltonian has

$$H_{21} = e^{2i\phi_{\mathrm{CP}B}} H_{12}$$

and $\eta_m = (\pm)e^{i\phi_{\mathrm{CP}B}}$.

Since $H_{21} = m_{12}^* + \frac{i}{2}\Gamma_{12}^* = e^{-2i\phi_{\mathrm{CP}B}}(m_{12} + \frac{i}{2}\Gamma_{12})$, this implies $m_{12} = |m_{12}|e^{i\phi_{\mathrm{CP}B}}$ and $\Gamma_{12} = |\Gamma_{12}|e^{i\phi_{\mathrm{CP}B}}$.

9.3.2.2 The Kaon as Approximate CP Invariant

Exactly this situation is **almost** true for the $K^0/\overline{K}^0$ system. The light K_S^0 decays to about 99.9% into the CP $= +1$ eigenstates $\pi^+\pi^-$ and $\pi^0\pi^0$, while the K_L^0 decays to one third into a CP $= -1$ eigenstate with 3 pions, the rest being mainly flavour specific semileptonic decays, and only 0.3% are to the CP $= +1$ two pion state. Therefore, a parametrization is chosen where $K_S^0 \approx K_+$ and $K_L^0 \approx K_-$. If we have a K_S^0 as decay product of the B, we are used to assign it a CP $= +1$ eigenvalue contribution to the whole final state. To be precise, this is only correct if the K_S^0 decays into a CP $= +1$ final state. In this case also a $K_L^0 \to \pi\pi$ will be assigned the same CP $= +1$ eigenvalue, i. e. the "K_S^0" denotes its final state rather than the undecayed particle, and a $K_S^0 \to \pi l \nu$ as a flavour specific state is not included in this use of the label K_S^0.

9.3.3 CP Violating Interference Effects in B Decays

The $B^0/\overline{B}^0$ meson system has a simple description in the Standard Model: One parameter x is sufficient to parametrize the oscillation, since $y = 0$ and $|\eta_m| = 1$ are good approximations.

CP violation in B decays (as in K decays) occurs always via interference of (at least) two amplitudes with different CP-even and CP-odd phases, in three different ways:

1. Direct CP violation $\Gamma(B \to X) \neq \Gamma(\overline{B} \to \overline{X})$ can be observed by final state counting experiments. It occurs from the interference of two decay amplitudes with different phases that transform as $\mathrm{CP}\,\phi = -\phi$ (CP-odd phases from the CKM matrix), and with different phases that transform as $\mathrm{CP}\,\delta = +\delta$ (CP-even phases from the strong interaction). Direct CP violation is not restricted to neutral mesons, but may also be observed in charged meson or baryon decays.
2. CP violation induces a small asymmetry in the oscillation probability $P(B^0 \to \overline{B}^0) \neq P(\overline{B}^0 \to B^0)$ due to $|\eta_m| \neq 1$. This is due to the interference of amplitudes with local (box diagram) and non-local intermediate states in $B/\overline{B}$ mixing.
3. The interference of mixed and unmixed amplitudes leads to lifetime dependent differences $\Gamma(B^0|_{t=0} \to X|_t) \neq \Gamma(\overline{B}^0|_{t=0} \to X|_t)$ for a common final state of B and $\overline{B}$ with asymmetry amplitude modulation $\propto \sin \Delta m\, t$. This is also called "CP violation from interference of oscillation and decay", or "mixing-induced CP violation". Here, the two interfering phases are phases from the CKM matrix that transform as $\mathrm{CP}\,\phi = -\phi$ and the phase $\frac{\pi}{2}$ between the coefficients $\cos x\frac{T}{2}$ and $i \sin x\frac{T}{2}$ from (9.36).

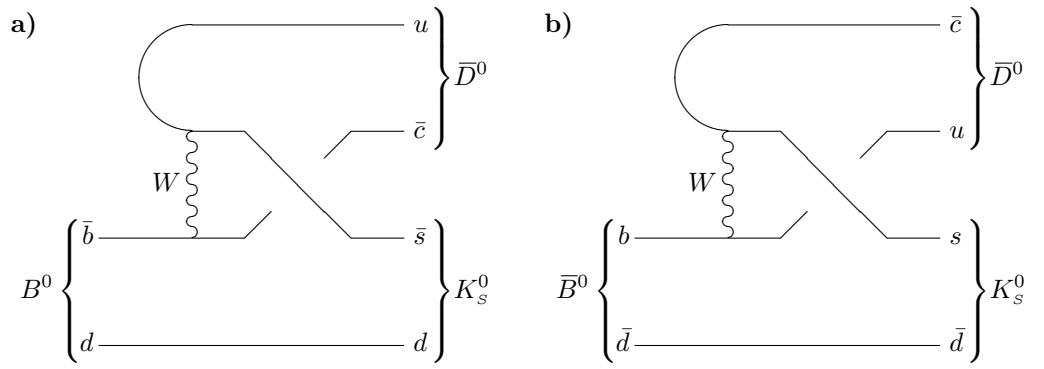

Fig. 9.12 Diagrams for $B^0 \to \overline{D}^0 K_S^0$ **(a)** and $\overline{B}^0 \to \overline{D}^0 K_S^0$ **(b)**.

The final state X can be a CP eigenstate, like $J/\psi\,(\pi\pi)_{K_S^0}$ (CP $= -1$) or $\pi^+\pi^-$ (CP $= +1$), or a state that can be reached from both B^0 mesons via different processes, like $B^0 \to \overline{D}^0 K_S^0$ and $\overline{B}^0 \to \overline{D}^0 K_S^0$ (figure 9.12).

In the Standard Model, CP violating interference can lead to almost maximum asymmetries. In many cases, large values are expected, and the time-dependence is a further handle to avoid misinterpretation of data.

9.3.4 Direct CP Violation

Decays with direct CP asymmetries require in the Standard Model at least two interfering channels with different CKM phase $\phi_{1,2}$ and different strong phases $\delta_{1,2}$. This defines the amplitudes

$$\begin{aligned} A(B^0 \to X) &= |A_1| e^{i\phi_1 + i\delta_1} + |A_2| e^{i\phi_2 + i\delta_2} \\ \overline{A}(\overline{B}^0 \to \overline{X}) &= |A_1| e^{-i\phi_1 + i\delta_1} + |A_2| e^{-i\phi_2 + i\delta_2} \end{aligned} \tag{9.84}$$

where $|A_1| e^{i\delta_1}$ and $|A_2| e^{i\delta_2}$ is unchanged due to CP invariance of the strong interaction. They contribute to the rates as

$$\begin{aligned} |A|^2 &= |A_1|^2 + |A_2|^2 + 2|A_1||A_2| \cos(\phi_1 - \phi_2 + \delta_1 - \delta_2) \\ |\overline{A}|^2 &= |A_1|^2 + |A_2|^2 + 2|A_1||A_2| \cos(\phi_2 - \phi_1 + \delta_1 - \delta_2) \end{aligned}$$

which are different if $\cos(\phi_2 - \phi_1 + \delta_1 - \delta_2) \neq \cos(\phi_1 - \phi_2 + \delta_1 - \delta_2)$. This is not the case if $\delta_1 = \delta_2$ or if $\phi_1 = \phi_2$. The difference is

$$\begin{aligned} |\overline{A}|^2 - |A|^2 &= 2|A_1||A_2|[\cos(\phi_2 - \phi_1 + \delta_1 - \delta_2) - \cos(\phi_1 - \phi_2 + \delta_1 - \delta_2)] \\ &= 4|A_1||A_2| \sin(\phi_1 - \phi_2) \sin(\delta_1 - \delta_2) \end{aligned}$$

The ratio of the amplitudes can be expressed as

$$\left| \frac{\overline{A}}{A} \right| = \frac{1 - \epsilon'_X}{1 + \epsilon'_X} \tag{9.85}$$

with a real parameter ϵ'_X. Due to the arbitrary phase factor $e^{-i\phi_{\mathrm{CP}B}}$ and the free CKM phases in A and $\overline{A}$ the complex ratio $\overline{A}/A$ itself is not an observable.

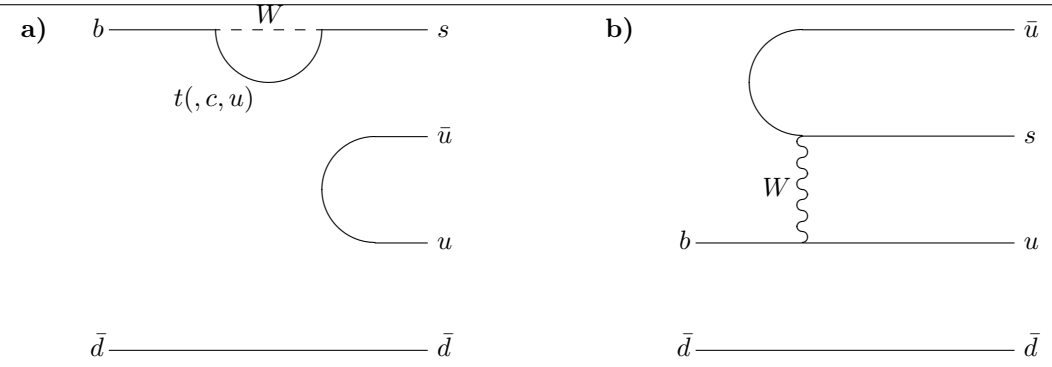

Fig. 9.13 Diagrams for $B^0 \to K^+\pi^-$: penguin **(a)** and tree **(b)**. The CKM elements for both amplitudes give a suppression of the tree diagram by a factor $\sim \lambda^2$.

The asymmetry is

$$\begin{aligned} a &= \frac{N(\overline{B} \to \overline{X}) - N(B \to X)}{N(\overline{B} \to \overline{X}) + N(B \to X)} \\ &= \frac{|\overline{A}|^2 - |A|^2}{|\overline{A}|^2 + |A|^2} \\ &= \frac{2|A_1||A_2| \sin(\phi_1 - \phi_2) \sin(\delta_1 - \delta_2)}{|A_1|^2 + |A_2|^2 + 2|A_1||A_2| \cos(\phi_1 - \phi_2) \cos(\delta_1 - \delta_2)} \end{aligned}$$

An example is the B decay to $K\pi$, where a rate asymmetry

$$a = \frac{N(\overline{B}^0 \to K^-\pi^+) - N(B^0 \to K^+\pi^-)}{N(\overline{B}^0 \to K^-\pi^+) + N(B^0 \to K^+\pi^-)}$$

with $|a| \lesssim 0.1$ is expected. In this example, the first amplitude is from a $b \to s$ penguin diagram (figure 9.13a) which has a dominant contribution from the t quark in the loop, with a CKM phase $\arg(V_{tb}^* V_{ts})$ and a $K\pi$ state with isospin $\frac{1}{2}$. The second amplitude occurs via a tree diagram $b \to u + \bar{u}s$ transition (figure 9.13b), with $\arg(V_{ub}^* V_{us})$ and isospin $\frac{1}{2}$ and $\frac{3}{2}$ amplitudes. The interference terms are proportional to $\sin\gamma' \sin(\delta_1 - \delta_2)$. Asymmetries of this type can also be observed in charged B decays, e. g. $B^\pm \to K^\pm\pi^0$.

The asymmetry is limited, however, by the ratio of amplitudes. This is approximately $P : \lambda^2 T$, where $P : T < 1$ reflects the suppression of the loop penguin diagram (P) with respect to a tree diagram (T) of same order. This ratio has been believed to be small, $P : T \sim \lambda^2$, which would allow indeed for large asymmetries, but is now known to be $\sim \lambda$ from the measurement of the $K\pi$ and $\pi\pi$ branching fractions.

CKM unitarity angles can only be extracted from those asymmetries when the strong phase difference is known. This can be obtained, however, from flavour SU(3) and isospin relations on a set of results from related channels.

9.3.4.1 Experimental Results

Experimental measurements of asymmetries of this type have been reported by various experiments.

The first evidence for CP violation was reported in 2004 by BABAR and BELLE[83] in the decay $B^0 \to K^-\pi^+$. No significant asymmetry is found in other decays by now (2012).

[83] BABAR Collab., Phys. Rev. Lett. **93**, 131801 (2004); Belle Collab., Phys. Rev. Lett. **93**, 191802 (2004).

9.3.5 CP Violation in the Oscillation

CP violation induces a small asymmetry in the oscillation probability $P(B^0 \to \overline{B}^0) \neq P(\overline{B}^0 \to B^0)$ due to $|\eta_m| \neq 1$. This is due to the interference of non-local amplitudes with the leading box diagram of $B/\overline{B}$ mixing. A CP-even phase is the $i = e^{i\pi/2}$ between m_{12} and Γ_{12}, while the CP-odd phases are the phases of the CKM matrix.

The oscillation asymmetry (9.43) starting with an initial B^0 meson can be expanded in δ_ϵ as

$$a(T) = \left.\frac{\dot{N}(B) - \dot{N}(\overline{B})}{\dot{N}(B) + \dot{N}(\overline{B})}\right|_T = \frac{\cos xT}{\cosh yT} + \delta_\epsilon \left(1 - \frac{\cos^2 xT}{\cosh^2 yT}\right) + \mathcal{O}(\delta_\epsilon^2) \tag{9.86}$$

which is for $y = 0$

$$a(T) \approx \cos xT + \delta_\epsilon \sin^2 xT = \cos xT + \frac{\delta_\epsilon}{2}(1 - \cos 2xT)$$

Starting with a $\overline{B}^0$ at $T = 0$ gives for the same asymmetry

$$\bar{a}(T) = \left.\frac{\dot{N}(B) - \dot{N}(\overline{B})}{\dot{N}(B) + \dot{N}(\overline{B})}\right|_T \approx -\cos xT + \frac{\delta_\epsilon}{2}(1 - \cos 2xT) \tag{9.87}$$

i. e. if $\delta_\epsilon < 0$ there are always more $B \to \overline{B}$ than $\overline{B} \to B$ oscillations. Using leptons as flavour tag the net asymmetry can be observed at the $\Upsilon(4S)$ by counting like-sign lepton pairs which originate directly from semileptonic neutral B meson decays. They occur in final states with mixing and show an asymmetry

$$a = \frac{N(B\overline{B} \to l^+l^+) - N(B\overline{B} \to l^-l^-)}{N(B\overline{B} \to l^+l^+) + N(B\overline{B} \to l^-l^-)} = \frac{1 - |\eta_m|^4}{1 + |\eta_m|^4} = \frac{2\delta_\epsilon}{1 + \delta_\epsilon^2} \tag{9.88}$$

constant in time. This asymmetry should be very small in the Standard Model and will be discussed below.

The quantity δ_ϵ is often quoted as $2\,\mathcal{R}e\,\epsilon_B$ which is incorrect, since the mixing parameter ϵ_m is convention-dependent. Neither $\mathcal{R}e\,\epsilon_m$ nor $\mathcal{I}m\,\epsilon_m$ nor $|\epsilon_m|$ are observables, only one function of this complex parameter

$$\delta_\epsilon = \frac{2\,\mathcal{R}e\,\epsilon_m}{1 + |\epsilon_m|^2}$$

is a measurable quantity and can indeed be observed as an CP violating asymmetry in $B/\overline{B}$ oscillation.

9.3.5.1 Theoretical Predictions

To leading order in Γ_{12}/m_{12} equation (9.25) yields

$$|\eta_m| - 1 = -\tfrac{1}{2}\,\mathcal{I}m\,\frac{\Gamma_{12}}{m_{12}} \approx \frac{2\pi}{S(m_t^2/m_W^2)}\,\frac{m_c^2}{m_W^2}\,\mathcal{I}m\,\frac{V_{cb}V_{cd}^*}{V_{tb}V_{td}^*} \tag{9.89}$$

from (9.58). This leads to a rough estimate of the convention-independent number

$$\delta_\epsilon \approx 1 - |\eta_m| \approx -2\pi\frac{m_c^2}{m_t^2}\,\frac{|V_{cb}||V_{cd}|}{|V_{tb}||V_{td}|}\,\sin\beta \sim -\frac{\sin\beta}{2000} \tag{9.90}$$

with $|\delta_\epsilon| \ll 1$ where β is the CKM unitarity angle in figure 9.1a. Since this result is based on a leading order quark diagram, the number should be taken only as an order of magnitude. In particular, at this level of precision it can not be used to measure β.

Replacing d with s, equation (9.90) can be used to estimate $\delta_{\epsilon s} \sim \sin\beta_s/2000 \sim 10^{-5}$. Again, large corrections to this simple calculation may be expected.

9.3.5.2 The Total Decay Rate

This same parameter can also been observed as an asymmetry in the time-dependent total decay rate of B and $\overline{B}$. This rate for an initially pure B^0 sample can be calculated as

$$\frac{\mathrm{d}N}{\mathrm{d}t} = N_0 \sum_X \int \mathrm{dPS}\,|\mathcal{M}|^2\,\delta(m_B - E_X)$$

The amplitude for $B|_{t=0} \to X|_{t=t}$ is derived from (9.36) as

$$\mathcal{M}(B^0 \to X) = e^{-imt-T/2} A \Big\{ \cos(x-iy)\frac{T}{2} + ir\sin(x-iy)\frac{T}{2} \Big\} \tag{9.91}$$

using the ratio

$$r := \frac{\eta_m \overline{A}}{A} \tag{9.92}$$

where $A = A(B^0 \to X)$ and $\overline{A} = A(\overline{B}^0 \to X)$ are the decay amplitudes of the flavour eigenstates, and the latter occurs in combination with the oscillation $B^0 \to \overline{B}^0$. The amplitude for $\overline{B}\big|_{t=0} \to X|_{t=t}$ is correspondingly

$$\overline{\mathcal{M}}(\overline{B}^0 \to X) = e^{-imt-T/2} \overline{A} \Big\{ \cos(x-iy)\frac{T}{2} + \frac{i}{r}\sin(x-iy)\frac{T}{2} \Big\} \tag{9.93}$$

As in direct CP violation, the asymmetry emerges from an interference of a CP-odd phase from the CKM matrix in η_m for mixing alone or in r for mixing and decay, and a CP-even phase, which is the $-i = e^{-i\pi/2}$ factor of the cos-term in both (9.91) and (9.93).

The decay rates are proportional to

$$\begin{aligned}
|\mathcal{M}|^2 &= e^{-T}\Big\{ |A|^2 \Big|\cos(x-iy)\frac{T}{2}\Big|^2 + |A|^2|r|^2 \Big|\sin(x-iy)\frac{T}{2}\Big|^2 \\
&\qquad + i\sin x\frac{T}{2}\cos x\frac{T}{2}(A^*\overline{A}\eta_m - A\overline{A}^*\eta_m^*) + \sinh y\frac{T}{2}\cosh y\frac{T}{2}(A^*\overline{A}\eta_m + A\overline{A}^*\eta_m^*)\Big\} \qquad (9.94)\\
&= e^{-T}|A|^2\Big\{\frac{1+|r|^2}{2}\cosh yT + \frac{1-|r|^2}{2}\cos xT + |r|\cos(\arg r)\sinh yT - |r|\sin(\arg r)\sin xT\Big\}\\
&= e^{-T}|A|^2\Big\{\frac{1+|r|^2}{2}\cosh yT + \frac{1-|r|^2}{2}\cos xT + \mathcal{R}e\,r\,\sinh yT - \mathcal{I}m\,r\,\sin xT\Big\} \qquad (9.94a)\\
|\overline{\mathcal{M}}|^2 &= e^{-T}|\overline{A}|^2\Big\{\frac{1+|r|^2}{2|r|^2}\cosh yT - \frac{1-|r|^2}{2|r|^2}\cos xT + \frac{\cos(\arg r)}{|r|}\sinh yT + \frac{\sin(\arg r)}{|r|}\sin xT\Big\}\\
&= e^{-T}\frac{|A|^2}{|\eta_m|^2}\Big\{\frac{1+|r|^2}{2}\cosh yT - \frac{1-|r|^2}{2}\cos xT + \mathcal{R}e\,r\,\sinh yT + \mathcal{I}m\,r\,\sin xT\Big\} \qquad (9.94b)
\end{aligned}$$

For the sum over all decays, we replace $\sum_X |A|^2 \to \Gamma$, $\sum_X |\overline{A}|^2 \to \Gamma$, $|r|^2 \to |\eta_m|^2$ and $\sum_X A^*\overline{A} \to \sum_X \langle B^0|\mathcal{H}_w|X\rangle\langle X|\mathcal{H}_w|\overline{B}^0\rangle = \Gamma_{12}$. From (9.27) one can write

$$\begin{aligned}
\sum_X \eta_m A^*\overline{A} = \eta_m\Gamma_{12} &= i\eta_m(H_{12} - H_{21}^*)\\
&= \frac{\Gamma}{2}\left[-ix(1-|\eta_m|^2) - y(1+|\eta_m|^2)\right]\\
&\approx \Gamma(1-\delta_\epsilon)\left[-ix\delta_\epsilon - y\right]
\end{aligned}$$

where the last line is an approximation for $\delta_\epsilon \ll 1$, which is good for all four meson pairs. This yields a total rate

$$\frac{\mathrm{d}N}{\mathrm{d}t} = N_0\,\Gamma\frac{1}{1+\delta_\epsilon}e^{-T}\Big\{\cosh yT + \delta_\epsilon\cos xT - y\sinh yT + x\delta_\epsilon\sin xT\Big\} \tag{9.95}$$

using $(1+|\eta_m|^2)\cdot(1+\delta_\epsilon)\equiv 2$. The total number of decays is the initial number of mesons N_0, as can be verified from

$$\begin{aligned}\int_0^\infty \frac{\mathrm{d}N}{\mathrm{d}t}\,\mathrm{d}t &= \frac{1}{\Gamma}\int_0^\infty \frac{\mathrm{d}N}{\mathrm{d}t}\,\mathrm{d}T = N_0\frac{1+|\eta_m|^2}{2}\left\{\frac{1}{1-y^2}+\delta_\epsilon\frac{1}{1+x^2}-y\frac{y}{1-y^2}+x\delta_\epsilon\frac{x}{1+x^2}\right\}\\ &= N_0\end{aligned} \tag{9.96}$$

In the approximation $y=0$ expected to be good for the B^0 the rate is

$$\frac{\mathrm{d}N}{\mathrm{d}t} = N_0\Gamma e^{-T}\left[1+\delta_\epsilon\cdot(-1+\cos xT + x\sin xT)\right]+\mathcal{O}(\delta_\epsilon^2) \tag{9.97}$$

An initially pure $\overline{B}^0$ sample gives the same rates with the replacement $\eta_m \longleftrightarrow 1/\eta_m$ and $\delta_\epsilon \longleftrightarrow -\delta_\epsilon$. The asymmetry (where the B flavour is understood as the one at $T=0$) is therefore

$$\begin{aligned}a(T) &= \left.\frac{\dot{N}(\overline{B}^0\to\text{anything})-\dot{N}(B^0\to\text{anything})}{\dot{N}(\overline{B}^0\to\text{anything})+\dot{N}(B^0\to\text{anything})}\right|_T\\ &= \delta_\epsilon\,(1-\cos xT - x\sin xT)\\ &= 2\delta_\epsilon\left(-\frac{x}{2}\sin xT+\sin^2\frac{xT}{2}\right)\end{aligned} \tag{9.98}$$

Another approximation, $\delta_\epsilon=0$, gives the total decay rate of the B_s from (9.95) as

$$\frac{\mathrm{d}N}{\mathrm{d}t} = N_0\,\Gamma e^{-T}\Big\{\cosh yT - y\sinh yT\Big\} \propto \Gamma_H e^{-\Gamma_H t}+\Gamma_L e^{-\Gamma_L t}$$

that has been used to obtain an upper limit on y_s.

9.3.5.3 Experimental Results

Experimental results using like-sign lepton pairs have been obtained at CLEO and at the B factories.

Measurements of the total asymmetry were performed at LEP. CPT conservation is assumed in these results. The present (2012) world average is

$$\delta_\epsilon = -0.0016\pm 0.0016$$

for the B^0 and

$$\delta_\epsilon = -0.0052\pm 0.0032$$

for the B_s meson.

9.3.6 CP Violation in Common Final States of B^0 and $\overline{B}^0$

The most pronounced manifestation of CP violation in the $B^0/\overline{B}^0$ system is observed in interference of oscillation and decay to final states common to B^0 and $\overline{B}^0$. The effect is largest for CP eigenstates, but may occur at any final state where the amplitudes of the mixed and unmixed decay can interfere:

$$\begin{array}{ccc} & \overline{B}^0 & \\ \nearrow & & \searrow \\ B^0 & \longrightarrow & X \end{array} \tag{9.99}$$

As in oscillation, the asymmetry is caused by an interference of a CP-odd phase from the CKM matrix in r and the CP-even phase $-i = e^{-i\pi/2}$ of the cos-term in both (9.91) and (9.93).

The simplest situation is the evolution of an isolated B^0 meson produced (e. g. incoherently in $b\bar{b}$ fragmentation) at $t = 0$ as a flavour eigenstate. An unambiguous flavour tag for the state at production time may be a charged state from the second b, which cannot mix. The amplitude for $B|_{t=0} \to X|_{t=t}$ is (9.91) where the ratio of the upper and lower path's amplitudes in (9.99) is

$$r := \eta_m \frac{\bar{A}}{A} = \frac{\langle \bar{B}^0 | B_L \rangle}{\langle B^0 | B_L \rangle} \frac{\langle X | \mathcal{H} | \bar{B}^0 \rangle}{\langle X | \mathcal{H} | B^0 \rangle} \tag{9.100}$$

The cos-term in (9.91) describes the lower path with pure $B/\bar{B}$ oscillation, while the sin-term is a true interference term that vanishes if $r = 0$. The amplitude for $\bar{B}|_{t=0} \to X|_{t=t}$ is (9.93). If X is a CP eigenstate, the ratio $\bar{A}/A$ is often just a phase, which includes the sign of the CP eigenvalue of X. The phase of the product r is independent of conventions, and is in fact an observable, as will be shown below. More general, A and $\bar{A}$ can have also different magnitudes, which in the absence of oscillation would still imply an asymmetry and corresponds to the direct CP violation of non-oscillating particles. This direct CP violation is responsible for the cos-term in (9.91) for final states that can be reached by both B^0 and $\bar{B}^0$. Figure 9.12 shows an example for this case, where the diagrams for $B^0 \to \bar{D}^0 K_S^0$ and $\bar{B}^0 \to \bar{D}^0 K_S^0$ are different. Another example is a mixture of CP eigenstates, as in the final state $D^{*+}D^{*-}$ which is CP $= -1$ for $L = 1$ and CP $= +1$ for $L = 0$ or 2.

The corresponding decay rates are proportional to $|\mathcal{M}|^2$ of (9.94a) and $|\overline{\mathcal{M}}|^2$ of (9.94b) where the oscillating interference term is proportional to

$$\tfrac{1}{2}(A^* \bar{A} \eta_m - A \bar{A}^* \eta_m^*) = \mathcal{I}m(A^* \bar{A} \eta_m) = |A|^2 |r| \sin \arg r = |A|^2 \cdot \mathcal{I}m\, r$$

and the relaxation part of the interference is proportional to $|r| \cos \arg r = \mathcal{R}e\, r$. For decays to CP eigenstates, $|r| = |\eta_m| \approx 1$ and the amplitude of the asymmetry oscillation is the sine of the phase angle $\arg r$. For decays like $B^0/\bar{B}^0 \to D^0 K_S^0$ where $|A| \neq |\bar{A}|$ and consequently $|r| \neq 1$, the asymmetry oscillation gets a physical dilution factor

$$D_P = \frac{2|r|}{1 + |r|^2} = \frac{2|A||\bar{A}|}{|A|^2 + |\bar{A}|^2}$$

to the $\sin xT$ term, and a mixing contribution as an additional $\cos xT$ term. Using the parameters[84]

$$\Omega_0 := \frac{2\,\mathcal{R}e\, r}{1 + |r|^2} = D_P \cos \arg r, \qquad \Lambda_0 := \frac{2\,\mathcal{I}m\, r}{1 + |r|^2} = D_P \sin \arg r, \qquad \Theta_0 := \frac{|r|^2 - 1}{|r|^2 + 1} \tag{9.101}$$

which are given by the two real numbers $\mathcal{R}e\, r$ and $\mathcal{I}m\, r$ and related via

$$\Omega_0^2 + \Lambda_0^2 + \Theta_0^2 = 1 \tag{9.102}$$

so that always two define the third one up to a sign. We can rewrite

$$|\mathcal{M}|^2 = e^{-T} |A|^2 \frac{1 + |r|^2}{2} \Big\{ \cosh yT - \Theta_0 \cos xT + \Omega_0 \sinh yT - \Lambda_0 \sin xT \Big\} \tag{9.94a'}$$

$$|\overline{\mathcal{M}}|^2 = e^{-T} \frac{|A|^2}{|\eta_m|^2} \frac{1 + |r|^2}{2} \Big\{ \cosh yT + \Theta_0 \cos xT + \Omega_0 \sinh yT + \Lambda_0 \sin xT \Big\} \tag{9.94b'}$$

[84] Another set of parameters in use is

$$S = \Lambda_0, \qquad C = \frac{1 - |r|^2}{1 + |r|^2} = -\Theta_0$$

(note the minus sign), and alternative names are $\mathcal{S} = \Lambda_0$ and $\mathcal{A} = \Theta_0$.

This corresponds to a general asymmetry function[85]

$$\begin{aligned} a(T) &= \left.\frac{\dot{N}(\overline{B}\to X)-\dot{N}(B\to X)}{\dot{N}(\overline{B}\to X)+\dot{N}(B\to X)}\right|_T = \frac{|\overline{\mathcal{M}}|^2-|\mathcal{M}|^2}{|\overline{\mathcal{M}}|^2+|\mathcal{M}|^2} \\ &= \frac{\Theta_0\cos xT+\Lambda_0\sin xT+\delta_\epsilon(\cosh yT+\Omega_0\sinh yT)}{\cosh yT+\Omega_0\sinh yT+\delta_\epsilon(\Theta_0\cos xT+\Lambda_0\sin xT)} \end{aligned} \tag{9.103}$$

The slightly simplified form as expected for the $B_s/\overline{B}_s$ system is

$$a(T) = \left.\frac{\dot{N}(\overline{B}_s\to X)-\dot{N}(B_s\to X)}{\dot{N}(\overline{B}_s\to X)+\dot{N}(B_s\to X)}\right|_T = \frac{\Theta_0\cos xT+\Lambda_0\sin xT}{\cosh yT+\Omega_0\sinh yT} = \frac{a_0\sin(xT+\phi_0)}{\cosh yT+\Omega_0\sinh yT} \tag{9.104}$$

where $\delta_{\epsilon s}=0$ (corresponding to $|\eta_{ms}|=1$) is used, which is believed to be a very good approximation. Under this condition, Θ_0 describes direct CP violation, and is for $X=\overline{X}$ equivalent to the time-integrated asymmetry parameter for self-tagging modes or $B^\pm$ decays

$$a = \frac{\dot{N}(\overline{B}\to\overline{X})-\dot{N}(B\to X)}{\dot{N}(\overline{B}\to\overline{X})+\dot{N}(B\to X)} = \Theta_0$$

while Λ_0 parametrizes the interference of oscillation and decay.

The parameter-triplet $(\Omega_0,\Lambda_0,\Theta_0)$ is forced to be on the unit sphere through (9.102), and can be given by the polar angle and azimuth (see figure 9.14)

$$\cos\theta_{\Omega\Lambda\Theta} = \frac{|r|^2-1}{|r|^2+1} = \sqrt{1-D_P^2}, \qquad \phi_{\Omega\Lambda\Theta} = \arg r$$

The physical dilution factor is $D_P=\sqrt{\Omega_0^2+\Lambda_0^2}$. The asymmetry amplitude at $T=0$ is

$$a_0 = \sqrt{\Lambda_0^2+\Theta_0^2} = \sqrt{1-\Omega_0^2}$$

and the phase is given by

$$\tan\phi_0 = \frac{\Theta_0}{\Lambda_0}$$

In the approximation $|\eta_m|=1$ and $y=0$ the rates are given by

$$\begin{aligned} |\mathcal{M}|^2 &= e^{-T}\left\{\frac{|A|^2+|\bar{A}|^2}{2}+\frac{|A|^2-|\bar{A}|^2}{2}\cos xT-|A||\bar{A}|\sin(\arg r)\,\sin xT\right\} \\ |\overline{\mathcal{M}}|^2 &= e^{-T}\left\{\frac{|A|^2+|\bar{A}|^2}{2}-\frac{|A|^2-|\bar{A}|^2}{2}\cos xT+|A||\bar{A}|\sin(\arg r)\,\sin xT\right\} \end{aligned} \tag{9.105}$$

These lead to an oscillating asymmetry as a function of the proper lifetime of the signal-B

$$a(T) = \left.\frac{\dot{N}(\overline{B}^0\to X)-\dot{N}(B^0\to X)}{\dot{N}(\overline{B}^0\to X)+\dot{N}(B^0\to X)}\right|_T = \Theta_0\cos xT+\Lambda_0\sin xT \tag{9.106}$$

[85] This definition of the asymmetry is consistent with the definition of r, however, the opposite sign $a\to -a$ is also used in the literature, leading to flipped signs in the coefficients. To add to the confusion, when checking signs one has also to distinguish $N(\overline{B}\to X)=N(B+X)$, where the right hand side denotes the flavour of the tag, and the left hand side the flavour of the signal at $T=0$.

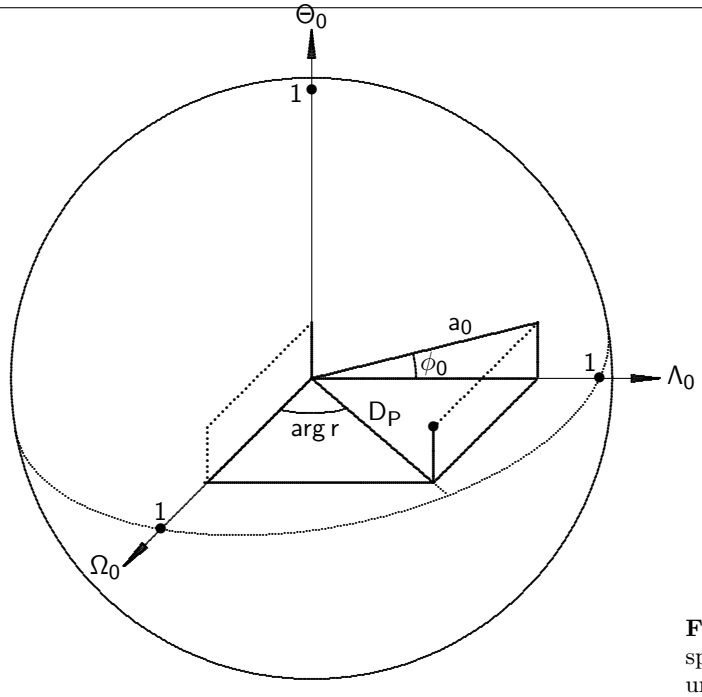

Fig. 9.14 The $(\Omega_0, \Lambda_0, \Theta_0)$ parameter space. All valid parameter sets are on the unit sphere.

where the B flavours are taken at $T = 0$, and the amplitudes are given by (9.101). If in addition $|A| = |\bar{A}|$, especially if X is a CP eigenstate, this simplifies further to $|r| = 1$:

$$\begin{aligned} |\mathcal{M}|^2 &= e^{-T}|A|^2\Big\{1 - \sin(\arg r)\sin xT\Big\} \\ |\overline{\mathcal{M}}|^2 &= e^{-T}|A|^2\Big\{1 + \sin(\arg r)\sin xT\Big\} \end{aligned} \tag{9.107}$$

The corresponding rates $\dot{N}(B^0|_{T=0} \to X) \propto |\mathcal{M}|^2$ and $\dot{N}(\overline{B}^0|_{T=0} \to X) \propto |\overline{\mathcal{M}}|^2$ are illustrated in figure 9.15. They show a time-dependent asymmetry

$$a(T) = \left.\frac{\dot{N}(\overline{B}^0 \to X) - \dot{N}(B^0 \to X)}{\dot{N}(\overline{B}^0 \to X) + \dot{N}(B^0 \to X)}\right|_T = \Lambda_0 \sin xT \tag{9.108}$$

with $\Lambda_0 = \sin\arg r$.

The dimensionless time variable is $T = t_s/\tau$ defined by the signal B lifetime t_s for incoherent $b\bar{b}$ production. For coherent $B\overline{B}$ production on the $\Upsilon(4S)$, it has to be replaced by $T = (t_s - t_t)/\tau$ where t_t denotes the second B meson in the $\Upsilon(4S)$ decay in a flavour tagging decay mode. Also, the factor e^{-T} has to be replaced by $e^{-|T|}$, which originates from the integration over the unobserved $t_s + t_t$. This is in full analogy to the mixing situation described in section 9.2.11, and will be discussed in more detail below.

9.3.6.1 CP Violation Described by r

The ratio r in (9.100) may include in fact all three types of CP violation:

- direct CP violation if $|\bar{A}/A| \neq 1$,
- CP violation in the oscillation if $|\eta_m| \neq 1$,
- and CP violation from interference of mixed and unmixed amplitudes if $\mathcal{I}m\, r \neq 0$.

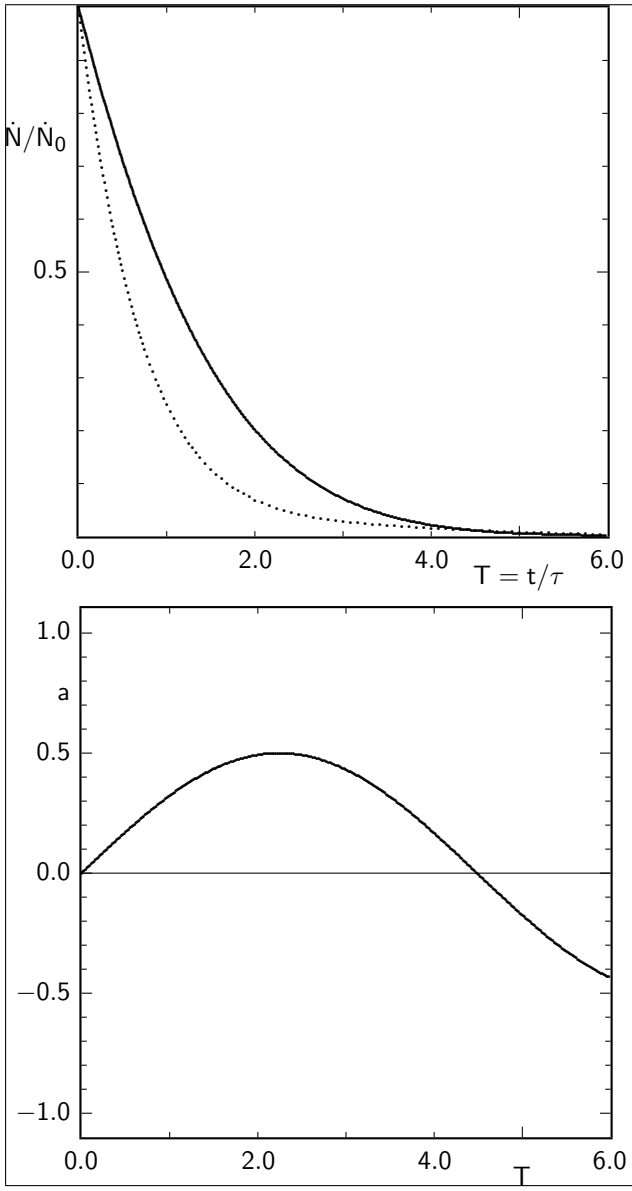

Fig. 9.15 Time dependent rate of $\overline{B}^0 \to J/\psi K_S^0$ (——) and $B^0 \to J/\psi K_S^0$ (·····) for $\Lambda_0 = \sin 2\beta = 0.5$ and $x = 0.70$. The lower plot shows the asymmetry $a(T)$.

If the small effect of CP violation in the oscillation is ignored, one can split the complex number r into two pieces, $|r| - 1$ describing direct CP violation and $\arg r$ describing the CP violating interference of mixed and unmixed amplitudes. The first can be derived from Θ_0 as

$$|r| = \sqrt{\frac{1+\Theta_0}{1-\Theta_0}} \tag{9.109}$$

Since

$$D_P = \sqrt{1-\Theta_0^2}$$

the phase is obtained as

$$\arg r = \arcsin \frac{\Lambda_0}{\sqrt{1-\Theta_0^2}} \tag{9.110}$$

and is dominated by Λ_0 for small values of Θ_0.

For B and B_s mesons, where $|\eta_m| = 1$ is a good approximation, we have $|r| \approx |\bar{A}/A|$. So here direct CP violation is given by

$$\frac{|\bar{A}|^2 - |A|^2}{|\bar{A}|^2 + |A|^2} = \frac{|r|^2 - 1}{|r|^2 + 1} = \Theta_0 \tag{9.111}$$

9.3.6.2 The Eigenstate Parametrization

Instead of the ratio (9.100) one may use in analogy to the terminology of kaon physics

$$\eta := \frac{A_H}{A_L} \tag{9.112}$$

where $A_{H,L} = A(B_{H,L} \to X)$ are the decay amplitudes of the mass (and width) eigenstates. If one leaves a free relative phase between B_H and B_L, one has to define, using (9.26)

$$\eta := \frac{A_H}{A_L}\frac{\langle B^0|B_L\rangle}{\langle B^0|B_H\rangle} = -\frac{A_H}{A_L}\frac{\langle \overline{B}^0|B_L\rangle}{\langle \overline{B}^0|B_H\rangle} \tag{9.113}$$

which is determined unambiguously. It is related to the ratio r via

$$\eta = \frac{1-r}{1+r} = i\tan i\frac{\ln r}{2}, \qquad r = \frac{1-\eta}{1+\eta} = i\tan i\frac{\ln \eta}{2}$$

The asymmetry parameters can be calculated as

$$\Omega_0 := \frac{1-|\eta|^2}{1+|\eta|^2}, \qquad \Lambda_0 := -\frac{2\,\mathcal{I}m\,\eta}{1+|\eta|^2}, \qquad \Theta_0 := -\frac{2\,\mathcal{R}e\,\eta}{1+|\eta|^2} \tag{9.114}$$

which implies

$$a_0 = \frac{2|\eta|}{1+|\eta|^2}, \qquad \phi_0 = -\frac{\pi}{2} - \arg\eta \Leftrightarrow \arg\eta = -\frac{\pi}{2} - \phi_0$$

or $\eta = -i|\eta|e^{-i\phi_0}$

9.3.6.3 Parameters for Conserved CP

The parameters $\Omega_0, \Lambda_0, \Theta_0$ describe also oscillation phenomena if CP is conserved.

The special cases $r = 0$ and $r = \infty$ correspond to a final state that occurs only from one flavour. The corresponding parameter set

$$\Omega_0 = 0, \qquad \Lambda_0 = 0, \qquad \Theta_0 = \mp 1$$

describes the pure $B\overline{B}$ oscillation

$$a(T) = \mp\cos xT$$

(for $\delta_\epsilon = 0$).

If there is a small, suppressed amplitude from the second flavour, but no CP violating phase difference, we have a real ratio $r \ll 1$. In this case, the parameters are

$$\Omega_0 = \frac{2r}{1+r^2} \approx 2r, \qquad \Lambda_0 = 0, \qquad \Theta_0 = \frac{r^2-1}{r^2+1} \approx -1$$

corresponding to an asymmetry

$$a(T) = \frac{-\cos xT}{\cosh yT + 2r \sinh yT}$$

In the case of final CP eigenstates and conserved CP, the values are $r = \pm 1$ and

$$\Omega_0 = \pm 1, \qquad \Lambda_0 = 0, \qquad \Theta_0 = 0$$

corresponding to

$$a(T) = 0$$

i. e. equal differential decay rates for B and $\overline{B}$.

9.3.6.4 The $B_s/\overline{B}_s$ Case

For the B_s meson, y is not negligible, and the asymmetry oscillation (9.106) is modulated as given by (9.104). For the simpler case $|r| = 1$ the asymmetry is

$$a(T) = \left.\frac{\dot{N}(\overline{B}_s \to X) - \dot{N}(B_s \to X)}{\dot{N}(\overline{B}_s \to X) + \dot{N}(B_s \to X)}\right|_T = \frac{\Lambda_0 \sin xT}{\cosh yT + \Omega_0 \sinh yT} \tag{9.115}$$

with $\Lambda_0 = \sin \arg r$ and $\Omega_0 = \cos \arg r$.

The envelope function modulating the asymmetry amplitude

$$f(T) = \frac{1}{\cosh yT + \Omega_0 \sinh yT} \tag{9.116}$$

has a maximum

$$f(T_0) = \frac{1}{\sqrt{1 - \Omega_0^2}} \qquad \text{at} \qquad T_0 = \frac{1}{2y} \ln \frac{1 - \Omega_0}{1 + \Omega_0} = -\frac{\operatorname{Artanh} \Omega_0}{y}$$

and a width

$$\text{FWHM} = \frac{2 \ln(2 + \sqrt{3})}{|y|} \approx \frac{2.634}{|y|}$$

The maximum asymmetry amplitude at $T = T_0$ is

$$\frac{a_0}{\sqrt{1 - \Omega_0^2}} = 1$$

due to (9.102). In the case $|r| = 1$ (where $\Theta_0 = 0$) the asymmetry amplitude is

$$\frac{\Lambda_0}{\sqrt{1 - \Omega_0^2}} = 1$$

This effect is illustrated in figure 9.16, using $x = 8$, $y = -0.2$, $\Theta_0 = 0$, and $\Lambda_0 = 0.2$, corresponding to $\Omega_0 = 0.9798$. The asymmetry amplitude is amplified to its maximum possible value of 1 at $T_0 \approx 11.5$, i. e. more than 11 mean lifetimes from production. At that time, only a fraction $e^{-T_0} \approx 10^{-5}$ of all B_s mesons is left. For more realistic smaller $|y|$ values, the maximum is even further out.

Note that both the sign of Λ_0 and Ω_0 change with the CP eigenvalue of an eigenstate. Therefore one of a pair of two always has the maximum on the negative T axis, which is not accessible in a jet production experiment.

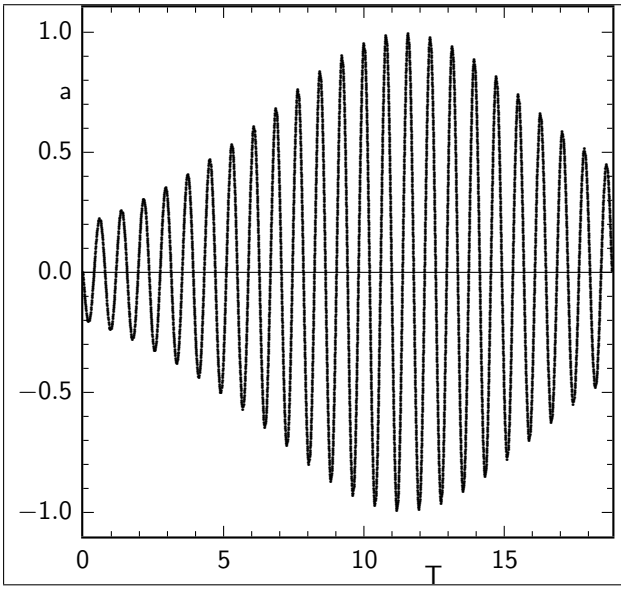

Fig. 9.16 Time dependent asymmetry for $B_s/\overline{B}_s \to$ CP eigenstate, assuming for $\Lambda_0 = -0.2$, $\Omega_0 > 0$, $x = 8$ and $y = -0.2$ (these unrealistic values are chosen for illustration of the effects).

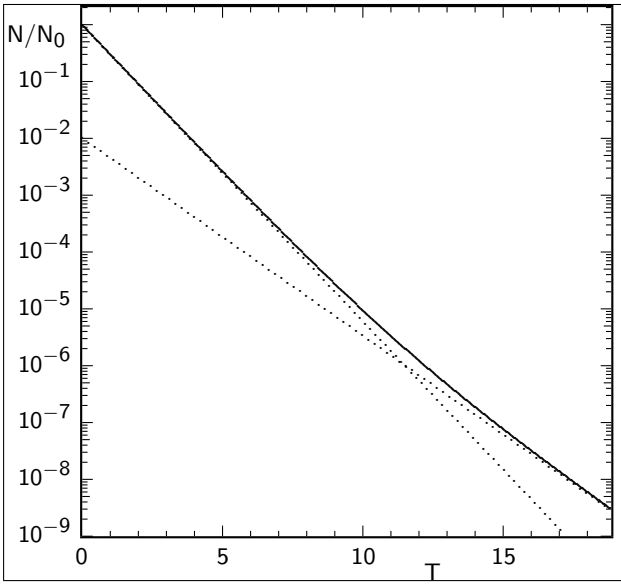

Fig. 9.17 The two components B_{sH} and B_{sL} of the $B_s + \overline{B}_s$ decay to a CP eigenstate for the parameter set of figure 9.16. The maximum CP asymmetry occurs at the point where the B_{sH} and B_{sL} components of this decay are equal.

The modulation function (9.116) can be rewritten as

$$f(T) = \frac{2}{(1+\Omega_0)e^{yT} + (1-\Omega_0)e^{-yT}}$$

The maximum corresponds to the minimum of the denominator, which is the position where

$$(1+\Omega_0)e^{yT} = (1-\Omega_0)e^{-yT}$$

or, multiplying with e^{-T} and using (9.24), where

$$(1+\Omega_0)e^{-t/\tau_L} = (1-\Omega_0)e^{-t/\tau_H}$$

This is exactly the point, where B_{sL} and B_{sH} contribute equally to the decay probability

$$\begin{aligned} |\mathcal{M}|^2 + |\overline{\mathcal{M}}|^2 &= 2e^{-|T|}|A|^2 \left\{\cosh yT + \cos\arg r \cdot \sinh yT\right\} \\ &= |A|^2 \left\{(1+\Omega_0)e^{-t/\tau_L} + (1-\Omega_0)e^{-t/\tau_H}\right\} \end{aligned} \tag{9.117}$$

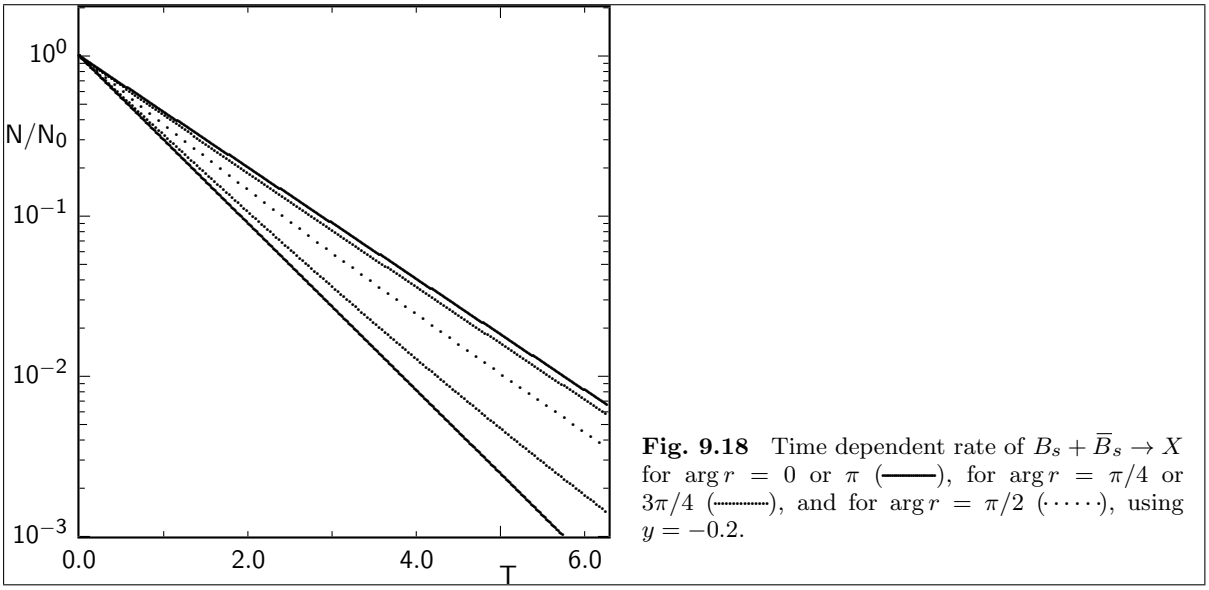

Fig. 9.18 Time dependent rate of $B_s + \overline{B}_s \to X$ for $\arg r = 0$ or π (——), for $\arg r = \pi/4$ or $3\pi/4$ (·····), and for $\arg r = \pi/2$ (· · · · ·), using $y = -0.2$.

as illustrated in figure 9.17. A completely equivalent point of view to the interference of $B_s \to X$ and $B_s \to \overline{B}_s \to X$ amplitudes is the picture of interfering B_{sL} and B_{sH} states. In this picture, it becomes obvious that the interference is maximum at the point where both states contribute with equal magnitude.

The time evolution of an equal, untagged mixture of B_s and $\overline{B}_s$ mesons is given by

$$|\mathcal{M}|^2 + |\overline{\mathcal{M}}|^2 = 2e^{-|T|}|A|^2 \frac{1+|r|^2}{2}\Big\{\cosh yT + \Omega_0 \sinh yT\Big\} \tag{9.118}$$

For decays into CP eigenstates ($|r| = 1$) the time dependence of the decay probability is simply (9.117), i. e. it is a sum of two exponential distributions with weights $(1 \pm \Omega_0) = (1 \pm \cos\arg r)$. This opens an alternative way to measure the CP violation parameter $\arg r$, as illustrated in figure 9.18 on a logarithmic scale. The upper and lower solid curve correspond to the CP conserving case $r = \pm 1$, where e. g. B_{sL} decays into either CP $= +1$ or CP $= -1$ eigenstates exclusively, and B_{sH} into the opposite one. The central curve corresponds to maximum CP violation, i. e. $\mathcal{R}e\, r = 0$, where both B_{sL} and B_{sH} decay into CP $= +1$ and CP $= -1$ eigenstates with the same probability, The other two curves correspond to $\cos\arg r = \pm 0.7$. Figure 9.17 shows an example with $\Omega_0 \approx 0.98$.

If $\arg r = 2\phi_{\mathrm{CKM}}$ is a large angle, a measurement of $\cos 2\phi_{\mathrm{CKM}}$ via the mixture of short and long lived states is complementary to a measurement of $\sin 2\phi_{\mathrm{CKM}}$ via an oscillating asymmetry function (9.115). Due to the large value of x_s, the latter requires a very precise measurement of the individual lifetimes and flavour tagging, while the decomposition of the short and long lived fractions can be done with untagged events and a modest resolution, but requires a large data sample.

9.3.6.5 CP Violation at the Υ(4S)

B meson pairs from $\Upsilon(4\mathrm{S})$ decay are initially in a CP $= +1, \mathrm{P} = -1, \mathrm{C} = -1$ eigenstate

$$|B^0(1)\overline{B}^0(2)\rangle - |B^0(2)\overline{B}^0(1)\rangle \tag{9.119}$$

with angular momentum $L = 1$. Their time evolution is described by (9.70a), where the two scaled times T_1 and T_2 may be taken as the decay times of the two mesons. By multiplying this state function with $\langle X(1)X(2)|\mathcal{H}(1)\mathcal{H}(2)$ where

$$\langle X(1)X(2)|\mathcal{H}(1)\mathcal{H}(2)|B^0(1)B^0(2)\rangle = \langle X(1)|\mathcal{H}|B^0(1)\rangle\,\langle X(2)|\mathcal{H}|B^0(2)\rangle = A_1 A_2$$

are the decay amplitudes of two B^0 mesons and amplitudes of other mixtures of $B(i)$ and $\overline{B}(j)$ yield products of A_i and $\overline{A}_j$ accordingly, one obtains an amplitude

$$\mathcal{M}_- := e^{i\phi_0} e^{-\frac{1}{2}(T_1+T_2)} \left[C_- \cos(x-iy) \frac{T_1-T_2}{2} + iS_- \sin(x-iy) \frac{T_1-T_2}{2} \right] \tag{9.120}$$

where ϕ_0 is a common, unobservable phase including the imt phases of two free B mesons, and the coefficients are

$$C_- = A_1\overline{A}_2 - \overline{A}_1 A_2, \qquad S_- = \eta_m \overline{A}_1 \overline{A}_2 - \frac{A_1 A_2}{\eta_m}$$

There can be always two non-zero amplitude factors separated, leaving coefficients like

$$\frac{C_-}{A_1\overline{A}_2} = 1 - \frac{\overline{A}_1}{A_1}\frac{A_2}{\overline{A}_2} = 1 - \frac{r_1}{r_2}, \qquad \frac{S_-}{A_1\overline{A}_2} = \frac{\eta_m \overline{A}_1}{A_1} - \frac{A_2}{\eta_m \overline{A}_2} = r_1 - \frac{1}{r_2}$$

These coefficients are **convention independent** factors similar to r: CP phases common to $A/\overline{A}$ and η_m cancel, and the exchange of quarks with antiquarks ensure that the product of CKM elements has each quark index in as many V as V^* (or, with the same phase, $1/V$) factors. From the general amplitude, we can derive various special cases listed in table 9.3.

The square $|\mathcal{M}_-|^2$ leads to a general formula which reads on the $\Upsilon(4S)$ with the final states X_1, X_2 from the two B^0 mesons

$$\dot{N}(B\overline{B} \to X_1 X_2) \propto e^{-2\Gamma t_1} e^{-T} (g_1 \cosh yT + g_2 \sinh yT + h_1 \cos xT + h_2 \sin xT) \tag{9.121}$$

with $T = T_2 - T_1 = \Gamma(t_2 - t_1)$ and

$$\begin{aligned} g_1 &= |C_-|^2 + |S_-|^2 \\ g_2 &= 2\,\mathcal{R}e(S_-^* C_-) \\ h_1 &= |C_-|^2 - |S_-|^2 \\ h_2 &= 2\,\mathcal{I}m(S_-^* C_-) \end{aligned}$$

Integrating over t_1 gives

$$\dot{N}(B\overline{B} \to X_1 X_2) \propto e^{-|T|} (g_1 \cosh yT + g_2 \sinh yT + h_1 \cos xT + h_2 \sin xT) \tag{9.122}$$

where the $|T|$ comes from the lower limit on t_1: if $T < 0$, possible values are restricted to $t_1 > -T = |T|$. For B^0 mesons, we can assume $\delta_\epsilon = 0$ and $y = 0$, which corresponds to the simpler equation

$$\dot{N}(B\overline{B} \to X_1 X_2) \propto e^{-2\Gamma t_1} e^{-T} (g_1 + h_1 \cos xT + h_2 \sin xT) \tag{9.123}$$

9.3.7 Time Integrated Asymmetries

The total rates are proportional to $\int_0^\infty |\mathcal{M}|^2 \,\mathrm{d}T$. Using (9.94) one obtains

$$\begin{aligned} \int_0^\infty |\mathcal{M}|^2 \,\mathrm{d}T &= |A|^2 \frac{1+|r|^2}{2} \left\{ \frac{1}{1-y^2} - \Theta_0 \frac{1}{1+x^2} + \Omega_0 \frac{y}{1-y^2} - \Lambda_0 \frac{x}{1+x^2} \right\} \\ \int_0^\infty |\overline{\mathcal{M}}|^2 \,\mathrm{d}T &= \frac{|A|^2}{|\eta_m|^2} \frac{1+|r|^2}{2} \left\{ \frac{1}{1-y^2} + \Theta_0 \frac{1}{1+x^2} + \Omega_0 \frac{y}{1-y^2} + \Lambda_0 \frac{x}{1+x^2} \right\} \end{aligned}$$

leading to an asymmetry

$$a_{\mathrm{int}} = \frac{(\Theta_0 + x\Lambda_0)(1-y^2)}{(1+y\Omega_0)(1+x^2)} \tag{9.124}$$

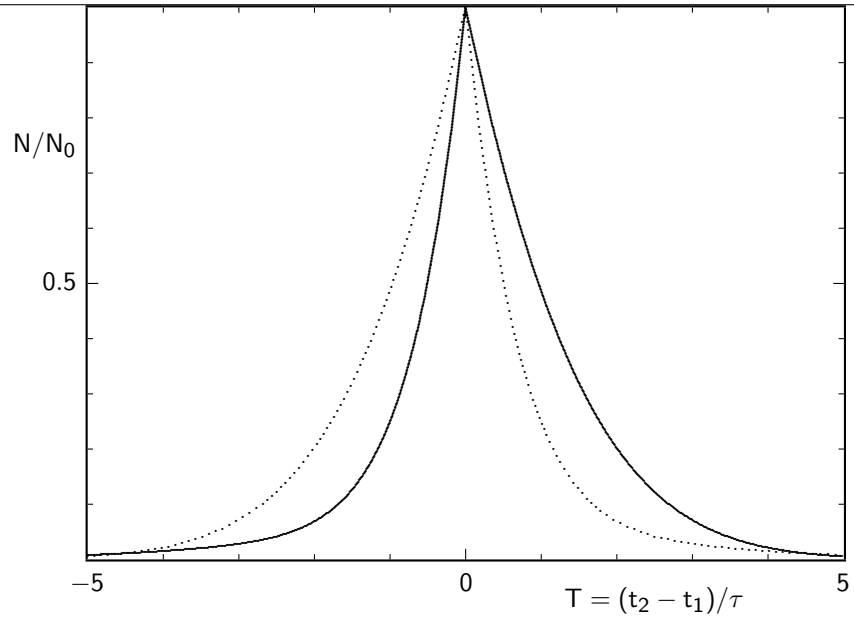

Fig. 9.19 Time dependent rate of $\Upsilon(4S) \to B^0 + J/\psi K_S^0$ (——) and $\Upsilon(4S) \to \overline{B}^0 + J/\psi K_S^0$ (·····) for $\sin 2\beta = 0.5$ and $x = 0.7$.

for $|\eta_m| = 1$. For $y = 0$ this simplifies to

$$a_{\text{int}} = \frac{\Theta_0 + x\Lambda_0}{1 + x^2} \tag{9.125}$$

Therefore, a time integrated measurement is only meaningful if one of the parameters is known, e. g. for $|r| = 1$ where $\Theta_0 = 0$, the asymmetry a_{int} determines Λ_0. In this case, the asymmetry is reduced by a dilution factor

$$D_{\text{int}} = \frac{x}{1 + x^2}$$

with respect to the amplitude Λ_0 of the time-dependent one, which is $D_{\text{int}} = 0.48$ for the B^0, and $D_{\text{int}} < 0.05$ for the B_s.

On the $\Upsilon(4S)$, the integration is from $-\infty$ to ∞, and e^{-T} is replaced by $e^{-|T|}$. Therefore, all odd components in $|\mathcal{M}|^2$ and $|\overline{\mathcal{M}}|^2$ lead to vanishing integrals, and the rates are

$$\int_{-\infty}^{\infty} |\mathcal{M}|^2 \, \mathrm{d}T = |A|^2 \frac{1 + |r|^2}{2} \Big\{ \frac{1}{1 - y^2} - \Theta_0 \frac{1}{1 + x^2} \Big\}$$
$$\int_{-\infty}^{\infty} |\overline{\mathcal{M}}|^2 \, \mathrm{d}T = \frac{|A|^2}{|\eta_m|^2} \frac{1 + |r|^2}{2} \Big\{ \frac{1}{1 - y^2} + \Theta_0 \frac{1}{1 + x^2} \Big\}$$

and the asymmetry is

$$a_{\text{int}} = \frac{\Theta_0}{1 + x^2} \tag{9.126}$$

for $|\eta_m| = 1$. A measurement without decay time information can therefore be used to determine Θ_0 alone. A determination of Λ_0 in this environment requires the measurement of the lifetime difference to the second, tagging B.

In the simple case where $\Theta_0 = 0$, the integrated asymmetry is $a_{\text{int}} = 0$ and hence cannot be used as an observable to determine the physical parameter Λ_0. However, if the time order is known,

$$a_{+/-\text{int}} = \frac{N(B^0 + X) - N(\overline{B}^0 + X)}{N(B^0 + X) + N(\overline{B}^0 + X)} \Big|_{t_s > t_t}$$

$$= -\left.\frac{N(B^0+X)-N(\overline{B}^0+X)}{N(B^0+X)+N(\overline{B}^0+X)}\right|_{t_s<t_t} = \Lambda_0\frac{x}{1+x^2}$$

would offer a partly time-integrated measurement with the same dilution as in (9.125), hence the same reduction in precision compared to the full time distribution analysis. This is of no practical use, since as the time information is available one would like to use it in the most effective way.

9.3.8 Final CP Eigenstates from B^0 or B_s Decays

Weak decay amplitudes can be described by (9.12) and (9.13). For CP eigenstates with eigenvalue ζ_X^{CP} their ratio is then given by

$$\frac{\overline{A}}{A} = \zeta_X^{CP} e^{-i(\phi_{\mathrm{CP}B}+2\arg V)} \tag{9.127}$$

where $\arg V$ is the phase angle of the CKM elements involved in A (i. e. the B^0 decay amplitude). Using the CKM representation (9.9) with $\eta_m = e^{i(\phi_{\mathrm{CP}B}-2\tilde{\beta})}$ results in

$$r = \zeta_X^{CP} e^{-2i(\arg V+\tilde{\beta})} \tag{9.128}$$

which is a convention independent phase factor[86] of a product of four or more CKM elements. It can be transformed into an ϵ-like parameter

$$\eta_X := \frac{1-r}{1+r} = i\zeta_X^{CP}\tan(\arg V+\tilde{\beta}) \tag{9.129}$$

which is, in contrast to ϵ_m defined by (9.25), convention independent, but is specific to a final state X.

A measurement of the angle $\beta = \arg(-V_{td}^* V_{tb} V_{cd} V_{cb}^*)$ in the CKM triangle (figure 9.1a) requires a decay with $\bar{b}\to\bar{c}+c\bar{d}$. Examples for final states with this quark content are $J/\psi\,\pi^0$ or D^+D^-. In these decays one has $r = \zeta_X^{CP} e^{-2i\beta}$.

Similarly, for other final states common to B and $\overline{B}$ the rephasing invariant net product of CKM elements in the combined amplitude/mixing phase ratio r is easily extracted using (9.9). A summary of common final states of B^0 and $\overline{B}^0$ is given in table 9.3. Since the spectator with a b quark is a $\bar{d}$ quark, the decay products of the b must have the net flavour of a d quark, accompanied by one or more quark antiquark pair.

Table 9.3 Examples of CP eigenstates as final states of B^0 and $\overline{B}^0$, and their sensitivity to the CKM phases. Only tree amplitudes are considered, penguins lead to modifications and in general also to direct CP violation. The asymmetry (9.108) has an amplitude $\Lambda_0 = -\zeta_X^{CP}\sin 2\phi_{\mathrm{CKM}}$.

b decay	$\prod$ CKM elements	angle ϕ_{CKM}	some final states
$b\to c\bar{c}d$	$V_{tb}^*V_{td}V_{cd}^*V_{cb}$	β	$(J/\psi\,,\psi',\eta_c\ldots)+(\pi^0,\eta,\rho^0\ldots),\ D^{(*)+}D^{(*)-}$
$b\to c\bar{c}s, s\to u\bar{u}d$	$V_{tb}^*V_{td}V_{cs}^*V_{cb}V_{ud}^*V_{us}$	$\beta-\tilde{\phi}_4-\tilde{\phi}_6$	$(J/\psi\,,\psi',\eta_c\ldots)+(K_S^0,K_S^0\pi^0\ldots)$
$b\to c\bar{c}s, s\bar{d}\to K_L^0$	$V_{tb}^*V_{td}V_{cs}^*V_{cb}V_{cd}^*V_{cs}$	β	$(J/\psi\,,\psi',\eta_c\ldots)+K_L^0$
$b\to u\bar{u}d$	$V_{tb}^*V_{td}V_{ud}^*V_{ub}$	$-\alpha$	$\pi\pi,\rho\rho\ldots$
$b\bar{d}\to u\bar{u}$	$V_{tb}^*V_{td}V_{ud}^*V_{ub}$	$-\alpha$	$\pi\pi\ldots,K^+K^-$
$b\to d$	$V_{tb}^*V_{td}V_{tb}^*V_{tb}$	0	$\pi^0\eta',\ldots$
$b\to s, s\to u\bar{u}d$	$V_{tb}^*V_{td}V_{ts}^*V_{tb}V_{ud}^*V_{us}$	β'	$(K_S^0,K_S^0\pi^0\ldots)+(\pi^0,\eta,\eta',\rho^0,\omega,\ldots)$
$b\to ss\bar{s}, \bar{s}\to u\bar{u}\bar{d}$	$V_{tb}^*V_{td}V_{ts}^*V_{tb}V_{ud}V_{us}^*$	β'	$(K_S^0,K_S^0\pi^0\ldots)+(\eta,\eta',\phi\ldots)$
$b\to s, s\bar{d}\to K_L^0$	$V_{tb}^*V_{td}V_{ts}^*V_{tb}V_{cd}^*V_{cs}$	$\beta'+\tilde{\phi}_4+\tilde{\phi}_6$	$K_L^0+(\pi^0,\eta,\eta',\rho^0,\omega\ldots)$
$b\to ss\bar{s}, \bar{s}d\to K_L^0$	$V_{tb}^*V_{td}V_{ts}^*V_{tb}V_{cd}V_{cs}^*$	$\beta'-\tilde{\phi}_4-\tilde{\phi}_6$	$K_L^0+K_L^0+(\eta,\eta',\phi\ldots)$

[86] This is a convenient recipe, but the alternative phase convention (9.15) leaves the mixing contribution real, and requires $r = \zeta_X^{CP} e^{-2i\arg V}$ determined by the decay amplitudes alone!

Only the dominant contribution to the box diagram for $B^0\overline{B}^0$ mixing and to the penguin transitions $b \to d$ and $b \to s$ are considered in table 9.3. Very small modifications to the phase angles ϕ_{CKM} will emerge from corrections to this approximation.

Also, many final states are reached by both tree and penguin amplitudes, specifically all direct $b \to q\bar{q}d$ final states can also be reached by the $b \to d$ penguin transition. In these cases, the true asymmetry has to be calculated using the sum of all amplitudes for A and $\overline{A}$, with additional unknown parameters that can typically not be resolved with a single asymmetry measurement.

A special case are final states with a K^0_S or K^0_L, since these states are no CP eigenstates, and the association with an "approximate eigenstate" is by convention rather than by a physical observable (see discussion in section 9.3.2). However, if one decays subsequently into a CP $= \pm 1$ eigenstate, the whole system can still be taken as a CP eigenstate, and be used to extract unitarity angles. These decays have even an advantage over direct decays to the $c\bar{c}d\bar{d}$ state, since they have less contributions from penguin diagrams due to the Cabibbo-allowed transition $W \to c\bar{s}$.

In the tables, the tree level decay $s \to u + \bar{u}d$ is used to determine the CKM phase angles. There may be penguin contributions as well, which modify the asymmetry. For a c quark in the loop, the relevant unitarity angle for $B^0 \to c\bar{c}K_{S,L}$ is exactly β, for a u quark it is the same as for the tree diagram, and for a t quark it is the small angle $\tilde{\phi}_2 + \tilde{\phi}_6$.

A more precise treatment of the whole system includes oscillation and decay of the kaons as well, leading to four amplitudes which all interfere:

$$\begin{aligned}
A_1 &:= A(B \to B|t_B) \cdot A(B \to c\bar{c}K) \cdot A(K \to K|t_K) \cdot A(K \to \pi\pi) \\
A_2 &:= A(B \to B|t_B) \cdot A(B \to c\bar{c}K) \cdot A(K \to \overline{K}|t_K) \cdot A(\overline{K} \to \pi\pi) \\
A_3 &:= A(B \to \overline{B}|t_B) \cdot \overline{A}(\overline{B} \to c\bar{c}\overline{K}) \cdot A(\overline{K} \to \overline{K}|t_K) \cdot A(\overline{K} \to \pi\pi) \\
A_4 &:= A(B \to \overline{B}|t_B) \cdot \overline{A}(\overline{B} \to c\bar{c}\overline{K}) \cdot A(\overline{K} \to K|t_K) \cdot A(K \to \pi\pi)
\end{aligned}$$

Here the oscillation amplitudes $A(K \to K)$ etc. depend on the kaon lifetime t_K. For $t_K = 0$ we have $A(\overline{K} \to K) = A(K \to \overline{K}) = 0$ and an oscillation $\Lambda_0 \sin \Delta m_B t_B$ with an amplitude $\Lambda_0 = \sin 2(\tilde{\beta} - \tilde{\phi}_6)$ as given in table 9.3. For other times t_K, the argument $\tilde{\beta} - \tilde{\phi}_6 \approx \tilde{\beta}$ changes by a phase angle of $\mathcal{O}(\lambda^4)$. This is small compared to $\tilde{\beta}$, so it still measures $\tilde{\beta}$ to that precision for any kaon lifetime.

If the final kaon is a K^0_L, it will usually be detected via its strong interaction—of a strangeness flavour component—with the detector material. Since the cross section for its $\overline{K}^0$ part is considerably larger than that of the K^0 part, only two amplitudes need to be considered:

$$\begin{aligned}
A_2 &:= A(B \to B|t_B) \cdot A(B \to c\bar{c}K) \cdot A(K \to \overline{K}|t_K \to \infty) \\
A_3 &:= A(B \to \overline{B}|t_B) \cdot \overline{A}(\overline{B} \to c\bar{c}\overline{K}) \cdot A(\overline{K} \to \overline{K}|t_K \to \infty)
\end{aligned}$$

Their ratio is

$$\frac{A_3}{A_2} = \frac{A(B \to B|t_B)}{A(B \to \overline{B}|t_B)} \cdot \frac{V_{cb}V^*_{cs}}{V^*_{cb}V_{cs}} e^{i\phi_{\mathrm{CP}K}} \cdot \frac{1}{-\eta_{mK}}$$

The last factor for the $K^0/\overline{K}^0$ system is obtained using the limits $T \to \infty$ of (9.36) as

$$\begin{aligned}
A(K \to \overline{K}) &= e^{-imt-T/2} \left[-i\eta_{mK} \sin(x - iy)\frac{T}{2} \right] \\
&= e^{-imt} e^{-T/2} \left[-i\eta_{mK} \frac{e^{(ix+y)T/2} - e^{(-ix-y)T/2}}{2i} \right] \to -e^{-imt} \frac{\eta_{mK}}{2} e^{(ix+y-1)T/2}
\end{aligned} \tag{9.130}$$

(the second term wins due to $y < 0$) and (9.37) as

$$A(\overline{K} \to \overline{K}) = e^{-imt-T/2} \left[\cos(x - iy)\frac{T}{2} \right] \to e^{-imt} \frac{1}{2} e^{(ix+y-1)T/2} \tag{9.131}$$

For the leading term in the box diagram we have

$$\eta_{m\,K} = e^{i(\phi_{\mathrm{CP}\,K} + 2\arg V_{cs}^{*2} V_{cd}^2)}$$

which yields

$$\frac{A_3}{A_2} \approx \frac{A(B \to B|t_B)}{A(B \to \overline{B}|t_B)} \cdot \frac{V_{cb} V_{cd}^*}{V_{cb}^* V_{cd}} \cdot (-1)$$

i. e. it behaves indeed as a $b \to c\bar{c}d$ state with CP $= -1$ (for an $L =$ even final state). The effect of regeneration in matter will complicate the situation in a full treatment of K_L^0 interactions. Different phase changes from elastic scattering of K^0 and $\overline{K}^0$ produce a coherent K_S^0 component. This implies that the K_S^0 component is "regenerated" even at long distances in the presence of matter, and CP-even $\pi\pi$ final states may occur that will dilute the asymmetry due to their opposite sign of ζ_X^{CP}, if they cannot be distinguished from the inelastic $\overline{K}$ interactions.

The angles to be measured via oscillation/decay interference include all the factor $V_{tb}^* V_{td}$ from mixing, which is one side in the bd triangle (9.7k). Hence only the adjacent angles α and β can be measured this way. Besides the small difference of the various combinations of β and ϕ_i angles in table 9.3, big differences may occur from contributions outside the Standard Model to loop (penguin) and tree decay diagrams. This may lead to different Λ_0 parameters for e. g. $J/\psi\, K_S^0$ and ϕK_S^0.

Similarly, interference in B_s oscillation can be used to measure the angles in the flat bs triangle (9.7l) given in table 9.4. One of them, $\gamma' = \tilde{\gamma} - \tilde{\phi}_2$, is identical to an angle in the tu triangle (9.7h), and differs from the third angle γ in the bd triangle (9.7k) only at order λ^2. This would allow a test of $\alpha + \beta + \gamma = \pi$ to $\mathcal{O}(\lambda^2)$.

Table 9.4 Examples of CP eigenstates as final states of B_s and $\overline{B}_s$, and their sensitivity to the CKM phases. The asymmetry (9.108) has an amplitude $\Lambda_0 = -\zeta_X^{CP} \sin 2\phi_{\mathrm{CKM}}$.

b decay	$\prod$ CKM elements	angle ϕ_{CKM}	some final states
$b \to c\bar{c}s$	$V_{tb}^* V_{ts} V_{cs}^* V_{cb}$	$\beta_s := \tilde{\phi}_2 + \tilde{\phi}_6$	$(J/\psi\,, \psi'\,, \eta_c \ldots) + (\eta, \phi \ldots), D_s^{(*)+} D_s^{(*)-}$
$b \to u\bar{u}s$	$V_{tb}^* V_{ts} V_{us}^* V_{ub}$	γ'	$\phi + (\pi^0, \rho^0 \ldots), K^{(*)+} K^{(*)-}$
$b \to u\bar{u}d, \bar{s} \to \bar{u}u\bar{d}$	$V_{tb}^* V_{ts} V_{ud}^* V_{ub} V_{us}^* V_{ud}$	γ'	$(\pi^0, \eta, \rho^0 \ldots) + (K_S^0, K_S^0 \pi^0 \ldots)$
$b \to u\bar{u}d, \bar{s}d \to K_L^0$	$V_{tb}^* V_{ts} V_{ud}^* V_{ub} V_{cs}^* V_{cd}$	$\gamma' - \tilde{\phi}_4 - \tilde{\phi}_6$	$(\pi^0, \eta, \rho^0 \ldots) + K_L^0$
$b \to s$	$V_{tb}^* V_{ts} V_{ts}^* V_{tb}$	0	$(\phi, \eta \ldots) + (\pi^0, \eta' \ldots)$
$b \to d, \bar{s} \to \bar{u}u\bar{d}$	$V_{tb}^* V_{ts} V_{td}^* V_{tb} V_{ud} V_{us}^*$	$-\beta'$	$(K_S^0, K_S^0 \pi^0 \ldots) + (\eta' \ldots)$
$b \to d, \bar{s}d \to K_L^0$	$V_{tb}^* V_{ts} V_{td}^* V_{tb} V_{cd} V_{cs}^*$	$-\beta' - \tilde{\phi}_4 - \tilde{\phi}_6$	$K_L^0 + (\eta' \ldots)$

If the given quark level transitions are the only contributions to a final state, the asymmetry with time is a simple $\sin 2\phi_{\mathrm{CKM}} \sin xT$ behaviour. However, many of the final states can be reached via loop graphs as well, often with different CKM elements involved. In this case, both direct CP violation via the interfering amplitudes and the oscillation/decay interference lead to more complex asymmetries with the matrix elements (9.105) and both a $\cos xT$ and $\sin xT$ term.

9.3.8.1 CP Eigenvalues of Some Final States

The most promising examples are for CP$(X) = -1$ the decay $B \to J/\psi\, K_S^0$ with $\Lambda_0 = \sin 2\beta$, and for CP$(X) = +1$ the decay $B \to \pi^+\pi^-$ with $\Lambda_0 = \sin 2\alpha$ up to corrections from the penguin amplitude. The CP eigenvalues of related channels can be constructed from the data listed in table 9.5.

States with several possible angular momenta, like vector vector final states, are typically a mixture of CP $= +1$ and -1 eigenstates. Helicity 0 dominance would simplify these analyses, since it is forbidden

Table 9.5 Examples of CP eigenstates relevant for B^0 decays, dependent on their relative orbital angular momentum L.

channel	L	CP	remarks
J/ψ		$+1$	
ψ'		$+1$	
χ		$+1$	
η_c		-1	
π^0		-1	
$K_S^0 \to \pi\pi$		$+1$	
K_L^0		-1	
$\rho^0 \to \pi^+\pi^-$	1	$+1$	
$K^{*0} \to K_S^0\pi^0$	1	$+1$	
$K^{*0} \to K_L^0\pi^0$	1	-1	
$K_2^{*0} \to K_S^0\pi^0$	2	-1	
$K_0^{*0} \to K_S^0\pi^0$	0	-1	
$J/\psi\, K_S^0$	1	-1	
$J/\psi\,(K^{*0} \to K_S^0\pi^0)$	0, 2	$+1$	helicities: $J_z = 0, \pm 1$
$J/\psi\,(K^{*0} \to K_S^0\pi^0)$	1	-1	helicities: $J_z = \pm 1$
$J/\psi\,(K_0^{*0} \to K_S^0\pi^0)$	1	$+1$	helicity: $J_z = 0$
$J/\psi\,(K_2^{*0} \to K_S^0\pi^0)$	2	-1	helicities: $J_z = \pm 1$
$J/\psi\,(K_2^{*0} \to K_S^0\pi^0)$	1	$+1$	helicities: $J_z = 0, \pm 1$
$\eta_c(K^{*0} \to K_S^0\pi^0)$	1	$+1$	
D^+D^-	0	$+1$	
$D^{*+}D^{*-}$	0, 2	$+1$	
$D^{*+}D^{*-}$	1	-1	
$\pi^+\pi^-$	0	$+1$	
$\rho^+\rho^-$	0, 2	$+1$	
$\rho^+\rho^-$	1	-1	

for $L = 1$ final states, and hence indicates a pure CP eigenstate. In general, though, these states have to be deconvolved via a partial wave analysis.

Many final states are particle antiparticle pairs. For these, the C operator introduces only one arbitrary phase as in (9.11), since for bosons $\mathrm{C}^2 = 1$, and hence

$$\mathrm{C}\,|X(1)\overline{X}(2)\rangle = e^{i\phi_C}e^{-i\phi_C}|X(2)\overline{X}(1)\rangle = |X(2)\overline{X}(1)\rangle$$

For pairs of spin 0 mesons, this implies

$$\mathrm{C}(|X(1)\overline{X}(2)\rangle \pm |\overline{X}(1)X(2)\rangle) = \pm(|X(1)\overline{X}(2)\rangle \pm |\overline{X}(1)X(2)\rangle) = \mathrm{P}(|X(1)\overline{X}(2)\rangle \pm |\overline{X}(1)X(2)\rangle) \quad (9.132)$$

where 1,2 stands for $|\boldsymbol{x}\rangle, |-\boldsymbol{x}\rangle$ or $|\boldsymbol{p}\rangle, |-\boldsymbol{p}\rangle$. Therefore, eigenstates of P are always also eigenstates of C with **the same** eigenvalue, hence a CP eigenvalue of $\zeta^{CP} = +1$.

9.3.8.2 The $B \to \pi\pi$ Decay

The decay $B^0 \to \pi^+\pi^-$ can proceed via a tree diagram $b \to u\bar{u}d$, with an amplitude $A_T \propto V_{ub}^* V_{ud}$, and via a penguin type diagram $b \to d$ with an amplitude $A_P \propto V_{tb}^* V_{td}$ (see figure 9.13 in section 9.3.4, with the s quark replaced by a d quark). The CP violating asymmetries are then determined by the ratio

$$r = \eta_m \frac{\overline{A}_T + \overline{A}_P}{A_T + A_P}$$

which has in general no simple relation[87] to the unitarity angles. This fact is often referred to as the "penguin pollution". The ratio of heavy to light B^0 eigenstates decaying into the CP-even $\pi^+\pi^-$ system is no longer given by (9.80), but rather by (9.81) with a parameter Ω_0 determined by magnitudes and phases of $\bar{A}_T$, A_T, $\bar{A}_P$ and A_P.

The tree diagram creates a four quark system $u\bar{u}d\bar{d}$ and can be decomposed into a $\Delta I = \frac{1}{2}$ component producing a $\pi^+\pi^-$ in the isospin $I = 0$ state, and a $\Delta I = \frac{3}{2}$ component producing a $\pi^+\pi^-$ in the isospin $I = 2$ state[88]. The penguin diagram creates only two quarks $d\bar{d}$ and can therefore produce a $\pi^+\pi^-$ only in the isospin $I = 0$ state.

The $I = 1$ final state is impossible for a pion pair since bosons are descibed by symmetric wave functions, and odd L and odd I combinations are antisymmetric. Hence L and I must be either both odd or both even. For B decays, $L = 0$ and therefore I can have only even values. This implies that the charged B^+ can not decay to $\pi^+\pi^0$ via the penguin diagram, which produces $u\bar{d}$ and hence $(I, I_3) = (1, 1)$.

Both amplitudes may differ by a strong phase δ_{20} which could give rise to CP violation in the decay. The Clebsch Gordan coefficients relating these amplitudes are given in table 9.6and will be discussed in detail below. The amplitudes in the language of the BSW model[89] are also given. The various factors $\sqrt{\frac{1}{2}}$ are from the π^0 wavefunction $|\pi^0\rangle = \sqrt{\frac{1}{2}}(|u\bar{u}\rangle - |d\bar{d}\rangle)$. The physical amplitudes may be modified by strong final state interactions. Since isospin is conserved in strong interaction, the isospin parametrization of the amplitudes is more general, and in addition not limited to the tree graph.

The weak phases involved in this CP violation from the interference of A_T and A_P and in the CP violation from the interference of oscillation and decay through A_T are both given by the factor

$$\frac{V_{ub}V_{ud}^*}{V_{tb}V_{td}^*} = -e^{i\alpha} \cdot \left|\frac{V_{ub}V_{ud}}{V_{tb}V_{td}}\right|$$

Therefore, the decay can be used to determine the unitarity angle α, and the amplitude ratio is

$$r = e^{2i\alpha}\frac{a_{T1/2} + a_{T3/2}e^{i\delta_{20}}/\sqrt{2} - a_P e^{-i\alpha}}{a_{T1/2} + a_{T3/2}e^{i\delta_{20}}/\sqrt{2} - a_P e^{i\alpha}} \tag{9.133}$$

where $T1/2$, $T3/2$, and P denote tree $\Delta I = \frac{1}{2}$, $\Delta I = \frac{3}{2}$, and penguin, respectively.

In the limit $|A_P| = 0$, the parameters are simply $r = e^{2i\alpha}$, $\Theta_0 = 0$ and $\Lambda_0 = \sin 2\alpha$.

If the phase difference δ_{20} is a multiple of π, i. e. if both isospin amplitudes of the tree process are relatively real,

$$r = e^{2i\alpha}\frac{|A_T| - |A_P|\cos\alpha + i|A_P|\sin\alpha}{|A_T| - |A_P|\cos\alpha - i|A_P|\sin\alpha}$$

and there is still $|r| = 1$, but the phase is a function of $|A_P|/|A_T|$ and α. This would be the case in a factorizing approach like the BSW model, which is in good agreement with exclusive two body decays from the $b \to c$ transition. However, final state interactions may be large in light quark final states, and could easily destroy this simple phase relation.

All of the above assumes t quark dominance in the penguin loop which is motivated by the large top quark mass. Including all three quarks u, c, t in the loop leaves 4 amplitudes, where standard CKM phases are taken from (9.9):

$$A_T = \left(a_{T1/2} + a_{T3/2}e^{i\delta_{20}}/\sqrt{2}\right)e^{i\tilde{\gamma}}$$

[87] M. Gronau, Phys. Rev. Lett. **63**, 1451 (1989); D. London, R. D. Peccei, Phys. Lett. **B223**, 257 (1989); B. Grinstein, Phys. Lett. **B229**, 280 (1989); H. Lipkin, Phys. Lett. **B357**, 404 (1995).

[88] There may also be $\Delta I = \frac{5}{2}$ from electromagnetic rescattering or non-standard model physics, but the final state is still $I = 0$ or $I = 2$.

[89] M. Bauer, B. Stech, M. Wirbel, Z. Phys. **C34**, 103 (1987).

Table 9.6 Spectator amplitudes (F = form factor, f = decay constant).

A	quark state	BSW model	$\Delta I = 1/2$		$\Delta I = 3/2$	
			$I=0$	$I=1$	$I=1$	$I=2$
	$B^0 \to d(\bar{u}u\bar{d})$	a_1	$\sqrt{\frac{1}{2}}$	$\sqrt{\frac{1}{2}}$	$-\sqrt{\frac{1}{2}}$	$\sqrt{\frac{1}{2}}$
T^{-+}	$\to \rho^-\pi^+$	$a_1 F_V f_P$	$\sqrt{\frac{1}{6}}$	$-\frac{1}{2}$	$\frac{1}{2}$	$\sqrt{\frac{1}{12}}$
T^{+-}	$\to \pi^-\rho^+$	$a_1 F_P f_V$	$\sqrt{\frac{1}{6}}$	$\frac{1}{2}$	$-\frac{1}{2}$	$\sqrt{\frac{1}{12}}$
$T^{\pm\mp} = \sqrt{\frac{1}{2}}\cdot(T^{+-}+T^{-+})$	$\to \pi^-\pi^+$ $(L=0)$	$a_1 F_P f_P$	$\sqrt{\frac{1}{3}}$	0	0	$\sqrt{\frac{1}{6}}$
	$B^0 \to d(\bar{d}u\bar{u})$	a_2	$\sqrt{\frac{1}{2}}$	$\sqrt{\frac{1}{2}}$	$-\sqrt{\frac{1}{2}}$	$\sqrt{\frac{1}{2}}$
T^{00}	$\to \rho^0\pi^0$	$a_2\sqrt{\frac{1}{2}}F_V\sqrt{\frac{1}{2}}f_P$	$-\sqrt{\frac{1}{6}}$	0	0	$\sqrt{\frac{1}{3}}$
	$\to \pi^0\rho^0$	$+a_2\sqrt{\frac{1}{2}}F_P\sqrt{\frac{1}{2}}f_V$				
T^{00}	$\to \pi^0\pi^0$	$\sqrt{2}\cdot a_2\sqrt{\frac{1}{2}}F_P\sqrt{\frac{1}{2}}f_P$	$-\sqrt{\frac{1}{6}}$	0	0	$\sqrt{\frac{1}{3}}$
	$B^+ \to u(\bar{u}u\bar{d})$	a_1	0	1	$-\frac{1}{2}$	$\sqrt{\frac{3}{4}}$
	$B^+ \to u(\bar{d}u\bar{u})$	a_2				
T^{0+}	$\to \rho^0\pi^+$	$a_1\sqrt{\frac{1}{2}}F_V f_P$		$-\sqrt{\frac{1}{2}}$	$\sqrt{\frac{1}{8}}$	$\sqrt{\frac{3}{8}}$
	$\to \pi^+\rho^0$	$+a_2 F_P\sqrt{\frac{1}{2}}f_V$				
T^{+0}	$\to \pi^0\rho^+$	$a_1\sqrt{\frac{1}{2}}F_P f_V$		$\sqrt{\frac{1}{2}}$	$-\sqrt{\frac{1}{8}}$	$\sqrt{\frac{3}{8}}$
	$\to \rho^+\pi^0$	$+a_2 F_V\sqrt{\frac{1}{2}}f_P$				
$T^{0+}_{+0} = \sqrt{\frac{1}{2}}\cdot(T^{0+}+T^{+0})$	$\to \pi^0\pi^+$ $(L=0)$	$a_1\sqrt{\frac{1}{2}}F_P f_P$		0	0	$\sqrt{\frac{3}{4}}$
	$\to \pi^+\pi^0$	$+a_2 F_P\sqrt{\frac{1}{2}}f_P$				

$$
\begin{aligned}
A_{P,t} &= a_{P,t}e^{-i\tilde{\beta}} \\
A_{P,c} &= -a_{P,c}e^{i\tilde{\phi}_6} \approx a_{P,c}e^{i\pi} \\
A_{P,u} &= a_{P,u}e^{-i\tilde{\gamma}}
\end{aligned}
$$

Employing unitarity relation (9.7k) to eliminate $V_{td}V_{tb}^*$ we can rewrite

$$
A_{P,t} = a_{P,t}\left[-\left|\frac{V_{ub}V_{ud}}{V_{tb}V_{td}}\right|e^{i\tilde{\gamma}} - \left|\frac{V_{cb}V_{cd}}{V_{tb}V_{td}}\right|\right]
$$

(ignoring $\tilde{\phi}_6$) and

$$
r = e^{2i\alpha}\frac{a_{0,2} + a_0 e^{i\delta}e^{i\gamma}}{a_{0,2} + a_0 e^{i\delta}e^{-i\gamma}} \tag{9.134}
$$

with

$$
a_{0,2} = |A_T| - a_{P,t}\cdot\left|\frac{V_{ub}V_{ud}}{V_{tb}V_{td}}\right| + a_{P,u}, \qquad a_0 = a_{P,c} - a_{P,t}\cdot\left|\frac{V_{cb}V_{cd}}{V_{tb}V_{td}}\right|
$$

for $I = 0, 2$ ($a_{0,2}$) and pure $I = 0$ (a_0) isospin final states. The principal decomposition into two amplites is the same as for the tree and t-penguin above, but the relative weak phase is γ and none of the two sub-amplitudes is pure tree, while one is pure penguin. It should also be emphasized that CKM unitarity is already assumed in this parametrisation. The strong phase difference is with respect to $A_{0,2}$ versus A_0 (with absolute values $a_{0,2}$ and a_0).

If the penguin amplitude is much smaller than the tree amplitude, the ratio

$$r = e^{2i\alpha}\frac{|A_T|e^{i\delta_{TP}} - |A_P|e^{-i\alpha}}{|A_T|e^{i\delta_{TP}} - |A_P|e^{i\alpha}}$$

can be used to determine the asymmetry amplitudes as taylor expansion in $|A_P/A_T|$ as

$$\begin{aligned}
\Lambda_0 &= \sin 2\alpha + 2\cos 2\alpha \sin\alpha \cos\delta_{TP}\frac{|A_P|}{|A_T|} + \mathcal{O}\left(\frac{|A_P|^2}{|A_T|^2}\right)\\
\Theta_0 &= \sin\alpha \sin\delta_{TP}\frac{|A_P|}{|A_T|} + \mathcal{O}\left(\frac{|A_P|^2}{|A_T|^2}\right)\\
\Omega_0 &= \cos 2\alpha - 2\sin 2\alpha \sin\alpha \cos\delta_{TP}\frac{|A_P|}{|A_T|} + \mathcal{O}\left(\frac{|A_P|^2}{|A_T|^2}\right)
\end{aligned}$$

If $|A_P/A_T|$ is known, e. g. from comparison of $K\pi$ and $\pi\pi$ final state branching fractions, the two phase angles α and δ_{TP} can be determined up to discrete ambiguities from a fit to the asymmetry (9.106) which determines Θ_0 and Λ_0.

For an arbitrary phase difference δ_{20} and penguin contribution, all parameters can be determined via additional measurements. The amplitudes for $B^0 \to \pi^+\pi^-$ (A_{+-}), $\overline{B}^0 \to \pi^+\pi^-$ ($\bar{A}_{+-}$), $B^0 \to \pi^0\pi^0$ (A_{00}), $\overline{B}^0 \to \pi^0\pi^0$ ($\bar{A}_{00}$), $B^+ \to \pi^+\pi^0$ (A_{0+}), and $B^- \to \pi^-\pi^0$ ($\bar{A}_{0-}$) are related to the four amplitudes $B \to \pi\pi_{I=0}$ (A_0), $\overline{B} \to \pi\pi_{I=0}$ ($\bar{A}_0$), $B \to \pi\pi_{I=2}$ (A_2), and $\overline{B} \to \pi\pi_{I=2}$ ($\bar{A}_2$) via Clebsch Gordan coefficients. Actually the final states with two different mesons have to be symmetrized, e. g. $\frac{1}{\sqrt{2}}(\pi^+\pi^- + \pi^-\pi^+)$. The two B mesons are related via the $\Delta I = \frac{3}{2}$ and $\Delta I = \frac{1}{2}$ Amplitudes of the $\bar{b} \to u\bar{u}d$ transition, combining with the $I = \frac{1}{2}$ spectator quark to $I = 0$ and $I = 2$ final states.

$$\begin{aligned}
A(\overline{B}^0 \to u\bar{u}d\bar{d}) &= \frac{1}{\sqrt{2}}A_2 + \frac{1}{\sqrt{2}}A_0\\
A(\overline{B}^+ \to u\bar{u}u\bar{d}) &= \sqrt{\frac{3}{4}}A_2
\end{aligned}$$

The amplitudes can be decomposed into $\pi\pi$ channels

$$\begin{aligned}
\overline{B}^0 \to \pi\pi_{I=2} &= \frac{1}{\sqrt{2}}\bar{A}_2 = \frac{1}{\sqrt{6}}\pi^+\pi^- + \sqrt{\frac{2}{3}}\pi^0\pi^0 + \frac{1}{\sqrt{6}}\pi^-\pi^+ = \frac{1}{\sqrt{3}}\bar{A}_{+-} + \sqrt{\frac{2}{3}}\bar{A}_{00}\\
\overline{B}^0 \to \pi\pi_{I=0} &= \frac{1}{\sqrt{2}}\bar{A}_0 = \frac{1}{\sqrt{3}}\pi^+\pi^- - \frac{1}{\sqrt{3}}\pi^0\pi^0 + \frac{1}{\sqrt{3}}\pi^-\pi^+ = \sqrt{\frac{2}{3}}\bar{A}_{+-} - \sqrt{\frac{1}{3}}\bar{A}_{00} \quad (9.135)\\
B^+ \to \pi^+\pi^0 &= \sqrt{\frac{3}{4}}\bar{A}_2 = \frac{1}{\sqrt{2}}(\pi^+\pi^0 + \pi^0\pi^+) = \bar{A}_{+0}
\end{aligned}$$

leading to

$$\begin{aligned}
\bar{A}_{+-} &= \sqrt{\frac{1}{3}}\bar{A}_0 + \sqrt{\frac{1}{6}}\bar{A}_2, \qquad \bar{A}_{00} = -\sqrt{\frac{1}{6}}\bar{A}_0 + \sqrt{\frac{1}{3}}\bar{A}_2, \qquad \bar{A}_{0-} = \sqrt{\frac{3}{4}}\bar{A}_2\\
A_{+-} &= \sqrt{\frac{1}{3}}A_0 + \sqrt{\frac{1}{6}}A_2, \qquad A_{00} = -\sqrt{\frac{1}{6}}A_0 + \sqrt{\frac{1}{3}}A_2, \qquad A_{0+} = \sqrt{\frac{3}{4}}A_2
\end{aligned}$$

and to the relations

$$\begin{aligned}
A_{+-} + \sqrt{2}\,A_{00} - \sqrt{2}\,A_{0+} &= 0\\
\bar{A}_{+-} + \sqrt{2}\,\bar{A}_{00} - \sqrt{2}\,\bar{A}_{0-} &= 0
\end{aligned} \quad (9.136)$$

which can be represented by triangles in the complex plane. The shapes of these triangles are determined by the lengths of their sides, i. e. the absolute values of the amplitudes, and the phase differences can then be calculated using triangle geometry.

The value of $|A_{0+}| = |\bar{A}_{0-}|$ is given by the B^+ branching fraction to $\pi^+\pi^0$ as

$$|A_{0+}|^2 = |\bar{A}_{0-}|^2 = f\frac{\tau(B^0)}{\tau(B^+)}\,\mathcal{B}(B^+ \to \pi^+\pi^0)$$

The factor f is common to all amplitudes, if we ignore the tiny difference in the phase space factor of the three channels.

Note that A_{0+} and $\bar{A}_{0-}$ are pure $I = 2$ amplitudes, hence the penguin with an $I = 1$ final state cannot contribute[90] (up to isospin-violating electromagnetic final state interactions).

The other two amplitudes can be reconstructed from the Θ_0 parameter of the asymmetry function (9.106),

$$\Theta_0 = \frac{|\bar{A}|^2 - |A|^2}{|\bar{A}|^2 + |A|^2}$$

and the sum of both branching fractions,

$$\begin{aligned} |A_{+-}|^2 + |\bar{A}_{+-}|^2 &= f \cdot \left[\mathcal{B}(B^0 \to \pi^+\pi^-) + \mathcal{B}(\overline{B}^0 \to \pi^+\pi^-)\right] \\ |A_{00}|^2 + |\bar{A}_{00}|^2 &= f \cdot \left[\mathcal{B}(B^0 \to \pi^0\pi^0) + \mathcal{B}(\overline{B}^0 \to \pi^0\pi^0)\right] \end{aligned}$$

In principle, the same method works for both final states. However, since there is no lifetime measurement, the difference $|A_{00}|^2 - |\bar{A}_{00}|^2$ can only be determined at the $\Upsilon(4S)$, where the rates integrated over all time differences are

$$\begin{aligned} f \cdot \mathcal{B}(B^0_{T=0} \to \pi^0\pi^0) &= (1-\chi)\,|A_{00}|^2 + \chi|\bar{A}_{00}|^2 \\ f \cdot \mathcal{B}(\overline{B}^0_{T=0} \to \pi^0\pi^0) &= (1-\chi)\,|\bar{A}_{00}|^2 + \chi|A_{00}|^2 \end{aligned} \tag{9.137}$$

and their asymmetry (9.126) depends only on one parameter Θ_0. The time integrated asymmetry (9.125) for a single B^0 or $\overline{B}^0$ produced in fragmentation depends also on Λ_0 which involves an unknown phase angle.

The analysis of the time dependent $\pi^+\pi^-$ asymmetry (9.106) provides $\Lambda_0 = 2\,\mathcal{I}m\,r/(1+|r|^2)$ and $\Theta_0 = (|r|^2-1)/(|r|^2+1)$ corresponding to the ratio

$$r = \eta_m \frac{\bar{A}_{+-}}{A_{+-}} = e^{i(2\alpha+\kappa)} \cdot \frac{|\bar{A}_{+-}|}{|A_{+-}|} \tag{9.138}$$

The parameter Θ_0 thus determines $|\bar{A}_{+-}|/|A_{+-}|$, which together with the total rate determines the sides $|\bar{A}_{+-}|$ and $|A_{+-}|$. This is equivalent to the extraction from the time integrated rates as described above for $\pi^0\pi^0$ via (9.137).

All these values can be used to construct the two triangles given by (9.136) from their three sides. The two amplitudes A_{0+} and $\bar{A}_{0-}$ can be made relatively real by a suitable choice of the CP phase $\phi_{\mathrm{CP}B}$. In this convention, $A_{0+)} = \bar{A}_{0-}$ and the two triangles can be drawn with this amplitude as a common base line. Then, the phase angle κ of $\bar{A}_{+-}/A_{+-}$ is the angle between the two sides corresponding to the amplitudes $\bar{A}_{+-}$ and A_{+-}. It can be determined up to a twofold ambiguity in magnitude, since the tips

[90] This can be seen directly on the quark level: $\bar{b}u \to \bar{d}u$ can pick up a $u\bar{u}$ or $d\bar{d}$ pair to form $\pi^+\pi^0$. However, the π^0 wave function is $\propto u\bar{u} - d\bar{d}$, therefore both contributions will cancel.

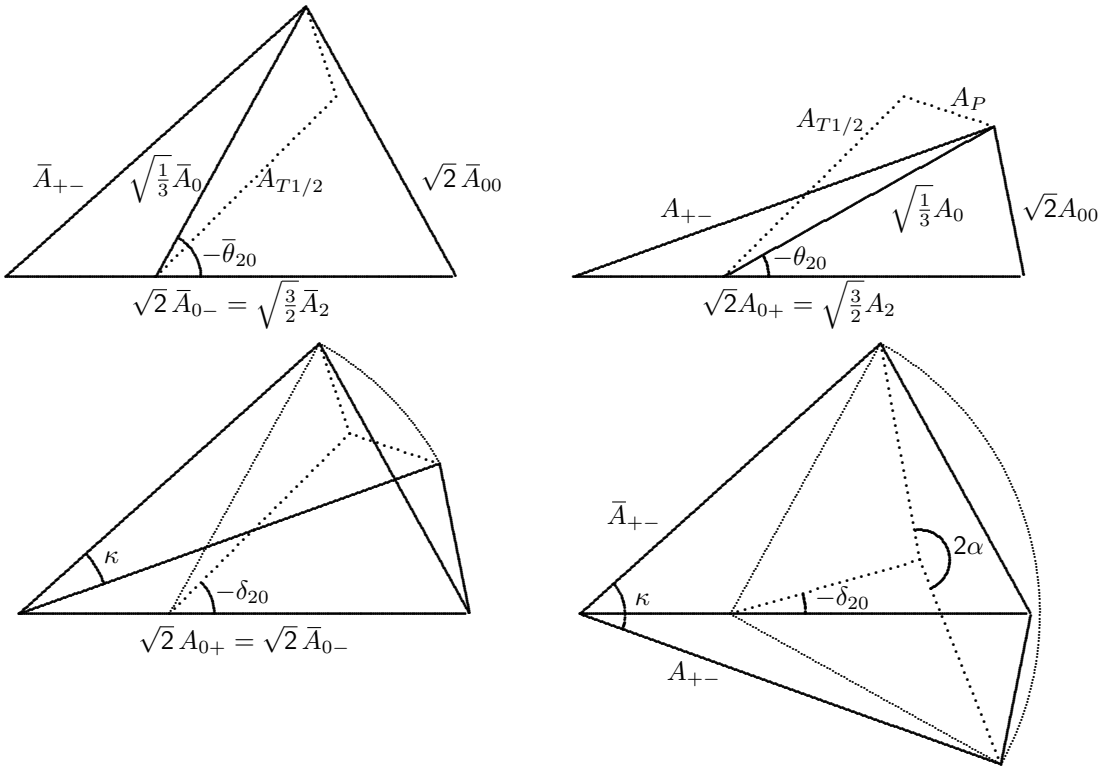

Fig. 9.20 Amplitude triangles for B and $\overline{B}$ to $\pi\pi$ are shown as the upper two plots. The dotted lines are the tree and penguin contributions to A_0 and $\bar{A}_0$, with a relative phase angle of $\pm\alpha$ to the tree amplitude, leading to $|A_0| = |\bar{A}_0|$. The lower left graph is the combination of the two triangles with the tips on the same side of the base line, corresponding to the dotted amplitudes shown in the upper plots. The lower right graph is the second solution with tips on different sides. It corresponds to a different composition of A_0 and $\bar{A}_0$ (not shown in the upper plots).

of the two triangles can be either on the same side of the base line or on opposite sides, and a twofold ambiguity in its sign.

Figure 9.20 illustrates the situation. The convention

$$\sqrt{\frac{1}{3}}A_0 = A_{T1/2} + A_P, \qquad \sqrt{\frac{1}{3}}\bar{A}_0 = \bar{A}_{T1/2} + \bar{A}_P$$

is used leading to

$$A_{T+-} = A_{T1/2} + \frac{\sqrt{2}}{3}A_{0+}, \qquad \sqrt{2}A_{T00} = -A_{T1/2} + \frac{2\sqrt{2}}{3}A_{0+}$$
$$\bar{A}_{T+-} = \bar{A}_{T1/2} + \frac{\sqrt{2}}{3}\bar{A}_{0-}, \qquad \sqrt{2}\bar{A}_{T00} = -A_{T1/2} + \frac{2\sqrt{2}}{3}\bar{A}_{0-}$$

and A_{0+}, $\bar{A}_{0-}$ are pure $\Delta I = \frac{3}{2}$.

The asymmetry amplitude Λ_0 can be calculated from (9.138) to be

$$\Lambda_0 = \frac{2}{1 + |\bar{A}_{+-}/A_{+-}|}\sin(2\alpha + \kappa)$$

The amplitude ratio is given by the second fit parameter Θ_0, and four κ values can be read from the triangles.

The ratio of B_H^0 to B_L^0 in this state is given by

$$\Omega_0 = \frac{2}{1 + |\bar{A}_{+-}/A_{+-}|} \cos(2\alpha + \kappa)$$

and is in general different from that for $\pi^0\pi^0$, since both the $|\bar{A}_{00}/A_{00}|$ ratio and θ_{00} differ.

An alternative way to use the triangles is obtained if the ratio r is expressed in isospin amplitudes:

$$r = e^{2i\alpha} \frac{|A_0| + |A_2| e^{i\theta_{20}}}{|A_0| + |A_2| e^{i\bar{\theta}_{20}}}$$

The angles θ_{20} and $\bar{\theta}_{20}$ can be read from the two upper triangles in figure 9.20, up to the ambiguous sign, as well as the amplitude ratio $r_{20} := |A_2/A_0|$. The asymmetry parameter

$$\begin{aligned} \Lambda_0 = & \frac{\sin\theta_{20} - \sin\bar{\theta}_{20} + r_{20}\sin(\theta_{20} - \bar{\theta}_{20})}{1 + r_{20}(\cos\theta_{20} + \cos\bar{\theta}_{20}) + r_{20}^2} r_{20}\cos(2\alpha) \\ & + \frac{1 + r_{20}(\cos\bar{\theta}_{20} + \cos\theta_{20}) + r_{20}^2\cos(\theta_{20} - \bar{\theta}_{20})}{1 + r_{20}(\cos\theta_{20} + \cos\bar{\theta}_{20}) + r_{20}^2} \sin(2\alpha) \end{aligned}$$

is then a function of these three parameters and 2α.

There are several ways to present a measurement of the $\pi^+\pi^-$ asymmetry in absence of clear knowledge of the penguin contribution. One can give the amplitudes Λ_0 and Θ_0 of the $\sin xT$ and $\cos xT$ terms, or give $|r|$ and a measure of the phase $\arg r$ like $\sin 2\alpha_{\text{eff}} := \sin\arg r = \mathcal{I}m\, r/|r|$. There are theoretical predictions relating α_{eff} with α. They are, however, based on the factorization assumption which is likely to be invalid for $b \to$light quark transitions.

A similar analysis can be used with the three pion decays $B \to \rho\pi \to \pi\pi\pi$, with common final states $\pi^+\pi^-\pi^0$ and $\pi^0\pi^0\pi^0$ to B^0 and $\overline{B}^0$ ($\rho^+\pi^-$ and $\rho^-\pi^+$ are no CP eigenstates). Here, one has five independent amplitudes from different $\rho\pi$ charge combinations, but also two more amplitudes ($\Delta I = \frac{1}{2}$ and $\Delta I = \frac{3}{2}$) leading to $I = 1$ final states. Phase differences can be calculated from the absolute values of the five amplitudes in complete analogy to the two pion case, with discrete ambiguities due to different orientation of the polygons. However, these ambiguities can be resolved from a measurement of the phase difference from the interference regions in the Dalitz plot. Therefore, the three pion channels offer not only higher rates, but also a unique solution for α in the Standard Model analysis.

At a high level of precision, further corrections have to be considered. The isospin analysis is based on the assumption that penguin type amplitudes produce only isospin 0 final states. This is not true for electroweak penguin diagrams, which may lead to $I = 2$ states with four light quarks hadronizing to $\pi\pi$, and which may contribute a small fraction to the decay. There are also other quarks besides the t in the loops, which modify the phase angles. While all these effects can be considered negligible in the first generation of CP violation experiments, inconsistent results could still emerge. They would indicate CP violating effects beyond the Standard Model, where the assumption of a description via the CKM matrix phases does not hold.

9.3.9 Measurement of Time Dependent Asymmetries of Neutral B Mesons

Experimental information on CP violation of B mesons produced in jets have been obtained by the CDF collaboration at the Tevatron, and with B mesons produced in $\Upsilon(4S)$ decays at the asymmetric colliders PEP II/BABAR and KEKB/BELLE.

The asymmetry described by (9.108) has been measured in the distribution of the signal B meson's proper lifetime or lifetime difference via its distance of flight and the momentum reconstructed from its decay products. The measurement is illustrated using the most abundant channel $B^0 \to J/\psi K_S^0$. Here

the asymmetry amplitude $\Lambda_0 = \sin 2\beta$ is related directly to the angle β in the CKM unitarity triangle, and (9.108) reads

$$a(T) = \Lambda_0 \sin xT$$

with $T = t/\tau$ and assuming $y = 0$. The example $J/\psi K_S^0$ can be replaced by many other final states which show a similar behaviour with the same or a different amplitude Λ_0. The integrated asymmetry is 0 at the $\Upsilon(4S)$ and diluted by the factor $x/(1+x^2) = 0.48$ in b jets.

In any experiment using the time-dependent asymmetry, the CP violating parameters are measured by the analysis of final states from a continuum or bound $b\bar{b}$ quark pair involving three main steps:

- The relevant B meson final states are reconstructed with a maximum signal-to-background ratio,
- the lifetime or lifetime difference is measured,
- and the initial beauty flavour of the B^0 (or B_s) at $T = 0$ is determined.

The latter, tagging, has already been discussed in section 9.2.12.1. In contrast to a pure frequency measurement as in $B\overline{B}$ oscillation, the determination of CP asymmetries includes measurements of oscillation amplitudes, which are diluted as given in (9.73). The bigger the dilution factor D, the smaller is the dilution, and the better is the sensitivity of the experiment. This effect is discussed quantitatively in the following section.

9.3.9.1 Observed Versus True Asymmetry

Using the example intruduced above with leptons as flavour tags, the asymmetry a is in an ideal case, where the flavour B^0 or $\overline{B}^0$ at $T = 0$ is known unambiguously from the lepton charge,

$$a(T) = \frac{\dot{N}(\overline{B}^0 \to J/\psi K_S^0) - \dot{N}(B^0 \to J/\psi K_S^0)}{\dot{N}(\overline{B}^0 \to J/\psi K_S^0) + \dot{N}(B^0 \to J/\psi K_S^0)} = \frac{\dot{N}(J/\psi K_S^0 \ + l^+) - \dot{N}(J/\psi K_S^0 \ + l^-)}{\dot{N}(J/\psi K_S^0 \ + l^+) + \dot{N}(J/\psi K_S^0 \ + l^-)}$$

In a real experiment, there are a few additional asymmetries involved at $\Upsilon(4S)$ decays, and even more at hadronic B factories using pp, $\bar{p}p$ or p nucleus collisions. The most obvious effect comes from the probability of wrong tagging of the initial flavour. These effects have already been discussed in section 9.2.12.1.

For a charged lepton tag with mistag probability w, i. e. a fraction w of leptons with the opposite charge compared to a lepton from $b \to cl\nu$, the observed number of initial B^0 and $\overline{B}^0$ mesons is

$$\begin{aligned} N_1 &\equiv \dot{N}(J/\psi K_S^0 + l^+) = (1-w) \cdot \dot{N}(\overline{B}^0 \to J/\psi K_S^0) + w \cdot \dot{N}(B^0 \to J/\psi K_S^0) \\ N_2 &\equiv \dot{N}(J/\psi K_S^0 + l^-) = (1-w) \cdot \dot{N}(B^0 \to J/\psi K_S^0) + w \cdot \dot{N}(\overline{B}^0 \to J/\psi K_S^0) \end{aligned}$$

and the observed asymmetry

$$a_{\text{obs}} = \frac{\dot{N}_1 - \dot{N}_2}{\dot{N}_1 + \dot{N}_2} = (1-2w) \cdot a = D \cdot a$$

is diluted as in the mixing case (9.73). In general we have the following diluting effects:

1. The production rates of B^0 and $\overline{B}^0$ are equal in experiments where the sum of all initial flavours is 0, as e^+e^- or $\bar{p}p$ annihilation, but different e. g. in pp collisions, due to the fact that an excess of 4 u-quarks and 2 d-quarks is present from the beginning. There are four different fragmentation probabilities:

$$\begin{aligned} f_0 &= N(B^0)/N(\bar{b}) \qquad & \bar{f}_0 &= N(\overline{B}^0)/N(b) \\ f_s &= N(B_s)/N(\bar{b}) \qquad & \bar{f}_s &= N(\overline{B}_s)/N(b) \end{aligned}$$

   This introduces an intrinsic asymmetry, which is not present at particle antiparticle colliders.

2. The second b-hadron used for tagging can have oscillated into its antiparticle with probability

$$\chi = \frac{N(\bar{b} \to l^-)}{N(\bar{b} \to l)} = f_0\chi_0 + f_s\chi_s$$
$$\bar{\chi} = \frac{N(b \to l^+)}{N(b \to l)} = \bar{f}_0\chi_0 + \bar{f}_s\chi_s$$

   Here χ is the average probability for $\bar{b} \to b$, and $\bar{\chi}$ for $b \to \bar{b}$ through mixing; χ_0 and χ_s denote the mixing probabilities of B^0 and B_s, respectively. Due to the coherent antisymmetric $B\overline{B}$ state in $\Upsilon(4S)$ decays, this effect is absent at B factories operating at the $\Upsilon(4S)$.

3. The lepton can be from semileptonic charm decay in the $b \to c$ cascade. Likewise, almost all tags have a chance to occur at the "wrong" charge. Part of this effect is even due to wrong particle identification of b decay products. This mistag probability w is present at all experiments, but is reduced if determined as a function of discriminating variables, as described below. This probability can be different for b and $\bar{b}$ tags due to asymmetric background and different efficiencies for positive and negative particles.

   This can be parametrized with the branching fractions B for $b \to l^-X$ and C for $b \to l^+X$ being

$$B \approx 2\left[\mathcal{B}(b \to l^-\nu X) + 0.18\,\mathcal{B}(B \to \tau^-\nu X) + 0.08\,\mathcal{B}(B \to D_s^- X)\right] \approx 0.24$$
$$C \approx \mathcal{B}(b \to cX) \cdot 2\,\mathcal{B}(c \to l^+\nu X) \approx 0.20$$

   and the charge-dependent efficiencies (including geometry, reconstruction and identification of leptons associated with a $B \to J/\psi K_S^0$ signal) $\varepsilon_{B\pm}$ for "right sign" leptons from the second b-hadron, and $\varepsilon_{C\pm}$ for "wrong sign" leptons, mainly from secondary charmed hadron decays. The given branching fractions illustrate the main contributions to both classes. Note that the resulting event numbers are about equal, if the efficiency is uniform over the whole phase space, and tagging power has to come from the use of kinematic differences of both lepton samples.

4. The lepton can be faked by π or K, with absolute multiplicities b_+ and b_- for faked positive and negative tag leptons, with

$$b_+ = N(\pi^+) \cdot \delta_\pi^+ \cdot \varepsilon_{\pi^+} + N(K^+) \cdot \delta_K^+ \cdot \varepsilon_{K^+}$$
$$b_- = N(\pi^-) \cdot \delta_\pi^- \cdot \varepsilon_{\pi^-} + N(K^-) \cdot \delta_K^- \cdot \varepsilon_{K^-}$$

   Here ε_X is the kinematic tagging acceptance and δ_X the misidentification probability for hadron X.

   Two sources of hadrons contribute in two different ways:

   - At hadron beam experiments, the charged hadron production through fragmentation yields $b_+ \neq b_-$ due to the initial quarks from the pp or pn state, with no correlation to the b flavour.
   - The charged hadron production through b-hadron decays may show a substantial charge asymmetry, which is correlated to the b flavour and therefore has also effective tagging power and mistag probability. This case is absorbed in the mistag probability w, which includes mistags from true and faked tag leptons. To include these misidentified hadrons, we just change the meaning of B and C above to represent all right- and wrong-sign tracks, and $\varepsilon_{B\pm}$ and $\varepsilon_{C\pm}$ to be the average probability that these tracks are (correctly or wrongly) identified as leptons.

5. Two b-hadrons with the same beauty may have been produced simultaneously. High rate hadronic b factories have a small chance to produce two $b\bar{b}X$ events in a single bunch crossing. In addition, single interactions like $pp \to b\bar{b}b\bar{b}X$ have a small non-zero frequency $\sim 10^{-5} \ldots 10^{-4}$ compared to all $pp \to b\bar{b}X$ events. These effects are typically below fractions of 10^{-4} which can safely be neglected.

   A related background is a $c\bar{c}X$ event that occurs together with a $b\bar{b}$ event, producing additional leptons from charmed hadron decays with no relation to the beauty flavour. Their effect is the same as from misidentified hadrons, and can be included in the fractions b_+ and b_- for the analytical calculation.

For b and $\bar{b}$ flavours as tags at $T = 0$ we have two event rates $\dot{N} = \mathrm{d}N/\,\mathrm{d}T$ as a function of the proper scaling lifetime T

$$\begin{aligned}\dot{N}(J/\psi\, K_S^0 \ + \bar{b}) &= (1+a)\cdot f_0 \cdot N\\ \dot{N}(J/\psi\, K_S^0 \ + b) &= (1-a)\cdot \bar{f}_0 \cdot N\end{aligned}$$

for given true asymmetry $a = a(T)$. Tagging the b or $\bar{b}$ with an electron or muon, the effects mentioned above give the following rates:

$$\begin{aligned}\dot{N}_1 = \dot{N}(J/\psi\, K_S^0 + l^+) = \ & (1-a)\cdot \bar{f}_0 \cdot [(1-\chi)\varepsilon_{B+}B + \chi\varepsilon_{C+}C + b_+]\cdot N\\ & + (1+a)\cdot f_0 \cdot [\bar{\chi}\varepsilon_{B+}B + (1-\bar{\chi})\varepsilon_{C+}C + b_+]\cdot N\\ \dot{N}_2 = \dot{N}(J/\psi\, K_S^0 + l^-) = \ & (1+a)\cdot f_0 \cdot [(1-\bar{\chi})\varepsilon_{B-}B + \bar{\chi}\varepsilon_{C-}C + b_-]\cdot N\\ & + (1-a)\cdot \bar{f}_0 \cdot [\chi\varepsilon_{B-}B + (1-\chi)\varepsilon_{C-}C + b_-]\cdot N\end{aligned} \tag{9.139}$$

The parameters b_- and b_+ are the fake rates from misidentification of hadrons that are not correlated with the b flavour.

Double tags, e. g. by a true plus a fake lepton, have been ignored in these formulae. However, in a more general tagging procedure that incorporates multiple particles for tagging, the same calculation can be used with appropriate translation of the meaning of the individual constants.

The normalization constant is

$$N = N(b\bar{b})\cdot \mathcal{B}(B^0 \to J/\psi\, K_S^0 \to l^+l^-\pi^+\pi^-)\cdot \varepsilon(T)\cdot e^{-|T|}$$

where ε is the reconstruction and trigger efficiency. It will cancel in all ratios.

The observed asymmetry a_{obs} is then

$$\begin{aligned}a_{\mathrm{obs}} &= \frac{\dot{N}_1 - \dot{N}_2}{\dot{N}_1 + \dot{N}_2}\\ &= \frac{2f_b d_b + d_\varepsilon + D_w\chi_{\mathrm{av}}\Delta_\chi - D_w D_m d_f + a\,[D_w D_m - d_f(2f_b d_b + d_\varepsilon + D_w\chi_{\mathrm{av}}\Delta_\chi)]}{1 + 2f_b + f_\varepsilon(\chi_{\mathrm{av}}\Delta_\chi - D_m d_f) + a\,[D_m f_\varepsilon - d_f(1 + 2f_b + \chi_{\mathrm{av}}\Delta_\chi f_\varepsilon)]}\end{aligned} \tag{9.140}$$

with

$$D_w = 1 - 2w, \qquad w = \frac{\varepsilon_C C}{\varepsilon_B B + \varepsilon_C C}, \qquad d_f = \frac{\bar{f}_0 - f_0}{2}$$

$$D_m = 1 - \bar{\chi} - \chi, \qquad \Delta_\chi = \bar{\chi} - \chi, \qquad \chi_{\mathrm{av}} = \frac{\bar{\chi} + \chi}{2}$$

$$f_b = \frac{(b_+ + b_-)}{\varepsilon_B B + \varepsilon_C C}, \qquad d_b = b_+ - b_-, \qquad \varepsilon_C = \frac{\varepsilon_{C+} + \varepsilon_{C-}}{2}, \qquad \varepsilon_B = \frac{\varepsilon_{B+} + \varepsilon_{B-}}{2}$$

$$d_\varepsilon = \frac{1}{2}(\varepsilon_{B+} - \varepsilon_{B-})(1-w) + (\varepsilon_{C+} - \varepsilon_{C-}), \qquad f_\varepsilon = \frac{1}{2}(\varepsilon_{B+} - \varepsilon_{B-})(1-w) - (\varepsilon_{C+} - \varepsilon_{C-})$$

or approximately, ignoring terms $\mathcal{O}(a^2)$,

$$a_{\mathrm{obs}} \approx I + D\cdot a \tag{9.141}$$

with an "intrinsic" asymmetry

$$I = \frac{2f_b d_b + d_\varepsilon + D_w\chi_{\mathrm{av}}\Delta_\chi - D_w D_m d_f}{1 + 2f_b + f_\varepsilon(\chi_{\mathrm{av}}\Delta_\chi - D_m d_f)}$$

and a "dilution factor"

$$D = D_m\cdot(1 - d_f^2)\cdot \frac{D_w(1+2f_b) - f_\varepsilon(d_\varepsilon + 2f_b d_b)}{(1 + 2f_b + f_\varepsilon(\chi_{\mathrm{av}}\Delta_\chi - D_m d_f)} = D_m\cdot D_t$$

where the dilution factor can be split into a tagging component D_t and a mixing component $D_m = 1 - \chi - \bar{\chi} \approx 0.78$ for b jets and $D_m = 1$ at the $\Upsilon(4S)$. The linear approximation holds very well for all practical purposes. Nonlinear corrections to (9.141) occur for $f_0 \neq \bar{f}_0$, $\varepsilon_{C+} \neq \varepsilon_{C-}$ or $\varepsilon_{B+} \neq \varepsilon_{B-}$, but are small due to the smallness of these asymmetries.

The rate of reconstructed tagged events is

$$\dot{N}_{\text{tot}} = \dot{N}_1 + \dot{N}_2 = (\varepsilon_B B + \varepsilon_C C + b_+ + b_-) \cdot [f_0 + \bar{f}_0 + a(\bar{f}_0 - f_0)] \cdot N$$

On the $\Upsilon(4S)$ a $B\overline{B}$ pair is produced exclusively and $T = 0$ is the decay time of the tag-B. There are no background tracks corresponding to $b_- = b_+ = 0$, no mixing $\chi = \bar{\chi} = 0$, and equal production rate $f_0 = \bar{f}_0$ and the relation (9.140) simplifies considerably to

$$a_{\text{obs}} = \frac{d_\varepsilon + D_w a}{1 + f_\varepsilon a} \approx (1 - 2w)a \tag{9.142}$$

There is no intrinsic asymmetry unless the detector has different acceptances for positive and negative particles, there is no mixing dilution, $D_m = 1$, and the dilution factor is related to the mistag probability simply as $D = D_t = 1 - 2w$. This tagging dilution, which is also a good first approximation in more complicated jet environments, can be expressed in the simple form

$$D_t = 1 - 2w = \frac{\text{right-sign} - \text{wrong-sign}}{\text{right-sign} + \text{wrong-sign}} \tag{9.143}$$

where "right-sign" and "wrong-sign" refers to the number of correct and wrong tags, respectively.

As will be shown in detail below, the error on the observed asymmetry amplitude is $\sigma_a \propto 1/\sqrt{N_1 + N_2}$. Therefore, the error on the asymmetry amplitude Λ_0 is

$$\sigma(\Lambda_0) = \frac{1}{D\sqrt{N_1 + N_2}} \sqrt{1 - (D\Lambda_0)^2} \approx \frac{1}{\sqrt{\varepsilon_t D^2 N_s}}$$

where N_s is the number of signal events, ε_t is the tagging efficiency, i. e. $\varepsilon_t N_s$ is the fraction of signal events with a flavour tag, and the approximation holds for small asymmetries $(D\Lambda_0)^2 \ll 1$. The performance of tagging can therefore be defined by the factor $(\varepsilon_t D_t^2)_{\text{eff}}$ which gives the effective reduction in number regarding statistical precision. It is known under many names. One is **separation**, since it is 1 if b and $\bar{b}$ can be separated perfectly event by event, and 0 if they cannot be distinguished. It is also called *effective tagging efficiency* since it is the tagging efficiency weighted by a measure of usefullness of a tag.

9.3.9.2 Effects of Vertex Resolution

The discussion of vertex resolution effects in section 9.2.14.1 applies also to CP violating asymmetry oscillations. Figure 9.21 shows one of the distributions

$$f(T) = e^{-|T|}(1 \pm \Lambda \sin xT)$$

describing decay rates to CP eigenstates on the $\Upsilon(4S)$ and its smearing from a convolution with a Gaussian. The asymmetry calculated from the smeared distribution is diluted and distorted. As an example, the dilution factor from (9.77) is $D_r > 0.995$ for the fully reconstructed $B^0 \to J/\psi K_s^0$ events at CDF. The asymmetric e^+e^- collider experiments are operating at moderate boosts much smaller than that of a B produced in a high energy jet, and are therefore more sensitive to resolution effects than jet experiments.

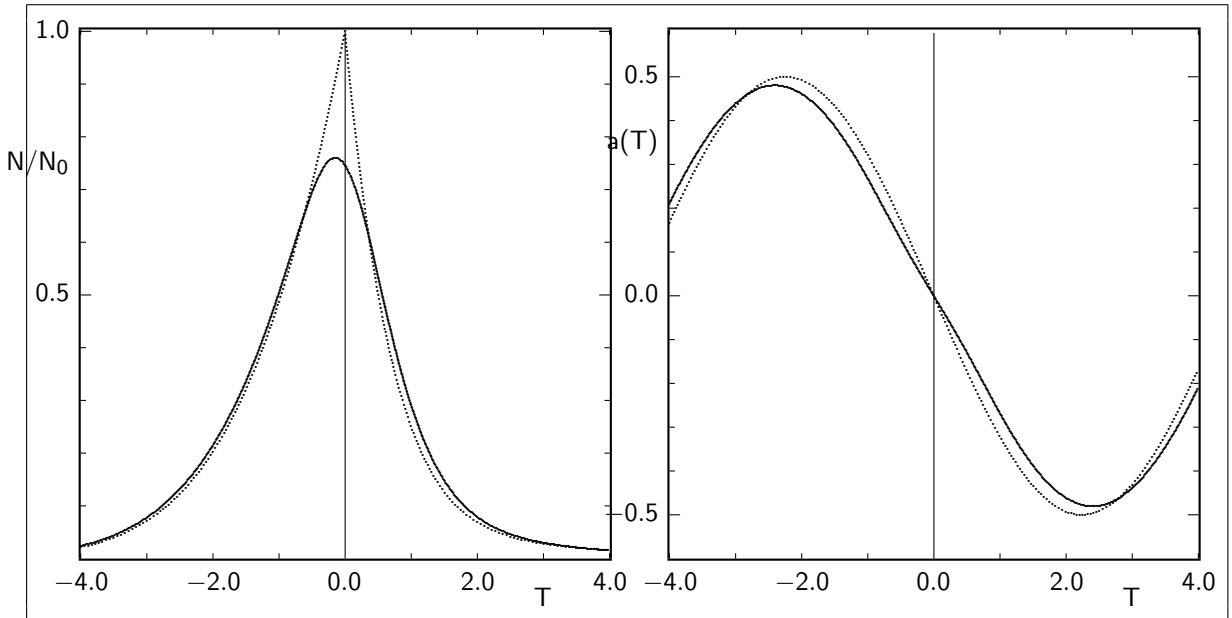

Fig. 9.21 Original (dotted) and smeared (solid line) distribution of $T = \Delta t/\tau$ and the corresponding asymmetry $a(T)$ assuming a Gaussian error in T with $\sigma_T = 0.4$, and the parameters $x = 0.7$, $\Lambda = 0.5$. The dilution factor from the approximation (9.77) is $D_r = 0.9616$ corresponding very precisely to the true reduced amplitude $\Lambda = 0.4808$.

9.3.10 CP Violation in K Meson Decays

CP Violation has first been observed[91] in 1964 in K^0 decays. As shown in figure 9.3, the neutral kaon system is characterized by all parameters x, y and $|\eta_m|$ having non-trivial values. This makes it much more complicated than the B meson system. The light K_S^0 decays to about 99.9% into the CP $= +1$ eigenstates $\pi\pi$ and can therefore be identified with a CP $= +1$ eigenstate $K_+^0 = \frac{1}{\sqrt{2}}(K^0 + \mathrm{CP}\, K^0)$, while $K_L^0 \approx K_-$. Using the convention $K_+^0 = \frac{1}{\sqrt{2}}(K^0 + \overline{K}^0)$, i. e. $\phi_{\mathrm{CP}K} = 0$, this can be written as

$$K_S^0 = \frac{1}{\sqrt{1+|\epsilon|^2}}(K_+^0 + \epsilon K_-^0)$$
$$K_L^0 = \frac{1}{\sqrt{1+|\epsilon|^2}}(K_-^0 + \epsilon K_+^0)$$

up to an arbitrary common phase factor.

In contrast to B mesons, where $y \ll x$, $\Delta\Gamma$ cannot be neglected for K mesons. Hence the mixing parameter is determined from (9.25)

$$\eta_m = -2\frac{m_{12}^* - \frac{i}{2}\Gamma_{12}^*}{\Delta m - \frac{i}{2}\Delta\Gamma}$$

The leading term for m_{12} from the box graph for $K^0/\overline{K}^0$ oscillation with a c quark in the loop yields

$$\arg m_{12} \approx e^{i\phi_{\mathrm{CP}K}} \frac{V_{cs}^{*2} V_{cd}^2}{|V_{cs}^2 V_{cd}^2|} = e^{i\phi_{\mathrm{CP}K}} e^{2i(\tilde{\phi}_4 + \tilde{\phi}_6)}$$

It can be shown that the corresponding

$$\arg \epsilon = \arg(x - iy) = -\arctan\frac{x}{y} \approx 43.5^\circ$$

[91] J. H. Christenson, J.W. Cronin, V.L. Fitch, R. Turlay, Phys. Rev. Lett. **13**, 138 (1964).

Within the same convention, the CKM elements in the dominant tree decay $s \to u + \bar{u}d$ are real, hence the invariant phases including this decay are identical to the phases put into η_m. A convention independent definition of ϵ similar to η_X in (9.129) is

$$\epsilon_0 = \eta_{\pi\pi,I=0} = \frac{1 - \eta_m \bar{A}_0/A_0}{1 + \eta_m \bar{A}_0/A_0} \tag{9.144}$$

where

$$A_0 = \langle \pi\pi, I = 0|\mathcal{H}|K\rangle = \sqrt{3}\langle \pi^+\pi^-, I = 0|\mathcal{H}|K^0\rangle$$
$$\bar{A}_0 = \langle \pi\pi, I = 0|\mathcal{H}|\overline{K}\rangle = \sqrt{3}\langle \pi^+\pi^-, I = 0|\mathcal{H}|\overline{K}^0\rangle$$

are the decay amplitudes into the $\pi^+\pi^-$ final state with isospin 0. This quantity is identical to

$$\epsilon_0 = \frac{\langle \pi^+\pi^-, I = 0|\mathcal{H}|K_L^0\rangle}{\langle \pi^+\pi^-, I = 0|\mathcal{H}|K_S^0\rangle}$$

defined as ϵ_K by Buras and Fleischer.

There are again three possibilities for CP violation.

1. Direct CP violations have only been observed for neutral kaon decays to $\pi\pi$, where they constitute a component in the asymmetries observed in interference of oscillation and decay. The effects are much smaller than the expected ones in B decays. The phenomenology is in complete analogy with equation (9.84), and will be discussed in more detail below.
2. CP violation in the oscillation can be observed using flavour specific decays like $K^0 \to \pi^- l^+ \nu$. The oscillation asymmetry (9.43) starting with an initial K^0 meson is dominated by the damped $\cos xT$ oscillation term seen in the lower diagram in figure 9.3. The expansion of the asymmetry in δ_ϵ according to (9.86) approaches $a(T) \to \delta_\epsilon$ at large times $T \gg 1$ where the long-lived state K_L^0 is the only remaining one. It is the same for an initial $\overline{K}^0$. Hence, there are more $\overline{K} \to K$ oscillations than $K \to \overline{K}$, leaving a net excess of K^0 mesons $a(\infty) = (3.27 \pm 0.12) \cdot 10^{-3} = \delta_\epsilon$ which has first been observed[92] in 1967.
3. A big fraction of neutral kaons decay not as a flavour specific state but as one of the CP eigenstates, e. g. $K_+^0 \to \pi^+\pi^-$ and $K_-^0 \to \pi^+\pi^-\pi^0$. The asymmetry from interference of oscillation and decay has rates determined by (9.94), and has been observed in all these modes.

The CP asymmetry in the $\pi^+\pi^-$ final state is a complex interplay between CP violation in oscillation $(1 - |r|)$ and a small phase angle $\arg r$. Therefore, the terminology of (9.112) has been applied which is based on the amplitudes for the two eigenstates, using the complex parameter

$$\eta_{+-} = \frac{\langle \pi^+\pi^-|\mathcal{H}|K_L^0\rangle}{\langle \pi^+\pi^-|\mathcal{H}|K_S^0\rangle}$$

with a phase $\phi_{+-} = \arg \eta_{+-}$. If the formalism used for the B system is applied defining $r_{+-} = \eta_m \bar{A}/A$ by the K^0 and $\overline{K}^0$ amplitudes as above, this parameter is an ϵ parameter for the final state $\pi^+\pi^-$ according to (9.129) and we get $\langle \pi^+\pi^-|\mathcal{H}|K_S^0\rangle = pA(1 + r_{+-})$ and $\langle \pi^+\pi^-|H|K_L^0\rangle = pA(1 - r_{+-})$ and

$$\eta_{+-} = \frac{1 - r_{+-}}{1 + r_{+-}} = -i \tan i\frac{\ln r_{+-}}{2}, \qquad r_{+-} = \frac{1 - \eta_{+-}}{1 + \eta_{+-}} = -i \tan i\frac{\ln \eta_{+-}}{2}$$

Since r_{+-} is an observable, this holds also for η_{+-}. The coefficients for (9.94) are

$$1 - |r_{+-}|^2 = 4\frac{\mathcal{R}e\, \eta_{+-}}{|1 + \eta_{+-}|^2}$$
$$1 + |r_{+-}|^2 = 2\frac{1 + |\eta_{+-}|^2}{|1 + \eta_{+-}|^2}$$
$$\mathcal{R}e\, r_{+-} = |r_{+-}| \cos(\arg r_{+-}) = \frac{1 - |\eta_{+-}|^2}{|1 + \eta_{+-}|^2}$$
$$\mathcal{I}m\, r_{+-} = |r_{+-}| \sin(\arg r_{+-}) = -2\frac{\mathcal{I}m\, \eta_{+-}}{|1 + \eta_{+-}|^2}$$

[92] D. E. Dorfan et al., Phys. Rev. Lett. **19**, 987 (1967); S. Bennett et al., Phys. Rev. Lett. **19**, 993 (1967).

The amplitude ratio is further modified by direct CP violation from

$$\begin{aligned}\overline{A} = \langle \pi^+\pi^-|\mathcal{H}|\overline{K}^0\rangle &= \langle \pi^+\pi^-|\,\mathrm{CP}(\mathrm{CP}\,\mathcal{H}\,\mathrm{CP})\,\mathrm{CP}\,|\overline{K}^0\rangle \\ &= e^{i\phi_{\mathrm{CP}K}}\langle \pi^+\pi^-|(\mathrm{CP}\,\mathcal{H}\,\mathrm{CP})|K^0\rangle = e^{i\phi_{\mathrm{CP}K}}A\frac{1-\epsilon'}{1+\epsilon'}\end{aligned}$$

where ϵ' describes the small difference in the amplitudes. Its origin within the Standard Model lies in the interference of tree and penguin diagrams, where hadronic penguins contribute only to the isospin 0 final state, while the tree graph and electromagnetic penguins have also a small isospin 2 component. The two isospin amplitudes have different strong phases, and penguin and tree have a different weak phase. Therefore there is a small direct CP violation according to (9.84), which would be observed even without oscillation.

The isospin decomposition of a two-pion system has been discussed above in section 9.3.8.2.

If we choose an overall phase to make the isospin 0 amplitude A_0 real, we may write the isospin 2 amplitude as

$$A_2 e^{i\phi}e^{i\delta_{20}} := \langle \pi\pi, I=2|\mathcal{H}|K\rangle$$

with A_2 real (being the absolute value of the amplitude) and δ_{20} being the strong phase difference, while ϕ is the weak phase difference. Then the amplitudes and their ratio are

$$\begin{aligned}A(K^0 \to \pi^+\pi^-) &= \sqrt{\frac{1}{6}}A_2 e^{i\phi}e^{i\delta_{20}} + \sqrt{\frac{1}{3}}A_0 \\ \overline{A}(\overline{K}^0 \to \pi^+\pi^-) &= e^{i\phi_{\mathrm{CP}K}}\left(\sqrt{\frac{1}{6}}A_2 e^{-i\phi}e^{i\delta_{20}} + \sqrt{\frac{1}{3}}A_0\right) \\ \frac{\overline{A}}{A} &\approx e^{i\phi_{\mathrm{CP}K}}\left(1 + \sqrt{\frac{1}{2}}\frac{A_2}{A_0}e^{i\delta_{20}}(e^{-i\phi} - e^{i\phi})\right) = e^{i\phi_{\mathrm{CP}K}}\left(1 - \sqrt{2}\frac{A_2}{A_0}e^{i\delta_{20}}\, i\sin\phi\right)\end{aligned}$$

and

$$\epsilon' = \sqrt{\frac{1}{2}}\, i\, \frac{A_2}{A_0}e^{i\delta_{20}}\sin\phi \tag{9.145}$$

Correspondingly we obtain

$$r_{+-} = \frac{\eta_m \overline{A}}{A} = \frac{1-\epsilon_0}{1+\epsilon_0}\cdot\frac{1-\epsilon'}{1+\epsilon'} \approx 1 - 2\epsilon_0 - 2\epsilon'$$

and

$$\eta_{+-} \equiv \eta_{\pi^+\pi^-} \approx \epsilon_0 + \epsilon' \tag{9.146}$$

Note that in contrast to (9.85) the ϵ' is complex and has a phase. This is possible since the arbitrary phase factors that could be shuffled freely between η_m and $\overline{A}/A$ are indeed distributed between the factors $\frac{1-\epsilon_0}{1+\epsilon_0}$ and $\frac{1-\epsilon'}{1+\epsilon'}$ by the definition of $\epsilon_0 = \eta_{\pi\pi,I=0}$. This fixes the phase of the second factor.

Using the 1996 world average, these numbers are

$$\begin{aligned}\phi_{+-} &= (43.56 \pm 0.56)^\circ \\ |\eta_{+-}| &= (2.290 \pm 0.020)\cdot 10^{-3} \\ |r_{+-}| &= 0.996687 \pm 0.000042 \\ \sin(\arg r_{+-}) &= -(3.156 \pm 0.043)\cdot 10^{-3} \\ r_{+-} &= 0.996682 - 0.003146\, i\end{aligned}$$

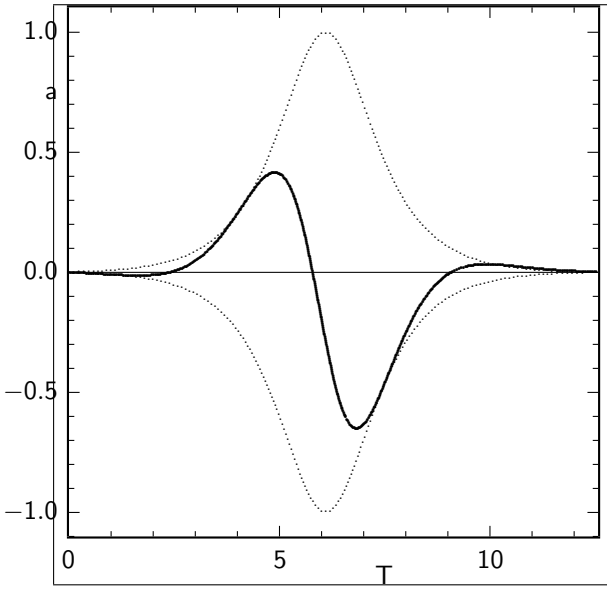

Fig. 9.22 Time dependent rate asymmetry $a(T)$ of $\overline{K}^0 \to \pi^+\pi^-$ and $K^0 \to \pi^+\pi^-$. $T = t/\bar{\tau}$ is the lifetime in units of $\bar{\tau} \approx 2\tau_S$, the inverse of the average width of K_L^0 and K_S^0. The dotted lines mark the envelope given by (9.116).

and the coefficients used in (9.94a′, b′) are

$$D_P = \frac{2|r_{+-}|}{1+|r_{+-}|^2} = 1 - 2(\mathcal{R}e\,\eta_{+-})^2 + \mathcal{O}(\eta_{+-}^4) = 0.999994$$

$$\Theta_0 = \frac{|r_{+-}|^2 - 1}{|r_{+-}|^2 + 1} = -2\,\mathcal{R}e\,\eta_{+-} + \mathcal{O}(\eta_{+-}^3) = -(3.318 \pm 0.045)\cdot 10^{-3}$$

$$\Lambda_0 = D_P \sin(\arg r_{+-}) = -2\,\mathcal{I}m\,\eta_{+-} + \mathcal{O}(\eta_{+-}^3) = -(3.156 \pm 0.043)\cdot 10^{-3}$$

$$\Omega_0 = D_P \cos(\arg r_{+-}) = 1 - 2|\eta_{+-}|^2 + \mathcal{O}(\eta_{+-}^4) = +0.999990$$

where the + sign for Ω_0 is determined by the CP value of the $\pi^+\pi^-$ eigenstate.

From (9.144) and (9.146) and with $|A_0| \approx |\bar{A}_0|$ (since the $\pi\pi$ final state in isospin 0 almost saturates the kaon decay) we have

$$|\eta_m| \approx \left|\frac{1-\epsilon_0}{1+\epsilon_0}\right| \approx \left|\frac{1-\eta_{+-}}{1+\eta_{+-}}\right|$$

Expressed in the η_{+-} variable, the squared matrix elements are

$$|\mathcal{M}|^2 = e^{-T}\frac{|A|^2}{|p|^2|1+\eta_{+-}|^2}\Big\{(1+|\eta_{+-}|^2)\cosh yT + (1-|\eta_{+-}|^2)\sinh yT + 2\,\mathcal{R}e\,\eta_{+-}\cos xT + 2\,\mathcal{I}m\,\eta_{+-}\sin xT\Big\} \tag{9.147}$$

$$|\overline{\mathcal{M}}|^2 = e^{-T}\frac{|A|^2}{|q|^2|1+\eta_{+-}|^2}\Big\{(1+|\eta_{+-}|^2)\cosh yT + (1-|\eta_{+-}|^2)\sinh yT - 2\,\mathcal{R}e\,\eta_{+-}\cos xT - 2\,\mathcal{I}m\,\eta_{+-}\sin xT\Big\}$$

which corresponds to the asymmetry function

$$a(T) = \frac{\dot{N}(\overline{K}^0 \to \pi^+\pi^-) - \dot{N}(K^0 \to \pi^+\pi^-)}{\dot{N}(\overline{K}^0 \to \pi^+\pi^-) + \dot{N}(K^0 \to \pi^+\pi^-)} = -\frac{2|\eta_{+-}|\cos(xT-\phi_{+-}) - \delta_\epsilon[|\eta_{+-}|^2 e^{yT} + e^{-yT}]}{|\eta_{+-}|^2 e^{yT} + e^{-yT} - 2\delta_\epsilon|\eta_{+-}|\cos(xT-\phi_{+-})}$$
$$\approx -\frac{2|\eta_{+-}|\cos(xT-\phi_{+-})}{|\eta_{+-}|^2 e^{yT} + e^{-yT}} \tag{9.148}$$

shown in figure 9.22, where the K flavour is understood to be the one at $T = 0$. The approximation in (9.148) is for $|\eta_m| = 1$ ($\delta_\epsilon = 0$). Although $\delta_\epsilon \approx 2\,\mathcal{R}e\,\eta_{+-}$ is of the same order as other terms, it is small compared to the maximum asymmetry, as can be seen in figure 9.22. The determination of ϕ_{+-} from (9.148) is only modulo 180°. Equivalent to the solution 43.4° is −136.7°.

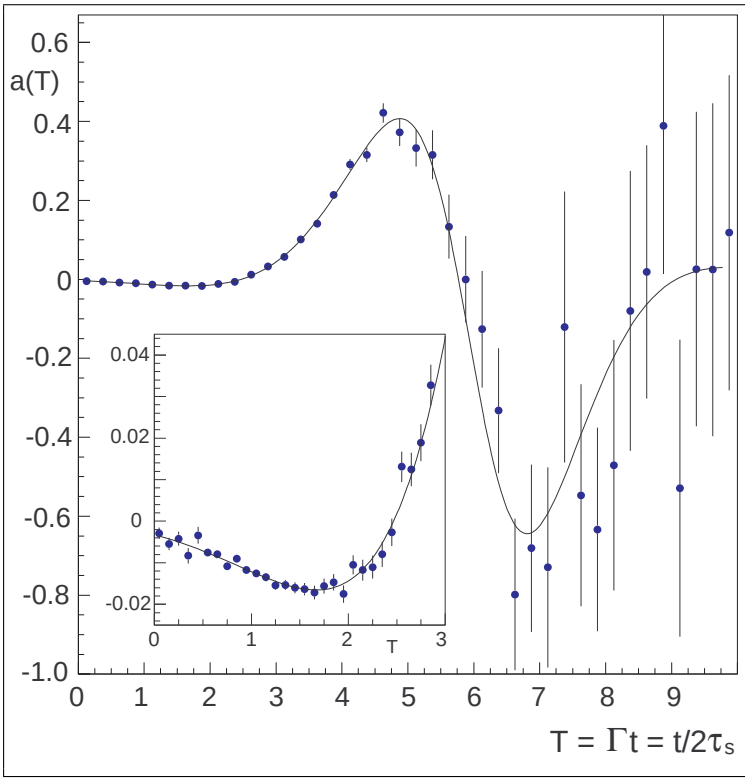

Fig. 9.23 Time dependent rate asymmetry $a(T)$ of $\overline{K}^0 \to \pi^+\pi^-$ measured by the CPLEAR collaboration. The insert shows the deviation from 0 also for small values of T.

This asymmetry has been nicely verified in a measurement by the CPLEAR collaboration [93], and is shown in figure 9.23. Note that instead of T the variable $t/\tau_S \approx 2T$ is used.

The phenomenology for the $\pi^0\pi^0$ state is similar, with a small change due to the different interference between

$$A(K^0 \to \pi^0\pi^0) = \sqrt{\frac{2}{3}} A_2 e^{i\phi} e^{i\delta_{20}} - \sqrt{\frac{1}{3}} A_0$$

$$\overline{A}(\overline{K}^0 \to \pi^0\pi^0) = e^{i\phi_{CPK}} \left(\sqrt{\frac{2}{3}} A_2 e^{-i\phi} e^{i\delta_{20}} - \sqrt{\frac{1}{3}} A_0 \right)$$

$$\frac{\overline{A}}{A} \approx e^{i\phi_{CPK}} \left(1 - \sqrt{2} \frac{A_2}{A_0} e^{i\delta_{20}} (e^{i\phi} - e^{-i\phi}) \right) = e^{i\phi_{CPK}} \left(1 + 2\sqrt{2} \frac{A_2}{A_0} e^{i\delta_{20}}\, i \sin\phi \right)$$

and

$$\epsilon'_{00} = -\sqrt{2} i \frac{A_2}{A_0} e^{i\delta_{20}} \sin\phi = -2\epsilon'$$

which finally leads to

$$\eta_{00} = \eta_{\pi^0\pi^0} \approx \epsilon_0 - 2\epsilon'$$

and hence

$$\epsilon' \approx \frac{\eta_{+-} - \eta_{00}}{3}$$

When we use $\epsilon_0 \approx \eta_{+-}$ to define $\epsilon \approx \epsilon_0$, the ratio is

$$1 - 3\frac{\epsilon'}{\epsilon} = \frac{\eta_{00}}{\eta_{+-}}$$

[93] CPLEAR Collab., R. Adler et al., Phys. Lett. **B363**, 243 (1995).

or calculating the absolute value and ignoring terms $\mathcal{O}(\epsilon'^2)$

$$1 - 6\,\mathcal{R}e\,\frac{\epsilon'}{\epsilon} = \left|\frac{\eta_{00}}{\eta_{+-}}\right|^2 = \frac{\frac{\Gamma(K_L^0\to\pi^0\pi^0)}{\Gamma(K_S^0\to\pi^0\pi^0)}}{\frac{\Gamma(K_L^0\to\pi^+\pi^-)}{\Gamma(K_S^0\to\pi^+\pi^-)}} \tag{9.149}$$

Experimental determination of this double ratio has lead to a significant confirmation of direct CP violation. Results are given in table 9.7.

Table 9.7 Experimental results

0 $3{\cdot}10^{-3}$	$\mathcal{R}e(\epsilon'/\epsilon)$ $[10^{-4}]$	experiment
	$(32 \pm 30$	E731A 1988)
	$(33 \pm 11$	NA31 1988)
	$-4 \pm 14 \pm 6$	(E731B 20% 1990)
	$7.4 \pm 5.2 \pm 2.9$	E731B final 1993
	23.0 ± 6.5	NA31 final 1993
	14.7 ± 2.2	NA48 2002
	19.2 ± 2.1	KTeV 2011
	16.8 ± 2.0	avg, $\chi^2 = 5.6/3 d.f.$

A more general description of the kaon system waiving CPT invariance can be found in the literature, e. g. in the book by Commins and Bucksbaum. The available results on the kaon system have reached an amazing precision on many parameters, but are all well compatible with the Standard Model.

9.3.10.1 CP Violation in Strange Baryon Decays

CP violation in strange baryon decays can be established as different levels of parity violation in baryon and antibaryon decay. An example is the decay $\Xi^- \to \Lambda\pi^-, \Lambda \to p\pi^-$ versus $\overline{\Xi}^+ \to \overline{\Lambda}\pi^+, \overline{\Lambda} \to \bar{p}\pi^+$, where the Λ polarization is used as an observable by the E871 experiment, who find no evidence from their measurement of the CP-violating parameter

$$A_{\Xi\Lambda} = \frac{\alpha_\Xi\alpha_\Lambda - \bar{\alpha}_\Xi\bar{\alpha}_\Lambda}{\alpha_\Xi\alpha_\Lambda + \bar{\alpha}_\Xi\bar{\alpha}_\Lambda} = (0.0 \pm 5.1 \pm 4.4)\cdot 10^{-4}$$

The α parameters are the decay-asymmetries from P violation in the coresponding two-body decays.

9.4 Messung der CKM-Parameter

9.4.1 V_{cd}

Myonpaare aus der Neutrino-Nukleon-Streuung:

Charm-Produktion mit Valenz und Seequarks

$$\nu_\mu d \to \mu^- c, \quad c \to s(d)\mu^+\nu_\mu \tag{9.150}$$

$$\nu_\mu d \to \mu^- u(c) \tag{9.151}$$

nur Seequarks

$$\begin{aligned}
&\nu_\mu s \to \mu^- c, \quad c \to s(d)\mu^+\nu_\mu \\
&\bar\nu_\mu \bar d \to \mu^+ \bar c, \quad \bar c \to \bar s(\bar d)\mu^-\bar\nu_\mu \\
&\bar\nu_\mu \bar s \to \mu^+ \bar c, \quad \bar c \to \bar s(\bar d)\mu^-\bar\nu_\mu
\end{aligned} \tag{9.152}$$

$$\begin{aligned}
&\nu_\mu s \to \mu^- u(c) \\
&\nu_\mu \bar u \to \mu^- \bar d(\bar s)
\end{aligned}$$

(schwere b-Quarks sind vernachlässigbar)

Wirkungsquerschnitte (4-Fermi-Wechselwirkung, $q^2 \ll m_W^2$):

$$\begin{aligned}
\frac{\mathrm{d}\sigma(\nu_\mu d \to \mu^- u)}{\mathrm{d}\Omega} &= \frac{\mathrm{d}\sigma(\bar\nu_\mu \bar d \to \mu^+ \bar u)}{\mathrm{d}\Omega} = |V_{ud}|^2 \frac{G_F^2 s}{4\pi^2} \\
\frac{\mathrm{d}\sigma(\nu_\mu \bar u \to \mu^- \bar d)}{\mathrm{d}\Omega} &= \frac{\mathrm{d}\sigma(\bar\nu_\mu u \to \mu^+ d)}{\mathrm{d}\Omega} = |V_{ud}|^2 \frac{G_F^2 s}{4\pi^2} \frac{(1+\cos\theta)^2}{2}
\end{aligned}$$

da nur linkshändige Fermionen und rechtshändige Antifermionen wechselwirken, also $\nu_{\mu L} d_L \to \mu_L^- u_L$ Gesamtspin $0 \to 0$, aber $\nu_{\mu L} \bar u_R \to \mu_L^- \bar d_R$ Gesamtspin $1 \to 1$ haben. Integriert ($\int \ldots \mathrm{d}\Omega$) wird

$$\begin{aligned}
\sigma(\nu_\mu d \to \mu^- u) = \sigma(\bar\nu_\mu \bar d \to \mu^+ \bar u) &= |V_{ud}|^2 \frac{G_F^2 s}{\pi} = \sigma_0 \\
\sigma(\nu_\mu \bar u \to \mu^- \bar d) = \sigma(\bar\nu_\mu u \to \mu^+ d) &= \frac{1}{3}|V_{ud}|^2 \frac{G_F^2 s}{\pi} = \frac{1}{3}\sigma_0
\end{aligned}$$

Der Wirkungsquerschnitt der Neutrino-Nukleon-Streuung kann daher auf Valenz- und Seequarks aufgeteilt werden ($f(...)$ = Anzahl pro Nukleon):

$$\begin{aligned}
\sigma(\nu_\mu N \to \mu^- X) &= \sigma_0 f(d_V) + \sigma_0 f(d_S) + \frac{1}{3}\sigma_0 f(\bar u_S) = \sigma_0 \left[f(d_V) + \frac{4}{3} f(x_S) \right] \\
\sigma(\bar\nu_\mu N \to \mu^+ X) &= \frac{1}{3}\sigma_0 f(u_V) + \frac{1}{3}\sigma_0 f(u_S) + \sigma_0 f(\bar d_S) = \sigma_0 \left[\frac{1}{3} f(u_V) + \frac{4}{3} f(x_S) \right] \\
\sigma(\nu_\mu N \to \mu^- X) - \sigma(\bar\nu_\mu N \to \mu^+ X) &= \sigma_0 \left[f(d_V) - \frac{1}{3} f(u_V) \right] \qquad (9.153) \\
\frac{\sigma(\nu_\mu N \to \mu^- X)}{\sigma(\bar\nu_\mu N \to \mu^+ X)} &= \frac{f(d_V) + \frac{4}{3} f(x_S)}{\frac{1}{3} f(u_V) + \frac{4}{3} f(x_S)} \qquad (9.154)
\end{aligned}$$

mit $f(x_S) := f(u_S) = f(\bar u_S) = f(d_S) = f(\bar d_S)$. Für ein **isoskalares Target**, $f(u_V) = f(d_V)$, ist die Differenz (9.153) proportional zu $\frac{2}{3} f(q_V)$, der Valenzquarks, daher ist $\frac{3}{2}[\sigma(\bar\nu_\mu N \to \mu^+ X) - \sigma(\bar\nu_\mu N \to \mu^+ X)]$ der Neutrinowirkungsquerschnitt mit einem Valenzquark. Das Verhältnis der Wirkungsquerschnitte (9.154) liegt zwischen 1 (nur Seequarks) und 3 (nur Valanzquarks), experimentell ist es etwa 2.

10. Neutrinooszillationen und -Massen

10.1 Zwei Neutrinos

Flavoureigenzustände μ,τ
Masseneigenzustände 2,3

$$\begin{aligned} |\nu_2\rangle &= |\nu_\mu\rangle \cos\theta_{23} - |\nu_\tau\rangle \sin\theta_{23} \\ |\nu_3\rangle &= |\nu_\mu\rangle \sin\theta_{23} + |\nu_\tau\rangle \cos\theta_{23} \end{aligned} \tag{10.1}$$

$$\begin{aligned} |\nu_\mu\rangle &= |\nu_2\rangle \cos\theta_{23} + |\nu_3\rangle \sin\theta_{23} \\ |\nu_\tau\rangle &= -|\nu_2\rangle \sin\theta_{23} + |\nu_3\rangle \cos\theta_{23} \end{aligned}$$

Näherung $m_2, m_3 \ll E$

$$p_i \approx E - \frac{m_i^2}{2E} \tag{10.2}$$

Zeitentwicklung eines Masseneigenzustands

$$|\psi_i(t)\rangle = |\nu_i\rangle\, e^{-iEt} e^{ip_i x}$$

Zeitentwicklung von $|\psi(0)\rangle = a_2|\nu_2\rangle + a_3|\nu_3\rangle$

$$\begin{aligned} |\psi(t)\rangle &\approx a_2 e^{-iE(t-x)} e^{im_2^2 x/2E}|\nu_2\rangle + a_3 e^{-iE(t-x)} e^{im_3^2 x/2E}|\nu_3\rangle \\ &= e^{-iE(t-x)} \Big[a_2 \cos\theta_{23} e^{im_2^2 x/2E}|\nu_\mu\rangle + a_3 \sin\theta_{23} e^{im_3^2 x/2E}|\nu_\mu\rangle \\ &\qquad -a_2 \sin\theta_{23} e^{im_2^2 x/2E}|\nu_\tau\rangle + a_3 \cos\theta_{23} e^{im_3^2 x/2E}|\nu_\tau\rangle \Big] \end{aligned}$$

Für einen Anfangszustand $|\nu_\mu\rangle$ ist[94]

$$\begin{aligned} a_2 &= \cos\theta_{23} \\ a_3 &= \sin\theta_{23} \\ |\psi(t)\rangle &\approx e^{-iE(t-x)} \Big[(\cos^2\theta_{23}\, e^{im_2^2 x/2E} + \sin^2\theta_{23}\, e^{im_3^2 x/2E})|\nu_\mu\rangle \\ &\qquad +(e^{im_3^2 x/2E} - e^{im_2^2 x/2E}) \cos\theta_{23} \sin\theta_{23}|\nu_\tau\rangle \Big] \end{aligned}$$

$$|\langle\nu_\mu|\psi(t)\rangle|^2 = 1 - 2\cos^2\theta_{23}\sin^2\theta_{23}\left(1 - \cos\frac{(m_3^2 - m_2^2)x}{2E}\right) = 1 - \sin^2 2\theta_{23}\sin^2\frac{(m_3^2 - m_2^2)x}{4E} \tag{10.3}$$

$$|\langle\nu_\tau|\psi(t)\rangle|^2 = 2\cos^2\theta_{23}\sin^2\theta_{23}\left(1 - \cos\frac{(m_3^2 - m_2^2)x}{2E}\right) = \sin^2 2\theta_{23}\sin^2\frac{(m_3^2 - m_2^2)x}{4E} \tag{10.4}$$

Für die praktische Rechnung:

$$|\langle\nu_\tau|\psi(t)\rangle|^2 = \cos^2\theta_{23}\sin^2\theta_{23}\sin^2\frac{((m_3c^2)^2 - (m_2c^2)^2)x}{\hbar c E}$$

---

[94] $\cos^4\alpha + \sin^4\alpha = \cos^4\alpha + (1 + \cos^4\alpha - 2\cos^2\alpha) = 1 - 2\cos^2\alpha\sin^2\alpha$,
$|a+b|^2 = |a|^2 + |b|^2 + 2|a||b|\cos(\arg a - \arg b)$,
$1 - \cos\alpha = 2\sin^2\frac{\alpha}{2}$
$4\sin^2\alpha\cos^2\alpha = \sin^2 2\alpha$

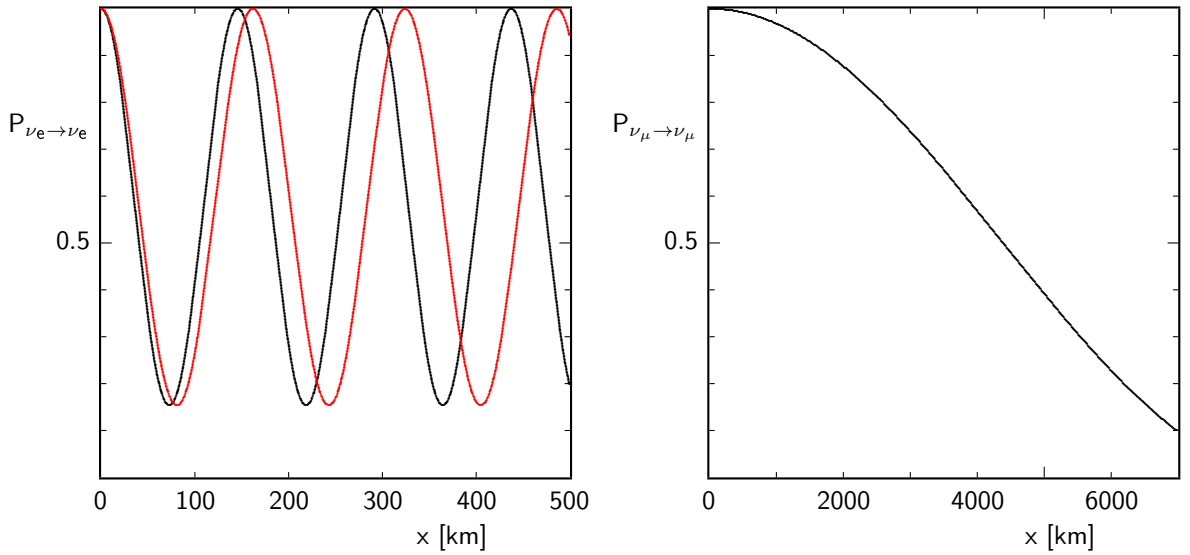

Fig. 10.1 Wahrscheinlichkeit für $\nu_e \to \nu_e$ bei $E = 4.5\,\text{MeV}$ und $E = 5.0\,\text{MeV}$ und $\nu_\mu \to \nu_\mu$ bei $E = 17\,\text{GeV}$ (CERN to Gran Sasso).

10.1.1 Massenmessung via Flugstrecke

Die Gleichungen (10.3) und (10.4) gelten für unendlich ausgedehnte ebene Wellen. Neutrinos als Punktteilchen erlauben eine Flugzeit- und Massenmessung. Die Interferenz zwischen Neutrinos verschiedener Masse kann nur innerhalb der Kohärenzlänge beobachtet werden.

Für gleiche Energie E, verschiedene Massen:

$$\Delta x = \Delta\beta t = \frac{\Delta p}{E} t \approx -\frac{\Delta(m^2)}{2E^2} t \tag{10.5}$$

und mit $v \approx 1$, d. h. $t \approx x$

$$\frac{\Delta x}{x} = \frac{\Delta t}{t} = -\frac{\Delta(m^2)}{2E^2}$$

Die Messung ist erst möglich, wenn die Unschärfe-Relation

$$\Delta p\, \Delta x \gtrsim 1$$

erfüllt ist. Andernfalls, d. h. wenn

$$\Delta p\, \Delta x \lesssim 1$$

sind keine Masseneigenzustände unterscheidbar und man hat eine **kohärente** Überlagerung verschiedener Massenzustände.

Mit (10.2) und (10.5) wird die Kohärenzbedingung

$$\Delta p \Delta x = \frac{(\Delta p)^2}{E} \cdot x = \frac{(\Delta m^2)^2}{4E^3} x \lesssim 1$$

$$x \lesssim \frac{4E^3}{(\Delta m^2)^2} = \frac{4}{\sqrt{\Delta m^2}} \left(\frac{E}{\sqrt{\Delta m^2}} \right)^3$$

Eine Massendifferenz $\sqrt{\Delta m^2} \approx 0.1\,\text{eV}$ entspricht[95] $\frac{4}{\sqrt{\Delta m^2}} \approx 10^{-2}\,\text{m}$. Mit Energien im GeV-Bereich wird daraus

$$x < 10^{24}\,\text{m} \approx 10^{13}\,\text{AE} \approx 10^{8}\,\text{pc}$$

[95] $1 \approx 0.2 \cdot 10^{-6}\,\text{eV m}$

Innerhalb dieser Flugstrecke ist keine Massenmessung durch Orts- und Impulsmessung möglich. Hätte ein Neutrino die Masse des s-Quarks von etwa $0.5\,\mathrm{GeV}$, ergäbe dieselbe Rechnung $x \lesssim 10\,\mathrm{fm}$.

10.2 Drei Neutrinos

Beispiel: Ein anfängliches ν_e der Energie E ist im Abstand x

$$|\langle\nu_e|\nu_e\rangle|^2 = 1 - P_{12}\sin^2\frac{x(m_2^2-m_1^2)}{4E} - P_{23}\sin^2\frac{x(m_3^2-m_2^2)}{4E} - P_{13}\sin^2\frac{x(m_3^2-m_1^2)}{4E} \tag{10.6}$$

oder

$$|\langle\nu_\mu|\nu_e\rangle|^2 = Q_{12}\sin^2\frac{x(m_2^2-m_1^2)}{4E} + Q_{23}\sin^2\frac{x(m_3^2-m_2^2)}{4E} + Q_{13}\sin^2\frac{x(m_3^2-m_1^2)}{4E} \tag{10.7}$$

mit Koeffizienten P und Q, die von dem PMNS-Matrixelementen abhängen.

$$\begin{aligned} P_{12} &= \sin^2(2\theta_{12})\cos^4\theta_{13} \\ P_{13} &= \sin^2(2\theta_{13})\cos^2\theta_{12} \\ P_{23} &= \sin^2(2\theta_{13})\sin^2\theta_{12} \end{aligned}$$

10.3 Oszillations-Phänomenologie

Zwei ineinander oszillierende Zustände haben die Zeitentwicklung

$$f(t) \sim e^{i\Delta E\cdot t}$$

wobei für kleine Differenzen $E\,\mathrm{d}E = m\,\mathrm{d}m$ gilt:

$$\Delta E = \frac{m\Delta m}{E} \approx \begin{cases} \Delta m & p \ll m \quad\Longrightarrow\quad E \approx m \\ \frac{\Delta m^2}{2p} & p \gg m \quad\Longrightarrow\quad E \approx p \end{cases} \tag{10.8}$$

Der erste Fall beschreibt die Oszillation von K, D und B-Mesonen, der zweite die Neutrino-Oszillation.

Im Ruhesystem des Teilchens ist $p = 0$, und es gilt immer der erste Fall. Die Oszillationsfrequenz der Neutrinos proportional Δm^2 ergibt sich dann aus der Lorentz-Transformation.

Im Neutrino-Ruhesystem ist $|\langle\nu|\Psi(t)|^2 \sim 1 - \cos(m_1 - m_2)t$. Im Laborsystem wird daraus nach einer Flugstrecke x mit

$$t = \frac{t_1+t_2}{2}, \qquad t_i = \frac{x}{\beta\gamma} = \frac{xm_i}{p_i} = \frac{xm_i}{E\sqrt{1-m_i^2/E^2}} \approx \frac{xm_i}{E}$$

$|\langle\nu|\Psi(t)|^2 \sim 1 - \cos(m_1^2 - m_2^2)x/2E$. Die unterschiedlichen Geschwindigkeiten der beiden Massen-Eigenzustände bedingen eine Unschärfe $|t_1 - t_2|$ des Neutrino-Ruhesystems!

10.4 MSW-Effekt

Mikheyev–Smirnov–Wolfenstein

10.5 Mischungsmatrix

PMNS-Matrix[96]

Für Dirac-Neutrinos (wie CKM-Matrix) :

$$\begin{aligned}\boldsymbol{U} &= \begin{pmatrix} 1 & 0 & 0 \\ 0 & c_{23} & s_{23} \\ 0 & -s_{23} & c_{23} \end{pmatrix} \begin{pmatrix} c_{13} & 0 & s_{13}e^{-i\delta_{13}} \\ 0 & 1 & 0 \\ -s_{13}e^{i\delta_{13}} & 0 & c_{13} \end{pmatrix} \begin{pmatrix} c_{12} & s_{12} & 0 \\ -s_{12} & c_{12} & 0 \\ 0 & 0 & 1 \end{pmatrix} \\ &= \begin{pmatrix} c_{12}c_{13} & s_{12}c_{13} & s_{13}e^{-i\delta_{13}} \\ -s_{12}c_{23} - c_{12}s_{13}s_{23}e^{i\delta_{13}} & c_{12}c_{23} - s_{12}s_{13}s_{23}e^{i\delta_{13}} & c_{13}s_{23} \\ s_{12}s_{23} - c_{12}s_{13}c_{23}e^{i\delta_{13}} & -c_{12}s_{23} - s_{12}s_{13}c_{23}e^{i\delta_{13}} & c_{13}c_{23} \end{pmatrix} \end{aligned} \tag{10.9}$$

$c_{ij} = \cos\theta_{ij}$, $s_{ij} = \sin\theta_{ij}$

$s_{ij} > 0$, $c_{ij} > 0$; $0 \leq \theta_{ij} \leq \pi/2$

10.5.1 Experimentelle Resultate

Stand Sep. 2014:

$$\begin{aligned} \Delta m^2_{12} &= (7.50 \pm 0.19) \cdot 10^{-5}\,\mathrm{eV}^2 \\ \sin^2\theta_{12} &= 0.304 \pm 0.013, \qquad \theta_{12} \approx 33^\circ \\ \Delta m^2_{23} &= (2.45 \pm 0.05) \cdot 10^{-3}\,\mathrm{eV}^2 \\ \sin^2\theta_{23} &\approx \tfrac{1}{2}, \qquad \theta_{23} \approx 45^\circ \\ \sin^2\theta_{13} &= 0.0218 \pm 0.0011, \qquad \theta_{13} \approx 9^\circ \end{aligned}$$

Hierarchieproblem: $1,2 \leftrightarrow 2,3$,

„natürliche Hierarchie“: kleine Massendifferenz zwischen 1 und 2, große zwischen 2 und 3, $\nu_1 \approx \nu_e$, $\nu_3 \approx \frac{1}{\sqrt{2}}(\nu_\mu + \nu_\tau)$

$\sin^2\theta_{23} = 0.452 \pm {}^{0.051}_{0.028}$

„invertierte Hierarchie“: große Massendifferenz zwischen 1 und 2, kleine zwischen 2 und 3 $\nu_2 \approx \nu_e$, $\nu_1 \approx \frac{1}{\sqrt{2}}(\nu_\mu + \nu_\tau)$

$\sin^2\theta_{23} = 0.579 \pm {}^{0.025}_{0.037}$

[96] Bruno Pontecorvo, „Mesonium and antimesonium“, Sov. Phys. JETP **6**, 429 (1957) and Zh. Eksp. Teor. Fiz. **33**, 549 (1957), [possibility of $\nu \leftrightarrow \overline{\nu}$ transitions]; B. Pontecorvo, „Inverse beta processes and nonconservation of lepton charge“, Sov. Phys. JETP **7**, 172–173 (1958) and Zh. Eksp. Teor. Fiz. **34**, 247 (1958); B. Pontecorvo, „Neutrino experiments and the question of leptonic-charge conservation“, Sov. Phys. JETP **26**, 984–988 (1968) and Zh. Eksp. Teor. Fiz. **53**, 1717–1725 (1967); S. Bilenky, B. Pontecorvo, „Lepton mixing and neutrino oscillations“ Phys. Rep. **41**, 225 (1978); Z. Maki, M. Nakagawa, S. Sakata, „Remarks on the Unified Model of Elementary Particles“, Prog. Theor. Phys. **28**, 870 (1962).

10.6 Majorana-Neutrinos

Die 4 Freiheitsgrade des Diracspinors können bei vollständig neutralen Teilchen auch anders aufgeteilt werden. So kann ein linkshändiges Neutrino das Antiteilchen des rechtshändigen Neutrinos sein.

Nach (5.7) ist

$$\psi_C = C\gamma^0\psi^* = i\gamma^2\psi^* \tag{10.10}$$

und für neutrale Teilchen kann man das Majorana-Feld

$$\psi_{1,2} = \frac{1}{\sqrt{2}}(\psi \pm \psi_C)$$

definieren. Diese Zustände sind ihre eigenen Antiteilchen mit $C = \pm 1$.

Majorana-Teilchen sind ihre eigenen Antiteilchen, sie können keine Ladungen tragen: alle elektrischen und magnetischen Momente sind 0.

Aus $\psi_{1,2}$ kann man jeweils rechts- und linkshändige Eigenzustände erzeugen. Es ist

$$\psi_{C;L} = \frac{i}{2}(1-\gamma_5)\gamma^2\psi^* = \frac{i}{2}\gamma^2(1+\gamma_5)\psi^* = i\gamma^2\psi_R^*$$

Mit

$$\psi_{1,2;R,L} = \frac{1}{\sqrt{2}}(\psi_{R,L} \pm \psi_{C;R,L})$$

werden die vier Spinor-Freiheitsgrade (statt üblicherweise durch $\psi_L, \psi_R, \psi_{C;L}, \psi_{C;R}$) bei Majoranateilchen durch $\psi_{1;L}, \psi_{1;R}, \psi_{2;L}, \psi_{2;R}$ repräsentiert.

Mögliche Massenterme im Lagrangian für einen Neutrinoflavour:

$$\begin{pmatrix} \bar\psi_L \\ \bar\psi_{C;R} \end{pmatrix} \begin{pmatrix} 0 & m_D \\ m_D & M_R \end{pmatrix} \begin{pmatrix} \psi_{C;L} \\ \psi_R \end{pmatrix} = m_D\bar\psi_L\psi_R + m_D\bar\psi_{C;L}\psi_{C;R} + M\psi_{C;R}\psi_R$$

(m_D = Diracmasse).

Die Massenmatrix kann diagonalisiert werden. Die Eigenwerte sind

$$\mu = \frac{M_R}{2} \pm \sqrt{\frac{M_R^2}{4} + m_D^2}$$

Für $m_D \ll M_R$

$$\mu_1 \approx M_R$$
$$\mu_2 = -m_\nu \approx -\frac{m_D^2}{M_R}$$

(Seesaw-Mechanismus). Das Minuszeichen von μ_2 muss durch Phasen der Majoranafelder kompensiert werden.

Für drei Familien ist

$$\mathbf{M} = \begin{pmatrix} 0 & \mathbf{m}_D \\ \mathbf{m}_D^+ & \mathbf{M}_R \end{pmatrix}$$

Durch die Gleichheit von ν und $\bar\nu$ wird die Leptonzahl um 2 Einheiten verletzt.

Dies erlaubt den neutrinolosen doppelten Betazerfall, bei dem zwischen den beiden Neutronen ein reelles Neutrino = Antineutrino ausgetauscht wird. Allerdings ist er wegen der Linkshändigkeit der schwachen Wechselwirkung um den Helizitätsfaktor $(m/E)^2$ unterdrückt.

Literatur

D. Griffiths, Einführung in die Elementarteilchenphysik, Akademie Verlag

D. Griffiths, Introduction to Elementary Particles, John Wiley & Sons

D. H. Perkins, Hochenergiephysik, Addison-Wesley

D. H. Perkins, Introduction to High Energy Physics, Cambridge University Press

C. Berger, Teilchenphysik – eine Einführung, Springer

C. Berger, Elementarteilchenphysik: Von den Grundlagen zu den modernen Experimenten, Springer

O. Nachtmann, Elementarteilchenphysik, Vieweg

Feldtheorie:

F. Halzen and A. D. Martin, Quarks and Leptons, John Wiley

M. E. Peskin and D. V. Schroeder, An Introduction to Quantum Field Theory, Addison Wesley

C. Itzykson and J. B. Zuber, Quantum Field Theory, McGraw Hill

Elektroschwache Wechselwirkung:

E. D. Commins, P. H. Bucksbaum, Weak Interactions of Leptons and Quarks, Cambridge University Press (enthält auch eine Diskussion der CPT-Verletzung)

CP-Verletzung:

G. C. Branco, L. Lavoura, J. P. Silva, CP Violation, Clarendon Press, Oxford (1999)

I. I. Bigi, A. I. Sanda, CP Violation, Cambridge University Press (2000)